THE USE OF SMALL SCALE FIRE TEST DATA FOR THE HAZARD ASSESSMENT OF BULK MATERIALS

by

MARIANNE FOLEY (MENG)

DOCTOR OF PHILOSOPHY

UNIVERSITY OF EDINBURGH

1995

DECLARATION

It is declared that this thesis and the results therein contained are the work of the author, herself, and have been produced under the supervision of Dr. D. D. Drysdale

Marianne Foley (MEng)

Edinburgh

April 1995

Abstract

An experimental study of fire testing of solid materials has been carried out to investigate whether or not these tests yield useful data for the burning of materials stored in bulk, for example in warehouses. Tests were performed using the Cone Calorimeter, the HSE third scale room/corridor rig, BS 5852 part 2, and some non-standard tests. The results have been compared and the problems with fire testing have been discussed with reference to the current literature and trends in fire testing. The additional complications of unusual material behaviour under exposure to heating have also been investigated.

In the third scale room/corridor test, where vertical, parallel samples are used, the separation distance between the samples was found to play a significant part in whether ignition of fire retarded samples could be achieved or not. A literature survey revealed a dearth of information on this subject. As this type of parallel configuration is found in warehouse storage as well as vertical ducts and cavities, an investigation was conducted into flames between vertical parallel walls. Measurements were made of total and radiative heat fluxes at the walls, flame and gas temperatures, and flame heights under a variety of conditions. It was found that the configuration of the system was very important, with the separation distance and fluid dynamics both having a major influence. Burner position, geometry and heat release rate were also varied and their influence assessed.

Statistical methods were employed to correlate the heat flux data and temperatures with the other variables, with excellent correlation coefficients for the equations developed. These have been compared with previous expressions developed for flames against vertical walls. Results from CFD work on two of the parallel wall cases of special interest were analysed and discussed with reference to the experimental results. The findings have implications for the fire testing of materials, and for the hazard assessment of materials stored in high rack storage. An understanding of potential exposure conditions in a real fire scenario are essential for the appropriate use of fire tests.

Acknowledgements

The author gratefully acknowledges the help and support from the following people during the course of this research:

Dougal Drysdale for his supervision, advice and encouragement.

Graham Atkinson, Chris Lea, and all at Fire Section, HSE, Buxton for their enthusiasm and ideas.

All the technicians in Civil Engineering at Edinburgh University, and Dave Bagshaw and Ed Belfield at HSE, without whom experimental work would have been impossible. Also the secretarial staff at Edinburgh for such friendly help.

The postgrad. students (and some RAs) in the Civil Engineering Department, whose friendship and advice prevented me giving up. Thanks especially to Pete Thompson and Pete Woodburn for reading parts of the thesis.

Thanks to all my friends in Edinburgh, who have done a great job of keeping me sane and cheerful, especially Graeme Wood for his understanding, patience and humour.

Finally, thanks to my parents and family who have always given me support in everything I've done.

This work was supported by a grant from the EPSRC and funding from the Health and Safety Executive.

Table of Contents

Chapter 5: Results

Chapter 6: Discussion

List of Figures

Figure (2.19) schematic pattern of burning area growth in Room/corner test

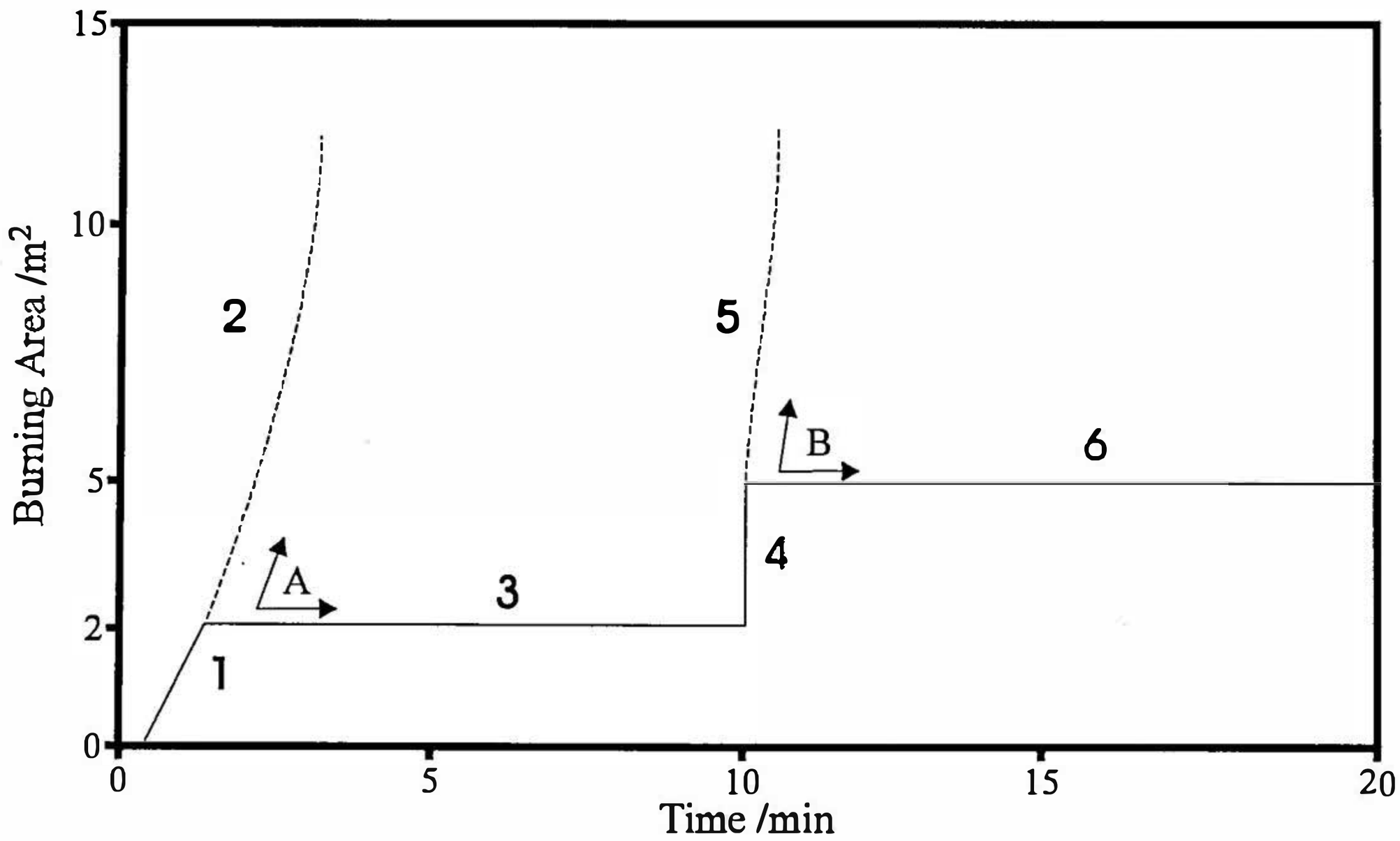

Nomenclature

a	separation between parallel vertical surfaces, m
A	heat release during peak period, $J.m^{-2}$
b	radius to the edge of a plume, m
B	buoyancy flux, $kg.m.s^{-3}$
$b_{\Delta T}$	plume radius up to $0.5\Delta T_0$, m
C	orifice plate coefficient, $kg^{0.5}m^{0.5}K^{0.5}$
c_p	specific heat capacity, $J.kg^{-1}.K^{-1}$
D	fire source diameter, or equivalent diameter, m
E	heat of combustion per gram oxygen, $J.g^{-1}$
g	acceleration due to gravity, $m.s^{-2}$
h	height of a vertical surface, m
h_{ig}	heat transfer coefficient, $kW.m^{-2}.K^{-1}$
ΔH_c	heat of combustion, $J.kg^{-1}$
ΔH_G	heat of gasification, $J.kg^{-1}$
I	light energy at detector in absence of smoke
I_o	light energy at detector in presence of smoke
k	extinction coefficient, m^{-1}
k	thermal conductivity, $W.m^{-1}.K^{-1}$, turbulence energy, m^2s^{-1}
k_g	thermal conductivity of air, $W.m^{-1}.K^{-1}$
k_m	apparent mixing length, m
l	flame height, m
l_{free}	flame height under free burning conditions, m
L	pathlength, m
Lp	pyrolysis length, m
L_m	mean beam length, m
m_i	sample initial mass, kg
m_f	sample final mass, kg
$\dot{m}$	mass flowrate of fuel vapour, $kg.s^{-1}$
$\dot{m}_a$	total mass flowrate, mass flowrate in incoming air, $kg.s^{-1}$
$\dot{m}_e$	mass flowrate in exhaust duct, $kg.s^{-1}$
$\dot{m}_f$	mass burning rate, specimen mass loss rate, $kg.s^{-1}$
$\dot{m}''_v$	fuel vaporisation rate, $kg.s^{-1}$
m_{O_2}	molecular mass of oxygen, $g.mol^{-1}$
m_{fuel}	molecular mass of fuel, $g.mol^{-1}$
M	molecular weight, $g.mol^{-1}$
N	nondimensional parameter
$\dot{n}$	molar flow rate, $mol.s^{-1}$
Δp	pressure drop across orifice plate, Pa
$\dot{q}$	heat release rate, kW
$\dot{q}''$	heat flux, $kW.m^{-2}$
$\dot{q}''_{cl}$	centreline wall heat flux, $kW.m^{-2}$

$\dot{q}''_p$	peak wall heat flux, $kW.m^{-2}$
$\dot{q}''_{rr}$	surface reradiation, $kW.m^{-2}$
$\dot{q}''_w$	wall heat flux, $kW.m^{-2}$
$\dot{q}''_r$	radiative heat flux, $kW.m^{-2}$
$\dot{q}''_c$	convective heat flux, $kW.m^{-2}$
$\dot{q}''_{crit}$	critical minimum heat flux for ignition, $kW.m^{-2}$
q''_{fs}	full scale heat release rate, $kW.m^{-2}$
q''_{bs}	180s average heat release rate in Cone at 25 $kW.m^{-2}$, $kW.m^{-2}$
$\dot{Q}$	total heat release rate, kW
$\dot{Q}_c$	convective heat flux, kW
$\dot{Q}_l$	heat release rate per unit length of fuel, $kW.m^{-1}$
Q^*	dimensionless heat release term
$\dot{Q}_l{}^*$	dimensionless heat release term
$\dot{Q}_{rec}{}^*$	dimensionless heat release term
r	stoichiometric ratio of air to volatiles by mass
r_o	oxygen to fuel mass ratio
t	time, s
t_{ig}	time to ignition, s
t_{fo}	time to flashover, s
T	plume temperature, K
T_b	apparent or brightness temperature, K
T_e	exhaust duct temperature, K
T_f	flame temperature, K
T_{ig}	ignition temperature, K
T_m	maximum temperature in the fire plume, K
T_s	solid temperature, K
T_∞	ambient temperature, K
T0	mean centreline temperature in plume, K
ΔT	mean excess temperature of flame above ambient, K
ΔT_0	mean excess temperature (above ambient) of plume centreline, K
u_c	characteristic velocity, $m.s^{-1}$
u_0	vertical velocity in the plume, $m.s^{-1}$
U_g	opposed flow air velocity, $m.s^{-1}$
V_o	voltage in the absence of smoke, Volts
V_i	voltage in the presence of smoke, Volts
$\dot{V}$	volume flowrate, $m^3.s^{-1}$
Vp	flame spread velocity, $m.s^{-1}$
w	longest side of rectangular fire source, length of line burner, m
x	height, m
$X^{A^0}_{O_2}$	measured mole fraction of O_2 in incoming air
$X^{A}_{O_2}$	measured mole fraction of O_2 in exhaust flow
$X^{o}_{O_2}$	actual fraction of O_2 in incoming air
$X^{o}_{H_2O}$	mole fraction of H_2O in incoming air
y	horizontal distance, m

z height, m

z_0 elevation of virtual source above origin, m

Greek Symbols

α entrainment coefficient

β expansion coefficient of air, K^{-1}

ε rate of dissipation of turbulence energy, m^2s^{-1}

κ flame absorption coefficient, m^{-1}

ρ density, $kg.m^{-3}$

ρ_o density in the plume, $kg.m^{-3}$

$\rho\infty$ density of ambient air, $kg.m^{-3}$

υ entrainment velocity, $m.s^{-1}$

ν',ν'' stoichiometric coefficients

ξ height above pyrolysis front, m

ϕ equivalence ratio

σ_f specific extinction area, m^2kg^{-1}

δ boundary layer thickness, m

γ constant, value depends on definition of flame height

τ sample thickness, m

Chapter 1

Introduction/Objectives

1.1 Introduction:

From the time that mankind discovered fire, it has been both a blessing and a curse in his life. On a positive note it provides power, heat, warmth and light, but the destructive potential of fire cannot be underestimated. Unwanted fires can cause the devastation of homes, businesses, and places of leisure and lead to injury and loss of life. The incidence of large fires has been increasing since 1988 (Scoones, 1994). In the UK. there was a 2.5 % increase in the number of large unwanted fires in 1991 compared with 1990 (Scoones, 1994) giving a total of 814 large (> £50,000) fires reported to the Fire Prevention Association (FPA) in that year. Of these 814 fires, 30% were in storage areas and accounted for 32.3% of the financial losses. Woodward (1989a) of FPA wrote that 'it can be stated quite positively that fires associated with storage areas are now one of the two dominant fire problems affecting the whole of the industry. The second is arson.'

The fact that a large percentage of fires are caused by arson gives reason for concern. On average, malicious fires tend to be about four times more expensive than accidental fires. There are several reasons for this: there is often more than one seat of fire, accelerants may be employed, fire protection equipment rendered ineffective, and the fires started in areas perceived to allow rapid fire development (Woodward, 1989b). The often rapid development of deliberate fires is also a danger for fire-fighters. Recent statistical analysis (Scoones, 1994) shows that of the 814 large fires in 1991, arson accounted for 50% of the total number of fires, whilst for warehouse fires in particular, arson was the cause of 39% of fires (Ward, 1985). Arson is therefore 'the most common *known* cause of fire outbreak' for the storage of bulk materials (Hymes and Flynn, 1989).

1.2 Fires in Warehouses

Warehouse fires are often serious because of the large amounts and diversity of material stored in them. Large areas of vertical combustible surfaces can exist in

high bays where the rate of upward flame spread is determined by heat transfer from the vertical flame to the fuel above and ahead of the burning area (Janssens, 1992). This is often considered to be the "worst" *orientation* for rapid fire development, but the *configurations* found in warehouses can lead to even more rapid fire growth than would be supposed. The storage arrays in warehouses provide vertical channels between adjacent stacks which offer an ideal pathway for rapid fire growth.

The size of warehouse fires gives rise to a considerable risk to fire-fighters and the variety of contents within gives cause for environmental and health concerns. There have been many cases where a large number of stored chemicals have lead to health risks to fire-fighters and people living in the vicinity (FPA Casebook of Fires, 1977, 1983, 1984, 1985). Many of these cases also demonstrated very rapid fire development due to the fire storage conditions and fire load. This was true of the UK's largest fire at an Army Ordnance depot in Donnington, where a fire in a high density warehouse caused £165 million damage and spread asbestos from the roof over a large area (FPA Casebook, 1984).

1.3 Fire Testing

The testing of materials stored in warehouses can be undertaken in various ways, although there is no standard test for stored goods. At present the Health and Safety Executive (HSE) use a one third scale room and corridor test facility to burn materials, many of which have been obtained by inspectors from various premises because they may present a possible hazard. The hazard assessment is based on rate of temperature rise and smoke production data. This medium scale test was developed because it was considered necessary to test materials on a larger scale with conditions that could be more representative, and therefore more suitable than laboratory scale tests, of real fire exposure conditions. Unfortunately, this scale of testing is expensive, time consuming, and generally cannot be used for the development or routine testing of materials.

Although their limitations are recognised, smaller scale test methods are required from an economic point of view, and the results from these need to be carefully examined before real fire behaviour can be confidently predicted from laboratory tests. The Cone Calorimeter is a small scale test method, becoming popular at the present time as it has been designed 'scientifically'. The advantages in the cost and

speed of testing have lead organisations such as the HSE to consider the use of the Cone Calorimeter as a replacement for larger scale tests. An investigation of the validity of using this small scale test, by comparison with third scale test data, and other small scale tests, is the main aim of this thesis, combined with an examination of the effects that geometry, ignition source and other physical factors may have on the heat transfer in the type of fire scenarios found in bulk storage configurations.

1.3.1 The Cone Calorimeter

In the Cone Calorimeter, the rate of heat release of a sample of material, 100 mm by 100 mm and up to 50 mm thick, is determined by oxygen consumption calorimetry. The rate of mass loss, oxygen, carbon dioxide, and carbon monoxide concentrations, air flow rate and combustion product optical density are recorded simultaneously. The rate of heat release under the given conditions can be calculated by using the principle of oxygen consumption (Thornton, 1917, Huggett, 1980), as described in chapter 2. The heat flux to the sample surface is produced by the use of a temperature controlled, cone shaped radiant heater which provides a radiation only flux. This apparatus was designed to measure the rate of heat release, mass loss rate and the production of CO_2 and CO under irradiance levels up to 100 kW/m^2. The irradiance level can be varied in order to study the behaviour of materials under different radiant intensities. The test conditions in the Cone Calorimeter are always well ventilated.

1.3.2 Other Applications of the Cone Calorimeter

1.3.2.1 Smoke Measurement

The Cone Calorimeter was originally designed to measure rate of heat release, but it has proved to be extremely versatile because the fire effluents, especially smoke, can readily be sampled and subjected to measurement. The relevance of data from the fuel-controlled burning of materials in small scale tests to real fires has still to be explored, although it is desirable as many tests use smoke production for hazard assessment (e.g. HSE, 1991, Nordtest, 1976). Finding relationships between the Cone smoke data and smoke production from real fires will be difficult as it will require careful analyses of the smoke yields in large scale fire tests. The production of smoke will also be apparatus dependent, as it is affected by the burning

conditions. Smoke is measured in several fire tests for hazard assessment, despite reservations about the reliability or usefulness of the results. Smoke yield is very sensitive to the conditions of burning, and in particular to the availability of air. In the early stages of a fire, well ventilated conditions are likely to exist, and the yield of smoke will be relatively low. The situation will change with the approach and onset of flashover, and it is known that the yield of smoke will increase (Drysdale and Abdul-Rahim, 1985). One of the aims of this thesis is to investigate smoke production in the Cone Calorimeter and compare these results with smoke produced under different conditions, for example under both fuel controlled and ventilation controlled conditions in the HSE third scale test. This is to help assess whether smoke yield is a realistic measurement or not on which to base hazard assessment.

1.3.2.2 Flame Spread Modelling

Other measurements made in the Cone Calorimeter have also been used to predict properties beyond the original scope that the apparatus was designed for. The time to ignition of samples under different imposed heat fluxes have been used to find the minimum or 'critical' heat flux necessary for ignition of the material, that is the maximum imposed flux, found by extrapolation, at which ignition would take an infinitely long time (Breazeale, 1988, Goff, 1991). This value is further used to calculate thermal inertia and predict the rate of upward flame spread over the material. There are several question marks over this use of Cone Calorimeter data, the first being the prediction of the minimum heat flux for ignition. Various researchers (Breazeale, 1988, Goff, 1991) have used equations based on heat flux as a function of $1/t_{ig}$ or $1/t_{ig}^{n}$, where t_{ig} is the time to ignition of the sample, to find the critical heat flux. Many of these are shown to be almost meaningless when the errors involved are taken into account (Whiteley, 1993). For other cases it is necessary to use different equations for thermally thick and thin samples (Mikkola and Wichman, 1989), although whether a sample can be classed as thick or thin also depends on the duration of exposure. The critical heat flux, found by any method, also depends upon the heat transfer boundary conditions in the system, which will make the value unique to the Cone Calorimeter and only of use for measurements made using the Cone. The problems inherent in finding the minimum critical heat flux for ignition mean that predictions based on this value will be subject to error.

Another problem with using Cone Calorimeter data for the prediction of flame spread, and even time to flashover in a room fire, is that in the Cone the sample is

only subjected to a radiative heat flux, whereas in a real fire convective heat transfer may be extremely important and may even dominate the heat transfer processes, especially in the early stages of a fire. Little work has been done to investigate the relative importance of convective and radiative heat transfer in various fire scenarios (Tamanini, 1979). No research has been conducted into how the time to ignition of a sample of material may be affected by imposing a specific heat flux by different heat transfer methods, such as a mixed mode convection and radiation, instead of radiative heat transfer only. In flame spread modelling based on times to ignition, it has to be assumed that the ignition time under an imposed irradiance is the same as under a mixed mode heat flux.

The question of using Cone Calorimeter data for flame spread modelling was addressed experimentally. Measurements were made to find the relative importance of the convective and radiative components of heat transfer, from a flame to a wall surface, under configurations representative of those that can be found in a warehouse fire and in the third scale room/corridor test. This was used to give an indication of how significant the convective heat transfer is and, from this, whether there may be a problem with using radiation-only in tests used to indicate the fire hazard a material may present in a real fire scenario.

1.3.3 The HSE Third Scale Room/Corridor Test

The HSE third scale room and corridor assembly is used to test materials suspected of being hazardous in the event of fire in a storage area. Large samples are used, approximately 5 kg of material, often separated into two halves with an ignition source placed between the vertical parallel faces. The room is closed except for an opening leading into a corridor at one side. One of the criteria for passing this test is based on the quantity of smoke produced by a sample, which is measured at the end of the corridor. As a large amount of material is used and the room is relatively small, the fire often moves to ventilation controlled conditions and the amount of smoke produced, per unit mass of sample, is far greater than would be found from a Cone Calorimeter test. One objective is to compare the smoke production under these conditions with the smoke produced in cone tests and further to assess whether smoke production from laboratory tests is a reasonable hazard indicator.

The third scale room test employs a British Standard No. 7 crib (BSI, 1982) as its ignition source. This crib is the largest of the seven standard ignition sources. It is placed between the two halves of the sample material, which are separated by a distance roughly equal to the width of the crib. The size of the ignition source may have the effect of overcoming any inherent ignition resistance that the material has and thus could produce a rapidly developing fire. The effect of the compartment will quickly become important through radiation from the walls and by preventing heat being easily removed by convection, both of which will lead to an increased rate of burning of the sample. A material which may not ignite under normal fire conditions, but which will burn rapidly under extreme heat fluxes, could then be given a high hazard rating in this test. One of the objectives of this work is to compare the fire development of a set of materials tested in these severe conditions to the rate of heat release found from the Cone Calorimeter, as well as the less severe and more common test for ignitability of upholstered composites, BS 5852 (BSI, 1982).

1.4 Conditions Affecting the Fire Hazard of Materials Stored in Bulk

Some knowledge of the conditions arising during warehouse fires needs to be gained in order to understand which, if any, of the current test methods is appropriate for assessing the fire hazard of materials stored in bulk. The storage configurations in warehouses are different from domestic dwellings and many industrial settings. Large amounts of materials are stored, giving large parallel vertical faces of combustible material with narrow channels between racks of materials. The exact configurations will affect the rate of development of an unwanted fire (Ingason, 1993). Fire protection is difficult in such circumstances and there is a need to understand the mechanism of fire spread in more detail to enable the risks to be quantified, and possibly reduced, by avoiding storage geometries which are particularly hazardous. The work in this thesis is aimed to be a *first step* towards understanding how the geometries in warehouses increase the fire risk.

To help increase the understanding of ignition and flame spread in warehouses, research was undertaken to identify the geometrical conditions which gave the highest levels of heat transfer to a sample surface and would therefore give the most rapid flame spread over a combustible material. The mechanisms by which heat transfer occurred also needed to be investigated and understood in order to help with

assessing which test methods and conditions would be relevant for materials to be stored in warehouses. Heat transfer under different conditions was also investigated experimentally to help increase understanding in this field so that appropriate measures may be taken to reduce the fire hazards in bulk storage and cease any unsafe practices.

Chapter 2

Fire Testing

2.1 Introduction:

In order to be able to select, design or use a fire test, one must first have an understanding of the different phases and processes occurring during the progression of a fire. In most real fire situations, it is behaviour within a compartment that is of interest. The stages that a compartment fire goes through are shown in figure (2.1), (Drysdale, 1985). The first event is ignition, after which the fire grows as if it were out in the open, unaffected by the compartment. This is the growth stage. The temperatures are fairly low, with combustion only initially happening in a localised vicinity. During the growth period, fire begins to spread, increasing in size and begins to interact with the compartment boundaries. The fire may, at this stage, follow one of two paths; it may undergo the transition to a fully developed fire, or if there is insufficient fuel, the fire will consume the combustibles and gradually die down. The transition to the fully developed fire is termed flashover and is characterised by a rapid spread of flame from mainly localised combustion to a fire that involves almost all the combustible material in the compartment.

It is during the fully developed period of a fire that the highest burning rates are seen, and along with that the highest compartment temperatures. Flames are often seen emerging from openings as the fire moves into a ventilation controlled regime, and fire may be spread to the rest of the building. Structural damage may occur during this stage, due to the high temperatures and heat release rates. As the combustible materials become consumed, the fire will gradually abate and the decay period is entered. The heat release rate drops and flaming ceases. Smouldering combustion may continue for some time, but there is overall cooling of the remaining materials.

The aim of a fire test should be to assess the behaviour of a material and its contribution to a possible fire at a certain known stage of a fire. Before this can be

done, it is necessary to understand the parameters that govern this progression of a fire.

In basic terms, fuel, oxygen and energy are required to cause a fire. This can be seen in its simplest form in a fire triangle, figure (2.2). The fire triangle has been used for some time to describe fire behaviour, but it was not until 1973 (Emmons, 1973) that the role of heat and mass transfer in these processes was discussed seriously. This showed that the fire triangle is an over simplification and can only be used for qualitative thinking of fire. Even the seemingly simple factors of fuel, oxygen and energy are themselves affected by a large number of variables making it apparent that fire is complex to describe; to quantitatively describe it and predict its course is almost impossible (Östman and Nussbaum, 1987). Many of the variables affecting the fire components were summarised and discussed by Steingeiser (1972).

The fuel is affected by its own chemical and physical properties, such as sample geometry and orientation, sample environment and age, density, thermal conductivity, specific heat capacity, heat of combustion, melting point etc. A different thickness or shape of a material can affect the burning properties, but it can also be affected by external factors such as its position within a room, the ventilation, the velocity and direction of air flow, the temperature of the air etc. The air can then affect the fuel and the fire. The fuel is in turn affected by the fire, flow rates to the fire may depend on the stage of the fire, the temperatures being generated, which are also influenced by the fuel. The heat release from the fire is significant also in that it transfers energy back to the fuel by radiation and convection, the radiation coming from the flame itself and from the surroundings.

Whilst the fire triangle may be useful to provide the qualitative picture, it obviously hides the complexity of the many variables affecting a fire. A far greater understanding of the physical laws, particularly heat and mass transfer, under different conditions is necessary to predict or describe fire behaviour. It is therefore evident that the fire performance of a material cannot be characterised solely by its physical and chemical properties, it is not in fact an intrinsic property but depends on the conditions that the material is exposed to.

2.2 Fire Testing Philosophy

The hazard associated with a material depends on its end use, certain applications are more hazardous than others. It is desirable to reduce this hazard down to an 'acceptable level'. The definition of this level depends, amongst other things, upon current awareness and public acceptability. In other words, it is not a scientific, quantifiable value and is seen to vary considerably between countries. However, there has been in recent years a move away from this situation, towards harmonised standard tests, especially within the European Community, which have been designed on better understood scientific principles. The International Organisation for Standardisation (ISO) has been working on developing and validating these new tests (Malhotra, 1975).

Early fire tests were based on a combination of experience and intuition, but moves have been made to design tests more rationally and scientifically so that specific fire parameters or scenarios were being tested for. The fire tests internationally can be categorised according to the stage in a compartment fire that they attempt to emulate:

- ease of ignition
- contribution to fire growth
- behaviour in fully developed fire

Other tests are aimed at measuring parameters that fall within both of the last two categories, such as the production of smoke and toxic gases. Within the fully developed category are tests for structural elements and structural materials, but these are outwith this review. The remaining tests are placed in one of the three sections, or in a fourth category, 'other tests', which covers smoke tests, as well as the one test for which there is no known property and which cannot be considered to be testing for behaviour at any part of a compartment fire (ASTM, 1977b). Although these tests have been subdivided so, it must be remembered that the tests have not been carefully designed to represent real fire conditions, and that the relevant physical processes have not been taken into consideration. Thus, none of the tests make any real attempt to emulate real heat transfer conditions at the suitable compartment fire stage, sample orientation and geometry is not intended to be representative and so on.

2.3 The National Fire Tests

The first event in the history of a fire is ignition, Figure (2.1). The ease by which a material ignites is therefore considered important and tests have been developed in different countries to investigate ignitability (e.g. BSI, 1982; JIS, 1966; DIN, 1975). The ease of ignition is influenced by the size, position and type of ignition source as well as any imposed heat flux.

After ignition has taken place, the first stage in a fire is the growth period. Most of the fire tests are aimed at assessing some parameter within this category (e.g. ASTM, 1977, TGL, 1975, Nordtest 1976 etc.). Flame spread is often taken into account in some way, and materials classified or ranked according to how quickly flame spreads over them, in each particular test, compared with other materials. An aim of tests within this category is to separate the materials which would quickly become involved in a fire from those that show a higher degree of resistance to flame spread.

To test a material for behaviour in a fully developed fire, parameters such as temperature rise and amount of material consumed under more severe exposure conditions are investigated. In a fully developed fire, it is desirable to know what contribution materials will make to the fire. This is relevant to the problem of structural failure and fire spread to other parts of a building. Between the fully developed region and the growth part of the fire is the transition period, flashover. Several tests (e.g. ASTM, 1979, BSI, 1981) used in the fully developed regime also test samples for fire growth at the higher levels that would be seen just prior to flashover, and these tests aim to rank materials according to high fire growth, leading to flashover and then their contribution to the fully developed fire.

The tests in these three categories can be used to show if a material has a high, medium or low fire contribution level (Troitzsch, 1983). Tests for production of smoke are less common than the previous types of tests, but are still used for ranking materials (e.g. ASTM, 1979b). Some of the previous tests include smoke measurement, which is used for hazard assessment as it is often the smoke from a fire that is the direct cause of death for fire fatalities. Thus, smoke production is often perceived as forming the major hazard in a unwanted fire. Tests dealing with special cases, such as finished products or specific end uses are not covered here.

A comprehensive review of the National tests was made in 1983 (Troitzsch, 1983), although it was aimed mainly at plastics testing. The variety of conditions employed in these tests is demonstrated in the following tables. The wide variety even within each of the categories outlined above, helps explain the difficulties in comparing data from the different tests. The National tests employed for this thesis, BS 5852 and the HSE third scale room/corridor test, are described in more detail, along with the tests discussed by Emmons (1974), comparing the results from six National tests (see section 2.3.5).

2.3.1 Ease of Ignition

The ignitability tests are the most simple in concept, materials are tested to discover if they will ignite under certain conditions, or if they can sustain burning once an ignition source has been removed. In the second respect, they can also deal with early fire spread; materials may fail a test because ignition occurs, flame spreads beyond a certain time or distance limit and the sample has then exhibited ignition and early fire growth. The sample geometry and orientation, ignition source position, size and type are all important factors within these tests. Ignition is easier at a sample edge, and sustained burning when an ignition source is removed occurs more easily for samples in a vertical orientation, due to characteristics of heat transfer. Therefore, not even the simplest type of tests can be considered to be apparatus independent. Three such tests are compared below, the conditions in each of the tests are seen to be different.

Table (2.1) criteria for ignition tests

Test	small burner (DIN, 1975)	JIS A1322 (JIS, 1966)
sample size	340 x 104 mm	300 x 200 x usual thickness
orientation	vertical	45º, 50 mm above tip of burner
ignition source	small burner at 45º angle, flame height 20 mm	burner 20 mm internal diameter, flame height 65 mm
duration	30 s	flame applied for 10, 20, 30s, 1, 2, 3 min
criteria	based on burning time and burning through of sample	based on charred length, afterflame time and afterglow

BS 5852: Part 2 Fire Test for Furniture

This standard test (BSI, 1982) is designed to test the ignitability of upholstered composites for seating, by the use of solid and gaseous flaming sources, table (2.2). It is one of the tests used in the experimental work for this thesis. Upholstery filling material is covered with the appropriate cover material and fabric interliner and two pieces are arranged at right angles on a small scale metal 'chair' frame, figure (2.3). An ignition source, which is either a butane flame or a wooden crib, is applied to the sample for a set time in the case of the gas flame or until the wood is consumed. The ignition source is applied at the join between the vertical and horizontal sections of the 'chair', so the sample is tested in both a horizontal and vertical orientation. In the case of the wood crib source, the maximum heat fluxes that the sample is exposed to will occur beneath the crib, on the horizontal surface. The criteria for passing or failing this test are based on the material behaviour after the ignition source has been removed. Flaming or smouldering combustion continuing after a set time after ignition source removal or burn out means that the sample has failed for that specific ignition source size. The material is also deemed to have failed if flame spreads to any of the extremities of the specimen, if the sample is consumed during the test or if it displays escalating combustion behaviour so that it is unsafe to continue the test and forcible extinction is required. In this way, the test is also taking early flame spread into account, although failure is based only on sustained ignition after removal of the ignition source. If a sample passes at a certain ignition source, the test must be repeated.

Table (2.2): details of test for BS 5852 part 2

sample	one piece 450 x 450 x 75 mm, one piece 450 x 300 x 75 mm of upholstery material covered in fabric cover and interliner for each test
test apparatus	steel rectangular frames hinged and lockable together, back frame 450 x 450 mm, base frame 450 x 300 mm sited in draught free environment with adequate supply of air and smoke removal
sample position	two pieces at right angles to each other, with ignition source at join
ignition source	sources 2 and 3, butane burner tube; source 2- 160 ml/min for 40s, source 3- 350 ml/min for 70s sources 4-7, wooden cribs of various construction. Mass of wood: crib 4 - 8.5g, crib 5 - 17g, crib 6 - 60g, crib 7 - 126g.
test duration	up to 60 min
criteria	pass at sources 2 and 3 if: -no flaming or progressive smouldering after 120s after flame removed -no signs of heat, smoke or glowing 30 min after burner removed pass at sources 4 - 7 if: -no flaming or smouldering 10 min after ignition of sources 4 + 5 or 13 min after ignition of sources 6 + 7 -no signs of heat, smoke or glowing 60 min after ignition of source material will fail if it does not meet the above or if it is essentially consumed during test, displays escalating combustion and has to be extinguished or flame front reaches extremities of sample

2.3.2 Growth Period

It is desirable to know how quickly a material will become involved in a fire, whether the flame spread rate will be high etc., in order that materials that lead or contribute to a rapidly developing fire, in which possible evacuation times are short, can be either avoided or added safety measures used. It is because of this that most tests can be said to fall in this category. Some measure early flame spread, others involve more severe conditions and aim to assess material behaviour in a fire close to flashover.

There are many parameters that affect the growth of a fire, as discussed earlier. Tests in this category employ many different conditions in order to assess materials, so it is inevitable that there will be discrepancies between the results. This is demonstrated in table (2.3) and in the more detailed descriptions of the tests examined by Emmons (1974).

Table (2.3) criteria for fire growth tests

test	ASTM D 635 (ASTM, 1977b)	Plattenrahmen (TGL, 1975)	NT Fire 004 (Nordtest, 1976)	ASTM E84-79a (ASTM, 1979a)
sample size	125 x 12.5 x usual thickness	500 x 190 mm, ≤ 30 mm thick	225 x 225 x 11 mm	0.51m x 7.32m x usual thickness
orientation and position	125 mm side horizontal, short side 45º to horizontal	vertical	4 samples attached to side and rear walls and ceiling	horizontal on tunnel ceiling
ignition source	Bunsen burner, blue flame 25 mm long	gas pipe burner with 8 jets	ring propane burner, 45 mm diameter, at 45º	2 gas burners, 88 kW, 190 mm below sample, 305 mm from tunnel end
duration	flame applied for 30s	1 min	10 min max.	10 min
criteria	based on mean rate of burning	based on flame extension beyond upper edge of sample	based on smoke temperature curves and smoke intensity	based on dist. travelled by flame front, and smoke density

Epiradiateur Test

This classification test (AFNOR, 1975) is used in France to test materials by the use of radiative heat sources, (figure 2.4) and was included in Emmons' comparison (1974). Rigid and flexible samples less than 5 mm thick are exposed to the radiative heat source and two pilot ignition flames. The time elapsed until flaming is supported, i.e. lasts for more than 5 seconds, on each side of the specimen is recorded, as is the maximum flame height every 30 seconds, and other behaviour such as smoke generation, glowing, burning droplets etc.

Three indices are used to classify the test material: a flammability index which uses the times taken to achieve flaming combustion at the top and bottom of the material, a spread index using the sum of the maximum flame lengths determined every 30 seconds, and an index of maximum flame length. These different indices represent an attempt to use a test to find parameters which are relevant to the different stages of fire development. The flammability index gives an indication of sustained ignition under these test conditions and imposed heat flux. The flame spread and flame length indices give an indication of the contribution a material would make to the fire growth period. This test varies from many other tests in this category in that it uses an imposed irradiance to help sustain combustion on the sample surface.

Table (2.4): details of test for the Epiradiateur test

sample	4 of 300 x 400 mm
position	inclined at 45^{o}
ignition source	500 W electric radiator inclined at 45^{o}, 30 mm above sample, giving 30 kW/m^{-2} 2 butane pilot flames to ignite combustible gases above and below sample
test duration	20 min
criteria	• classification from non-flammable to moderately flammable if sample passes test, higher flammability materials fail and must be assessed using a different method

BS 476 : Part 7. Surface spread of flame test

Like the Epiradiateur, this uses a radiant heat source for the testing of materials, this being the British standard test (BSI, 1987) as shown in figure (2.5). A pilot flame is applied for the first minute of the test and the time required for the flame front to reach various reference marks on the sample are noted. The flame spread at 1.5 min and the final flame spread are used to categorise materials in classes 1 - 4, of which only 1 - 3 are acceptable for use under the building regulations, 1 being the lowest flame spread. The radiant panel provides the imposed heat flux to the sample, but in this test it is not a constant flux over the sample surface. It falls with distance travelled by the flame as the sample is perpendicular to the panel. The heat transfer

conditions in this case will therefore be very different than those for the Epiradiateur, or tests that have no imposed irradiance. Table (2.5) details the conditions and criteria for the test.

Table (2.5): details of test for BS 476 : Part 7

sample	6-9 of 885 x 270 x 50 mm (max.)
position	vertical, 885 mm side perpendicular to radiant panel
radiant and ignition source	gas fired radiant panel, giving 32.5 kW/m^{-2} at 75 mm from panel surface (i.e. at the closest end of the sample) gas pilot flame, 75-100 mm, impinging on sample at same side as radiant panel
test duration	10 min
criteria	• classified in groups 1 - 4, depending on distance travelled by the flame at 1.5 min and end of test

This test method has also previously been employed in Belgium and Denmark, with some alterations. The construction of the radiant panel in the Belgian test was different, whilst the Danish test used a different classification method for the materials, based on the radiant heat flux at the point where the flame ceased propagation. These three versions of basically the same test were considered as independent tests in Emmons' comparison of results (1974). As there was little correlation between the results for the tests, (see section 2.3.5), small alterations in either design or criteria must have a large influence on the outcome of the test.

NEN 3883 Contribution to Flashover

This (NEN, 1975) was another of the flammability tests considered by Emmons (1974). It tests materials under the conditions found towards the end of the growth period, just before flashover, and aims to assess under what conditions each material will contribute to flashover. Flashover is judged to have occurred when a second sample (see figure 2.6), which does not have a burner applied to it, burns for longer than 5 s. At least three tests are performed, at different power settings of the electric filaments. The power necessary to cause flashover at 5 and 15 minutes is inter- or extrapolated from the data gathered. These values are used to classify the materials. The conditions are summarised in table (2.6).

Table (2.6): details of test for NEN 3883

samples	16 samples, 295 x 295 x max. 75 mm (50 mm for melting materials)
sample position	2 samples vertical and parallel with separation distance of 160 mm
ignition and heat sources	12 electric filaments, variable output (190-2250 W), 80 mm from samples pipe burner, 10 mm dia., 9 openings at 30 mm apart, flame length 20 mm, 70% H_2, 30% Nat. gas ≈500W, 25 mm from first test sample
duration	until flashover
criteria	classification, depends on energy supply needed to give flashover at 5 or 15 min

2.3.3 Fully Developed Fire Tests

These are tests where the material is tested under high heat fluxes, or in a compartment where flashover takes place. Two of the National tests in this category are compared, along with the Health and Safety Executive's medium scale compartment test.

Brandschacht test

This was the final one of the tests to be included in Emmons' paper (1974). For a material to be classified in the B1 and A2 categories in the German standards, they are tested in the Brandschacht test (DIN, 1978), figure (2.7) and must satisfy the requirements shown in tables (2.7 and 2.8). It is a rigorous test to assess whether a material would be involved significantly in a developed fire. Combustible materials can be given a low flammability status if they pass and materials meeting the higher standard, A2, can be termed 'non-combustible'. The samples are tested under heat flux conditions which may exist in a developed fire rather than simply the early fire growth period. The samples are tested vertically in a situation where cross radiation will occur, both of these conditions adding to the severity of the test. The contribution to a fire is assessed by the amount of material that survives the test, and

the temperature of the combustion gases is effectively an indication of heat release rate, although it cannot be quantified.

Table (2.7) class B1 specifications

sample	4 of 190 x 1000 mm x original thickness (up to 80 mm)
position	vertical, samples at 90^{o} to each other
ignition source	ring burner
test duration	10 min
criteria	material passes if: • average value of remaining material is at least 150 mm, with no one piece being completely burnt away • mean smoke gas temperature is not greater than 200 ^{o}C • no other unsatisfactory indications

Table (2.8) class A2 specifications

sample	4 of 190 x 1000 mm x original thickness (up to 80 mm)
position	vertical, samples at 90^{o} to each other
ignition source	ring burner
test duration	10 min
criteria	material passes if: • average value of remaining material is at least 350 mm, with no one piece less than 200 mm in length • mean smoke gas temperature is not greater than 125 ^{o}C • the back of any sample does not flame • no other unsatisfactory indications

BS 476 : Part 6. Fire propagation test.

This British test (BSI, 1981), was developed to enable further classification of materials which had been given a class 1 rating in the BS 476 Part 7 Flame Spread test (BSI, 1987). It takes into account heat release from the material by continuous measurement of the temperature in the chimney (figure 2.8), the values of which are

compared with a calibration curve. Indices are calculated from this comparison at different intervals from the start of the test. They are so weighted that an early high temperature rise will register unfavourably for the sample. The heat release to the sample is altered during the test so the material is exposed to conditions nominally found at the different stages of the growth and developed stages of a fire, table (2.9). The continuous measurement of temperature during the test is a means of assessing a materials potential contribution to a fully developed fire.

Table (2.9): details of test for BS 476: Part 6

sample	min. 3, max. 5, of 225 x 225 x 50 (max.) mm
position	vertical
radiant and ignition sources	two 1000 W electric elements with variable output (initially not on, 1800 W after 2 min 45 s and 1500 W after 5 min); 45 mm from sample gas pipe burners, internal diameter 9 mm, with 14 x 1.5 mm holes at 12.5 mm separation, 3 mm from sample, flame applied from the start of the test, 25 mm above bottom of the exposed face of the sample
test duration	20 min
conclusion	• Various indices are used to assess whether sample can be given class 0, a demanding subset of class 1.

The HSE Medium Scale Test

Although not strictly one of the National tests as it is not a standard test, the Health and Safety Executive medium scale test method (Wharton, 1990; HSE, 1991) is used by the HSE in the UK for the hazard assessment of materials in bulk storage. Larger amounts of material are used than in the previous tests, ideally 5 kg, although for low density materials 3 kg is often used instead, table (2.10). The apparatus consists of a third scale room and corridor assembly (figure 2.9) with the corridor divided into two passageways by a horizontal divider. The lower passageway provides ventilation for the material burning in the chamber while the upper one provides an exit path for the smoke and combustion products produced during the test. The combustion products are collected by a hood, duct, and fan system at the end of the corridor. The chamber is $1m^3$ in volume and the corridor 1m high, 0.5m wide and 6m long. The sample is placed in the chamber, usually around the ignition source, a

British Standard Number 7 crib (BSI, 1982). To increase the severity of the test, materials are often either cut into two halves, placed facing each other with the crib between them, or placed in a horseshoe shape around the crib.. The opening from the room chamber to the laboratory is sealed, so that air can only enter via the corridor, and the test commences. Continuous measurement is made of smoke optical density in a duct above the end of the corridor and of temperature in the corridor just outside the burning chamber. The aim of this test, unlike most of the others, is to assess material fire hazard once the material is burning. The ignition source size is large, to ensure that all materials will ignite so that their behaviour in a fully-developed fire can be investigated. Thus the assessment of solid flammability is made by ranking materials on their behaviour in this type of fire. Conditions are often ventilation controlled, giving very different results from the previous well ventilated tests, as the aim is for this test to be more representative of 'real' fire conditions.

Table (2.10): details of test for the HSE third scale room/corridor test

sample	5 kg sample, unless density is too low to fit this in apparatus, then 3 kg
test apparatus	sealed room, 1m^3 connected to open-ended corridor 1m high, 0.5 m wide and 6m long. Corridor partitioned horizontally down centre. Duct above end of corridor to collect combustion gases and measure smoke optical density
sample position	wrapped around ignition source in horseshoe shape or in two halves facing each other with ignition source between
ignition source	British Standard No. 7 wood crib
test duration	30 min
criteria	hazard level based on smoke obscuration and max. vent (measured in corridor just outside test chamber) rate of temp. rise: high if - smoke obscuration $\geq$ 400 m^{3}ODml - max. vent temp rise $\geq$ 700^{o}C/min normal if - smoke obscuration < 400 m^{3}ODml - max. vent temp rise < 700^{o}C/min

2.3.4 'Other' Tests

Several other tests exist, mainly to measure smoke production (e.g. ASTM, 1979b, DIN, 1966, GOST, 1980), one of which is covered briefly below, table (2.11). The oxygen index test (ASTM, 1977b) is also mentioned, as it is a widely used test which has the unique status of measuring behaviour under conditions which cannot arise in a real fire; there is no known property related to this test. Burning under fuel rich conditions is not being simulated as the test is carried out at ambient temperature and with no imposed heat flux.

Table (2.11): details of 'other' tests

test	NBS smoke chamber (ASTM, 1979b)	oxygen index test (ASTM, 1977b)
sample size	76 x 76 x 25 mm (max.)	150 x 6 x 3 mm
orientation and position	vertical, parallel to radiant heat source	vertical
ignition and heat source	vertical furnace, 76 mm opening giving heat flux on sample of 25 kWm^{-2}. propane micro burner, 6.4 mm away from and above lower edge of sample. Used for flaming tests, not smouldering	gas pilot flame applied to upper end of sample
duration	20 min or 3 min after min. light transmission	until minimum $[O_2]$ of an O_2/N_2 mixture required to sustain combustion is reached
criteria	based on optical density	based on oxygen index $=100 \times O_2/(O_2 + N_2)$

2.3.5 Problems with the National Tests

As stated earlier, a large number of variables affect the development and behaviour of a real fire, many of which depend on and affect each other. As it is impossible to

measure all of these together, the above laboratory tests are used in an attempt to identify and quantify the important parameters. However, the results from these tests cannot then be used for prediction of fire behaviour as they are over simplified and unrepresentative of a fire scenario. Other tests are therefore needed, and used, to attempt to assess the behaviour of larger objects in a real fire situation. These are much more expensive and cannot be used for material screening. Ideally, correlations from carefully controlled and designed small scale tests with results from these more meaningful large tests are needed. The above tests, along with a plethora of other National tests, are far removed from the ideal of correlation with large tests or real fire prediction. As seen in the description of the tests, they are primarily aimed at many different points within the development of a fire and, despite often attempting to describe the same characteristic such as ignitability, flame spread rate and combustibility, there is little correlation between the results.

In the 1960s, a working group (ISO WG4) of the International Organisation for Standardisation (ISO) carried out a Round Robin of seven of the National tests. Scarcely any correlation was found between different tests and none at all between different laboratories. The serious nature of this disagreement was shown by one material, phenolic foam wallboard. It was the most hazardous material according to Denmark's test but the safest of the 24 materials according to Germany's test methods. The lack of correlation between the results was demonstrated by Emmons (1974). He showed that the random scatter from selecting numbered cards from a box was only slightly greater than the scatter of the test results. More recently, this issue was re-examined and the situation was found to have only improved very slightly (Östman and Nussbaum, 1987). This highlights the startling inadequacies of the National tests, which must call into question their relevance to any real fire scenario. The reason for these discrepancies is that the conditions vary widely between tests. The heat transfer plays a vital part in controlling fire behaviour, but it has been given no serious consideration in design of any of these tests. The importance of understanding the heat transfer and other physical processes cannot be underestimated, as was highlighted some time ago (Emmons, 1973).

2.4 The 'Reaction-To-Fire' Tests

After the above Round Robin, it was decided by ISO not to adopt any of the existing fire tests to form an international standard, but instead to develop simple, basic tests aimed at investigating the parameters which have a significant influence on the course of the initiating fire and which could provide data for use in predicting real fire behaviour. These 'reaction-to-fire' tests should allow estimation of familiar parameters in a simple and logical way. The parameters to be tested are ignitability, combustibility, flame spread, and heat release. The intention behind the tests was to ascertain whether or not a material becomes involved in a fire, its contribution to flame spread and its tendency to propagate and add to a fire by preheating other materials. Other fire properties such as smoke generation and toxicity of fire gases are influenced by the way in which a material burns and becomes involved in a fire. These are then secondary properties, but can also be measured in the reaction-to-fire tests. The overall desire was to find test methods that gave results that were apparatus-independent, ones which revealed fundamental material behaviour. These results could then be used to develop fire models that could be used for predictions of fire behaviour, in a way that data from the National tests could not.

2.4.1 What Are the 'Reaction-to-Fire' Tests ?

Ignition can occur due to the influence of convection or radiation, with or without a pilot flame (piloted and autoignition respectively). The different stages of a fire are represented by the level of heat flux the material is subjected to, from the initiating fire up to the fully developed fire, the heat fluxes being of the order of; 0-15 kWm^{-2} for the ignition tests to represent the first item ignited, higher to investigate ignition at different stages of the fire, 15-25 kWm^{-2} for the growth period, around 30 kWm^{-2} for flashover, and above this for the fully developed fire. One can, in this way, determine whether or not a material will initiate a fire when exposed to a small ignition source, if it contributes to flashover by becoming involved during the growth period, and if it will contribute significantly to a developed fire by exhibiting a high heat release rate, leading to potential structural failure and flame spread beyond the confines of the original compartment.

Simple flame spread tests are a more sophisticated type of ignition test, where a material is exposed to an ignition source and an additional heat flux to encourage

flame spread. The aim is to find the radiation intensity at which the flame no longer spreads. The simplest flame spread tests use simply an ignition source without additional heat flux, whilst the more severe enable the convection from the flame itself to contribute to the overall heat transfer to the sample, by testing the specimen in a vertical orientation.

The rate at which heat is released from a material in a fire is important because of its influence on the rate of fire growth, a high heat release rate just after ignition has important implications for the rapid initial fire growth, contributing to the development to flashover and the fully developed fire. The significance of this for successful evacuation from buildings cannot be underestimated.

2.4.2 The International Organisation for Standardisation Tests

The reaction-to-fire tests have been developed under the auspices of ISO/TC92 (Malhotra, 1975). This technical committee was established in 1961 to develop test methods for assessing the fire performance of building materials and components. In 1979, a reorganisation left TC92/SC1 in charge of the reaction-to-fire tests. Some of the test methods developed before the introduction of oxygen calorimetry are discussed below.

2.4.3 ISO/DP 5657. Ignitability of Building Materials.

This test (ISO, 1979) was the first of the series intended to characterise the fundamental parameters which help determine the early stages of a developing fire, in other words the first of the reaction-to-fire tests for building materials. It is only ignitability that is being examined in this test, with a sample passing the test at a given heat flux if it does not ignite in 15 minutes of testing. The apparatus, figure (2.10) uses a truncated-cone electric heater to subject samples to heat fluxes up to 50 kWm^{-2}, table (2.12). The specimen, which can be up to 70 mm thick, is located 22 mm below the heater by means of a pressing plate and counterweight. The first test is carried out at 50 kWm^{-2}. The sample is placed in position beneath the heater and the ignition system operated. This comprises a small propane flame which is moved from above the cone heater to 10 mm above the sample surface every 4 seconds, where it is held for 1 second before being withdrawn. If the material does not ignite at this heat flux, after 5 samples have been tested, then it has passed at 50 kWm^{-2}. If

it fails at this level, the tests are repeated at a lower flux to find the irradiance level that the material will pass at. Tests continue in this way down to 10 kWm^{-2}.

Table (2.12): details of test for ISO/DP 5657

sample	5 of 165 x 165 x 70 mm (max.) for each irradiance level, 50,40,30,20 and 10 kWm^{-2}
position	horizontal; samples are masked so that a circle 140 mm in diameter is irradiated
ignition source	• cone heater, variable irradiance level, 22 mm above sample surface • propane pilot flame, 10 mm long, which can be moved towards and away from sample, from above heater to 10 mm above sample surface
test duration	until sample ignites, up to 15 min
criteria	• sample passes an irradiance level if it does not ignite within 15 min • if sample fails an irradiance, next level down is tested for until 'pass flux' is found

2.4.4 ISO/DP 5658. Spread of flame of building materials.

The apparatus in shown in figure (2.11). It can be used to test lining materials for walls, ceilings, and floors by being able to present the sample in the vertical and both horizontal positions (ISO, 1977b). A radiant panel is employed as the heat source and a gas flame provides a pilot ignition source, table (2.13). The radiant panel is allowed to reach a steady temperature, then the pilot flame positioned such that it will impinge on the sample at an angle of 20^{o} to its surface, at approximately 20 mm from the sample edge closest to the radiant panel. About 50 mm of the 80 mm pilot flame should impinge on the sample surface. Once all this has been set up the sample can be placed in the holder and the time taken for the flame front to reach various marked positions, between 50 mm and 750 mm from the radiator, along the surface are recorded. The test is complete once the flame self extinguishes or the flame has reached the far end of the sample.

Table (2.13): details of test for ISO/DP 5658

sample	3 of 800 x 155 x 40 mm (max.) for each orientation, wall, ceiling and floor
position	sample end 100 mm from panel wall: 450 mm side of radiant panel horizontal, sample vertical, long (800 mm) horizontal side 45º to radiant panel ceiling: 450 mm side of radiant panel vertical, sample horizontal at top of panel, long side at 90º to radiant panel floor: 450 mm side of radiant panel vertical, sample horizontal at bottom of panel, long side at 90º to radiant panel
ignition/heat source	-vertical propane fired radiant panel, 300 x 450 mm, irradiance level 62 kWm^{-2} at surface, surface temperature 750 ^{o}C -propane pilot flame, 80 mm long, impinges on sample 20 mm from edge nearest to radiator
test duration	until flame self extinguishes or reaches end of sample
criteria	if end of sample is not reached, distance travelled and time to extinction are recorded

2.4.5 The 'LIFT' Test

This test (ASTM, 1990a) was designed to measure ignition and lateral flame spread. The samples are in the vertical orientation and are exposed to an external irradiance from a radiant panel, which is also mounted vertically, at an angle of 15º to the sample, figure (2.12). The tests for ignition and flame spread are carried out separately, using different sized samples. The first test performed is the ignition test, which uses a square specimen, exposed to a roughly uniform heat flux across its surface. A pilot acetylene/air flame, applied above the sample, is employed to give piloted ignition of the volatiles being given out from the material. This part of the test is first carried out at an irradiance level of 30 kWm^{-2}. If ignition occurs within 20 minutes, the ignition time is noted and the irradiance level reduced by 5 kWm^{-2}, and the test repeated. This process is continued until the minimum heat flux necessary to cause ignition is found. If the sample does *not* ignite at 30 kWm^{-2}, the tests are repeated at heat fluxes *increasing* in increments of 5 kWm^{-2}.

The flame spread part of the test is then carried out. The radiant panel is set to an irradiance level 5 kWm^{-2} higher than the minimum that was necessary to cause ignition. A longer sample is used in this test, with the irradiance at the sample surface falling along the specimen, because of the angle between the sample and the panel. A preheat period is allowed, calculated from the ignition test, before the pilot flame is applied above the sample. The time of arrival of the flame front at 25 mm increments along the sample is recorded. The time and position at which the flame front progression ceases are noted. Calculations are made of flame spread and flame heating parameters, along with a thermal inertia and minimum surface temperature necessary for ignition. The aim is to use these values for predicting material ignition and flame spread behaviour. The test conditions are summarised in table (2.14).

Table (2.14): details of test for the LIFT test

sample	ignition test: 155 x 155 mm. flame spread test: 155 x 800 mm
position	vertical
ignition/heat source	acetylene/air pilot flame 180 mm long applied to the flow of vapours above top of sample, vertical radiant panel, 483 x 30 mm at 15° to sample. Heat flux can be set in range 10-50 kWm^{-2} at 50 mm from hot end of sample. For flame spread test set at 5 kWm^{-2} above minimum flux for ignition at 50 mm from hot end , found from ignition test. Heat flux falls along sample surface for flame spread test, but is fairly constant over the sample used in the ignition test.
test duration	ignition test: until ignition or 20 min flame spread test: until flame spread ceases
conclusion	ignition test: minimum heat flux and time to ignition are found, surface temperature at ignition and thermal inertia calculated flame spread test: flux and temperature necessary for flame spread, a flame spread parameter and a flame heating parameter are calculated

2.4.6 ISO Smoke Box

The ISO smoke box (ISO, 1980) consists of interconnecting decomposition and measuring chambers (figure 2.13). Located in the decomposition chamber is the ignitability test device of ISO/DP 5657 (1979), which comprises a cone heater which can provide and irradiance level between 10 and 50 kWm^{-2}, in this case without an ignitor. Smoke is produced in the decomposition chamber and is drawn through a duct system by a fan, into the measuring chamber, the smoke being recirculated throughout the test. The smoke density is measured continuously by a tungsten halogen lamp light source and light detector, table (2.15). The irradiance is first set to 50 kWm^{-2} and the test sample (covered with aluminium foil with a hole cut out so that a circle of the sample 140 mm in diameter is exposed to the heat flux) is placed in the sample holder. The sample is tested at this irradiance for 15 minutes, and the test repeated under these conditions a further four times. This procedure is then repeated at 40, 30, 20 and 10 kWm^{-2}. Maximum smoke density and time to ignition can be measured and the averages at each irradiance level are calculated.

Table (2.15): details of test for the ISO Smoke Box

sample	max. 5 of 165 mm x 165 mm x ≤ 70 mm for each irradiance
position	horizontal sample is covered with aluminium foil so that a circular area 140 mm in diameter is irradiated
test chamber	consists of decomposition chamber containing a radiant heat source, connected by an upper and lower duct to the measuring chamber in which the smoke density measuring system is located, total volume $1.3m^3$
heat source	ISO/DP 5657 ignitability radiant heater without pilot flame, irradiance variable from 10 to 50 kWm^{-2}
photoelectric measuring device	light source with optics, horizontal light path (length 360 mm), light detector and amplifier
test duration	15 min
conclusion	determination of max. smoke density and where relevant time to ignition

2.4.7 Drawbacks of 'reaction-to-fire' tests

As these tests are established on a more sound scientific basis than the earlier National tests, they are able to measure one or two key fire parameters, which may be used in fire models and to further improve the level of knowledge of fire science. However, the effects of other factors such as ventilation, geometry, effect of a compartment etc. cannot be assessed in these tests. Therefore, only general trends can be examined and results cannot be used to predict the course and behaviour of a real fire. This means that results are still apparatus dependent. In order to take account of external factors, large scale tests must be performed.

2.5 Large Scale Tests

These are desirable to assess the behaviour of materials or finished products under real or end-use conditions, although they are in general prohibitively expensive for general purposes. Initially these were carried out in a rather ad-hoc way, in that an attempt was made to simulate the real fire conditions, but none was made to standardise or lay down any exact conditions. Later, large scale tests were done on a more scientific basis whereby certain conditions were specified such as; fire load, ventilation, ignition source etc. Malhotra (1976) defined the first test types, where all attempts are made to closely match real fire conditions, such as using a real ignition source and enclosure conditions, as 'realistic' tests. The second, more scientific tests, he classified as 'partially realistic'.

Large scale test data can be used to confirm the laboratory scale findings, something which is especially important for new materials, or conversely these data can be used to assess the suitability of small scale tests.

Large scale tests have been favoured in the field of transport, as the conditions in which a fire may develop are somewhat different than building fires. Full scale tests have been performed for aircraft, ships, and trains. Full scale test data have also been obtained for entire houses, but these tests, like the transport ones, have proved to be extremely expensive. A move has been made away from these type of experiments, without losing the advantages of more realistic fire conditions, by the use of 'compartment' tests. A compartment is a closed spatial element in which a fire can develop and flashover can occur. Examples of compartments are rooms in

buildings, train carriages and cabins in ships. Various parameters such as ignition source, measurement methods, arrangement of test specimen etc. can be defined and more realistic data obtained than for bench scale tests. These tests are however still far more expensive than the laboratory scale equivalent, are more time consuming, and do not have the advantage of a standard methodology.

In recent years there has been a move within the fire community to try to standardise large scale fire tests, although it is surprising that no attempts were made prior to this as large scale testing is certainly not a new development. However, attempts to standardise these tests and to compare data from different large scale tests could not really succeed until a reliable and easily measurable way of finding the rate of heat release from a fire could be found.

2.6 Oxygen Consumption Calorimetry

The theory of oxygen consumption calorimetry is based on pioneering work carried out by Thornton in 1917. He showed that, for the combustion of organic liquids and gases, a similar amount of heat was released per unit mass of oxygen consumed for a wide range of these substances. This theory was based on the assumption of the complete combustion of pure chemical compounds and uses the enthalpies of combustion for these reactions. In 1968 and in 1974 attempts were made to utilise this principle to determine the heat release rates of different materials. Hinkley suggested that this could be used to measure the heat release rates of wood cribs, (Hinkley *et al.*, 1968) but it was in 1974 that the first large laboratory scale tests using the oxygen consumption principle were performed, with the results being published later (Parker, 1977). Materials were tested in the ASTM E84 tunnel test and oxygen measurements used to determine the heat release rate. In 1979 oxygen consumption techniques were applied to the pyrolysis of Douglas fir and ponderosa pine trees (Sussott *et al.*, 1979). The researchers adapted a 'Reaction Coulometer' gas chromatograph detector (RCD) for the thermal analysis of solids. Oxygen was generated, rather than air being used, and detected by a closed loop electronic control system. The depletion in oxygen level caused by the combustion process was detected and then oxygen was generated to replace that consumed. The output of the RCD was proportional to the amount of oxygen generated for combustion and so the heat release rate could be calculated.

The first small scale test aimed specifically at fire testing based on this theory followed (Krause and Gann, 1980) with alterations to the Ohio State University Rate of Heat Release Calorimeter (Smith, 1972; ASTM, 1977) which under normal conditions used temperature measurements of exhaust gas to compare rate of heat release indirectly. Tests were carried out, using methane as a reference fuel, on several different types of materials with various behaviour patterns. The conventional temperature measurement method, using a thermocouple, and oxygen consumption calorimetry were performed concurrently and the results compared to theoretical heat release rate values from known fuel flow rates. For most cases the thermocouple data gave significantly lower values for rate of heat release than the oxygen measurement method. For cases where the measured rate of heat release could be compared with theoretical values, the temperature measurement method gave lower values than these whereas results from the oxygen method corresponded well with the theory. Krause and Gann (1980) put forward a theory for the difference in calculated heat release between the two methods based on studies of the convective and radiative partitioning of heat from burning materials (Tewarson, 1976). They stated that the convective component is efficient in the heating of the air flow but is less so in heating solid surfaces such as the chamber walls. The radiative component behaves in the opposite manner. The thermocouple method therefore, is excellent at detecting the heat transferred to the air, resulting in elevated air temperature, but is poorer where radiation is concerned since this energy is transmitted to the chamber walls and some of it is conducted away. This theory (Krause and Gann, 1980) was supported by the results from the combustion of polyoxymethylene, which were similar for the two measurement methods. This substance burns, like methane, with a virtually non-luminous flame so the radiative component is almost negligible. The overall conclusions from this work are that the oxygen consumption technique can be used for the measurement of rate of heat release without the problems of the separation between convection and radiation from the burning sample and therefore is more accurate. This was an important finding which helped confirm the value of this technique.

It was also in 1980 that another significant discovery helped promote the oxygen consumption technique. The work done by Thornton (1917) had been on pure organic materials and had used data for complete combustion. Huggett (1980) took this work further and applied it to the fuels found in real fires and fire experiments. He first presented data for organic gases and liquids but used slightly different values of enthalpies of combustion than the standard ones, as his took into account

the products more likely to be found in a fire. The heats of combustion per gram of oxygen consumed all fell within approximately 3% of the average of -12.72 kJg^{-1} O_2, despite a wide variety of fuels being used. When the author investigated the results for synthetic polymers, he found a similar trend for the heats of combustion per gram of oxygen consumed, despite the materials having large differences in the heats of combustion per gram of fuel consumed. Again all the values were within only 4% of the average, -13.02 kJg^{-1} O_2. Finally the heats of combustion for fuels of natural origin, such as may be found in large quantities in real fires, were investigated. The heats of combustion per gram of oxygen were again found to be nearly constant and only slightly higher, at -13.21 kJg^{-1} O_2, than for the synthetic polymers. Huggett also investigated the effect of incomplete combustion on these results and found that, for most applications, the assumption of constant heat release per unit of oxygen consumed would be sufficiently accurate. He concluded that the heat release from conventional fuels involved in fires can be taken as 13.1 kJ per gram of oxygen consumed, with an accuracy of 5% or better. This work meant that the oxygen consumption principle could now be used without detailed knowledge of heats of combustion for different and composite fuels. The fire testing community were now in a position to develop tests with confidence based on Thornton's discovery in 1917.

2.6.1 Development of the Equations

The original theory of heat of combustion for oxygen was put forward by Thornton (1917) that, because of different stoichiometries, the heat of combustion per gram of oxygen can be written as

$$E = \Delta Hc / r_o \qquad (2.1)$$

where $r_o = m_{O_2} / m_{fuel}$, the stoichiometric oxygen to fuel ratio

therefore

$$\Delta H_c = E \frac{m_{O_2}}{m_{fuel}} \qquad (2.2)$$

If the net heat of combustion per gram of fuel consumed, ΔHc, and the molar mass ratio of oxygen to fuel is known, the heat of combustion per unit gram of oxygen can

be calculated. When these are not known, it is acceptable to assume a value of 13.1 kJ/g oxygen (Huggett, 1980). These rules imply that it is sufficient to measure the oxygen consumed within a system to be able to calculate the net heat released. Most simply, it is necessary to have equations dealing with the calculation of rate of heat release based on air flow rate into a system, oxygen concentration in the exhaust duct and the volume flow in the duct. Such equations were developed and refined further to take into account the production of CO, which leads to a significantly different amount of heat produced per unit mass of oxygen consumed than when CO_2 is formed (Parker, 1984). Corrections must be made if large amounts of CO are produced. Parker (1984) developed equations using an oxygen/nitrogen ratio as a means of expressing the rate of heat release when readings are taken from the oxygen analyser rather than the oxygen concentration arising in the exhaust duct. The difference between these is the removal of water vapour between the duct and the analyser, as the gases must be dried before sampled by the analyser. Since volume flow of air into the system cannot be measured directly in many cases, Parker also presented equations to calculate rate of heat release from measurements of volume flow of combustion gases in the exhaust duct. These equations allowed the oxygen consumption principle to be applied to many fire testing situations. Janssens (1991) also developed similar equations, but avoided the need for measurement of volumetric flow rates as these equations were specifically aimed at full scale testing. Different gas analyser combinations that can be used were discussed and the calculation methods for these were given.

2.6.2 The Equations

Janssens (1991) set out the problem of developing the equations in a simple and logical manner, as shown in the diagram below (figure 2.14)

Figure (2.14): Mass flows for oxygen consumption equations

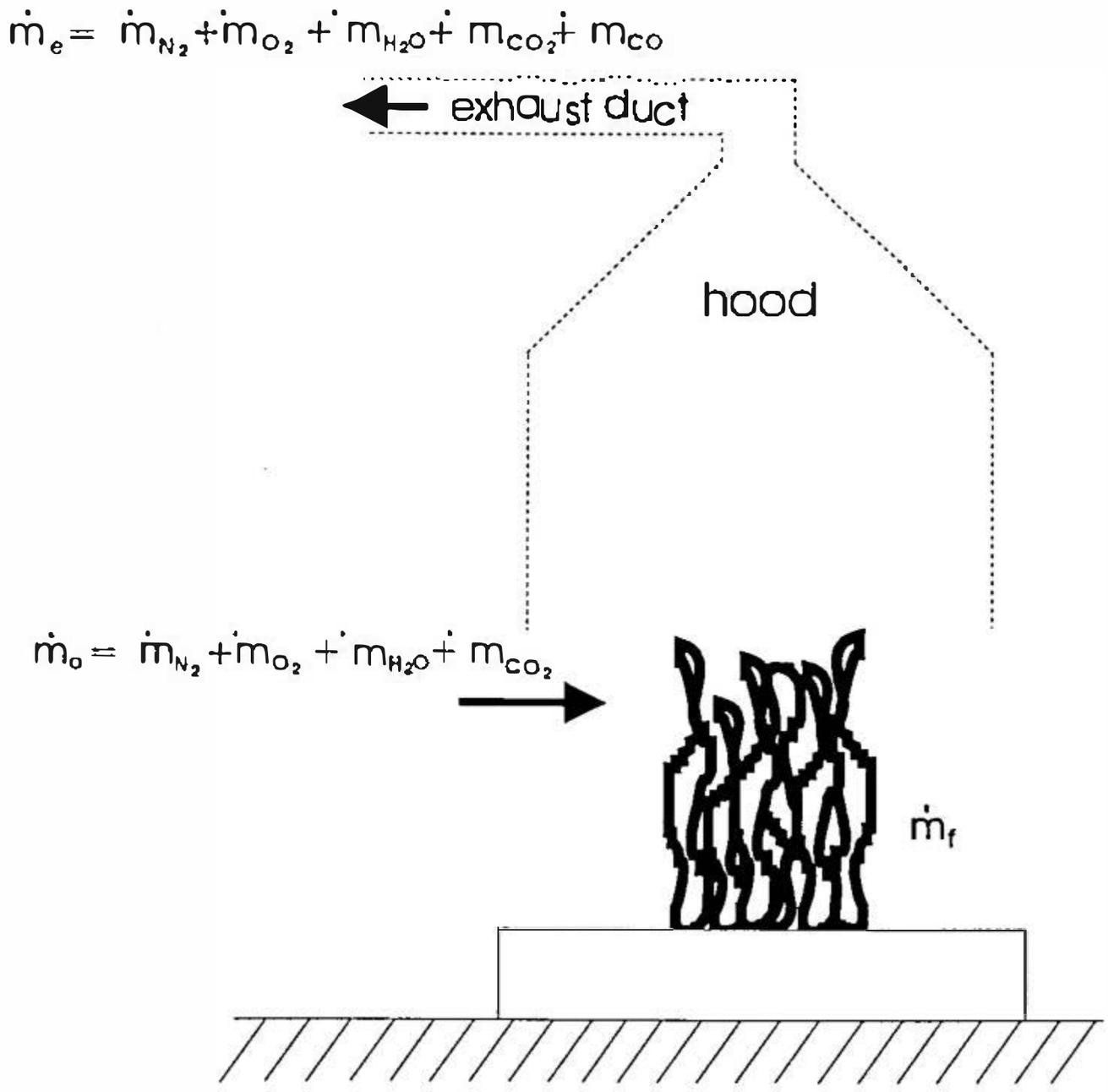

The rate of heat release can then be expressed in equation 2.3 as

$$\dot{q} = E\left(\dot{m}_{O_2}^{0} - \dot{m}_{O_2}\right) \qquad (2.3)$$

where $\dot{m}_{O_2}^{0}$ = the mass flow rate of oxygen into the system (g / s)

$\dot{m}_{O_2}$ = the mass flow rate of oxygen in the duct (g / s)

E = the heat released per gram of oxygen consumed (kJ / g)

If CO_2 and H_2O are trapped and CO is ignored, the sample gas is only O_2 and N_2. In the oxygen analyser, the percentage or molar fraction of oxygen in the gas is measured, equations 2.4 and 2.5

$$X_{O_2}^{A^0} = \frac{\dot{n}_{O_2}^0}{\dot{n}_{O_2}^0 + \dot{n}_{N_2}^0} = \frac{\dot{m}_{O_2}^0 / M_{O_2}}{\dot{m}_{O_2}^0 / M_{O_2} + \dot{m}_{N_2}^0 / M_{N_2}} \qquad (2.4)$$

$$X_{O_2}^{A} = \frac{\dot{n}_{O_2}}{\dot{n}_{O_2} + \dot{n}_{N_2}} = \frac{\dot{m}_{O_2} / M_{O_2}}{\dot{m}_{O_2} / M_{O_2} + \dot{m}_{N_2} / M_{N_2}} \qquad (2.5)$$

where $X_{O_2}^{A^0}$ = analyser oxygen reading inflow

$X_{O_2}^{A}$ = analyser oxygen reading outflow

$\dot{n}$ = molar flow rate (moles / s)

M = molecular weight (g / mol)

Assuming N_2 is conserved and does not participate in the combustion reactions, $\dot{m}_{N_2}^0$ is equal to $\dot{m}_{N_2}$. Equations 2.3, 2.4 and 2.5 simplify to equation 2.6 (Janssens, 1991)

$$\dot{m}_{O_2}^0 - \dot{m}_{O_2} = \frac{X_{O_2}^{A^0} - X^{A}{}_{O_2}}{\left(1 - X_{O_2}^{A^0}\right)\left(1 - X_{O_2}^{A}\right)} \dot{m}_{N_2} \frac{M_{O_2}}{M_{N_2}} \qquad (2.6)$$

It can further be assumed that, even if the water vapour cannot be trapped and analysed, the moisture content of the incoming air is known. If the air is at temperature T_a, pressure p_a, and has a relative humidity of RH%, the mole fraction of water vapour in the incoming air can be given by

$$X_{H_2O}^0 = \frac{RH\%}{100} \frac{p_s(T_a)}{P_a} \qquad (2.7)$$

where $p_s(T_a)$ = saturation pressure of water vapour at temperature T_a (Pa)

The saturation pressure as a function of temperature can be obtained graphically (Janssens, 1991).

Equation 2.8 (Janssens, 1991) for the heat release rate takes into account the varying water content in air in laboratory testing.

$$\dot{q} = E\left[\frac{X_{O_2}^{A^0} - X_{O_2}^{A}}{1 - X_{O_2}^{A}}\right]\frac{M_{O_2}}{M_a}\dot{m}_a(1 - X_{H_2O}^{0}) \qquad (2.8)$$

However, in most cases it is impossible to measure the incoming air flow rate, m_a, and this is not equal to the exhaust flow rate. It is therefore necessary to have an equation that uses the mass flow rate of the exhaust gases in place of that of the incoming gases.

Consider the combustion of methane in air

$$CH_4 + 2O_2 + 7.52N_2 \rightarrow CO_2 + 2H_2O + 7.52N_2 \qquad (2.9)$$

The incoming air comprises 2 moles of oxygen and 7.52 moles of nitrogen, giving a total of 9.52 moles of incoming air. The exhaust gas is made up of 2 moles of water vapour, 7.52 moles nitrogen and 1 mole of carbon dioxide, giving 10.52 moles. Therefore, it can be said that the volume of incoming gas has increased by 9.52/10.52 = 1.105 by the time it reaches the exhaust. This factor is labelled α, and is named the 'expansion' factor (Janssens, 1991), although this name is slightly misleading as expansion implies heating. In a test set-up only a fraction of the oxygen is depleted from the incoming air, therefore;

$$\dot{m}_e = (1 - \phi)\dot{m}_a + \alpha\phi\dot{m}_a \qquad (2.10)$$

where $\dot{m}_e$ = mass flow rate in exhaust duct (kg/s)
The oxygen depletion factor, ϕ, is, (Janssens, 1991):

$$\phi = \frac{\dot{m}_{O_2}^{0} - \dot{m}_{O_2}}{\dot{m}_{O_2}} = \frac{X_{O_2}^{A^0} - X_{O_2}^{A}}{\left(1 - X_{O_2}^{A}\right)X_{O_2}^{A^0}} \qquad (2.11)$$

It is now possible to substitute $\dot{m}_e$ in place of $\dot{m}_a$ in equation 2.8

$$\dot{q} = E\frac{M_{O_2}}{M_a}\left(\frac{\phi}{1+\phi(\alpha-1)}\right)m_e\left(1-X^0_{H_2O}\right)X^{A^0}_{O_2} \qquad (2.12)$$

The molecular mass of O_2 is 32 kg/kmol and the molecular mass of air is 28.96 kg/kmol, therefore

$$\frac{M_{O_2}}{M_a} = 1.10 \qquad (2.13)$$

and from the flow measuring technique in the duct,

$$\dot{m}_e = C\sqrt{\frac{\Delta p}{T_e}} \qquad (2.14)$$

where Δp = pressure differential over flow measuring device in exhaust duct (Pa)

T_e = temperature in exhaust duct (K)

C = orifice plate coefficient ($kg^{0.5}m^{0.5}K^{0.5}$)

also it can be assumed (Janssens, 1991)

$1 - X^0_{H_2O} \approx 1$ and

$\alpha = 1.105$.

Therefore equation 2.12 can be expressed as

$$\dot{q} = \frac{\Delta H_c}{r_0}1.1\,C\sqrt{\frac{\Delta p}{T_e}}\left(\frac{X^{A^0}_{O_2} - X^A_{O_2}}{1.105 - 1.5X^A_{O_2}}\right) \qquad (2.15)$$

where $X^{A^0}_{O_2}$ and $X^A_{O_2}$ are oxygen analyser readings of incoming and exhaust gases respectively.

This equation was included in the Cone Calorimeter standard (ASTM, 1990).

If CO_2 is measured rather than trapped, and CO is ignored, the oxygen depletion factor becomes

$$\phi = \frac{X_{O_2}^{A^0}\left(1 - X_{CO_2}^{A}\right) - X_{O_2}^{A}\left(1 - X_{CO_2}^{A^0}\right)}{X_{O_2}^{A^0}\left(1 - X_{O_2}^{A} - X_{CO_2}^{A}\right)} \qquad (2.16)$$

Then by using the same equations as for O_2 measurement only,

$$\dot{q} = \frac{\Delta H_c}{r_0}\ 1.1\ C\sqrt{\frac{\Delta p}{T_e}}\left[\frac{\phi}{1 - \phi + 1.105\phi}\right]X_{O_2}^{0} \qquad (2.17)$$

where: $X_{O_2}^{0} = X_{O_2}^{A^0}\left(1 - X_{H_2O}^{0}\right)$

2.7 Test Methods Based on Oxygen Consumption

Once the equations had been developed and testing using the oxygen consumption principle, as previously described, had proved that this technique could be used successfully, the development of experiments for testing of materials, both large and small scale using this method became a priority. Whilst work was being carried out on the design of small scale methods, the large scale tests were being performed. One laboratory, the Swedish National Testing Institute, developed a full scale room fire test in which all the fire gases leaving the room were drawn through a duct and sampled for oxygen content to calculate the rate of heat release (Wickström *et al.*, 1983). The heat release rate was also determined by analysing the heat balance of the fire room. The authors came to the conclusion that the latter method was far less accurate due to the difficulty in assessing wall heat losses, convective heat losses through the doorway, and variations in temperature and gas velocity. Therefore they decided that this method of calculation was unsuitable in the attempts to find a standard large scale test method, whereas the oxygen consumption technique proved to be far more promising. The main objective of their work was to develop a room/corner test method for the testing of surface lining materials. They also suggested that their test method could be useful in determining the validity of results from small scale tests. Another of the first large scale tests developed using this method was the National Bureau of Standards Furniture Calorimeter (Babrauskas *et al.*, 1982). This was designed specifically to utilise the oxygen consumption principle to determine the rate of heat release for the full scale burning of pieces of furniture.

Although it was now easier to develop large scale standard test methods, using the oxygen consumption theory, large scale tests were still too expensive and difficult to perform when compared with the bench scale National tests. What was required was a small scale test using oxygen consumption to measure rate of heat release and that required high speed data acquisition systems and extremely accurate measuring equipment.

2.7.1 The Cone Calorimeter

Development work began on a small scale test method after the publication of Huggett's work (Huggett, 1980) on the heat of combustion per unit of oxygen consumed. This principle was fundamental to the development of the small scale test. In 1982, the first paper was published on this work (Babrauskas, 1982). Some initial work began by various researchers and standards organisations (Janssens and Minne, 1982, Levin *et al.,* 1983, Green and Bilger, 1984, Peacock and Braun, 1984) to investigate the testing of different materials using this piece of equipment and in 1984 the full description of the Cone Calorimeter was published in an international journal (Babrauskas, 1984). This did not include the measurement of visible smoke and soot; that was to follow later.

In the Cone Calorimeter, figure (2.15), the rate of heat release is determined by combustion product gas flow and oxygen depletion, while the rate of mass loss is recorded simultaneously. Small samples, 100 mm by 100 mm and up to 50 mm thick, are heated by the use of a temperature controlled truncated-cone shaped radiant heater which provides a uniform heat flux across the sample surface and allows flames and fire gases through it into the duct.. The samples can be subjected to irradiance levels up to 100 kW/m^2, as determined by a 12.5 mm diameter Gardon type total heat flux meter, and can be tested in either the vertical or horizontal orientation. The sides and base are protected by aluminium foil and the sample then mounted on a refractory pad. For standard testing, the sample is mounted in a specimen holder. Additional refractory pad is used if the sample is less than 50 mm thick, to bring the sample surface in line with the top of the sample holder. A separation of 25 mm is maintained between the cone heater and the sample surface.

The sample can be tested for piloted and non-piloted ignition, the piloted version uses a spark ignitor placed 13 mm above the centre of a horizontal specimen and 3

mm above the face plane of a vertical sample. A high accuracy oxygen analyser is used as the changes in oxygen concentration are small due to the large amount of dilution from the air being drawn into the system. Because of this, the analyser must have a high degree of stability and low noise. The equations used are those for heat release rate with water vapour and carbon dioxide removed, equations 2.13 and 2.14. Mass loss measurements are made with the use of a load cell with a live load range of 500g and a mechanical tare of seven times its live load capacity, allowing the use of heavy sample holders without compromising the mass loss resolution. Effective heat of combustion for the sample material is also calculated as part of the operation. The instrument was seen to demonstrate a linearity generally to within 5% and over the major operating region to within 2%. Noise was also to within 2%. Fuels of known combustion characteristics were investigated and the values for heat of combustion were found to be accurate to within the noise level of the apparatus (Babrauskas, 1984). These levels of accuracy are now written into the standard (e.g. ASTM, 1990)

The advantage of this apparatus over other standard tests, because it employs oxygen consumption calorimetry, is in the parameters it measures. The rate of heat release from a material subjected to an imposed heat flux is important for understanding its behaviour in 'real' fires. Using the 'FAST' fire computer model, a parametric study of the hazard of upholstered furniture was performed, using large scale oxygen consumption data (Babrauskas, 1983), to explore the impact of changes in the burning properties of furniture items (Bukowski, 1985). Burning properties consisted of smoke production, burning rate, heat of combustion and toxicity. Other variables included room dimensions, open and closed doors, and wall materials. The study revealed that reducing the burning rate by a factor of two produced a significantly greater increase in time to hazard than any other variable examined, this benefit being seen regardless of changes to the other parameters. This shows that knowledge of the variables related to the burning rate is essential. Subsequent experimental work confirmed the importance of heat release rate on time to untenable conditions in a room fire (Babrauskas Peacock, 1992). Measurement of the rate of heat release provides the means to assess burning rate. The heat release rate enables engineers to gain a scientific understanding of the 'size' of a fire. Until the correct parameters are measured, it is impossible to predict full-scale fire behaviour based on small-scale tests. This is the most useful aim for fire tests.

2.7.1.1 Applications of the Cone Calorimeter

2.7.1.1.1 Smoke and Toxic Gases

Although the Cone Calorimeter was designed to measure rate of heat release, the ease with which it can be used to measure both smoke and toxic gases has encouraged researchers to investigate hazard analysis based on measurements of smoke production from the cone. The smoke extinction is measured simply with a monochromatic Helium-Neon laser. Details of the units for measurement of smoke in the Cone Calorimeter and other test methods are given in Appendix A. For the Cone Calorimeter, the units and calculations for smoke measurement are (Babrauskas, 1988, 1991);

$$k = c\sigma_f \tag{2.18}$$

where k = extinction coefficient (m^{-1})

c = concentration of smoke in the measuring volume (kg/m^3)

σ_f = specific extinction area (m^2/kg)

The extinction coefficient, k is calculated according to equation 2.19

$$\frac{I}{I_0} = e^{-kL} \tag{2.19}$$

where L= pathlength (m)

I_0 = light intensity collected at the detector in the absence of smoke

I = light intensity at the detector in the presence of smoke

The specific extinction area is computed in the Cone Calorimeter as

$$\sigma_f = \frac{k\dot{V}}{\dot{m}_f} \tag{2.20}$$

where $\dot{V}$ = volume flowrate of exhaust gas m^3/s

$\dot{m}_f$ = specimen mass loss rate kg/s

This measurement technique and the above equations form part of the American standard (ASTM E 1354, 1990).

The Cone Calorimeter can also be used to measure toxic gases. The standard cone measures CO, CO_2 and reduced O_2. This can be extended to HCN and HCl, with other gases deemed to be harmful to be considered later (Babrauskas, 1988).

A Round Robin on 11 materials involving 12 laboratories (Mikkola, 1992) demonstrated that the time to ignition measurements in the Cone Calorimeter showed better repeatability and reproducibility than other test methods, including the ISO ignitability test (ISO, 1986), possibly because of strict design and operating codes, and also the scientific basis of design. The smoke measurement repeatability was at the same level as for the ignition times, but the reproducibility was poorer. Study of the results lead to the conclusion that with experience of operating the cone, it was possible to obtain reasonable results for smoke production.

Results of specific extinction area from the Cone Calorimeter have been used successfully for comparison of materials (Hume and Pettett, 1990). For example, one series of tests showed that the addition of melamine to polyurethane foam decreased the yield of smoke from samples tested in the cone, and increased the time to peak release rate of smoke.

Although initially the smoke measurement seems promising, it does not form part of the International and British Standards for the Cone Calorimeter (ISO, 1990; BSI, 1993). The reason for this may lie in the difficulty of correlating these smoke measurements to other test methods, and to 'real' fires. Correlation of Cone Calorimeter and NBS Smoke chamber (ASTM, 1980) results for tests with carpet tiles proved impossible (Hirschler, 1992). This does not necessarily indicate a problem with the results from the cone, but in fact appears to be a problem with the NBS smoke chamber as other tests indicate (Hirschler 1991). However, initial tests comparing the rate of and total smoke production (see Appendix A for definition) from the Cone Calorimeter with the room corner test for 11 building materials did not reveal any simple correlation (Östman, 1991). These less encouraging results could only be expected and certainly did not mean that smoke measurement in the cone was any worse than in other test methods. A comprehensive and thorough review prior to the cone found few, if any, correlations between small and full-scale smoke test data (Quintiere, 1982).

However, some more positive comparisons have been made. A reasonable correlation was found between small scale and large scale smoke emission results provided that the mass loss rate of the fuel was kept the same at the two scales (Mulholland *et al.*, 1988). Whilst this may not really be practical, it served to indicate that correlations and comparisons may exist, but that they are possibly not as simple as the ones first sought.

The most promising approach seems to be use of a combination of rate of heat release and smoke obscuration (Mulholland *et al.*, 1988). The results demonstrate the importance of burning rate on the smoke production. Since burning rate and rate of heat release are closely related, it is logical to assume that the heat release rate must form part of any correlation between small and large scale smoke tests. Comparisons between the Cone Calorimeter smoke results and the room corner test were found to be reasonable when smoke production per heat release was used (Östman, 1988). As these two variables depend on ventilation conditions and size and shape of flames, it cannot be assumed that universal correlations may exist from the success of these tests, further study would be needed to assess whether these parameters could be used for predictive purposes. A more recent study (Heskestad and Hovde, 1994) revealed good relationships between the smoke production normalised by heat release rate in the Cone Calorimeter and a full scale room test, the CSTB fire test (Hognon, 1992). The smoke production in full scale was seen to only be around 45-60% of that on small scale, a fact that was attributed to secondary combustion in the hot smoke layer. This serves to reduce the smoke produced in the ventilation controlled burning regime, which produces more smoke than fuel controlled burning, and thus may hinder relationships between bench and full scale smoke data.

A similar approach has also been used for the Cone Calorimeter and the Ohio State University (OSU) calorimeter (Hirschler, 1991b). Here two new parameters were defined, both of which depended on rate of heat release and smoke obscuration. The smoke parameter (peak rate of heat release x average specific extinction area) for the Cone Calorimeter and smoke factor (total smoke x peak rate of heat release) for the OSU calorimeter. These gave a reasonably satisfactory correlation for a set of 17 materials (Hirschler, 1991). The correlation coefficients obtained were of the order of 74-88%, with the average being 79%. These are statistically significant, although the exact relationships do not appear to have been found, if exact relationships exist.

Correlations with the NBS smoke chamber and the cone and OSU calorimeter were only around 1% which is statistically insignificant and suggests that unrelated properties are being measured. This further confirms the earlier suggestion that the smoke measurements in the NBS smoke chamber are the problem, not measurements in the cone.

Although the above approaches may indicate that it will soon be possible to model large scale smoke production from small scale tests, it is misleading in that for 'real' fires, the conditions are often ventilation controlled, a situation which leads to increased smoke emission (Drysdale and Abdul-Rahim, 1985, Rasbash and Pratt, 1979). Recent attempts to rectify this have included the design of a modified Cone Calorimeter in which the air supply is controlled, and either nitrogen or carbon dioxide added to produce vitiated conditions (Mulholland *et al.*, 1991). Smoke yields were found to be insensitive to vitiation for the solid materials tested (less than 30% change) when the oxygen concentration was decreased from 21% to 14%. From observations of 'real' fires, this does not seem to be modelling fire behaviour in ventilation controlled conditions.

2.7.1.1.2 Time to ignition and flame spread modelling

The time to ignition is used to calculate critical minimum imposed heat flux for ignition, which can be used, sometimes along with rate of heat release, in predictions of flame spread (e.g. Janssens, 1992; Delichatsios *et al.*, 1991; Wickström *et al.*, 1992). The Cone Calorimeter allows collection of radiant ignition data over a wide range of controlled irradiances, in horizontal or vertical orientation. For most of the models developed to date, testing is performed in the horizontal position. Data from such tests have been seen to be both repeatable and reproducible (Östman and Tsantaridis., 1990).

The next step, in most cases, is to use these ignitability data to find the critical imposed heat flux necessary to cause ignition of a sample. This is not a new approach; ignition data from other test methods has been used previously to find the critical heat flux (Lawson and Simms, 1952; Simms, 1963). As the irradiance level is increased, the time to ignition decreases in all cases. A typical plot of ignition time (t_{ig}) versus heat flux ($\dot{q}''$) is shown in figure (2.16) (Scudamore *et al.*, 1991). The ignition time tends to infinity as the heat flux tends to $\dot{q}''_{crit}$. The critical heat flux is defined as the heat flux at which the time to ignition is infinite i.e., it is

theoretically the minimum heat flux necessary to cause piloted ignition. Ignition models (Janssens, 1992; Delichatsios *et al.*, 1991) have been developed based on this to find the minimum heat flux. The simplest approach is to assume that $1/t_{ig}$ varies linearly with heat flux and the intercept at $1/t_{ig} = 0$ gives the critical value of heat flux, figure (2.17). Whilst this approach appears reasonable and is certainly simple, when 95% confidence limits were imposed on a set of data (Whiteley, 1993), the critical heat flux for one set of conditions ranged from 2.7 to 22.6 kW/m^2. Clearly this is unacceptable.

A more sophisticated approach, based on heat transfer theory for thermally thick solids, is to plot $1/(t_{ig})^{1/2}$ versus $(\dot{q}'')$. This straight line plot, figure (2.18), still gives quite a large confidence range and very different answers than the above method (Whiteley, 1993). Instead of using either of these equations individually, it has been proposed that $1/t_{ig}$ should be plotted against $(\dot{q}'')$ for thermally thin samples, whereas for thick samples $1/(t_{ig})^{1/2}$ should be employed (Mikkola and Wichman, 1989). The difference for the two thermal thicknesses arises from heat transfer theory for thin slabs and semi-infinite solids. For thermally thin materials exposed to radiative heating and cooling convectively, Simms (1963) used a 'lumped thermal capacity' approach (e.g. Drysdale, 1985) to show that the time to ignition of the material was directly proportional to the thermal capacity per unit area, $\tau\rho c$. τ is the thickness of the slab. The limiting heat flux for a thermally thick material, both from theory and experiment (Lawson and Simms, 1952; Simms, 1963), depends upon $(t_{ig})^{1/2}$. This was shown by Simms (1963) in correlations of 'cooling modulus' versus 'energy modulus' for significant amounts of data on piloted ignition of wood. However, whether a sample is thermally thick or thin depends on the duration of the imposed heat flux. A thermally thin sample is one which is thin enough to assume that no temperature gradients exist in the sample, the rear surface temperature being the same as the front. In a thermally thick sample, temperature gradients exist. The sample can only be considered to be thermally thick as long as the rear surface is not affected by the heat flux at the top surface, and it remains at ambient temperature. This was seen for data tested under long duration times (Simms, 1963) where the correlation of cooling modulus with energy modulus diverged. For intermediate cases, it follows that $(t_{ig})^{-n}$ should be plotted against $(\dot{q}'')$, where $0.5<n<1$.

Another approach (Delichatsios *et al.*, 1991) has been proposed, where $1/(t_{ig})^{1/2}$ is plotted against;

$\dot{q}'' - 0.64\dot{q}''_{crit}$ $\quad\quad$ $\dot{q}'' > \dot{q}''_{crit}$

$\dot{q}'' - \dot{q}''_{crit}$ $\quad\quad$ $\dot{q}'' > 3\dot{q}''_{crit}$

Having chosen the method of finding the critical heat flux for ignition the thermal inertia of the material and the surface temperature at ignition can be found. To demonstrate the method used, a step-by-step approach using the work of Janssens (1992) is shown below:

a. Plot $(1/t_{ig})^{0.547}$ versus $(\dot{q}'')$, Janssens method for materials which are not obviously thermally thick or thin

b. find $\dot{q}''_{crit}$, the intercept with the abscissa of a straight line fit through the data

c. find the surface temperature at ignition (T_{ig}) from the equation;

$$\frac{\dot{q}''_{crit}}{(T_{ig} - T_\infty)} = 0.015 + \sigma \frac{(T_{ig}^4 - T_\infty^4)}{(T_{ig} - T_\infty)} \qquad (2.21)$$

d. find the total heat transfer coefficient at ignition, h_{ig}, from the equation;

$$h_{ig} = \frac{\dot{q}''_{crit}}{(T_{ig} - T_\infty)} \qquad (2.22)$$

e. measure the slope on the curve produced in step (a)

f. compute the apparent thermal inertia, $k\rho c$ as:

$$k\rho c = h_{ig}^2 \left[\frac{1}{0.73[\text{slope}]\dot{q}''_{crit}} \right] \qquad (2.23)$$

This process has several areas of possible error. The first, as mentioned above, is in finding the critical heat flux, the second is in calculating the ignition temperature. the coefficient quoted here, 0.015 is the convective heat transfer coefficient at the surface of the sample. This value was calculated from tests on wood products using the LIFT apparatus (Janssens, 1992). For vertical orientation in the Cone Calorimeter, a value of .0135 $kWm^{-2}K^{-1}$ is suggested. These values have not been investigated for other products, and it cannot be assumed that they can be used with confidence for all cases.

The calculated value of $k\rho c$ is then used in various equations, depending on exact conditions, for flame spread rate (m/s) such as opposed flow spread (Janssens, 1992; De Ris, 1969)

$$V_p = \frac{U_\infty k_g \rho_\infty C_g \left(T_f - T_{ig}\right)^2}{k\rho c \left(T_f - T_s\right)^2} \qquad (2.24)$$

where U_g = opposed air flow velocity (m/s)

k_g = thermal conductivity of air (kW/mK)

T_s = solid temperature (K)

T_f = flame temperature (K)

or (Janssens, 1992):

$$V_p = \frac{\phi}{k\rho c \left(T_f - T_s\right)} \qquad (2.25)$$

ϕ = opposed flow flame spread parameter (kW^2m^{-3})

ϕ has been evaluated for many materials (Quintiere and Harkleroad, 1984) by finding $k\rho c$ and T_{ig} from the LIFT apparatus (ASTM, 1990b).

Rate of flame spread and rate of heat release measurements, either together or separately, are used to predict what will happen in large scale tests and in 'real' fires based on results from small scale tests. One parameter that can be considered is the time to flashover in a room fire for surface lining materials (Östman and Nussbaum, 1988). In this correlation it is simply the heat release that is used, and an empirical relationship between the heat release and the time to flashover was sought from Cone Calorimeter, ISO (1986) and NORDTEST (1986) room fires. Direct correlations could not be found, instead the best relationship was:

$$t_{fo} = a \times \frac{t_{ig}\sqrt{\rho}}{A} + b \qquad (2.26)$$

where t_{fo} = time to flashover in full-scale test (s)

t_{ig} = time to ignition (s) in Cone Calorimeter at 25 kW/m^2

A = heat release (Jm^{-2}) during peak period at 50 kW/m^2

ρ = density of material (kgm^{-3})
a = constant, 2.76×10^6 ($J(kgm)^{-0.5}$)
b = constant, -46.0 (s)

The addition of density reflects the importance of thermal inertia on the growth of room fires. Eleven materials were tested but the relationship cannot be generalised to other materials without further research. A difficulty with the model is that an effective density has to be input. For non-homogeneous materials, this may not always be easy to estimate accurately.

Another model for behaviour in the room/corner test, based on results from the Cone Calorimeter uses the time to ignition in the cone and the complete heat release rate curve to predict the fire growth in the large scale (Wickström and Göransson, 1992). Three major assumptions were made to form the model: the burning area growth rate and the heat release rate are decoupled; the burning area growth rate is proportional to the ease of ignition, i.e. the inverse of the time to ignition in the Cone Calorimeter, and the history of the heat release rate per unit area is the same on a large scale as it is on small scale. Tests in the Cone Calorimeter are performed at 25 kW/m^2 only and the ignitability data used to calculate large scale burning area growth rate. The heat release rate is then calculated by assuming that the heat release rate per unit area as a function of time will be the same as in the Cone tests. This means that it is assumed that all parts of the tested product will burn the same way on a large scale as on a small scale. This will clearly not be realistic for many products, for example thermally bonded polyester wadding that is vacuum wrapped and tested on large scale will destroy its wrapping and expand rapidly towards an ignition source giving a high burning rate and heat release rate. The same material tested on small scale will not be subjected to the confines of the wrapping, shrinks away from an ignition source and often will not ignite (Atkinson, 1992). It is also clearly incorrect to assume that a material will burn the same way in a real fire where heat fluxes to the material will be varying, whereas in the Cone the irradiance in constant. For many building and wall lining materials, however, this assumption, although a large simplification, seems to be reasonable for comparison between these two tests.

The flame spread at the beginning of the room/corner test is divided into two parts. First the area behind the gas burner is ignited, the size of which is assumed to be the same for all materials. The second part is concerned with the growth of the burning

area. This is calculated as a given function of time, as long as a certain surface temperature is reached, this being calculated using ignitability and heat release data from the Cone Calorimeter. The schematic of the model is shown in figure (2.19). The area behind the burner ignites first (1) and burns at a certain heat release rate. Products then behave in one of two ways, depending upon whether they achieve the critical temperature; either there is progressive flame spread that will come to involve the entire room (2) or there is no further flame spread outside of the burner flame area (3). In the room/corner test, the burner heat output is increased to 300 kW after ten minutes. At this point the flaming area behind the burner will increase (4) and the same scenario for flame spread arises, namely the there is progressive flame spread which will eventually involve the whole room (5) or there is no further flame spread (6). The exact equations used in forming the model are not given here, but the analysis seems to be sound, based on tests on 13 products. However, only 25 kW/m^2 was considered in the Cone tests and the large scale burning rate is assumed to match that of the small scale at this heat flux, which is unrealistically low for many fire scenarios. Another disadvantage of this approach was that it could not model materials which did not go to flashover. This was later improved (Karlsson, 1993) by applying a thermal theory for concurrent-flow flame spread to the underside of a ceiling, thus including a possible retreat of the flame. The problems with both this and the earlier model are that preheating of the material is only assumed to come from radiation from the flame and this radiation is assumed to be of constant intensity over the flame length, and zero beyond that. Also, at the time of publication, no sensitivity testing had been carried out on the various assumptions made.

Concurrent flame spread theory had previously been applied for modelling purposes for the room corner test (Magnusson and Sundström, 1985). The basic flammability data in this case came from the ISO ignitability test (ISO, 1979) but the data could also be obtained in the same way from the Cone Calorimeter. The main model is developed on parameters obtained from ASTM room tests (ASTM, 1982).

Flame spread modelling is also used with the Cone Calorimeter data to predict the flame spread results in the LIFT (ASTM, 1990b) apparatus (Jianmin, 1990, 1992). Again, the heat release rate from a material tested in the cone at 25 kW/m^2 is used, along with a number of ignition times at several, at least two, imposed irradiance levels. The ignitability obtained from the cone is used, as previously shown, to obtain the thermal properties, $k\rho c$, of the material and the surface temperature at

ignition. The heat balance equation is written by considering conduction into the sample, natural convection, radiation from the flame and radiation from the imposed heat source. The large number of assumptions made in this model, without any justification, means that its validity must be questioned. For example, the flame in the LIFT apparatus is assumed to be plane, parallel to the sample surface with the distance between it and the sample being proportional to the heat release rate in the Cone Calorimeter at an irradiance level of 25 kWm^{-2}. The heat release rate for black PMMA, 25 mm thick, is taken as reference data, presumably as this material is tested more frequently than any other. The flame temperature is taken as constant over all the burning sample, at 1300K, with all heat transfer from the flame assumed to be by radiation. The use of radiation as the only mechanism of heat transfer from the flame has been criticised (Thomas, 1993; Quintiere, 1993). Many researchers (e.g. Quintiere, 1981; De Ris, 1969) have identified conduction and convection through the gas phase as the main means of heat transfer from the flame to the fuel ahead of the pyrolyzing zone. Whilst radiation does have a role to play, it cannot be considered the main mechanism of heat transfer for this case. The emissivity of the flame in this model (Jianmin, 1990, 1992) is assumed to be related to the smoke generation rate from the material in the Cone Calorimeter at 25 kWm^{-2}. Again, the emissivity is calculated by comparison with data for PMMA, for which the flame emissivity is assumed to be 0.45. This was also criticised by Thomas (1993). For the system under consideration, flame thickness is of the order of a few centimetres, giving flame emissivities of approximately 0.05-0.10 (Thomas, 1993). Thomas also showed that in this case conduction could not be neglected. Also, smoke generation results are not as repeatable and reproducible as other measurements in the Cone, further increasing the errors for this assumption. Another unjustified assumption is that for the flame duration, taken to be related to the time in the Cone that the heat release rate is greater than 60% of the maximum, at 25 kWm^{-2}, the critical irradiance and the average rate of heat release from the Cone, during the period that the heat release rate is within 60% of the maximum. Many other assumptions are made in forming this model, with few supported by any experimental research. Certainly detailed tests would have to be made before this model could be used with any confidence. This is especially important if, as suggested (Jianmin, 1992), predictions of LIFT data rather than experimental data could be used in flame spread models based on LIFT data (e.g. Karlsson and Magnusson, 1992).

The aim of work like this is to examine the consistency between the small scale tests by trying to show that flame spread in one test can be predicted from properties

obtained from the other. If successful, this would indicate that the thermal properties of a material and the ignition temperature can be found successfully from the Cone Calorimeter, increasing confidence in their use for modelling large scale flame spread, as well as increase understanding of the properties measured and the combustion conditions.

Finally, research has been aimed at using the Cone Calorimeter to predict what will happen to entire pieces of furniture in a fire. Parker *et al.* (1991) compared chair burns in a room with burns under a furniture calorimeter and the materials in a Cone Calorimeter. Correlations were obtained between total rate of heat release of full scale chairs and the three minute average heat release rate of material combinations in the Cone Calorimeter at an external irradiance of 35 kW/m^2. For the chairs tested, the total heat release rate of 65 kW in the furniture calorimeter was found to be equivalent to a 3 minute average heat release rate of 87 kW/m^2 in the Cone Calorimeter. The correlations obtained were based on only ten tests, and no investigation of different irradiance levels in the Cone Calorimeter was made. The heat flux of 35 kW/m^2 was chosen as it is the heat flux specified in the proposed NFPA 246A standard for the use of the Cone Calorimeter for upholstered furniture (Babrauskas, 1989). Calculations of the upper layer temperature in the room were made, using HAZARD 1 (Bukowski *et al*, 1989) with the measured heat release rates in the room as input data.

There are many discrepancies within the results and conclusions drawn. Comparisons were made between the tests using only the materials which had a three minute average heat release rate of less than 180 kW/m^2 when tested in the Cone, even though this was the case for only five out of the ten foam combinations. The authors state that the material combinations with this low rate of heat release do not show significant involvement of the foam filling in furniture calorimeter tests, with the exception of one sample. This means that this does not hold true for 20% of the five samples. Again, these low heat release rate samples are said to pass the room test, based on temperature above the chair, although two chairs exceeded the upper temperature criteria in the room test but gave three minute average heat release rates of less than 87 kW/m^2 when tested in the Cone.

The furniture calorimeter and room fire test data cannot even be compared satisfactorily, although they both use full scale chairs, as, for the over half the chairs the peak heat release rate is such that heat feedback in the room causes increased rate

of burning, above that seen for the furniture calorimeter. For peak heat release rates less than 600 kW, the two tests give reasonable agreement for the small number of samples studied. The rationale behind using the 180 s average heat release from the Cone tests is also not clear. Certainly of interest is the heat release rate in the early part of the test, the rate of heat release rate, as this will give an indication of how quickly a material may become involved in a real fire situation, but this does not justify the use of the 3 minute average. Lastly, of concern is the poor repeatability of measurements in duplicate tests. Six tests in the room were duplicated and measurements made of temperature and heat release rate. The latter was calculated from rate of mass loss in several cases. In the worst case, one temperature rise measurement was 38°C, whilst its duplicate was 204°C. The average variation from the mean for each pair of tests was ± 19.9% for the temperature measurements and ± 20.4% for the heat release rate data. Further work would be necessary on these and other materials to use the correlation with any confidence and to apply it to other chairs and material combinations.

Another approach (Babrauskas and Krasny, 1985) to the same problem, in this case trying to predict behaviour in the furniture calorimeter from Cone results has yielded an equation based on the Cone Calorimeter heat release rate, the combustible mass of the chair, the type of material and the style of the item:

$$q''_{fs} = 0.63 q''_{bs} (\text{mass factor})(\text{frame factor})(\text{style factor}) \qquad (2.27)$$

where q''_{fs} = full scale heat release rate

q''_{bs} = 180s average heat release rate in Cone Calorimeter at 25 kW/m^2

mass factor = combustible mass (kg)

frame factor = 1.66 non combustible frame material
0.58 melting plastic
0.30 wood
0.18 charring plastic

style factor = 1.0 plain, primarily rectilinear construction
1.5 ornate, convolute shapes
intermediate values for intermediate shapes

The value of 25 kW/m^2 for testing in the Cone was decided after tests at 25, 30, 40, and 50 kW/m^2. The only criterion, however, for selecting this value was the lowest coefficient of variation for predicting a proportionality factor for each set of results, rather than basing the choice on any theoretical or 'real-fire' scenario ideas. Again, the 180 s average is used for heat release rate, although in this case it was chosen out of 60, 120, 180, 240 and 300 s averages, plus peak values, as giving the best fit with the data. The correlations obtained rely on limited data, only around ten materials and fewer different styles of chairs, and are therefore restricted in their possible use.

2.7.1.2 Cone Calorimeter Discussion

All the above show ways in which the Cone Calorimeter is being used beyond its original design intentions. Researchers have hoped that the measurement of rate of heat release, a more fundamental and 'scientific' approach to fire testing than has previously been adopted, will allow small scale testing to virtually replace the need for large scale tests. However, this must be approached with caution, the conditions employed in the Cone Calorimeter are not representative of those appearing in many 'real' fires and it is real fire behaviour that fire engineers need to be concerned with, not simply large or small scale representations of them. Results from any test method, large or small scale, will be dependent on the test conditions. Comparisons and correlations of data from different test methods can only be successful if the fundamental properties measured, and the conditions of test, are the same. This also applies to developing models using test data to predict behaviour in real fires. It is because of this that there are restrictions on the use of fire tests. Finally, before a material can be tested with confidence, it is necessary to understand both the exposure conditions in the test method and those that may exist in the usage of the product.

2.8 Conclusions

There exists a large number of fire tests for materials which measure various properties under many different conditions. Whilst the tests may be used to compare materials under the test conditions, their relevance to 'real' fire conditions is questionable. The main purpose of fire testing should be to gain an indication of the way in which a material will become involved in and influence the course of a fire. It is also desirable to gain results that will be able to be used in modelling and

predicting fire behaviour under different conditions. The Cone Calorimeter appears to be the most useful of the test methods for these purposes, as the rate of heat release and time to ignition measurements that can be made are based on sound scientific theory, and indications from researchers investigating this apparatus are that the results may be useful for modelling purposes. Additional measurements, such as specific extinction area, are not as reliable or useful, but it is not really this that the Cone Calorimeter was designed to measure. It must be recognised that materials tested under well-ventilated, small scale conditions may behave differently in a ventilation controlled situation, and that geometry will have an influence on fire behaviour. These cannot be taken into account in the current small scale tests. It is also vital to have some knowledge of 'real' fire conditions, in order to subject samples to severe, yet realistic, exposure levels and configurations.

Figure (2.1) The course of a compartment fire

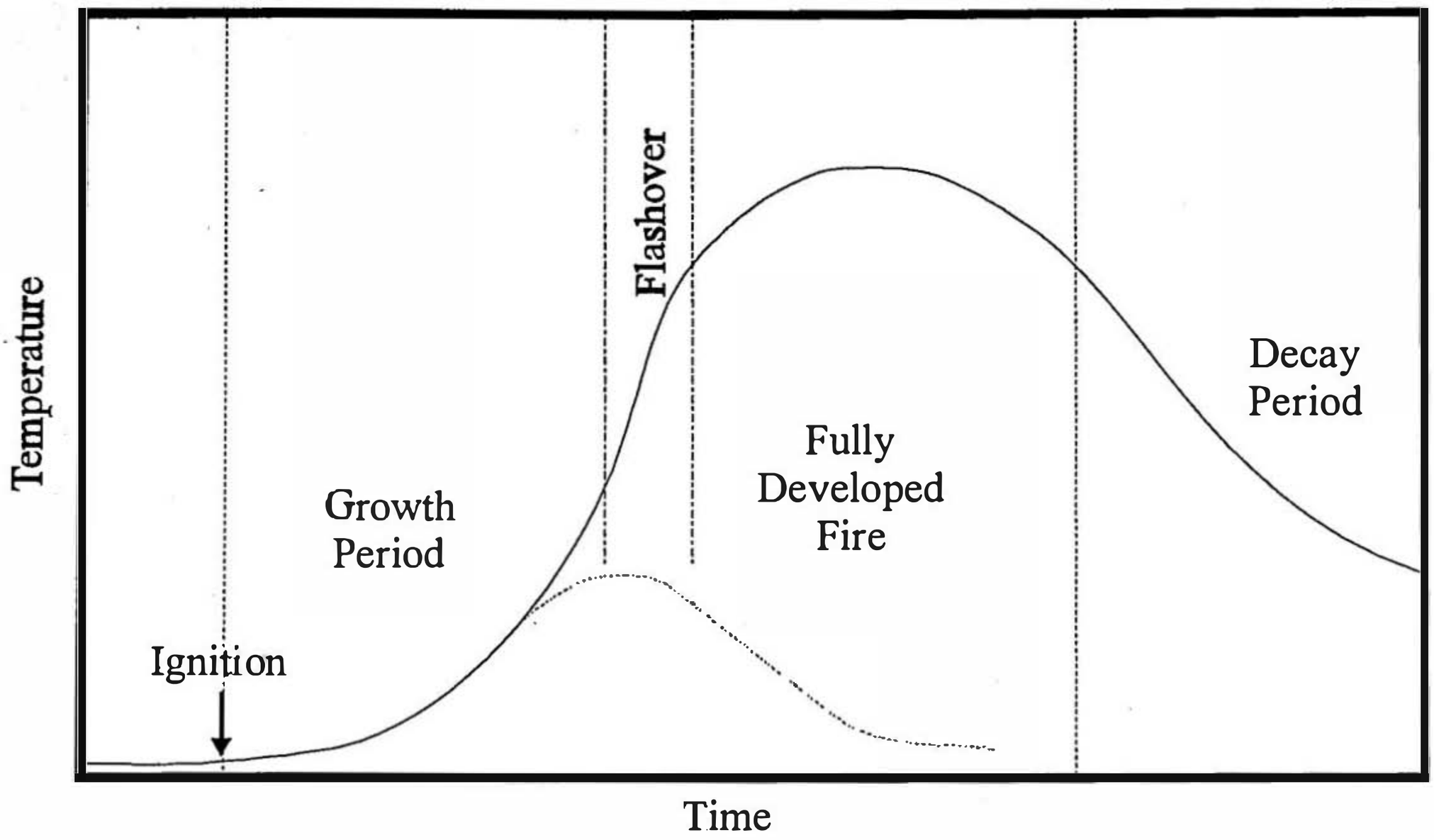

Figure (2.2) Emmons' Fire Triangle

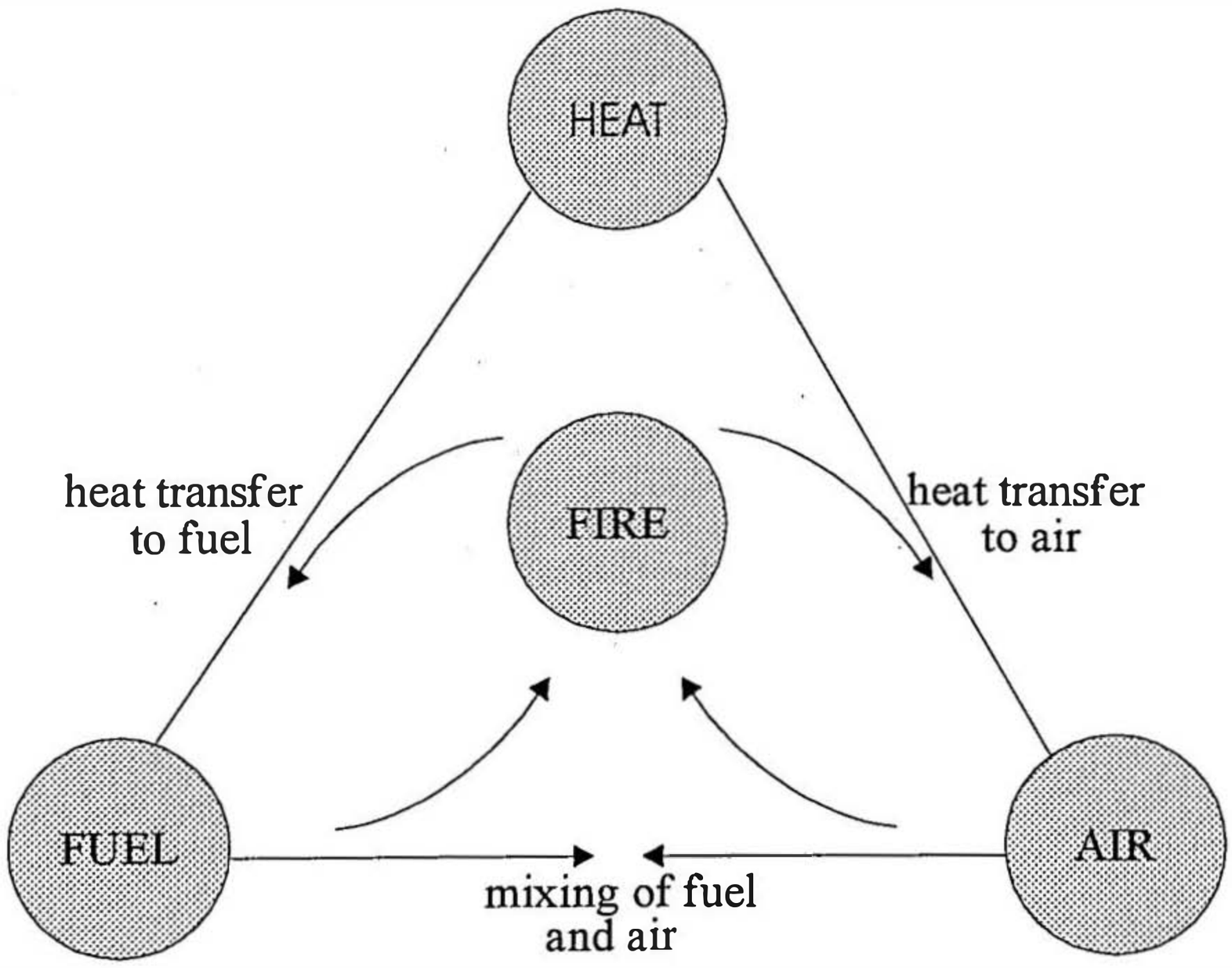

Figure (2.3) BS 5852 Ignitability test for upholstered composites

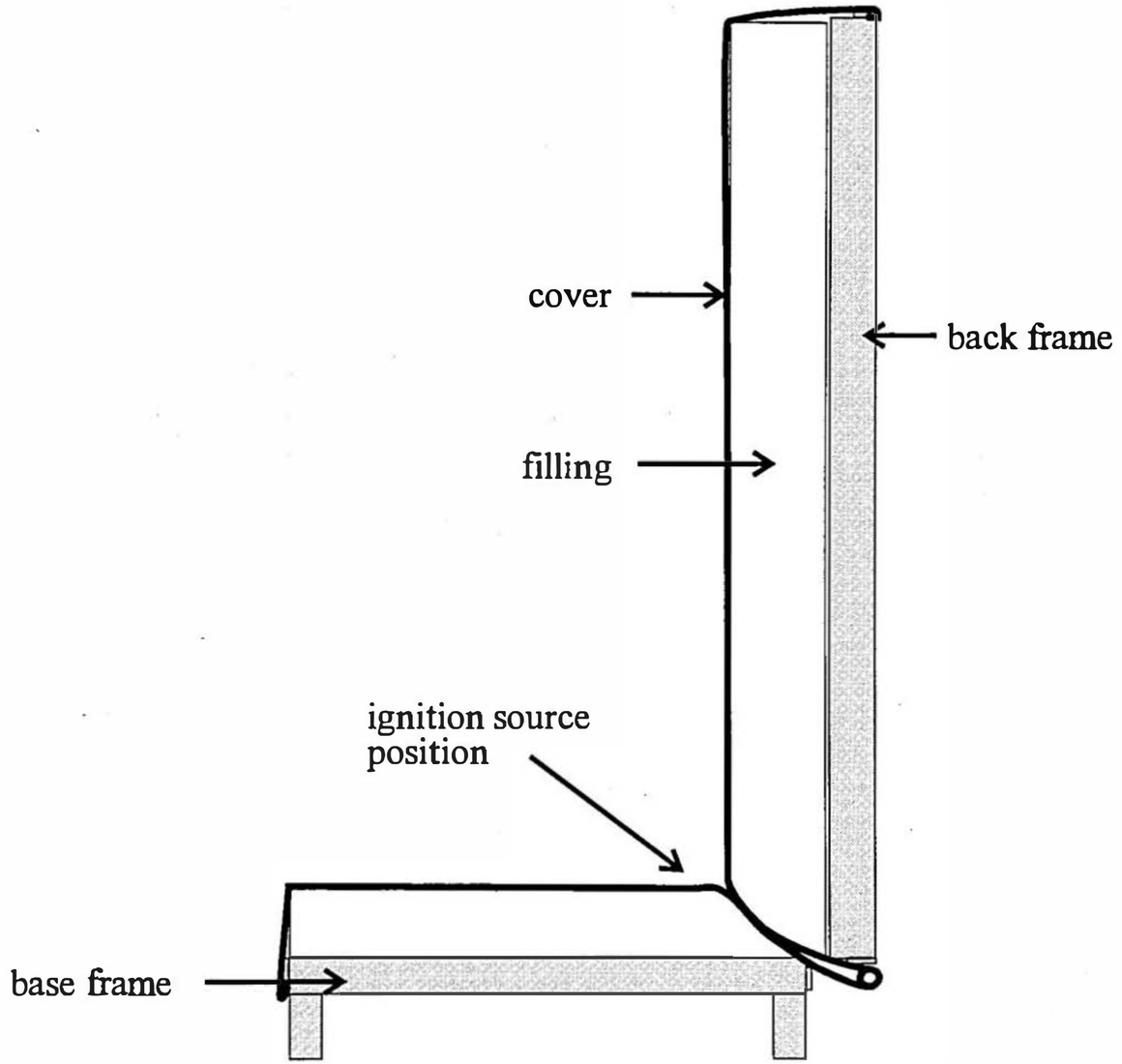

Figure (2.4): Epiradiateur test cabin

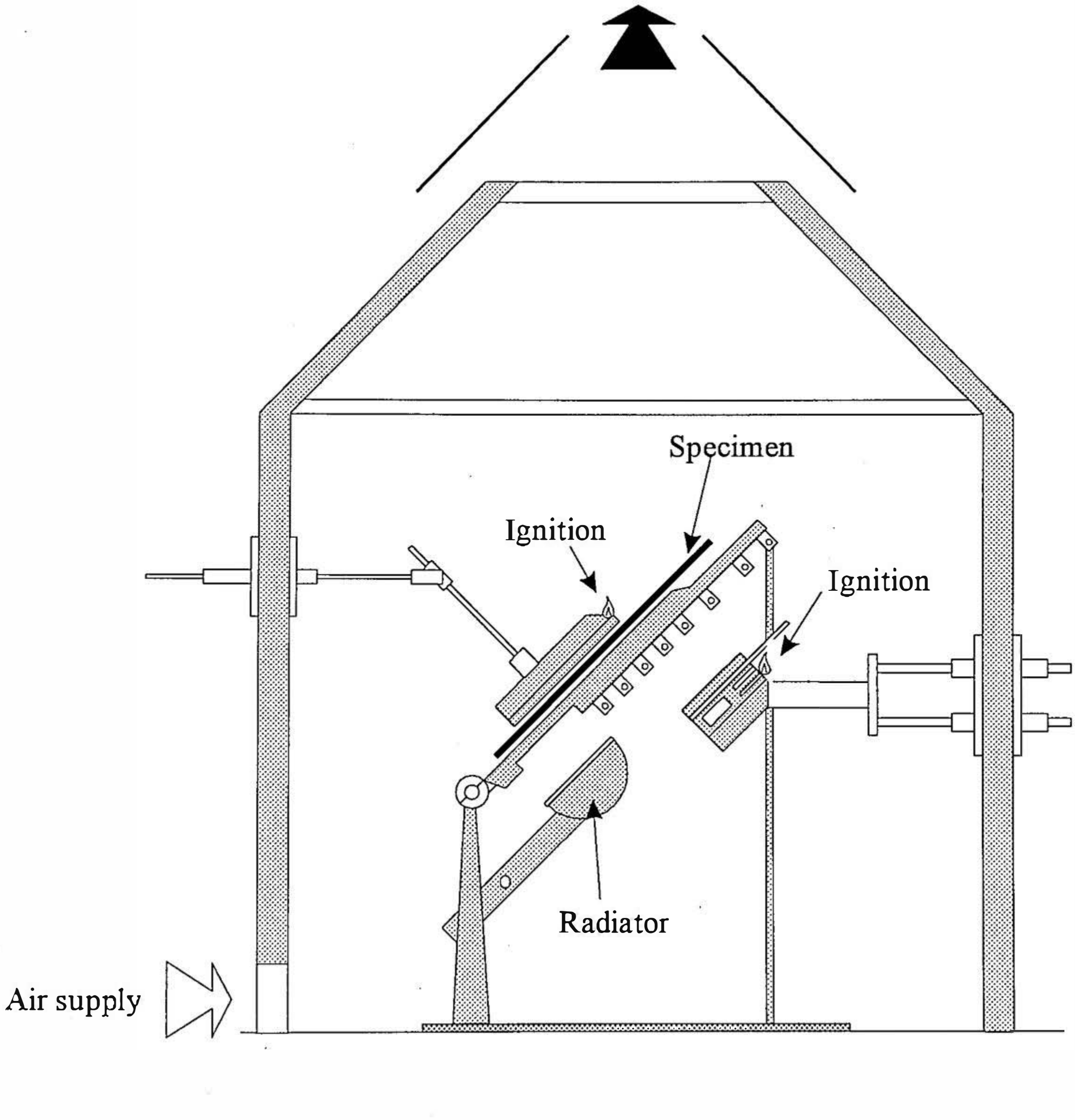

Figure (2.5): BS 476 Part 7
Surface Spread of Flame Test

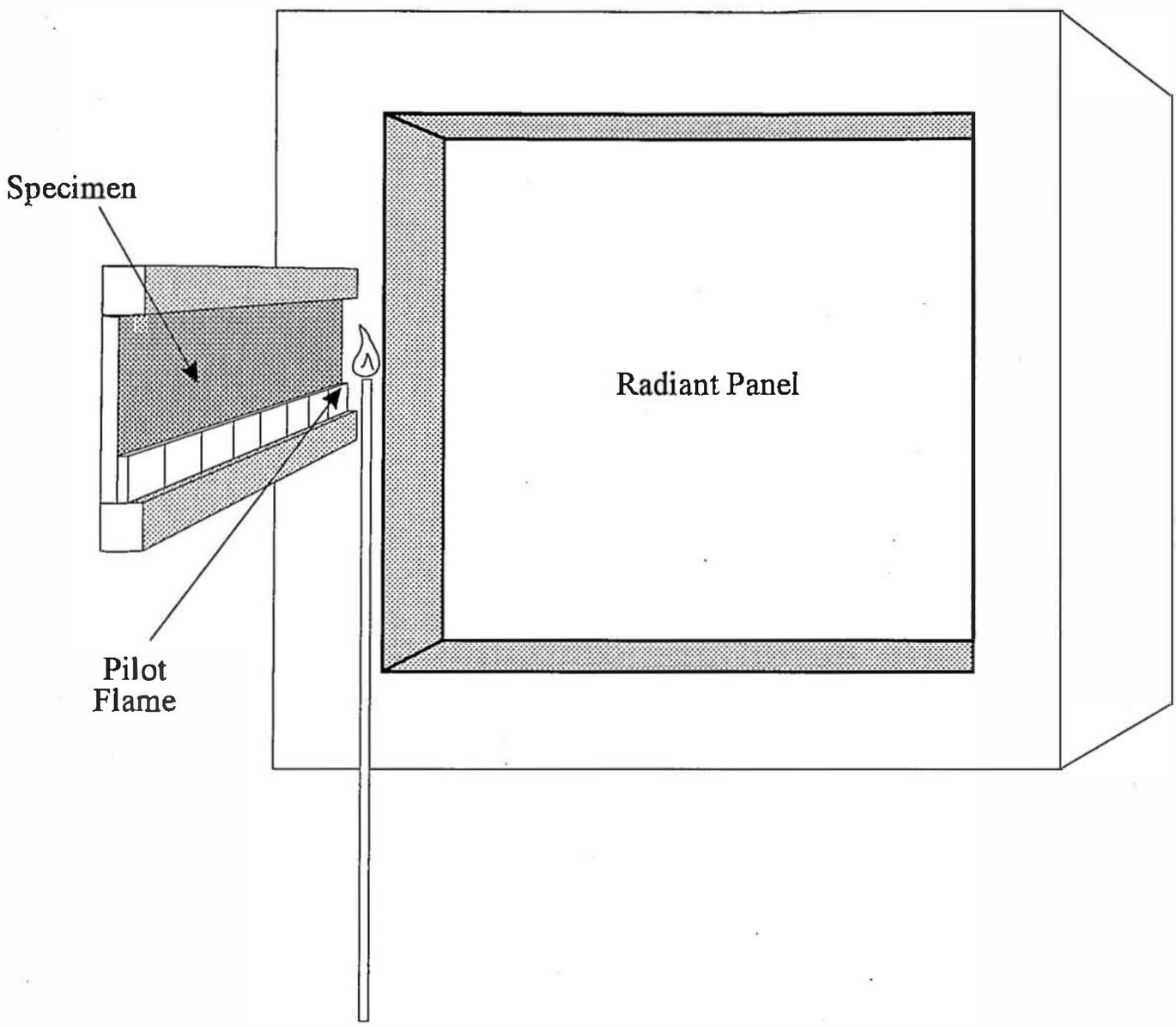

Figure (2.6): NEN 3883 Apparatus for testing flashover

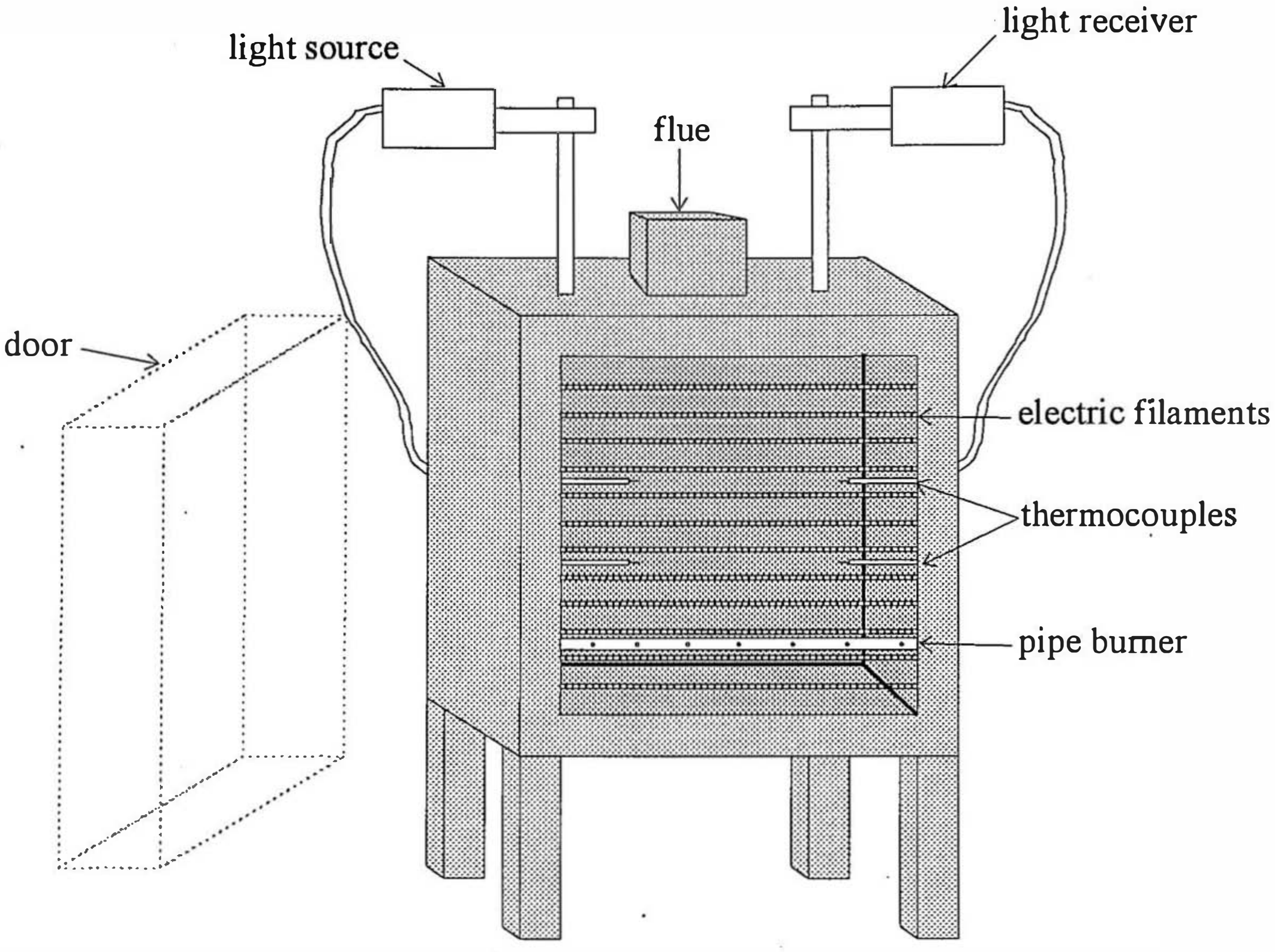

Figure (2.7): Brandschacht test

Figure (2.8) BS 476 Part 6 Fire Propagation Test Apparatus

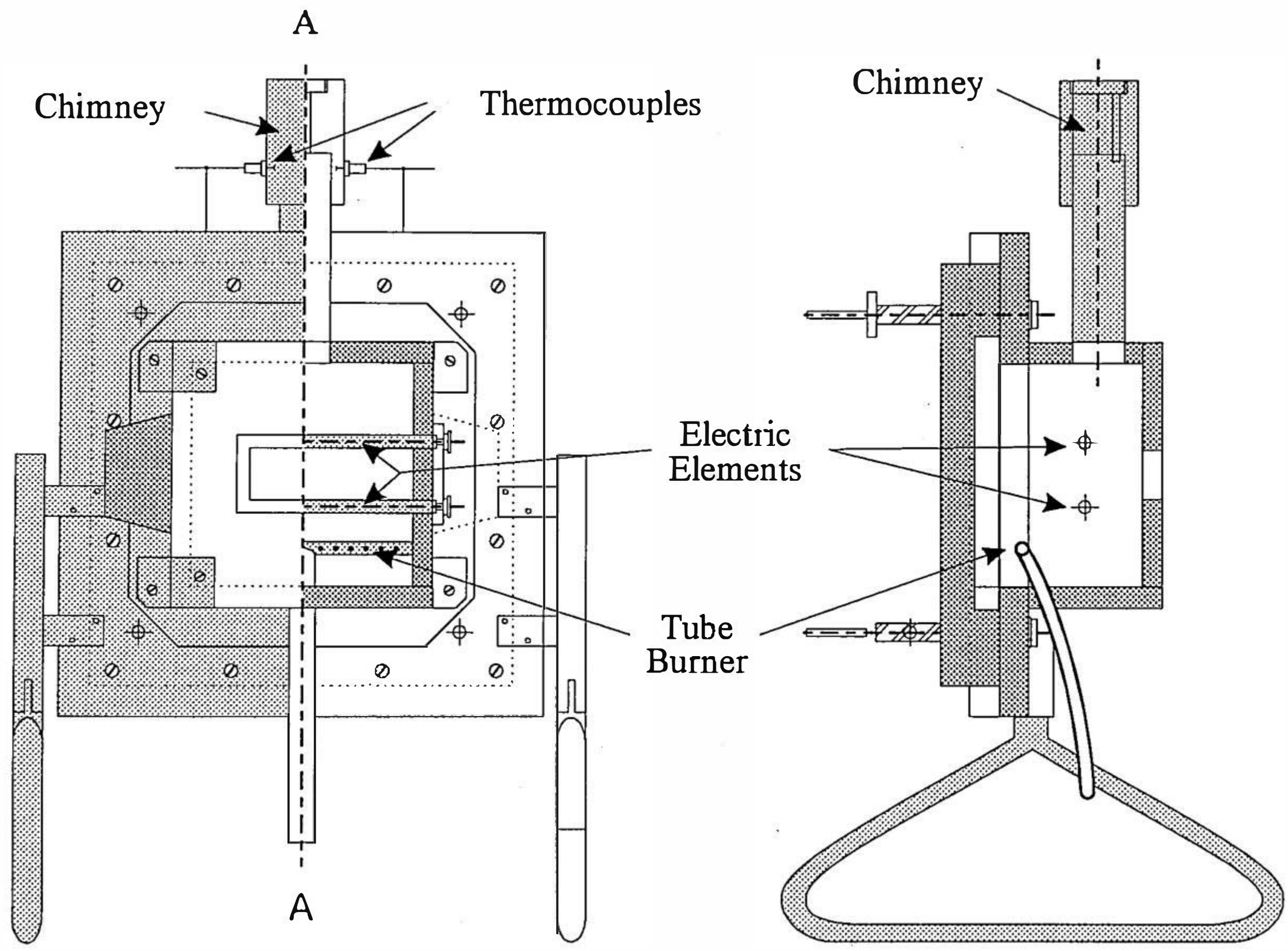

Figure (2.9): The HSE Medium Scale Fire Test

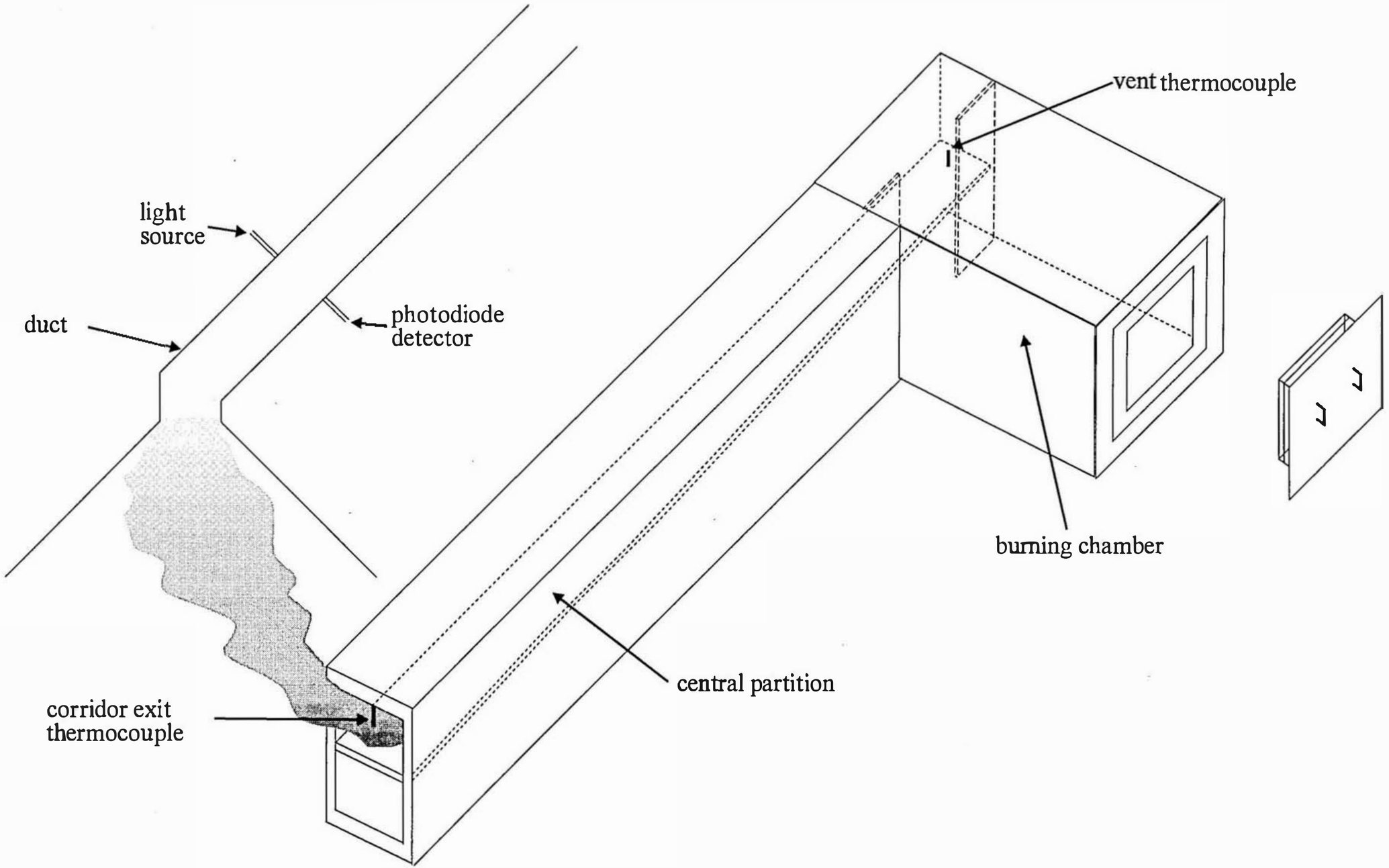

Figure (2.10): Schematic of ISO 5657 Ignitability Test

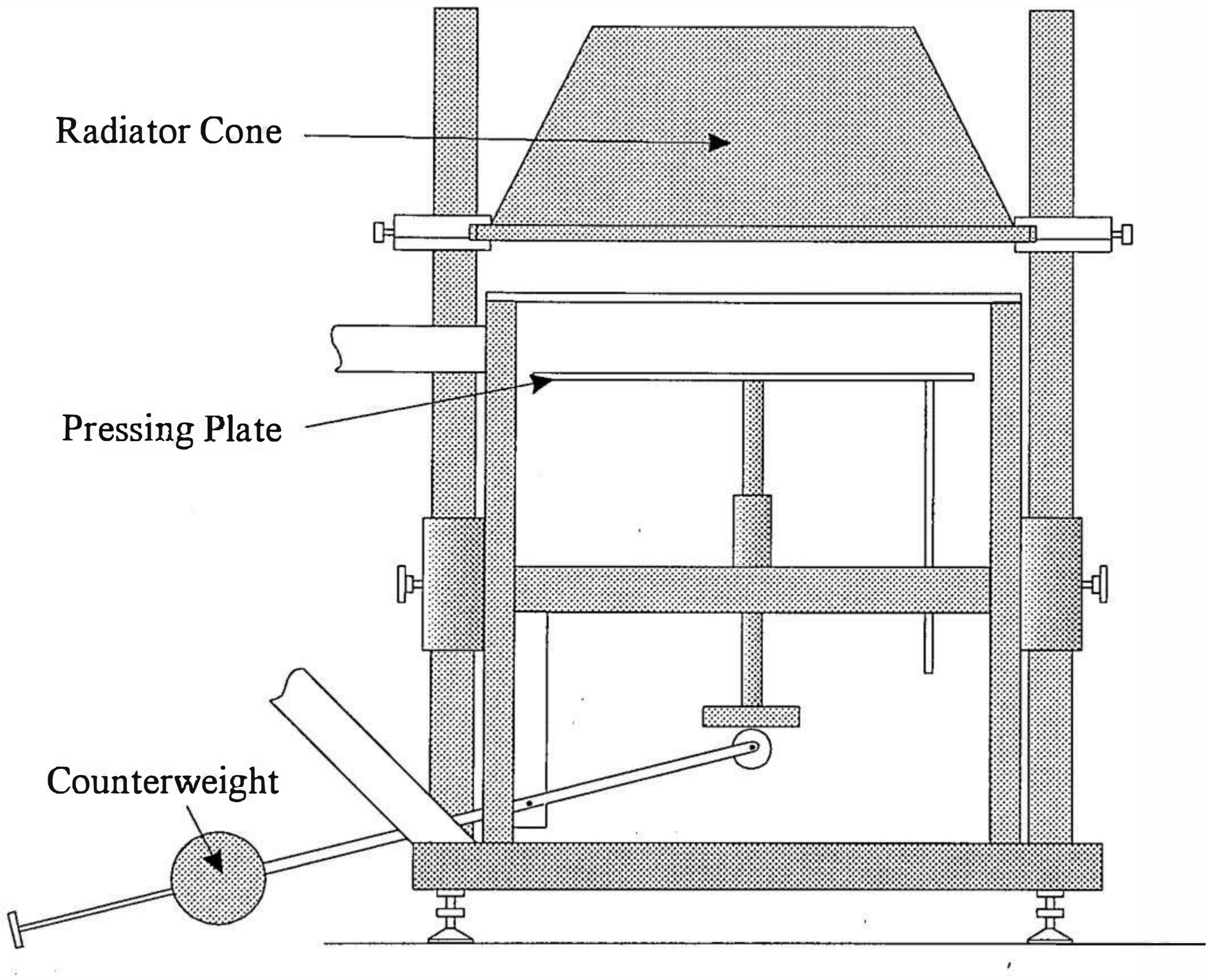

Figure (2.11) ISO 5658 Spread of Flame Apparatus

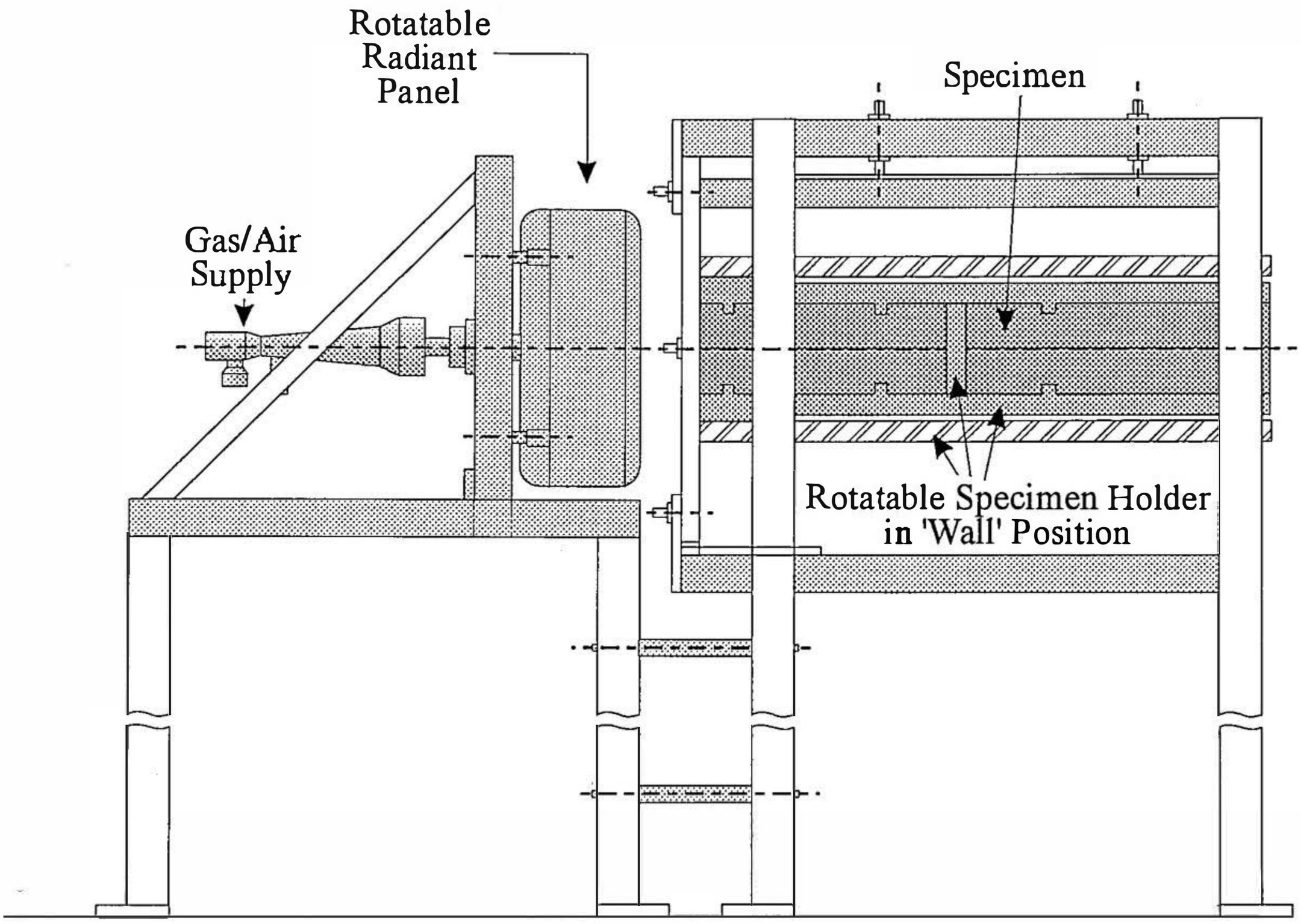

Figure (2.12): The LIFT Apparatus

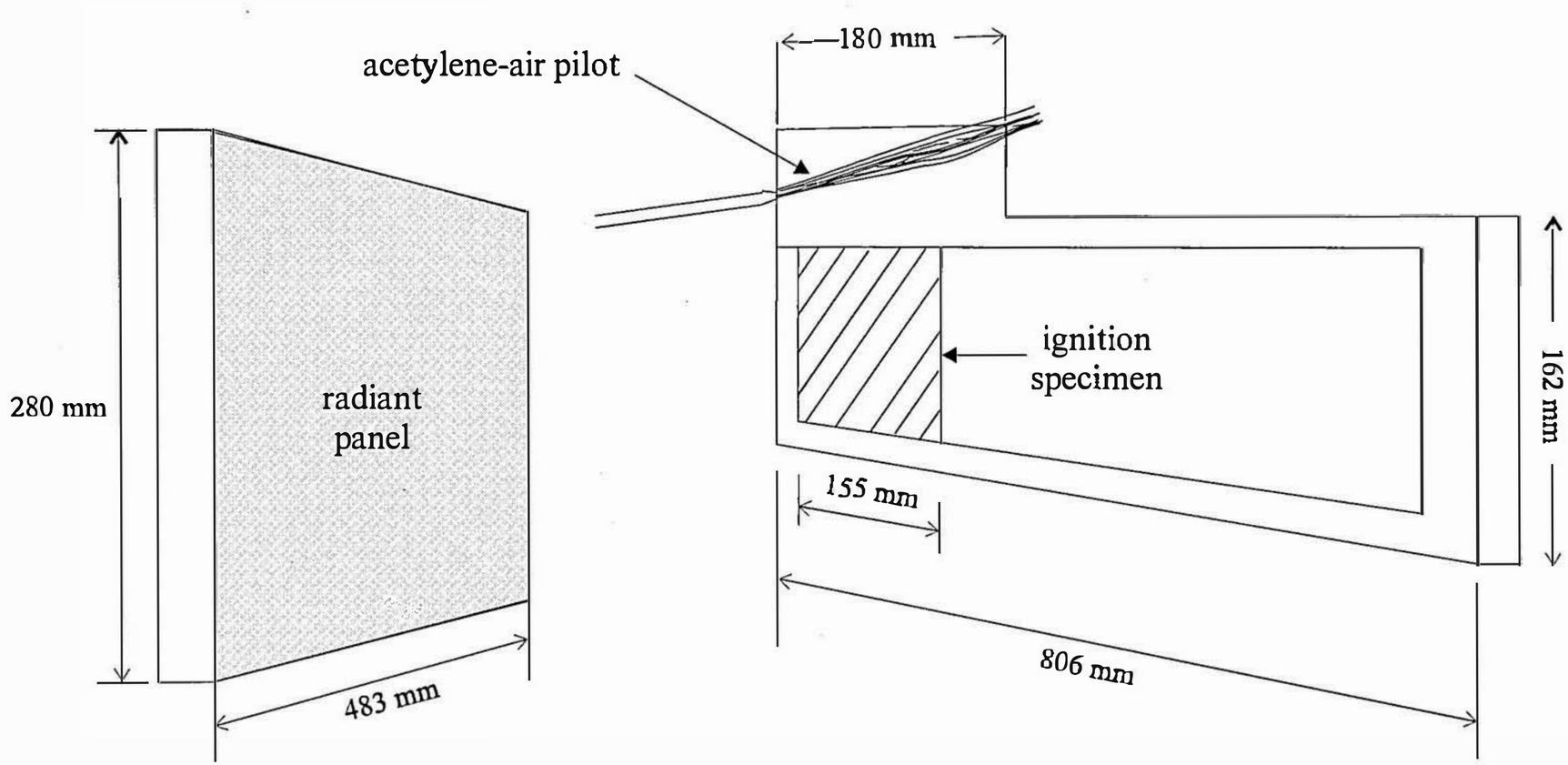

Figure (2.13) ISO Smoke Box

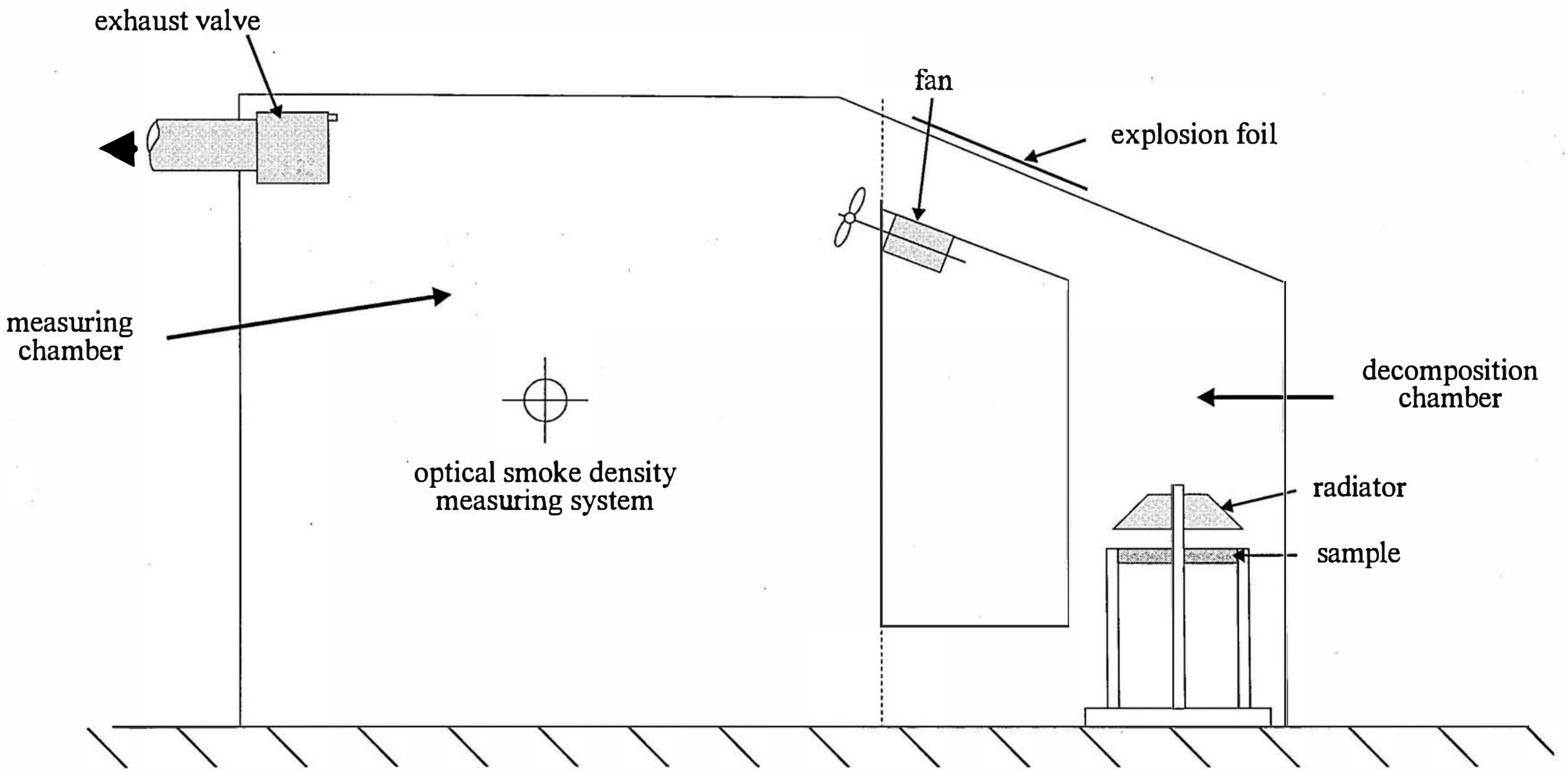

Figure (2.15): The Cone Calorimeter

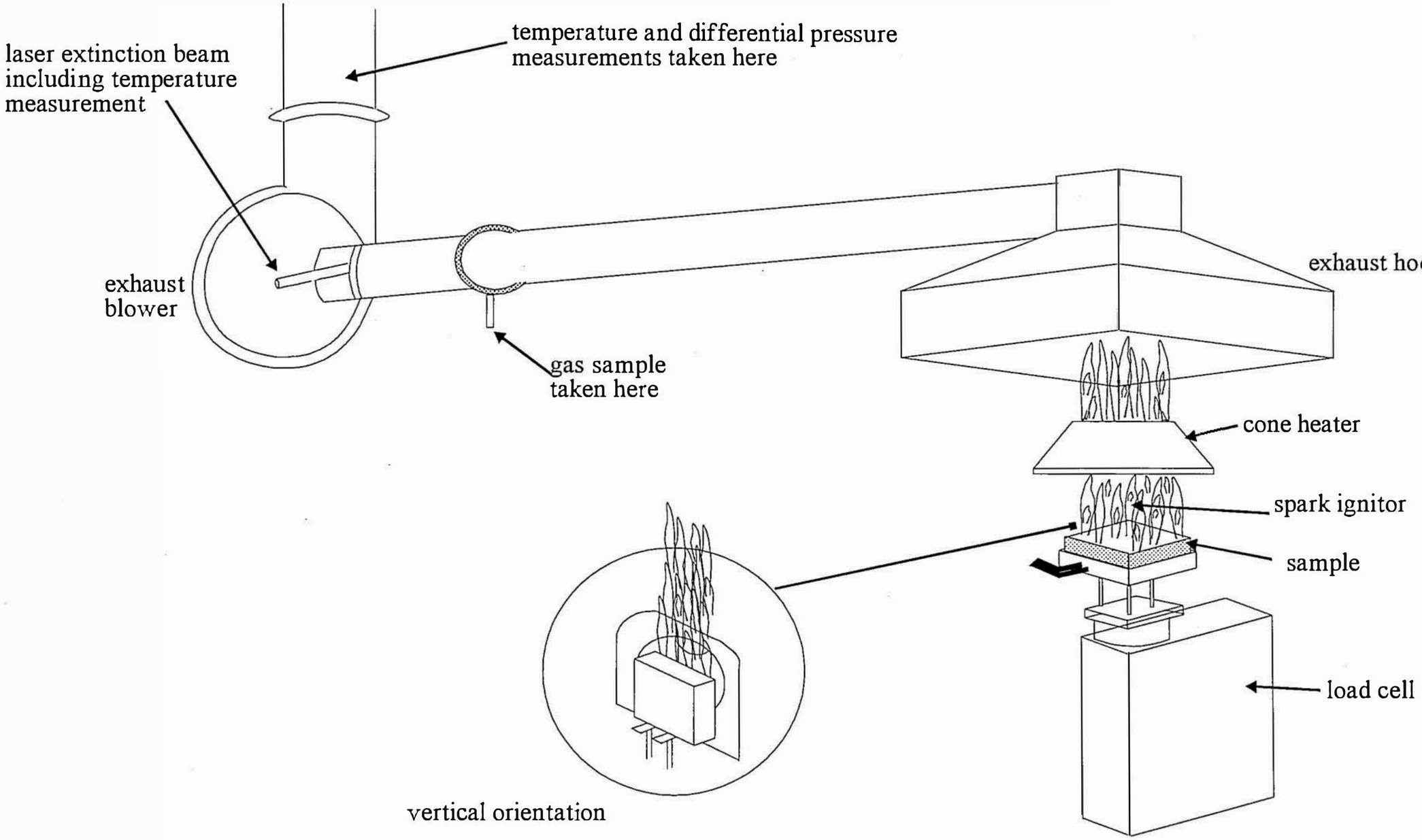

Figure (2.16): t_{ig} as a function of imposed heat flux

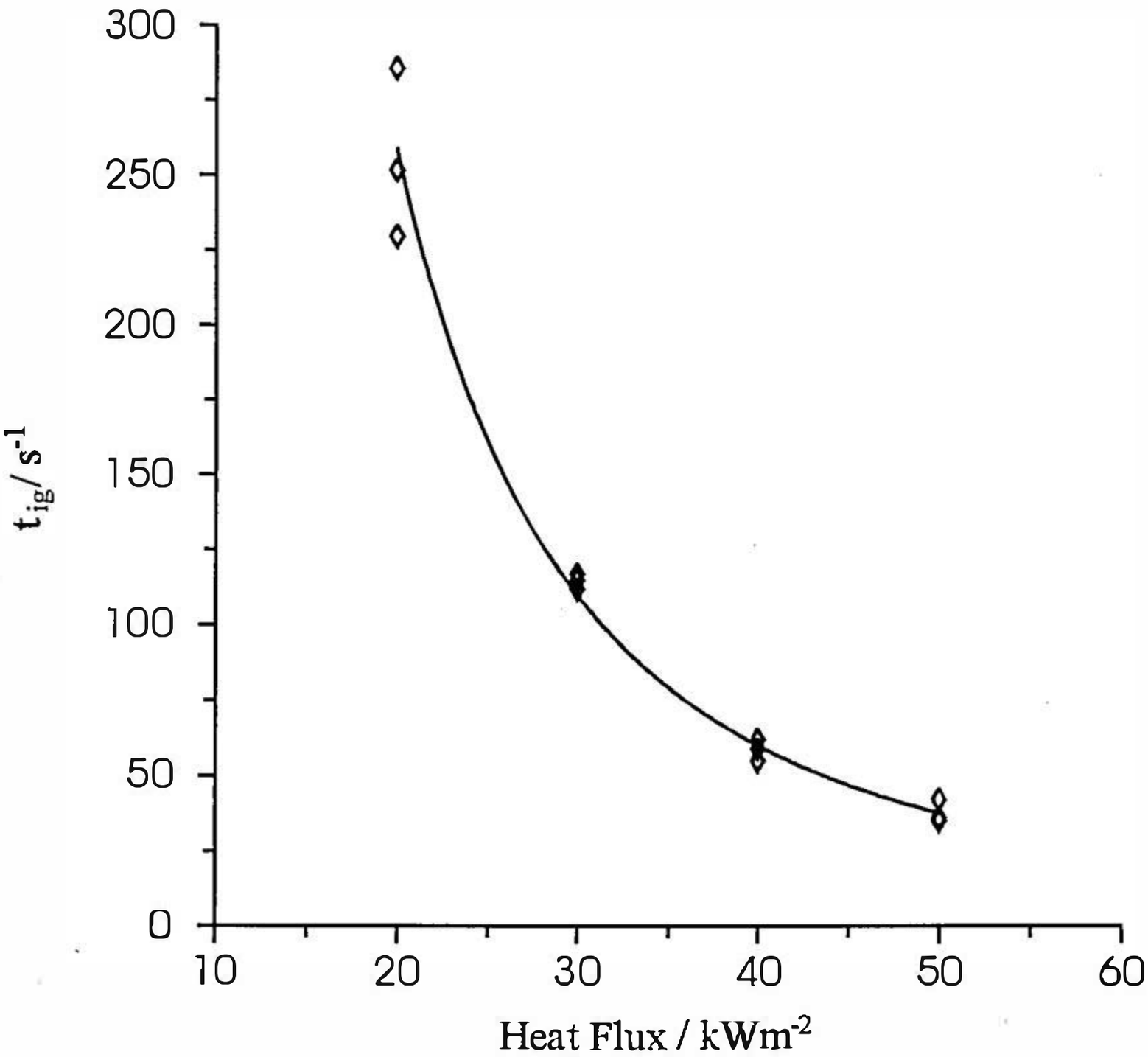

Figure (2.17): $1/t_{ig}$ as a function of imposed heat flux

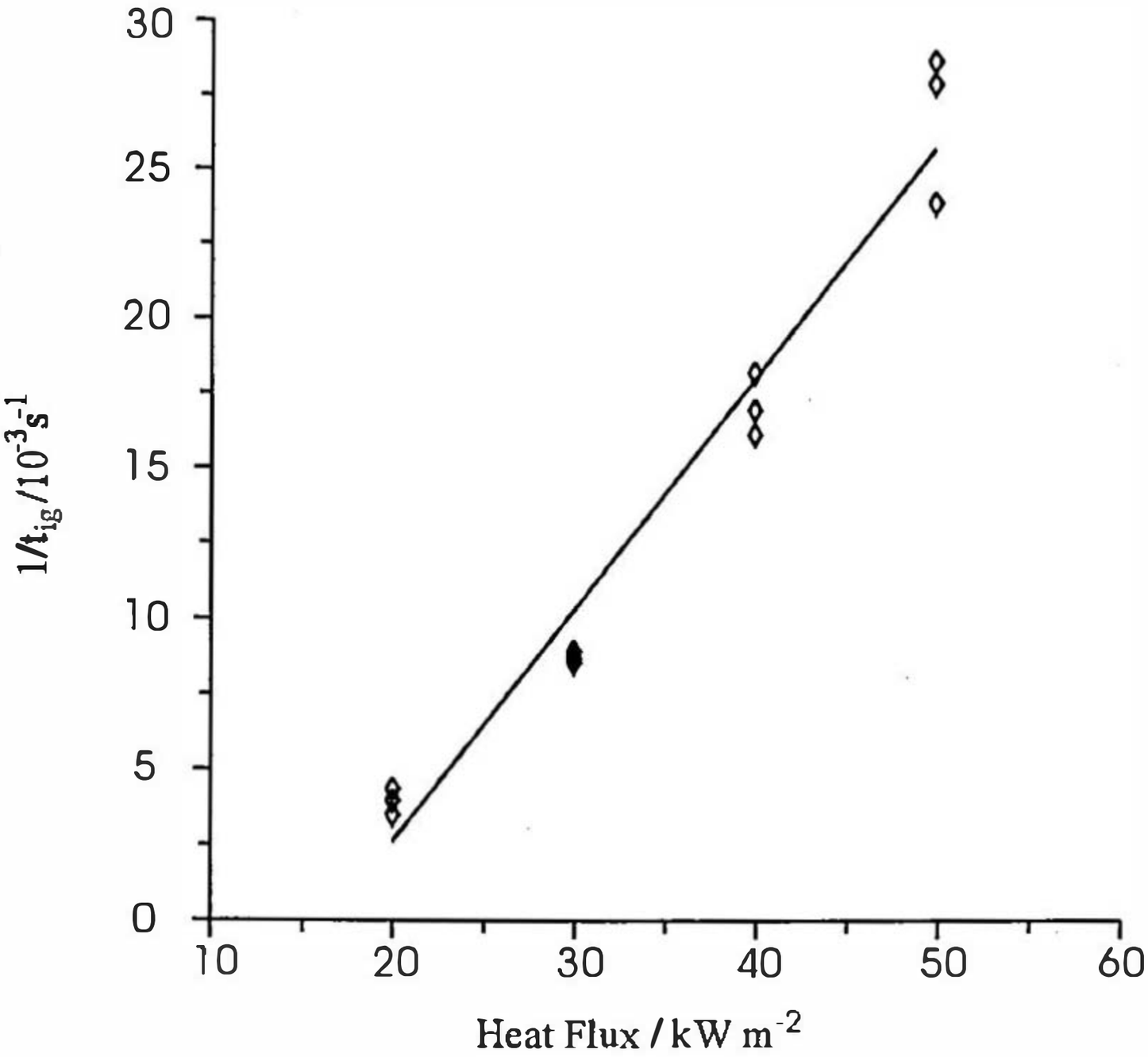

Figure (2.18): $1/(t_{ig})^{1/2}$ as a function of imposed heat flux

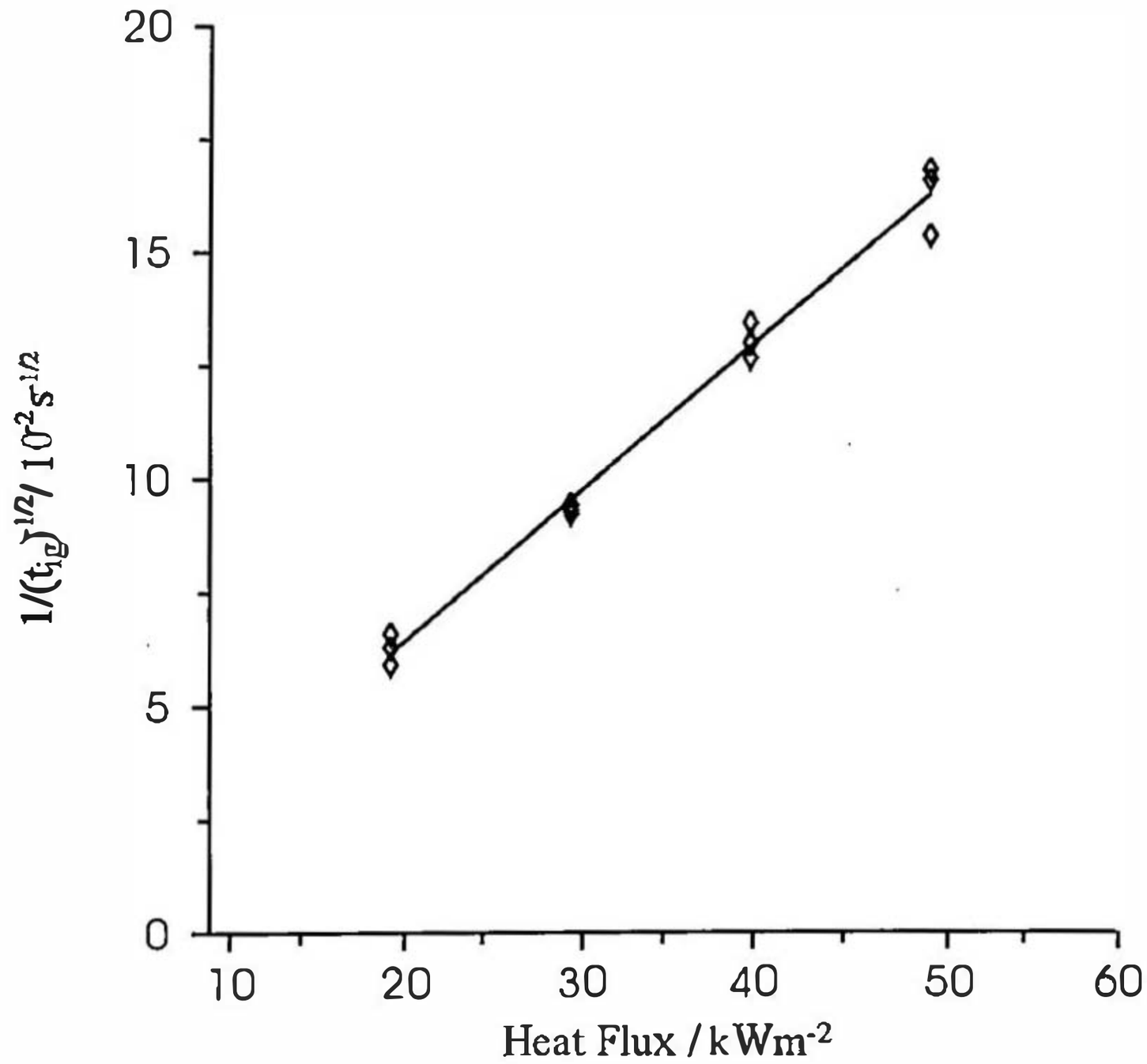

Figure (2.19) schematic pattern of burning area growth in Room/corner test

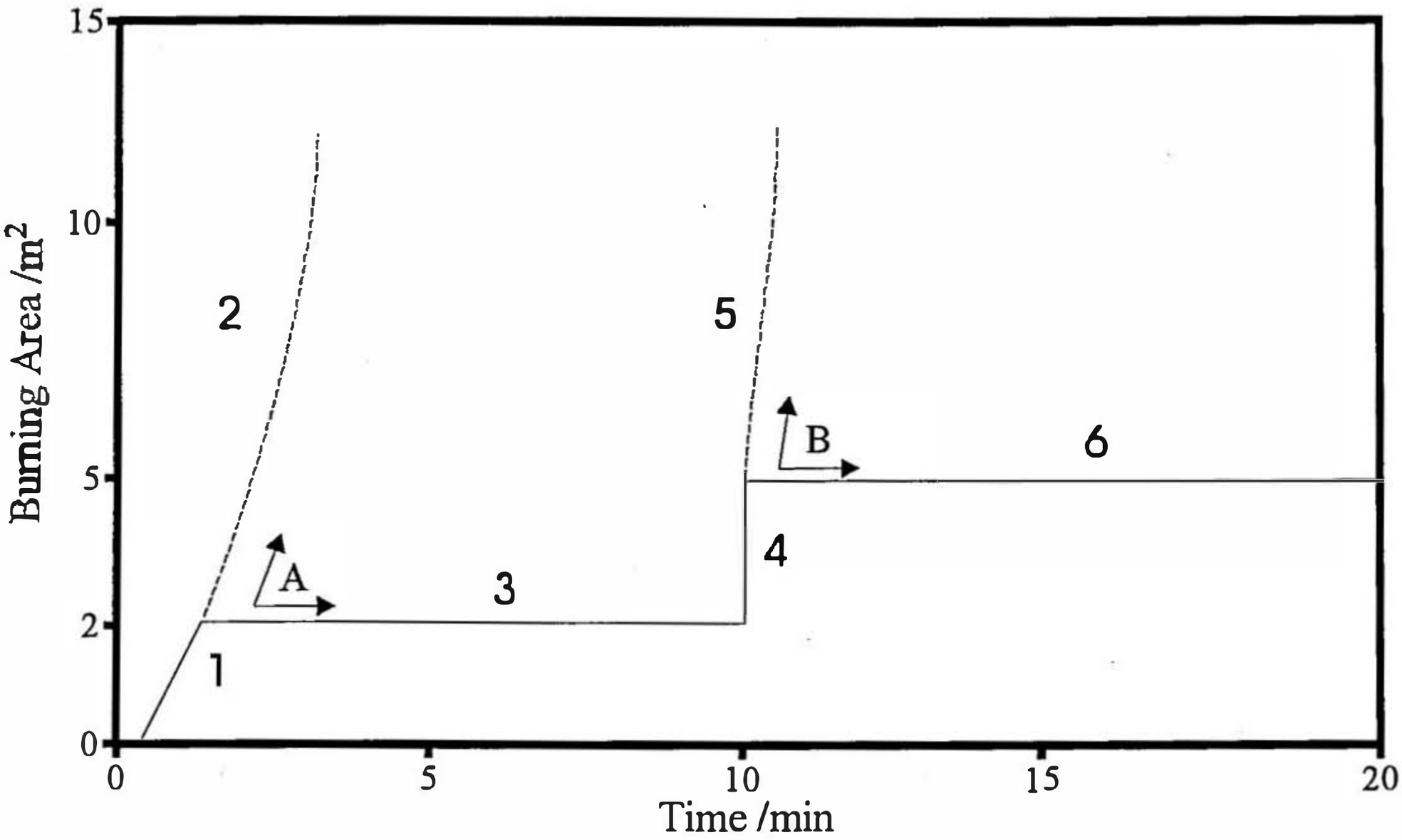

Chapter 3

Flames and the Fire Plume

3.1 Introduction

In order to be able to interpret data from fire tests, as well as being able to select appropriate tests, one must have an understanding of the different physical processes involved in a fire. This knowledge is also necessary to understand the potential exposure conditions within a fire. The heat fluxes and temperatures associated with ignition and flames are of importance for flame spread and fire development in real fires and for the testing of materials. The following sections contain a review of the relevant experimental and theoretical research published in the field.

3.2 Ignition

'Ignition may be defined as that process by which a rapid, exothermic reaction is initiated, which then propagates and causes the material involved to undergo change, producing temperatures greatly in excess of ambient.' (Drysdale, 1985). For flaming combustion, which is of interest for this thesis, gaseous fuel mixes with air, reacts with the oxygen and liberates heat. In the process, the fuel is converted to various combustion products. The fuel must always be in the form of a gas before it can undergo flaming combustion, therefore solid and liquid fuels must first be gasified before combustion can take place. This process requires heat energy to produce the vapours, and must be great enough to provide a high enough flow of volatiles to give a flammable fuel/air mixture. Once this criterion has been satisfied, ignition can occur provided that; there is either a source of pilot ignition or the rate of heat transfer to the material from the heat source is sufficient to provide vapours whose temperature is high enough for them to react spontaneously as they mix with air. The first of these processes in known as piloted ignition, the second is autoignition. If a material is exposed to a flame, as in a fire, the flame acts as both the source of heat energy and the ignition source. If the surface is heated by radiation only, for example from an electric heater, the volatiles require either a separate ignition source for piloted ignition or high enough heat transfer for

autoignition. In the majority of fires, and almost all of those involving solid materials rather than gaseous fuel, ignition occurs via piloted ignition, and it is this process that most ignition tests investigate. Figure (3.1) demonstrates the scenario for piloted ignition.

3.2.1 Sources of Energy and Ignition

In fire testing of solid materials, the source of ignition may also be the heat energy source, as mentioned above, or it may simply be a spark or small pilot flame. In the second case, the heat energy necessary to provide the flow of volatiles must be provided independently, often an electric heater. This type of system has the advantage of easy control of both heat and ignition source. Where the heat and ignition source are provided together, the selection of this source is extremely important. It should subject the sample to a severe, yet realistic, level of exposure. In many of the fire tests described in Chapter 2, the heat source is a radiant heater and ignition is effected by a pilot flame or spark, for example the Cone Calorimeter (ISO, 1990). In other tests, the source of heat energy gives radiative and convective heat transfer to the surface in the form of a flame, which also acts as the ignition source. The flame for this type may come from combustion of solid fuels, for example a wood crib (BSI, 1985), or from a gas burner (e.g. ISO, 1986).

The intensity of the gaseous ignition sources can be reasonably easily controlled, compared with using a solid flaming ignition source. In the BS 5852 ignitability test for upholstered materials (BSI, 1982), the ignition sources used to test the materials consist of various sizes of wooden crib. Whilst these solid ignition sources may be more representative of the majority of 'real' sources of ignition, mean coefficients of variance of above 17% for the maximum heat flux below these cribs have been recorded (Paul and Christian, 1987). This variation leads to potential unreliability of ignition tests using these sources, especially for materials of marginal ignitability. It is therefore theoretically and practically better to employ gas flames, electrical heaters and the like as these are more reproducible. However, these too have problems associated with their use; the difficulty of equating different types of standard source with each other and with real fire sources. Some research has also indicated that ignition is influenced not only by the level of radiation but also by spectral characteristics of that radiation (Hallman *et al.*, 1972; Drysdale and Thomson, 1990).

The use of these reproducible sources, despite concerns about spectral emissivity, remains the most satisfactory approach. There is still the question of what level of intensity is produced by the selected ignition source, and whether this is appropriate. The incorrect choice of ignition source for a fire test can produce anomalous and inconsistent hazard ratings and, for large scale tests, may have an effect on the validation of laboratory scale test methods. For full scale room tests, the ignition source must be representative of 'real' potential ignition sources. For example, the maximum rate of heat release from T.V.s, chairs, and curtains has been found to be of the order of 100 kW to 200 kW (Ahonen *et al.*, 1984). Tests performed using this order of magnitude for propane burners in room fire tests found that it was not simply the ignition power that influenced fire development, but that the burner geometry was significant (Ahonen *et al.*, 1987). Altering the size of the burner varied the relation between radiation and convective heat transfer from the flame to the sample material, large burners with thicker flames giving a higher proportion of radiation. This caused the sample to ignite at different times and in different places on a vertical wall. The burner geometry will influence the heat flux distribution at the wall, changing the material's response to a given burner heat release rate.

The exposure conditions at a vertical wall were found not only to be dependent on ignition source size and intensity, but also on the position of the source with relation to the wall (Williamson *et al.*, 1991). Increasing the distance of the burner from the wall reduced the heat flux measured at the surface of the wall. Three burner 'stand-off distances', 0, 5, and 10 cm, were investigated for various burner heat release rates with the three distances giving quite different flame exposures at the wall. The burner against the wall gave the most severe conditions, with the heat flux being virtually uniform from the bottom to the top of the wall. Heat fluxes of up to 60 kWm^{-2} were imposed for the entire height of the walls in a corner. This is approximately double the values recorded for wall flames and line burners (Quintiere *et al.*, 1986). Moving the burner away from the wall probably allowed entrainment of cool air between the flame and the wall at the lower portion of the wall, giving convective cooling and only periodic flame attachment. This gave lower heat fluxes at the wall.

These differences in heat flux intensity at a sample surface are significant. The material behaviour depends upon the imposed heat flux, with ignition times varying approximately inversely with the square of the incident heat flux (Quintiere *et al.*,

1986). This underlines the importance of understanding the exposure conditions and physical processes in a fire test and in real fire scenarios. Knowledge of potential conditions for different fire scenarios, configurations, etc. is essential before fire tests can be confidently used for predictive purposes. Furthermore, a fundamental understanding of basic flame behaviour is necessary. For the case of warehouse fires, understanding of the behaviour of flames at walls and in confined spaces is required.

3.3 The Fire Plume

McCaffrey (1979) showed that the fire plume above a free-standing 300 mm square burner consisted of three distinct regions, namely

1. the near field, above the surface of the burner, where there is persistent flame and an accelerating flow of burning gases. This is known as the flame zone.
2. a region in which there is intermittent flaming and a near constant flow velocity, known as the intermittent zone
3. the buoyant plume which is characterised by decreasing velocity and temperature with height

As conditions within these three regions are very different, the equations developed to describe the physical behaviour, such as rate of change of temperature and velocity with height, are not the same. The concepts and equations developed by various researchers are described below, both for the axisymmetric plume and for line plumes.

3.3.1 The Axisymmetric Plume

This is the plume issuing from square and circular heat sources.

3.3.1.1 The Buoyant Plume

In this region, a buoyant gas stream rises up from a source of heat into air unaffected by the fire. The rising gases are normally turbulent unless the fire is very small. Along the centreline of the plume, the temperature and gas velocity decrease with height. The driving force within the plume is buoyancy caused by density

differences between the hot combustion gases and the cooler ambient air, and is given by the product $g(\rho_\infty-\rho)$. Viscous drag within the fluid provides the resisting force, and the ratio of these opposing forces is given by the Grashof number. The plume is cooled by the entrainment of ambient air and becomes broader and the flow velocity decreases with height. The temperature of the plume is dependent on the height and the strength of the fire source.

These properties were used in the derivation of equations to describe the plume temperatures and velocities. The first plume theories assumed (Morton *et al.*, 1956); a point source of buoyancy, for example a point fire source; that the air entrainment velocity at the edge of the plume was proportional to the local vertical plume velocity; that the profiles of vertical velocity and buoyancy force in the horizontal sections are of a similar form at all heights and that variations of density within the field of motion are negligible compared to the ambient density.

These assumptions, along with the further one that the profiles are uniform, allowed the conservation equations for continuity, momentum and buoyancy to be written (Morton *et al.*, 1956)

momentum:

$$\frac{d}{dz}(u_0^2 b^2) = b^2 g \frac{(\rho_\infty - \rho_0)}{\rho_\infty} \qquad (3.1)$$

continuity:

$$\frac{d}{dz}(u_0 b^2) = 2\, u_0 \alpha\, b \qquad (3.2)$$

buoyancy:

$$\frac{d}{dz}\left(b^2 u_0 g \left(\frac{\rho_\infty - \rho_0}{\rho_\infty} \right) \right) = 0 \qquad (3.3)$$

z is the distance above the point source of the plume; b is the radius of the plume; u_0 is the vertical velocity in the plume, α is the entrainment coefficient (where entrainment velocity $v = u_0\alpha$); ρ_0 is the density in the plume, varying with height, and ρ_∞ is the density of the ambient air. Integration of equation (3.3) gives;

$$\left(b^2 u_0 g \left(\frac{\rho_\infty - \rho_0}{\rho_\infty}\right)\right) = const = \mathrm{B} \qquad (3.4)$$

B is the buoyancy flux in the plume, which remains constant at all heights. The convective heat in the plume can be related to this flux by the equation;

$$\dot{Q}_c = \rho\, u \pi b^2 c_p (T_0 - T_\infty) = u b^2 \pi c_p (\rho_\infty - \rho_0) T_\infty \qquad (3.5)$$

by use of the ideal gas law. T_0 is the plume temperature and T_∞ is the ambient temperature. B can be expressed in terms of the convective heat release rate by use of the two equations above;

$$B = g(\pi c_p T_\infty \rho_\infty)^{-1} \dot{Q}_C \qquad (3.6)$$

Solutions to equations (3.1), (3.2), and (3.4) were developed (Morton *et al.*, 1956) the important relationships being;

$$b \propto z \qquad (3.7)$$

$$u_0 \propto A^{1/3} \dot{Q}_c^{1/3} z^{-5/3} \qquad (3.8)$$

$$\Delta T_0 \propto \left(A^{2/3} T_\infty / g\right) \dot{Q}_c^{2/3} z^{-5/3} \qquad (3.9)$$

where $A = g / c_p T_\infty \rho_\infty$. These equations are the weak plume (small density deficiency) relations for point sources. In reality, a buoyant fire source will not be a point source, but will have a finite area. The correction is made for this by introducing a 'virtual origin' or 'virtual source location'. The term z for height will be replaced by $z - z_0$, where z_0 is the elevation of the virtual origin above the source. In addition, the weak plume theory must be extended (Morton *et al.*, 1956) to take into account the large density deficiencies that occur in fire plumes. To do this, it is necessary to move away from the assumption that the flow profiles are uniform, and this adds error to the numerical coefficients in the resulting equations (Heskestad, 1988).

Instead, equations have been developed using the 'strong plume theory' where large density deficiencies are taken into account. The theoretical equations for this plume

theory have been well supported by experimental measurements. Heskestad (1984) made measurements of mean excess temperature and mean velocity in the plume and found that they obeyed the following relations

$$b_{\Delta T} = 0.12(T_0/T_\infty)^{1/2}(z - z_0) \tag{3.10}$$

$$\Delta T_0 = 9.1\left[T_\infty/(g c_p^2 \rho_\infty^2)\right]^{1/3} \dot{Q}_c^{2/3}(z - z_0)^{-5/3} \tag{3.11}$$

$$u_0 = 3.4\left[g/(c_p \rho_\infty T_\infty)\right]^{1/3} \dot{Q}_c^{1/3}(z - z_0)^{-1/3} \tag{3.12}$$

$b_{\Delta T}$ is the plume radius up to the point where the temperature rise has fallen to $0.5\Delta T_0$. The set of three equations above are known as the strong plume relations and are valid only at and above the point of mean flame height, which will be discussed in the section dealing with flame height correlations.

If z_0, the elevation of the virtual origin above the source, is negative, the virtual origin lies below the fire source. The origin is often assumed to be coincident with the fuel surface, but this assumption is only satisfactory for predictions far removed from the source. The position of the virtual origin must be known in order to make accurate predictions in the vicinity of the fire source.

3.3.1.2 Virtual Source

The virtual source or origin of a fire is defined as the equivalent point source position of the finite area fire. The simplest way of determining the virtual origin of a test fire is from temperature data along the plume axis. The use of equation (3.11), giving a plot of $\Delta T_0^{-3/5}$ versus z should yield a straight line whose intercept with the z axis occurs at z_0. The problems associated with obtaining accurate data; radiation affecting temperature readings, temperature readings not being taken exactly on the plume centreline, and data averaging errors, mean that this approach is often impractical or inaccurate.

Studies of this type have been conducted by several researchers (McCaffrey, 1979; Heskestad, 1981; Kung and Stavrianidis, 1981) using pool fires and Heskestad interpreted these results using a model based on his work on flame height

correlations (Heskestad, 1983a). After some simplifications, he proposed the following relation

$$\frac{z_0}{D} = 0.083\frac{\dot{Q}^{2/5}}{D} - 1.02 \qquad (3.13)$$

Cetegen *et al.* (1984) used a different approach to the problem of identifying the virtual source position. They carried out fire experiments using circular natural gas burners in which measurements were made of air entrainment into the plume. Using entrainment theory for a point source, they developed equations to predict the virtual origin for burners whose top surfaces were either above the floor of the laboratory or mounted flush with it

$$\frac{z_0}{D} = 0.0659\frac{\dot{Q}^{2/5}}{D} + c \qquad \frac{Q^{2/5}}{D} > 16.5 \qquad (3.14)$$

$$\frac{z_0}{D} = 0.01015\left(\frac{\dot{Q}^{2/5}}{D}\right)^{5/3} + c \qquad \frac{Q^{2/5}}{D} \leq 16.5 \qquad (3.15)$$

For the burner mounted flush with the floor, c = -0.50, for non-flush mounted c = -0.80. These relations can be written in terms of a nondimensional parameter, Q^*, where

$$Q^* = \dot{Q}/(\rho_\infty c_p T_\infty g^{1/2} D^{5/2}) \qquad (3.16)$$

such that

$$\frac{z_0}{D} = 1.09Q^{*2/5} + c \qquad Q^* > 1 \qquad (3.17a)$$

$$\frac{z_0}{D} = 1.09Q^{*2/3} + c \qquad Q^* \leq 1 \qquad (3.17b)$$

c remains the same as for equations (3.14) and (3.15) (Cetegen *et al.*, 1984).

This nondimensional parameter was used in correlations in the same year (Hasemi and Tokunaga., 1984a) in work on a virtual origin based on temperature

measurements in plumes from gas burners. The following correlations were suggested;

$$\frac{z_0}{D} = 2.4\left(Q^{*2/5} - 1\right) \qquad Q^* \geq 1 \tag{3.18}$$

$$\frac{z_0}{D} = 2.4\left(Q^{*2/3} - Q^{*2/5}\right) \qquad Q^* < 1 \tag{3.19}$$

Under normal ambient conditions, the nondimensional character can be replaced and the equations written in terms of the familiar $Q^{2/5}/D$, with all units being metric.

$$\frac{z_0}{D} = 0.145\frac{\dot{Q}^{2/5}}{D} - 2.4 \qquad \frac{Q^{2/5}}{D} \geq 16.5 \tag{3.20}$$

$$\frac{z_0}{D} = 0.0224\left(\frac{\dot{Q}^{2/5}}{D}\right)^{5/3} - 0.145\frac{\dot{Q}^{2/5}}{D} \qquad \frac{Q^{2/5}}{D} < 16.5 \tag{3.21}$$

These various correlations have been plotted and compared to one another (Heskestad, 1988) and found to yield fairly similar results, despite their diverse approaches to the problem. This indicates that the researchers are close to the solution of the problem, but at present it is impossible to select the most accurate relations due to the errors arising in experimental results.

3.3.1.3 The Flame and Intermittent Zones

Flame is seen in the flame zone and the intermittent zone, as defined at the beginning of this section. In the flame zone, persistent flame is observed, whilst in the intermittent region regular oscillations occur with a frequency that is dependent on the area of the burning surface, this frequency falling with increase in area (Porscht, 1971). The oscillations are generated by instabilities at the boundary between the fire plume and the surrounding air, leading to vortex-like structures. The intermittency of the flame at a given point decreases from unity, when the flame is seen there continuously, in the lower region, close to a burner or fuel source, eventually down to zero in the buoyant plume (McCaffrey, 1979).

A desirable parameter to measure or calculate is the mean flame height, as this is important in rate of fire growth in compartments. Zukoski *et al.* (1981) defined the mean flame height as the point where the flame had an intermittency of 50 percent. They also discovered that visual observations of flame height were some 10-15 percent higher than determinations made photographically. As it is not always possible to measure flame height, several correlations have been developed based on experimental data and theory.

3.3.1.4 Flame Height Equations

The important parameters in the modelling of flame height were first derived by Thomas *et al.* (1961) by the application of dimensional analysis to the fire problem. They defined the tip of the flame as the point at which sufficient air had been entrained into the flame to give the complete combustion of the volatiles. With buoyancy as the force dominating the process, the following relationship was derived

$$\frac{l}{D} = f\left(\frac{\dot{m}^2}{\rho^2 g D^5 \beta \Delta T}\right) \tag{3.22}$$

where l is the flame height above the fuel surface, D is the diameter of the fuel bed, $\dot{m}$ and ρ are the mass flowrate and density of the fuel vapour, ΔT is the average temperature excess above ambient of the flame, g is the acceleration due to gravity and β is the expansion coefficient of air. They also obtained empirical relations based on experiments with wooden crib fires;

$$\frac{l}{D} \propto \left(\frac{\dot{Q}_c}{D^{5/2}}\right)^{0.61} \tag{3.23}$$

or
$$l \propto \frac{\dot{Q}_c^{0.61}}{D^{0.5}} \tag{3.24}$$

This equation is valid for $3 < l/D < 10$, whilst for $l/D \leq 2$, the relationship is almost linear;

$$\frac{l}{D} \propto \frac{\dot{Q}_c}{D^{5/2}} \tag{3.25}$$

For larger values of l/D, such that l/D > 6, Zukoski *et al.* (1981) plotted data from a large number of sources and found that flame height was virtually independent of fuel bed or burner diameter;

$$\frac{l}{D} \propto \left(\frac{\dot{Q}_c}{D^{5/2}}\right)^{2/5} \propto \frac{\dot{Q}_c^{2/5}}{D} \tag{3.26}$$

The most important relation to note in the above equations is that of the rate of heat release with the diameter of the fuel bed or burner. For scaling, the heat release rate must scale with $D^{5/2}$. This comes from the use of certain significant dimensionless groups in scaling. The relevant group, in this case the Froude number, is maintained constant in small scale models, at the same value as may be found in full scale conditions. The Froude number is the relevant one in this case as the viscous forces present are far less significant than the buoyancy forces that drive the flow in a flame. This type of relationship can be seen in the flame height correlations, in work on the buoyancy plume and in the relations described later for temperatures in the fire plume.

Heskestad (1983b) also used a form of this relationship in his correlation work on flame heights, developed from a large amount of experimental data

$$\frac{l}{D} = 15.6(N)^{1/5} - 1.02 \tag{3.27}$$

where D is the diameter of the fuel bed or bumer. For non-circular fuel sources, the diameter is replaced by an effective diameter such that $\pi D^2/4$ = the area of the fire source. N is a nondimensional parameter, defined as

$$N = \left[\frac{c_p T_\infty}{g\rho_\infty^2 (\Delta H_c/r)^3}\right]\frac{\dot{Q}^2}{D^5} \tag{3.28}$$

ΔH_c is the heat of combustion, r is the stoichiometric ratio of air to volatiles by mass, $\dot{Q}$ is the total heat release rate (kW) as given by

$$\dot{Q} = \dot{m}_f \Delta H_c \tag{3.29}$$

where $\dot{m}_f$ is the mass burning rate. All other symbols are as defined for all previous equations. As $\Delta H_c/r$ is within the range of 2900 to 3200 kJ/kg for many liquid and gaseous fuels, an average of 3000 kJ/kg can be taken and, under normal ambient conditions, equation (3.27) can be rewritten as

$$l = 0.235\dot{Q}^{2/5} - 1.02D \qquad (3.30)$$

3.3.1.5 Temperature and Velocity Correlations

The three regions within the total fire plume, as defined at the beginning of this section, were identified by McCaffrey (1979) following his experiments with methane burning on a 0.3 m porous burner. Measurements of gas velocities and average temperatures on the centreline above the burner demonstrated the three different regimes clearly. Each region of the plume gave different correlations for temperature and velocity, although all retain the $z/\dot{Q}^{2/5}$ parameter;

centreline velocity:
$$\frac{u_0}{\dot{Q}^{1/5}} = k\left(\frac{z}{\dot{Q}^{2/5}}\right)^{\eta} \qquad (3.31)$$

centreline temperature
$$\frac{2g\Delta T_0}{T_0} = \left(\frac{k}{C}\right)^2\left(\frac{z}{\dot{Q}^{2/5}}\right)^{2\eta-1} \qquad (3.32)$$

where the following conditions apply:

Table (3.1) - values of coefficients for equations (3.31) and (3.32)

	buoyant plume	intermittent zone	flame zone
k	1.1 $m^{4/3}/kW^{1/3}.s$	1.9 $m/kW^{1/5}.s$	6.8 $m^{1/2}/s$
η	-1/3	0	1/2
$z/\dot{Q}^{2/5}$ / $m/kW^{2/5}$	> 0.2	0.08 - 0.2	< 0.08
C	0.9	0.9	0.9

The different regions of the fire plume can be easily seen on a plot of ΔT versus $z/\dot{Q}^{2/5}$, with each portion of the plume showing a different gradient on this graph.

3.3.2 The Line Plume

The majority of work has concentrated on the axisymmetric plume, as described previously. There is, however, one major piece of work (Lee and Emmons, 1961) on the line plume which develops the equations in the plume in the same way as the axisymmetric plume was treated earlier (Morton *et al.*, 1956).

Both a theoretical and experimental approach were used, with measurements made of temperature above the flames. Both approaches were aimed at the buoyant plume, with no consideration being given to flame heights or temperatures. For the theoretical model, the fire is replaced by a horizontal source of heat, momentum and energy, of infinite length and finite width. Local density differences were assumed small in comparison with the ambient density, the assumption made to develop the weak plume equations for the axisymmetric plume (Morton *et al.*, 1956). The other assumptions were; transverse accelerations were small in comparison with vertical accelerations and that turbulent mixing in the vertical direction was small compared with that in the horizontal direction (these two assumptions mean that pressure essentially has no horizontal variation), flow is considered symmetrical in the y-direction (in the horizontal plane, normal to the wall), and entrainment is proportional to the vertical velocity, as for the axisymmetric plume (Morton *et al.*, 1956). The entrainment coefficient, α, is therefore defined the same.

The assumptions allowed theoretical development of the equation governing continuity, vertical momentum and buoyancy.

vertical momentum:

$$\frac{d}{dz}\left(u_0^2 b\right) = 2^{1/2}\lambda g b \frac{(\rho_\infty - \rho_0)}{\rho_\infty} \tag{3.33}$$

continuity:

$$\frac{d}{dz}\left(u_0 b\right) = \frac{2}{\pi^{1/2}}\alpha u_0 \tag{3.34}$$

buoyancy:

$$\frac{d}{dz}\left(u_0 b g(\rho_\infty - \rho_0)\right) = 0 \tag{3.35}$$

λ is a universal constant associated with length scale, all other variables are as defined for the axisymmetric plume equations.

Various transformations are used by the authors and three different sets of equations developed for different modified Froude numbers. The Froude number, modified by factors to account for; the Gaussian distribution of the plume, the difference between velocity and buoyancy profiles, and the actual effective density difference is given by:

$$F = \left(\frac{2}{\pi}\right)^{1/4} \left(\frac{\alpha}{\gamma} \frac{\rho_0}{\rho_\infty - \rho_0}\right)^{1/2} \frac{u}{(gb)^{1/2}} \tag{3.36}$$

The equations at F=1 are those for a line plume and maintain the vertical velocity constant, at F<1 they are for a restrained source where the plume velocity is relatively too small, and F>1 they are for a plume velocity which is too high, such as in a heated jet. The two latter cases are outwith the field of this review. It is of interest however to note that for F<1 the plume grows slowly or even contracts to raise the local Froude number, whilst for F>1 the plume grows more rapidly, decreasing the velocity. Both cases approach the case of F=1 as height increases.

For the case of F=1, solutions to the equations were found, with the important relationships being;

$$b \propto z \tag{3.37}$$

$$u_0 \propto \dot{Q}_c^{1/3} \tag{3.38}$$

$$\frac{\rho_0 - \rho\infty}{\rho_0} \propto z^{-1} \dot{Q}_c^{2/3} \tag{3.39}$$

The velocity for this case is therefore constant, the plume width increases with height and the buoyancy is inversely proportional to height. Also, for a finite width line source, the whole convection column can be regarded as arising from a line source situated at a distance $z_0 = \pi^{1/2} b_0 / 2\alpha$ below the real source (Lee and Emmons, 1961).

The experimental data were found to fit the predictions well, with data from a non-luminous flame lying in the region of $F<1$, while plumes from acetone flames were in the lower region for low burning rates and in the region of $F>1$ for higher burning rates.

3.4 Flames at Walls

The behaviour of flames against a wall and in corners has been investigated by several researchers in an attempt to increase understanding both of the science of flames and the more practical problems of ignition and flame spread. Ahmed and Faeth (1974) presented the first significant paper addressing this topic. Turbulent natural convection fires at the base of vertical walls, with the burning surface simulated by wicks soaked in liquid fuel, were investigated and measurements made of radiative and convective heat fluxes to the wall from the plume above the pyrolysis zone. Results were found to agree well with solutions of boundary layer equations and integral equations for a turbulent compressible boundary layer, assuming a one-step reaction;

$$\nu'_{F(fuel)} + \nu'_{o(oxygen)} \rightarrow \nu''_{p(products)} \qquad (3.40)$$

Measurements showed that the gas temperatures were highest in the pyrolysis zone, decreasing in both combusting and non combusting portions of the plume. An unconfined line plume exhibits a nearly constant maximum temperature until combustion is complete (at the mean flame height), but the fire plume against the wall is not adiabatic and so demonstrates the decreasing temperature even within the combusting region.

Measurements of flame height under different conditions show that laminar wall flames are 2-3 times longer than turbulent wall flames, when the flame length is normalised by the length of the pyrolysis zone. The model developed (Ahmed and Faeth, 1974) for burning rate appears to be fortuitously good as the radiation from the flame to the burning surface was not taken into account; although this varies from 0-86 % of the total surface heat flux, with laminar flames giving the lowest radiative fluxes and fully turbulent flames giving high radiation. No real

explanation can be provided for this, although overestimates of convection were thought to have an influence.

It is generally assumed that flame height and therefore plume temperature at a specific height would be higher for a flame against a wall than in the unconfined case, due to the decrease of entrainment of air into the flame, but it is necessary to be able to quantify these increases. A simple and practical approach to the problem of calculating these parameters for a fire source against a wall or in a corner is to assume an imaginary fire source, of the same intensity as the real one, on the opposite side of the wall. Calculations are performed using the relationships presented above for the real and imaginary sources together, assuming an unconfined source. The values obtained are for a fire source twice as large as the one at the wall and four times as large as the one in a corner and so must be scaled down. This method has the advantage of simplicity but does not take into account any wall heat losses, friction or wall effects on turbulence.

The above approach was compared with correlations modified from those developed for unconfined plumes (Hasemi and Tokunaga, 1984b). Measurements of temperature and flame height were made to modify the previous equations (Hasemi and Tokunaga, 1984a) for confined conditions. Table (3.2) compares the flame height correlations for the imaginary source method with those developed by various researchers in this field. Correlations are presented for both line and square burners, in unconfined space, against a wall and in a corner.

Table (3.2) - flame height correlations

Author	burner geometry	burner position	equation	conditions
Hasemi and Tokunaga, (1984b)	square	unconfined	$\frac{l}{D} = \gamma Q^{*n}$	n=2/3, $Q^* < 1$ n=2/5, $Q^* > 1$ $\gamma = 3.5$ flame tips $\gamma = 1.8$ continuous flame
Hasemi and Tokunaga, (1984a)	square	wall	$\frac{l}{D} = \gamma Q^{*2/5}$	$\gamma = 3.5$ flame tips $\gamma = 2.2$ continuous flame
Hasemi and Tokunaga, (1984a)	square	corner	$\frac{l}{D} = \gamma Q^{*2/3}$	$\gamma = 4.3$ flame tips $\gamma = 3.0$ continuous flame
imaginary method	square	wall	$\frac{l}{D} = \gamma Q^{*n}$	$Q^* > 2^{1/4}$, $\gamma = 4.6$, n=2/5 $Q^* < 2^{1/4}$, $\gamma = 4.4$, n=2/3
imaginary method	square	corner	$\frac{l}{D} = \gamma Q^{*n}$	$Q^* \geq \sqrt{2}$, $\gamma = 6.5$, n=2/5 $Q^* < \sqrt{2}$, $\gamma = 5.6$, n=2/3
Hasemi (1984)	line	unconfined	$\frac{l}{D} = \gamma Q_l^{*n}$	$n \rightarrow 2/3$ as $Q_l^* \rightarrow \infty$
Hasemi (1984)	line	wall	$\frac{l}{D} = \gamma Q_l^{*n}$	n=2/3, $Q_l^* > 1$ n=0.8, $Q_l^* < 1$ $\gamma = 6.0$ flame tips $\gamma = 2.8$ continuous flame
Sugawa *et al.* (1991)	line	unconfined	$\frac{l}{D} = 4.2 Q_{rec}^{*2/3}$	$0.2 < Q_{rec}^* < 50$ flame tip
Sugawa *et al.* (1991)	square / circular and line	unconfined	$\frac{l}{D} = k_m^{2/(2n+3)} Q_{rec}^{*2/(2n+3)}$	line: n=0, k_m=8.6 square/circular: n=1, k_m=28
Sugawa *et al.* (1991)	line	wall	$\frac{l}{D} = 6.3 Q_{rec}^{*2/3}$	$0.2 < Q_{rec}^* < 50$ flame tip
Quintiere and Cleary, (1994)	line	wall	$\frac{l}{w} = 6.81 Q^{*2/3}$	where $Q^* = \dot{Q} / (\rho_\infty c_p T_\infty g^{1/2} w^{5/2})$

where $Q^*_l = \dot{Q}_l / (\rho_\infty c_p T_\infty g^{1/2} D^{3/2})$ and $Q^*_{rec} = \dot{Q} / \rho_\infty C_p T_\infty g^{1/2} wD$. k_m is an apparent mixing factor in the flame up to the tip, w is the length of a burner, i.e. the longest

side, *l* is the flame height and D is the shorter side of a rectangular burner for the correlations that use both *w* and D.

For a square burner at a wall, the flame height is approximately proportional to $Q^{*2/5}D$ (Hasemi and Tokunaga, 1984a), and from the definition of Q^*, this implies that the height of the flame against a wall should be a function of heat release rate and independent of fuel size. In this case the height at the tip of the flame coincides with that in the unconfined case for $Q^* > 1$. Comparison of these equations with the imaginary source method shows that the imaginary source method gives errors up to 30% for $Q^* > 2^{1/4}$ at the wall and $Q^* < \sqrt{2}$ in a corner. Sugawa's correlations (Sugawa *et al.*, 1991) for an unconfined line burner give slightly higher results than Hasemi (Hasemi and Tokunaga, 1984a, 1984b). The expression for a line source against a wall was, however, very close to that developed by Hasemi (1984) for the flame tip. The approach used by Sugawa (Sugawa *et al.*, 1991) was to model the presence of a wall by considering its effect on air entrainment into the flame. Their experiments demonstrated that flame geometry, for both single and multiple flames depended very strongly on entrainment into the flame, but little on configuration of the fuel bed.

3.4.1 Flame Temperature

One of the above papers (Hasemi and Tokunaga, 1984b) also included research on flame temperatures for confined flames, both at a wall and in a corner. This included the significant finding that the development of the temperature profile in the direction normal to the wall is not very pronounced, whilst the parallel profile is almost the same as for the unconfined case. This means the decrease in excess temperature with height is reduced, with the maximum excess temperature at each height being approximately proportional to the inverse of the height above the fuel surface. The growth of the plume in the direction normal to the wall is less than in the parallel direction and an elliptical pattern arises. This means, for the use of the concept of virtual heat source, the horizontal distance of T/T_m should develop in the shape of a half ellipse, with the long axis coincident with the wall. The results are given in table (3.3).

Table (3.3) - temperature correlations

burner position	z_o	T_m	z'
wall	$z_0 = (2.5 - 0.7Q^*)Q^{*2/5}D$	$4600/z'^{5/3}$	>3
corner	$z_0 = (3.6Q^{*2/5} - 3.3Q^{*2/3})D$	880	<2.5
corner	$z_0 = (3.6Q^{*2/5} - 3.3Q^{*2/3})D$	$2200/z'$	$2.5 \leq z' \leq 3.6$
corner	$z_0 = (3.6Q^{*2/5} - 3.3Q^{*2/3})D$	$5100/z'^{5/3}$	$3.6 \leq z'$

where $z' = (z + z_0) / Q^{*2/5} D$

Higher temperatures have been measured, at set heights, in the plume for flames against walls and in corners than for unconfined fire sources as has been shown in the above work and the imaginary source method underestimates this. The correlation for a flame against a wall is similar to one developed later for experimental data on square propane burners against vertical walls (Back *et al.*, 1991).

3.4.2 Wall Heat Flux

To analyse the wall heat flux data, Hasemi (1984) plotted the measured wall flux at a thermally thin wall versus $x/Q_l^{*2/3}D$, and found four distinct regions;

1. $x/Q_l^{*2/3}D < 1$

   this corresponds to the lower part of the solid flame, $\dot{q}''_w$ increases with height

2. $1 \leq x/Q_l^{*2/3}D < 2.8$

   this applies in the upper part of the solid flame. $\dot{q}''_w$ remains approximately constant with height and appears to be a weakly increasing function of Q_l^*. The flame thickness is almost constant with height.

3. $2.8 \leq x/Q_l^{*2/3}D < 10$

   this is the transition region, characterised by the intermittency of the flame. The slope is steepest here, with all the data points falling onto

$$\dot{q}''_w \approx 45\left(x / Q_l^{*2/3} D\right)^{-5/2} \qquad (3.41a)$$

4. $x/Q_l^{*2/3}D \geq 10$

this is the buoyant plume, above the flame. The heat flux here can be represented by

$$\dot{q}''_w \approx 2.5\left(x / Q_l^{*2/3} D\right)^{-1.3} \qquad (3.41b)$$

this is a less certain relation than the one above as fewer data were collected within this region, but it appears to be satisfactory.

The increase of $\dot{q}''_w$ with height adjacent to the lowest section of the flame is consistent with the idea of a cool recirculation region just above the fuel surface which has been seen in investigations of flame temperature and gas species (Bouhafid *et al.*, 1988). This was also observed in the heat flux measurements made by Back (Back *et al.*, 1991) for flames from square propane burners where the maximum heat fluxes occurred 30 cm above the fuel surface for their larger fires. For the majority of their test fires, they observed three regions within the flame;

1. $z/l \leq 0.4$,

this is the lower part of the flame, the centreline heat flux is given by

$$\dot{q}''_{cl} = \dot{q}''_p \quad \text{where } \dot{q}''_{cl} \text{ is the centreline heat flux}, \ \dot{q}''_p \text{ is the peak total incident heat flux} \qquad (3.42a)$$

2. $0.4 \leq z/l \leq 1.0$

this is the intermittent section of the flame where the incident heat flux decreases linearly to 20 kW/m^2

$$\dot{q}''_{cl} = \dot{q}''_p - \frac{5}{3}\left(\frac{z}{l} - \frac{2}{5}\right)\left(\dot{q}''_p - 20\right) \qquad (3.42b)$$

3. $z/l \geq 1.0$

this is the region above the flame height where the heat flux at the wall decays according to the 5/3 power of height above the flame

$$\dot{q}''_{cl} = 20\left(\frac{z}{l}\right)^{-5/3} \qquad (3.42c)$$

Measurements were also made of the wall heat fluxes laterally away from the centreline. The correlations obtained were for two different flame regions; above and below the average flame height.

1. $y/(0.5\mathrm{D}) < 1.0$

$$\dot{q}'' = \dot{q}''_{cl} \exp\left(-\left(\frac{y}{0.5\mathrm{D}}\right)^2\right) \qquad (3.43a)$$

2. $y/(0.5\mathrm{D}) > 1.0$

$$\dot{q}'' = 0.38\dot{q}''_{cl}\left(\frac{y}{0.5\mathrm{D}}\right)^{-1.7} \qquad (3.43b)$$

It was found that the radiative heat fluxes beyond the edge of the source in many cases were sufficient to allow lateral flame spread on the wall. This is not the case for line or wall flames and approaches based on these are not expected to be able to predict flame spread on walls exposed to adjacent item flames.

However, one of the aims of formulating this type of correlation has been to use them in the prediction of flame spread. Flame spread rate calculations can be performed using the assumption that ignition and flame spread occur as a result of the inert heating of a solid material to an ignition temperature. The study of flames against walls continued in this way (Hasemi, 1985), with equations developed for flame spread velocity;

semi-infinite thick combustible wall

$$\mathrm{V_p} = \left\{\int_0^{\infty} \dot{q}''_w\left(\xi + \mathrm{L_p}\right)/\sqrt{\xi d\xi}\right\}^2 \Big/ \pi k\rho \mathrm{c_p}\left(\mathrm{T_{ig}} - \mathrm{T_\infty}\right)^2 \qquad (3.44a)$$

thermally thin wall (insulated) with Newtonian cooling

$$V_p = \frac{1}{\rho c_p d\left(T_{ig} - T_\infty\right)} \int_0^\infty \dot{q}''_w\left(\xi + L_p\right) d\xi \qquad (3.44b)$$

The parameters ρ, c_p, k and T_{ig} are material properties which are determined by thermometric measurements. ξ is the height above the pyrolysis front and L_p is the pyrolysis length. The integrals in these equations can be estimated by formulating the distribution of $\dot{q}''_w$ as a function of height above the pyrolysis front.

To contribute further to the understanding of flame spread, an equation was formulated for the relationship between flame height and incident heat flux at a vaporising surface;

$$\begin{aligned} l &= \gamma \left(\Delta H_c \int_0^{L_p} \dot{m}''_v dx \,/\, \rho_\infty c_p T_\infty \sqrt{g\, L_p^3} \right)^n L_p \\ &= \gamma \left(\Delta H_c \int_0^{L_p} \left(\dot{q}''_w - \dot{q}''_{rr}\right) dx \,/\, \Delta H_G \rho_\infty c_p T_\infty \sqrt{g\, L_p^3} \right)^n L_p \end{aligned} \qquad (3.45)$$

where γ = const., value depends on definition of flame height.

Comparison of this correlation with experimental data from other researchers (Orloff *et al.*; 1974, Kishitani, 1984) showed that, although the estimation slightly under-predicted the flame height, it was consistent and reasonably close to the experimental data.

Recently data were taken from several of the above sources for line fires against walls, square burner flames against walls and in corners, and window flames impinging on a wall (Quintiere and Cleary, 1994). The correlations for flame heat flux were investigated in terms of configuration and fuel properties. In the theoretical work, the authors began with the simple heat flux statement;

$$\dot{q}'' = \dot{q}''_c + \dot{q}''_r \qquad (3.46)$$

where

$$\dot{q}''_c = h(T_f - T_\infty) \tag{3.47}$$

and

$$\dot{q}''_r = \sigma T_f^4 \left(1 - e^{-\kappa L_m}\right) \tag{3.48}$$

using a mean beam length approximation L_m.
Equation (3.46) is made dimensionless;

$$\frac{\dot{q}''}{\sigma T_f^4} = \frac{h}{\sigma T_f^3}\left(1 - \frac{T_\infty}{T_f}\right) + \left(1 - e^{-\kappa L_m}\right) \tag{3.49}$$

h, the heat transfer coefficient, is a function of position and the fluid properties in general, whilst L_m is a function of the geometry of the flame. For flames against surfaces, the mean beam length will depend on the nature of the fire.

For a wall flame or flame from a line burner, $L_m \leq 2\delta$, where δ is the boundary layer thickness, based on an optically thin infinite slab approximation. For burner flames against walls;

$\frac{L_m}{D} = \text{function}\left(\frac{l}{D}\right)$, where D is the dimension of a side and l is the flame height.

The centreline temperature in general correlates as a universal function of $x/Q^{*2/5}D$, where Q^* is defined as in equation (3.16). Temperatures and heat fluxes from flames should roughly depend on flame length, so l is a suitable scale factor for x. Hence, $h/\sigma T_f^3$ and T_∞/T_f should be functions of x/l for the most part. Let $T_f = (T_f / T_\infty)T_\infty$, and rewrite equation (3.49) as

$$\frac{\dot{q}''}{\sigma T_\infty^4} = \left(\frac{T_f}{T_\infty}\right)^4 \left[\frac{h}{\sigma T_f^3}\left(1 - \frac{T_\infty}{T_f}\right) + \left(1 - e^{-\kappa L_m}\right)\right] \tag{3.50}$$

Since κL_m can be represented as κD times some function of l/D, for a given flame configuration;

$$\frac{\dot{q}''}{\sigma T_\infty^4} = \frac{h}{\sigma T_f^3}\left(\frac{T_\infty}{T_f} - 1\right) + \left(1 - e^{-\kappa D_f (l/D)}\right) \tag{3.51}$$

$$\text{or } \frac{\dot{q}''}{\sigma T_\infty^4} = \text{function}\left(\frac{x}{l}, \frac{y}{l}, \frac{l}{D}, \kappa D\right)$$

D is the characteristic fire dimension with respect to radiant heat transfer to the wall. For a line fire it is related to the boundary layer thickness; for the square burner it is the side dimension; and for the window it is the equivalent diameter.

Analysis of the data for the line fire gives

$$l = 0.0667\left(\frac{\dot{Q}}{w}\right)^{2/3} \tag{3.52}$$

where w is the length of the burner and $\dot{Q}$ is the rate of heat release. To make the equation dimensionless;

$$\frac{l}{w} = \frac{0.0667}{w}\left(\frac{\dot{Q}}{w}\right)^{2/3} \tag{3.53}$$

$$= 0.0667\left(\frac{\dot{Q}}{w^{5/2}} \frac{\rho_\infty C_p \sqrt{g T_\infty}}{\rho_\infty C_p \sqrt{g T_\infty}}\right)^{2/3}$$

specifying $\rho_\infty = 1.1$ kg/m^3, $C_p = 1.0$ kJ/kgK, g = 9.81 m/s^2 and $T_\infty = 298$ K,

$$\frac{l}{w} = 6.81 Q^{*2/3} \tag{3.54}$$

as given in table (3.2), where Q^* is defined in terms of w rather than D (see equation (3.16)).

For a square burner against a wall, the authors used a previous correlation (Hasemi and Tokunaga, 1984a) for continuous flame height, table (3.2) to calculate the flame height for a set of data that did not include measurements of flame height. These were then used to plot heat flux against x/l. Different curves appear for different l/D

or κD, where κ was taken as 13.3 m^{-1} for propane flames. As κD increased, $\dot{q}''$ increases. For flames in a corner, the flame heights were again calculated using correlations for a continuous flame (Hasemi and Tokunaga, 1984a), table (3.2). The data showed, since D was fixed in this case, that changes in *l*/D must be due to changes in supply rate of propane. Also as the corner flame heat flux became more uniform as *l*/D increased, it appears that, if radiation is the principle component, the flame is becoming thicker over its length as *l*/D increases.

Heat flux was seen to increase as y/D approached zero, i.e., close to the corner. This is apparently due to reradiation from the wall surfaces. Also, there appears an implied family of curves increasing in heat flux as *x*/*l* decreases, i.e., closer to the base of the flame or for larger flames. Again, for a fixed *l*/D, an increase in κD, where κ is the flame absorption coefficient, causes an increase in heat flux, as would be expected from considerations of flame radiation. The case for the window flames is outside the scope of this review.

Overall, this work shows that the heat flux distribution can be reasonably scaled with flame length and that the heat flux distribution is similar with distance from the source normalised with the flame length.

3.4.3 Combustible Walls

The previous work was based on tests for burners against incombustible walls, but to accurately predict flame spread velocities and flame heights for flames spreading over combustible materials, experiments had to be carried out to investigate whether these correlations could be applied to 'real' fire situations. Quintiere *et al.* (1986) performed experiments on six combustible materials in the same way as Hasemi (1984) and compared their data to that for the incombustible walls. Flame height was found, as in Hasemi's work to be proportional to $Q^{*2/3}$, although the data for the materials is more scattered, as would be expected. Measurements made of wall heat flux showed an apparent universal distribution when plotted against height/flame height, although the authors expressed concern that this could be changed by changes in energy release rate and radiation effects. Data from the burning materials showed the relationship $\dot{q}''_w \propto x^{-p}$, where p ~ 2.4 and *x* is height, which is consistent with the findings of Ahmed and Faeth (1974).

3.5 Parallel Surfaces

A study in 1961 on spray combustion (Toong, 1961) addressed the question of interaction between two parallel fuel plates, which provided droplets for burning in an oxidising stream. The researcher found that decreasing the separation between these plates increased the evaporation or sublimation rate at the fuel surface while, at the same time, decreasing the combustion rate at the flame front. The flame length of a burning fuel droplet was predicted to increase as other droplets were brought closer, as was burning rate, provided the flames remained separate. This was due to changes in the air flow and entrainment. Although the results were never aimed at solving fire problems, they showed the importance of air flow patterns and interference from a parallel surface on flame, and therefore fire, behaviour.

Apart from studies like the one above, it had also been frequently observed outside the research laboratory that free burning between two solid fuel surfaces is more intense than the burning of a single surface, in many cases materials in parallel burning fiercely when a single surface could not sustain combustion. The classic example of this is a log fire; a single log will not burn on its own unless preheated. This principle has also been used in the fire testing of materials, in the Brandschacht test (DIN, 1978) to give the most severe test conditions. This behaviour had been attributed on various occasions to two different possible causes;

1. the containment of radiation being emitted by flames or hot surfaces within the channel between the surfaces, known as cross-radiation, and
2. a fluid dynamic 'chimney effect' involving the confinement of hot combustion products.

In 1974, research was published from work in the US (Kim *et al.*, 1974) on this problem of vertical parallel fuel surfaces and the effect on fire behaviour, with the possible aim of developing materials flammability tests. The analysis ignored radiation effects.

This experimental and theoretical work found that a fuel set up under these conditions shows three burning regimes, depending on the geometrical arrangement of the channel between the two surfaces, $h/(a/2)^4$, where h is the height of the fuel surfaces and a is the separation between them. For small $h/(a/2)^4$, i.e. shorter fuel

surfaces or wider channels between the parallel surfaces, the burning is less dependent on the existence of the opposite surface and the total burning rate is proportional to $h^{3/4}$, which is the case for a single wall. If $h/(a/2)^4$ is large, i.e. if the channel between the fuels is sufficiently high and narrow, the fuel consumes the oxidant close to the bottom of the vertical fuels and the total burning rate is independent of the channel height but proportional to a^3, the cube of the separation between the surfaces. Between these two extremes lies a transition regime.

The results for this non-radiative burning theory show a reduced burning for the two surfaces as compared with a single surface. The authors conclude that radiation is probably the dominant factor in the increased burning between vertical parallel surfaces under 'real' conditions, as the non-radiative model does not predict the increased burning. The previous suggestion of a fluid dynamic 'chimney effect' cannot cause this as the fluid dynamic confinement actually causes a decrease in the steady burning rate by restricting the access of oxidant to the fire. However, as this study only considered laminar burning, whilst in most cases for real fires the burning is turbulent, and experiments were for non-radiative conditions, further work would be needed to confirm the causes of increased burning intensity between parallel surfaces.

More detailed experimental work was carried out at Factory Mutual Research (Tamanini, 1979) to address the problem of fire spread in rack storage. 'Combustible' vertical walls, created using porous walls and liquid fuel, were burned in single and parallel configurations and measurements taken of radiative and convective heat fluxes. The radiative component was found to increase with height whilst the convective decreased. Even for tests using methanol for which the flame is generally assumed to give out negligible radiation, the radiative component was important close to the top of the walls. The inclusion of the parallel wall gave up to a 40 % increase in burning rate, the maximum being at a wall spacing about equal to 20 % of the wall height. Burning rate initially increases as separation between the walls decreased from the maximum investigated (413 mm). As the separation was further decreased however, the burning rate dropped, although the exact point where this change occurred was not identified. Certainly at the lowest separations, 38 and 25 mm, the burning rates are less than at the greater ones. The data suggest that the burning rate at the smaller separation distances is controlled by convective heat transfer, whilst at the larger separations radiation becomes important.

At around the same time in Japan, investigations of burning vertical parallel surfaces were proceeding as part of research into downward flame spread (Kurosaki *et al.*, 1978). Experiments were performed on the downward spread of flame on vertical sheets of paper. The flame spread rate was found to depend on the separation distance between parallel sheets, not on the width of the paper. The burning behaviour could be separated into three distinct regimes;

1. the smallest separation ($\leq$ 3 mm) has a low flame spread rate, with no flame in the gap between the sheets. This lack of flame in the gap is attributed to the inability of oxygen from the ambient air to diffuse into the gap. This means that there is no radiative heat transfer from a flame in the gap to the inner surface of the paper. Also radiation from the opposite flame and embers is negligible as the configuration factor is small. The temperature profiles show that there is no convective heat transfer to the inner surface of the unburnt paper in the 'preheat' zone, thus the total heat transfer to the unburnt paper is due only to heat transfer from outside of the channel between the paper. This heat transfer rate is estimated to be approximately half that for a single sheet and the measured flame spread rate is seen to be approximately half that for a single sheet.
2. In the transition zone (3 mm $< a <$ 5 mm), an intermittent flame appears in the gap between the sheets. The flame spread rate here is not stable enough to allow calculation of a steady flame spread rate. This is the transition zone between the narrow and wide regions.
3. Wider gap region, ($a \geq$ 5 mm). A stable flame is seen between the sheets, merging into one large flame engulfing both sheets when 5 mm $\leq a \leq$ 10 mm. The flames were separate when $a \geq$ 10 mm. In this regime, flame spread rate is greater than for a single sheet and passes through a maximum at 10 mm $\leq a \leq$ 20 mm, then asymptotically approaches the rate for a single sheet as separation is increased.

The measurements of temperature in the wider gap region show the gradients on the temperature surface at any point to be independent of the separation distance and therefore the convective heat transfer is considered to be independent of separation distance. If this is the case, then it must be the radiative transfer from the opposite flame and embers that alters the flame spread rate, causing it to increase in this regime with decreasing separation. In all cases, the convective heat transfer appears to play the major role, with radiation supplementing this in the space between the sheets at certain separation distances and thus producing a maximum in the flame

spread curve. These findings agree with the trends seen by Tamanini (1979), for upward flame spread, and indicate that, although it appears to be increases in radiation that leads to enhanced burning, the convective component of the heat transfer is very significant. The importance of the convective component was further confirmed (Most *et al.*, 1988) in a study which showed that as the separation between two walls decreased, with either one or both burning, the dominant mode of heat transfer changed from radiative to convective as the character of the flow changed from natural to forced convection as the flow accelerated.

More recently, a research report (Ingason, 1993) detailed results from a set of experiments from apparatus which was representative of conditions in two dimensional rack storage. The racks consisted of incombustible boxes stacked with gaps between them to represent storage on shelves. Two sets of racks were set up facing each other, separated by a vertical channel. Walls were erected at each end of the boxes to create two dimensional conditions. Air could enter the system via the horizontal channels between the layers of boxes. Measurements were made of flame height, temperature and air flow.

For the smallest separation between the racks, a = 50 mm, the ratio of l/l_{free}, the flame height in a rack storage divided by the flame height for a freely burning line burner, is around 2.5-2.9. At double the separation, a = 100 mm, the ratio is around 1.9-2.3. The mass flow rate, or entrained air, at each tier is nearly doubled when the flue width is doubled. This increase in entrained air may explain the reduction in flame height when the flue width is increased.

Two distinct regions are seen on a graph of centreline temperature in the gap versus dimensionless height (z/l where z is the height and l is the mean height for the tip of the flame). Below about half the flame height, in the region of continuous flame, the temperature is nearly constant, as found by McCaffrey (1979), at around 870 ^{o}C. Above this it starts to decrease, giving the two regimes seen previously (McCaffrey, 1979), and is ~ 450 ^{o}C at the mean flame tip. The author observed that the narrower the channel, the slightly higher the flame temperature.

A plot of (z/h) versus ($\dot{m}_a$/a), where $\dot{m}_a$ is the mass flow rate in the vertical channel between the racks and h is the height of the racks, showed that the mass flow rate through each tier did not change much with large changes in heat output from the burner. It also revealed a relationship between the amount of air passing through

each tier and the vertical channel width; the mass flow rate increases linearly with the width. Variation of horizontal flue height was found to have a negligible effect on the vertical flue flow. The ratio of air entrained to stoichiometric air required for combustion = ϕ and is defined as the equivalence ratio. Under free burning conditions this has been found to be up to 10 at the flame tip (Delichatsios, 1988). When a flue width of 100 mm, the largest investigated, was used, ϕ was approximately 10, as for unconfined burning. For the smallest separation, a = 50 mm, ϕ = 6. An overall relationship for the conditions investigated was found to be approximately ϕ = 7.5 at the flame tip.

The curve fit of a plot of flame height versus $\dot{Q}_l/a$, where $\dot{Q}_l = \dot{Q}/w$, the heat release rate per metre, gave;

$$l = 6.15\text{x}10^{-4}\left(\dot{Q}_l/a\right) + 0.307 \qquad (3.55)$$

Thus, in a two dimensional system with a constant geometrical width, the height of the flame tip tends to increase linearly with heat output.

The importance of separation between two vertical parallel combustible walls has shown that the steady burning rate and heat flux to the walls increase as the separation decreases, reaching a maximum at a separation of around 15% of the wall height (Bellin, 1991). As the separation is further decreased, these values fall, probably due the inefficiency of combustion. The upward flame spread rates over the PMMA walls investigated, before steady burning was achieved, increase with decreased separation between the walls. This helps to confirm why fire development in many warehouses is rapid, showing that not only are higher heat fluxes produced but also that the upward flame spread rate is higher in these type of configurations. The results from this author follow the same trends as Tamanini (1979), but the burning rates at small separations are higher than Tamanini predicted and are lower than predicted for larger separations.

3.6 Summary

Wall heat fluxes, flame temperature distributions and flame heights are influenced by several factors. Geometry plays a significant part in the behaviour of flames, with flames at walls yielding higher flame temperatures at a given height than their

unconfined counterparts. A parallel wall has a considerable influence on the heat transfer and burning behaviour, with the separation between two surfaces being of importance. It is necessary to test materials under realistic exposure conditions in order to assess the hazard a material may present in an unwanted fire. To be able to test under appropriate conditions, and to understand potential hazards, for example for materials to be stored in high rack storage, knowledge of the possible conditions arising in these scenarios is necessary. The influence of parallel surfaces needs to be investigated further as well as the effect of reduced air entrainment on heat fluxes.

Figure (3.1) The scenario for piloted ignition

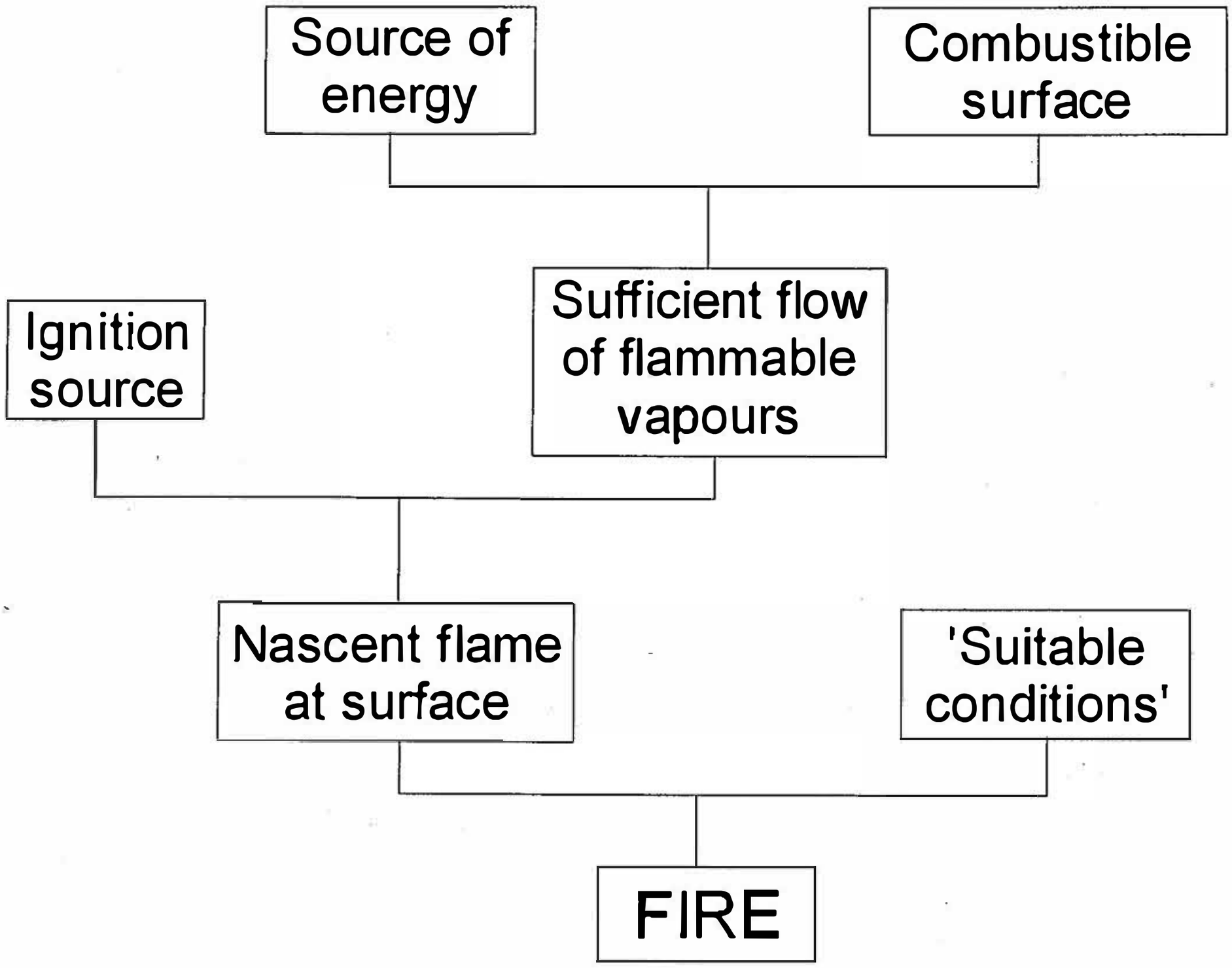

Chapter 4

Experimental

4.1 Introduction

The experimental programme was intended to investigate the hazard assessment of bulk stored materials, by achieving a number of specific, practical objectives. The first aim was to identify those storage conditions for bulk materials which may increase the fire hazard by increasing the heat fluxes occurring in the event of an unwanted fire, thereby increasing the likelihood of ignition and high flame spread rates. Another objective was to gain an increased understanding of flame behaviour at walls and in channels between parallel walls. Measurements were made of flame height, flame temperature, and total and radiative heat flux distribution across vertical, parallel, incombustible walls from flames from propane burners.

Several tests which are used within the fire community employ smoke measurement for hazard assessment of materials. The exposure conditions within these tests can be very different, as outlined in Chapter 2. The use of smoke production from materials tested in the Cone Calorimeter as a means of hazard assessment was investigated and results from the cone were compared with smoke results from the HSE medium scale room/corridor assembly, which operates under very different conditions.

Other parameters which are used for the fire hazard assessment of materials include rate of heat release, rate of temperature rise, continued flaming or smouldering etc. Three main test methods were investigated in this study; the Cone Calorimeter, the HSE medium scale room/corridor assembly and the British Standard test for furniture, BS 5852. All involve different exposure conditions and measure different parameters. One part of this experimental work involved using these tests for a set of materials and investigating how the ranking of the samples varied from test to test. Further investigation was also carried out into the HSE medium scale test. The separation between parallel samples was investigated, air flow patterns to the sample surfaces were changed and ignition source size was altered. More instrumentation

than that normally required for the standard test was included. Oxygen consumption, carbon dioxide and carbon monoxide analysers were included as well as load cells for rate of mass loss measurements.

4.2 The Parallel Wall Tests

Two vertical monolux boards, 610 mm long, 813 mm in height and 25 mm thick, were placed in parallel, figure (4.1). For some tests the 'walls' were standing on a closed kaoboard base, 40 mm thick, 600 mm long and 600 mm wide, which did not allow air flow beneath the walls, for others a 40 mm gap was left between the bottom of the walls and the laboratory bench. A propane burner between the walls provided flames at two propane flow rates, 5 and 9 litres per minute. These correspond to heat release rates of approximately 7.0 kW and 12.5 kW respectively, assuming complete combustion. The propane flow rate was adjusted manually by the use of a rotameter. Various measurements were made, although not all were made for all conditions. Measurements included total heat flux, radiative heat flux, temperature measurements using thermocouples, temperature measured using an optical pyrometer, and flame height. Different burner types and positions were investigated. Each experiment was approximately of nine minutes duration. The first five minutes of a test were performed with an extract fan on, to allow the walls to heat up to a near constant temperature. For the final four minutes the extract fan was turned off, thereby preventing forced air flows other than those naturally induced by the flame. The apparatus was located in a large laboratory, where radiation from walls was not a factor and where movement of air could be considered to be mainly influenced by the flame. In most cases, except where specified, data were recorded at a rate of 1 Hz for the final three minutes of the test, using a 'Microlink' data logger with the 'Windspeed' or 'Windmill' software. The values used in calculations and on graphs were the averages calculated over the last minute of the test, to ensure that steady state had been achieved. Data were saved to a PC and the processing done using the Microsoft Excel spreadsheet package. Some experiments were carried out more than once to check the repeatability of this experimental procedure. Some were also run over a longer period of time to ensure that the system had time to reach near stable conditions in the normal test duration. The walls were allowed to cool down between tests to ensure the same starting conditions. The general parameters which were varied included; separation distance between the walls, burner type, position and flow rate, and the presence of the base.

The specific test geometry, conditions and measurements are detailed in the following sections.

4.2.1 The Buxton Tests

In these sets of tests, the vertical, parallel walls, as described above, were set up with the base in position. The propane burner in this case was a circular glass bead bed burner with a diameter of 75 mm embedded in the kaoboard base, so that the top of the burner was level with the base of the monolux walls. The burner was located at a position which was equidistant from either end of the walls, and, in most cases, in the centre of the channel between the walls. Measurements were made of both total heat flux and temperature at various locations across and up the wall. One wall was instrumented as shown in figure (4.2) for the heat flux measurements, using Gardon type, water cooled heat flux meters, with the other wall blank. The instrumentation remained the same for the other series of tests measuring total heat flux, described in the following sections. Since only four heat flux meters were available for these experiments, heat fluxes could be measured at four positions on the wall during one test, four tests were carried out to obtain the distribution of flux across the wall. The holes not being used for heat flux meters during a test were plugged with kaowool to prevent airflow through them. The heat flux meters were wiped clean between tests with damp cotton wool to prevent the build up of soot over a series of tests.

In some cases, the ends of the walls were partially blocked to alter the air flow pattern. This was not very successful as it caused the flame to flip over, moving away from the centreline position and distorting the pattern of readings. Despite this, these tests have been included because they did give some indication of the importance of the effect of altering the air flow. In another two sets of tests, the burner was not in the centre of the channel, but was kept against one wall, whilst the other wall was moved away to alter the separation. The case of an infinite separation was considered by removing the blank wall and performing the tests with just one wall. Measurements were also made using a British Standard No. 7 wood crib (BSI, 1982) in place of the burner. This was always placed in the centre of the channel between the walls. Table (4.1) shows the test parameters used for the measurement of total heat flux in this series of tests.

Table (4.1) - the burner propane flow rate (l/min) or 'ignition' source investigated at each separation and each measurement position across the wall. All tests included measurements at four heights on the wall.

	horizontal distance from centreline/mm			
separation /mm	0	50	100	150
60	5 9	5 9	5 9	5 9
100	5 9	5 9	5 9	5 9
∞	5 9	–	–	–
80	No. 7 crib	No. 7 crib	No. 7 crib	No. 7 crib
120*	5 9	–	–	–
140*	5 9	–	–	–
100+	5 9	–	–	–
70+	5 9	–	–	–

Note: tests denoted by '* ' are with the burner beside the instrumented wall
those denoted by '+' are with the ends partially blocked; 100 mm separation is restricted to 60 mm at the end and the 70 mm separation is restricted to 27 mm at the end.

The influence of the various parameters on temperature were investigated for the Buxton tests. Thirty two thermocouples were pushed through small holes in various locations on one of the monolux walls, as shown in figure (4.3). The distance that the thermocouples were pushed through the holes varied, to alter the thermocouple tip location within the gap. Three distances were investigated; one with the tips in the centre of the separation between the walls, one with the thermocouples pushed quarter of the way into the channel and the last with the tips located 3 mm into the channel, i.e. almost flush with the wall. The separation distance between the walls was varied, as was the propane flow rate and therefore heat release rate from the burner. Tests were also carried out using a British Standard No. 7 wood crib, which

gave a minimum wall separation of 80 mm. Larger separations for this ignition source were also investigated. A collection rate of 1 Hz was used for the data acquisition, using the type of data logging system described above. Readings of temperature were taken for a period of 6 minutes, until steady state had been achieved. The values were averaged over the last 100 s of the test, as the temperatures were reasonably constant at that time. Symmetry was assumed so that temperatures measured at the same position either side of the vertical centreline could be averaged and a value quoted for temperature at a certain height and distance from the centreline, without making any distinction between left and right of the centreline. As these values of temperature were very similar before averaging, the assumptions seems justified as well as allowing simpler and clearer comparison of data and the identification of trends. Tests with the ends of the walls partially blocked were repeated. These again had the problem of the flame being pushed over, making the averaging of the temperature data impossible. The exact conditions used for each test are shown in table (4.2)

Table (4.2) - thermocouple depth into channel between walls (mm) for each separation and flaming source

	flaming source		
separation /mm	propane, 5 l/min	propane, 9 l/min	BS No. 7 crib
60	30, 15, 3	30, 15, 3	-
100	50, 25, 3	50, 25, 3	50
80	40, 20, 3	40, 20, 3	40, 20, 3
100^{+}	50	50	-
70^{+}	35	35	-
60^{+}	30	30	-

Note the tests denoted by '+' are with the ends partially blocked; 100 mm separation is restricted to 60 mm at the end, the 70 mm separation is restricted to 27 mm at the end and the 60 mm separation is restricted to 20 mm.

4.2.2 The EU Total Heat Flux Tests

The tests performed at Edinburgh University (EU) involved the use of line burners rather than circular. The line burner was made from 10 mm o.d. stainless steel pipe, 600 mm in length. It was made in the form of a T-piece to allow it to be moved easily into different positions between the walls. One millimetre diameter holes were drilled into the pipe, at a distance of 10 mm apart. To construct the final burner, the line burner was inverted in a stainless steel trough, 15 mm x 15 mm x 640 mm long. This was then filled with sand to reduce the effect of momentum of the gases coming out of the burner. In the following work this set up will be referred to as the sandbed burner. For both types of line burner, experiments were performed with both the open and closed base configurations. Different separations were investigated, using the same wall set up and instrumentation described for the heat flux tests in the previous section.

Three burner positions were investigated; in the centre of the gap between the walls, against the instrumented wall, and against the opposite wall. The length of the burner was kept parallel to the walls. The separation between the walls was varied for different tests and the corresponding heat fluxes measured. The situation of infinite separation, no cross-radiation, was considered by performing tests with the blank wall removed. This could only be done for the case where the burner was situated against the instrumented wall, since there is no equivalent configuration for the burner in the centre of the channel. Tests were done with the base both in place and removed. The exact configurations investigated are shown in tables (4.3) and (4.4).

Table (4.3) - the base configurations investigated for the line burner, for each separation and burner position. All tests were carried out at both 5 and 9 l/min propane and measurements taken at all four heights and horizontal positions.

	burner position		
separation /mm	centre of channel	against instrumented wall	against opposite wall
60	open closed	open closed	open
100	open closed	open closed	open
140	open closed	open closed	open
∞	–	open closed	–

Table (4.4) - the base configurations investigated for the sandbed burner, for each separation and burner position. All tests were carried out at both 5 and 9 l/min propane and measurements taken at all four heights and horizontal positions.

	burner position		
separation /mm	centre of channel	against instrumented wall	against opposite wall
60	open closed	open closed	open closed
100	open closed	open closed	open closed
140	open closed	open closed	open closed
∞	–	open closed	–

4.2.3 Radiation Measurements

Tests were carried out in order to try to separate the radiative and convective components of the heat transfer occurring between the walls. To achieve this, two radiometers were used to replace the total heat flux meters in the parallel vertical wall set-up. They were Schmidt-Boelter type with a sapphire window, water cooled and with air blown across the front of the detector in order to prevent soot deposition. The air was supplied from a small pump which produced only a low flow rate so that the air flow would not interfere with the flame or the hot combustion gases. The data collection was the same as that described above, except for the case when the flame was against the instrumented wall. In this case, soot deposition became a problem so the sampling rate was increased to 2 Hz. The walls in this case were allowed to warm up for 5 minutes with the fan on and 150s with the fan off before the radiometers were inserted into their holes. Collection of data was performed for approximately 90 s, although the averaging of data could not always be carried out over this whole time period as a very noticeable decrease in radiative flux was observed after about 30 s. When this was the case, data were only averaged over the first 30 s of collection.

Measurements of radiation were made for the line burner only. Combinations of open and closed bases, two propane flow rates, different burner positions and various separations were investigated as shown in table (4.5).

Table (4.5) - the base configurations investigated for the line burner, for each separation and burner position. All tests were carried out at both 5 and 9 l/min propane and measurements taken at all four heights and horizontal positions.

	burner position		
separation /mm	centre of channel	against instrumented wall	against opposite wall
60	open closed	–	–
100	open closed	open	open
140	open closed	open	–
∞	-	open	-

The same procedure as for the total heat flux tests for moving the radiometers and plugging the holes with kaowool was used, except that in this case there were only two heat flux meters. Twice as many tests were required to obtain a radiation distribution across the wall

4.2.4 Flame Heights

Measurements of flame height were taken for the line burner against the wall and in the centre of the channel between the walls. Both burner propane flow rates were used and the two base configurations were investigated. The flame height was measured in two ways; visually during the test and from videotape recordings taken of each test. A measuring stick beside the apparatus was used as the reference point for both methods. To obtain the readings from the tape, approximately 30-40 measurements were taken at random times during the test, by pausing the tape and measuring off the flame height at that instant. These were then averaged to gain the average flame height. Two flame heights were obtained for each test; the average height of the flame tip and the height of the solid flame region. The second of these was again obtained visually during the test and from videotape. To obtain this reading form the tape, the same procedure as above was adopted, but the solid flame height was taken as the minimum value obtained over the 30 or 40 readings. Measurements were also made of the flame height for the unconfined flame, i.e. for

the burner standing alone with no walls present. The conditions investigated are summarised in table (4.6).

Table (4.6) base configuration investigated for each separation and burner position. Measurements were made at both 5 and 9 l/min propane and readings obtained for the flame heights at the tip and at the top of the solid flame region.

	burner position	
separation /mm	centre of channel	against instrumented wall
60	open closed	open closed
100	open closed	open closed
140	open closed	open closed
∞ (one wall)	_	open closed
no walls	open closed	_

4.2.5 Flame Temperature

Flame temperature readings were taken for the line burner between the parallel walls at Edinburgh University. A portable infrared thermometer (Minolta Cyclops 52) was used instead of thermocouples. This equipment requires the emissivity to be set before readings are taken. In this case the emissivity was set to unity, the value of a 'blackbody'. As the emissivity of the flame was in reality less than this, the readings obtained were less than the actual temperature. The temperature reading is known as the 'apparent' or 'brightness' temperature. This is related to the actual temperature by

$$T = \frac{T_b}{\varepsilon^{1/4}} \qquad (4.1)$$

where T_b = brightness temperature /K

ε = emissivity

T = actual temperature /K

As propane produces a very sooty flame, the emissivity will be high and the actual temperature should not be much higher than the measured one. Use of the brightness temperature allows comparison of flame temperatures under different conditions, without the need to know the emissivity.

Temperature measurements were taken using the 'Cyclops' on continuous mode. The data were logged using a Minolta Data Processor DP-C. Calculations of the mean and standard deviation were also performed. Two measurements were obtained for each set of conditions; the temperature near the tip of the flame and the temperature in the solid flame region. The measurements at the tip could not be considered to be as reliable as those in the solid flame, as the flame tip moved in and out of sight of the Cyclops. The readings for the burner in the centre of the channel are less reliable than for the flame at the wall, because the flame tip was less clearly defined, and flickered more than for the flame at the wall.

4.2.6 Blockage Ratio Tests

Tests were carried out at Edinburgh University to assess the influence that restricting the air flow would have on the heat fluxes produced at the walls in the parallel wall configuration. The apparatus was moved to a 13.5m^2 smoke chamber in which a flammable gas detector was installed for safety reasons. It could no longer be assumed that radiation from surrounding walls did not influence results, and that air flow patterns were natural. This meant that it was not necessarily possible to compare the results from these tests with the previous ones, so 'control' tests had to be carried out with no end restriction of air flow. The conditions in these control tests were nominally the same as for some of the previous EU tests. The smoke chamber was vented at the top during the test, with the use of a fan only on low power, to prevent any considerable influence of forced air flows on the results. After the control tests were completed, the end blockage was introduced by placing pieces of monolux board, 10 mm thick, at the ends of the walls, figure (4.4). Two pieces were used at each end, to maintain the symmetry of the system. Blockage

ratios of a half and a quarter of the separation distance were investigated, along with tests where both ends were completely sealed off. Measurements of total heat flux were taken at various separations and both burner flow rates.

4.3 Fire Tests

4.3.1 Smoke Experiments

Smoke measurements were made from experiments using three different test apparatus; the Cone Calorimeter, an ignition apparatus, also using a cone shaped heater, located within a 13.5m^2 smoke chamber, and the HSE medium scale room/corridor test facility. Two main series of tests were carried out; one to investigate whether or not the Cone Calorimeter produced results comparable to those under free-burning conditions, the second to investigate whether a relationship existed between the cone smoke results, under well-ventilated conditions, and the HSE medium scale test where conditions move to ventilation controlled burning. The first series of tests will be referred to as the EU smoke tests, the second are the Buxton smoke tests.

4.3.1.1 The EU Smoke Tests

This series involved tests on a set of materials in the Cone Calorimeter and the ignition apparatus in a smoke chamber, referred to here as the smoke box tests. Both operate under well-ventilated conditions, with cone shaped heaters, of the same size, providing the radiant flux to the sample. The main differences between the two pieces of apparatus are that;

(a) the Cone Calorimeter uses a fan to draw air past the sample, at a known flow rate in the duct whilst the ignitability apparatus in the smoke chamber simply moves air by the effect of the flame, and
(b) the Cone Calorimeter uses monochromatic light for the dynamic measurement of smoke, whilst white light is used for static measurement in the chamber.

The difference in the methods of smoke measurement should not affect the results, however, as it has been shown that dynamic and static methods give good agreement provided that the static measurement is made before accumulated smoke has aged

too much (Atkinson and Drysdale, 1989). Also, tests were carried out when the Cone Calorimeter was fairly new to the fire testing field, to ensure that monochromatic light and white light gave similar results, and this was shown to be the case (Östman and Tsantaridis, 1991). Another difference between the two test methods is the sample size. In the Cone Calorimeter, 100 mm square samples are tested, placed on a refractory blanket and sample holder. An edge frame is usually used for keeping the sample in place during the test. For the smoke box tests, the sample size is 65 mm square, placed within an edge frame holder and secured by incombustible kaoboard beneath the sample.

4.3.1.1.1 Cone Calorimeter Tests

In the Cone Calorimeter, specimens are burned in ambient air conditions, while being subjected to a predetermined irradiance within the range 0-100 kW/m^2. The exhaust gas flow rate, the specimen mass loss rate and the specific extinction area (see Appendix A) are measured. It is used to measure the contribution that the material under test can make to the rate of smoke evolution during its involvement in a fire. The smoke measuring system comprises a helium-neon laser, photodiode detector and appropriate electronics to derive the extinction coefficient and to set a zero reading after calibration with two neutral density filters of different optical density. The smoke meter electronics find the extinction coefficient, k, from

$$k = \frac{1}{L}\ln\left(\frac{I_0}{I}\right) \tag{4.2}$$

where L = pathlength over which measurement is taken, 0.1 1m

I_0 = intensity of light in the absence of smoke

I = intensity of light in the presence of smoke

The average specific extinction area is then calculated from

$$\sigma_{f(avg)} = \frac{\sum_i V_i k_i \Delta t_i}{m_i - m_f} \tag{4.3}$$

where $\dot{V}$ = exhaust volume flow rate

t = time

m_i = initial sample mass

m_f = final sample mass

Several fuels and fuel composites were tested for smoke production using the Cone Calorimeter in this series of tests. Two solid fuels were investigated; black polymethylmethacrylate (PMMA) and a combustion modified (with melamine) polyurethane foam (PUF). One liquid fuel was used; 95% pure *n*-hexane, and two solid-liquid composites were tested; PMMA chips with methanol and polystyrene chips with hexane.

4.3.1.1.1.1 PMMA Tests

Black PMMA was tested using the Cone Calorimeter sample holder, both with and without an edge frame, at four different irradiance levels. The Cone Calorimeter standard (ASTM, 1990) was followed for preparation of samples for testing. For each set of conditions, three tests were performed and the average taken. The same exposure levels were used to test PMMA in the Cone Calorimeter, but the same sample holder and sample size was used as in the ignitability apparatus. These tests were also carried out three times to find the average. The tests are summarised in Table (4.7).

Table (4.7) - irradiance levels (kW/m^2) used for PMMA cone tests for different sample conditions

100 mm sample, no edge frame	100 mm sample, edge frame	65 mm sample, ignitability test sample holder
30	30	30
25	25	25
20	20	20
15	15	15

4.3.1.1.1.2 PUF Tests

The combustion modified polyurethane foam was tested in the Cone Calorimeter under five irradiance levels; 30, 27.5, 25, 22 and 20 kW/m^2. A sample thickness of 25 mm was used, with the standard sample size for the cone, (100 mm)^2. An edge frame was used to restrain the sample and each test was performed in triplicate according to the standard (ASTM, 1990).

4.3.1.1.1.3 The Hexane Tests

In these tests, no external irradiance was applied to the sample, as hexane can burn without a supporting heat flux. The hexane was burned in a 100 mm diameter petri dish, which was wrapped in aluminium foil. The petri dish was placed on the Cone Calorimeter sample holder, without the edge frame, and 50 ml of 95% pure *n*-hexane was pipetted into the dish. The hexane was ignited using a match. Although the cone heater was not used to provide an external irradiance, the influence of its position during the test on the specific extinction area produced from the sample was investigated. The heater was placed in the horizontal position at two different heights, as well as in the vertical position and also completely removed from the Cone Calorimeter. Tests with the heater removed, and one set for the heater vertical, were carried out with the doors to the Cone Calorimeter open. Some designs of Cone Calorimeter, such as PL Thermal Sciences, include doors around the heater and sample, but others do not include this feature because it is not a part of any of the cone standards. Table (4.8) shows the different test conditions for hexane. Each test was carried out five times to obtain the average specific extinction area.

Table (4.8) cone heater positions for *n*-hexane tested in the Cone Calorimeter

heater position
horizontal, 65 mm above sample
horizontal, 25 mm above sample
vertical, doors closed
vertical, doors open
removed

4.3.1.1.1.4 Solid with Liquid Fuel Tests

Two solid fuels were investigated without the use of an imposed irradiance. Instead, a liquid accelerant was employed to ignite the sample, after which combustion could be sustained. The first fuel composite was 20g of clear PMMA chips with 17g of methanol as the accelerant. The second was 15g of polystyrene chips with 4.5g of *n*-hexane. Several different combinations were tested, before these were chosen, to assess which combinations would burn without an external heat flux. The materials were tested in the petri dish, as for the *n*-hexane above. Tests were performed for both fuel composites with the cone heater removed and also with it 25 mm above the sample surface, but providing no irradiance. Each test was performed five times and the average of the results was calculated.

4.3.1.1.2 The Smoke Box Tests

These tests utilised the 'EU ignitability apparatus', as used previously by Thomson and Drysdale (1987). This is shown in figure (4.5). The heater height above the sample and the heater temperature could both be altered to change the irradiance to the sample. The samples were 65 mm square and were wrapped around the back and edges in aluminium foil, except where stated, as for the standard Cone Calorimeter tests. They were placed in a sample holder as shown in figure (4.6). Piloted ignition was effected by manual application of a non-luminous hydrogen diffusion flame at the end of a horizontal swing arm. This ignitability apparatus was set up in a 13.5m^3 smoke chamber, constructed of incombustible monolux walls with windows in each wall. Entry to the chamber was through a doorway constructed in one wall. Smoke was collected in the sealed chamber during a test, then evacuated via a closable duct and fan at the top of the chamber. The smoke produced was collected and monitored continuously by an obscuration meter and data logger (Microlink). The data were collected using the Microsoft 'Windspeed' collection package. The obscuration meter consisted of a white light source and a photocell receiver. The voltage output from the receiver was converted to the obscuration value by the use of equation (4.4).

$$\log \frac{V_0}{V_i} = \log \frac{I_0}{I} \qquad (4.4)$$

where V_0 = voltage in the absence of smoke

V_i = voltage in the presence of smoke

I_0 = light energy collected at the detector in the absence of smoke

I = light energy at the detector in the presence of smoke

The linearity of this relationship was verified by measuring the voltage output for a series of different neutral density filters of known optical density. The total smoke produced by a sample was calculated using the maximum value of obscuration measured during a test, by equation (4.5):

$$D_0 = \frac{V}{Lm}\log\left(\frac{I_0}{I}\right) \qquad (4.5)$$

where D_0 = smoke potential, m^3ODm1/kg

V = volume of smoke chamber, m^3

L = pathlength, m

m = mass of sample consumed, kg

The pathlength is the distance between the light source and the detector and, in this case, is 2.19 m. Smoke measurement units are discussed in Appendix A.

Tests were carried out using this experimental set up with some of the same fuels as tested in the Cone Calorimeter; PMMA, PUF, and *n*-hexane. These are covered in more detail in the following sections.

4.3.1.1.2.1 PMMA Tests

Black PMMA samples, 65 mm square, were tested under the cone heater in the ignitability apparatus in the smoke box. The samples were placed in the sample holder and the heater was located 98 mm above the sample surface. The heat flux to the sample surface was altered by changing the heater temperature. Four heat fluxes were investigated; 30, 25, 20, and 15 kW/m^2. Each test was carried out in triplicate and the average taken. The specific extinction area for the samples was calculated from equation (4.6)

$$SEA = D_0 \times \ln(10) \qquad (4.6)$$

where SEA = specific extinction area, m^2/kg

4.3.1.1.2.2 PUF Tests

Combustion-modified polyurethane foam samples, which were 25 mm thick, were tested with the experimental set up described above. The sample holder was used, the samples were positioned 98 mm below the cone heater and four heat fluxes were investigated by altering the heater temperature. Tests were done at 15, 20, 25 and 30 kW/m^2. Triplicate tests were carried out at all irradiances, except 15 kW/m^2, where only one test was performed. This heat flux level only produced flaming combustion for a few seconds, which was followed by smouldering combustion. Therefore, the results could not easily be compared to the other cases and tests were not continued.

4.3.1.1.2.3 Hexane Tests

Tests with 95% pure *n*-hexane were carried out in the smoke chamber in two different configurations: in the ignitability apparatus, with the heater off, and with the sample on the sample holder, which was simply located on the floor of the smoke chamber. A petri dish was used, as described in section 4.3.1.1.1.3 for Cone Calorimeter tests with hexane. Three different heater heights were investigated for the tests with the sample placed beneath the cone shaped heater. All tests were carried out at least three times and the data averaged. The conditions are summarised in Table (4.9).

Table (4.9) sample and cone heater positions investigated

sample position
in ignitability apparatus, 98 mm below heater
in ignitability apparatus, 65 mm below heater
in ignitability apparatus, 25 mm below heater
on sample holder located on chamber floor
directly on chamber floor

4.3.1.2 The Buxton Smoke Tests

This series of tests involved the use of the Cone Calorimeter and the HSE medium scale room/corridor assembly (see chapter 2 for description). The tests were carried out on a set of conventional and combustion-modified flexible polyurethane foams. The seven materials that were used are listed in Table (4.10) below. It was not possible to obtain the exact formulation of the foams, but it was known whether they were combustion-modified or not. The chemical composition and formulation is not important in this case, as no detailed analysis will be carried out on this basis. Use of this set of materials does allow comparison of the smoke produced by a known set of materials under different conditions.

Table (4.10) - the set of foams for the Buxton smoke tests

Foam sample and type	Isocyanate	foam ref.	density/kgm^{-3}
'M Waterlily' CMHR	MDI	A	35.9
'G Waterlily' CMHR version 2	MDI	B	35.3
'T' conventional ex Draka NV	TDI	C	31.8
HR(yellow), ex Metzeler Gmbh	TDI	D	31.2
'Waterlily'	MDI	E	34.2
CMHR (blue) ex British Vita UK	TDI	F	32.2
CMHR 'PUF' as used in previous sections	unknown	G	24.6

4.3.1.2.1 Cone Calorimeter Tests

The above set of foams were tested in the Cone Calorimeter, according to the standard (ASTM, 1990). Tests were performed in triplicate for five irradiance levels, except for the PUF which was tested under twelve irradiance levels prior to testing of the other samples in order to gain a general understanding of which irradiance levels were appropriate to test the foams under. A suitable range of conditions was necessary to be able to observe difference in behaviour for the different materials. The conditions imposed for each material are shown below, in Table (4.11).

Table (4.11) - exposure levels for each material in the Cone Calorimeter tests

Foam Number	irradiance level /kWm^{-2}
A	50, 40, 30, 20, 15
B	50, 40, 30, 20, 15
C	50, 40, 30, 20, 15
D	50, 40, 30, 20, 15
E	50, 40, 30, 20, 15
F	50, 40, 30, 20, 15
G	50, 40, 35, 30, 27.5, 25, 22, 20, 18.5, 17, 16, 15

4.3.1.2.2 HSE Medium Scale Test

The set of foams were tested in the HSE medium scale room/corridor test assembly. Foam G was tested several times. Initially, this material was tested with only smoke and mass loss measurements taken for the duration of the test (test CMHR93). In the second test (CMHR1) smoke measurements were not taken, but all other measurements were (see 4.3.2.3). This test was non-standard, as only a very small amount of the sample was consumed initially. A second ignition crib was then inserted, after the end of the first experiment, and measurements continued. The next test using this sample (CMHR2) also did not burn significantly, and the remaining sample was used for test CMHR3. For both of these, all measurements including smoke production were taken. All samples were conditioned together for

at least a month, with the majority conditioned for over a year. Smoke measurement in the medium scale test is made dynamically using white light and a photocell detector. The relationship between the voltage output and the light energy, equation (4.4), is only really applicable to low smoke output. When the optical density becomes very high, such as for the tests where the combustion moves to ventilation-controlled conditions, this relationship becomes non-linear. To establish the relationship for the light source and detector used in the HSE apparatus, many readings were taken of voltage output at different optical densities, using neutral density filters. The sensitivity of the position of the light image on the detector was investigated by moving the detector slightly off line from the light emitter. This should have the effect of altering the actual voltage readings, but the ratio between the voltage outputs in the presence and absence of 'smoke' should be maintained. The final equation obtained for the smoke detector was

$$O.D.=\left[-b+\left(b^2+4c\ln\{aV_0/V\}\right)^{1/2}\right]/2c \qquad (4.7)$$

where O.D. = optical density

const. a = 0.9981324643

const. b = 2.366572088

const. c = -0.2367822749

Data were recorded using a 'Microlink' data logger with 'Windspeed' software. Calculations and data processing were carried out using Microsoft Excel.

4.3.2 Other Hazard Assessment Methods

Three hazard assessment test methods were investigated in this section of the research: the Cone Calorimeter, the British Standard test for furniture - BS 5852, and the HSE medium scale test facility. In these tests, parameters other than smoke production were measured and used to classify materials. The tests were generally carried out in accordance with the existing protocol or standard for each method and comparisons were made between the results. Tests were performed using the set of foams described in table (4.10).

4.3.2.1 Cone Calorimeter Tests

The samples were tested according to the standard (ASTM, 1990) under the conditions listed in table (4.11). The samples were tested in the horizontal orientation, which did not allow melting, flowing, or dripping to affect the combustion process. The times to ignition were recorded and the rate of heat release measurements were taken using oxygen consumption calorimetry, as described in Chapter 2. Data were averaged over at least three tests, with the calculations carried out using the Microsoft Excel spreadsheet.

4.3.2.2 BS 5852

Part 2 of this test method (BSI, 1982) is the British Standard test for ignitability of furniture by flaming sources, and is described in Chapter 2. Part 1, (BSI, 1979), uses the same apparatus, but ignition is effected by a smouldering cigarette. The tests that were carried out as part of this research deviated from the standard in that there was no cover material and interliner over the foam samples. The aim of the test in this context was to compare various different types of foam, not composites for seating. Results from this test were qualitative rather than quantitative, but it was possible to compare the different materials by their behaviour in this test. For part one, each material was set up in the 'chair' configuration and a smouldering cigarette placed at the join of the two pieces. If, once the cigarette has self-extinguished, the sample had not ignited, the test was repeated for a cigarette in a different position. All samples that did not begin to burn after two such attempts were classified as having passed this part of the test, and were then tested according to BS 5852 Part 2.

In part 2 of this test method, each material was tested using a British Standard No. 4 crib. Those that passed this ignition source, as defined in Chapter 2, underwent a repeat test. If the material still passed a 'pass' was recorded at this ignition source, i.e. P4 (pass at ignition source 4), and the material was then tested using the No. 5, then the No. 6 crib, and finally the No. 7. Once a material failed at an ignition source, a 'fail' was recorded for that source size, e.g. F6, and no further tests were performed. The only difference between the fail criteria used in these tests and the standard criteria is that a sample was not failed if it had burned through its depth. The reason that this was not taken as a fail criteria was that most samples did burn through in places, as they did not have the protection of the cover material. The criteria of continued flaming or smouldering, almost complete consumption of the sample, flame spread horizontally to reach an edge, and accelerated burning which lead to necessary extinguishment of the sample, were all retained as indicative of failure.

The wood cribs were constructed according to the standard (BSI, 1982), and conditioned before use. The tests were carried out in a 13.5m^2 smoke chamber, with a door kept open and an extract fan on 'low' to allow movement of air and prevent accumulation of smoke. CO_2 extinguishers and sand were used to extinguish the samples, where necessary. The test apparatus was mounted over a thin sheet of aluminium foil which influenced the tests in that it allowed accumulation of dripped materials; the supalux floor of the smoke chamber absorbed some of the liquid foam if the aluminium was not in place, although it was often not extinguished if still burning on contact with the floor. The melted material was allowed to accumulate in order to prevent damage to the smoke chamber and to allow continued burning of the material. The ignition source sizes that each material was subjected to are shown in the results section, chapter 5.

4.3.2.3 The HSE Medium Scale Tests

The same set of materials was tested in the HSE medium scale room/corridor assembly. The foam samples, each of approximately 5 kg in mass, were split into two halves before being tested. The two halves were placed on the floor of the HSE test rig, facing each other, with a BS No. 7 ignition crib (BSI 1982) between them. Ignition was effected by the ignition crib, and standard continuous measurements of vent and corridor exit temperatures and smoke obscuration were taken. The smoke measurement was made, as described in section 4.3.1.2.2. Additional

instrumentation included oxygen, carbon dioxide and carbon monoxide analysers and load cells for continuous mass loss measurements. The inclusion of the oxygen analyser allowed the rate of heat release to be calculated, as the volume flow rate in the duct was known. The analysers were first calibrated with known compositions of gases. The oxygen analyser was zeroed using oxygen-free nitrogen and spanned using atmospheric air, whilst the carbon monoxide and carbon dioxide analysers were calibrated using firstly atmospheric air, then a gas composed of nitrogen with 0.75% CO and 5% CO_2. The voltage outputs were measured during calibration, to obtain an accurate correlation between gas input and signal output. The load cell arrangement involved passing aluminium poles through the base of the test chamber, above the level of the floor, then placing a false floor upon these for the sample to be tested on. The poles rested upon load cells at one end and a mass balance at the other, which together carried all the mass of the sample, false floor and poles. The load cells were initially calibrated such that a 1 mVolt increase in output corresponded to a 1g loss in mass. After placing the test sample on the false floor, the load cells and balance were zeroed. A mass of 400g was then placed beside the sample and the load cells checked to ensure that no other part of the system was carrying any of the mass. As this was often initially the case, it was an essential procedure to obtain accurate mass loss measurements. The outputs from the load cells were logged continuously during each test, and video recordings were made of the mass balance, with the video timer used to match these measurements with the load cells. The mass loss measurements could not be considered accurate for the duration of the tests, as the poles often deformed under the intense heat within the chamber, and the load would then be supported elsewhere, rather than on the load cells. Despite this, the measurements could be considered sound during the initial part of the tests, the point of failure usually being obvious, characterised by sharp spikes on the mass loss curve. Some non-standard tests were performed (see 4.3.1.2.2). For most of the tests a sampling rate of 1 Hz was used, except for the CMHR93 and for the test on foam F (British Vita Blue), where the sampling rate was 10 Hz. These were the first tests performed, this sampling rate was later judged to be too high. The data logging system was that described in section 4.3.1.2.2. The sampling rate of the data logger was checked against the video timer and a stopwatch to ensure that all were operating correctly, which was the case.

4.3.3 Further Investigations

This section of the experimental program consisted of more involved and detailed studies into the HSE medium scale test facility. Non-standard tests were carried out using this apparatus to gain a deeper understanding of the exposure conditions existing in the tests and the subsequent material behaviour during a test. Much of the work was based on findings and ideas generated from the parallel wall tests (section 4.2).

4.3.3.1 The HSE Medium Scale Test

Non-standard tests were carried out using rigid polyurethane foam in order to further understand the processes occurring in this apparatus, and to investigate the influence of parameters that would be important in warehouse storage. The separation distance between the two halves of the sample was altered for some tests, whereas in others the ignition source size was changed. The influence of air flow, and storage on pallets or directly on the floor, was investigated by either placing the samples straight on to the floor of the test apparatus, as for the standard test protocol, or by raising them off the floor. This is comparable to the closed and open base configurations of the parallel wall tests. All the foam materials were cut from sheets to approximately 60 x 60 x 6 cm and kept upright and parallel by small steel poles pushed through each corner. The exact configurations and materials investigated are listed below:

rigid polyurethane foam: ('closed base') ~~(PIR)~~

80 mm separation: no. 7 crib
no. 7 crib, outside test apparatus
no. 4 crib
no. 3 butane flame
no. 2 butane flame

60 mm separation: no. 3 butane flame

40 mm separation: no. 3 butane flame
no. 2 butane flame
no. 3 butane flame for the duration of the no. 2 source
no. 2 butane flame for the duration of the no. 3 source

10 mm separation: no. 1 match source

For the no. 7 crib, the separation between the samples was the same as the width of the crib. For the other ignition sources, the gap was larger than the sources, and the ignition source was placed against one face of the sample.

Polyisocyanurate (PIR)

After preliminary tests using the PIR foam with the smaller standard ignition sources and separations, tests were performed using the no. 7 crib and the 80 mm separation. In the first set of tests the specimens were placed directly on the false floor of the third scale combustion room, in the second the samples were elevated by 7 cm. During the first one of these tests, the samples fell over and the test had to be repeated.

Phenolformaldehyde (PHF)

Sheets of this material were placed parallel in the third scale room, with an ignition source between them. Samples were tested at a 40 mm separation using a no. 3 butane flame and a no. 4 crib. A no. 7 crib was used as the ignition source for tests with samples 80 mm apart and with the base either open or closed. A final test used the 80 mm sample separation, a closed base, and a No. 7 crib, with the materials set up outside of the third scale room. The smoke and combustion gases were collected and readings taken. This test allowed observation of the material behaviour on exposure to heat and flame.

Figure (4.1) Parallel wall setup

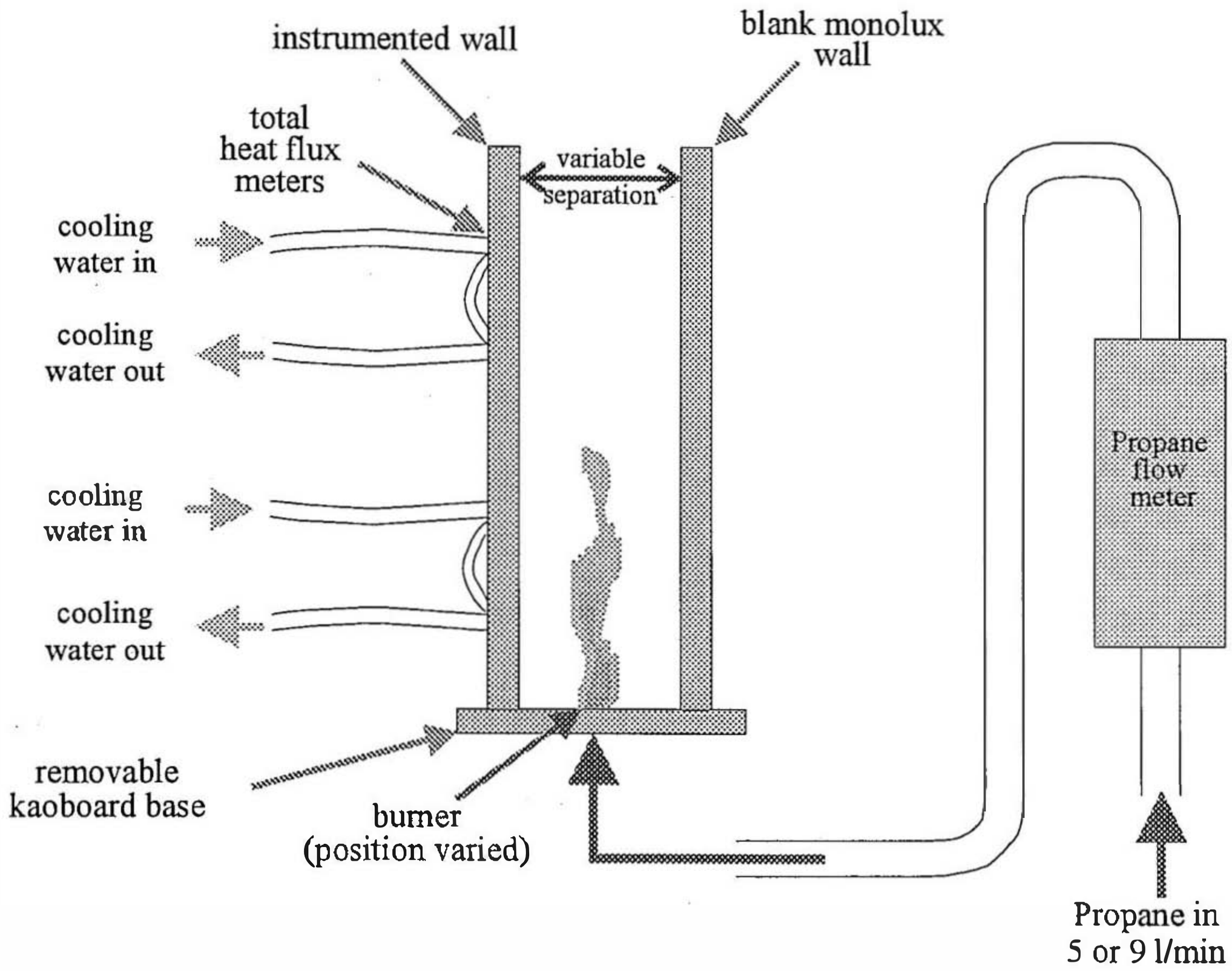

Figure (4.2) Instrumented Wall for Heat Flux Measurement

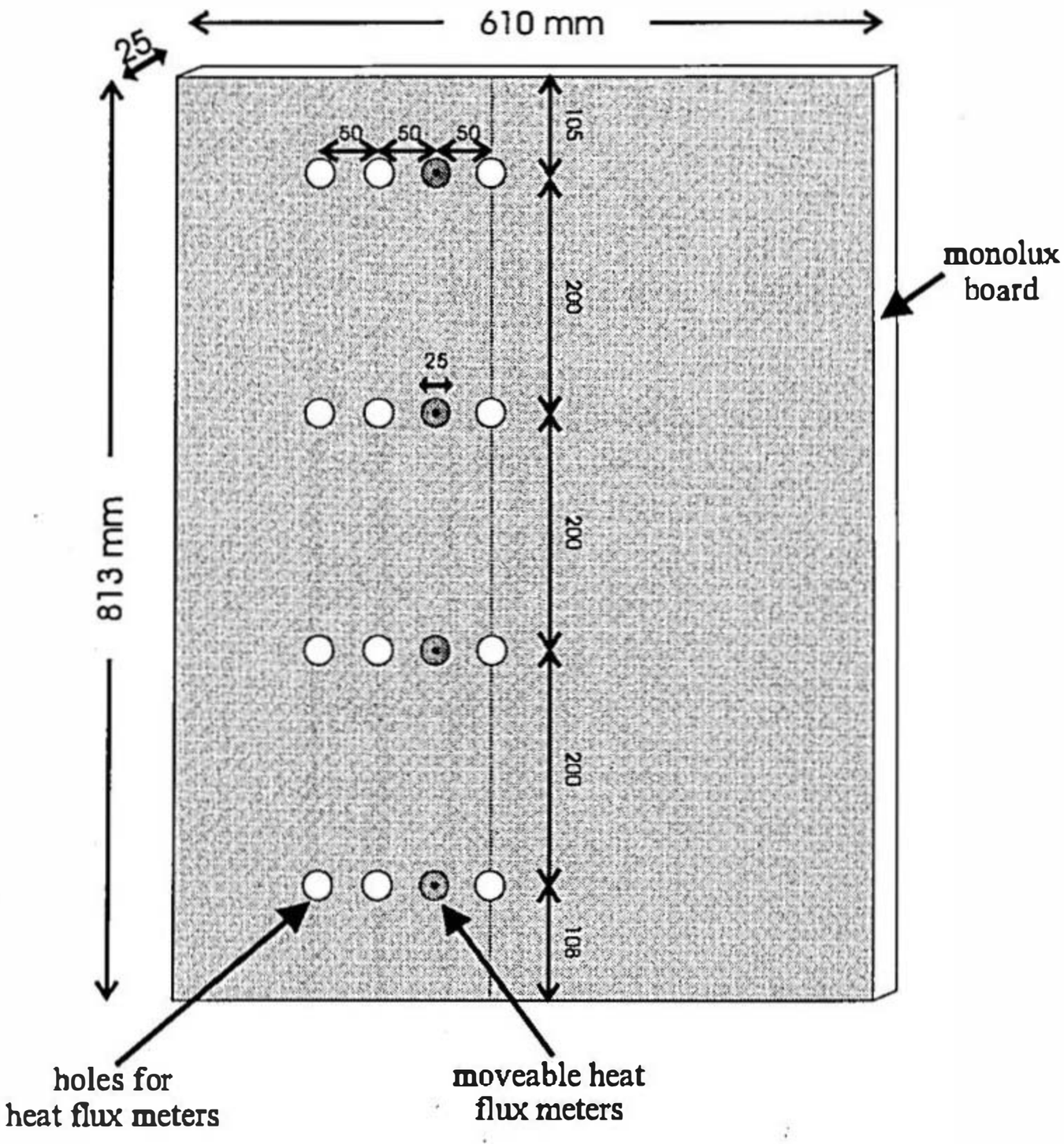

Figure (4.3) Instrumented Wall for Temperature Measurement

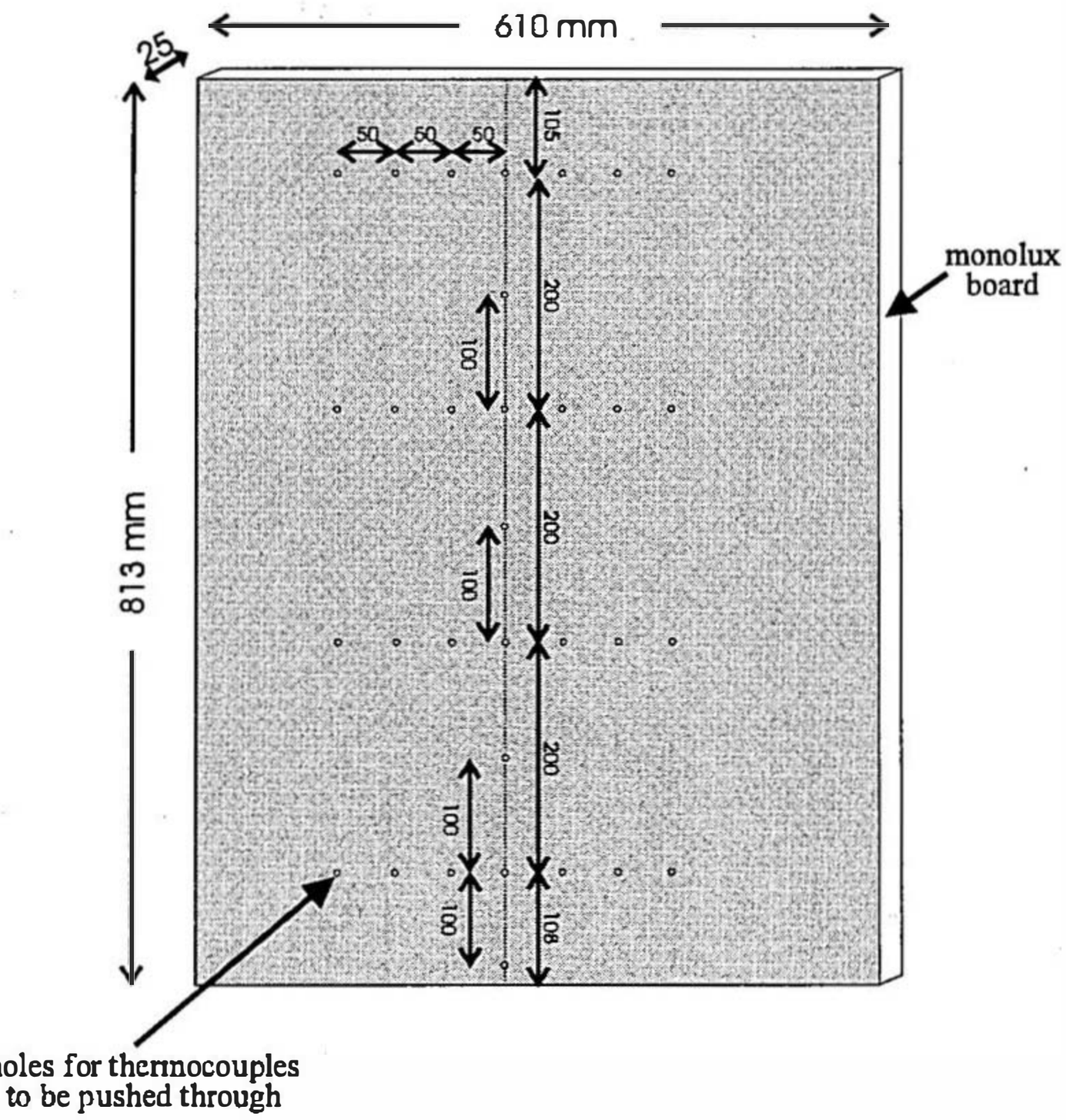

Figure (4.4) Parallel wall setup for flow restriction tests

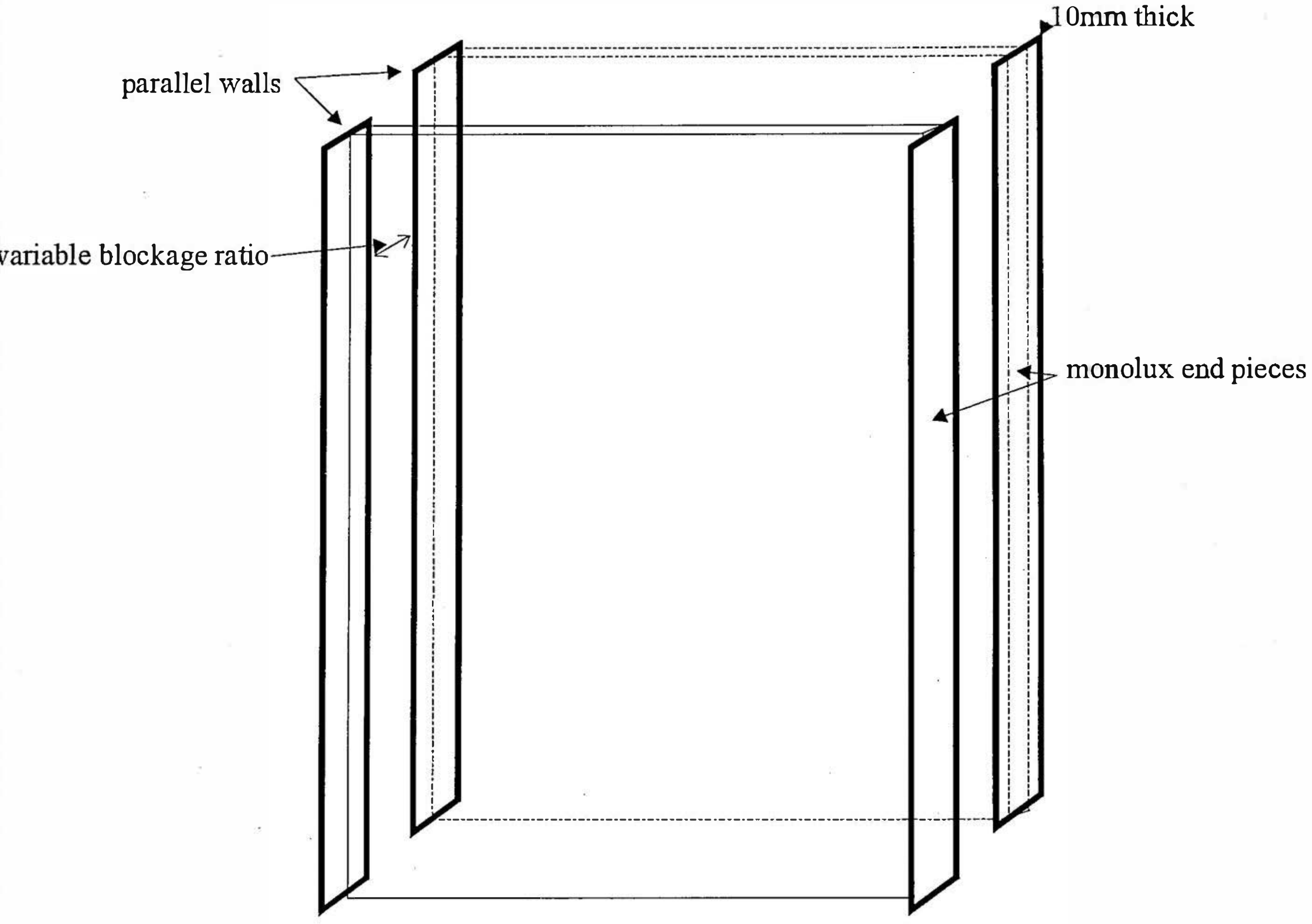

Figure (4.5) E.U. ignitability apparatus

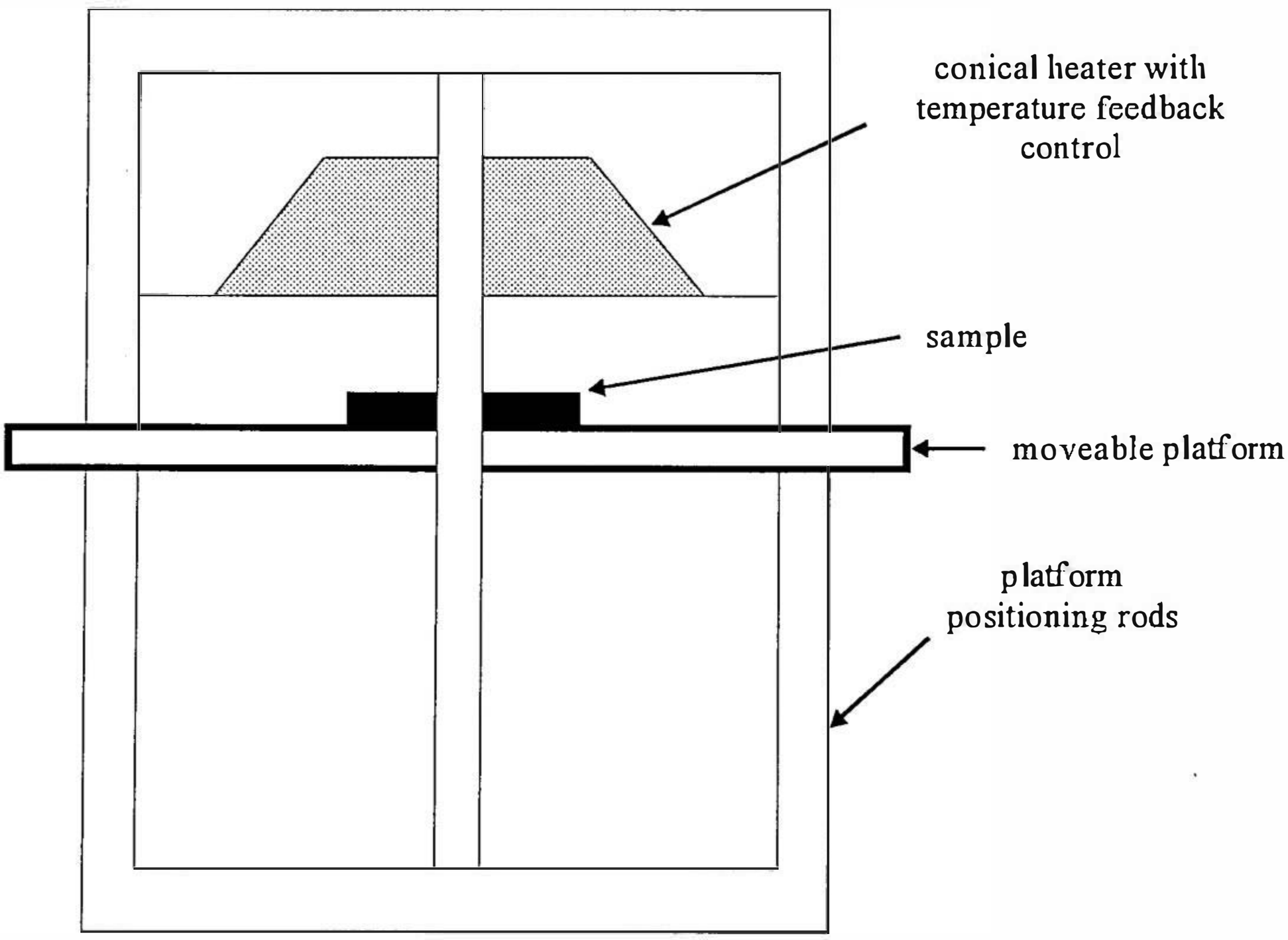

Figure (4.6) sample holder for ignitability apparatus

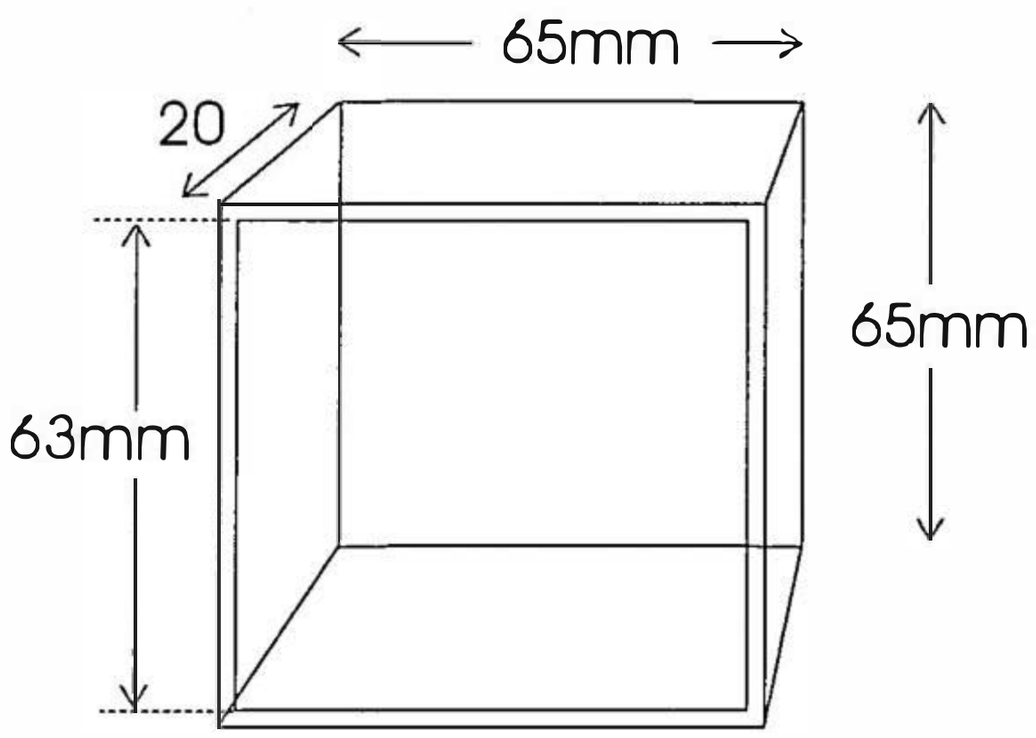

Chapter 5

Results

5.1 Introduction

The results from all the experiments described in the preceding chapter are given in the following sections. No discussion of the meaning of the results is included, this is covered in Chapter 6.

5.2 The Parallel Wall Tests

5.2.1 The Buxton Tests

This series of tests was performed using the circular burner and closed base, as described in section 4.2.1.

5.2.1.1 Heat Flux Measurements

Measurements of total heat flux were taken at four heights; 108, 308, 508, and 708 mm above the burner surface, and four positions across the wall; 0, 50, 100, and 150 mm across the wall from the centreline, giving a distribution of 16 positions in all. A burner propane flowrate of 5 l/min gives a heat release rate of approximately 7 kW, 9 l/min gives 12.5 kW. Results are shown in table (5.1).

Table (5.1) - total heat flux /kWm^{-2} measured at each position under different conditions, Buxton tests

			height /mm			
separation /mm	propane flowrate /l/min	dist. across wall /mm	108	308	508	708
60	5	0	43.28	46.28	26.32	14.50
60	9	0	42.69	60.58	58.04	43.09
60	5	50	13.32	25.49	18.10	11.79
60	9	50	17.68	40.59	43.41	30.48
60	5	100	5.92	11.33	8.68	5.83
60	9	100	8.27	18.34	21.75	16.56
60	5	150	2.52	4.80	3.88	2.56
60	9	150	4.27	9.27	11.36	8.56
100	5	0	21.56	21.79	11.27	6.16
100	9	0	32.48	36.31	28.30	17.34
100	5	50	11.10	15.86	9.51	5.77
100	9	50	17.35	27.64	24.04	15.93
100	5	100	5.47	8.84	5.80	3.89
100	9	100	9.54	15.59	14.32	9.70
100	5	150	2.23	3.73	2.42	1.80
100	9	150	4.92	7.97	7.39	4.91
120*	5	0	18.08	13.10	12.27	7.20
120*	9	0	22.55	19.56	25.33	15.45
140*	5	0	16.08	12.64	7.88	4.88
140*	9	0	22.71	19.97	17.03	9.78
100^{+}	5	0	17.26	17.60	8.62	4.77
100^{+}	9	0	26.38	45.24	29.54	19.47
70^{+}	5	0	23.56	30.27	15.10	9.29
70^{+}	9	0	24.68	43.61	35.52	23.84
∞	5	0	21.27	18.93	10.79	6.33
∞	9	0	23.63	18.88	11.68	7.09
80	No. 7 crib	0	24.32	29.15	11.02	6.18

where the tests denoted by '* ' are with the burner beside the instrumented wall
those denoted by '+' are with the ends partially blocked; 100 mm separation is restricted to 60 mm at the end and the 70 mm separation is restricted to 27 mm at the end.

5.2.1.2 Temperature Measurements

Measurements of temperature were made at thirty two positions on the wall, as shown in figure (4.3). Symmetry was assumed at either side of the vertical centreline and the results given below, table (5.2) - table (5.5), are the average of

two positions for those off centre. The data collection and averaging are described in Chapter 4.

Table (5.2) - temperature measurements /^{o}C, rounded up to the nearest degree, at the different positions and conditions for the thermocouples pushed halfway into the centre of the channel between the walls, Buxton tests

			height /mm							
separation /mm	propane flow rate /l/min	distance. across wall/mm	8	108	208	308	408	508	608	708
60	5	0	225	776	754	686	609	524	444	372
60	9	0	196	751	787	790	774	733	676	614
60	5	50	-	253	-	458	-	400	-	297
60	9	50	-	326	-	563	-	591	-	517
60	5	100	-	100	-	173	-	217	-	191
60	9	100	-	125	-	278	-	372	-	350
60	5	150	-	61	-	82	-	93	-	113
60	9	150	-	75	-	134	-	194	-	208
100	5	0	235	748	688	592	470	354	271	222
100	9	0	220	773	763	712	623	534	440	366
100	5	50	-	194	-	366	-	256	-	177
100	9	50	-	292	-	487	-	413	-	300
100	5	100	-	90	-	124	-	131	-	117
100	9	100	-	133	-	218	-	243	-	204
100	5	150	-	59	-	70	-	64	-	72
100	9	150	-	83	-	114	-	125	-	125
80	5	0	252	780	704	615	522	419	334	278
80	9	0	187	764	762	728	657	609	541	478
80	5	50	-	196	-	354	-	306	-	218
80	9	50	-	288	-	491	-	496	-	403
80	5	100	-	92	-	115	-	154	-	145
80	9	100	-	122	-	224	-	294	-	273
80	5	150	-	60	-	70	-	71	-	81
80	9	150	-	75	-	114	-	150	-	158
100^{+}	5	0	-	600	503	415	326	264	230	201
100^{+}	9	0	-	691	644	591	523	469	407	351
70^{+}	5	0	-	733	655	561	470	395	326	273
70^{+}	9	0	-	731	-	765	-	645	-	512
60^{+}	5	0	-	509	518	573	-	516	406	376
60^{+}	9	0	-	578	-	549	-	384	-	252

Table (5.3) - temperature measurements /^{o}C, rounded up to the nearest degree, at the different positions and conditions for the thermocouples pushed quarter of the way into the channel between the walls, Buxton tests

			height /mm							
separation /mm	propane flow rate /l/min	distance. across wall/mm	8	108	208	308	408	508	608	708
60	5	0	214	792	783	725	615	529	429	351
60	9	0	158	146	808	811	119	724	649	583
60	5	50	-	245	-	487	-	405	-	283
60	9	50	-	271	-	566	-	575	-	485
60	5	100	-	107	-	197	-	215	-	180
60	9	100	-	116	-	256	-	342	-	286
60	5	150	-	67	-	89	-	96	-	98
60	9	150	-	73	-	119	-	168	-	171
100	5	0	509	609	572	515	428	343	266	218
100	9	0	205	745	762	723	641	569	482	409
100	5	50	-	201	-	340	-	260	-	185
100	9	50	-	294	-	497	-	458	-	344
100	5	100	-	94	-	140	-	150	-	130
100	9	100	-	124	-	229	-	279	-	237
100	5	150	-	62	-	74	-	81	-	81
100	9	150	-	82	-	114	-	147	-	143
80	5	0	327	706	654	578	491	411	328	265
80	9	0	210	689	728	704	645	595	521	448
80	5	50	-	288	-	420	-	330	-	223
80	9	50	-	373	-	545	-	506	-	388
80	5	100	-	106	-	191	-	196	-	158
80	9	100	-	172	-	303	-	336	-	282
80	5	150	-	66	-	90	-	99	-	98
80	9	150	-	98	-	164	-	195	-	186

Table (5.4) - temperature measurements /^{o}C, rounded up to the nearest degree, at the different positions and conditions for the thermocouples pushed 3 mm into the channel between the walls, Buxton tests

			height /mm							
separation /mm	propane flow rate /l/min	distance across wall/mm	8	108	208	308	408	508	608	708
60	5	0	179	573	561	550	490	406	297	251
60	9	0	139	544	591	637	642	596	504	464
60	5	50	-	255	-	402	-	302	-	201
60	9	50	-	296	-	491	-	499	-	414
60	5	100	-	124	-	213	-	189	-	126
60	9	100	-	142	-	285	-	330	-	252
60	5	150	-	73	-	104	-	93	-	72
60	9	150	-	85	-	142	-	173	-	144
100	5	0	345	41	434	424	348	255	206	161
100	9	0	224	563	558	555	495	414	362	290
100	5	50	-	197	-	304	-	210	-	137
100	9	50	-	315	-	451	-	370	-	255
100	5	100	-	111	-	165	-	137	-	92
100	9	100	-	160	-	276	-	268	-	182
100	5	150	-	75	-	92	-	75	-	59
100	9	150	-	108	-	154	-	156	-	114
80	5	0	285	551	499	469	385	293	237	183
80	9	0	164	592	628	622	570	495	452	380
80	5	50	-	228	-	347	-	242	-	152
80	9	50	-	281	-	489	-	431	-	316
80	5	100	-	121	-	177	-	152	-	98
80	9	100	-	153	-	272	-	290	-	202
80	5	150	-	76	-	94	-	76	-	62
80	9	150	-	98	-	148	-	155	-	125

Table (5.5) - temperature measurements /^{o}C, rounded up to the nearest degree, at the different positions and conditions for the Number 7 crib between the walls, Buxton tests

			height /mm							
separation /mm	thermocouple depth /mm	dist. across wall/mm	8	108	208	308	408	508	608	708
100	50	0	709	877	752	615	454	336	250	210
100	50	50	-	274	-	216	-	208	-	155
100	50	100	-	141	-	72	-	79	-	95
100	50	150	-	82	-	60	-	44	-	50
80	40	0	791	870	751	598	426	309	232	190
80	40	50	-	316	-	171	-	199	-	150
80	40	100	-	117	-	63	-	80	-	93
80	40	150	-	68	-	54	-	39	-	45
80	20	0	584	756	733	488	343	274	219	189
80	20	50	-	238	-	216	-	191	-	149
80	20	100	-	108	-	62	-	88	-	93
80	20	150	-	68	-	51	-	42	-	50
80	3	0	365	405	578	497	297	186	147	117
80	3	50	-	305	-	185	-	125	-	87
80	3	100	-	115	-	73	-	58	-	50
80	3	150	-	67	-	49	-	30	-	30

5.2.2 The Edinburgh University Tests

5.2.2.1 Total Heat Flux Measurements

The variables altered for these tests were heat flux meter position, separation between the walls, burner flow rate, burner type, burner position and base configuration.

5.2.2.1.1 Line Burner Tests

The results are given in table (5.6) - table (5.10).

Table (5.6) - total heat fluxes /kWm^{-2} at different positions and conditions for the closed base configuration and the line burner situated in centre of the channel, EU tests

			height /mm			
separation /mm	propane flow rate l/min	distance across wall /mm	108	308	508	708
100	5	0	23.97	9.28	4.91	3.58
100	5	50	24.27	9.04	4.38	4.02
100	5	100	21.55	5.89	2.70	2.58
100	5	150	19.95	3.24	1.46	1.53
100	9	0	39.38	16.28	7.85	6.86
100	9	50	43.58	16.65	7.57	6.01
100	9	100	41.30	12.50	5.73	4.71
100	9	150	41.89	8.20	3.31	3.02
140	5	0	11.15	5.30	3.05	2.55
140	9	0	19.60	8.45	4.30	3.46
140	5	50	11.72	5.49	2.90	2.53
140	9	50	21.84	8.85	4.42	3.60
140	5	100	10.89	4.02	2.11	2.03
140	9	100	21.18	7.89	3.71	2.95
140	5	150	8.54	1.83	0.71	0.94
140	9	150	17.60	4.45	1.77	1.55
60	5	0	66.06	21.62	9.86	5.84
60	9	0	114.64	51.18	21.76	13.41
60	5	50	62.85	16.88	7.65	5.57
60	9	50	114.64	41.28	17.00	10.20
60	5	100	42.25	8.36	4.05	3.57
60	9	100	97.14	23.93	9.07	7.29
60	5	150	25.64	3.78	1.55	1.95
60	9	150	71.12	12.53	4.10	3.50

Table (5.7) - total heat fluxes /kWm^{-2} at different positions and conditions for the closed base configuration and the line burner against the instrumented wall, EU tests

			height /mm			
separation /mm	propane flow rate l/min	dist. across wall /mm	108	308	508	708
140	5	0	29.34	8.79	3.29	2.88
140	9	0	35.75	17.08	5.65	5.30
140	5	50	28.17	7.47	3.08	2.65
140	9	50	34.29	15.61	5.59	4.36
140	5	100	31.09	5.55	1.92	1.90
140	9	100	39.51	13.17	3.74	3.13
140	5	150	26.14	6.29	2.01	1.62
140	9	150	34.47	9.47	4.15	2.69
100	5	0	35.07	9.51	3.52	3.26
100	9	0	43.34	19.05	7.50	5.27
100	5	50	29.10	9.86	4.40	3.89
100	9	50	36.38	17.02	7.79	6.90
100	5	100	26.57	7.57	2.81	2.50
100	9	100	33.14	16.00	6.45	5.47
100	5	150	23.04	9.29	2.61	1.81
100	9	150	37.16	19.41	4.71	3.40
60	5	0	47.99	20.60	8.52	6.61
60	9	0	69.32	48.29	19.16	12.00
60	5	50	42.73	18.75	8.01	7.14
60	9	50	62.81	44.69	19.67	12.15
60	5	100	44.33	11.65	4.63	4.85
60	9	100	65.18	32.79	13.11	9.29
60	5	150	22.67	6.06	2.72	2.20
60	9	150	59.48	18.31	7.40	4.94
∞	5	0	22.72	5.32	2.24	1.66
∞	9	0	24.49	10.43	3.89	2.81
∞	5	50	20.94	4.64	2.03	1.59
∞	9	50	20.57	8.42	3.44	2.73
∞	5	100	14.00	4.48	2.14	2.12
∞	9	100	14.97	7.40	3.24	2.95
∞	5	150	13.91	4.00	2.08	1.57
∞	9	150	14.21	6.87	2.96	2.42

Table (5.8) - total heat fluxes /kWm^{-2} at different positions and conditions for the open base configuration and the line burner in the centre of the channel, EU tests

			height /mm			
separation /mm	propane flow rate /l/min	dist. across wall /mm	108	308	508	708
100	5	0	8.89	4.43	3.97	3.40
100	9	0	20.25	8.77	6.38	4.90
100	5	50	9.08	4.96	4.23	3.57
100	9	50	20.64	10.33	7.14	5.49
100	5	100	8.90	5.32	3.57	2.78
100	9	100	19.14	10.07	5.99	4.42
100	5	150	9.61	3.75	2.13	1.70
100	9	150	20.64	6.80	3.46	2.58
60	5	0	14.40	6.74	5.48	4.07
60	9	0	30.36	12.48	8.48	6.15
60	5	50	10.16	6.29	4.65	3.44
60	9	50	30.72	12.51	8.50	5.35
60	5	100	9.93	5.53	3.07	2.34
60	9	100	29.92	11.90	5.67	3.61
60	5	150	10.97	4.42	2.02	1.64
60	9	150	31.01	10.50	4.27	2.98
140	5	0	6.83	2.94	2.78	2.33
140	9	0	14.05	5.88	4.37	3.35
140	5	50	7.01	3.90	3.02	2.51
140	9	50	14.34	5.92	4.12	3.33
140	5	100	7.17	3.29	2.32	1.93
140	9	100	14.38	6.22	3.60	2.90
140	5	150	7.79	2.17	1.52	1.23
140	9	150	15.40	4.54	2.44	1.89

Table (5.9) - total heat fluxes /kWm^{-2} at different positions and conditions for the open base configuration and the line burner against the instrumented wall, EU tests

			height /mm			
separation /mm	propane flow rate /l/min	dist. across wall /mm	108	308	508	708
100	5	0	35.45	5.89	3.40	2.46
100	9	0	53.44	13.52	6.03	3.44
100	5	50	34.95	5.42	3.13	2.57
100	9	50	54.29	14.60	6.31	3.56
100	5	100	40.44	6.58	3.58	2.35
100	9	100	50.47	14.23	5.54	2.91
100	5	150	34.23	6.14	2.71	1.62
100	9	150	46.12	14.11	4.53	2.39
60	5	0	43.24	8.50	5.53	3.59
60	9	0	71.86	19.37	10.44	5.58
60	5	50	44.44	8.40	4.41	3.08
60	9	50	81.83	18.87	8.06	4.65
60	5	100	44.15	8.53	4.15	2.44
60	9	100	74.41	17.55	6.23	3.15
60	5	150	39.50	5.20	2.04	1.67
60	9	150	67.26	11.73	3.46	2.04
60	5	150	43.37	6.32	2.43	1.87
60	9	150	74.38	10.10	3.50	2.62
140	5	0	36.00	7.46	3.96	2.42
140	9	0	42.35	14.56	5.59	3.30
140	5	50	34.98	7.44	3.40	2.21
140	9	50	41.67	15.77	6.00	3.30
140	5	100	36.56	5.70	2.87	1.78
140	9	100	42.78	12.08	4.85	2.79
140	5	150	32.10	5.14	2.62	1.31
140	9	150	35.63	10.98	4.66	2.28
∞	5	0	35.51	5.30	2.93	1.84
∞	9	0	40.64	13.68	5.32	2.87
∞	5	50	40.61	4.67	2.51	1.84
∞	9	50	49.40	9.85	4.24	2.58
∞	5	100	35.03	3.85	2.34	1.70
∞	9	100	44.00	7.36	3.47	2.33
∞	5	150	39.02	3.81	2.37	1.53
∞	9	150	45.51	10.02	5.00	2.51

Table (5.10) - total heat fluxes /kWm^{-2} at different positions and conditions for the open base configuration and the line burner against the opposite wall, EU tests

			height /mm			
separation /mm	propane flow rate /l/min	dist. across wall /mm	108	308	508	708
100	5	0	17.98	5.60	2.41	2.02
100	9	0	27.60	16.15	5.71	3.60
100	5	50	19.97	6.24	2.74	2.22
100	9	50	28.85	16.06	5.92	3.99
100	5	100	18.86	5.31	2.51	1.94
100	9	100	27.44	13.87	5.08	3.12
100	5	150	18.81	4.94	1.95	1.36
100	9	150	25.94	12.54	4.13	2.36
60	5	0	25.02	6.48	3.78	3.15
60	9	0	39.15	19.72	7.99	4.63
60	5	50	24.77	7.13	3.84	2.84
60	9	50	37.26	20.68	8.10	4.26
60	5	100	25.98	6.93	3.19	2.26
60	9	100	36.97	19.12	6.74	3.91
60	5	150	25.01	6.37	2.28	1.62
60	9	150	35.02	17.67	5.22	2.89
140	5	0	14.79	6.45	2.36	1.52
140	9	0	20.85	13.34	4.92	2.56
140	5	50	15.31	6.90	2.53	1.59
140	9	50	20.81	13.51	5.00	2.60
140	5	100	14.80	6.40	2.45	1.54
140	9	100	20.27	12.72	4.79	2.49
140	5	150	13.78	5.77	2.06	1.33
140	9	150	18.65	11.62	4.04	2.12

5.2.2.1.2 Sandbed Burner Tests

A series of tests was carried out using the sandbed line burner, for which the effect of momentum of the gases from the burner should be less then for the normal line burner. Tests were done with the burner in different positions, various separations were investigated, the burner flow rate changed and the base either open or closed. The results are given in tables (5.11) - (5.16).

Table (5.11) - total heat fluxes /kWm^{-2} at different positions and conditions for the closed base configuration and the sandbed burner in the centre of the channel, EU tests

			height /mm			
separation /mm	propane flow rate /l/min	dist. across wall /mm	108	308	508	708
100	5	0	23.72	7.84	4.84	3.41
100	9	0	46.62	17.61	8.63	5.31
100	5	50	23.65	7.56	4.53	3.20
100	9	50	49.22	19.98	9.11	5.34
100	5	100	18.96	5.99	3.48	2.59
100	9	100	46.78	14.62	6.7	4.25
100	5	150	20.21	3.22	2.12	1.84
100	9	150	40.67	9.89	4.55	2.95
60	5	0	56.48	15.97	8.46	4.72
60	9	0	105.83	46.97	20.36	9.49
60	5	50	58.43	20.26	9.48	5.67
60	9	50	116.77	55.52	21.94	11.17
60	5	100	51.16	15.66	7.72	4.57
60	9	100	81.17	31.12	12.13	6.55
60	5	150	33.94	7.02	3.50	2.54
60	9	150	58.25	17.43	7.40	4.11
140	5	0	16.78	4.94	3.58	2.67
140	9	0	31.54	11.21	6.34	4.31
140	5	50	15.02	6.17	2.22	2.89
140	9	50	28.61	12.60	6.54	4.40
140	5	100	12.63	4.37	2.90	2.36
140	9	100	26.44	10.48	5.24	3.66
140	5	150	13.45	3.08	2.06	1.86
140	9	150	27.01	7.50	3.95	2.84

Table (5.12) - total heat fluxes /kWm^{-2} at different positions and conditions for the closed base configuration and the sandbed burner against the instrumented wall, EU tests

			height /mm			
separation /mm	propane flow rate /l/min	dist. across wall /mm	108	308	508	708
140	5	0	35.29	11.97	4.93	3.02
140	9	0	41.57	20.70	8.57	4.83
140	5	50	32.91	12.51	4.68	3.25
140	9	50	37.40	20.70	7.75	4.93
140	5	100	30.13	10.21	4.33	2.86
140	9	100	36.88	18.44	7.11	4.05
140	5	150	24.50	9.71	3.87	2.44
140	9	150	35.81	14.36	6.27	3.68
100	5	0	42.15	12.47	6.03	3.77
100	9	0	50.93	25.94	10.60	5.68
100	5	50	37.46	12.38	5.62	3.94
100	9	50	53.15	27.03	10.52	6.05
100	5	100	35.77	11.65	5.13	3.40
100	9	100	45.57	25.04	8.66	4.82
100	5	150	31.77	5.24	1.95	1.43
100	9	150	35.24	13.81	4.99	2.90
60	5	0	51.25	20.34	9.17	5.55
60	9	0	71.21	49.90	22.52	10.66
60	5	50	48.64	18.88	7.60	5.40
60	9	50	66.01	47.63	20.99	10.45
60	5	100	45.54	9.66	4.37	3.53
60	9	100	63.83	34.44	12.90	7.73
60	5	150	33.69	3.64	1.95	2.05
60	9	150	53.35	15.71	6.55	3.97
∞	5	0	29.98	13.19	4.92	2.80
∞	9	0	37.00	27.20	10.14	4.08
∞	5	50	27.50	10.19	3.74	2.51
∞	9	50	38.10	21.54	7.85	4.06
∞	5	100	24.11	9.61	3.79	2.55
∞	9	100	37.50	15.27	6.85	3.69
∞	5	150	20.36	7.02	3.68	2.32
∞	9	150	28.25	13.17	5.92	3.62

Table (5.13) - total heat fluxes /kWm^{-2} at different positions and conditions for the closed base configuration and the sandbed burner against the opposite wall, EU tests

			height /mm			
separation /mm	propane flow rate /l/min	dist. across wall /mm	108	308	508	708
60	5	0	42.54	21.09	8.13	4.87
60	9	0	66.14	41.02	16.74	7.96
60	5	50	33.25	16.09	6.08	4.04
60	9	50	59.70	36.99	14.14	7.44
60	5	100	28.53	9.40	3.71	3.02
60	9	100	51.13	27.85	10.52	5.59
60	5	150	21.52	5.59	2.15	1.68
60	9	150	34.16	15.24	6.15	3.45
100	5	0	19.34	7.43	3.53	2.59
100	9	0	31.80	18.09	7.80	4.64
100	5	50	21.60	8.31	3.64	2.58
100	9	50	33.40	18.67	7.74	4.58
100	5	100	21.78	7.51	2.78	1.76
100	9	100	30.21	17.22	6.38	3.31
100	5	150	19.07	6.16	2.09	1.26
100	9	150	27.78	13.47	4.38	2.12
140	5	0	15.40	6.41	2.41	1.53
140	9	0	23.89	13.86	5.56	3.09
140	5	50	17.03	7.52	2.90	1.81
140	9	50	24.75	14.94	6.04	3.44
140	5	100	15.10	7.12	2.68	1.61
140	9	100	22.06	13.94	5.47	2.96
140	5	150	12.69	5.48	2.05	1.22
140	9	150	19.04	11.22	4.21	2.21

Table (5.14) - total heat fluxes /kWm^{-2} at different positions and conditions for the open base configuration and the sandbed burner in the centre of the channel, EU tests

			height /mm			
separation /mm	propane flow rate /l/min	dist. across wall /mm	108	308	508	708
60	5	0	25.52	12.61	6.00	4.41
60	9	0	48.14	29.74	10.48	7.83
60	5	50	24.29	8.93	6.55	5.09
60	9	50	42.41	23.14	11.52	7.66
60	5	100	20.54	6.54	5.43	4.13
60	9	100	42.89	19.86	10.01	6.46
60	5	150	18.32	7.95	2.72	2.15
60	9	150	39.94	17.49	5.69	3.51
100	5	0	20.97	7.95	4.02	3.35
100	9	0	36.17	16.68	7.09	5.04
100	5	50	11.96	5.00	4.42	3.69
100	9	50	24.53	11.66	7.24	5.46
100	5	100	14.91	4.69	4.43	3.25
100	9	100	28.55	11.22	7.27	4.98
100	5	150	10.57	5.17	2.84	2.10
100	9	150	24.08	10.49	4.45	3.15
140	5	0	13.01	5.41	3.01	2.58
140	9	0	20.62	8.85	5.04	3.90
140	5	50	9.42	3.96	3.40	2.98
140	9	50	18.37	8.45	5.45	4.36
140	5	100	11.61	3.25	3.25	2.82
140	9	100	19.06	7.61	4.54	3.76
140	5	150	8.24	3.43	2.35	1.82
140	9	150	17.12	6.57	3.55	2.62

Table (5.15) - total heat fluxes /kWm^{-2} at different positions and conditions for the open base configuration and the sandbed burner against the instrumented wall, EU tests

			height /mm			
separation /mm	propane flow rate /l/min	dist. across wall /mm	108	308	508	708
60	5	0	50.29	10.44	5.22	4.05
60	9	0	71.94	33.86	13.71	7.39
60	5	50	49.46	9.06	5.75	4.56
60	9	50	68.34	33.68	10.59	6.17
60	5	100	41.18	6.84	4.73	3.03
60	9	100	67.08	22.51	8.85	5.45
60	5	150	36.65	6.72	2.77	2.02
60	9	150	58.55	19.41	5.99	3.48
100	5	0	30.73	8.63	4.11	3.30
100	9	0	49.82	22.44	8.95	5.43
100	5	50	30.35	6.65	4.19	2.77
100	9	50	48.35	20.36	7.68	4.67
100	5	100	28.66	6.40	3.88	2.72
100	9	100	41.02	17.57	6.64	4.33
100	5	150	29.20	5.08	3.50	2.19
100	9	150	40.22	12.12	6.42	3.24
140	5	0	36.50	9.47	4.32	2.73
140	9	0	42.00	18.15	6.61	4.00
140	5	50	35.34	5.93	3.44	2.43
140	9	50	44.99	16.54	6.10	3.92
140	5	100	32.18	6.19	3.33	2.62
140	9	100	36.71	14.26	6.03	4.07
140	5	150	24.32	5.15	3.33	2.09
140	9	150	36.71	13.00	6.30	3.68
∞	5	0	36.52	7.02	3.01	2.16
∞	9	0	39.27	17.71	5.39	3.52
∞	5	50	31.29	3.74	2.54	1.96
∞	9	50	38.38	12.39	5.04	3.44
∞	5	100	29.89	3.50	2.33	1.63
∞	9	100	37.40	12.78	4.64	2.94
∞	5	150	29.59	3.27	2.38	1.72
∞	9	150	35.88	11.00	4.11	2.80

Table (5.16) - total heat fluxes /kWm^{-2} at different positions and conditions for the open base configuration and the sandbed burner against the opposite wall, EU tests

			height /mm			
separation /mm	propane flow rate /l/min	dist. across wall /mm	108	308	508	708
60	5	0	30.03	14.24	6.92	4.58
60	9	0	48.83	33.06	13.16	7.31
60	5	50	30.99	15.44	4.79	3.86
60	9	50	42.82	34.41	11.31	6.97
60	5	100	27.68	10.66	4.68	3.09
60	9	100	40.75	27.96	11.23	5.06
60	5	150	24.41	8.95	2.75	1.72
60	9	150	35.21	20.48	6.95	3.05
100	5	0	20.27	9.25	3.64	2.37
100	9	0	27.52	19.02	7.54	4.04
100	5	50	19.60	9.94	3.30	2.30
100	9	50	27.46	17.50	7.27	4.15
100	5	100	18.91	8.25	3.06	1.93
100	9	100	26.67	16.22	6.51	4.03
100	5	150	17.50	6.14	2.69	1.70
100	9	150	25.44	14.85	5.95	2.81
140	5	0	14.05	8.36	3.29	1.84
140	9	0	20.23	14.89	6.37	3.36
140	5	50	14.05	8.29	3.01	1.74
140	9	50	20.09	14.29	6.17	3.40
140	5	100	13.88	7.50	3.01	1.68
140	9	100	19.52	13.90	5.69	3.08
140	5	150	13.57	6.45	2.64	1.66
140	9	150	18.84	13.35	5.24	2.65

5.2.2.2 Radiation Measurements

The radiation measurements were made for the line burner only, at various separations, burner positions, flowrate and base configurations. The results are given in tables (5.17) - (5.19).

Table (5.17) - radiative heat fluxes /kWm^{-2} at different positions and conditions for the open base and the line burner in the centre of the channel, EU tests

				height /mm			
burner position	Separation /mm	propane flow rate /l/min	dist. across wall /mm	108	308	508	708
centre	100	5	0	4.50	0.68	0.25	0.29
centre	100	9	0	10.26	1.82	0.58	0.49
centre	100	5	50	3.90	0.65	0.24	0.30
centre	100	9	50	9.60	1.69	0.51	0.47
centre	100	5	100	4.35	0.67	0.24	0.30
centre	100	9	100	10.16	1.65	0.48	0.46
centre	100	5	150	3.88	0.58	0.18	0.25
centre	100	9	150	8.98	1.39	0.35	0.35
centre	60	5	0	7.79	1.86	0.52	0.47
centre	60	9	0	21.41	6.37	1.11	0.82
centre	60	5	50	8.39	2.09	0.49	0.45
centre	60	9	50	18.54	5.48	1.29	0.94
centre	60	5	100	8.32	1.66	0.32	0.36
centre	60	9	100	19.48	4.35	0.89	0.75
centre	60	5	150	7.56	0.95	0.18	0.27
centre	60	9	150	17.95	2.80	0.50	0.50
centre	140	5	0	3.97	0.75	0.22	0.27
centre	140	9	0	7.83	1.76	0.41	0.37
centre	140	5	50	4.19	0.85	0.24	0.28
centre	140	9	50	8.35	2.00	0.42	0.38
centre	140	5	100	3.96	0.82	0.21	0.26
centre	140	9	100	7.52	1.32	0.25	0.26
centre	140	5	150	4.15	0.73	0.18	0.24
centre	140	9	150	7.71	1.43	0.26	0.27

Table (5.18) - radiative heat fluxes /kWm^{-2} at different positions and conditions for the open base and the line burner against a wall, EU tests

				height /mm			
burner position	Separation /mm	propane flow rate /l/min	dist. across wall /mm	108	308	508	708
inst.wall	100	5	0	5.73	1.02	0.28	0.28
inst.wall	100	9	0	13.64	3.71	0.54	0.45
inst.wall	100	5	50	5.36	0.77	0.21	0.25
inst.wall	100	9	50	13.51	2.93	0.46	0.37
inst.wall	100	5	100	5.58	0.89	0.24	0.26
inst.wall	100	9	100	13.40	2.92	0.49	0.38
inst.wall	100	5	150	4.74	0.76	0.19	0.24
inst.wall	100	9	150	11.49	2.82	0.35	0.33
inst.wall	140	5	0	4.73	0.91	0.23	0.24
inst.wall	140	9	0	8.45	2.70	0.40	0.33
inst.wall	140	5	50	4.95	1.11	0.24	0.25
inst.wall	140	9	50	9.92	3.00	0.50	0.39
inst.wall	140	5	100	4.97	0.97	0.22	0.25
inst.wall	140	9	100	9.82	2.51	0.42	0.33
inst.wall	140	5	150	3.45	0.95	0.22	0.23
inst.wall	140	9	150	7.89	2.43	0.45	0.35
inst.wall	∞	5	0	4.07	0.26	0.10	0.23
inst.wall	∞	9	0	7.15	0.75	0.15	0.27
inst.wall	∞	5	50	3.22	0.30	0.10	0.22
inst.wall	∞	9	50	5.87	0.86	0.17	0.26
inst.wall	∞	5	100	2.25	0.32	0.11	0.23
inst.wall	∞	9	100	4.59	0.68	0.17	0.26
inst.wall	∞	5	150	2.59	0.34	0.10	0.22
inst.wall	∞	9	150	5.17	0.60	0.17	0.26
opp.wall	100	5	0	9.75	2.28	0.29	0.28
opp wall	100	9	0	16.19	8.14	1.08	0.54
opp wall	100	5	50	9.40	2.14	0.3	0.29
opp wall	100	9	50	15.86	8.27	0.97	0.50
opp wall	100	5	100	9.15	2.04	0.27	0.27
opp wall	100	9	100	15.20	7.65	0.85	0.46
opp wall	100	5	150	7.52	1.50	0.17	0.20
opp wall	100	9	150	12.80	6.14	0.58	0.30

Table (5.19) - radiative heat fluxes /kWm^{-2} at different positions and conditions for the line burner and the closed base, EU tests

				height /mm			
burner position	separation /mm	propane flow rate /l/min	dist. across wall /mm	108	308	508	708
centre	60	5	0	24.24	4.55	1.15	0.77
centre	60	9	0	51.78	18.67	3.93	1.95
centre	60	5	50	22.12	4.83	0.95	0.67
centre	60	9	50	46.70	15.91	3.19	1.70
centre	60	5	100	15.74	2.96	0.56	0.48
centre	60	9	100	28.95	7.73	1.88	1.15
centre	60	5	150	13.69	1.78	0.31	0.32
centre	60	9	150	34.34	6.22	1.03	0.66
centre	140	5	0	34.77	0.78	0.25	0.27
centre	140	9	0	10.68	2.34	0.53	0.43
centre	140	5	50	5.04	0.95	0.29	0.29
centre	140	9	50	10.08	2.28	0.56	0.46
centre	140	5	100	4.42	0.87	0.25	0.28
centre	140	9	100	9.00	1.97	0.50	0.43
centre	140	5	150	4.76	0.78	0.20	0.26
centre	140	9	150	10.29	1.60	0.39	0.36
centre	100	5	0	7.61	1.44	0.44	0.40
centre	100	9	0	16.11	4.29	1.06	0.75
centre	100	5	50	8.02	1.63	0.46	0.42
centre	100	9	50	16.52	4.25	1.06	0.75
centre	100	5	100	7.37	1.41	0.35	0.37
centre	100	9	100	16.41	3.83	0.87	0.67
centre	100	5	150	7.13	0.96	0.24	0.30
centre	100	9	150	13.69	1.78	0.31	0.32

5.2.2.3 Flame Height Measurements

Measurements were made of flame heights, visually during the test and from video recordings, at different wall separations for the line burner, with both the open and closed base configurations, and the burner against a wall and in the centre of the channel, table (5.20). The line burner was used as the flame source.

Table (5.20) - flame height for solid flame region and at the flame tip under different conditions, EU tests

				flame height /mm		
base	burner position	separation /mm	propane flow rate /l/min	(video) solid	(video) tip	(visible) tip
open	wall	∞	5	190	215	270
open	wall	∞	9	250	290	390
open	wall	140	5	170	200	250
open	wall	140	9	260	290	400
open	wall	100	5	170	210	250
open	wall	100	9	250	280	400
open	wall	60	5	170	190	210
open	wall	60	9	240	280	350
open	centre	140	5	140	150	170
open	centre	140	9	170	200	240
open	centre	100	5	150	160	160
open	centre	100	9	180	210	250
open	centre	60	5	150	170	170
open	centre	60	9	200	240	260
open	free-standing	no walls	5	130	150	190
open	free-standing	no walls	9	200	220	260
closed	wall	∞	5	230	280	370
closed	wall	∞	9	320	380	490
closed	wall	140	5	220	280	350
closed	wall	140	9	250	360	480
closed	wall	100	5	180	250	310
closed	wall	100	9	240	315	400
closed	wall	60	5	230	350	450
closed	wall	60	9	330	420	600
closed	centre	140	5	120	160	160
closed	centre	140	9	150	210	240
closed	centre	100	5	130	170	210
closed	centre	100	9	160	230	290
closed	centre	60	5	180	260	400*
closed	centre	60	9	240	355	550*
closed	free-standing	no walls	5	150	170	200
closed	free-standing	no walls	9	180	220	280

* flame is noticeably pulsating, reaching greater flame heights than recorded here

5.2.2.4 Flame Temperature Measurements

These are the measurements made using the Cyclops infrared thermometer for the line burner, table (5.21). The standard deviation of the continuously collected data is given in brackets.

Table (5.21) - flame temperatures for the solid flame region and in the intermittent flame region under different conditions, standard deviation in brackets, EU tests

				flame temperature /K	
base	burner position	separation /mm	propane flow rate /l/min	solid flame region	intermittent flame region
open	wall	∞	5	1431(70)	1201(158)
open	wall	∞	9	1546(50)	1181(95)
open	wall	140	5	1511(46)	1261(50)
open	wall	140	9	1504(78)	1199(51)
open	wall	100	5	1520(13)	1255(10)
open	wall	100	9	1560(47)	1274(20)
open	wall	60	5	1424(112)	1186(92)
open	wall	60	9	1515(3)	1246(62)
open	centre	140	5	1457(13)	1301(49)
open	centre	140	9	1424(230)	1243(102)
open	centre	100	5	1490(32)	1172(129)
open	centre	100	9	1451(33)	1255(212)
open	centre	60	5	1601(9)	1134(92)
open	centre	60	9	1521(53)	1156(4)
open	free-standing	no walls	5	1418(56)	1114(134)
open	free-standing	no walls	9	1370(71)	1282(160)
closed	wall	∞	5	1324(7)	1153(41)
closed	wall	∞	9	1436(39)	1090(52)
closed	wall	140	5	1303(28)	1163(98)
closed	wall	140	9	1417(33)	1200(73)
closed	wall	100	5	1398(11)	1266(93)
closed	wall	100	9	1457(21)	1166(142)
closed	wall	60	5	1366(86)	1130(68)
closed	wall	60	9	1437(2)	1182(132)
closed	centre	140	5	1464(35)	1128(90)
closed	centre	140	9	1397(70)	1328(45)
closed	centre	100	5	1452(1)	1321(124)
closed	centre	100	9	1472(18)	1306(184)
closed	centre	60	5	1445(4)	1169(94)
closed	centre	60	9	1532(45)	1138(64)
closed	free-standing	no walls	5	1388(16)	1110(78)
closed	free-standing	no walls	9	1481(78)	1151(85)

5.2.2.5 Blockage Ratio Tests

The total heat fluxes (kWm^{-2}) under different conditions and end blockage ratios are given in tables (5.22) - (5.33).

Table (5.22) total heat fluxes /kWm^{-2} at different positions and conditions for the open base, line burner against instrumented wall, 140 mm wall separation, EU tests

				height /mm			
separation /mm	blockage ratio	propane flow rate /l/min	dist. across wall /mm	108	308	508	708
140	0	5	0	36.07	10.90	2.96	2.30
140	0	9	0	48.35	32.35	8.46	5.19
140	0	5	50	35.76	10.05	2.89	2.11
140	0	9	50	45.10	26.27	7.99	4.25
140	0	5	100	34.56	10.22	2.67	2.08
140	0	9	100	46.98	22.47	6.52	3.89
140	0	5	150	33.17	6.49	1.99	1.47
140	0	9	150	44.50	17.12	3.97	2.32
140	0.25	5	0	43.25	13.84	4.68	3.65
140	0.25	9	0	65.00	27.91	9.24	4.12
140	0.25	5	50	44.19	13.05	4.15	2.89
140	0.25	9	50	58.99	20.28	6.72	4.57
140	0.25	5	100	42.75	10.33	2.92	2.10
140	0.25	9	100	63.97	23.93	6.98	3.58
140	0.25	5	150	35.15	7.18	1.69	1.20
140	0.25	9	150	58.53	17.30	4.53	2.72
140	0.5	5	0	36.16	14.06	5.08	3.82
140	0.5	9	0	59.86	31.17	10.89	5.66
140	0.5	5	50	37.72	14.68	4.10	2.96
140	0.5	9	50	53.64	27.07	9.09	4.36
140	0.5	5	100	35.64	9.33	2.39	1.45
140	0.5	9	100	54.77	19.34	5.65	3.07
140	0.5	5	150	32.20	5.52	1.70	0.99
140	0.5	9	150	48.92	12.20	3.07	1.75
140	1	5	0	29.78	15.96	4.04	2.82
140	1	9	0	44.55	18.01	5.64	3.20
140	1	5	50	28.54	12.72	4.49	3.07
140	1	9	50	41.32	13.31	3.98	3.36
140	1	5	100	29.25	11.12	3.57	2.88
140	1	9	100	33.12	8.37	4.60	2.92
140	1	5	150	21.28	5.04	1.64	1.67
140	1	9	150	36.49	7.65	3.36	2.01

Table (5.23) total heat fluxes /kWm^{-2} at different positions and conditions for the open base, line burner against instrumented wall, 100 mm wall separation, EU tests

				height /mm			
separation /mm	blockage ratio	propane flow rate /l/min	dist. across wall /mm	108	308	508	708
100	0	5	0	38.25	17.00	4.50	3.34
100	0	9	0	47.37	37.60	13.24	5.94
100	0	5	50	39.83	16.09	4.12	2.90
100	0	9	50	48.56	31.21	10.63	5.03
100	0	5	100	39.97	12.93	3.45	2.10
100	0	9	100	48.92	24.90	6.52	3.64
100	0	5	150	38.12	5.77	2.19	1.31
100	0	9	150	48.38	18.66	4.57	2.76
100	0.25	5	0	45.71	13.99	4.62	3.20
100	0.25	9	0	70.75	24.59	8.68	5.97
100	0.25	5	50	43.97	12.23	3.35	2.62
100	0.25	9	50	67.95	24.56	6.85	4.35
100	0.25	5	100	43.51	13.63	3.32	2.02
100	0.25	9	100	62.89	24.64	7.17	3.34
100	0.25	5	150	38.82	9.06	1.88	1.27
100	0.25	9	150	65.73	17.97	4.55	2.31
100	0.5	5	0	43.25	12.33	4.48	3.91
100	0.5	9	0	69.83	27.50	9.62	6.55
100	0.5	5	50	42.06	10.45	3.83	2.72
100	0.5	9	50	62.34	21.05	8.42	4.96
100	0.5	5	100	39.89	10.20	2.98	2.21
100	0.5	9	100	63.23	22.86	8.18	4.07
100	0.5	5	150	37.86	8.57	1.71	1.03
100	0.5	9	150	58.90	18.64	4.51	2.42
100	1	5	0	28.50	10.66	4.52	3.43
100	1	9	0	38.20	14.97	6.69	4.57
100	1	5	50	26.38	8.16	3.33	2.13
100	1	9	50	33.29	15.54	5.73	3.22
100	1	5	100	19.15	5.35	2.41	1.88
100	1	9	100	25.15	11.49	4.11	2.81
100	1	5	150	18.60	5.96	2.95	1.58
100	1	9	150	26.93	9.68	4.35	2.02

Table (5.24) total heat fluxes /kWm^{-2} at different positions and conditions for the open base, line burner against instrumented wall, 60 mm wall separation, EU tests

				height /mm			
separation /mm	blockage ratio	propane flow rate /l/min	dist. across wall /mm	108	308	508	708
60	0	5	0	53.52	21.89	5.60	4.92
60	0	9	0	70.31	48.66	18.72	10.55
60	0	5	50	50.22	22.16	5.70	3.27
60	0	9	50	69.83	43.75	13.57	5.20
60	0	5	100	52.90	13.47	3.97	2.09
60	0	9	100	68.65	36.02	9.81	4.16
60	0	5	150	48.20	5.06	0.79	0.81
60	0	9	150	66.34	20.00	5.10	2.41
60	0.25	5	0	60.56	13.91	5.65	4.76
60	0.25	9	0	90.95	33.91	13.67	9.65
60	0.25	5	50	55.52	15.20	5.14	3.71
60	0.25	9	50	87.37	34.20	12.53	6.75
60	0.25	5	100	55.92	13.80	3.97	2.58
60	0.25	9	100	83.69	33.17	8.46	4.96
60	0.25	5	150	47.11	11.44	2.40	1.44
60	0.25	9	150	78.60	38.12	6.11	3.09
60	0.5	5	0	60.28	15.07	6.10	2.60
60	0.5	9	0	91.30	32.74	13.67	9.83
60	0.5	5	50	58.54	16.27	5.88	4.19
60	0.5	9	50	80.91	32.05	12.20	6.68
60	0.5	5	100	57.38	15.72	4.03	2.93
60	0.5	9	100	82.04	25.00	10.76	4.40
60	0.5	5	150	46.17	8.89	1.56	1.15
60	0.5	9	150	75.70	24.73	5.42	2.83
60	1	5	0	39.09	29.13	5.42	2.22
60	1	9	0	50.28	39.57	15.21	6.71
60	1	5	50	41.25	25.30	8.11	3.79
60	1	9	50	51.49	37.76	14.85	7.01
60	1	5	100	37.42	20.44	6.91	4.02
60	1	9	100	52.11	37.42	11.27	5.72
60	1	5	150	34.25	10.71	5.15	4.31
60	1	9	150	52.53	16.58	6.53	3.89

Table (5.25) total heat fluxes /kWm^{-2} at different positions and conditions for the open base, line burner in the centre of the channel, 140 mm wall separation, EU tests

				height /mm			
separation /mm	blockage ratio	propane flow rate /l/min	dist. across wall /mm	108	308	508	708
140	0	5	0	7.57	2.42	1.68	1.57
140	0	9	0	13.51	5.52	4.18	3.14
140	0	5	50	7.75	2.77	1.25	1.16
140	0	9	50	14.65	6.01	3.26	1.79
140	0	5	100	7.47	2.56	0.87	0.82
140	0	9	100	13.92	5.99	2.85	1.42
140	0	5	150	6.82	1.53	0.28	0.31
140	0	9	150	12.75	4.51	2.02	0.66
140	0.25	5	0	6.90	2.44	2.01	1.87
140	0.25	9	0	13.09	6.18	4.61	3.51
140	0.25	5	50	6.59	2.71	1.95	1.95
140	0.25	9	50	13.89	6.76	4.27	2.64
140	0.25	5	100	6.68	2.60	1.07	1.18
140	0.25	9	100	13.65	6.18	3.45	1.89
140	0.25	5	150	6.32	2.02	0.74	0.80
140	0.25	9	150	12.51	4.24	2.01	1.14
140	0.5	5	0	5.93	3.30	2.15	2.23
140	0.5	9	0	11.03	4.26	3.66	3.58
140	0.5	5	50	6.06	3.04	2.31	2.17
140	0.5	9	50	11.05	5.02	3.91	3.31
140	0.5	5	100	5.94	2.20	1.68	1.55
140	0.5	9	100	11.08	5.79	3.13	2.40
140	0.5	5	150	5.95	1.78	0.76	0.79
140	0.5	9	150	11.21	3.86	1.61	1.26
140	1	5	0	3.85	1.60	1.23	1.32
140	1	9	0	6.16	2.95	2.15	2.10
140	1	5	50	3.47	1.65	1.31	1.45
140	1	9	50	5.71	2.90	2.36	1.87
140	1	5	100	3.39	1.92	1.23	1.47
140	1	9	100	5.60	3.06	2.30	2.25
140	1	5	150	3.42	1.59	1.35	1.42
140	1	9	150	5.94	2.91	2.41	2.09

Table (5.26) total heat fluxes /kWm^{-2} at different positions and conditions for the open base, line burner in the centre of the channel, 100 mm wall separation, EU tests

				height /mm			
separation /mm	blockage ratio	propane flow rate /l/min	dist. across wall /mm	108	308	508	708
100	0	5	0	10.19	4.67	2.85	3.09
100	0	9	0	19.41	9.37	5.31	4.98
100	0	5	50	10.18	4.41	2.78	2.75
100	0	9	50	19.99	8.39	5.03	4.27
100	0	5	100	10.17	3.48	1.84	1.97
100	0	9	100	19.77	7.46	3.96	3.28
100	0	5	150	9.25	2.85	0.99	1.30
100	0	9	150	18.39	6.41	2.28	1.97
100	0.25	5	0	10.07	2.87	2.58	2.88
100	0.25	9	0	22.18	10.21	5.85	5.20
100	0.25	5	50	10.35	4.54	2.73	2.86
100	0.25	9	50	22.99	9.65	5.54	4.61
100	0.25	5	100	9.87	4.97	1.87	1.90
100	0.25	9	100	23.34	8.07	4.25	3.34
100	0.25	5	150	9.40	2.40	0.50	0.78
100	0.25	9	150	21.51	7.31	2.29	1.88
100	0.5	5	0	10.52	5.54	2.88	3.39
100	0.5	9	0	20.27	9.22	4.99	4.88
100	0.5	5	50	10.48	4.39	2.81	2.77
100	0.5	9	50	19.71	8.34	5.02	4.26
100	0.5	5	100	9.26	2.74	1.63	1.73
100	0.5	9	100	19.35	6.46	3.94	3.10
100	0.5	5	150	9.13	2.91	0.77	1.12
100	0.5	9	150	18.75	6.68	2.00	1.78
100	1	5	0	4.02	2.80	1.34	1.97
100	1	9	0	7.54	5.03	2.68	2.98
100	1	5	50	3.46	1.76	1.23	1.67
100	1	9	50	7.17	3.16	2.29	2.88
100	1	5	100	3.91	1.48	1.14	1.83
100	1	9	100	6.50	2.93	2.62	2.61
100	1	5	150	3.59	1.63	0.97	1.63
100	1	9	150	6.61	2.35	2.05	2.65

Table (5.27) total heat fluxes /kWm^{-2} at different positions and conditions for the open base, line burner in the centre of the channel, 60 mm wall separation, EU tests

				height /mm			
separation /mm	blockage ratio	propane flow rate /l/min	dist. across wall /mm	108	308	508	708
60	0	5	0	16.80	9.36	5.90	4.40
60	0	9	0	35.71	18.44	11.95	8.65
60	0	5	50	15.96	7.90	5.54	3.46
60	0	9	50	35.10	18.03	10.17	6.66
60	0	5	100	15.11	6.57	3.51	2.47
60	0	9	100	34.19	18.12	7.44	4.61
60	0	5	150	14.41	6.12	2.03	1.16
60	0	9	150	33.55	11.62	4.05	2.62
60	0.25	5	0	12.23	4.68	4.57	4.73
60	0.25	9	0	30.63	15.26	9.56	8.42
60	0.25	5	50	12.83	6.47	4.40	3.87
60	0.25	9	50	30.59	14.96	6.54	6.15
60	0.25	5	100	12.67	5.74	2.96	2.55
60	0.25	9	100	30.78	14.08	7.00	4.46
60	0.25	5	150	11.19	4.93	1.22	1.23
60	0.25	9	150	28.36	12.40	3.76	2.35
60	0.5	5	0	14.26	6.30	5.33	5.35
60	0.5	9	0	30.11	14.29	10.17	8.95
60	0.5	5	50	13.64	6.73	5.20	4.95
60	0.5	9	50	28.18	14.54	9.71	8.04
60	0.5	5	100	13.67	4.99	3.90	3.41
60	0.5	9	100	28.74	12.34	7.89	5.41
60	0.5	5	150	12.86	4.98	1.88	1.72
60	0.5	9	150	28.57	11.83	4.71	2.98
60	1	5	0	6.68	2.61	2.51	2.79
60	1	9	0	14.06	4.71	4.41	4.19
60	1	5	50	6.90	2.41	1.81	3.07
60	1	9	50	13.80	4.27	3.68	4.37
60	1	5	100	6.80	2.91	2.01	2.92
60	1	9	100	13.45	5.11	4.21	4.80
60	1	5	150	6.78	1.69	1.96	2.99
60	1	9	150	12.40	3.31	3.31	4.21

Table (5.28) total heat fluxes /kWm^{-2} at different positions and conditions for the closed base, line burner against instrumented wall, 140 mm wall separation, EU tests

				height /mm			
separation /mm	blockage ratio	propane flow rate /l/min	dist. across wall /mm	108	308	508	708
140	0	5	0	37.83	13.18	2.91	2.21
140	0	9	0	47.69	26.36	7.65	5.01
140	0	5	50	38.62	10.43	3.39	2.42
140	0	9	50	46.99	21.81	7.93	3.98
140	0	5	100	35.89	8.94	2.71	1.89
140	0	9	100	45.85	18.88	6.14	3.39
140	0	5	150	27.33	4.98	1.71	1.28
140	0	9	150	45.36	10.24	3.11	1.98
140	0.25	5	0	42.63	12.30	4.37	1.67
140	0.25	9	0	56.09	19.76	7.18	3.76
140	0.25	5	50	41.91	9.55	3.26	1.52
140	0.25	9	50	56.44	17.17	6.95	3.54
140	0.25	5	100	39.17	9.06	3.95	1.35
140	0.25	9	100	53.81	16.20	6.17	2.69
140	0.25	5	150	34.94	6.19	2.29	0.38
140	0.25	9	150	50.18	14.75	4.53	1.78
140	0.5	5	0	30.08	6.11	2.79	2.22
140	0.5	9	0	50.84	12.96	5.07	3.60
140	0.5	5	50	29.90	6.79	2.29	1.49
140	0.5	9	50	50.46	11.61	5.01	2.77
140	0.5	5	100	29.23	6.78	1.74	1.03
140	0.5	9	100	46.98	11.96	3.50	1.76
140	0.5	5	150	27.86	3.57	0.87	0.54
140	0.5	9	150	44.97	9.58	2.54	1.12
140	1	5	0	35.39	8.13	2.78	2.20
140	1	9	0	63.12	27.14	10.95	4.46
140	1	5	50	32.28	7.75	2.66	1.75
140	1	9	50	60.58	23.59	7.81	3.83
140	1	5	100	31.73	7.14	2.46	1.19
140	1	9	100	58.98	21.56	7.41	4.49
140	1	5	150	33.71	5.96	1.74	1.86
140	1	9	150	55.47	20.87	7.45	5.40

Table (5.29) total heat fluxes /kWm^{-2} at different positions and conditions for the closed base, line burner against instrumented wall, 100 mm wall separation, EU tests

				height /mm			
separation /mm	blockage ratio	propane flow rate /l/min	dist. across wall /mm	108	308	508	708
100	0	5	0	42.86	14.34	5.60	3.57
100	0	9	0	56.03	30.80	11.06	6.20
100	0	5	50	40.69	15.11	6.02	3.39
100	0	9	50	55.63	27.38	9.61	4.84
100	0	5	100	39.10	9.17	3.95	1.35
100	0	9	100	55.86	16.29	5.90	3.57
100	0	5	150	26.42	4.72	1.93	0.45
100	0	9	150	49.39	9.45	3.49	1.91
100	0.25	5	0	39.64	11.48	4.14	3.56
100	0.25	9	0	59.20	20.79	8.09	5.75
100	0.25	5	50	38.10	10.64	4.46	3.05
100	0.25	9	50	59.06	20.14	8.24	4.97
100	0.25	5	100	37.27	10.27	3.20	2.00
100	0.25	9	100	56.01	19.68	6.88	3.40
100	0.25	5	150	35.61	5.95	0.99	0.89
100	0.25	9	150	56.21	14.56	3.82	2.14
100	0.5	5	0	37.29	9.26	3.87	2.81
100	0.5	9	0	59.80	15.26	7.24	4.97
100	0.5	5	50	33.97	8.86	2.48	1.61
100	0.5	9	50	57.99	16.79	5.52	3.30
100	0.5	5	100	29.58	4.88	1.21	0.91
100	0.5	9	100	53.85	12.79	4.13	1.92
100	0.5	5	150	22.37	2.94	0.55	0.56
100	0.5	9	150	51.78	9.13	2.28	1.12
100	1	5	0	47.09	14.51	6.37	4.14
100	1	9	0	74.39	33.62	13.00	6.94
100	1	5	50	45.37	14.88	5.19	3.14
100	1	9	50	71.31	29.97	11.69	6.14
100	1	5	100	41.80	12.31	3.78	2.47
100	1	9	100	71.83	28.27	10.32	5.33
100	1	5	150	38.80	9.84	3.25	2.70
100	1	9	150	69.02	22.64	8.41	5.27

Table (5.30) total heat fluxes /kWm^{-2} at different positions and conditions for the closed base, line burner against instrumented wall, 60 mm wall separation, EU tests

				height /mm			
separation /mm	blockage ratio	propane flow rate /l/min	dist. across wall /mm	108	308	508	708
60	0	5	0	62.73	24.64	10.31	7.03
60	0	9	0	93.25	51.59	20.58	12.66
60	0	5	50	56.72	19.72	8.20	5.40
60	0	9	50	89.26	44.71	17.47	8.38
60	0	5	100	46.27	13.03	5.03	3.38
60	0	9	100	73.33	27.16	10.32	5.27
60	0	5	150	34.43	6.97	2.86	2.20
60	0	9	150	66.08	15.86	5.50	2.90
60	0.25	5	0	59.96	22.19	8.50	6.03
60	0.25	9	0	92.48	49.64	17.53	10.49
60	0.25	5	50	53.88	16.70	5.86	3.42
60	0.25	9	50	93.70	33.31	12.55	6.19
60	0.25	5	100	49.60	9.30	2.21	1.58
60	0.25	9	100	83.31	20.41	5.75	3.00
60	0.25	5	150	42.53	4.89	0.99	0.87
60	0.25	9	150	76.78	12.39	3.17	1.50
60	0.5	5	0	66.09	19.20	6.42	4.00
60	0.5	9	0	91.93	41.25	15.59	9.27
60	0.5	5	50	60.49	10.84	3.36	1.86
60	0.5	9	50	91.32	25.53	9.57	4.79
60	0.5	5	100	46.18	6.21	1.15	0.81
60	0.5	9	100	79.77	16.86	4.85	2.12
60	0.5	5	150	31.59	3.35	0.35	0.40
60	0.5	9	150	63.53	9.67	2.22	1.07
60	1	5	0	55.30	16.05	5.16	3.11
60	1	9	0	100.80	49.25	15.25	7.21
60	1	5	50	54.30	15.76	4.63	2.84
60	1	9	50	100.88	48.73	14.63	6.05
60	1	5	100	46.14	15.41	4.89	2.92
60	1	9	100	96.68	45.93	15.33	6.21
60	1	5	150	46.73	13.41	5.65	3.06
60	1	9	150	92.47	28.69	10.51	4.89

Table (5.31) total heat fluxes /kWm^{-2} at different positions and conditions for the closed base, line burner in the centre of the channel, 140 mm wall separation, EU tests

				height /mm			
separation /mm	blockage ratio	propane flow rate /l/min	dist. across wall /mm	108	308	508	708
140	0	5	0	11.54	5.48	2.82	2.49
140	0	9	0	21.01	10.45	5.17	4.07
140	0	5	50	11.76	3.62	1.66	1.84
140	0	9	50	22.07	8.11	3.70	3.10
140	0	5	100	10.19	2.29	0.88	1.08
140	0	9	100	20.49	5.89	2.33	1.94
140	0	5	150	9.12	1.83	0.30	0.59
140	0	9	150	18.00	4.55	1.49	1.19
140	0.25	5	0	12.36	6.06	3.18	2.84
140	0.25	9	0	21.38	10.57	5.68	4.21
140	0.25	5	50	11.66	4.10	2.05	1.87
140	0.25	9	50	21.49	8.49	3.87	2.98
140	0.25	5	100	10.92	2.66	1.13	1.27
140	0.25	9	100	20.27	5.97	2.32	1.98
140	0.25	5	150	9.61	1.63	0.38	0.65
140	0.25	9	150	17.61	4.18	1.36	1.10
140	0.5	5	0	16.69	6.62	3.45	2.60
140	0.5	9	0	28.95	12.46	6.56	4.35
140	0.5	5	50	15.99	4.92	2.42	1.46
140	0.5	9	50	28.08	10.07	4.70	3.33
140	0.5	5	100	14.02	2.99	1.22	0.93
140	0.5	9	100	25.34	6.81	2.79	2.18
140	0.5	5	150	11.38	2.17	0.59	0.69
140	0.5	9	150	20.24	4.91	1.51	1.24
140	1	5	0	14.47	6.09	2.34	2.41
140	1	9	0	37.30	15.96	8.03	4.60
140	1	5	50	15.98	5.34	3.05	2.51
140	1	9	50	32.75	14.02	7.32	4.38
140	1	5	100	15.58	6.45	3.13	2.53
140	1	9	100	30.22	15.43	7.40	4.65
140	1	5	150	13.40	4.11	2.99	2.19
140	1	9	150	29.49	12.07	5.64	3.94

Table (5.32) total heat fluxes /kWm^{-2} at different positions and conditions for the closed base, line burner in the centre of the channel, 100 mm wall separation, EU tests

				height /mm			
separation /mm	blockage ratio	propane flow rate /l/min	dist. across wall /mm	108	308	508	708
100	0	5	0	17.52	7.26	4.35	3.64
100	0	9	0	35.69	16.04	8.43	6.13
100	0	5	50	15.96	6.17	3.35	2.74
100	0	9	50	33.93	12.70	6.53	4.56
100	0	5	100	14.70	3.36	1.80	1.92
100	0	9	100	30.64	8.60	3.61	2.67
100	0	5	150	12.29	1.99	0.50	0.85
100	0	9	150	26.33	5.99	1.88	1.34
100	0.25	5	0	20.49	9.83	5.26	3.80
100	0.25	9	0	38.26	18.41	8.99	6.38
100	0.25	5	50	20.29	7.42	3.82	2.49
100	0.25	9	50	36.04	14.21	6.33	4.53
100	0.25	5	100	17.02	3.86	1.51	1.73
100	0.25	9	100	32.64	9.01	3.44	2.79
100	0.25	5	150	14.51	2.35	0.48	0.93
100	0.25	9	150	27.54	6.10	1.70	1.29
100	0.5	5	0	22.01	8.64	4.52	3.48
100	0.5	9	0	45.82	19.08	9.08	5.85
100	0.5	5	50	20.79	6.21	2.64	2.26
100	0.5	9	50	41.73	14.37	6.39	4.16
100	0.5	5	100	18.31	3.68	1.35	1.34
100	0.5	9	100	37.11	10.24	3.71	2.51
100	0.5	5	150	15.91	2.35	0.47	0.73
100	0.5	9	150	31.76	6.73	2.18	1.45
100	1	5	0	33.28	11.50	5.43	3.62
100	1	9	0	60.55	27.04	13.09	6.71
100	1	5	50	32.66	11.43	5.03	3.34
100	1	9	50	58.05	25.22	12.27	6.37
100	1	5	100	29.08	9.98	4.31	3.26
100	1	9	100	53.96	23.05	10.88	5.91
100	1	5	150	28.38	8.46	3.77	2.85
100	1	9	150	46.42	23.51	9.25	5.38

Table (5.33) total heat fluxes /kWm^{-2} at different positions and conditions for the closed base, line burner in the centre of the channel, 60 mm wall separation, EU tests

				height /mm			
separation /mm	blockage ratio	propane flow rate /l/min	dist. across wall /mm	108	308	508	708
60	0	5	0	46.21	17.85	9.17	6.54
60	0	9	0	77.50	40.41	20.68	13.57
60	0	5	50	40.43	12.27	6.43	5.17
60	0	9	50	75.86	31.52	14.70	9.65
60	0	5	100	30.82	8.05	3.40	3.23
60	0	9	100	63.99	21.97	8.60	5.62
60	0	5	150	26.82	5.11	1.47	1.48
60	0	9	150	54.93	4.79	4.79	3.00
60	0.25	5	0	48.53	20.77	10.20	7.39
60	0.25	9	0	87.30	42.27	20.41	12.96
60	0.25	5	50	40.62	11.86	6.10	3.97
60	0.25	9	50	76.83	34.24	14.98	9.04
60	0.25	5	100	33.62	7.62	3.28	2.45
60	0.25	9	100	65.94	19.98	7.37	4.37
60	0.25	5	150	26.61	3.71	0.89	0.66
60	0.25	9	150	59.51	11.42	3.52	2.16
60	0.5	5	0	61.52	19.19	7.94	5.51
60	0.5	9	0	102.68	48.43	20.13	12.22
60	0.5	5	50	42.99	11.88	4.53	3.32
60	0.5	9	50	83.04	30.64	11.96	6.45
60	0.5	5	100	36.78	7.12	2.01	1.84
60	0.5	9	100	72.26	19.04	5.77	3.28
60	0.5	5	150	27.63	2.99	0.32	0.56
60	0.5	9	150	62.08	10.64	2.64	1.57
60	1	5	0	58.38	16.17	5.87	4.10
60	1	9	0	100.26	40.60	12.96	6.58
60	1	5	50	54.26	16.18	6.19	4.18
60	1	9	50	94.53	38.11	11.77	6.20
60	1	5	100	43.45	14.61	5.37	4.08
60	1	9	100	87.14	30.59	10.05	5.33
60	1	5	150	42.64	12.12	4.73	3.45
60	1	9	150	82.52	24.01	7.84	4.38

5.3 Smoke Tests

5.3.1 The EU Smoke Tests

Table (5.34) gives the smoke results from Cone Calorimeter tests on black PMMA, table (5.35) gives the cone results for CMHR polyurethane foam, the hexane cone test results are shown in table (5.36) and the solid/liquid fuel composite results are in table (5.37). PMMA test results from the ignitability apparatus in the some box are shown in table (5.38), those for CMHR PUF are in table (5.39) and table (5.40) gives the smoke results for hexane in the smoke box test.

5.3.1.1 Cone Calorimeter Measurements

The results shown are the average of three tests which were are carried out according to the standard (ASTM, 1990), except where the smaller sample size is used; in this case the sample holder is the one from the EU ignitability apparatus, and for the hexane tests where a petri dish is used, as described in Chapter 4. Apart from these differences, everything else is performed according to the standard.

5.3.1.1.1 PMMA Tests

Table (5.34) - Specific extinction area /m^2kg^{-1} for black PMMA tests in the Cone Calorimeter

	sample size and frame condition		
imposed irradiance /kWm^{-2}	100 cm^2, no edge frame	100 cm^2, edge frame	(65 mm)^2, edge frame
30	104.1	107.6	135.2
25	-	98.8	128.9
20	106.2	88.3	126.2
15	104.9	90.9	115.3

5.3.1.1.2 PUF Tests

Table (5.35) - Specific extinction area /m^2kg^{-1} for CMHR polyurethane foam tests in the Cone Calorimeter with an edge frame

imposed irradiance //kWm^{-2}	SEA /m^2kg^{-1}
30	188.2
27.5	194.3
25	196.6
22	176.3
20	143.7

5.3.1.1.3 Hexane Tests

The results given below are the average of five tests, with the standard deviation given in brackets. No external irradiance is used.

Table (5.36) - Specific extinction area /m^2kg^{-1} for hexane tests in the Cone Calorimeter for different heat and sample positions. The sample is always tested in the horizontal orientation.

heater position	SEA /m^2kg^{-1}
horizontal, 65 mm above sample	101.9(4.17)
horizontal, 25 mm above sample	105.8(5.56)
vertical	127.5(4.72)
vertical, doors open	131.7(1.56)
removed completely	135.1(1.13)

5.3.1.1.4 Solid with Liquid Fuel Tests

The results given in table (5.37) are the average of five tests, with the standard deviation given in brackets.

Table (5.37) - specific extinction area /m^2kg^{-1} for the solid and liquid fuel tests with and without heater in the Cone Calorimeter

Fuel	heater position	SEA /m^2kg^{-1}
PMMA + methanol	removed	36.9(2.00)
PMMA + methanol	horizontal, 25 mm above sample	37.6(2.73)
polystyrene + hexane	removed	1153.8(27.40)
polystyrene + hexane	horizontal, 25 mm above sample	1099.7(48.33)

5.3.1.2 The Smoke Box Tests

Results from the smoke tests using the ignitability apparatus in the smoke chamber are given in tables (5.38) to (5.40). The values shown are the average of three tests, calculated from the maximum values of $\log(V_0/V)$ recorded during a test.

5.3.1.2.1 PMMA Tests

Table (5.38) - specific extinction area /m^2kg^{-1} for black PMMA tested under different irradiances, smoke box tests

imposed irradiance /kWm^{-2}	SEA /m^2kg^{-1}
30	179.6
25	171.1
20	145.9
15	141.8

5.3.1.2.2 PUF Tests

Table (5.39) - specific extinction area /m^2kg^{-1} for CMHR polyurethane foam tested under different irradiances, smoke box tests

imposed irradiance /kWm^{-2}	SEA /m^2kg^{-1}
30	203.8
25	177.2
20	148.9

5.3.1.2.3 Hexane Tests

These were carried out with no external irradiance. The sample and heater were always in the horizontal position.

Table (5.40) specific extinction area /m^2kg^{-1} for hexane tested at different sample positions, smoke box tests

sample position	SEA /m^2kg^{-1}
98 mm below heater	50.7
65 mm below heater	52.7
25 mm below heater	33.9
on floor of chamber	80.5

5.3.2 The Buxton Smoke Tests

5.3.2.1 Cone Calorimeter Tests

These tests were carried out according to the standard (ASTM, 1990). The values given for average specific extinction area are the average values over three tests. The foam types corresponding to the given letters are shown in Chapter 4. Table (5.41) gives the results for the more detailed, and preliminary tests done with CMHR foam, table (5.42) shows the results for all the foams.

Table (5.41) - average SEA /m^2kg^{-1} for CMHR under different irradiance levels in the Cone Calorimeter

imposed irradiance /kWm^{-2}	average SEA /m^2kg^{-1}
50	232.6
40	206.9
35	205.5
30	188.2
27.5	194.3
25	196.6
22	176.3
20	143.1
18.5	162.5
17	148.3
16	145.7
15	133.5

Table (5.42) - average SEA /m^2kg^{-1} for each foam under different irradiance levels in the Cone Calorimeter

	imposed irradiance /kWm^{-2}				
Foam	50	40	30	20	15
A	236.3	230.5	227.3	735.9*	605.1*
B	282.6	273.7	282.3	236.6	1173.7*
C	203.2	197.1	183.6	176.1	154.2
D	317.9	303.7	289.0	240.3	247.1
E	389.6	406.9	388.1	358.8	327.5
F	285.1	266.8	248.4	212.1	183.5
G	232.6	206.9	188.2	176.3	133.5

where * denotes no ignition

Table (5.43) - peak SEA /m^2kg^{-1} for each foam under different irradiance levels in the Cone Calorimeter

	imposed irradiance /kWm^{-2}				
Foam	50	40	30	20	15
A	236.3	230.5	227.3	735.9*	605.1*
B	282.6	273.7	282.3	236.6	1173.7*
C	203.2	197.1	183.6	176.1	154.2
D	317.9	303.7	289.0	240.3	247.1
E	389.6	406.9	388.1	358.8	327.5
F	285.1	266.8	248.4	212.1	183.5
G	232.6	206.9	188.2	176.3	133.5

Table (5.44) - total smoke, D_0 /m^3ODm1/kg, for each foam under different irradiance levels in the Cone Calorimeter

	imposed irradiance /kWm^{-2}				
Foam	50	40	30	20	15
A	104.68	102.12	115.49	330.55*	272.34*
B	127.51	123.02	124.84	174.75	526.22*
C	90.37	85.81	82.76	78.66	67.82
D	140.18	136.15	128.32	105.11	94.39
E	172.94	177.21	170.79	155.67	141.98
F	125.99	118.34	108.98	93.27	152.21
G	104.55	90.17	82.09	63.70	81.08

Table (5.45) - rate of rate of smoke production, (D_0/s^2) x 1000, m^3ODm1/kgs^2, for each foam under different irradiance levels in the Cone Calorimeter

	imposed irradiance /kWm^{-2}				
Foam	50	40	30	20	15
A	.447	.172	.118	.015	.012
B	.481	.390	.353	.054	.011
C	.631	.539	.659	.631	.388
D	.292	.425	.383	.296	.141
E	.578	.387	.316	.206	.369
F	.856	.314	.279	.268	.072
G	.240	.190	.223	.166	.090

5.3.2.2 HSE Medium Scale Tests

Table (5.46) total smoke, m^3ODm1, total smoke per kg, m^3ODm1/kg, total before ventilation controlled burning or peak, m^3ODm1, early rate of rate of smoke production and rate of rate of smoke production up to ventilation control or peak, m^3ODm1/s^2

Foam	total smoke	total smoke per kg	pre-vent smoke	early rate of rise /10^{-3}	rate of rise to vent. /10^{-3}
A	1444.69	267.61	243.84	0.5	13.6
B	2066.00	355.63	76.87	5.1	61.8
C	2043.25	427.68	210.64	29.1	134.6
D	1870.16	350.35	81.78	4.2	130.3
E	2176.71	427.52	350.86	5.8	70.8
F	1176.30	230.73	374.90	14.7	74.3
G(2)	70.41	116.38	40.62	1.9	6.9

5.4 Other Hazard Assessment Methods

Tables (5.47) - (5.50) show results from tests on the set of foams given in table (4.10).

5.4.1 Cone Calorimeter Tests

Table (5.47) - Results of time to ignition (t_{ig}) /s, rates of heat release (RHR), peak and average /kWm^{-2}, and time to peak RHR under various imposed irradiance levels ($\dot{q}''$) for the CMHR preliminary tests. Each result is the average of at least three tests, with the standard deviation for the av. RHR shown in brackets.

$\dot{q}''$ /kWm^{-2}	t_{ig}/s	av. RHR /kWm^{-2}	repeatability of av. RHR	peak RHR /kWm^{-2}	time to peak RHR /kWm^{-2}
50	3.0	141.2(25.0)	70.0	460.2	56.7
40	3.0	154.4(61.8)	173.1	425.1	60.0
35	6.0	101.0(17.1)	47.7	372.3	58.0
30	3.0	130.5(27.6)	77.4	480.6	55.7
27.5	5.3	123.0(8.3)	23.3	354.3	49.3
25	6.7	71.2(8.8)	24.6	345.7	49.3
22	6.0	111.8(26.4)	73.4	335.2	54.7
20	7.7	111.0(3.6)	10.1	408.5	65.0
18.5	7.7	93.5(4.1)	11.4	305.3	56.0
17	9.3	93.1(24.2)	67.7	380.9	76.0
16	9.7	103.0(37.6)	105.4	364.0	84.7
15	11.0	102.4(32.4)	90.8	382.5	74.5

Table (5.48) - Results of time to ignition (t_{ig}) /s, rates of heat release (RHR), peak and average /kWm^{-2}, and time to peak RHR under various imposed irradiance levels ($\dot{q}''$) in the Cone Calorimeter

$\dot{q}''$ /kWm^{-2}	Foam	t_{ig}/s	av. RHR /kWm^{-2}	peak RHR /kWm^{-2}	time to peak RHR /kWm^{-2}
50	A	5.3	151.6	455.9	71.7
50	B	5.0	141.5	497.9	40.0
50	C	2.3	184.9	564.9	48.3
50	D	3.7	164.6	528.4	40.0
50	E	3.7	179.2	712.7	51.7
50	F	4.3	185.2	478.3	285.1
50	G	3.0	141.2	460.2	56.7
40	A	6.7	147.0	428.1	81.7
40	B	6.0	145.0	463.6	50.0
40	C	3.0	148.1	438.1	53.3
40	D	6.3	156.2	458.4	56.7
40	E	5.7	172.8	525.5	60.0
40	F	5.0	160.8	424.7	65.0
40	G	3.0	154.4	425.1	60.0
30	A	46.7	133.6	381.0	103.3
30	B	7.7	134.7	390.6	65.0
30	C	5.0	153.2	431.8	70.0
30	D	6.0	129.6	406.4	60.0
30	E	7.0	173.1	425.5	61.7
30	F	5.3	165.7	408.7	80.0
30	G	3.0	130.5	480.6	55.7
20	A	NI	1.0	3.7	5.0
20	B	177.3	130.6	400.4	200
20	C	6.0	135.7	405.5	66.7
20	D	6.0	125.2	356.1	61.7
20	E	8.3	125.4	362.7	78.3
20	F	8.3	126.3	379.3	58.3
20	G	7.7	111.0	408.5	65.0
15	A	NI	0.4	3.2	5.0
15	B	NI	0.6	4.6	5.0
15	C	9.0	112.9	360.3	61.7
15	D	11.0	91.2	234.3	68.3
15	E	12.0	144.2	414.5	75.0
15	F	21.0	108.1	371.3	90.0
15	G	11.0	102.4	382.5	74.5

Table (5.49) fire growth calculated values for Cone Calorimeter tests: rate of rate of heat release from ignition to peak heat release rate /kW/s, time from ignition to peak, /s, fire growth coefficient, α_f (see Chapter 6 for details),/kW/s^2

$\dot{q}$"/kWm^{-2}	Foam	RRHR/kWs^{-1}	t/s	α_f/kW/s^2
50	A	555.45	70	7.935
50	B	1174.16	35	33.547
50	C	1053.10	45	23.402
50	D	1063.22	35	30.378
50	E	1034.97	50	20.699
50	F	868.33	35	24.81
50	G	842.48	41	20.548
40	A	464.74	75	6.196
40	B	772.18	45	17.160
40	C	885.72	45	19.683
40	D	700.02	60	11.667
40	E	717.60	55	13.047
40	F	613.65	55	11.157
40	G	630.75	52	12.130
30	A	197.34	105	1.879
30	B	500.68	65	7.703
30	C	625.79	60	10.430
30	D	570.54	55	10.373
30	E	588.24	60	9.804
30	F	424.80	80	5.310
30	G	552.68	60	9.211
20	A	*	*	*
20	B	36.28	210	0.1728
20	C	508.06	65	7.816
20	D	425.98	60	7.100
20	E	504.34	55	9.170
20	F	438.09	60	7.302
20	G	388.87	64	6.076
15	A	*	*	*
15	B	*	*	*
15	C	460.94	55	8.381
15	D	185.87	85	2.187
15	E	408.36	70	5.834
15	F	76.17	85	0.896
15	G	152.09	77	1.975

Table (5.50) CO/CO_2 values for Cone Calorimeter tests: peak, average over test, and rate of rise from ignition to peak. All values are based on a volumetric ratio

$\dot{q}''$/kWm^{-2}	Foam	av. CO/CO_2	peak CO/CO_2	rate of rise/s
50	A	0.1268	0.4221	0.00146
50	B	0.2529	0.3100	0.00090
50	C	0.0290	0.2067	0.02111
50	D	0.1249	0.4902	0.04770
50	E	0.0898	0.2806	0.02137
50	F	0.1416	0.4404	0.03995
50	G	0.0630	0.6425	0.05904
40	A	0.2098	0.9043	0.00304
40	B	0.3764	1.2123	0.00413
40	C	0.0402	0.1866	0.00033
40	D	0.1057	0.5782	0.00222
40	E	0.1185	0.3725	0.00148
40	F	0.0988	0.4388	0.00174
40	G	0.0307	0.3864	0.02926
30	A	0.1746	1.3002	0.00447
30	B	0.3898	2.4202	0.00855
30	C	0.0259	0.2792	0.02293
30	D	0.0935	0.4348	0.00148
30	E	0.1449	0.0317	0.00163
30	F	0.0402	0.3611	0.03474
30	G	0.0296	0.5714	0.05172
20	A	0.2091	0.3022	0.00031
20	B	0.1090	0.4735	0.00109
20	C	0.0182	0.1514	0.01266
20	D	0.0164	0.1115	0.00654
20	E	0.0260	0.1359	0.00613
20	F	0.0646	0.2859	0.01063
20	G	0.0384	0.4303	0.02793
15	A	0.0599	0.0784	0.00029
15	B	0.0376	0.0719	0.00011
15	C	0.0241	0.0923	0.00306
15	D	0.0167	0.1155	0.00511
15	E	0.0175	0.1067	0.00467
15	F	0.2040	0.3298	0.00050
15	G	0.0305	0.0967	0.00265

5.4.2 BS 5852

Part 1 of the test, (BSI, 1979), in which a mock-up of a seat and back is subjected to ignition by a smouldering cigarette, showed that none of the uncovered foams would ignite with this ignition source. The results for Part 2 of the test are shown in table (5.51).

Table (5.51) results of BS 5852 part 2 for set of foams

	ignition source				
Foam	crib 4	crib 5	crib 6	crib 7	ranking
A	pass	pass	fail		4
B	pass	pass	pass	fail	1=
C	fail	fail			5=
D	pass	pass	pass	fail	1=
E	fail	fail			5=
F	pass	pass	pass	fail	1=

where pass = two tests, fail = one or two.

Crib 7: D and F failed on the basis of lateral spread of flame, although flames self-extinguished within 13 min. B continued to burn beyond 13 minutes

5.4.3 HSE Medium Scale Tests

Continuous measurements were made of oxygen, carbon dioxide, carbon monoxide, mass loss, and various temperatures. For the majority of tests temperature was recorded at the vent (between the corridor and the combustion chamber), at the corridor exit, in the duct at the point of gas sampling, and the ambient. For two tests temperature was taken further along in the duct, close to where the smoke was measured. Data for all these are given in tables (5.52) - (5.55)

Table (5.52) CO/CO_2 values for third scale tests: peak ,average over test, early rate of rise (first 30s) and rate of rise from ignition to ventilation control or peak. All values are based on a volumetric ratio and have been multiplied by 10^3

Foam	av. CO/CO_2	peak CO/CO_2	early rate of rise/s	rate of rise/s
A	157.0	328.9	1.40	0.67
B	213.8	423.1	0.92	1.16
C	217.0	715.9	3.18	1.23
D	307.2	712.0	1.17	1.51
E	199.6	461.3	0.84	1.04
F	165.3	326.0	0.58	0.50
G	14.8	30.6	0.80	0.35

Table (5.53) -temperature measurements in third scale tests; T_a is ambient temperature, T_2 is the temperature in the duct at the gas sampling point, T_3 is the corridor exit temperature and T_4 is the vent temperature. All values are given in degrees Celsius and rates of temperature rise are in ^0C/minute. Times to peak values are in seconds.

	Foam						
	A	B	C	D	E	F	G(2)
T_a	15	19	20	22	17	-	16
av. T_2	19	24	25	24	24	-	16
av. T_3	143	221	230	184	230	-	57
peak T_3	333	353	333	324	343	-	136
t at peak/s	943	662	371	542	603	-	180
av. T_4	384	531	522	432	554	651	127
peak T_4	863	941	814	881	916	863	451
t at peak/s	957	598	364	520	560	528	163
max. rate of T_4 rise on 4s basis	1125	535	998	710	926	664	544
rate of T_4 rise from ign. to vent. cont. or peak	81.84	266.0	292.2	345.1	265.9	196.6	211.8

Table (5.54) -mass loss measurements /kg in third scale tests

Foam	initial mass/kg	total mass loss/kg
A	5.792	5.792
B	5.810	5.810
C	5.271	5.271
D	5.321	5.321
E	5.681	5.681
F	5.591	5.591
G(2)	4.951	0.606

Table (5.55) -rate of heat release values, calculated from oxygen concentration measurements in third scale tests

Foam	av. RHR /kW	av. peak RHR /kW	total HR/mass /MJ/kg	RRHR up to vent. cont. or peak/kWs^{-1}	early RRHR (30s)/kWs^{-1}	α_f /$10^{-2}kWs^{-2}$
A	187.2	247.8	10.44	1.280	3.704	12.345
B	181.4	279.1	23.94	2.697	2.420	8.068
C	257.2	310.8	25.86	4.870	3.039	10.130
D	136.0	273.9	17.10	5.035	3.164	10.546
E	198.7	285.3	26.72	4.072	4.378	14.595
F	179.1	232.3	17.10	2.587	1.568	2.121
G(2)	25.6	67.5	13.94	2.457	2.457	8.190

5.5 Further Investigations

5.5.1 HSE Medium Scale Test

Tests were carried out with parallel rigid polyurethane foam sheets at different separations between the pieces, with different British Standard (BSI, 1982) ignition sources and ignition source duration. Measurements were made of oxygen, CO and CO_2 concentration as well as smoke production rate, mass loss rate and various temperatures. Tables (5.56)-(5.59) give these results.

Table (5.56) - test conditions for rigid polyurethane foam in third scale test

Test no.	separation/mm	ignition source	duration	ignition
rig807	80	7	-	yes
rig807b*	80	7	-	yes
rig804	80	4	-	yes
rig803	80	3	70	no
rig802	80	2	40	no
rig603	60	3	70	no
rig403	40	3	70	yes
rig402	40	2	40	no
rig403t2	40	3	40	yes
rig402t3	40	2	70	no
rig101	10	1	-	no

where * indicates test performed outside the third scale rig

Table (5.57): heat release, temperature, CO/CO_2, and smoke results for rigid foam in third scale test. Rates of heat release measured in kW, rates of increase of heat release in kW/s, total heat release in MJ/kg, rate of smoke production in m^3ODm1/s (m^2/s), rate of increase of smoke production in m^2/s^2, total smoke in m^3ODm1/kg, temperature in ^oC, rates of temperature rise in ^oC/min calculated from ignition to peak, mass loss in kg and mass loss rates in kg/s.

	rig807	rig807b	rig804	rig403	rig403t2
RHR_{peak}	195.23	225.38	174.58	140.71	140.68
$RHR_{avg.}$	41.03	54.45	37.63	30.75	31.79
total HR	12.853	18.892	6.464	6.756	9.026
RRHR	1.695	2.675	3.681	1.337	1.076
smoke prod. rate, peak	7.612	6.767	8.889	7.482	5.465
smoke prod rate, avg.	1.812	1.013	1.309	1.496	1.622
total smoke	441.29	514.30	497.76	440.36	546.25
rate of smoke prod rate/10^{-2}	6.79	16.69	37.90	22.43	15.32
CO/CO_2,peak/10^{-2}	2.10	1.19	2.61	19.58	16.61
CO/CO_2,avg/10^{-2}	1.02	0.43	0.89	6.75	6.28
(rate of rise of CO/CO_2)/10^{-3}	0.813	0.277	1.29	8.16	4.68
vent T,peak	671.8	-	493.5	428.0	362.2
vent T rate of rise	3.081	-	8.654	5.157	4.538
mass loss	1.1766	0.6398	0.6287	0.8967	0.7009
rate of mass loss,peak/10^{-3}	6.7	3.3	6.3	6.2	4.1

Tests were also performed using polyisocyanurate foam (PIR) at a separation of 80 mm with a no. 7 wood crib, as smaller ignition sources did not give rise to ignition. In one test, PIR807c, the samples were placed simply on the false floor of the third scale room, in the others the samples were elevated by 7 cm to provide an air gap beneath the samples. In the first of the elevated tests, PIR807o, the samples fell over during the test, giving a different burning pattern and ruining the mass loss measurements. This was therefore repeated, test PIR807ob. The rate of heat release measurements could not be quantified for this test, as they were small and obscured by the noise of the analyser. All quantities are the same as defined above.

Table (5.58) - smoke, heat release, temperature, CO, CO_2 and mass loss data for polyisocyanurate in third scale tests. Rates of heat release measured in kW, rates of increase of heat release in kW/s, total heat release in MJ/kg, rate of smoke production in m^3ODm1/s (m^2/s), rate of increase of smoke production in m^2/s^2, total smoke in m^3ODm1/kg, temperature in ^oC, rates of temperature rise in ^oC/min calculated from ignition to peak, mass loss in kg and mass loss rates in kg/s.

	PIR807c	PIR807o	PIR807ob
RHR_{peak}	137.90	119.37	106.11
$RHR_{avg.}$	25.44	31.17	-
total HR	4.84	-	-
RRHR	3.704	3.851	-
smoke prod. rate, peak	2.196	1.873	1.973
smoke prod rate,$_{avg.}$ /10^{-2}	35.25	44.42	36.28
total smoke	353.09	-	321.62
rate of smoke prod rate /10^{-2}	0.944	1.517	1.478
$CO/CO_{2,peak}$ /10^{-2}	7.09	1.35	1.362
$CO/CO_{2,avg.}$ /10^{-2}	2.123	0.421	0.356
(rate of rise of CO/CO_2) /10^{-3}	0.289	0.116	0.106
vent T, peak	318.5	318.8	312.5
vent T rate of rise	0.9915	1.1008	1.224
mass loss	0.4502	-	0.4422
rate of mass loss, peak /10^{-3}	1.51	-	1.82

The final set of tests in the HSE third scale room/corridor test was on phenolformaldehyde. No ignition was obtained using a no. 3 source with a separation of 40 mm. With a no. 4 crib at this separation, the material appeared to crumble and smother the crib, preventing ignition. More successful tests were carried out using a no. 7 crib at the 80 mm separation, in both the elevated and floor positions. Only a small amount of the material burned in each case and large amounts crumbled and covered the cribs. Rate of heat release measurements could not be obtained as the oxygen consumption was very low and hidden by the analyser noise. Mass loss measurements were impossible as material was scattered away from the load cells. The actual material behaviour was observed in a test outside the

third scale rig. The elevated test is PHF807o, the closed PHF807c and the outside test is PHF807cb.

Table (5.59) - temperature, smoke and CO/CO_2 data for phenolformaldehyde third scale tests. Rate of smoke production in m^3ODm1/s (m^2/s), rate of increase of smoke production in m^2/s^2, total smoke in m^3ODm1/kg, temperature in ^oC, rates of temperature rise in ^oC/min calculated from ignition to peak.

	PHF807o	PHF807c	PHF807cb
vent T, peak	252.0	153.4	-
rate of vent T rise	0.83	0.43	-
avg. smoke prod. rate/10^{-2}	7.6	1.9	1.6
peak smoke prod. rate/10^{-2}	35.8	10.2	9.1
total smoke /(m^3ODm1)	15.39	6.404	5.733
(rate of rate of smoke prod.)/10^{-3}	2.498	1.152	0.560
CO/CO_2, peak /10^{-2}	8.1	0.8	7.1
CO/CO_2, avg. /10^{-2}	3.6	0.4	2.5
(CO/CO_2,rate of rise) /10^{-3}	0.47	0.04	0.30

Chapter 6

Discussion

6.1 Introduction

For the fire hazard assessment of materials stored in bulk, both the potential behaviour of the materials in a fire and any added hazards from the particular storage conditions must be understood. Fire tests are aimed at developing knowledge of the former, although it is rarely obvious how to use these results to provide insight into the hazards associated with materials. Simply ranking materials on the basis of behaviour in given tests may be misleading. The problem of the specific hazard of certain storage conditions requires non-standard tests aimed at increasing the fundamental understanding of fire science. The research for this project is separated into these two areas; first, an investigation into the problems of fire testing of solid materials, with experiments being carried out using three standard and one non-standard test method with various materials, second, a study of the geometrical conditions which affect both the fire behaviour of materials under tests that employ parallel vertical surfaces and, more importantly, the potential development of a fire in a warehouse.

6.2 Fire Testing of Flammable Solid Materials

To have any understanding of how hazardous a material may be in a fire, testing is essential. Factors such as ease of ignition, flame spread rate, production of smoke and toxic gases, and rates of heat release need to be examined before deciding whether a particular material may be put to a certain usage or stored in a certain way. However, as discussed in Chapter 2, these are not intrinsic properties of a material, but rather they depend upon the fire conditions. The behaviour of a material will change with altered exposure conditions, geometry, scale etc. These general problems with fire testing can be broadly separated into two categories: the test conditions and the material behaviour. In the first category, a specific test provides a

specific set of conditions under which a material will be tested. As these conditions vary between tests, so the reaction of a sample will also vary, and the results from different tests will lead to different conclusions about the hazardous nature of a material, as was demonstrated by Emmons (1974). The second category deals with how material behaviour can render the results from a test meaningless, for example by acting in such a way as to alter the exposure conditions. Some tests have provisions for dealing with unusual behaviour, but attempting to suppress a material's normal behaviour may also be a move away from understanding how the material will perform in a real fire and the hazard it may present. This section of the discussion is divided into these two categories; test conditions and material behaviour.

6.2.1 Test Conditions

There are many very different sets of conditions employed in the fire testing of solid materials. In Chapter 2, the sectioning of these tests into which part of a fire they attempted to represent was discussed. This was done on the basis of exposure to heating and the parameters being measured. Thus, the heat flux, or related parameter, that the sample is tested under is one of the most important conditions to be considered in a fire test. The test chamber is also important. In a compartment fire the heat transfer to the sample changes throughout the test, as radiation from compartment walls and trapped hot gases increases. A compartment fire may also move from fuel controlled to ventilation controlled burning, which greatly affects the fire behaviour and results. Therefore the ventilation conditions must be considered when examining data from a fire test. The ignition source size, type and position are significant factors influencing the subsequent progression of a fire. These are also variables in the fire test scenarios, as mentioned in Chapter 2.

The sample's own physical form is also important in affecting the outcome of a fire test. The orientation and geometry affect both the material behaviour and the exposure conditions to the sample surface. Keeping a sample in place or allowing it to swell or melt away, for example may have a pronounced effect on the results from a test, and therefore the perceived hazardous nature of the material. Each of the aforementioned test conditions are discussed separately below.

6.2.1.1 Ventilation

For a fully developed fire outside a compartment, or one within a compartment where the fire load is low or the ventilation openings are large, such that there is sufficient ventilation for the fire to be unaffected by the size of the ventilation openings, the rate of heat release from the fire is controlled by the surface area and burning characteristic of the fuel. This is known as a 'fuel-controlled' fire, and the combustion is efficient with relatively little unburned combustible material. If, however, the ventilation openings in a compartment fire are reduced, the burning rate is found to depend strongly on the size of the ventilation opening (Kawagoe, 1958). The heat release rate is controlled by the rate at which air for combustion can enter the compartment. This is the 'ventilation-controlled' regime, characterised by a reduced combustion efficiency and large amounts of smoke and unburned materials issuing from the compartment. Flames are often seen emerging from ventilation openings as flammable vapours burn outside the compartment where oxygen is available.

Several parameters can be measured in order to attempt to classify or rank potential material behaviour in a developed fire; rate of heat release, smoke production, toxic gas production, rate of mass loss, and other, more test specific parameters. The values of these for fire tests employing the two different ventilation regimes are unlikely to be the same as the controlling influences are different. The above parameters, and the way in which they vary in fuel and ventilation controlled tests, are considered below, and any similarities investigated. Data from tests in the HSE third scale room/corridor, the Cone Calorimeter and a smoke box are discussed in detail.

6.2.1.1.1 Rate of Heat Release

In a ventilation controlled fire, the rate of heat release is governed by the amount of air available to the burning fuel. This means that in a compartment fire, the peak heat release rate in that compartment will be the same for any fuel that moves into the ventilation controlled regime. This can be seen in the results from the third scale room/corridor test with flexible foams (Table (5.55)). The average peak heat release rate for the foams that burned in the ventilation controlled regime was approximately 287 ($\pm$ 23.5) kWm^{-2}. Higher heat release rates will be seen where combustion also took place for part of the time outside the compartment, as seen by flames issuing

from the end of the corridor when unburnt volatiles burned on mixing with air. This was the case for foam C, and, for a shorter time, foam E. The maximum average peak value was seen for foam C. The foams that did not enter ventilation controlled burning demonstrated lower peak heat release rates, from around 68 kWm^{-2} to 248 kWm^{-2}, with the lowest value being for a foam that did not burn completely, and the highest for Foam A, which entered ventilation controlled burning only briefly, after a relatively slow developing fire.

Overall, however, the results do demonstrate that the peak heat release rate cannot be used to distinguish between the hazardous nature of materials, when the samples are tested under ventilation controlled conditions in a compartment fire test. It is for these reasons that the total heat released during this type of fire test also cannot be used to rank or assess materials. The actual values of peak rate of, and total, heat release are dependent upon the conditions of test, such as ventilation openings, fuel loading, geometry etc.

In the fuel controlled burning regime, the rate of heat release is governed by the sample geometry and the burning characteristics of the fuel. This indicates that the rate of heat release is a test result that can be used in the hazard assessment of materials. The heat release rate is important as it influences the spread of flame from one item to adjacent ones. Also of importance for storage of materials is how quickly a burning material will reach its peak rate of heat release; short times indicate high flame spread rates, which can affect escape times and the overall time to fully developed burning. These are significant in hazard assessment, both from the point of view of potential fire casualties and the level of damage that could be caused by an unwanted fire. In the experimental work for this thesis, the rate of heat release is measured during Cone Calorimeter tests, as well as in the set of HSE third scale tests with the flexible foams. Although the room/corridor burning becomes controlled by the ventilation, in the early stages it is fuel controlled, and as such it can be compared to the results from the Cone Calorimeter.

Comparison, for the foam samples, of the rates of increase in rate of heat release up to the peak heat release rate for the Cone Calorimeter tests at different heat fluxes, table (5.49), were made with the rates of increase of heat release rate from ignition up to where ventilation controlled burning became dominant in the third scale room/corridor test, table (5.55). There appeared to be no relationship between the data for the HSE test and those for the Cone tests at heat fluxes other than 30

kWm^{-2}, with correlation coefficients (r^2) of only 20.5-39%. (The statistical techniques are discussed in section 6.3). A comparison with rate of increase in rate of heat release in the Cone at 30 kWm^{-2}, however, showed that there was a strong relationship between this and the rate of increase of heat release rate in the third scale test, with a correlation coefficient of 89.8%. All the flexible foam results were used to obtain this result. The equation obtained was

$$\ln(\text{RHRR in TSR}) = -5.46 + 1.10\ln(\text{RHRR in Cone at 30 kWm}^{-2}) \quad (6.1)$$

where RHRR = rate of increase in rate of heat release, kW/s
TSR = HSE third scale room/corridor test

The data are shown in figure (6.1). The flexible foams behave differently under different heat flux levels in the Cone Calorimeter, with the ranking order changing at each value. It is for this reason that it is possible to obtain a good correlation for one heat flux and not with any of the others. The significance of the 30 kWm^{-2} may be that this is approximately the value necessary to cause flashover in a compartment fire (Drysdale, 1995), and the heat release rate increases at a sufficient rate in most of these tests to give flashover and ventilation controlled burning.

The rate of 'vent temperature' rise in the HSE test can also be compared with the rate of increase in rate of heat release in the Cone Calorimeter at 30 kWm^{-2}. Although this is obviously a very test dependent measurement, it is used by the HSE to separate materials into 'high' and 'normal' risk categories. The maximum rate of temperature rise over a 4 second period (Atkinson, 1994) is calculated. If this is greater than 700°C/min, the material is ranked as having a high hazard and is considered as one which may lead to flashover when involved in a fire. The problem with using this method of calculating the rate of temperature rise is that the 4 second period is very short and may provide unrepresentative results. For calculations in this thesis both the maximum rate of vent temperature rise as calculated in this way, table (5.41), and the average rate of vent temperature rise from ignition to the maximum temperature, or ventilation control, are considered. Ignition is judged as being the point where the temperature begins to increase.

X 553

The two methods of calculating rate of temperature rise, using the flexible foam results, do not give the same ranking order and are therefore not compatible. This was further shown by correlating the results from these two methods, which only

gave an r^2 value of 4.6%, showing no statistically significant relationship between the two rates of temperature rise. Further investigation was therefore necessary to determine which, if either, of the values was realistic or useful. To do this, the rates of temperature rise were compared with the rate of increase in heat release rate in the third scale room/corridor, and with the rate of increase in rate of heat release in the Cone Calorimeter at 30 kWm^{-2}. There was no relationship between the temperature rise calculated over the 4 seconds and the rate of increase in heat release rate in either the Cone Calorimeter or the HSE third scale rig, with correlation coefficients of 0%. This confirms the view that the peak rate of temperature rise calculated over 4 seconds does not indicate anything about the material being tested and should not be used to rank materials.

The rate of temperature rise from ignition to peak or ventilation control gave a more encouraging result. When correlated with the rate of increase in rate of heat release in the third scale test for the flexible foams, the equation obtained was

$$\ln(\text{rate of temp. rise}) = 0.211 + 0.951 \ln(\text{RHRR in TSR}) \qquad (6.2)$$

This gave an r^2 value of 87.7% and is shown in figure (6.2). The rate of temperature rise calculated this way is related closely to the rate of increase in rate of heat release, and as such is representative of the hazard presented by a material. Comparison of the vent temperature rate of rise with the rate of increase in rate of heat release at 30 kWm^{-2} in the Cone Calorimeter gave (figure 6.3):

$$\ln(\text{rate of temp. rise}) = -5.46 + 1.13 \ln(\text{RHRR in Cone, 30 } kWm^{-2}) \quad (6.3)$$

In this case the correlation coefficient (r^2) is 90%, again demonstrating that this rate of temperature rise is better than the current method of calculation.

Rates of development of pre-flashover compartment fires have been found to display approximate parabolic growth after an initial incubation period (Heskestad, 1982), figure (6.4), given by equation 6.4:

$$\dot{Q} = \alpha_f (t - t_o)^2 \qquad (6.4)$$

where α_f = fire growth coefficient (kW/s^2)

t_o = incubation period (s)

$\dot{Q}$ = heat release rate (kW)

The coefficient α_f shows how quickly a fire develops, the higher it is, the faster the fire is developing. This can be used to compare Cone Calorimeter and third scale room results in the very early, post-ignition, stage. In the later stages of the room fire, the geometry of the compartment will have an effect. It would be expected that the very early growth in the room fire could be compared to Cone Calorimeter results from lower heat flux tests than 30 kWm^{-2}, as the samples experience lower heat fluxes than 30 kWm^{-2} in the room fire, generated only from the ignition crib and early surface flames, without the later contribution of radiation from the walls, hot gases and larger surface flames. The α_f values for the first 30 seconds after ignition in the third scale flexible foam tests were compared with those from ignition to peak for the Cone Calorimeter at various heat flux levels, tables (5.49) and (5.55). The best correlation obtained was for the Cone Calorimeter tests at 15 kWm^{-2}, with a correlation coefficient of 63.2%. Although this by no means indicates a good correlation, ones for the other heat flux levels gave coefficients of 0-8%. This suggests that the growth of the early stage of the room/corridor fire is related to the fire growth of a material exposed to an external heat flux of 15 kWm^{-2}. This figure is much lower than that associated with flashover, but once the compartment begins to have an effect heat fluxes will increase towards the levels seen at flashover and material behaviour will change accordingly.

6.2.1.1.2 CO/CO_2 Ratio

The amount of CO produced from a burning material is higher in a ventilation controlled situation than in fuel controlled burning as there is insufficient oxygen for complete combustion. As carbon monoxide is a toxic gas, and is the most common cause of death for victims of house fires (e.g. Watson, 1994), the amount of CO produced by burning materials is of concern. The Cone Calorimeter measures the rate of CO and CO_2 production, but the results are not generally used for hazard assessment, as the is Cone Calorimeter well ventilated and would not produce the same sort of levels of CO as seen in a real fire. The ratio between the gases during combustion could, perhaps, be considered as one of the criteria for hazard ratings of materials, although this particular study could not give any indications of that, as there was not a wide range of materials investigated. The experimental results obtained did show an overall increase in CO/CO_2 with increasing imposed heat flux in the Cone Calorimeter, table (5.50).

In the third scale rig, the CO/CO_2 ratios were far higher than the values measured in the Cone, up to 3.5 times higher for the peak values in the Cone at 50 kWm^{-2} and 7.75 times higher than those at 15 kWm^{-2}. The average values are also higher in the room/corridor test than in the Cone Calorimeter, especially for the foams that have a prolonged ventilation controlled burning period, and up to eighteen times that for the fuel controlled burning in the Cone Calorimeter, table (5.52). The materials that did not enter ventilation control, or had only a short ventilation controlled period, showed higher average CO/CO_2 ratios than for the Cone tests at low heat fluxes, but lower ratios than for the Cone tests at the higher fluxes. The exception to this is 'British Vita Blue', which, although it did not move to ventilation control, produced a higher CO/CO_2 ratio in the third scale test than in the Cone. The burning of this foam in the room test was, however, very unusual. This was the only one of the foams that melted quickly and burned as a pool fire, but its burning in this particular test was interfered with by a false floor in the combustion chamber used for making the load cell measurements. The liquid foam ran beneath the floor and burned, shielded from the radiation from the chamber walls. Air flow into this space would also have been restricted, probably leading to this higher than expected CO/CO_2.

It was not possible to find a relationship between the peak, average, and rate of rise of CO/CO_2 between the third scale room/corridor test and the Cone Calorimeter results for the foams, at any heat flux. They may be related, but a wider range of materials would be necessary to investigate this further.

The results from the Cone Calorimeter should be treated with caution. In some instances, for example foam B at 30 kWm^{-2}, the peak CO/CO_2 ratio at the end of the test was greater than 2. This does not seem reasonable. This is regularly observed in the standard output from the Cone software, where the CO and CO_2 values are divided by the mass loss. High values at the end of the test are attributed to the poor mass loss readings at this point. However, that can not be used to explain the results here, as mass loss is not used. It may be a fault of the analyser or unusual behaviour by the foam.

6.2.1.1.3 Smoke

The major proportion of fire fatalities is attributed to the inhalation of smoke and toxic gases. Smoke production is therefore perceived, at least by the general public,

as one of the most hazardous qualities of a material. It is, however, not an intrinsic material property, but depends very much on the conditions of burning. The amount of smoke produced from a burning material is greatly increased under ventilation controlled conditions (Drysdale and Abdul-Rahim, 1985). The Cone Calorimeter offers well-ventilated conditions throughout the duration of a test and cannot therefore be expected to produce the same quantities of smoke that are seen from a 'real' ventilation controlled fire. However, as measurement of smoke during Cone tests is very simple, recording the smoke produced, as 'specific extinction area' has become commonplace, although it does not form part of the ISO or British Standards for this apparatus. The relevance of the smoke data obtained under conditions of well-aerated, free burning to real fires has still to be explored. It seems more likely that the smoke produced in the Cone Calorimeter could be relevant to the early stages of a fire; however, this has never been put to the test.

To investigate smoke production in the Cone, a series of experiments was carried out to compare the smoke yields from three different fuels burning under conditions of adequate ventilation in a large smoke chamber with those obtained in the Cone Calorimeter. This comparison is between a 'static' and a 'dynamic' measurement. Atkinson and Drysdale (1989) showed that there was good agreement between the static and dynamic measurements of smoke *from the same fire*, provided that the static measurement was made before the accumulated smoke had aged significantly. Accordingly, in this study, the maximum smoke yields in the 'smoke box' were compared with the Cone Calorimeter measurements (Foley and Drysdale, 1994).

The fuels used are listed in section 4.3.1.1.1. Liquid n-hexane was identified as the most convenient as it could be burned in the open, without any imposed heat flux. The solid fuels had to be heated. This was achieved in the large smoke box using an apparatus originally constructed to study the ignition of combustible solids (Thomson and Drysdale, 1987). In effect, this was a simplified version of the ISO Ignitability Test Apparatus (BSI, 1987), using the same conical heater but with a smaller sample. The results, expressed as the 'specific extinction area'[1] values are summarised in Tables (5.34)-(5.40) in units of m^2kg^{-1}. The figures quoted in Tables (5.34)-(5.37) are based on the cumulative smoke yield over the duration of the test, and are calculated by dividing the total smoke produced by the total mass consumed

[1]N.B. Specific extinction area is defined as the extinction area of the smoke produced per unit mass of volatile material burned. This method of presentation is used only because it is the one incorporated into the Cone Calorimeter software.

as one of the most hazardous qualities of a material. It is, however, not an intrinsic material property, but depends very much on the conditions of burning. The amount of smoke produced from a burning material is greatly increased under ventilation controlled conditions (Drysdale and Abdul-Rahim, 1985). The Cone Calorimeter offers well-ventilated conditions throughout the duration of a test and cannot therefore be expected to produce the same quantities of smoke that are seen from a 'real' ventilation controlled fire. However, as measurement of smoke during Cone tests is very simple, recording the smoke produced, as 'specific extinction area' has become commonplace, although it does not form part of the ISO or British Standards for this apparatus. The relevance of the smoke data obtained under conditions of well-aerated, free burning to real fires has still to be explored. It seems more likely that the smoke produced in the Cone Calorimeter could be relevant to the early stages of a fire; however, this has never been put to the test.

To investigate smoke production in the Cone, a series of experiments was carried out to compare the smoke yields from three different fuels burning under conditions of adequate ventilation in a large smoke chamber with those obtained in the Cone Calorimeter. This comparison is between a 'static' and a 'dynamic' measurement. Atkinson and Drysdale (1989) showed that there was good agreement between the static and dynamic measurements of smoke *from the same fire*, provided that the static measurement was made before the accumulated smoke had aged significantly. Accordingly, in this study, the maximum smoke yields in the 'smoke box' were compared with the Cone Calorimeter measurements (Foley and Drysdale, 1994).

The fuels used are listed in section 4.3.1.1.1. Liquid n-hexane was identified as the most convenient as it could be burned in the open, without any imposed heat flux. The solid fuels had to be heated. This was achieved in the large smoke box using an apparatus originally constructed to study the ignition of combustible solids (Thomson and Drysdale, 1987). In effect, this was a simplified version of the ISO Ignitability Test Apparatus (BSI, 1987), using the same conical heater but with a smaller sample. The results, expressed as the 'specific extinction area'[1] values are summarised in Tables (5.34)-(5.40) in units of m^2kg^{-1}. The figures quoted in Tables (5.34)-(5.37) are based on the cumulative smoke yield over the duration of the test, and are calculated by dividing the total smoke produced by the total mass consumed

---

[1]N.B. Specific extinction area is defined as the extinction area of the smoke produced per unit mass of volatile material burned. This method of presentation is used only because it is the one incorporated into the Cone Calorimeter software.

as specified in the ASTM standard (ASTM, 1990b) (cf. Rasbash's "smoke potential" (Rasbash and Philips, 1978)). The results from measurements in the smoke box were calculated from the maximum optical density of the smoke which accumulated in the volume (13.5m^3), using the expression:

$$SEA = -\frac{V}{mL}\ln\left(\frac{I}{I_o}\right) \qquad (6.5)$$

where SEA is specific extinction area (m^2/kg), V is the volume of the smoke box (m^3), m is the mass of material burned (kg), L is the path length over which the optical density is measured (m), and I and I_O are the intensities of light falling on a photocell L m from a light source, in the presence and absence of smoke, respectively. The units used are described in detail in appendix 1.

It can be seen from tables (5.34)-(5.40) that significant differences exist, but the differences are not consistent. *n*-hexane consistently showed a lower smoke yield in the smoke box than in the Cone Calorimeter, although the same container (a 100 mm Petri dish) was used in both sets of experiment. Of the solids, the results from the polyurethane foam were in reasonable agreement, but PMMA apparently gave *more* smoke when measured in the box, compared to the Cone. Unfortunately, the sample holder from the Cone Calorimeter was too large to be placed under the conical heater in the smoke box, and a 60 mm diameter sample had to be used. To examine whether or not this could account for some of the differences observed in the PMMA results, the sample holder from the ignition apparatus was used to carry out some measurements in the Cone Calorimeter. As can be seen from Table (5.34), the smaller sample gave an increased SEA, but still not as high as the smoke box result.

Apart from the presence of the conical heater in the Cone Calorimeter, it is anticipated that the hexane results would be strictly comparable as the same 'sample holder' (Petri dish) was used in both sets of experiments, and no imposed heat flux was required, as the firepoint of hexane is below room temperature. To determine the effect of the presence of the cone heater, a set of experiments was carried out in which the cone was moved into its vertical position, i.e. out of direct line of the flames rising from the Petri dish fire (although there was still some impingement), and the smoke measurements repeated. The smoke yield was observed to *increase* by about 20%, giving an even greater difference between the Cone and the smoke

box tests. When the conical heater was completely removed from the Cone Calorimeter, a measured smoke yield was obtained which was even higher, 30% greater than with the heater in its "horizontal orientation".

To examine the way in which the cone heater affects the yield of smoke from solid fuels, it is necessary to burn them in the absence of supporting radiation. It proved impossible to ignite PMMA slabs, but it was found that a 100 mm diameter tray containing 20 g of PMMA pellets could be ignited successfully using 20 ml of methanol as an 'accelerant'. Methanol had the additional advantage of yielding no smoke, so that the smoke yield could be attributed entirely to the plastic. Similar experiments were carried out with polystyrene pellets, but 6 ml of hexane had to be used to ensure reproducible burning of 15 g of the polystyrene. These tests showed that there was no significant difference in the smoke yield with the cone heater removed and with it in place 25 mm above the sample. This is probably due to the fact that the flames produced from the solid fuels were very small, well below the level of the bottom of the heater. This contrasted with the tests using hexane (and with the solid plastics under an imposed heat flux) in which the flames were large, reaching up through the cone heater into the duct for the duration of the test. It appears that the interaction between the cone heater and the flame interferes with the smoke production process, although it is impossible to investigate the magnitude of the effect for the solids as large flames can only be produced with an imposed heat flux.

From these results, it appears that the Cone Calorimeter does not provide smoke data that can be compared in a simple fashion with free burning data. The smoke yields measured using the dynamic system of the Cone Calorimeter are sufficiently different from the accumulated smoke yields from free burning to raise the question of the value of using the Cone Calorimeter even to 'rank' materials on the basis of their smoke potential.

More important is whether the smoke data can give any information on the yields of smoke from 'real' compartment fires, ones in which ventilation controlled burning takes over. Data from tests in the Cone and the HSE third scale room/corridor test using the set of flexible foams were examined to see if there was any relationship. Far more smoke was produced per unit mass of fuel burned in the third scale test than in the Cone Calorimeter, Tables (5.44) and (5.46), with the exception of the cases in the Cone where ignition did not take place and the mass losses were very

small. Previous research has shown that more smoke per unit mass is produced during ventilation controlled burning in the third scale rig than during the fuel controlled early part of the test (Atkinson, 1989). This was also seen here, although in less quantitative terms, as the mass loss data were not sufficiently reliable. However, it was clear that the early stage of the fire produced much less smoke than the later, full developed part. The different types of burning gave not only numerically different smoke production rates, there was also no relationship between the average and peak rates of smoke production and the total smoke produced in the two tests.

The rate of increase in smoke production rate (m^3ODml/s^2) were also investigated, similar in idea to the rates of increase in rate of heat release. This could be an important parameter to consider, as how quickly a material in a fire reaches its maximum rate of smoke production is as important for escape considerations as the rate of increase in rate of heat release. The rate of increase in smoke production rate in the very early part of the compartment fire, the first thirty seconds, could be compared with the rate of increase in rate of smoke production in the Cone Calorimeter at 20 kW/m^2, tables (5.33) and (5.34), and figure (6.5). This gave an r^2 value of 80.3% for the equation

$$\text{early } RRD_o \text{ in TSR} = -0.00157 + 44.2\ RRD_o \text{ in Cone at } 20\ kW/m^2 \quad (6.6)$$

The correlation coefficient is highest at this heat flux level, and lies in the range 37.8-71% for the other fluxes. This indicates that the compartment has little influence on the burning behaviour and the material burns under the influence of only the wood crib and the flames then present. This is the same as for the rate of increase in rate of heat release in the early stages of the third scale fire test. Comparing the rate of increase in rate of smoke production from ignition up to ventilation control or peak smoke production rate in the third scale test with the rate of increase in rate of smoke production from ignition to peak in the Cone Calorimeter tests, the values obtained can be correlated successfully at the higher heat fluxes, the best are obtained at 40 kW/m^2. Here an r^2 value of 85.8% is found for the equation

$$RRD_o \text{ in TSR} = -.0521 + 355\ RRD_o \text{ in Cone at } 40\ kW/m^2 \quad (6.7)$$

The graph is shown in figure (6.6). The correlation coefficient falls to 73.5% at 50 kW/m^2, and is between 19.7 and 71.1% for the lower heat fluxes. Once the compartment has an influence on the burning behaviour of the sample under test, the results are more compatible with the higher heat flux tests as the sample is subjected to heat transfer from the hot walls and combustion gases, as well as the larger flames on the surface.

Despite the reasonable correlations with the data from the Cone Calorimeter and the third scale room/corridor test, the actual values are very different and the peaks, averages and total smoke do not give the same ranking order at all. The smoke production is not a fundamental property, but depends upon the test conditions, as shown by many authors (e.g. Drysdale and Abdul-Rahim, 1985). The relevance of any smoke test data to smoke production in a real fire must be questioned, and results not used without understanding, otherwise any conclusions reached will be misguided and meaningless. More work is required on the mechanism of smoke formation in fires under a wide range of conditions before it will be possible to judge if and how smoke yield data from tests such as the Cone Calorimeter, or even the ventilation controlled tests in the third scale room/corridor test, can be used confidently as input to fire safety engineering design calculations.

6.2.1.2 Ignition Source

The influence that ignition sources can have on subsequent fire development was discussed in Chapter 3, section 2. The choice of ignition source for fire testing is far more complicated than would first appear. It may be desirable for the source to be representative of potential real sources, but reproducibility then becomes a problem. Wooden cribs, such as the British Standard ones used in BS 5852, provide a solid fuel ignition source, which may seem to be at least more representative of real ignition sources than gas flames, but it has been shown that the reproducibility from these very careful defined solid sources is poor (Paul and Christian, 1987). The alternative is to use a reproducible source which can only represent a real source in the level of heat flux or heat release rate that it provides to the material under test. Gas flames and electrical heaters are employed to provide this. A gas flame has the advantage that it gives both radiative and convective heat transfer, whereas an electrical heater provides only radiation. This problem will be discussed more fully in the next section. When using a gas or solid burning material, which provides both

the heat and piloted ignition source, it is necessary to identify the factors which alter the exposure conditions provided by the source to the material.

An ignition source provides either a constant or a varying heat output over either a strictly defined time period or one that depends on the burning rate of the ignition source material. For sources such as gas burners, both the heat release rate and the time can be controlled easily. Solid sources can only be controlled in either respect by the amount of material present and the method of construction of the source. They will be influenced by the developing fire itself, which will alter the burning rate of the ignition source. Of the two, the gas flames are more reproducible. Both the heat output and the duration of exposure influence the subsequent behaviour of a sample under test. The position of the ignition source in relation to the test material has also been found to have a significant affect, by changing the ignition source position the heat flux to the sample can be altered (Williamson *et al.*, 1991). Even gas burner geometry which is independent of heat output has been shown to have an effect (Ahonen *et al.*, 1987), as discussed in section 3.2.

The effect of ignition source size, duration and position have been investigated for the third scale room/corridor test. This employs a British Standard No. 7 wood crib, placed between two parallel halves of the test material. The separation distance of the sample surfaces is 80 mm, the width of the crib. The influence of separation distance is discussed in the second half of this chapter, both in the context of this test and that of storage conditions in warehouses. In order to discuss the influence of ignition source, it is only necessary to understand that reducing the separation between two parallel surfaces increases the heat flux at the sample surface and therefore increases the likelihood of ignition, and reduce the time taken to ignition.

Rigid polyurethane foam sheets were tested in the parallel configuration with the standard ignition source and with smaller cribs and gas flames, as described in Chapter 4, with the results given in tables (5.56) and (5.57). When the separation was 80 mm, ignition and burning of the samples occurred with the no. 7 crib and the no. 4 crib, but not with the no. 3 and 2 gas flames. For the no. 7 source, the crib touched both samples surfaces, whereas the smaller sources were placed against one face. No ignition was achieved with the no. 3 gas flame at a separation of 60 mm, but it was successful at 40 mm. The material did not ignite at this separation with the no. 2 source. The difference between the numbers 2 and 3 sources is both the gas flowrate to the burner and the duration of burning. The no. 2 source is 157

ml/min of butane for 40 seconds, the no. 3 is 344 ml/min for 70 seconds. To examine the relative importance of these two factors, tests were carried out with the number 2 gas flowrate for the no. 3 duration, i.e. 157 ml/min for 70 s, and the no. 3 flowrate for the duration of the no. 2 source, 344 ml/min for 40 s. For this material, of fairly low density, ignition occurred with the higher gas flowrate for the shorter duration of time, but not the lower flowrate for longer. Thus the heat output from the burner is more important, in this case, than the duration of burning. This cannot be considered to be universally applicable, however, as the reaction of a material to a heat source depends upon the material properties such as thermal conductivity (e.g. Drysdale, 1985). The foams have a low thermal inertia, which means that they heat up quickly at the surface. For those with a high thermal inertia, where heat can be dissipated into the material more quickly and the surface layers heat up more slowly, the duration of an ignition source may become more important.

More generally, the total heat release from the material decreased as the ignition source size decreased, probably as less material was consumed. The average and peak rates of heat release were slightly lower for the smaller sources, table (5.57) The vent temperature in the test chamber also decreased as the source size was reduced.

The selection of an ignition source affects the outcome of a fire test and must therefore be appropriate to the aims of the fire test. If the ignitability of the material is being investigated careful choice of source is required, along with a good understanding of the exposure conditions provided by each source. If, however, the aim of the test is to assess what contribution a material makes to the fully developed stage of a fire, the selection of source may not be so important, and could simply be chosen to be large enough to ensure that most materials achieve fully developed burning or flashover in a room fire test. This is the objective of the HSE third scale test.

6.2.1.3 Heat Flux

The alternative to using an ignition source that provides the heat flux to a sample is to use an electrical heater with a small pilot flame or spark ignition source. In this case the heat flux comes from the heater rather than the ignition source, as discussed in section 3.1. In Chapter 2, several tests were described that employed these two

approaches to fire testing. In this section the influence of heat flux in both the Cone Calorimeter and third scale room/corridor tests is discussed.

The level of heat flux provided to the sample surface is very important in determining the fire behaviour. Ignition and flame spread occur as a result of heating a material to its ignition temperature, and thereby producing a flow of volatiles from the material sufficient to allow combustion. The time this takes depends on the level of heating the sample is subjected to. Flame spread equations, e.g. (3.37a) and (3.37b) (Hasemi, 1985) demonstrate the importance of heat flux at the sample surface for flame spread. Electrical heaters can impose different levels of irradiance on samples. The irradiance levels can be used to represent different stages in a real fire, as mentioned in Chapter 2. In this way a test can be used to assess whether or not a material will ignite easily with just a small ignition source, giving around 10-15 kW/m^2. A higher heat flux is used to assess whether the material will become involved in the growth period fire to significantly increase the likelihood of flashover or not, and the highest heat fluxes to see if it may contribute significantly to a fully developed fire, thereby increasing the chances of structural damage and higher risk to fire-fighters.

Examples of these different types of behaviour are demonstrated in the flexible foam Cone Calorimeter tests, tables (5.47) to (5.49). Foam C, the conventional, non-fire retarded foam, undergoes ignition at 15 kW/m^2 which would indicate that this material would ignite very early in a fire. The fire retarded 'Waterlily' foams, A and B do not ignite until the external irradiance level is 30 and 20 kW/m^2 respectively. This suggests that these samples would not ignite in the early period of a fire, and would only become involved in the later growth stage. Flashover occurs once the heat flux is around 30 kW/m^2. The contribution that a material makes to the fully developed fire can be considered by examining the rate of heat release at an imposed heat flux of 30 kW/m^2 and above. A high rate of heat release indicates that the material has the potential to cause a large fire, possibly leading to further flame spread, for example beyond an original compartment, and to structural damage. Foams F and C demonstrate this higher rate of heat release at the highest irradiance level. At the lower heat fluxes, the rate of heat release is also important. Whilst the times to ignition at these fluxes may show how quickly a material could become involved in a small fire, the heat release rate indicates how quickly a material could cause other items to heat up and ignite, which is obviously of consideration for fire spread in warehouse storage. The aforementioned foams which indicated a

significant contribution in a developed fire do not demonstrate the highest rates of heat release at the lower heat fluxes, these are shown by foams C and E. Therefore, the hazard presented by a material can alter at different stages of a fire.

The rate of increase in rate of heat release is a parameter that is never really discussed, except, perhaps in terms of time to peak heat release rate. It is, however, important in terms of fire development, it is the acceleration of a fire towards its peak burning. If an ignited material takes a long time to reach its peak burning, it follows that it will take longer for surrounding materials to receive the sufficient heat flux for their ignition than if the original material accelerated rapidly from ignition to its maximum rate of heat release. It is therefore not sufficient to consider only the peak rate of burning that a material is capable of, but also the time it takes to get there. This, too, will vary with the imposed heat flux. This was discussed, in the context of early fire growth, in section 6.2.1.1. Generally, the rate of increase in rate of heat release increases with increasing irradiance in Cone Calorimeter tests, although it appears that for the high heat release materials, such as the non-fire retarded foams, the rate of heat release rate reaches a maximum and is then approximately the same for the medium to high heat flux levels.

The choice of imposed heat flux level in fire testing is therefore an important decision. Like the choice of ignition source size in the tests without external heating, the heat flux must be selected to represent the part of a fire that is of interest. The heat release rate and the rate of increase in rate of heat release both change with heat flux, and these are crucial to the subsequent development of a real fire. Results from fire tests under different heat fluxes must be interpreted carefully, with consideration for the fact that behaviour at one stage of a fire does not necessarily indicate any overall fire behaviour or behaviour at a different stage of a fire. For example, models of flame spread that use Cone Calorimeter data at only 25 kW/m^2 (e.g. Wickström and Göransson, 1992) may never predict accurately the flame spread rates seen in a real fire, as the test heat flux will only be matched in a real fire for a short time. In the early growth period it will be less, whilst later, just before and after flashover, the heat fluxes will be higher. This particular model is only aimed at early growth on wall lining materials, but may not even be using appropriate heat fluxes for that period.

A material tested in a compartment fire test is also subjected to external heat fluxes, after the ignition and early growth of the fire, once the compartment starts to have an

effect. Radiation from the compartment walls and from hot smoke and gases that build up in the compartment, even though it may be vented, both provide external heating on the sample. This is not easily controlled by test conditions, nor is it usually measured. It forms a feedback mechanism with the material itself; a sample that ignites and releases heat will gradually build up heat in the walls and hot gases above the sample. The higher the heat release rate from the material, the more rapidly the radiation from the walls and gases increases. This in turn increases the heat flux to the sample and therefore the rate of heat release from the material. Thus, the external heat flux is constantly changing, and depends on the material itself.

The influence of radiation from hot gases was seen clearly in the rigid polyurethane foam tests in the HSE third scale test, tables (5.56) and (5.57). In the test with an 80 mm separation and a no. 4 crib as the ignition source, the samples did burn, but were not completely consumed. The internal facing surfaces were burned over the entire surface, and on one sample the flame had travelled through the thickness of the material at one point. Flame had reached the rear face, the external facing surface, and had partially consumed material there. However, the flame had only spread across the upper part of the external face of the vertical sample, and there existed a very distinct line halfway down the face, between the burned material and the untouched. This is caused by the falling heat flux from the hot gases above the samples. The irradiance from the hot smoke layer to the sample was higher close to the top of the sample, as that is closer to the hot gases. This heat flux falls with distance away from the gases, in a way analogous to the flame spread test BS 476 (BSI, 1987a), until the point is reached where the imposed heat flux is insufficient to support downward flame spread. As the internal surfaces were fully consumed down to floor level, the heat flux on these surfaces must have been from radiation and convection from the flames, rather than from radiation from the smoke layer. The test with the same conditions, except for the larger no. 7 ignition crib, gave burning over almost all of the external surfaces, as the higher heat flux provided by the larger crib caused a higher burning rate and heat release rate from the foam, which in turn gave a higher smoke layer temperature, with a deeper smoke layer, and more heat transfer to the walls. This would then give higher radiation from the smoke layer and walls back to the external surfaces of the samples and allow burning to be supported over the entire surface.

Whilst this method of providing an external heat flux cannot really be controlled, it is extremely test dependent, both in terms of compartment dimensions and sample

size, geometry and orientation. Once again, results must be used with caution and understanding, and correlations with data from other test methods should not be expected. Just as materials give different ranking orders when tested under different irradiance levels in the Cone Calorimeter and when different parameters are considered (see flexible foam results, tables (5.47)-(5.50)), so it must be expected that the various conditions in compartment fire tests will also give different results and hazard ratings. Measuring conditions during compartment fire tests may help in understanding the material behaviour in the test.

6.2.1.4 Sample Restraint

For some materials, which display slightly unusual behaviour in fire conditions, the method used to keep the sample in place can influence the test result. Tests which do not allow a sample to regress from or swell towards an ignition source will produce different results from those that do not restrain the sample to a certain position. For example the Cone Calorimeter standard recommends use of a wire grid over samples that swell. This will be discussed more fully in the 'materials behaviour' section of the discussion. It is also a test condition problem, for example a material which drips will probably do better in the oxygen index test, as the material flows away from the ignition source.

6.2.1.5 Sample Geometry and Orientation

In different tests, samples may be tested in a horizontal orientation, either facing upwards or downwards, in a vertical orientation, or at an angle. Tests specify many different specimen shapes, sizes and positions. All these factors have a large part to play in the development of a fire, from ease of ignition to flashover. The sample geometry and orientation affect both the material behaviour and the exposure conditions, and these are discussed separately below.

6.2.1.5.1 Material Behaviour

Samples may not behave in the same way on a small and large scale. The use of results solely from a small scale test may therefore be inappropriate, and possibly even dangerous. An example cited earlier was the case of vacuum packed thermal wadding, Chapter 2. Use of the third scale room/corridor test did reveal some unexpected behaviour of rigid and flexible foams, which would not be apparent on a

small scale. The flexible foam F, British Vita blue, melted during the third scale test to form a pool fire, as mentioned in section 6.2.1.1. This behaviour which was not seen with the other flexible polyurethane foams. It was also not observed in the Cone Calorimeter, where this foam gave very high heat release rates at the higher heat fluxes. No account can therefore be taken of the fact that the material may melt and flow away from the heat source in real fire hazard assessment, when using Cone test data.

In the third scale test, the rigid polyurethane foam burned initially on the inward facing surfaces only. A gradual build up of volatiles within the material caused the back face to bulge and tear open and allowed the passage of flame to the rear face. This behaviour would not be seen on small scale or in the horizontal orientation, but is important as it allowed the rear surface material to become involved in the fire, giving a higher heat release and greater duration of burning as more material was consumed, both of which would be important in a real fire scenario. Similar observations were made for the polyisocyanurate foam, which also demonstrated this behaviour, although it occurred more explosively in this case, with large areas of the foam rear surface ripping apart due to build up of volatiles.

The phenolformaldehyde, when exposed to an ignition source, crumbles violently with a popping noise, into a large number of small pieces which cover the ignition source and protect the remaining foam from it. Each time part of the sample is exposed to heat, the material demonstrates this behaviour, whether it is the top surface or a newly uncovered layer. Whilst a Cone Calorimeter test, for example, may show this crumbling behaviour, it would not demonstrate the way in which an ignition source can become covered in the small pieces which burn so slowly that a no. 7 crib was still smouldering under unaffected foam pieces over half an hour after the crib had been presented to the material. This also could not have been observed with the samples in a horizontal position.

Different types of material behaviour that cause problems in fire testing will be discussed later in this chapter in more detail. It is clear, however, that sample geometry and orientation will have an effect of the outcome of certain tests, depending upon the material behaviour. The advantage of larger scale tests is that they may reveal this behaviour in a way that small scale tests cannot.

Sample geometry also has an effect on material behaviour with respect to thermal thickness. A material can be regarded as thermally thin provided that the Biot Number is less than 0.1, and $Bi = hL/k$, where L is the thickness of the sample. A thermally thin material is one in which there are no temperature gradients through the material. Thickness therefore plays a significant part in this behaviour. A thermally thick material is one in which temperature gradients do exist through the solid. Semi-infinite behaviour, where the rear face is assumed not to be reach a temperature significantly above ambient, can be assumed if $L > 2\sqrt{\alpha t}$, where t is the duration of exposure to the heat source and α is the thermal diffusivity, $k/\rho c$. In this case, the thickness is again important, as well as the duration of heating. The thicker a sample of a certain material is, the longer it can be exposed to a given heat source before the rear surface is affected and heat losses from there become important.

The time to ignition for a thermally thin sample depends upon the thickness, density and the thermal capacity. The thinner a material the easier it is to ignite. The time to ignition of a thermally thick material depends upon the thermal inertia ($k\rho c$). Materials that have a low value of thermal inertia, such as the flexible polyurethane foams, heat up quickly at the sample surface, cannot conduct heat away through the sample very quickly, and consequently ignite rapidly. For all materials, the time to ignition depends not only upon the heat flux to the sample, but also the heat losses. These change with different material thickness, as discussed above, and with sample orientation. The concept of a 'critical minimum heat flux' necessary to cause piloted ignition for a given material, must therefore be regarded with caution, it can only apply to the conditions of test, and will be altered by even such changes as orientation, sample thickness, sample geometry etc.

6.2.1.5.2 Exposure Conditions

The geometry, orientation and position of samples under test have an influence over the actual exposure conditions of the sample. The most striking example during this experimental program was the separation of the parallel samples in the third scale room/corridor test. In initial tests with Foam G, ignition and reasonably rapid development to a ventilation controlled fire occurred in one case, whilst in a seemingly identical test no ignition was achieved. This difference would have meant the foam being given either a 'high' or 'normal' fire hazard rating, which it turn could mean the difference in a warehouse situation of special fire and escape precautions or not. The only apparent difference between the two cases was a small

difference in separation between the two sample surfaces; in the first case the samples had been pushed firmly against the ignition crib, whilst in the second there was a very small gap present. This led to further research on heat fluxes from flames between parallel surfaces, which will be discussed in detail in the second half of this chapter. This simple observation also shows that the sample position is important in determining the exposure conditions to the samples themselves. The parallel surface configuration is used in other test methods, e.g. Brandschacht (DIN, 1978). This configuration provides a cross-radiation heat transfer situation, the level of which will grow with the rate of heat release from the samples, giving a feedback mechanism for increased rate of burning. The convective component of the heat transfer may also be increased with different sample position and geometry, this will be discussed for the case of parallel vertical surfaces in the second part of this chapter.

The separation distance between the parallel surfaces in the third scale test also has an effect on the burning behaviour of the material; reducing the separation in the rigid foam tests increased the rate of smoke production, the total smoke produced, and the rate of increase in rate of smoke production, table (5.57). The CO/CO_2 ratios were also increased significantly.

The orientation of samples under test affects the exposure conditions, especially when considering flame spread. The flame spread can be regarded as a series of ignition steps, all of which depend on raising the surface temperature to that which is sufficient to give the necessary flow of volatiles for sustained combustion. The ignition source is provided by the flame front itself, whilst the heat source comes both from the flame front and any external heat sources. The heat transfer from the flame front to the surface is greatly affected by the sample orientation and the direction of flame travel. For horizontal surfaces, without any wind effects, the heat transfer occurs by radiation from the flame to the surface normal to the flame, by conduction through the solid and air, and by conduction and convection through the vapour/air mixture at the surface. These processes provide greater heat transfer than is the case for downward spread of flame over vertical surfaces. Here, the heat transfer occurs only by conduction through the solid and air. This therefore is slow and often needs a supporting external heat flux, as was seen in the case of the rigid polyurethane foam, described in section 6.2.1.3. The most efficient heat transfer, giving rise to the highest flame spread rates, is seen for vertically upward flame spread. In this case the flame lies against the sample surface, filling the boundary

layer and transferring heat by convection and radiation. The rate of temperature rise to the ignition temperature is rapid, leading to the very high rates of flame spread seen in this case. Since materials behave differently under different levels of heat flux, and since heat losses and material behaviour can be altered by changing orientation, fire tests using the horizontal position will give different results from those with a vertical position.

The use of data taken from horizontal tests for prediction of vertical flame spread must be treated with caution. One notable example was for testing of urethane insulation board. (Williamson and Baron, 1973). The classification of this product after tests in the Steiner Tunnel (ASTM, 1979a), where the material covers the ceiling of a tunnel, showed a flame spread rating of less than 25, which is generally recognised by building codes to be 'non combustible'. The material could therefore be used in escape routes and suchlike. The same material tested in a vertical orientation, in a corner test with a burning wastebasket as the ignition source demonstrated ease of ignition and rapid flame spread. It was further generally found that polymeric materials with a low flame spread classification in the Steiner Tunnel showed intense combustion in the corner test (Williamson and Baron, 1973). The Cone Calorimeter is generally used in the horizontal position; it is more convenient to perform the test in this way. The data, however, are frequently used in flame spread modelling, for which the focus is upward vertical flame spread as this is the worst flame spread case. The use of different orientation in fire tests, with some tests even being carried out at an angle, further complicates the task of comparing results from fire tests. This has been proven to be unsuccessful for the National tests, and it may also be unacceptable to use 'reaction-to-fire' test data from horizontal tests in vertical flame spread models without further research and justification.

6.2.2 Material Behaviour

Although the behaviour of materials has been mentioned in several sections, that was in the context of how test conditions affected a material and the usefulness of the results. Conversely, the material behaviour itself may alter the conditions it is exposed to. Many tests for solid materials were designed with 'ideal' behaviour in mind, that is samples that stay in place without any changes in geometry or phase, except for the production of gaseous volatiles for combustion. This is not only true

for the National tests, but the Cone Calorimeter (ISO, 1990) and the Room/Corner test (ISO, 1986) were original designed for wall lining materials, which in general obey these criteria. The calibration of the Cone Calorimeter is performed using a much-tested material; polymethylmethacrylate. This gives a reasonably constant heat release rate once the maximum rate of burning has been achieved, and its repeatability and reproducibility are good (Babrauskas, 1984). Within the test instructions for the Cone is provision for materials that display intumescent or unusual behaviour, by placing a wire grid over the sample. However, although this may appear to keep the test standard, it does prevent any observation or testing of the material in the way that it would behave in a real fire, and it is often materials that do not behave in a 'normal' way that are of most interest. There are several distinct ways in which a sample may behave that calls into question the validity of the fire test, or may complicate the results; a specimen may regress, melt, char, swell, spall, or delaminate. These are discussed below in each category.

6.2.2.1 Regressing

A material which regresses from a heat source experiences a reduction in the heat flux at the sample surface. This may reduce the chance of ignition or reduce the early rate of flame spread. The flexible foams tested in the Cone Calorimeter regressed at the lower heat fluxes at a rate which prevented ignition, but at the higher heat fluxes, ignition occurred rapidly, before there was any significant regression. The times to ignition will be altered by the regression process, making flame spread modelling of these materials very difficult.

6.2.2.2 Melting

Materials that melt, partially or completely, are often present both in warehouse storage and in domestic dwellings. Some polyurethane foams used in furniture display this behaviour. The melting process allows material to move away from a heat or ignition source, and takes energy out of the system. However, the molten material may ignite and drip, causing the fire to spread away from the solid bulk of the sample. In small scale tests, this behaviour cannot normally be seen. Those that use the horizontal orientation for testing these materials do not demonstrate this at all.

In the third scale tests done during this research, one foam, F, melted to form a pool fire, as described in section 6.2.1.1.2, giving different results from those that did not melt. In a real fire, the melting process could be very important. It may be that the physical conditions would allow the melt to run off from the fire, via for example drainage channels in a warehouse, and either not burn or burn more slowly without the high heat fluxes generated by the main part of a fire. Alternatively, the liquid could ignite and burn as a pool fire beneath or beside the solid material mass, giving high burning rates. The spreading of the pool could also help spread the fire quickly to other items in the fire compartment.

The second type of behaviour was observed during the BS 5852 part 2 (BSI, 1982) flexible foam tests. In this set of tests Foam A, which gave good results in the Cone Calorimeter, failed with a number 6 crib, thereby falling behind B, D, and F which passed this ignition source, table (5.39). The reason for failure was that burning, molten droplets of foam formed a pool beneath the 'seat', which then burned under the foam and gave direct flame impingement on parts of the solid sample, increasing the melting rate and so enlarging the burning pool. This behaviour was also noted with Foams C and E which failed with a no. 4 crib.

The BS 5852 results appear to be at variance with the Cone Calorimeter results, as Foam A is the superior in the latter. The difference must lie in the difference of the tests. In the Cone, heating is by radiation with spark ignition of the vapours, whilst in the BS 5852 test, the crib rests directly on the material, transmitting heat by radiation and convection, as well as bearing down on the surface in such a way as to enhance penetration through to the base of the horizontal slab. Droplets of the polymer melt can then run down and fall below the rig: if a pool fire results, this will dominate subsequent behaviour.

It is not clear why Foam B was able to withstand crib no. 6 and Foam A failed. Foam B is inferior in its performance in the Cone Calorimeter; other factors must be considered. For example, if the viscosity of the melt from Foam A was significantly lower than that from B, the rate of formation of a pool of polymer melt may be sufficiently rapid to overcome heat losses to the surface below and allow a localised 'flashover' to occur in the confined space between the floor and the underside of the 'seat'. It would be appropriate to carry out further investigation on rates of melt formation. This example has, however, demonstrated that a single small scale test cannot be relied upon to provide all the necessary data for hazard assessment of

many materials. For both of the cases described here, the Cone Calorimeter gave no indication of the type of behaviour observed in the third scale room corridor test or the BS 5852. Whilst the latter may be an unsophisticated test, it is capable of giving an indication of larger scale fire behaviour.

In view of the importance of the melting process for fire development, materials that may display this behaviour should be tested in the vertical orientation on a large enough scale to be able to observe whether or not melting does occur and how it affects the outcome. Medium scale tests appear adequate, but the scale of samples used in tests such as the Cone Calorimeter may be insufficient to allow observation of melting and dripping, with most Cone tests being unsatisfactory as the standard method of test is to use the horizontal orientation.

6.2.2.3 Charring

Char layers are formed by some materials when they are exposed to heating which is insufficient to give rise to ignition and flaming combustion. The heating causes thermal decomposition which releases fuel vapours. Smouldering combustion often occurs, which is the reaction where heat released in the surface oxidation causes thermal decomposition of the unaffected fuel adjacent to the char. The criteria for smouldering combustion is formation of a solid porous char layer that allows ingress of air. Several materials may undergo this type of reaction; e.g. wood, rubber latex foam, some leathers, certain polyurethane foams, and some phenol formaldehyde foams (Drysdale, 1985). The porous layer of char formed on the surface of a material can significantly affect the results from a fire test. One example of char formation affecting test results was observed in tests of combustion modified polyurethane foam (Atkinson, 1989). Only a small amount of the material under test burned when exposed to a 500g wood crib. The author attributed this failure to burn completely to the foam forming an insulating layer of char that shielded the molten plastic beneath from radiation from the flame above, thereby cutting off the flow of volatiles. A brittle dome of char covering a pool of yellow, liquid plastic remained at the end of testing. This behaviour obviously alters the outcome of a fire test significantly, and is another factor that complicates the use of fire test data for hazard assessment of materials.

6.2.2.4 Swelling and Spalling

Materials generally behave 'better' on a small scale and in a horizontal position, as discussed in section 6.2.1. The purpose of preventing any unusual material behaviour is to maintain uniformity of testing, with all samples tested under the same conditions. Samples that swell up towards a heat or ignition source increase the heat flux at the sample surface, increasing the likelihood of ignition and reducing the times to ignition. Such behaviour, along with the ripping open of material changing the sample geometry, was observed in the third scale tests, as described in section 6.2.1.5.1. This behaviour may ruin standard tests, but if repressed then no account can be taken of it in hazard assessment.

The scattering of small pieces of crumbled material from phenolformaldehyde tests drastically altered the effect the ignition source could have on the material, in the third scale tests, table (5.59). This foam could smother a small ignition source, with even larger ones being covered, thereby preventing the source from affecting any surrounding materials. Whilst a Cone Calorimeter or other small scale test may show that the material did not easily ignite, it would not reveal this behaviour, which actually acts to reduce the hazard to other materials, for example in storage with it. Although the larger wood cribs, e.g. no. 7, were not extinguished by the material covering them, flaming combustion ceased and only smouldering could be maintained. The advantage of this in an unwanted fire could be considerable, but small scale tests cannot really be used to assess this.

6.2.2.5 Delamination

Material combinations that demonstrate delamination present a different hazard level when they are permitted to do this than when this behaviour is repressed. Delamination can provide thin layers of material which can ignite and spread flame quicker than the thicker material combination. The use of sample holders and edge frames can prevent this occurring, and can give misleading results.

6.2.3 Conclusions

The difficulty of using fire tests to predict real fire behaviour of materials cannot be underestimated. Results tend to be apparatus and test protocol dependent. Many

factors influence the results for even well-behaved materials. Those that do not stay in place and remain geometrically constant prove even more difficult to deal with. These are often the materials of interest and cannot be dismissed. Tests must be performed to gain an insight into potential material behaviour, even if the tests are initially only for observation purposes. A decision could then be made concerning the appropriate laboratory scale test, if any, for the material. One of the most important factors for hazard assessment is how the material will behave physically in a fire, and this must be understood before any further data can be used. Results from tests can also only be used if the test conditions, and how these affect the material response, are understood.

6.3 Geometry in Storage and Testing

The observation of the effect of separation on the ignition of slabs of Foam G (section 6.2.1.5.2.) indicated the importance of geometry in fire development. Whilst this has obvious implications for testing, both in this particular test method and others that employ parallel surfaces such as the Brandschacht test (DIN, 1978), a more important consideration is that of separation between racks of materials in warehouse fires. It is desirable to understand what storage geometries give rise to the worst exposure conditions in a warehouse fire, both to avoid these and to help in the selection of appropriate fire tests. It is therefore important to gain a deep insight into the fundamental behaviour of flames against vertical surfaces, especially between parallel surfaces. There is currently a shortage of information on vertical fire spread in confined spaces, despite the fact that is recognised that this is a common mechanism for rapid fire growth, and has now led to multiple fire fatalities in buildings (e.g. at the Summerland Fire) (Silcock and Hinkley, 1974). Assessing the hazard of combustible materials which may be used in such geometries requires an understanding of the effect of such geometries on ignition and flame spread characteristics. Two factors need to be considered:

(a) how the configuration affects the ease with which materials can be ignited by a given ignition source,
(b) once ignited, how the configuration influences the rate of fire development.

Tests were carried out to investigate the importance of separation distance, ignition source position, ignition source power and size, and geometrical factors which

influence the flow characteristics such as open/closed base and end restrictions. These are described in detail in Chapter 4 and the measurements of wall heat fluxes, temperatures and flame heights are given in Chapter 5. The influence of the different factors studied are now discussed, along with an investigation into the relative fraction of heat transfer by radiation and convection from calculation and measurement. All measurements are made under steady state conditions.

6.3.1 Separation

The effect that reducing the separation between the parallel walls has on the total heat flux at one of the walls is shown clearly in figure (6.7). Just a small decrease in the separation distance causes a significant increase in the heat flux, for all the burner types and for both the open and closed base configurations, with the highest increases giving up to a six fold increase in heat flux as the separation is decreased from 140 mm to 60 mm. This trend is consistent with findings of other researchers under different conditions (e.g. Toong, 1961; Kim *et al.*, 1974), although the heat fluxes were not seen to go through a maximum, then decrease with a further decrease in separation as was observed in some cases (Tamanini, 1979). The trend is most noticeable for the closed base configuration, which is affected more as air can only be entrained horizontally through the gap at the ends of the walls and not vertically from below them. Flame heights also increase with decreasing separation. The increase in heat flux with decrease in separation distance has obvious implications for the storage of bulk materials, as well as for the testing of materials with relation to their future storage conditions. For example, the Cone Calorimeter may be used to give information on the ignitability of materials and, along with certain models, this can be used to assess flame spread. However, the irradiance level in the Cone Calorimeter must be appropriate to the end use or storage conditions of the material. The heat fluxes produced from flames under different conditions, such as those created when separation distances are altered, and those situations which may lead to unexpected values must be understood.

The point at which the opposite wall becomes important is of interest. For the line burner tests with the burner in the centre of the channel, (section 5.2.2.1.1), the separation distance has an effect at all three separations investigated, although these could not be compared with a single wall as the burner could not be in the centre of an infinite gap. With the line burner against the instrumented wall, and an open

base, the wall heat fluxes for the 140 mm separation are slightly less than for the single wall case; the parallel wall is having little effect. This effect was seen by Kim *et al.* (1974) where short fuel surfaces or wide channels between parallel surfaces demonstrated the independence of the burning from the opposite wall. This is also the case for the 100 mm separation with the lower burner heat output, but for the higher heat release rate the heat fluxes are higher at 100 mm separation than for the single wall. The wall heat fluxes are higher for both burner flow rates at the 60 mm separation. Therefore, the influence of the opposite wall depends upon the size of the heat/ignition source between the parallel surfaces, as well as the separation distance itself. In the closed base configuration, the opposite wall gives higher heat fluxes than a single wall for all cases, suggesting the importance of air flow patterns on the system. This will be discussed in more detail later.

In the 'Buxton' tests where a circular burner was used, the temperature measurements increase with decreasing separation. This is especially noticeable with increasing height, probably due to flame extension caused by reducing the air entrainment on reducing separation, although flame heights were not measured. As the base was closed off, air could only enter through the gap at the end of the walls. As entrainment is therefore a function of separation, and flames are elongated by reduced entrainment (Hasemi and Tokunaga, 1984a; Sugawa *et al.*, 1991) so reducing the separation between the walls will increase the flame height.

6.3.2 Burner Position

The position of an ignition source can affect the outcome of a fire test, as discussed in Chapter 3. Parallel wall tests done for this thesis included ones with the line burner and the sandbed burner against each of the walls and in the centre of the channel between the walls. In the majority of cases, the heat flux to the wall is greatest with the burner against that wall, figure (6.8). This is in agreement with previous findings (Williamson *et al.*, 1991). Moving the burner away from the wall allows the convective cooling of the wall, reducing the measured heat flux. The convective heating from the flame will also be reduced in this way. In the case of the open base, the heat fluxes at the instrumented wall are higher with the burner against the opposite wall than in the centre of the channel. This is probably due to an increase in cross-radiation with the burner against a wall, increasing the temperature of the opposite wall will increase the radiation from it to the

instrumented wall. This is considered in more detail in the section discussing convection and radiation.

The burner positions have a slightly different effect in the closed base configuration. In general, the heat fluxes are higher for the burner at the instrumented wall, and higher with the burner at the opposite wall than with it in the centre of the channel. This, however, is not the case with the smallest, 60 mm, separation between the two walls. In this situation, the heat fluxes at the wall are up to 67% higher with the burner in the centre of the channel than against the wall. The reason for this is that, for this particular separation and base configuration, the flame fills the entire width of the channel, impinging for part of the time on *both* walls. This leads to high rates of cross-radiation, as well as increased convective heat transfer. When the burner is located against either of the walls, the flame attaches itself to the wall and does not impinge on the opposite wall.

The burner position also affects the flame height, and therefore heat flux distribution, tables (5.6)-(5.10). Flame heights are greater for flames against walls than for unconfined flames, as found by Hasemi and Tokunaga (1984b). With the open base configuration and the line burner against a wall, the flame tip heights agree well with Hasemi's equation, table (3.2), to predict flame height. The agreement for solid flames is, however, poor, with the measurements made here being higher than Hasemi's, figure (6.9). The closed base, figure (6.10), shows higher readings for both solid flame and flame tip than the prediction for wall flames. This is understandable as the previous predictions were based on single walls; the parallel case further restricts air flow to the flames, especially in the closed base configuration, causing flame extension. The reduction of the wall separation to 60 mm with the closed base gives the greatest flame heights of all the cases.

The flame heights for the burner in the centre of the channel are lower than for the burner at a wall, and therefore cannot be compared with the predictions for confined flames. The results have been compared with Hasemi's predictions for unconfined flames, table (3.2). The flame heights generally increase with decreasing separation, and are the highest for the 60 mm separation. This is caused by the reduced entrainment with the smaller separations. The open base configuration, figure (6.11), gave lower flame tips than the prediction, although the measured results are for the mean flame height and the prediction is for the height of the flame tip, which would explain the difference. The mean flame height is the one at which the flame

is present 50% of the time. The solid flame heights are greater than the predicted ones, as expected due to some degree of flow restriction. The closed base gives larger flames than the open, with the flame height again generally increasing with decreasing separation, as shown in figure (6.12). The predictions of solid flame height always underestimate the measured values here, with the flame tip height being overestimated, although the measured values are again the mean flame height rather than the tip.

Apart from the exceptional case of the 60 mm wall separation with the burner in the centre of the channel, the likelihood of ignition and high rates of flame spread will be increased with an ignition source placed against a vertical material surface, rather than at some distance from it. Along with the presence of parallel surfaces, this is a factor to be considered in hazard assessment.

6.3.3 Burner Output

The heat release rate of an ignition source plays an important part in the level of heating a material is exposed to and its consequent behaviour. Previous studies (e.g. Williamson *et al.*, 1991, Hasemi, 1984) have found the heat output to be one of the factors governing the heat fluxes measured at walls for burners against a wall or in a corner. In this study, two heat release rates from the propane burners were investigated; 7 and 12.5 kW. As expected, the higher burner heat release rates gave higher heat fluxes at the wall and higher temperatures, both in the Buxton tests as measured by thermocouples at different depths into the channel, and the flame temperatures measured using the infrared thermometer. The exact influence of the burner heat release rate on wall heat flux will be considered mathematically in the section dealing with correlations.

6.3.4 Burner/Ignition Source Geometry

The wall heat flux distribution from a simple line burner, a sandbed line burner, a circular burner and a British Standard No. 7 crib were all investigated. The geometries of the heat sources were expected to affect the heat fluxes and the heat flux distributions to the wall, as the flame shape would be altered. It has also been suggested that burner geometry influences the relative components of radiation and convection, and that different burner geometries have been shown to affect the wall

exposure conditions (Ahonen *et al.*, 1987). This would influence the subsequent course of an unwanted fire. A typical set of heat flux distributions are shown in figure (6.13).

The circular burner gives the highest heat fluxes along the vertical centreline of the wall, the heat flux falling with increasing distance across the wall. The differences between the centreline flux and those further across the wall decrease with height. This is because the difference in heat flux is greater between flame and hot gases than between the centreline combustion products and the outer edge combustion products. The temperature profiles reveal the same trend, with the highest temperatures being recorded along the centreline, falling across the wall. The highest temperatures occur in the centre of the channel between the walls, and fall towards the walls, figure (6.14). The flame heights, although not measured, appear far greater for this burner geometry than for the line burners, as shown by the relatively high heat fluxes at the greater heights. This is expected as the fuel is released over a smaller area of the channel.

The line burners give higher heat fluxes close to the base of the walls, with more uniformity across the wall than the circular burner, especially with the open base. The heat flux falls with height, significantly in the lower half of the wall opposite the flame, and less markedly towards the top where the heat is transferred to the wall only from hot combustion gases together with radiation from the opposite wall, e.g. figure (6.15). The simple line burner and the sandbed burner give a similar pattern, with slightly higher heat fluxes close to the base of the wall for the sandbed burner.

The wood crib does not provide the same steady state burning as the gas burners, as the available fuel is consumed without replacement. The maximum heat flux measured at the wall with the number 7 crib was about 30 kWm^{-2} at 300 mm above the base of the walls, figure (6.16). This was greater than the maximum for the circular burner heat release rate of 7 kW at a separation of 100 mm, but less than the same heat release rate at the 60 mm separation. The temperature measurements show higher maximum temperatures for the crib than the gas burner at similar positions, but only close to the crib. The maximum temperatures are lower for the crib than the burner further from the source. The temperature also falls across the wall more rapidly for the crib than the burner. These differences in temperature and heat flux distribution highlight the differences between gas burners and solid fuel

ignition sources, and the potential problems associated with using gas flames to represent real sources.

The different heat flux distributions given by various ignition source types and geometries are important for material testing and for fire development. Subsequent flame spread will depend upon the ignited area and its geometry, due to the differences in vertical and lateral flame spread rates. The potential heat flux and/or temperature distributions arising from different ignition sources are an important consideration in both fire testing and hazard assessment.

6.3.5 Open/Closed Base

The flow characteristics of the parallel wall system could be altered by either having an air gap between the walls and the laboratory bench, or by preventing air entrainment beneath the walls by use of a kaoboard base. The open and closed base configurations occur in warehouse storage when materials are stacked on pallets or directly on the ground. The results from these tests, tables (5.6)-(5.16), show the significant influence that air flow has on the flame and heat transfer characteristics of this configuration. The heat fluxes at the wall are generally higher with the closed base than with it open, especially with the burner in the centre of the channel. In the most extreme case the wall heat flux is almost four times as large for the closed base than the open, tables (5.6) and (5.8). This is for the smallest separation between the walls, the burner in the centre of the channel, and the highest burner heat release rate. When the base is open, cool air can enter the system beneath the walls, providing air for combustion, and reducing the convective heat transfer to the walls when the burner is in the centre of the channel. With the burner in the centre of the gap, the flame behaves as a reasonably uniform sheet between the two walls.

When the base is closed, air can only enter horizontally through the gap at the ends of the two walls, meaning higher air velocities between the walls, in order to provide sufficient air for combustion. Cool air does not come between the flame and the walls as easily, and the flame is pushed towards the centreline of the walls by the incoming air from the sides. This is seen in the contour plot for the 60 mm separation, burner in the centre of the channel and the 12.5 kW heat release, figure (6.17a) and can be compared with the plot for the open base, figure (6.17b). In this, the most extreme case, with the closed base the flame can be seen to fill the entire

width of the channel to access sufficient combustion air. The flame impinges on both of the walls and the heat fluxes at the walls are very large, from the increase in flame radiation from the thicker flame, the increase in cross radiation due to flame impingement on both walls, and from convection. The heat transfer will be studied more closely in the section covering radiation and convection. The flame behaviour for the open and closed bases in this particular case is shown in photographs of the two flames, figure (6.18).

Results also indicating the importance of convection and air movement have been obtained from investigations of tunnel fires using zone and field CFD models (Kumar, 1992, Beard, 1995a). In the first of these, the radiative heat fluxes at the tunnel floor for a 200 litre petrol fire in the 300m long Zwenberg Tunnel (Feizlmayr, 1976) were simulated using the Fire Research Station's field model, JASMINE and a special tunnel fire version, TUNFIRE. Radiation hazard assessments were made based on unacceptable pain-threshold levels at certain points on the tunnel floor. With an air velocity of 2 m/s, this unacceptable level extended to about 70m downstream of the fire, whilst with the higher velocity of 4 m/s, the hazardous heat flux extended only to 22m downstream. This increase in the available air provided a reduction in convective heat transfer, similar to that observed in the parallel wall tests. The second paper on the effect of ventilation in tunnel fires (Beard, 1995a) considered the problem of an HGV burning in the Channel Tunnel. The effect of ventilation was assessed by predicting the fire size necessary at one burning HGV to cause ignition of a second item, a target HGV, using the zone model FIRE-SPRINT A1,. At an air flow velocity of 2 m/s, the necessary fire size is 55.2 MW, at 2.5 m/s it is 72.6 MW and at 3 m/s the critical fire size cannot be reached at all. Although the author has stated that the actual numerical values cannot be considered to be accurate (Beard, 1995b), the trend is expected to be the same in experiment. That is, increasing the air flow rate causes a reduction in convective heat transfer by increased entrainment of cool air, which reduces the downstream heat fluxes.

An understanding of the conditions which may lead to unusual ignition or flame spread behaviour in an unwanted fire is necessary in order to select adequate fire protection measures and escape facilities for employees. The difference in results between the open and closed bases was not expected, but the significance of generating extremely high heat fluxes cannot be underestimated. Taken simply, this result indicates that it would be preferable to store materials on raised pallets in warehouses which allow the air to pass vertically between them. On a more

fundamental level, it shows that further work should be done to improve the understanding of heat transfer from flames in confined spaces.

6.3.6 Flow Restriction

Flow restrictions occur in warehouses in corridors between stacks of pallets, and the effect of these is therefore of interest. The tests performed to investigate the effect of air flow restrictions on wall heat fluxes did not demonstrate the unusually high heat fluxes at the wall for the closed base and the 60 mm separation (tables (5.6) and (5.33)). The apparatus in this case was slightly different from all the previous tests, as the monolux boards were mounted on metal frames in such a way that the burner could not be embedded in the kaoboard base for the closed base tests. Although the base was the same, the burner now sat on top of the base, which allowed air to flow past the burner before the point at which the gas was released. This was the cause of the lower heat fluxes as the flame in this case did not spread out to fill the entire width of the channel as previously. This was shown to be the case on comparing the heat fluxes for these tests with no end restriction with the previous results. Those for the open base, both with the burner in the centre of the channel and against the wall, are similar within an expected scatter of data. The experiments with the closed base and the burner in the centre gave similar results for the largest separation, 20-24% lower heat flux values for this set than the previous for the 100 mm separation, and up to 34% lower for the 60 mm separation. The tests with the burner at the wall demonstrated the opposite trend, with the heat fluxes for this set of experiments being 16-25% higher than previously.

It was anticipated that the two sets of data would not be the same, which was the reason behind carrying out the new 'control' set of experiments with no end restriction before investigating the effect of altering the air flow, see section 4.2.6. All conditions were then kept constant, except for the insertion of monolux board to alter the blockage ratio at the end of the walls (sections 4.2.6 and 5.2.2.5).

No simple relationship between the changes in heat flux with blockage ratio was obvious. Altering the flow restriction had different effects under different conditions. The wall heat fluxes, for the open base and the burner at the wall, (tables (5.22)-(5.24)) increase as the blockage ratio is increased from zero to 1/2, figure (6.19). This is due to the increased turbulence and flame heights caused by reducing

entrainment. However, the heat fluxes are considerably lower with the total end restriction. This is the result of the inefficiency of combustion caused by preventing the easy entrainment of oxygen. It is comparable to the decrease in heat fluxes, burning rates and flame spread rates seen by other researchers for small parallel surface separation distances (e.g. Kurosaki *et al.*, 1978, Tamanini, 1979, and Bellin, 1991). The exception to this trend is at 308 mm above the burner, with the smallest wall separation, where the heat fluxes are slightly higher for the total flow blockage than without, this probably being caused by slight flame extension.

The heat fluxes for the burner in the centre of the channel, with the open base, (tables (5.25)-(5.27)) were similar, falling slightly, for the open ends and the 1/4 and 1/2 blockage ratios, for all the wall separations, figure (6.20). The total end restriction again gave lower heat fluxes, for the same reason as for the burner at the wall.

The effect of the flow restriction was different for the closed base than the open. With the burner at the wall, figure (6.21) from tables (5.28)-(5.30), the heat fluxes do not change much as the blockage ratio is altered from zero up to 1/2. The centreline fluxes decreased slightly whilst those further away from the centreline increased. The total restriction causes an increase in the heat fluxes, again with the centreline ones sometimes being reduced whilst those across the wall are increased. This means that the heat fluxes become more constant across the wall with increasing restriction. The heat fluxes with the burner at the wall are greater for the closed base, with the total end restriction, than the open, for all separations. For the 140 mm separation, the heat fluxes are fairly similar for both open and closed bases at all except the total blockage, whilst for the 100 mm separation, the open ends, as well as the total restriction, gave higher heat fluxes for the closed base. The smallest wall separation gave higher heat fluxes for the closed base in all cases.

The flow restrictions for the closed base have more influence with the burner in the centre of the channel, tables (5.31)-(5.33). The heat fluxes increase as the blockage ratio is increased, figure (6.22), with the total restriction providing the highest heat fluxes of all. The flow restrictions have a greater effect with decreasing wall separation. This is the opposite trend from the open base wall heat fluxes. In all cases for the burner in the centre, the heat fluxes are higher for the closed base than the open, as the reduced entrainment increases turbulence and flame extension.

For almost all the experimental configurations, higher heat fluxes were produced with the burner against the wall than with it in the centre of the channel. The exception to this was the 60 mm separation with the 1/2 and total end restrictions, where some of the measured heat fluxes over the wall were higher with the burner in the centre. The closed base with the burner in the centre of the channel gave higher heat fluxes than the open base with the burner at the wall for the 60 mm separation, with both total and no end restriction, and for 100 mm separation with the total blockage. The largest wall separation always had higher heat fluxes for the wall burner than the burner in the centre of the channel, even when the first was with the open base and the second with a closed base.

Generally, restricting the air flow to a parallel wall system could, under certain circumstances, enhance flame spread, although reduced combustion efficiency could result in slower spread of flame. This reduced efficiency may also present a problem in certain fire situations as it could lead to a build up of flammable smoke, with the potential for explosion and spreading fire outside the confines of the initial compartment etc.

6.3.7 Radiative and Convective Heat Transfer

Heat is transferred from flames mainly by convection and radiation. The relative importance of each of these under different conditions is of interest, both to increase understanding of heat transfer from flames and to improve fire protection measures. The 'Buxton' series of tests, with the circular burner in the centre of the channel, both total heat flux and temperature in the channel were measured. As a first step towards understanding the heat transfer through the system, calculations were made of radiative heat transfer from one wall to the opposite one. The wall temperature was assumed to be equal to the measured temperature 3 mm into the channel. Whilst this is not accurate, the aim was to obtain heat fluxes of the right order of magnitude, to investigate the radiative heat transfer from the opposite wall. Emissivity from the soot-covered walls was assumed to be unity. The method of configuration factors was used where $\dot{q}'' = \phi.\varepsilon.T^4$ and ϕ is the configuration factor. The configuration factors at each point of interest (i.e. the places where heat flux measurements were taken) were calculated from each section of the grid drawn on the opposite wall. The heat fluxes from each of the grid sections to the measurement point were calculated from $\dot{q}'' = \phi.\varepsilon.T^4$, with the heat flux at each measurement

point given by the sum of the heat fluxes from each grid section. A detailed description of this method can be found in, e.g. (Drysdale, 1985, pp. 62-67). The configuration factors were calculated using the equation (McGuire, 1953)

$$\phi(\alpha,S)=\frac{1}{2\pi}\left\{\sqrt{\frac{\alpha S}{1+\alpha S}}\tan^{-1}\sqrt{\frac{\alpha/S}{1+\alpha S}}+\sqrt{\frac{\alpha/S}{1+\alpha/S}}\tan^{-1}\sqrt{\frac{\alpha S}{1+\alpha/S}}\right\} \quad (6.8)$$

where $S = L_1/L_2$ and $\alpha = (L_1 \times L_2)/D^2$

L_1 and L_2 are the length and height of the boards, D is the separation between them.

The grids used in the calculation of configuration factors at various points and the heat fluxes at the measurement points are shown in figures (6.23)-(6.26). The configuration factors from each part of the grid to each of the sixteen measurement points were calculated, the configuration factors at each point were summed and the heat flux calculated using the average of the temperatures on the bottom and the top of the grid section. In the interests of brevity, and because the calculation process is reasonably simple, the large number of the configuration factors have not been listed. Instead summary tables of the measured (total) and calculated (radiative) heat fluxes for the three cases considered are included below. It is worth noting at this point that flame temperatures measured using the infrared thermometer with the line burner did not reveal any dependence of temperature on separation, burner heat release rate, burner position or open/closed base configuration. Temperatures at a given height may increase as separation is decreased, due to flame extension, but the temperatures within the flame itself are not increased and do not therefore contribute to increases in radiation and convection.

Table (6.1) 100 mm separation, 7 kW

Ref. Point	Height /mm	Dist. from centreline /mm	Calculated radiative flux /kWm^{-2}	Measured total heat flux /kWm^{-2}
A1	108	0	2.36	21.56
A2	108	50	1.93	11.10
A3	108	100	1.18	5.47
A4	108	150	0.63	2.23
B1	308	0	4.04	21.79
B2	308	50	3.35	15.86
B3	308	100	2.09	8.84
B4	308	150	1.11	3.73
C1	508	0	2.52	11.27
C2	508	50	2.17	9.51
C3	508	100	1.46	5.80
C4	508	150	0.81	2.42
D1	708	0	0.76	6.16
D2	708	50	0.71	5.77
D3	708	100	0.51	3.89
D4	708	150	0.30	1.80

Table (6.2) 60 mm separation, 7 kW

Ref. Point	Height /mm	Dist. from centreline /mm	Calculated radiative flux /kWm^{-2}	Measured total heat flux /kWm^{-2}
A1	108	0	6.70	43.24
A2	108	50	4.44	13.32
A3	108	100	1.96	5.92
A4	108	150	0.77	2.52
B1	308	0	11.84	46.36
B2	308	50	8.23	25.49
B3	308	100	3.85	11.33
B4	308	150	1.50	4.80
C1	508	0	7.36	25.15
C2	508	50	5.57	18.10
C3	508	100	2.92	8.68
C4	508	150	1.20	3.88
D1	708	0	2.17	13.79
D2	708	50	1.74	11.79
D3	708	100	1.00	5.83
D4	708	150	0.45	2.56

Table (6.3) 60 mm separation, 12.5 kW

Ref. Point	Height /mm	Dist. from centreline /mm	Calculated radiative flux /kWm^{-2}	Measured total heat flux /kWm^{-2}
A1	108	0	8.37	42.69
A2	108	50	5.87	17.68
A3	108	100	2.78	8.27
A4	108	150	1.13	4.27
B1	308	0	19.38	60.58
B2	308	50	14.27	40.59
B3	308	100	7.12	18.34
B4	308	150	2.83	9.27
C1	508	0	18.76	58.04
C2	508	50	14.74	43.41
C3	508	100	7.91	21.75
C4	508	150	3.21	11.36
D1	708	0	7.75	43.09
D2	708	50	6.34	30.48
D3	708	100	3.58	16.56
D4	708	150	1.51	8.56

The calculated heat fluxes range from around 10 - 38% of the measured values, with the lower values being in the path of the flame, especially towards the base of the walls. Discrepancies may well exist because of the assumptions made for the calculations, but the fact that they are largest in the flame indicates that convective heat transfer, which was not calculated here, dominates. There will also be a contribution from radiation from the flame, again not taken into account here.

In order to investigate the heat transfer, an experimental program was undertaken where measurements of radiation as well as total heat flux allowed comparison of the relative importance of radiation and convection in different configurations. The line burner was used, rather than the circular as in the calculations above. The radiation varies from about 2.8 - 70% of the total heat flux, varying with burner position, heat release rate, separation between the walls, base configuration, and position on the wall, tables (5.17)-(5.19). In general, the convective component

dominates most of the time. Radiation plays a greater role close to the base of the walls, in line with the flame, and a lesser role closer to the top of the walls.

Both the total and radiative heat fluxes at the wall decrease with increasing separation between the parallel walls, tables (5.17)-(5.19). With the *closed base* and the line burner in the centre of the channel, the convective component falls most as the separation is increased, with a less significant decrease in radiation with increased separation. Therefore as separation between two vertical parallel surfaces is decreased the increase in hazard is caused by a rise in both convection and radiation, but it is the increase in the convective component that plays the greatest part. Convection is the dominant mode of heat transfer in all except the greatest separation and propane flow rate, where the radiative heat transfer makes up 54% of the heat transfer. In this case convection has been reduced by allowing greater entrainment of cool air and by reduced turbulence. Radiative heat transfer from the flame will remain similar as for the smaller separations, whilst cross radiation between the walls will also decrease with increased separation.

Convection has greater dominance for the closed base configuration than the open. For example, with the 60 mm separation distance and the burner in the centre of the channel (no tests were carried out for the closed base with the burner at the instrumented wall), the radiation close to the flame is increased by about 50% by closing the base. The convection is increased by around 180%. The increase in radiation will arise from the restricting the access of air for combustion, causing a thickening of the flames. The photograph, figure (6.18) shows this effect. The more significant increase in the convection is due to air flow patterns in the system.

The open base, tables (5.17) and (5.18), gives a different trend. Again, both the total and radiative fluxes decrease with increasing separation for the line burner in the centre of the channel, but it is the radiative component that falls by a greater fraction when the separation is increased from 60 mm to 100 mm, with the radiative heat transfer falling by up to 50% and the total flux by one third. Radiation and convection are almost equally important over the height of the flame for the 100 mm separation, whilst the radiation accounts for up to 70% of the total heat flux at the same point with the smaller separation. Radiation will be dominant as convection is reduced by the entrainment of cool air from beneath the walls. As expected, the heat fluxes fall with height, and radiation becomes relatively less important. With an increase in separation to 140 mm, both the radiative and the convective heat transfer

decrease, but this time it is the convective part that falls by a greater fraction, making the radiative component more significant for the overall heat transfer in this case than for the 100 mm separation.

With the line burner against the instrumented wall, open base, table (5.18), both the total and the radiative heat fluxes are higher than for the burner in the centre of the channel. The fraction of radiation is lower; the convective component is more important with the burner against the wall than with it moved away from the wall, with the radiation in this case being up to only 26% of the total heat flux. This is compatible with the idea that cool air can come between the flame and the wall with the burner moved off the wall, reducing the convective heating to the wall. In that case, the radiation forms a higher fraction of the heat transfer than when no cool air could come between the flame and the wall. The relative importance of the radiation falls as the separation distance is increased, and is lowest when there is only a single wall.

The burner against the opposite wall to the instrumented one gave lower total heat fluxes than for the burner against the instrumented wall, but higher ones than with the burner in the centre of the channel. The radiative flux was actually higher in this set up than for either of the other two burner positions. The fraction of radiation to the total heat flux was slightly higher than for the centre burner (e.g. 51% for burner in centre and 59% for the burner at the opposite wall) and much greater than for the burner at the instrumented wall, (which gave, for example, 25.5%). This indicates that the radiative heat transfer to a vertical surface parallel to one which has a flaming ignition source against it, where cool air can enter the system from beneath the vertical surfaces, is actually higher than that to the surface with the ignition source against it. More tests would be required to generalise, nevertheless, this shows the potential importance of cross radiation and flame radiation in parallel configurations, cavities etc.

The open and closed bases lead to different heat transfer patterns. The total and radiative fluxes are higher for the closed base than the open, especially close to the centreline, and the difference becomes more noticeable with decreasing separation between the walls. The relative importance of the radiation and convection changes with the different base configuration. Convection, although the most significant heat transfer mode in most cases, becomes by far the dominant method with the closed base. Cool air cannot flow between the flame and the walls in this case, convective

heat transfer is high as hot combustion gases come into contact with the walls. The heat fluxes decrease with height, the convective component becomes gradually less important, and becomes similar for the open and closed base configurations. Higher heat fluxes close to the top of the wall for the closed base than the open are now due to higher radiation for the closed base, rather than convection. At the top of the walls, the heat fluxes are similar for the open and closed bases.

The relative importance of the convection and radiation is not merely of scientific interest. To be able to reduce the hazard of ignition and rapid flame spread in a warehouse, or other vertical, parallel surface situations such as vertical ducts and cavities, and to be able to design tests and apply test data, an understanding of the heat transfer involved is crucial. For example, convection could be reduced by ensuring air gaps are available in bulk storage situations. Without the knowledge of the role of convection, radiation could be thought of as the problem and protective measures only considered with relation to this. Therefore, a good understanding of the heat transfer is important, making experiments such as those carried out for this thesis of importance. Further work investigating this for different configurations is required to extend the knowledge further.

6.3.8 Regression Analysis

Data for heat fluxes and temperatures have been obtained for flames between vertical parallel walls under several different conditions. To investigate whether there are any relationships between the results and the variables, regression analysis has been undertaken.

6.3.8.1 Introduction

For many experimental sets of data, it is desirable or even necessary to find a model for the relationship between several variables. The most common method used is the Pearson product moment correlation coefficient. This is the correlation coefficient normally used in scientific work to establish correlation between two variables x and y. It is given by:-

$$r = \frac{\sum (x - \bar{x})(y - \bar{y})}{\sqrt{\sum (x - \bar{x})^2 \sum (y - \bar{y})^2}} \qquad (6.9)$$

Its value lies between -1 and +1, although it is often the modulus of the number that is quoted for simplicity. The closer the data points are to forming a straight line, the nearer the correlation coefficient is to -1 or +1. If there is almost no association between x and y, the coefficient will be close to zero, although the converse is not true. The correlation coefficient only gives an indication of how closely the points lie on a straight line. If the relationship between them is a power relationship and gives a curve, the correlation coefficient will be very low. It is advisable to plot data where possible to ensure that this is not the case. This correlation equation can still be used for variables with a power relationship, but the calculations must be performed using the logarithms of the variables, to give the straight line.

Whilst correlation demonstrates how much association there is between two variables, regression analysis is used to find the best equation which describes the relationship between two variables. Again, these methods can only be applied to linear relationships. The relationship between heat fluxes at walls, wall separation distance, heat output, vertical and horizontal distance, and burner length are not simple ones but it is nonetheless desirable to obtain equations relating these parameters that can be used for predictive purposes. The conversion of data to natural logarithms enables linear regression to be used as the points then approximately fall on a straight line. Once in this form it is then relatively straight forward to search for the relationships and obtain the relevant equations.

6.3.8.2 Theory

The regression work carried out to examine the fairly complex relationships required several stages, but in order to explain clearly the theory and procedure, the response of wall heat flux to changes in one of the developed parameters will be considered. The use of a single input variable and response mean that the regression can easily be displayed graphically in Cartesian form. It is not difficult to expand this theory and practice to consideration of several variables.

Regression analysis provides a straight line through a set of data using the method of least squares to find the smallest sum of squared deviations of data from the best fit line. The equation of this line can be determined and a coefficient of determination found. This R^2 coefficient is simply the square of the correlation coefficient given by equation (6.9). It also has two other more general interpretations; it is the square

of the correlation between the observed and fitted y values and the fraction of variation in y that is explained by the fitted equation. The closer the R^2 coefficient is to 1.0, the closer the data will be to the fitted equation.

The use of regression analysis requires that several conditions must be met, at least approximately:

1. The relationship between x and y should be a straight line.
2. For each value of x, the amount of variation in the population of y values should be about the same. This variance is called the variance of y about the regression line and is denoted by σ^2. Correspondingly, σ is the standard deviation of y about the regression line.
3. For each value of x, the distribution of y values in the population should be approximately normal.
4. The y values obtained from the equation should be approximately independent. These are not independent if the amount by which a value of y differs from the mean is related to the amount that other y values differ from the mean.

The following example is used to explain the regression analysis. The case examined is for the wall centreline heat fluxes, two parallel walls, open base, line burner against the instrumented wall, with a term included for the separation between the walls. In figure (6.27), $\ln(q''_w)$ versus $\ln\left(x(a/D)^{0.36}/\mathrm{Q}_l^{*2/3}D\right)$ is approximately a straight line. (The experimental variables have been lumped together in this dimensionless group using this regression method, as discussed later in section 6.3.8.3.2, with this equation being (6.24)). The line plotted through the data is the best fit line calculated from the least mean squares method. Using these data, the spreadsheet in figure (6.28) was constructed. The input data, x and y are shown in the relevant columns, the other columns contain calculated parameters required to obtain the best fit equation, establishing if the parameters are statistically significant, and to allow confidence and prediction intervals to be calculated. 'Fitted y' is the set of data calculated from the equation of a straight line

$$y = a + bx \tag{6.10}$$

where a and b are found from general statistics (e.g. Ross, 1987,)

of the correlation between the observed and fitted y values and the fraction of variation in y that is explained by the fitted equation. The closer the R^2 coefficient is to 1.0, the closer the data will be to the fitted equation.

The use of regression analysis requires that several conditions must be met, at least approximately:

1. The relationship between x and y should be a straight line.
2. For each value of x, the amount of variation in the population of y values should be about the same. This variance is called the variance of y about the regression line and is denoted by σ^2. Correspondingly, σ is the standard deviation of y about the regression line.
3. For each value of x, the distribution of y values in the population should be approximately normal.
4. The y values obtained from the equation should be approximately independent. These are not independent if the amount by which a value of y differs from the mean is related to the amount that other y values differ from the mean.

The following example is used to explain the regression analysis. The case examined is for the wall centreline heat fluxes, two parallel walls, open base, line burner against the instrumented wall, with a term included for the separation between the walls. In figure (6.27), $\ln\left(q''_w\right)$ versus $\ln\left(x(a/D)^{0.36}/\mathrm{Q}_l^{*2/3}D\right)$ is approximately a straight line. (The experimental variables have been lumped together in this dimensionless group using this regression method, as discussed later in section 6.3.8.3.2, with this equation being (6.24)). The line plotted through the data is the best fit line calculated from the least mean squares method. Using these data, the spreadsheet in figure (6.28) was constructed. The input data, x and y are shown in the relevant columns, the other columns contain calculated parameters required to obtain the best fit equation, establishing if the parameters are statistically significant, and to allow confidence and prediction intervals to be calculated. 'Fitted y' is the set of data calculated from the equation of a straight line

$$y = a + bx \tag{6.10}$$

where a and b are found from general statistics (e.g. Ross, 1987,)

$$b = \frac{\sum (x - \bar{x})(y - \bar{y})}{\sum (x - \bar{x})^2} \tag{6.11}$$

and

$$a = \bar{y} - b\bar{x} \tag{6.12}$$

where x is the input parameter, y is the response parameter, $\bar{x}$ is the average value of x, $\bar{y}$ is the average value of y and a and b are constants. The calculated values of a and b are given in the spreadsheet, figure (6.28), beneath the x and y data columns. The equation of the best fit line is thus calculated as

$$\ln(q''_w) = 3.74 - 1.40 \ln\left(x(a/D)^{0.36} / Q_l^{*2/3} D \right)$$

giving the overall equation as (6.13)

$$q''_w = 42.18\left(x(a/D)^{0.36} / Q_l^{*2/3} D \right)^{-1.4}$$

The standard deviation of y about this line is calculated and given as 's'. This is the estimate of the population standard deviation σ. The lower this value, the closer the measured y values are to the calculated best fit line. s is given by the equation below

$$s = \sqrt{\frac{\sum (y - \textit{fitted } y)^2}{n-2}} \tag{6.14}$$

where *fitted y* are the calculated values of y for each x value, from equation (6.10) and n is the number of data points. The standard deviation given above has (n-2) degrees of freedom and is used in all formulae for standard deviations. All t-tests and confidence limits will be based on this s, and all will therefore have (n-2) degrees of freedom. In this example, the number of degrees of freedom is (24-2) = 22.

Standard deviation is also calculated for the coefficients a and b using the equations given

$$s_a = \sqrt{\frac{s^2 \sum x^2}{n.\sum (x-\bar{x})^2}} \tag{6.15}$$

$$s_b = \sqrt{\frac{s^2}{\sum (x-\bar{x})^2}} \tag{6.16}$$

When trying to find an equation which gives the relationship between all the parameters, it is necessary to be able to tell which parameters are statistically significant and therefore must form part of the final equation, and which do not affect the fitting of the results. It is by use of this knowledge that a correlation equation can be developed in stages and it was the use of this that enabled factors such as $(a/D)^{0.36}$ to be found relevant and integrated into the solution. The test of significance is carried out by testing each parameter against a null hypothesis, i.e. where the coefficient is zero. The value found from this calculation is compared with the relevant value taken from a Student *t*-test table (e.g. Chatfield, 1983), in this case the value shown at the top of the spreadsheet, figure (6.28) for a 95% confidence limit. If the calculated value is higher than the *t*-test one, the parameter can be said to be statistically significant as a predictor for the output. The larger the value, the more influence the parameter has on the *y* value.

The calculated *t* value is found from

$$t = \frac{\text{coefficient}(a,b,\text{etc}) - \text{hypothesised value}(=0)}{\text{estimated st. dev.of coefficient}} \tag{6.17}$$

The values for *t* are shown beside those for *a* and *b* in the spreadsheet. As can be seen, these are both statistically very significant. This is not unexpected as the coefficient *b* gives the exponent in equation (6.13) and *a* the coefficient and this equation has already been found and known to work. This *t* test is however very useful for finding the important parameters for inclusion in a predictive equation, as mentioned earlier.

The R^2 value, page 234, has also been calculated to find the percentage of variation in *y* values explained by the equation. The higher this value, the better the equation

is at predicting an output. The calculation to find this coefficient is performed using equation (6.18):

$$R^2 = 1 - \frac{\sum(y - \textit{fitted } y)^2}{\sum(y - \bar{y})^2} \tag{6.18}$$

The last column on the right of the spreadsheet contains the residuals data, i.e. the difference between the observed y value and the calculated one. The residuals are used as a test to check that the linear best fit is adequate. If the residuals are plotted against the input variable, x, figure (6.29), and the points are scattered around the zero residual line, then the linear equation is an adequate predictor of the output. If however, the points follow a trend, e.g., at low values of x the residuals are high, as x increases the residual value decreases and then increases again, then a different form of regression such as a polynomial should be sought.

Confidence and predictive intervals are used to predict what will happen for other tests and sets of data. The confidence interval gives an estimate of the population mean of all response (y) values at any given input value. The predictive interval is the estimate for a single output value. In other words, the confidence interval gives the estimated mean if a series of experiments were to be performed and the prediction interval gives the values between which each single data point is expected to fall. Greater uncertainty is expected for the prediction interval as it deals with only a single value, and therefore a wider interval is predicted. The equations below give the confidence and predictive intervals. For the values of t previously found, these equations give the 95% intervals.

$$\text{confidence interval} = \textit{fitted } y \pm t(\text{st. dev. fit}) \tag{6.19}$$

$$\text{prediction interval} = \textit{fitted } y \pm t\sqrt{(\text{st. dev. fit})^2 + s^2} \tag{6.20}$$

where (st. dev. fit.) is given by

$$\text{st. dev. fit.} = s.\sqrt{\frac{(x - \bar{x})^2}{\sum(x - \bar{x})^2} + \frac{1}{n}} \tag{6.21}$$

and is the standard deviation of the fitted y values.

The calculated values for confidence and prediction interval are shown at the bottom of the spreadsheet for a selection of x data and fitted y values. These intervals are shown on figure (6.30) along with the experimental data. This is for the data with the highest correlation coefficient and narrow confidence and prediction intervals are shown, with all the measured data falling into the prediction interval. Figure (6.31) drawn from a second spreadsheet, which has not been included for brevity, is for the lowest correlation coefficient of all the final proposed equations. A larger number of data were used in this case, 96 points across the whole of the wall, see equation (6.34), and the intervals are seen to be larger than in the previous case. However, only five data points fall outside the prediction interval, and these are not out by a significant amount. As a far wider range of data has been included in this correlation, this is not an unsatisfactory result.

From simple linear regression, the theory can be extended to include several input variables, with the dependence of one variable on several others being found. All the parameters can be treated in the same way as described, but graphical representation becomes impossible when there are more than two input variables. Analysis of more than two variables at one time prevents the plotting of data to check for a curve rather than a straight line. It is often easier to tackle the problem in a series of steps of two variables in order to allow graphical representation and therefore see whether a non-linear relationship exists.

6.3.8.3 Analysis of Data

Equations have been developed, using the statistics package 'Minitab', for the case of the line burner at the wall, both for a single wall and with the second wall at all the separations, and for the burner in the centre of the channel between the two walls. The dimensionless parameter Q_l^* as defined by Hasemi (1984) is used in all cases, where $Q_l^* = \dot{Q}_l / \left(\rho_\infty C_p T_\infty g^{1/2} D^{3/2} \right)$ and $\dot{Q}_l$ is the heat release rate per unit length of burner. All relationships are empirical and are based on correlations of the data from these tests. Regression analysis was performed using the natural logarithms of all parameters to obtain equations that use one variable to help explain the variation in another variable. From these regressions, a power relationship could be found and correlation coefficients determined. The correlation coefficient shows the fraction of variation in $\dot{q}_w''$ (the total heat flux) that is explained by the fitted equation. The

closer this value to 1, the more accurately the equation describes the data. Other dimensionless groups than the ones presented here, for example those identified by Quintiere and Cleary (1994), (equation 3.44), and ones using flame heights, were investigated. However, there was an insufficient range of data to make it worthwhile examining the effect of κD, as used previously (Quintiere and Cleary, 1994), and a preliminary check on using flame height in the dimensionless groups was not encouraging. It may be preferable to use image analysis techniques for determining the flame heights accurately, in which case it may be possible to incorporate them into these equations. However, whilst the presence of the flame will affect the heat flux to the wall, it appears that any alterations in the flame height caused by changing the parallel wall configuration are not a significant factor in altering the heat flux. The use of burner length, D, in the correlations is as a scaling parameter only, rather than being used in formal dimensional analysis. The burner length was not varied, and is only therefore a scaling parameter for linear dimensions.

6.3.8.3.1 Single wall, burner against the instrumented wall

The data are shown in figures (6.32) and (6.33).

Open base, centreline fluxes only

As this is the centreline there is no term included for distance across the wall. The equation best found to describe the fluxes at the wall was

$$\dot{q}_w'' = 104.95\left(x/\mathrm{Q}_t^{*2/3} D \right)^{-1.55} \qquad (6.22)$$

with a correlation coefficient of 0.993.

Closed base, centreline fluxes only

$$\dot{q}_w'' = 51.07\left(x/\mathrm{Q}_t^{*2/3} D \right)^{-1.29} \qquad (6.23)$$

This has a correlation coefficient of 0.987

As it is more useful for practical reasons to be able to estimate the heat flux at a wall away from the centre of an ignition source, correlations have been developed to describe the heat flux at any point across the wall. The horizontal term y' is the distance from the edge of the wall nondimensionalised with the line burner length D, $y'=y/D$, the burner length being the same as that of the wall.

Open base, all wall heat fluxes

Whilst the data are slightly more scattered here than on the centreline, as seen in figure (6.34), the correlation still has a very high coefficient of 0.990.

$$\dot{q}''_w = 136.8\left[x\Big/\left(\mathrm{Q}_l^{*2/3} D(y'/D)^{0.25}\right)\right]^{-1.56} \tag{6.24}$$

Closed base, all wall heat fluxes

$$\dot{q}''_w = 51.81\left[x\Big/\left(\mathrm{Q}_l^{*2/3} D(y'/D)^{0.35}\right)\right]^{-1.14} \tag{6.25}$$

The correlation coefficient, r, is 0.979 and the data are shown in figure (6.35).

Data from experiments on heat transfer from a line burner to a thin wall carried out by Hasemi (1984) have been plotted in Figures (6.32) (centreline only) and (6.34) (all relevant results) for comparison with the present data, although the experimental conditions were different. Hasemi used a thermally thin wall which had an open base but closed sides: it was considered (Hasemi, 1994) that this matched the present open base arrangement most closely, although the effect of the closed sides is not known. The agreement is very good. Not surprisingly, the data which he obtained for a line burner against an isothermal wall did not show the same correlation, falling well outside (below) the scatter of the present data.

6.3.8.3.2 Parallel walls, burner against the instrumented wall

The first equations derived are for the centreline heat fluxes only and are of the same form as the single wall tests in that a relationship is found between $\dot{q}''_w$ and $x/\mathrm{Q}_l^{*2/3} D$. This does not take into account the increase in heat flux caused by decreasing the separation between the walls. The equations are first developed

without the separation term included to assess the importance of separation on this different configuration. The graphs are shown in figures (6.36a) and (6.37a).

Open base, centreline heat fluxes

$$\dot{q}_w'' = 104.53\left(x/\mathrm{Q}_l^{*2/3} D\right)^{-1.4} \tag{6.26}$$

Although there is no allowance for the different separations, the r value remains high, at 0.979.

Closed base, centreline heat fluxes

$$\dot{q}_w'' = 89.5\left(x/\mathrm{Q}_l^{*2/3} D\right)^{-1.16} \tag{6.27}$$

Here the r value is much lower, 0.893, showing that there is another important factor missing from this correlation. This is not an unexpected finding as the graph in figure (6.7) shows the separation has a significant influence on the wall heat flux. The next two equations improve upon the previous ones by including a term for the separation, *a*, nondimensionalised by the burner length, *D*. The plots of these show the improvement, figures (6.36b) and (6.37b).

Open base, centreline heat fluxes

$$\dot{q}_w'' = 42.18\left[x(a/D)^{0.36}/\mathrm{Q}_l^{*2/3} D\right]^{-1.4} \tag{6.28}$$

The inclusion of the separation term improved the correlation from 0.979 to 0.991, showing that the separation does have some influence on the heat fluxes generated at the wall. When the separation term is taken out of the larger power equation, it can be seen that the heat flux depends on $(a/D)^{-0.5}$, or the inverse of the square root of the separation.

Closed base, centreline heat fluxes

$$\dot{q}_w'' = 12.74\left[x(a/D)^{0.905}/\mathrm{Q}_l^{*2/3} D\right]^{-1.16} \tag{6.29}$$

In this case the separation has a greater effect, with the heat flux depending on $(a/D)^{-1.05}$. The improvement in the correlation with the addition of the separation term is far greater for the closed base than for the open, increasing from 0.893 to 0.970. This further confirms the more important role the separation between the walls plays in this restricted air flow case.

Again it is desirable to have equations which can predict the heat flux at all points on the wall, so correlations have been sought which include the (y'/D) term as used for the single wall case.

Open base, all wall heat fluxes

The separation term introduced in the equation (6.28) is kept constant and the horizontal distance is included.

$$\dot{q}''_w = 67.38\left[x(a/D)^{0.36} \Big/ \left(\mathrm{Q}_l^{*2/3} D(y'/D)^{0.38} \right) \right]^{-1.47} \qquad (6.30)$$

This shows that as the distance from the edge of the wall increases, the heat flux increases. y' reaches a maximum at the centreline, where it equals 0.5, and the heat flux also reaches a maximum at this point. The horizontal distance does not have a very large influence, as for the open base situation the heat flux remains reasonably constant across the wall. The heat flux is proportional to $y'^{0.56}$. The correlation coefficient is 0.987.

Closed base, all wall heat fluxes

$$\dot{q}''_w = 23.31\left[x(a/D)^{0905} \Big/ \left(\mathrm{Q}_l^{*2/3} D(y'/D)^{2/3} \right) \right]^{-1.2} \qquad (6.31)$$

The horizontal distance has a greater effect in this case than for the open base as can be seen in the contour plots, figure (6.17). The heat flux falls away towards the edge of the wall, as air cannot enter from beneath the walls and so is entrained at a greater velocity from the sides of the walls. This will lead to a higher rate of cooling close to the edges and also visibly pushed the flame over towards the centreline of the walls. The heat flux is proportional to $y'^{0.8}$, with a correlation coefficient of 0.962.

The graphs in figures (6.38a) and (6.38b) show these relationships for the open and closed base configurations. The results for the different separations are reasonably evenly distributed along the curve, showing that the separate data sets all obey the same relationship.

6.3.8.3.3 Parallel walls, line burner in the centre of the channel

For the burner in the centre of the gap, there can be no single wall configuration, as the gap is infinite. For the parallel wall situation, equations have again been developed for the heat fluxes on the centreline and then extended to include the horizontal position. It was found that the separation term was always necessary in this case to obtain a satisfactory correlation. It was also found that the relationships best able to describe the data included the term $Q_l^* D$ rather than the previously used $Q_l^{*2/3} D$. These are shown in figures (6.39) and (6.40).

Open base, centreline heat fluxes

$$\dot{q}_w'' = 12.85\left[x(a/D)^{1.04} / Q_l^* D\right]^{-0.741} \qquad (6.32)$$

This had a correlation coefficient of 0.979. The heat flux depends on the separation to the power of -0.77, whereas for the open base with the burner at the wall it was $(a/D)^{-0.5}$. The separation is therefore of more influence in this case.

Closed base, centreline heat fluxes

$$\dot{q}_w'' = 8.23\left[x(a/D)^{1.7} / Q_l^* D\right]^{-1.02} \qquad (6.33)$$

The separation term is seen to be more important here than for the burner at the wall, as the heat flux is influenced by $(a/D)^{-1.73}$, rather than $(a/D)^{-1.05}$. This is confirmed by the fact that it was impossible to obtain a reasonable correlation coefficient without inclusion of the separation term. For this equation the correlation gives a coefficient of 0.987.

These equations were then extended to the flux distribution across the wall and the term y'/D included.

The graphs in figures (6.38a) and (6.38b) show these relationships for the open and closed base configurations. The results for the different separations are reasonably evenly distributed along the curve, showing that the separate data sets all obey the same relationship.

6.3.8.3.3 Parallel walls, line burner in the centre of the channel

For the burner in the centre of the gap, there can be no single wall configuration, as the gap is infinite. For the parallel wall situation, equations have again been developed for the heat fluxes on the centreline and then extended to include the horizontal position. It was found that the separation term was always necessary in this case to obtain a satisfactory correlation. It was also found that the relationships best able to describe the data included the term $Q_l^* D$ rather than the previously used $Q_l^{*2/3} D$. These are shown in figures (6.39) and (6.40).

Open base, centreline heat fluxes

$$\dot{q}_w'' = 12.85\left[x(a/D)^{1.04} / Q_l^* D\right]^{-0.741} \qquad (6.32)$$

This had a correlation coefficient of 0.979. The heat flux depends on the separation to the power of -0.77, whereas for the open base with the burner at the wall it was $(a/D)^{-0.5}$. The separation is therefore of more influence in this case.

Closed base, centreline heat fluxes

$$\dot{q}_w'' = 8.23\left[x(a/D)^{1.7} / Q_l^* D\right]^{-1.02} \qquad (6.33)$$

The separation term is seen to be more important here than for the burner at the wall, as the heat flux is influenced by $(a/D)^{-1.73}$, rather than $(a/D)^{-1.05}$. This is confirmed by the fact that it was impossible to obtain a reasonable correlation coefficient without inclusion of the separation term. For this equation the correlation gives a coefficient of 0.987.

These equations were then extended to the flux distribution across the wall and the term y'/D included.

Open base, all wall heat fluxes

$$\dot{q}''_w = 22.71\left[x(a/D)^{1.04} \Big/ \left(Q_l^* D(y'/D)^{0.86}\right)\right]^{-0.797} \qquad (6.34)$$

The horizontal distance has more influence for the burner away from the wall than for it against, with the heat flux dependent on $(y'/D)^{0.69}$. The equation gives a correlation coefficient of 0.956.

Closed base, all wall heat fluxes

$$\dot{q}''_w = 23.94\left[x(a/D)^{1.7} \Big/ \left(Q_l^* D(y'/D)^{1.34}\right)\right]^{-1.04} \qquad (6.35)$$

This equation shows a dependence of heat flux on horizontal distance to the power of 1.39, again larger than for the burner against the wall and for the open base. The correlation coefficient in this case is 0.957.

6.3.8.3.4 Temperatures in the channel between two walls

The heat transfer in any system depends, amongst other things, upon the temperature on the various components of the system. Measurement of temperature is often made and temperatures discussed as representing hazard. Understanding the factors which influence temperature can increase understanding of heat transfer. Correlations were carried out using the statistical package, 'Minitab', for flame temperature, as measured using thermocouples pushed through small holes in the monolux walls into the channel, with the other variables. The distribution of thermocouples across the wall is shown in figure (4.3), the temperatures being recorded halfway into the channel, a quarter of the way in and at a depth in of 3 mm. The temperature data are from the tests performed at HSE using a circular propane burner and a closed base. The flame produced from this configuration was tall and narrow. The development of the equations was carried out on a step by step basis, obtaining the power relationship for one or two variables at a time, as previously. T_m is the measured temperature in Kelvin, T_a is the ambient temperature, Q^* is the nondimensional heat release rate as defined previously, D is the diameter of the

circular burner, b is the depth into the channel perpendicular to the wall, h is the height of the wall, and the other variables are as previously described.

Centreline temperatures in the centre of the channel

$$\frac{T_m}{T_a} = 3.82 - 0.743\left(\frac{a}{D}\right)^{.85}\left(\frac{x}{Q^{*.88}D}\right) \qquad (6.36)$$

This shows that the temperature is dependent on the separation. It also varies with height and the heat release rate. The correlation coefficient for the above expression is r = 0.979.

The data can also be fitted to a polynomial, with an improved correlation coefficient:

degree	r
0	0
1	0.980
2	0.980
3	0.990
4	0.995

where the polynomial expression is

$$\frac{T_m}{T_a} = 3.29 + 1.29(eqn) - 2.11(eqn)^2 + 0.0792(eqn)^3 - 0.0966(eqn)^4$$

and the (eqn) is the whole right hand side of equation (6.36). The best fit lines are shown in figure (6.41).

Centreline temperatures, all depths into the channel

See figure (6.42)

$$\frac{T_m}{T_a} = 0.94 + 2.984\left(\frac{b}{a}\right)^{.077} - .659\left(\frac{a}{D}\right)^{.85}\left(\frac{x}{Q^{*.88}D}\right) \qquad (6.37)$$

r = 0.959. The temperature increases with depth into the channel.

Again this can be improved, but only slightly, by fitting the data to a polynomial of the form

$$\frac{T_m}{T_a} = 1.415 + 1.09 \times 10^{-3}(eqn) - 9.81 \times 10^{-7}(eqn)^2 + 1.25 \times 10^{-8}(eqn)^3 - 1.11 \times 10^{-11}(eqn)^4$$

where (eqn) is the right hand side of equation (6.37).

degree	r^2
0	0
1	0.959
2	0.959
3	0.964
4	0.964

all temperatures between the walls

$$\frac{T_m}{T_a} = -0.132 + 3.55\left\{\left[\left(\frac{b}{a}\right)^{.039}\left(\frac{y'}{D}\right)^{1.1} Q^{*1/3}\right] \Big/ \left[\left(\frac{x}{h}\right)^{.0169}\left(\frac{a}{D}\right)^{.207}\right]\right\} \qquad (6.38)$$

r = 0.894, figure (6.43).

The temperature further varies across the wall, as would be expected from the tall, narrow flame shape. Although the correlation coefficient is reasonable, it appears that there may be more variables influencing the flame temperature than have been included here. Flame height is an obvious one, which was unfortunately not recorded. The lower correlation coefficient may also be caused by a greater scatter of experimental data.

6.3.8.3.5 Radiative Heat Fluxes

The relationship between radiative and convective heat transfer from flames is important. Fire protection measures may be more effective if the dominant heat

transfer mechanism is known, and fire prevention may be more successful. Knowing the relative importance of each of these under different conditions will improve the understanding of heat transfer and flame spread.

Regression analysis has been carried out for the measured radiation at a wall, for the line burner at the instrumented wall and in the centre of the channel, with the base both open and closed and the separation and burner gas flow rate altered. The relationship that the radiative heat fluxes have with these variables is investigated, as well as the relationship they have with the total heat fluxes. $\dot{q}_r''$ is the radiative heat flux (kWm^{-2}). The equations are only applicable for $\dot{q}_r''>0$.

6.3.8.3.5.1 Regression for radiation only

This is the series of correlations comparing the radiative fluxes with the other variables, without the inclusion of the total heat fluxes.

Single wall, open base, line burner at instrumented wall

$$\dot{q}_r'' = -0.132 + 6\left[\frac{(x/D)}{Q_1^{*0.53}(y'/D)^{0.083}}\right]^{-1.72} \qquad (6.39)$$

The correlation coefficient is 0.981, the data shown in figure (6.44). The radiative heat flux is dependent, as for the total flux, on the height, horizontal distance, and burner heat release rate. It is less dependent on the horizontal distance than the total heat flux is ($\dot{q}_r'' \propto (y'/D)^{0.14}$, $\dot{q}_w'' \propto (y'/D)^{0.39}$). The height has slightly more influence on the radiation, whilst the heat release rate affects the total heat flux very slightly more than the radiative flux.

Parallel walls, open base, line burner at the instrumented wall

$$\dot{q}_r'' = 0.128 + 20.8\left[\frac{x(a/D)^{0.15}}{Q_1^{*0.7} D(y'/D)^{0.124}}\right]^{-1.81} \qquad (6.40)$$

This is shown in figure (6.45). The correlation coefficient in this case is 0.978. The radiative heat flux is considerably less dependent on the separation than is the total

flux ($\dot{q}''_r \propto (a/D)^{-0.27}$, $\dot{q}''_w \propto (a/D)^{-1.09}$). The height again has more effect on the radiation, as does the heat release rate, whilst the total heat flux is affected more than the radiation by the horizontal position.

Parallel walls, open base, line burner in the centre of the channel

$$\dot{q}''_r = -0.039 + 8.07\left[\frac{x(a/D)^{0.53}}{Q_1^{*0.7} D(y'/D)^{0.29}}\right]^{-1.72} \qquad (6.41)$$

The correlation coefficient is 0.981, figure (6.46). The separation in this case has slightly more influence on the radiative heat transfer than the total, the height has considerably more effect on radiative heat flux than it does on the total, and the heat release rate is also more important here. Only the horizontal distance is more important for the total heat flux. This shows that radiation, for the open base with the burner in the centre of the channel, is the most influential heat transfer mechanism.

Parallel walls, closed base, line burner in centre of channel

$$\dot{q}''_r = 0.0233 + 3.75\left[\frac{x(a/D)^{0.83}}{Q_I^{*0.76} D(y'/D)^{0.47}}\right]^{-1.8} \qquad (6.42)$$

The correlation gives a coefficient of 0.973, shown in figure (6.47). The separation in this case is important, but it does have more influence in governing the total heat transfer than the radiative, meaning that it alters the convection to a greater extent than the radiation. The same is true for the horizontal position, which would be expected from observations of the flame being pushed over by the air flows at the edges of the walls, this would cause a significant change in heat flux away from the centreline. Both the height and the heat release rate affect the radiation slightly more than the convective component of heat transfer.

The radiative heat fluxes are higher for the parallel wall case than the single wall. This would be expected due to the effects of cross radiation. The radiative heat fluxes are also increased by placing the burner against the wall, rather than in the

centre of the channel. The radiation is higher for the closed base than the open, with the separation distance playing a more important role.

6.3.8.3.5.2 Regression for radiation with total heat flux

Correlations were sought to relate the radiative and total heat fluxes, both simply and by including the other relevant variables. These equations show the relative importance of the radiation, and therefore the importance of the convective heat transfer. They are only applicable for $\dot{q}_r'' \geq 0$, the additional coefficients which imply a negative radiative heat flux for zero total heat flux arise from the use of least mean squares to find the equation. The correlations can only be used with confidence within the range of this study.

Single wall, open base, line burner at instrumented wall

$$\dot{q}_r'' = -0.219 + 0.113\dot{q}_w'' \tag{6.43}$$

with a correlation coefficient of 0.954. This correlation can be improved by including the other variables:

$$\dot{q}_r'' = 0.04 + 0.237\dot{q}_w'' - 6.2\mathrm{Q}_1^{*0.906} - 0.27(x/D)^{-1.72} \tag{6.44}$$

giving a new coefficient of 0.969.

Parallel walls, open base, line burner at instrumented wall

$$\dot{q}_r'' = -0.491 + 0.217\dot{q}_w'' \tag{6.45}$$

with r = 0.954. Again this is improved by taking other variables into account.

$$\dot{q}_r'' = -1.25 + 0.111\dot{q}_w''^{1.22} + 38\mathrm{Q}_1^{*} - 1.8(a/x)^{1.7} \tag{6.46}$$

r = 0.979.

Parallel walls, open base, line burner in centre of channel

$$\dot{q}_r'' = -1.93 + 0.649\dot{q}_w'' \qquad (6.47)$$

This has a coefficient of 0.960. Including the other variables gives a correlation coefficient of 0.972 with the equation:

$$\dot{q}_r'' = 0.59 + 0.675\dot{q}_w'' \; -98.4\mathrm{Q}_1^{*1.2} + 0.493(a/x)^{1.2} - 3.12(y'/D) \qquad (6.48)$$

Parallel walls, closed base, line burner in centre of channel

$$\dot{q}_r'' = -1.02 + 0.406\dot{q}_w'' \qquad (6.49)$$

r = 0.979. Inclusion of the other variables gives:

$$\dot{q}_r'' = 0.826 + 0.401\dot{q}_w'' \; +1.64(a/x)^{1.16} - 5.45(y'/D)^{0.844} \qquad (6.50)$$

and a correlation coefficient of 0.983.

The importance of radiation is greater for the parallel wall case than for the single wall, for example $\dot{q}_r'' \approx 0.217\dot{q}_w''$ for the parallel case, burner at wall and only about $0.113\dot{q}_w''$ for the single wall. For the open base configuration, radiation is also relatively more important for the burner in the centre of the channel than at the wall, $\dot{q}_r'' \approx 0.649\dot{q}_w''$ with the burner in the centre, $\dot{q}_r'' \approx 0.217\dot{q}_w''$ with the burner against the wall. The actual values are higher with the burner against the wall, so this means that when the burner is moved to the centre of the channel, the convective component falls by the greater fraction. With the burner in the centre and the open base, the radiation is the dominant mode of heat transfer, whilst convection dominates with the burner at the wall. The radiation falls with increasing height and, towards the top of the walls, it is similar for both the burner positions.

All heat fluxes are higher for the closed base than the open, but the relative importance of the radiation is less ($\dot{q}_r'' \approx 0.406\dot{q}_w''$ for the closed base and approximately $0.649\dot{q}_w''$ for the open base with the burner in the centre of the channel). This shows that the convective component is increased by a greater fraction than the radiation when the flow is restricted by closing off the base.

6.3.8.6 Conclusions

The equations developed using the regression analysis allow comparison of the heat fluxes and temperatures under different conditions. They should not be used for predictions outside the range of this study, (although those for the single wall and open base give good agreement with Hasemi's data (1984)), without further tests to extend their validity. It would be useful to know the effects of overall scale and height to separation ratios, for example, and these data cannot provide this. They do, however, give an indication of the factors that are important, and an insight into the conditions that lead to different wall heat fluxes. This is the first time that these factors have been identified in this way and quantified. They demonstrate that there is a significant difference between burning behaviour at single walls and at parallel surfaces.

6.3.9 Computation Fluid Dynamics

The flow and temperature fields for the exceptional case, where a closed base gave wall heat fluxes up to four times the values for the open base, was simulated using computational fluid dynamics (CFD). The code used was 'FLOW3D', with the setting up and runs carried out by Dr. C. J. Lea of HSE. The data from the CFD are used here to compare with the experimental results. The position of the system within a room is shown in figure (6.48). The symmetry of the experiment was exploited for the simulation purposes, a plane of symmetry was taken vertically parallel with the walls, through the centre of the burner. A second plane of symmetry was taken vertically perpendicular to the walls, at the centre of the wall length. The computation was thus performed with one quarter of the geometry, figure (6.49). The grid used is shown in figures (6.50)-(6.52).

The details of the physics, numerics and boundary conditions are given below.

<u>Physics</u>

3-d simulation

Fully compressible flow

k-ε turbulence model

Eddy-break-up combustion model (rate of fuel consumption depends on a computed turbulent time scale)

Transient simulation with fuel supply rate increased linearly over 30s, from 0s, followed by 10s steady (40s total)

Numerics

Planes of symmetry assumed at the mid plane of the burner and bisecting the walls at their mid-position. Only one quarter of the geometry is simulated

Grid size 34 x 46 x 43 = 67252 cells, as shown in figures (6.50)-(6.52)

3rd-order differencing scheme for convection

First-order accurate time-stepping

Convergence assessed on mass, momentum and ε residuals.

Boundary Conditions

Constant pressure boundary over enclosure floor for open base

All solid surfaces adiabatic

Initial k and ε specified, detailed below, velocities set zero, initial temperature 293K

Radiative heat transfer was not modelled so heat energy from the flame was transported by convection only, which is likely to over predict temperatures. The initial momentum of the fuel from the burner was not taken into account. This was decided after a run using a non-combusting propane supply into the system showed the momentum efflux from the system was far in excess of that entering due to the propane alone. In these circumstances it was judged permissible not to match the momentum influx to the domain, and just specify a fuel mass source.

6.3.9.1 Open Base Run Details

Run 1: To 40s, with a time step of 1s. The fuel supply rate was ramped up to the maximum over the first 30s.

Run 2: Restart of run 1 for one 1s time step, but with a solution forced to take between 1000 and 1200 iterations so that convergence is better and a comparison could be made with the solution at 40s.

The temperature field from the second run appeared identical to that from the first, so the code was assumed to be well-converged.

6.3.9.2 Closed Base Run Details

Run 1: To 40s, with a time step of 1s. The fuel supply rate was ramped up to the maximum over a period of 30s.

This gave an unsatisfactory solution, with negative temperatures, the solution appeared to diverge from poor initial conditions.

Run 2: To 5s, with a time step of 0.5s. Same fuel supply rate as previously. Initial k and ε were now set to 0.01 and 0.5 respectively, rather than the default 10^{-4}. This was to give an initial time-scale reciprocal of 50 times longer than in run 1, and hence a reaction rate 50 times larger.

The solution now appeared to be giving physically plausible values.

Run 3: as run 2, but up to 40s.

Although this was physically plausible, the solution was not well-converged, based on the momentum, mass flow and rate of dissipation of turbulence energy.

Run 4: restarting from run 3 for one time step to 40.5s, but forcing the calculation to perform between 900 and 1000 iterations, similar to the process used for the open base.

The solution showed no better convergence than the previous one. To investigate whether the flow was very time-dependent, a final run was performed.

Run 5: restarting from run 3, i.e. from 40s, up to 42s with a time step of 0.05s. The minimum number of iterations was 100, the maximum was 200.

The solution now converged towards a definite steady-state, with good overall convergence in each time-step. There was no time-dependency of the flow.

6.3.9.3 Velocity Profiles

The velocity vector plots for the open base simulations are shown in figures (6.53)-(6.55). The first two are the same view, but different scales, the third is the view looking at the face of the wall. The vectors shown in this third figure are for the velocities in the plane directly above the burner. The figures looking on to the end of the wall, (6.53) and (6.54) show the velocity distribution across the width of the channel. The open base shows high velocities directly above the burner, falling towards the wall. The velocity profile across the width of the channel for the closed base, figures (6.56) and (6.57), reveals only a slightly lower velocity at the wall than in the centre of the channel, the velocity gradient across the channels is therefore far less than for the open base. The velocities are higher for the closed base, both across the channel and at each height.

Comparing the profiles across the wall, figures (6.55) and (6.58), the open base velocities are higher at the end of the wall, but lower at the centreline, than those for the closed base. The closed base vectors demonstrate greater horizontal components of air flow towards the centreline. These flow patterns are compatible with air only being able to enter from the sides with the closed base; it was observed that the flame was pushed over towards the centreline in this case. This explains the higher dependence of the heat flux on horizontal position in the closed case, equations (6.32) and (6.33). The plots for the closed base indicate a greater mass outflow rate from the top of the walls than appears to be possible given the small indicated mass-inflow rates through the open sides. This was checked by performing a mass balance, using numerical values from the CFD calculation. This showed that the mass was actually well-conserved. This was backed up by the very small overall mass residual, of approximately 0.03 g/s, which is 0.75% of the mass inflow. The small area over which the air and combustion products flow out of the domain for this case is demonstrated in figure (6.59). This is the view at the top of the wall, with the nearest vectors being those at the centreline of the system. Using this view, it is easier to see how the mass balance can be correct, the velocities at the top are large but the area is small compared with the inflow.

6.3.9.4 Temperature Profiles

Temperature contours have been plotted from the CFD simulation. Figures (6.60)-(6.62) show the open base temperatures, in the same planes and using the same

scales as for the velocity profiles of figures (6.44)-(6.46). Those for the closed base are shown in figures (6.63)-(6.65). Taking the extent of intermittent flaming to correspond to approximately 800-900K, the results indicate that, for the open base, the flame fills the width of the burner, but does not extend as far as the sides of the walls. This is shown in figures (6.60) and (6.61). This result corresponds well with the experimental observations of flame shape, as shown in figure (6.18). The closed base configuration reveals a different flame shape, both experimentally in figure (6.18) and in the simulation, figures (6.63) and (6.64). Using the same criterion for the presence of the flame, flame can be seen to fill the width of the channel, touching the walls. Flame is present for the entire height of the wall, with combustion even occurring above the walls. Experimental observations show that flame does fill the width of the channel. Flame is also seen above the top of the walls, with the flame pulsating between approximately 520 mm and 800 mm above the burner. Flame is therefore seen intermittently at the top of the walls. When flame is present, the temperature will be greater than 900K, whilst when flame is not present it will be lower than this. The k-ε turbulence model used for solving this problem diffuses the various properties fairly quickly and therefore does not easily demonstrate any time dependence. The values for temperature etc. are average values, and in this way will represent an average for the intermittent flaming.

The temperature profiles in the plane parallel to the wall show the effect of the air flow on temperature and therefore heat transfer. Figures (6.62) and (6.65) show the profiles in the plane above the burner for the open and closed base configuration respectively, whilst figures (6.66) and (6.67) show the same thing, but for the plane just in front of the wall. The temperature falls faster towards the edges of the wall for the closed base than the open, giving slightly higher values closer to the edge for the open base. This trend was also observed for the measured heat fluxes, figures (6.15) and (6.17). The temperatures are higher close to the centreline for the closed base. The actual values of temperature in the cells just in front of the wall have been extracted at the points where heat flux measurements were taken. These are shown in table (6.4), demonstrating the far higher temperatures for the closed base scenario and the higher temperatures towards the edge of the wall for the open base scenario. Far higher temperatures are found for the closed base, as the flame is impinging on the wall and there is flame present in the computational cell next to the wall. The open base does not have flame close to the wall, the temperatures at the wall are lower than those assumed necessary for intermittent flaming.

Table (6.4) Temperatures /K in the cell next to the wall (x=0.03 m) for the open and closed base

height z/mm	dist. across wall y/mm	open base temp.	closed base temp.
108	0	384	1070
108	50	385	842
108	100	397	381
108	150	472	313
308	0	649	1330
308	50	676	438
308	100	654	293
308	150	378	293
508	0	698	1500
508	50	721	545
508	100	470	293
508	150	297	293
708	0	716	1640
708	50	693	586
708	100	379	306
708	150	294	293

6.3.9.5 Summary

The CFD simulation has demonstrated the processes which lead to the enhanced heat fluxes at the wall with the closed base in these tests. The air flows into the system are different for the two base configurations, giving different flame behaviour between the vertical parallel walls (see figure (6.18)). This, in turn, gave rise to greater temperatures and therefore the higher measured wall heat fluxes in the closed base case, and the lower values with the base open. Numerical values of various factors have not been compared, as temperature measurements were not made and heat transfer to the wall was not simulated. This would certainly be of interest for further work, both for increasing understanding of heat transfer between parallel surfaces and for helping to test CFD predictions under these circumstances. The use of modelling techniques such as CFD has the potential to reduce the number of fire tests necessary in many situations, and to aid in understanding of potential fire behaviour.

6.4 Summary

Fire tests have been carried out using several different materials under various conditions. Some of the problems of fire testing have been highlighted, and comparisons made of the results. The results from the well-ventilated Cone Calorimeter give good comparison with those from the third scale room/corridor test only before the ventilation controlled burning regime is entered. Once that regime has been reached, the burning depends on different factors from fuel controlled combustion. This implies that well ventilated tests cannot be used to represent post-flashover, ventilation-controlled fires. Material behaviour, such as melting, needs to be taken into account in hazard assessment, and therefore tests are needed to investigate this behaviour. The relevance of fire test data to 'real' compartment fires has been discussed. The conditions that exist in either a fire test or a compartment fire significantly affect the outcome of the fire. Geometry plays a crucial part in this, both for fire testing and for real fire development. Factors such as separation between vertical parallel surfaces, found in the HSE third scale room/corridor test, warehouse storage, and cavities, have been investigated experimentally and found to influence the heat fluxes at the wall. Burner/ignition source position and heat release rate, ignition source geometry, and flow restrictions are all variables influencing the course of a fire, with correlations used to show the effect they each have on heat flux and temperature. The relative fractions of convective and radiative heat transfer have been found to alter under different conditions, and correlation equations have again been used to demonstrate this. The burning in parallel wall configurations is seen to be different from single walls, which has implications both for fire testing and for hazard assessment. Further work is required into this area to extend the correlations developed here and to further improve the understanding of flames between parallel walls.

Figure (6.1) Graph of correlation equation for rate of increase of heat release rate in TSR and Cone

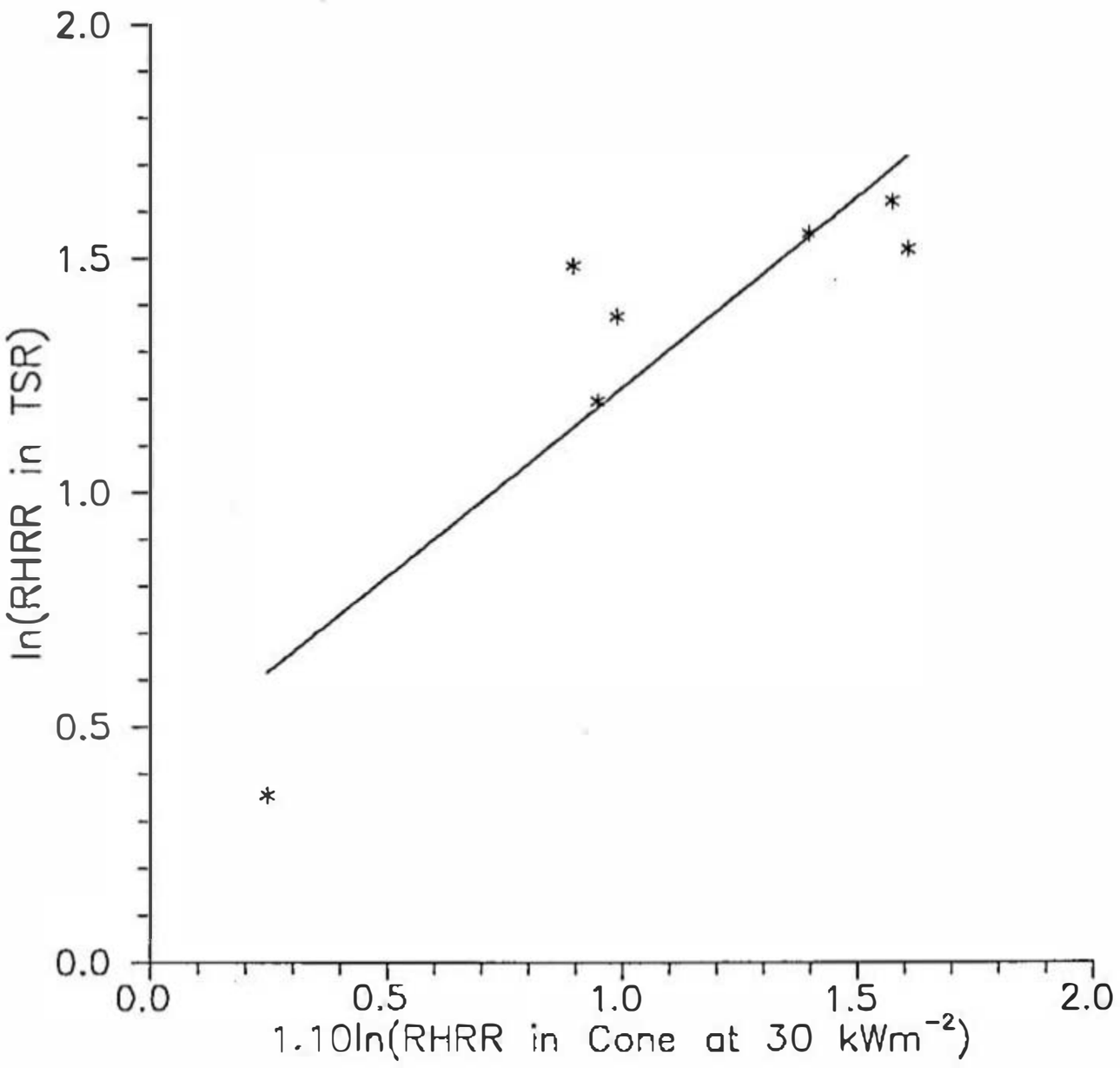

Figure (6.2) Graph of correlation equation for rate of increase of vent temperature rise and rate of increase of heat release rate in TSR

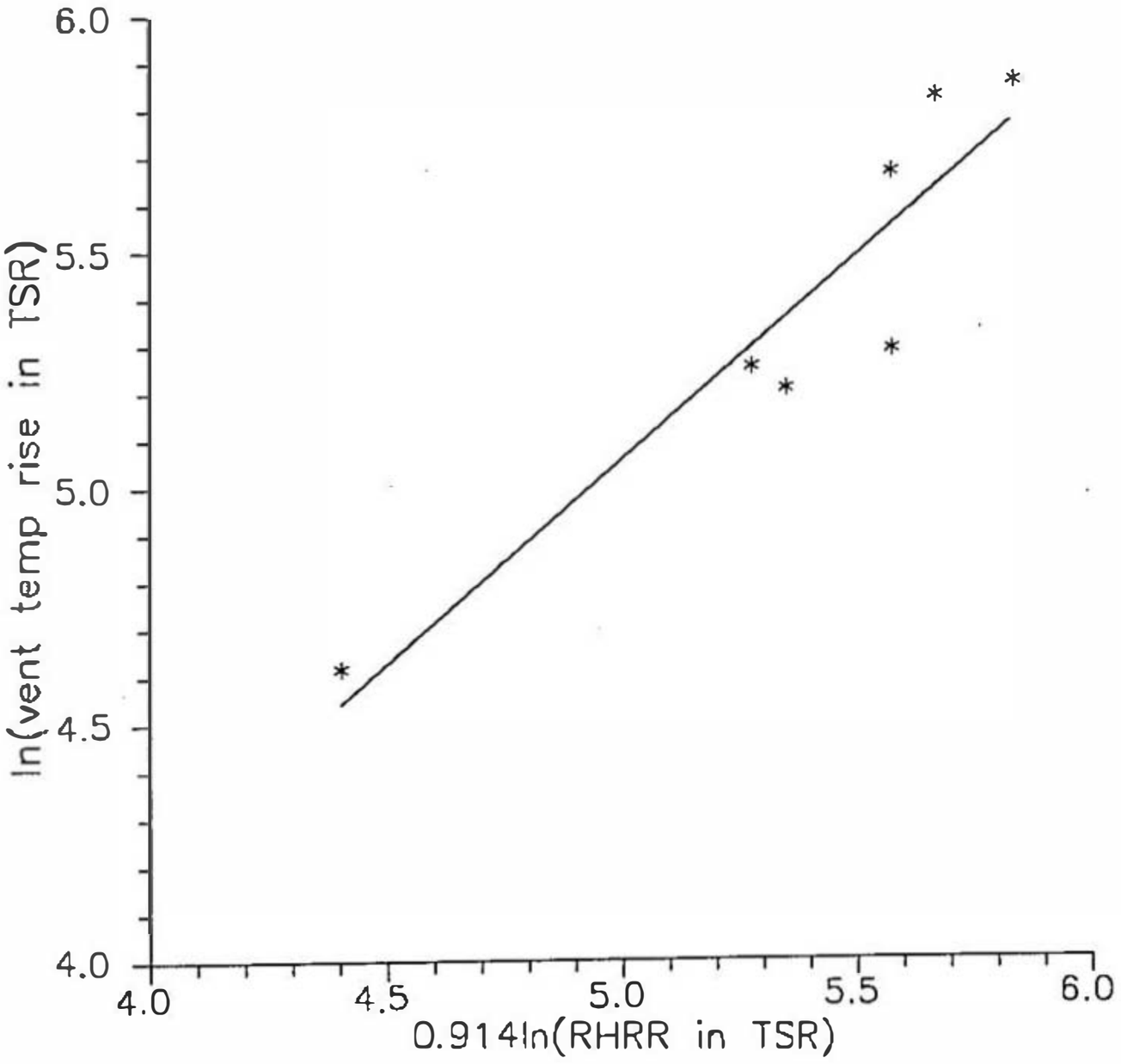

Figure (6.3) Graph of correlation equation for TSR rate of vent temperature rise with rate of increase of heat release rate in Cone at 30 kW/m^2

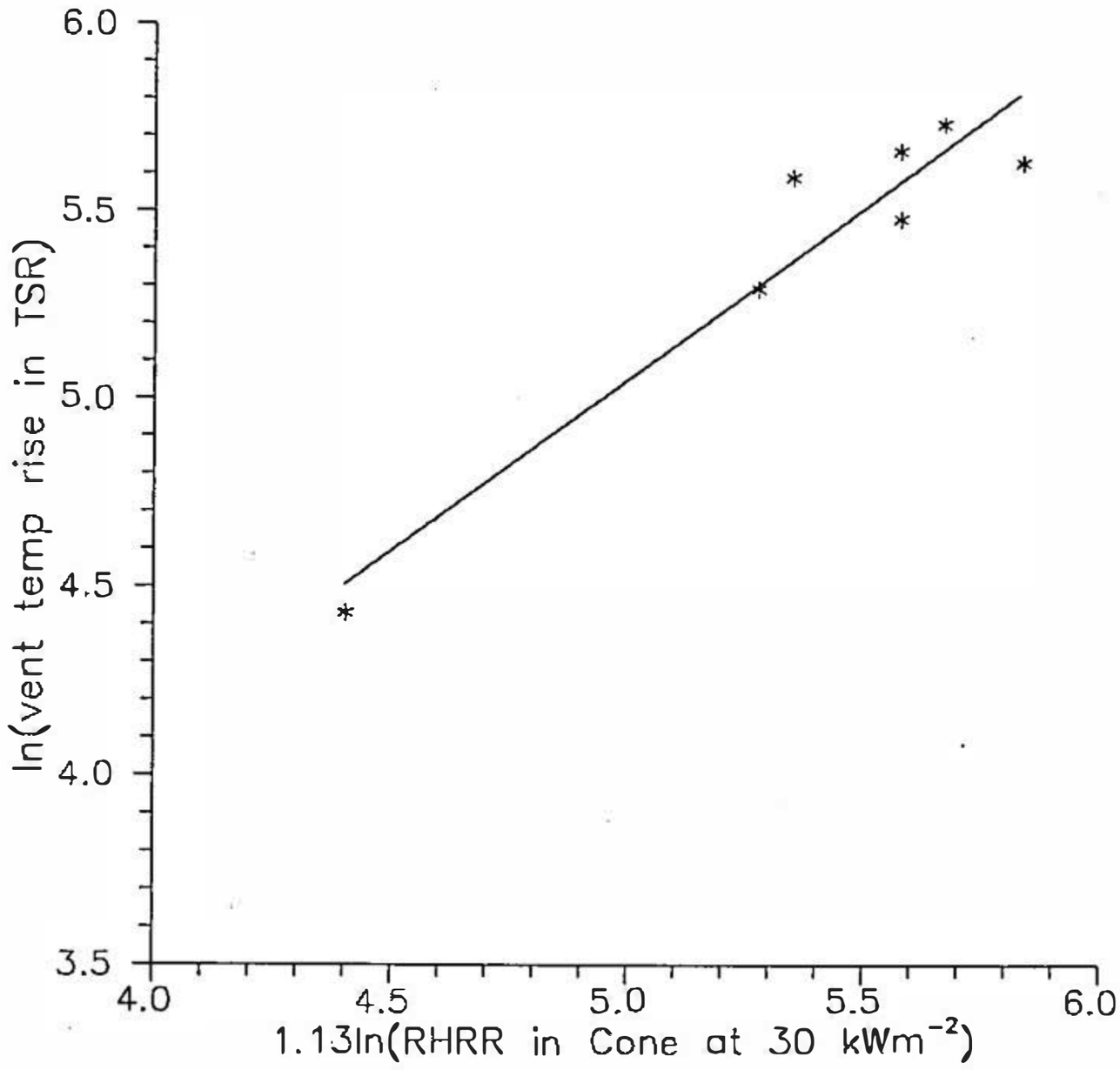

Figure (6.4) Growth of compartment fire for two fire growth coefficients

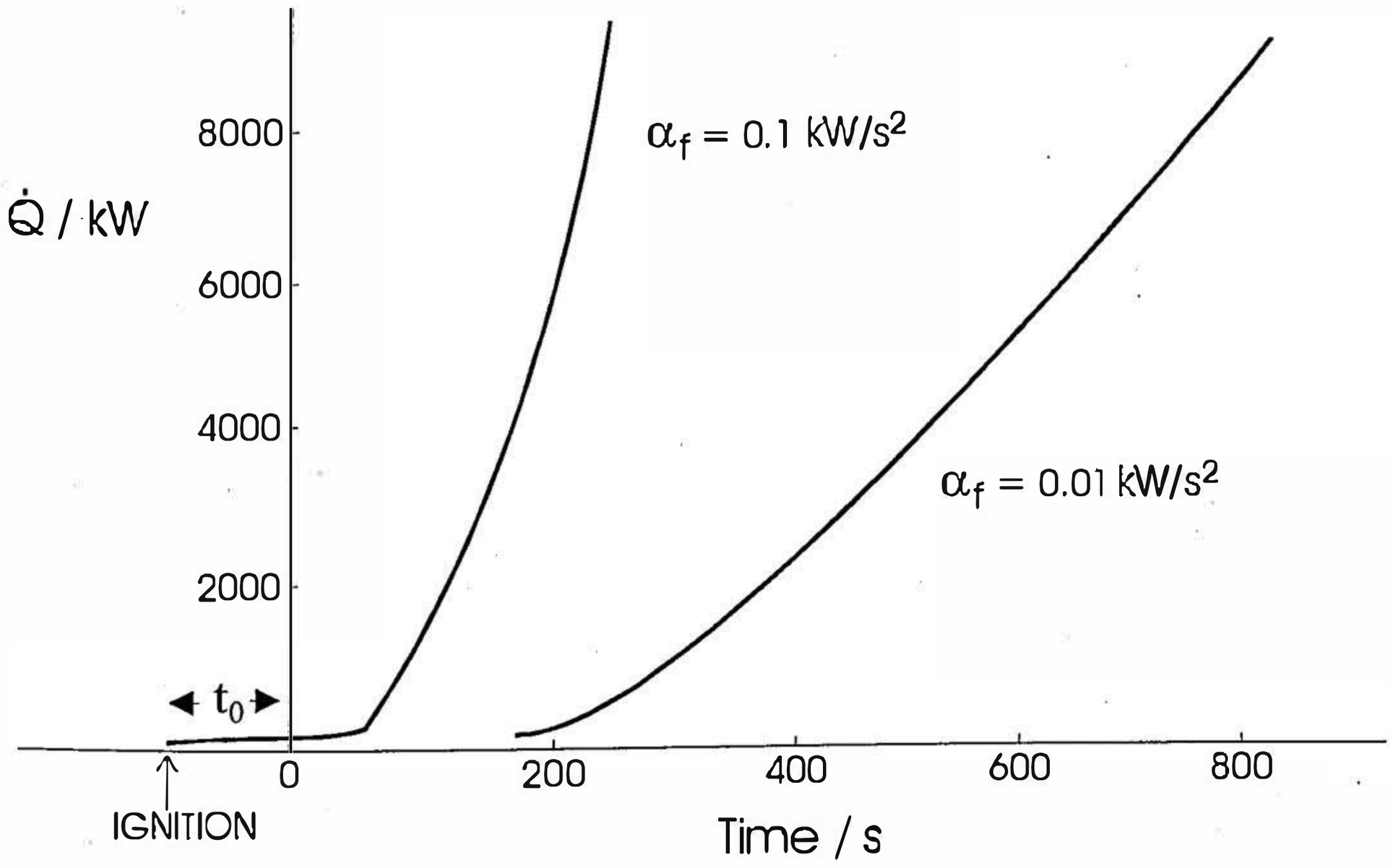

Figure (6.5) Graph of correlation equation for early rate of increase of smoke production rate with rate of increase of smoke production rate in Cone at 20 kW/m^2

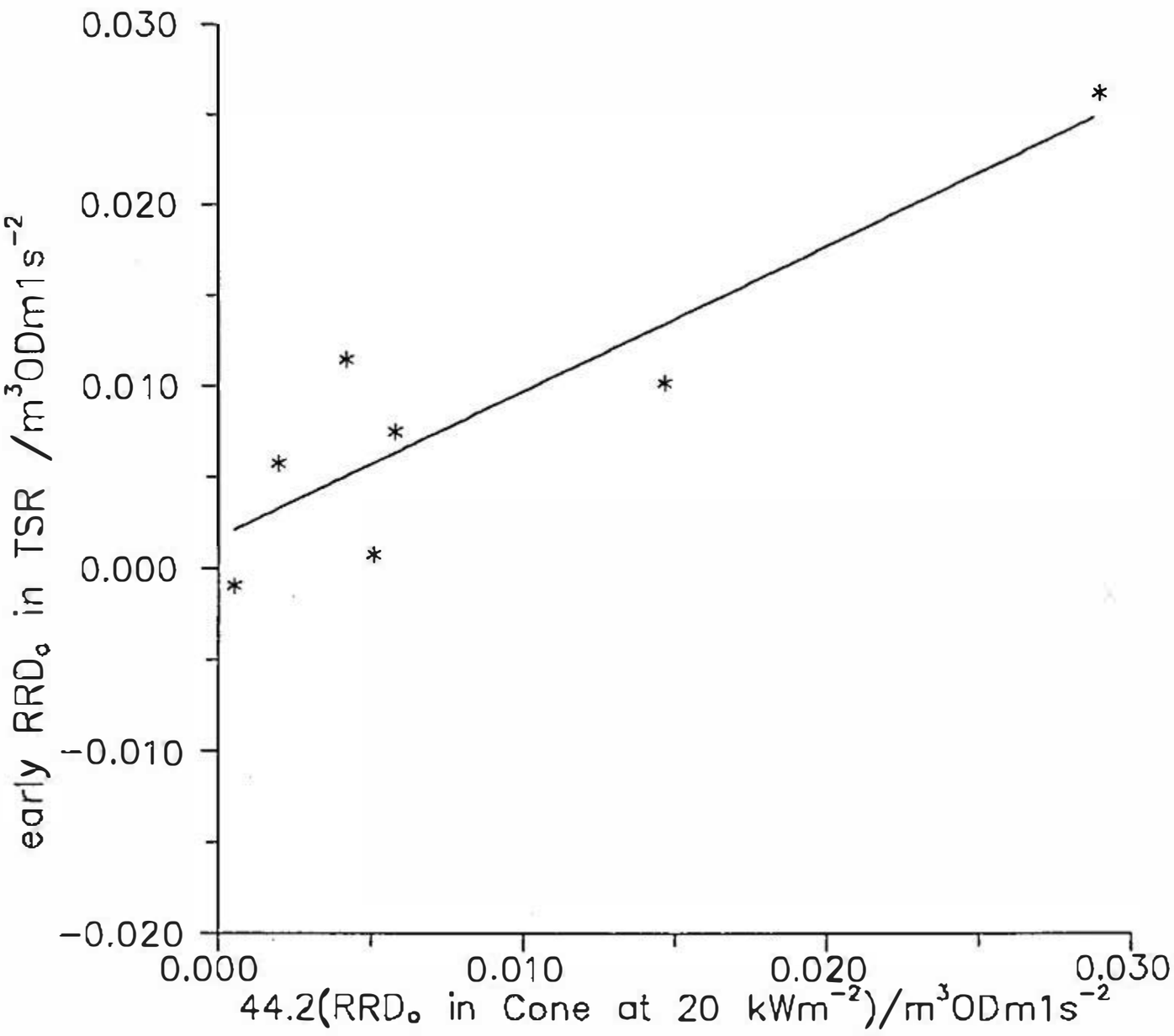

Figure (6.6) Graph of correlation equation for rate of increase of smoke production rate in TSR with rate of increase of smoke 2 production rate in Cone at 40 kW/m

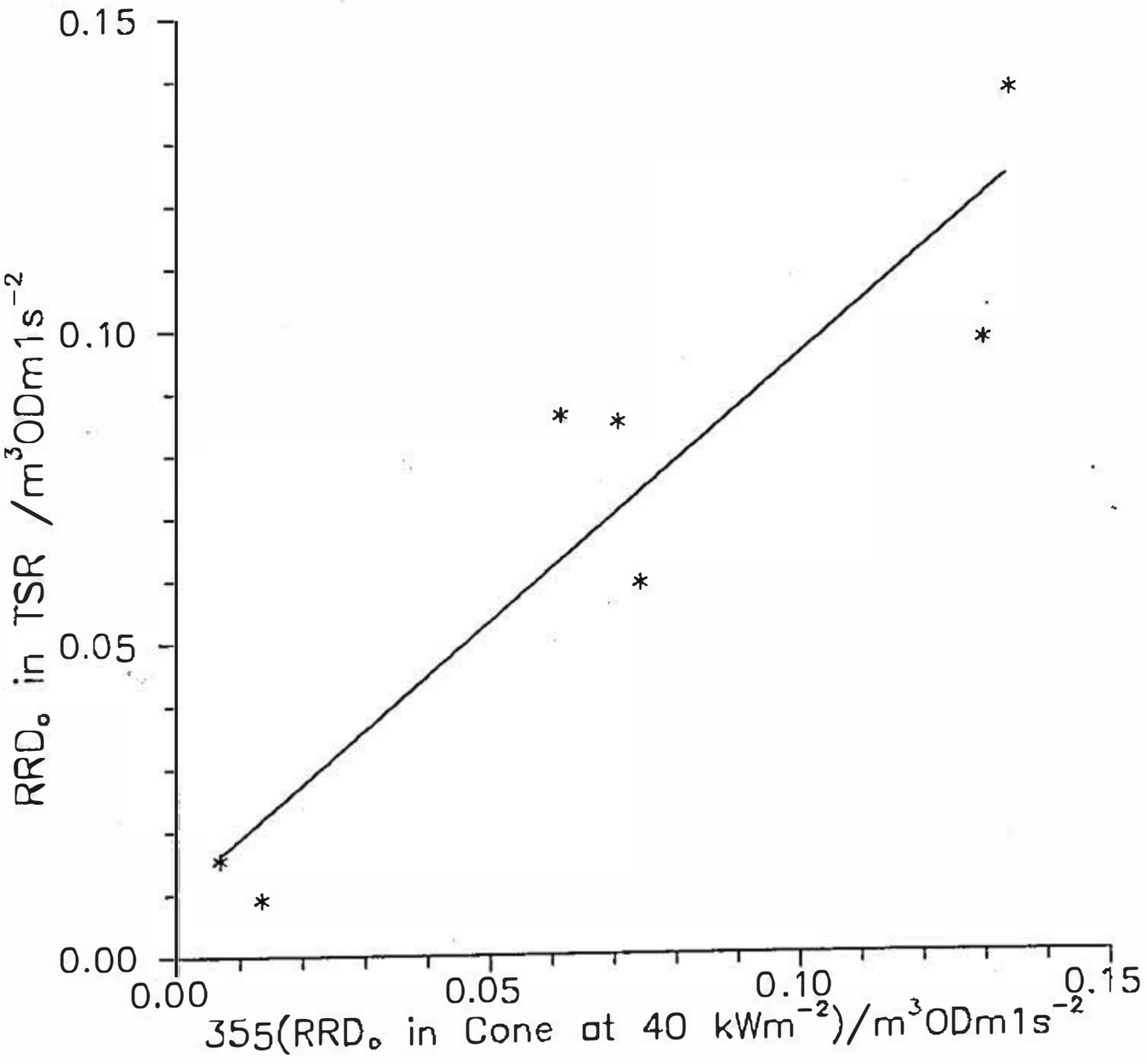

Figure (6.7) Heat Flux as a function of 1/Wall Separation, burner against the instrumented wall
$\dot{Q}$ = 12.5 kW, centreline fluxes only; △ 108 mm above burner, ◊ 308 mm above burner,
☆ 508 mm above burner, * 708 mm above burner,

(a) Open Base

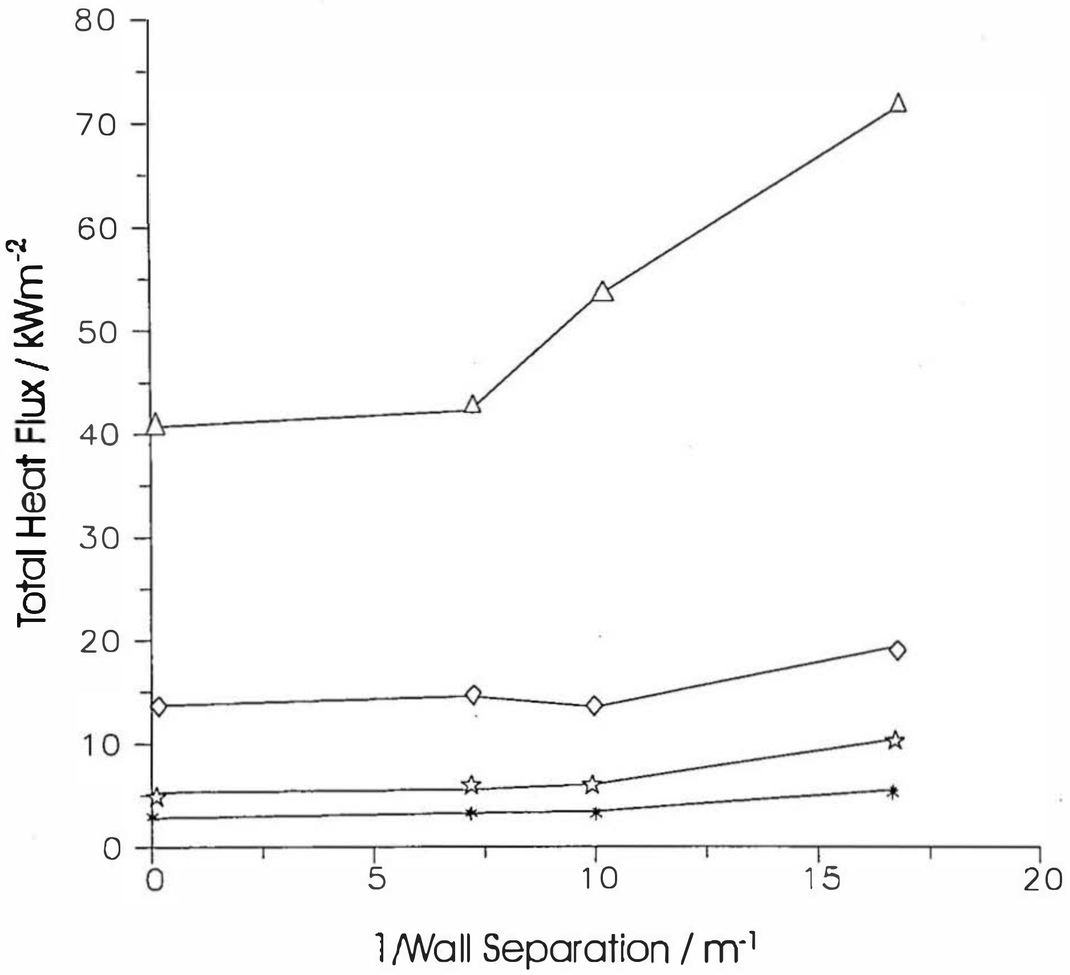

(b) Closed Base

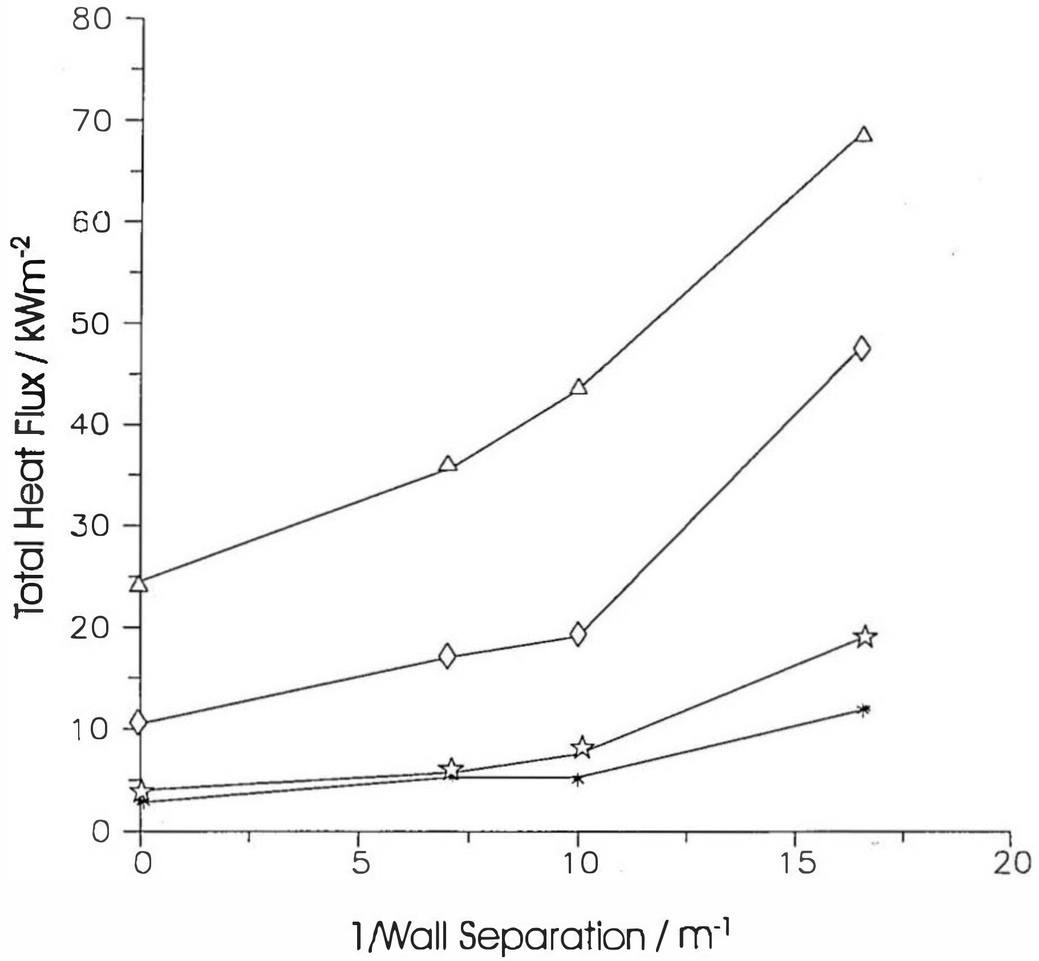

Figure (6.8) Heat Flux as a function of Height, burner at different positions, $\dot{Q}$ = 7 kW, centreline fluxes only

△ burner at instrumented wall ☆ burner in centre ◊ burner at opposite wall

(a) Closed Base, 60mm Separation

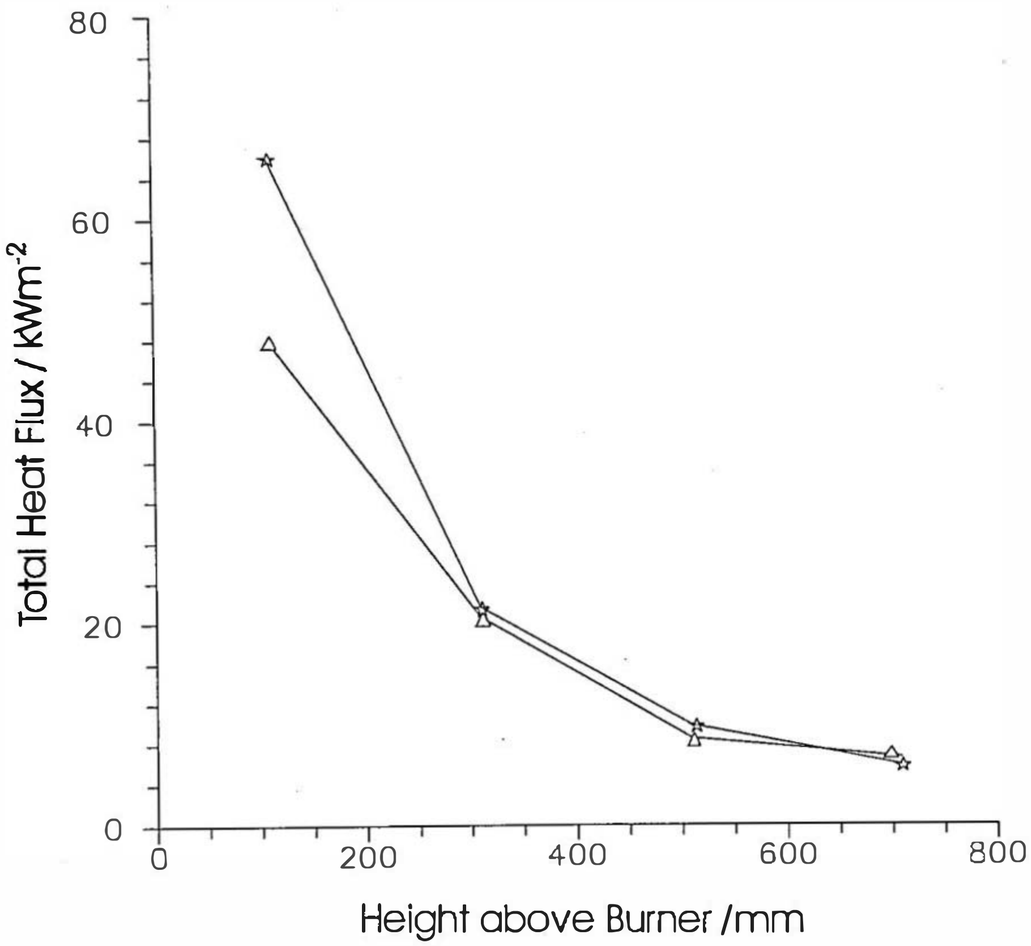

(b) Open Base, 100mm Separation

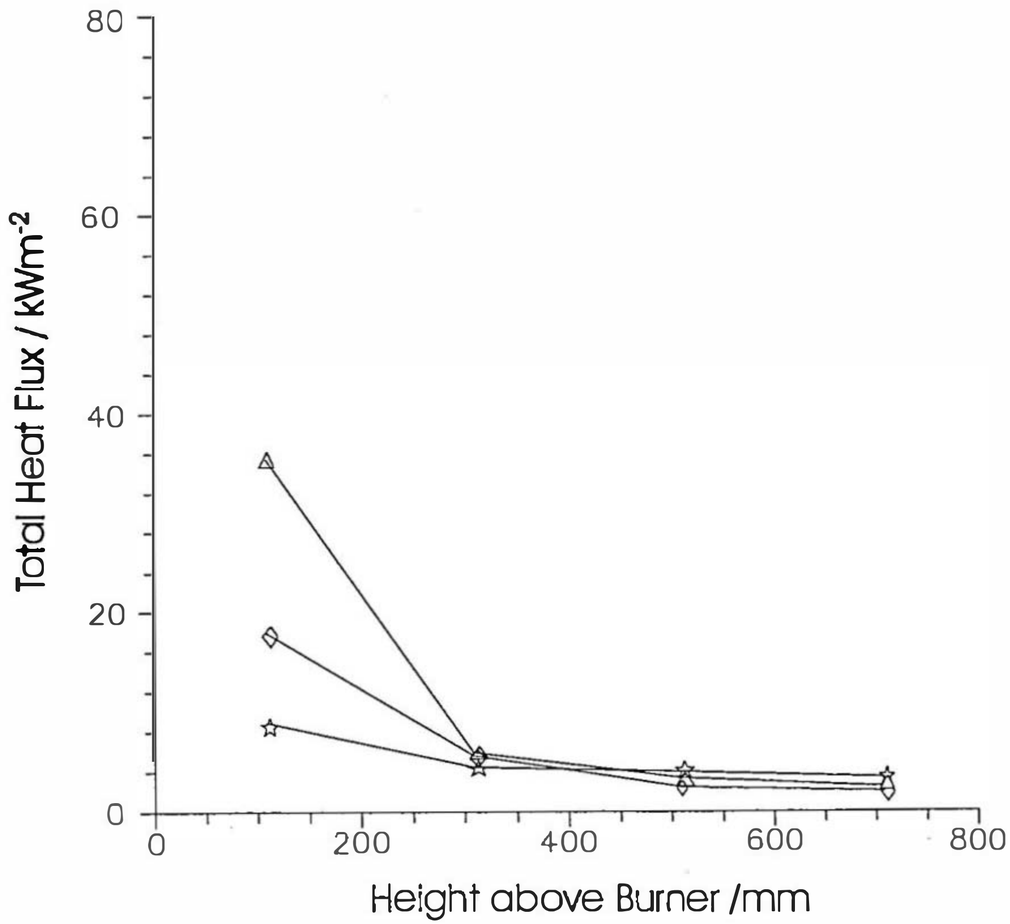

Figures (6.9)-(6.12) Flame heights for line burner between parallel walls, compared with Hasemi's predictions

Figure (6.9) open base, flames against wall

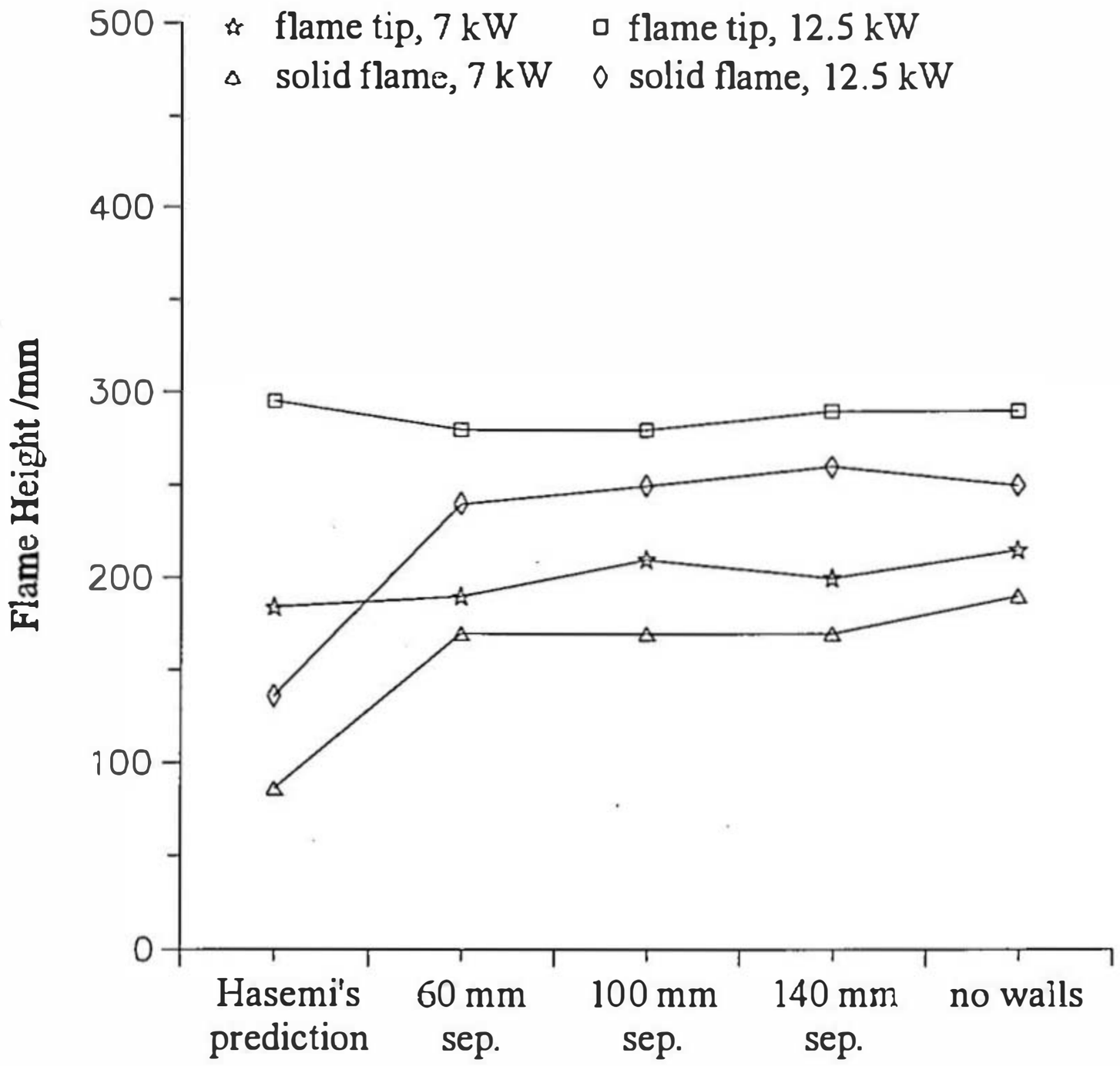

Figure (6.10) closed base, flames against wall

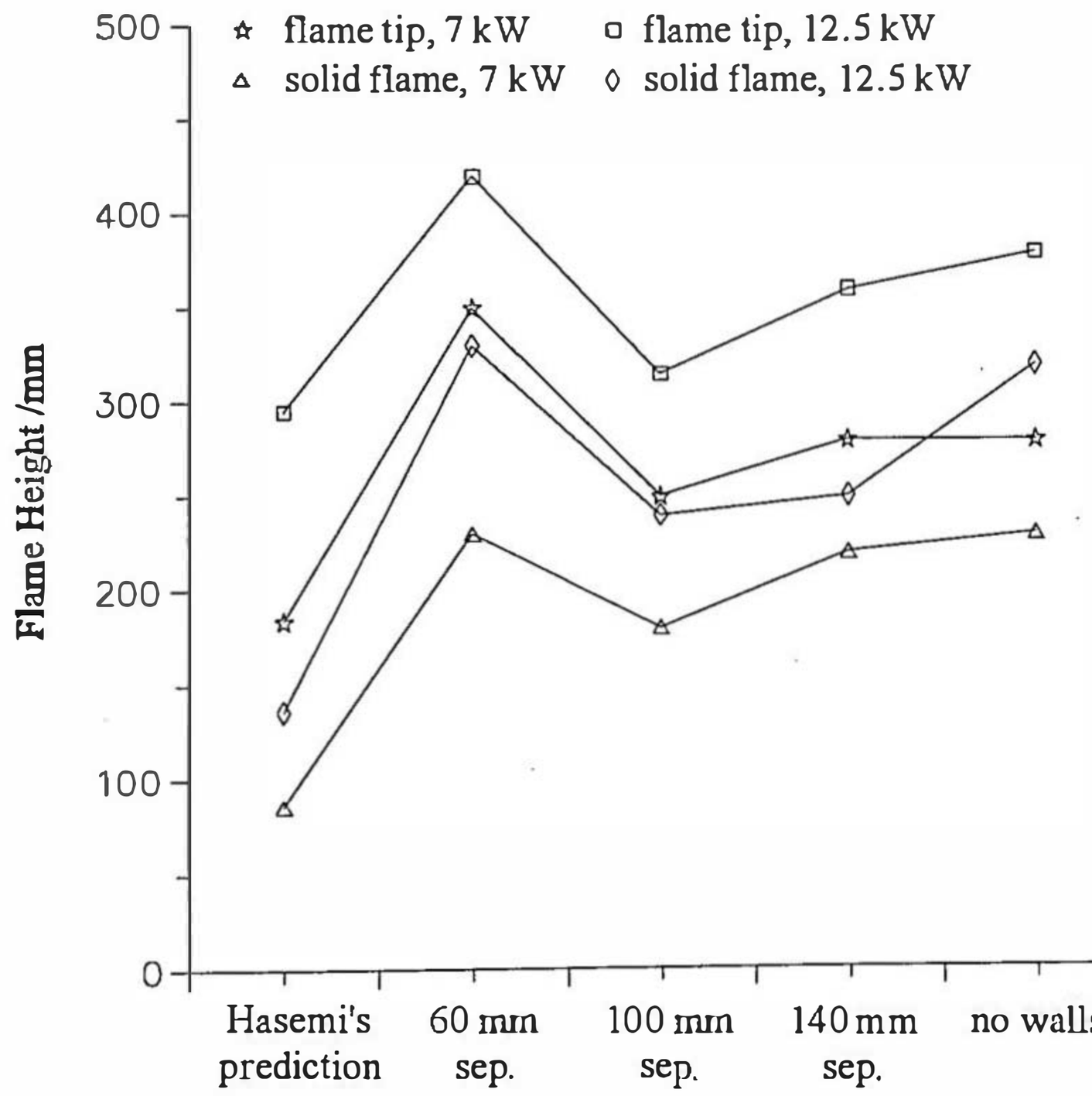

Figure (6.11) open base, unconfined (centre of channel) flames

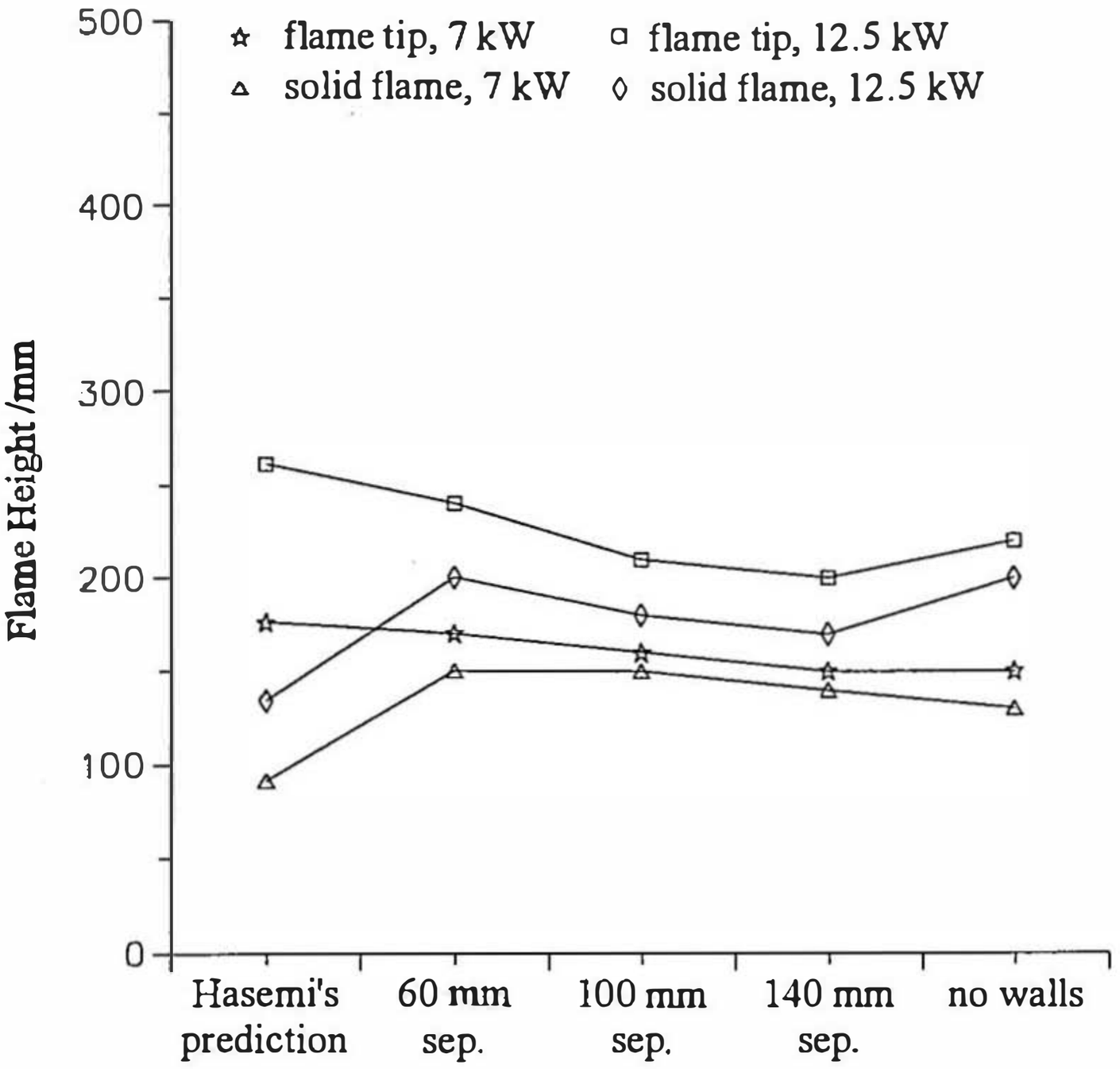

Figure (6.12) closed base, unconfined (centre of channel) flames

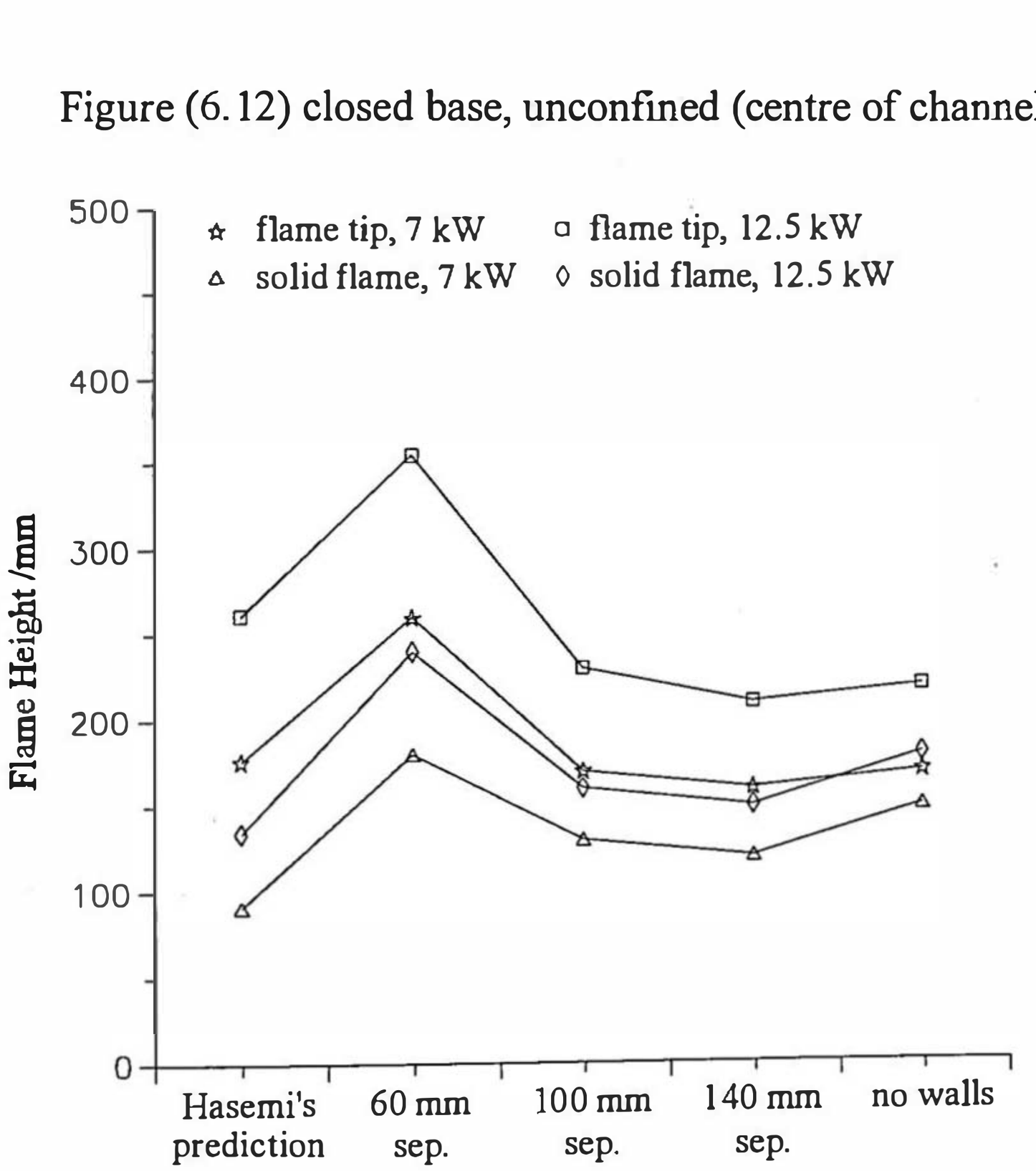

Figure (6.13) Contour maps of total heat flux distribution /kWm^{-2}
100 mm separation, closed base, 12.5 kW,
burners in the centre of the channel

(a) circular burner

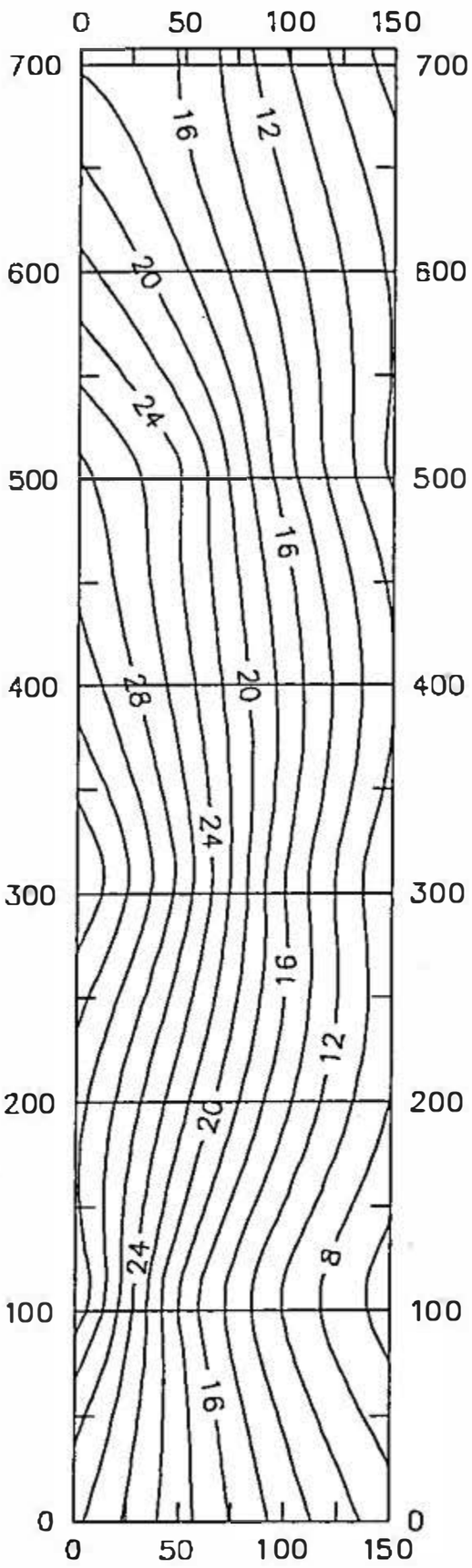

(b) line burner

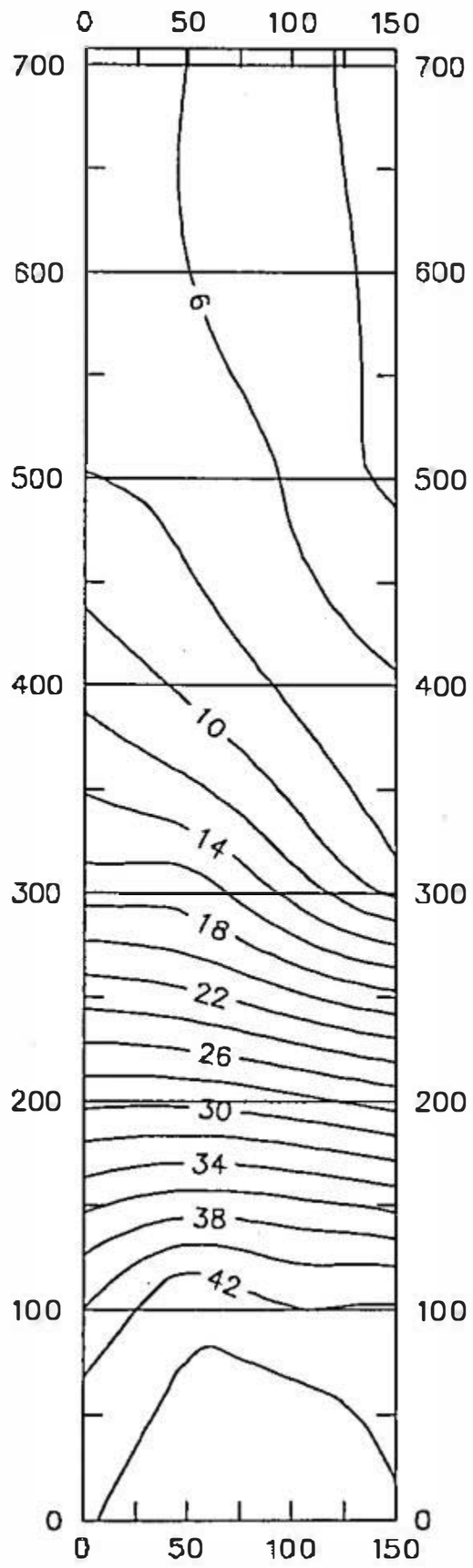

(c) sandbed burner

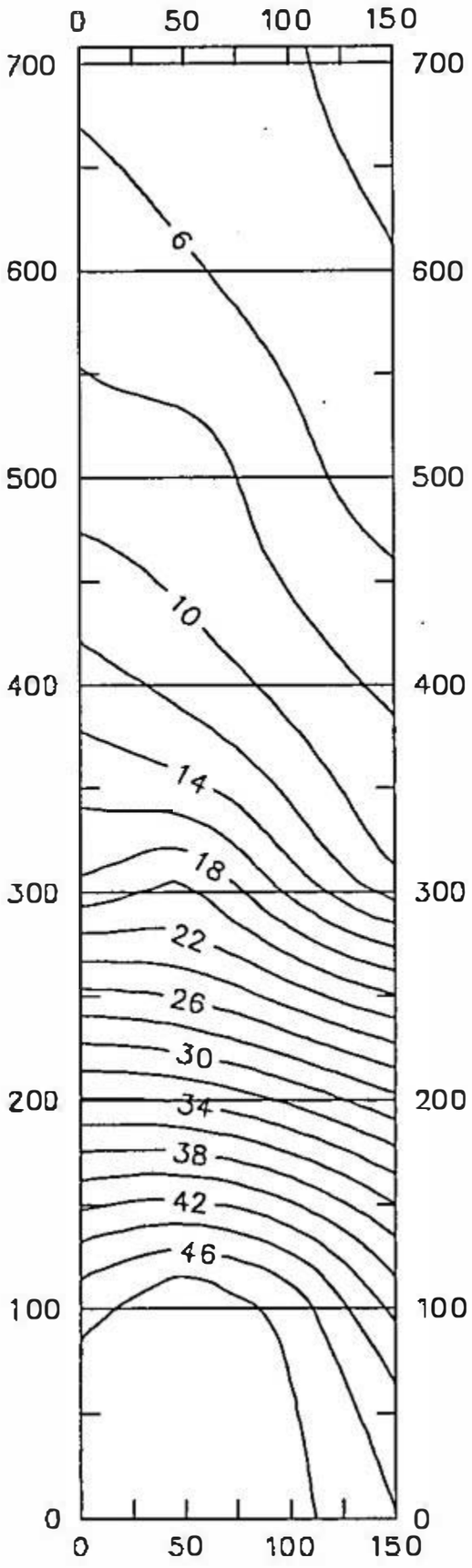

Figure (6.14) Centreline temperature versus depth into channel, separation 80mm, 7 kW, closed base, circular burner in centre

height above burner: ⛌ 108mm, □ 208mm, △ 308mm, ◊ 408mm, ☆ 508mm, + 608mm, ✳ 708mm,

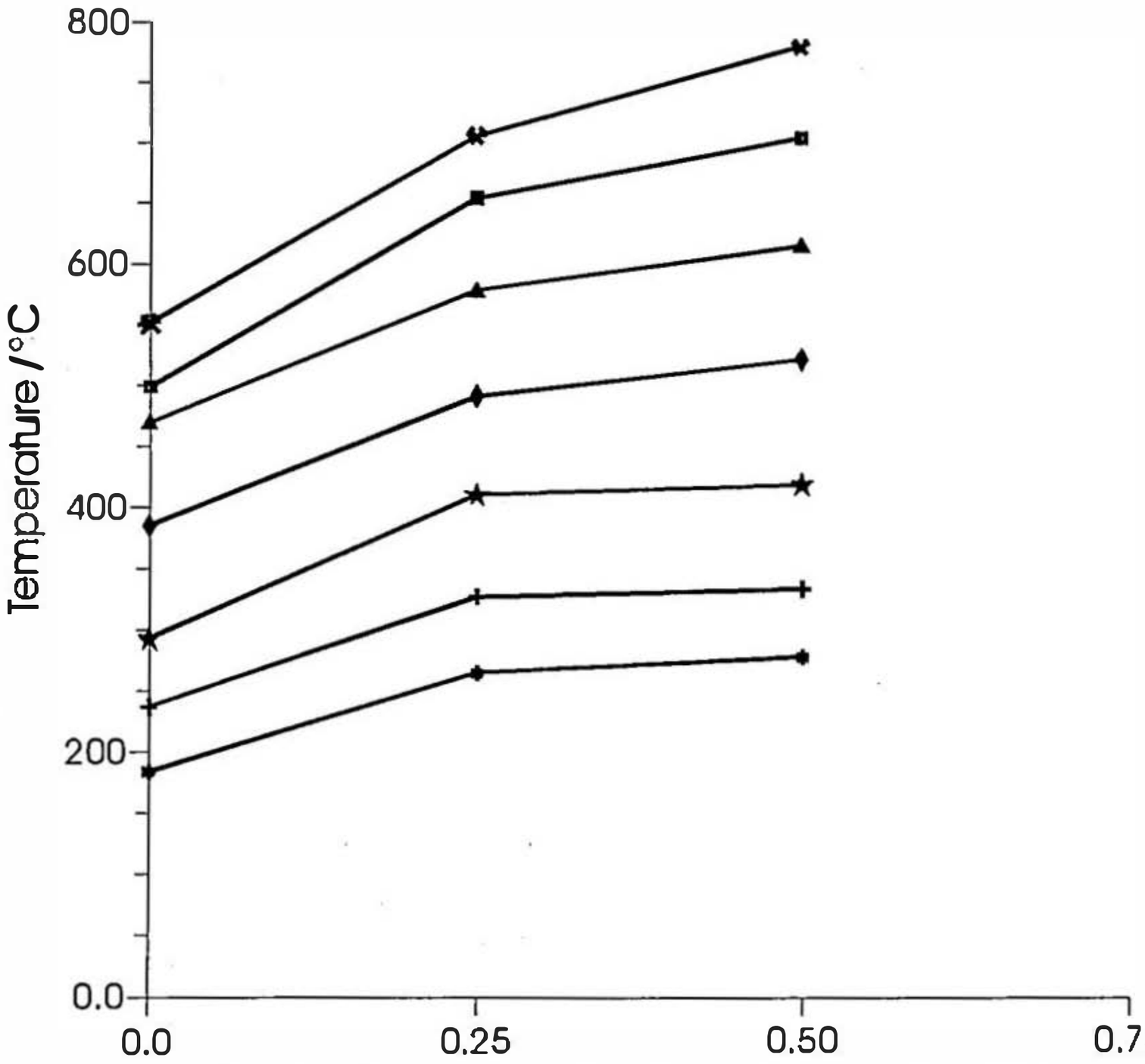

Figure (6.15) Total heat flux versus height, 60mm separation, open base, line burner at instrumented wall, 7 kW
distance across wall from centreline:
△0mm, ◊50mm, ☆100mm, ✣150mm

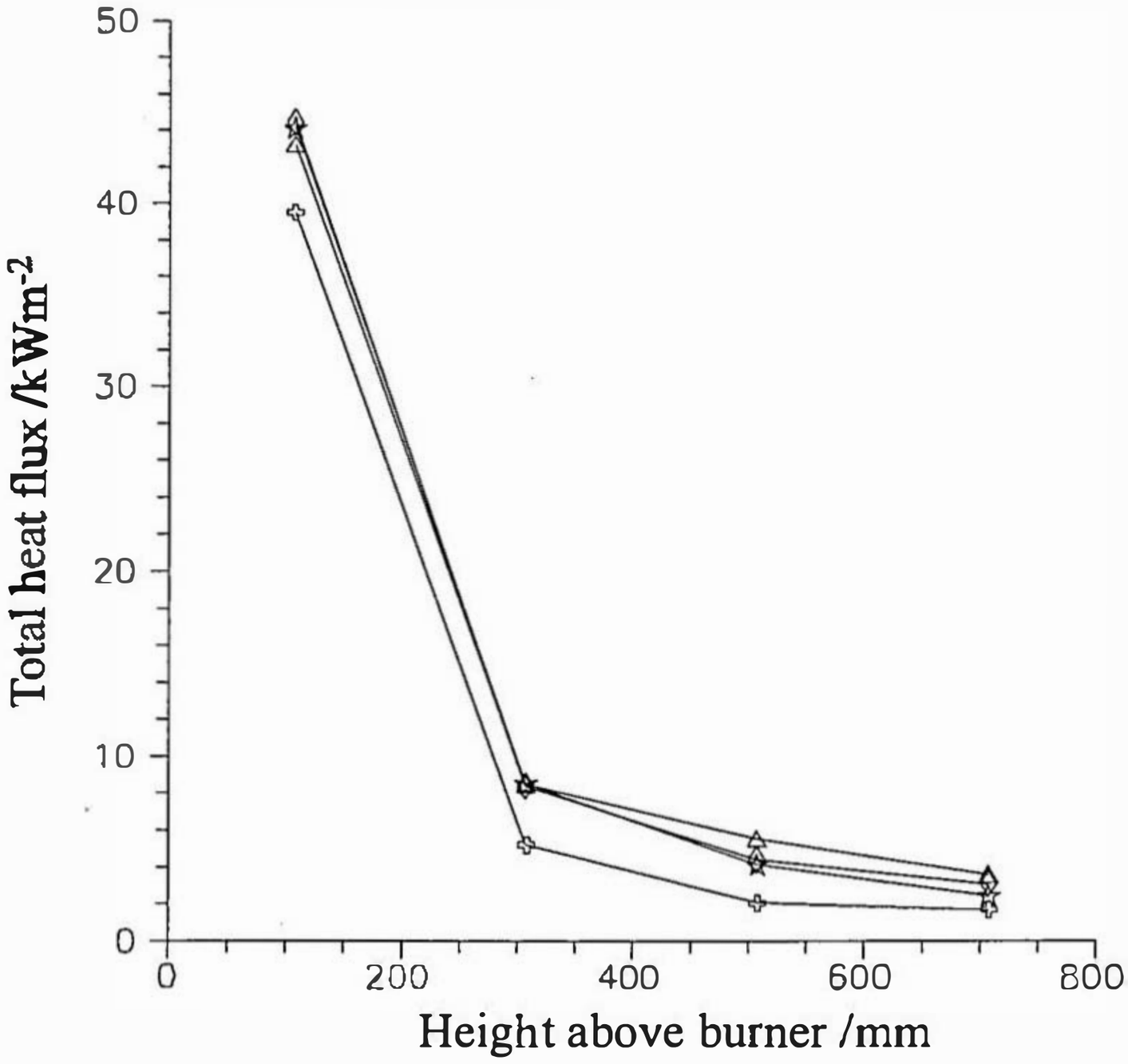

Figure (6.16) Centreline total heat flux versus height above crib base, No. 7 crib, 80mm separation

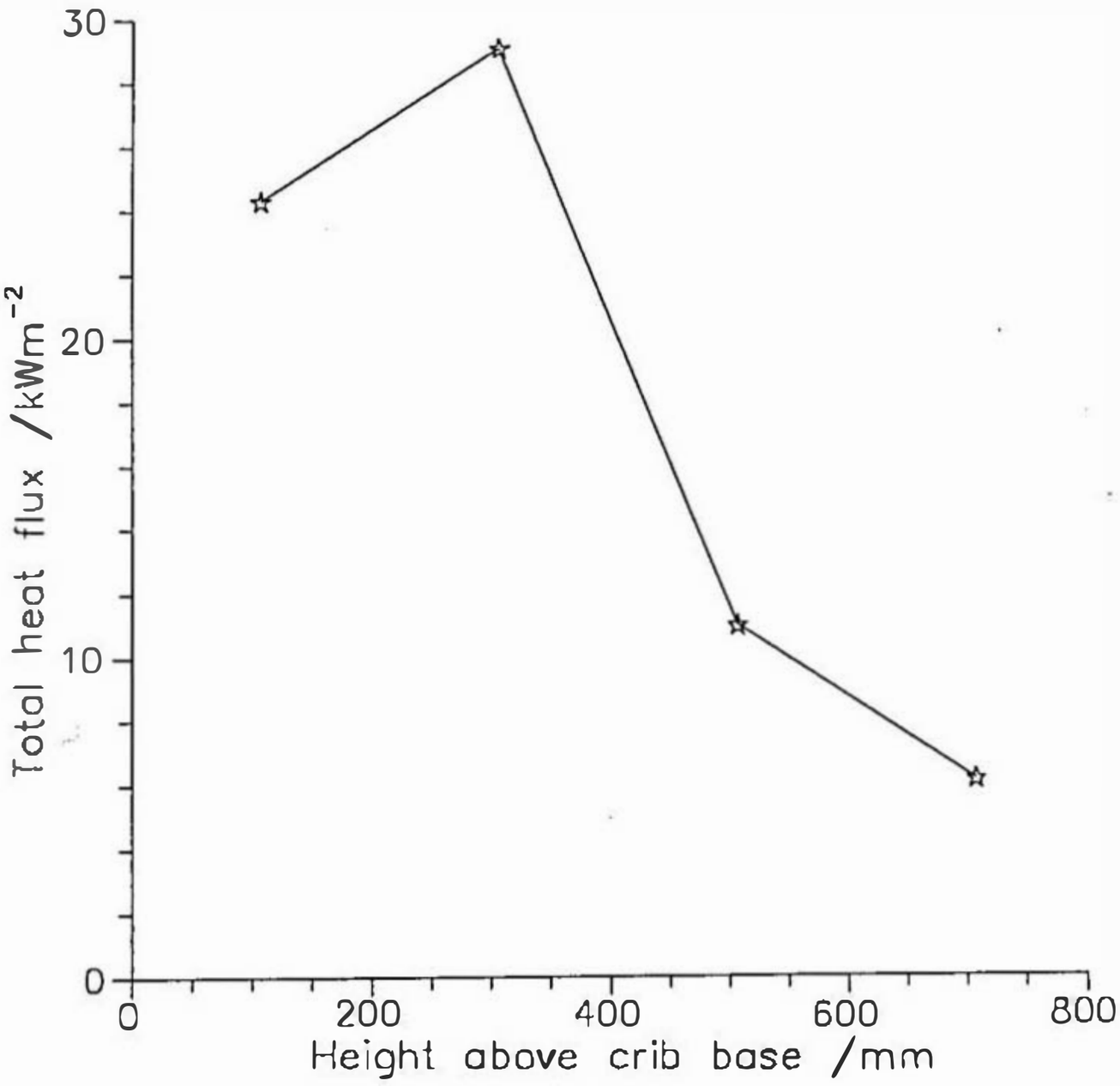

Figure (6.17)

Contour Maps of Total Heat Flux /kWm^{-2} over the Wall,
60 mm Separation, $\dot{Q}$ = 12.5 kW
Line Burner in the Centre of the Channel

(a) Closed Base

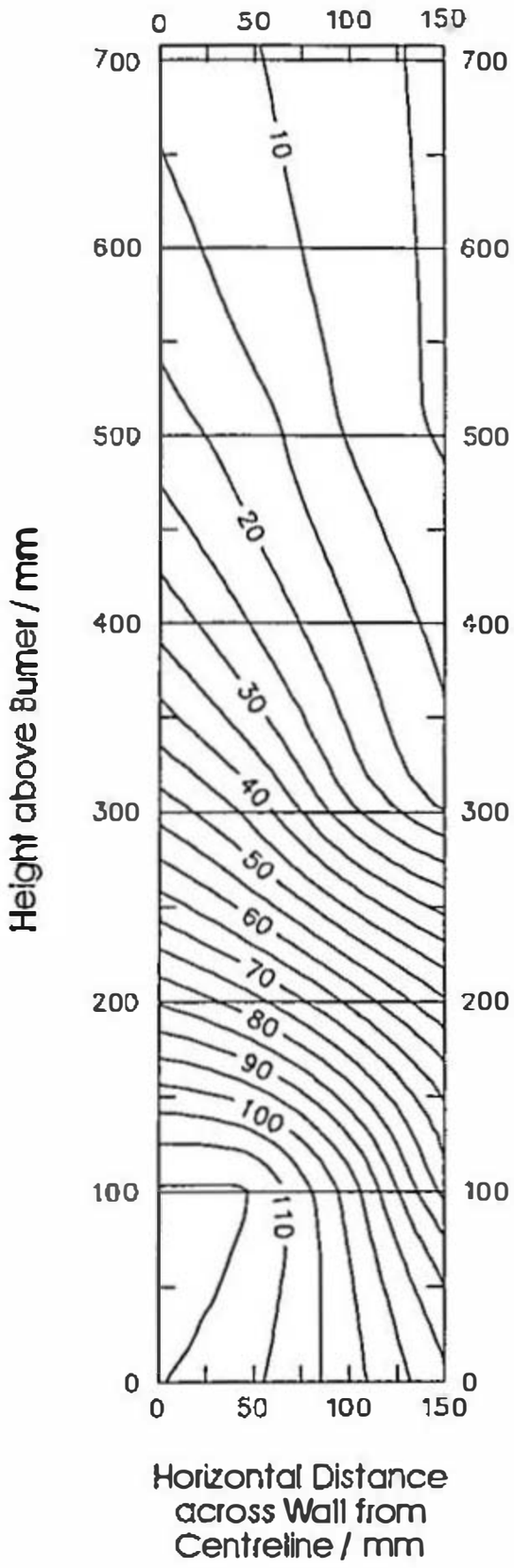

(b) Open Base

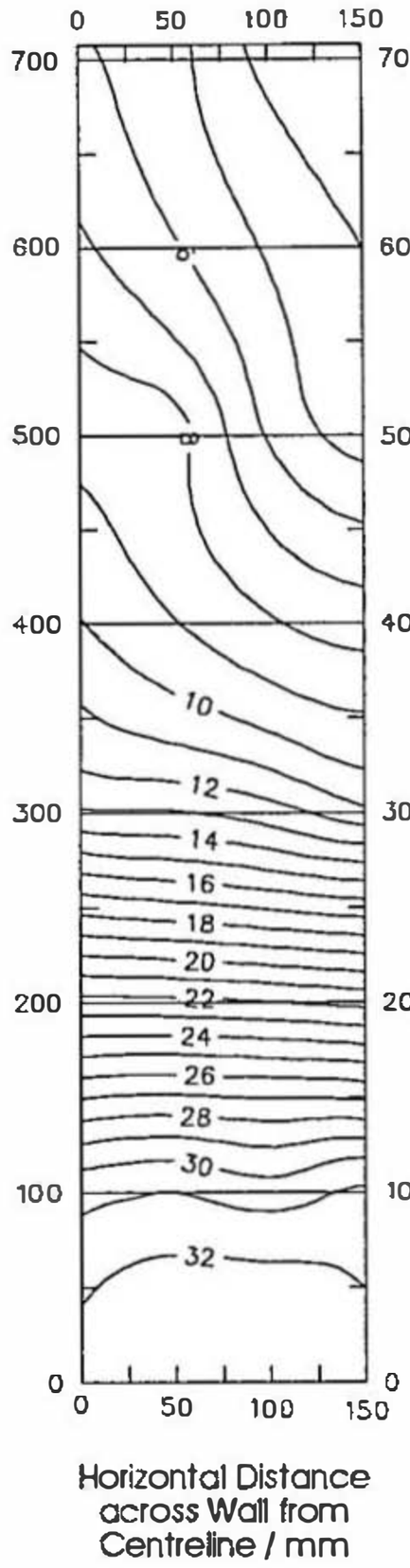

Figure (6.18) Photographs of closed and open base respectively,
60mm separation, Q=12.5 kW

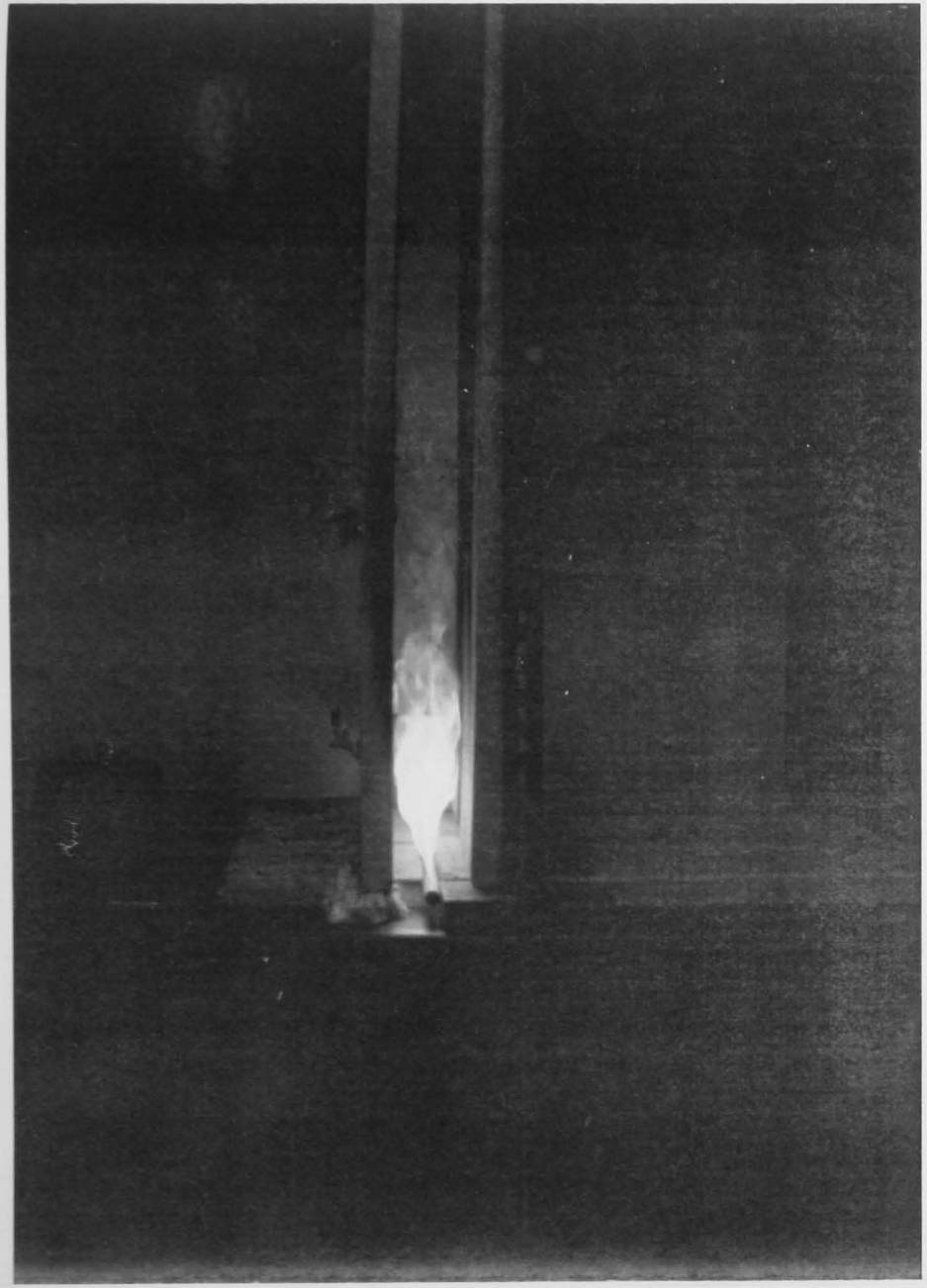

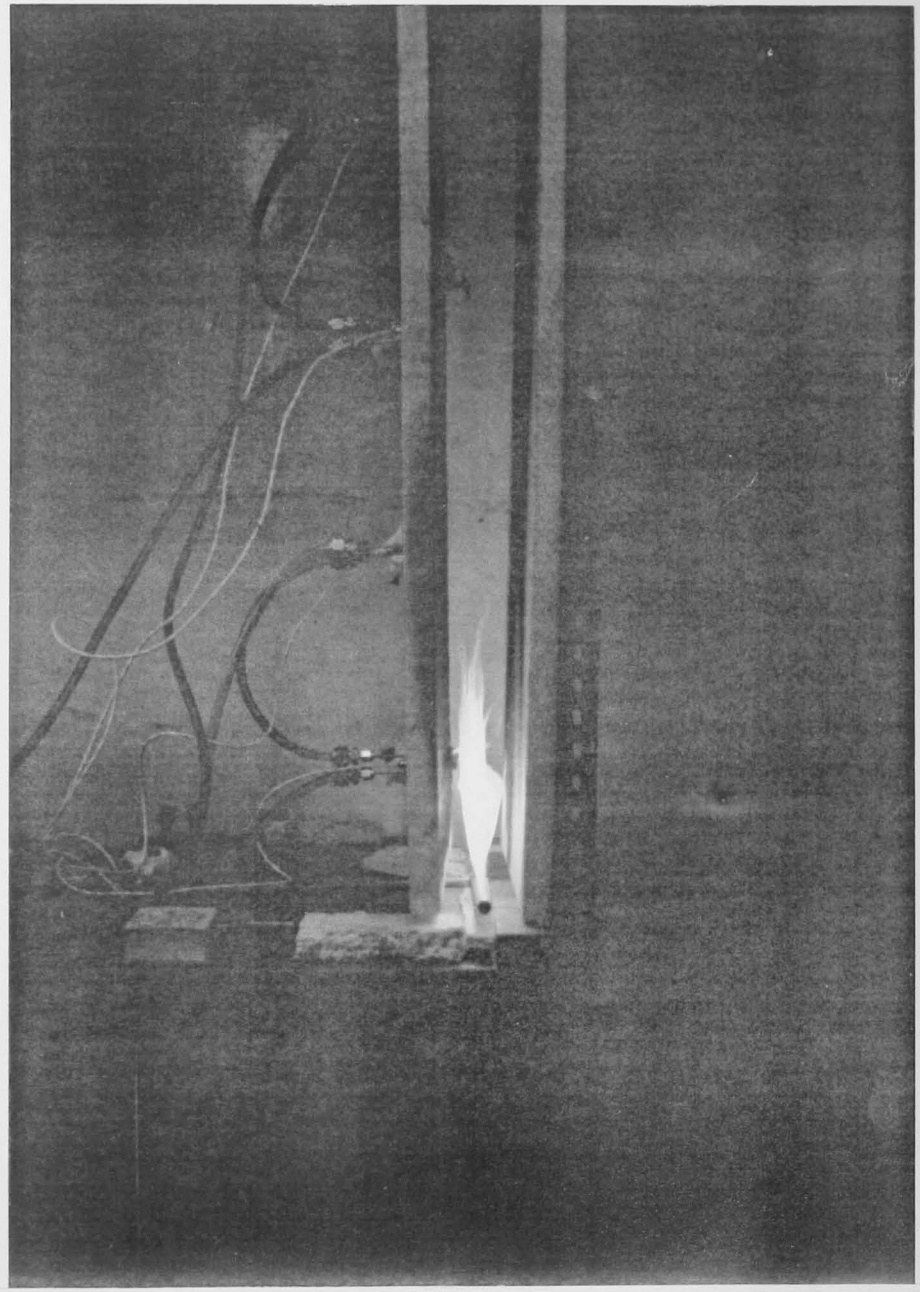

Figure (6.19) Heat flux as a function of end blockage ratio,
100 mm separation, open base, burner against instrumented wall.
Height above burner: △ 108 mm, ◊ 308 mm, ☆ 508 mm, * 708 mm

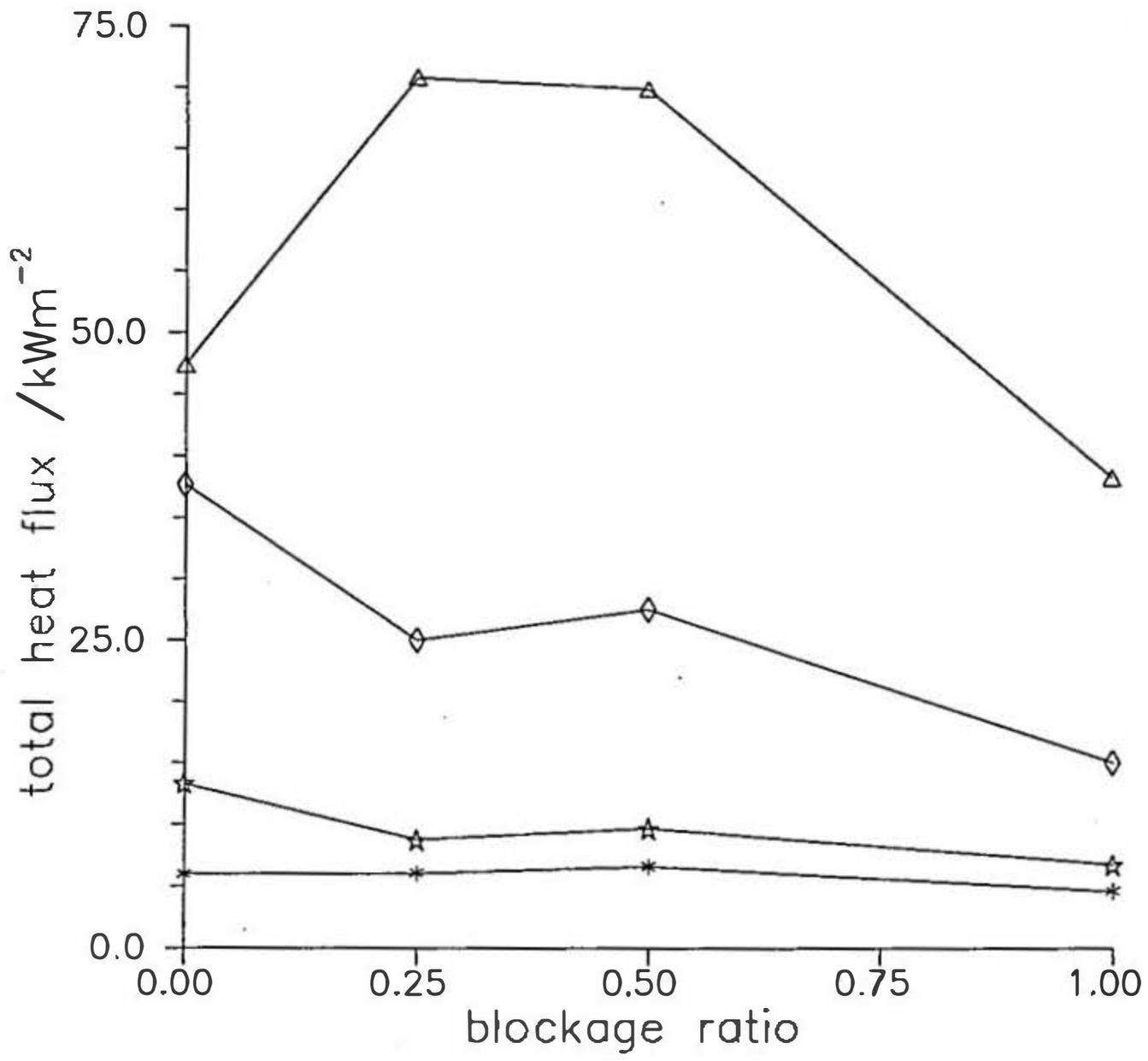

Figure (6.20) Heat flux as a function of end blockage ratio,
100 mm separation, open base, burner in centre of channel.
Height above burner: △ 108 mm, ◊ 308 mm, ☆ 508 mm, * 708 mm

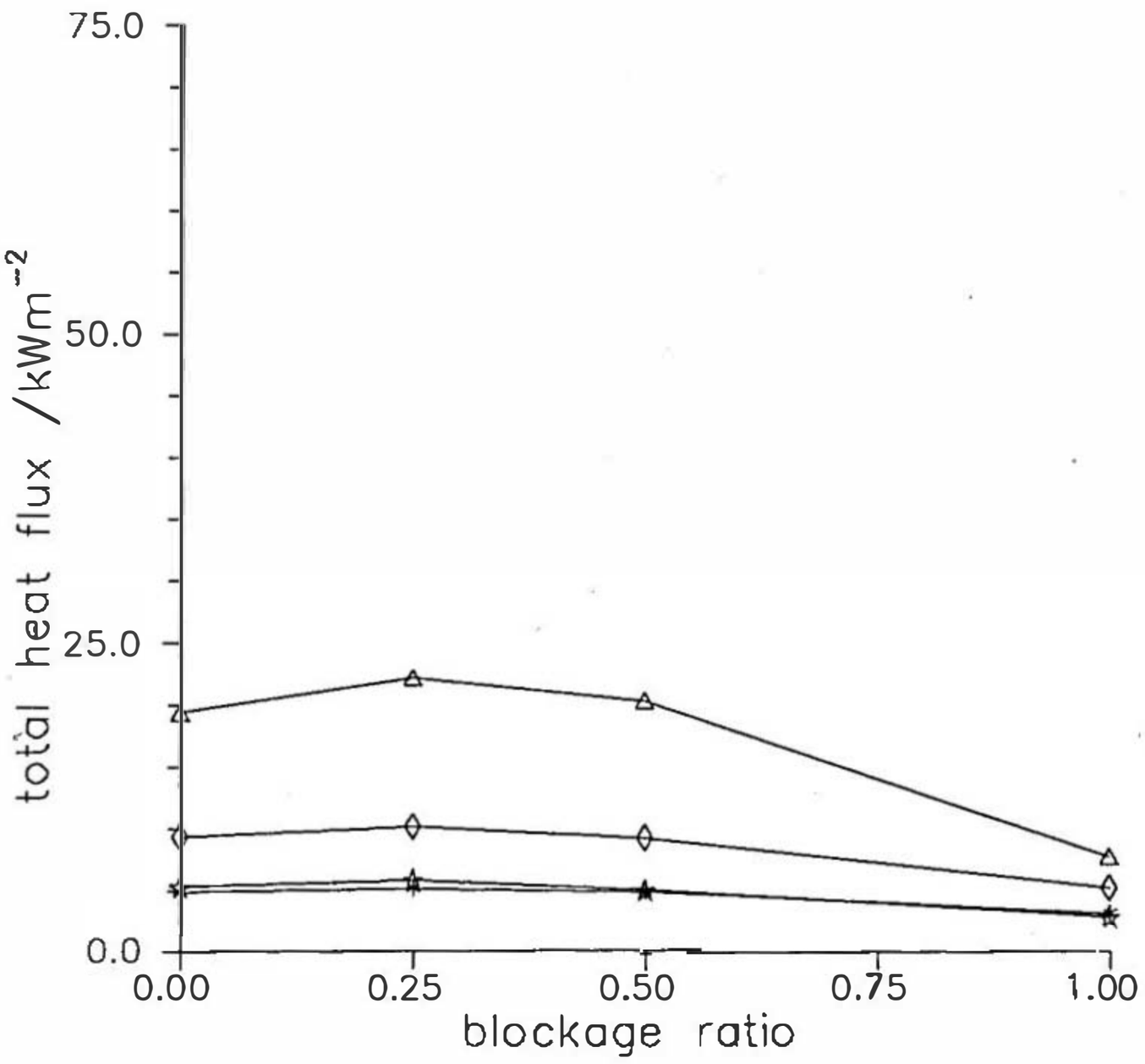

Figure (6.21) Heat flux as a function of end blockage ratio,
100 mm separation, closed base, burner against instrumented wall.
Height above burner: △ 108 mm, ◊ 308 mm, ☆ 508 mm, * 708 mm

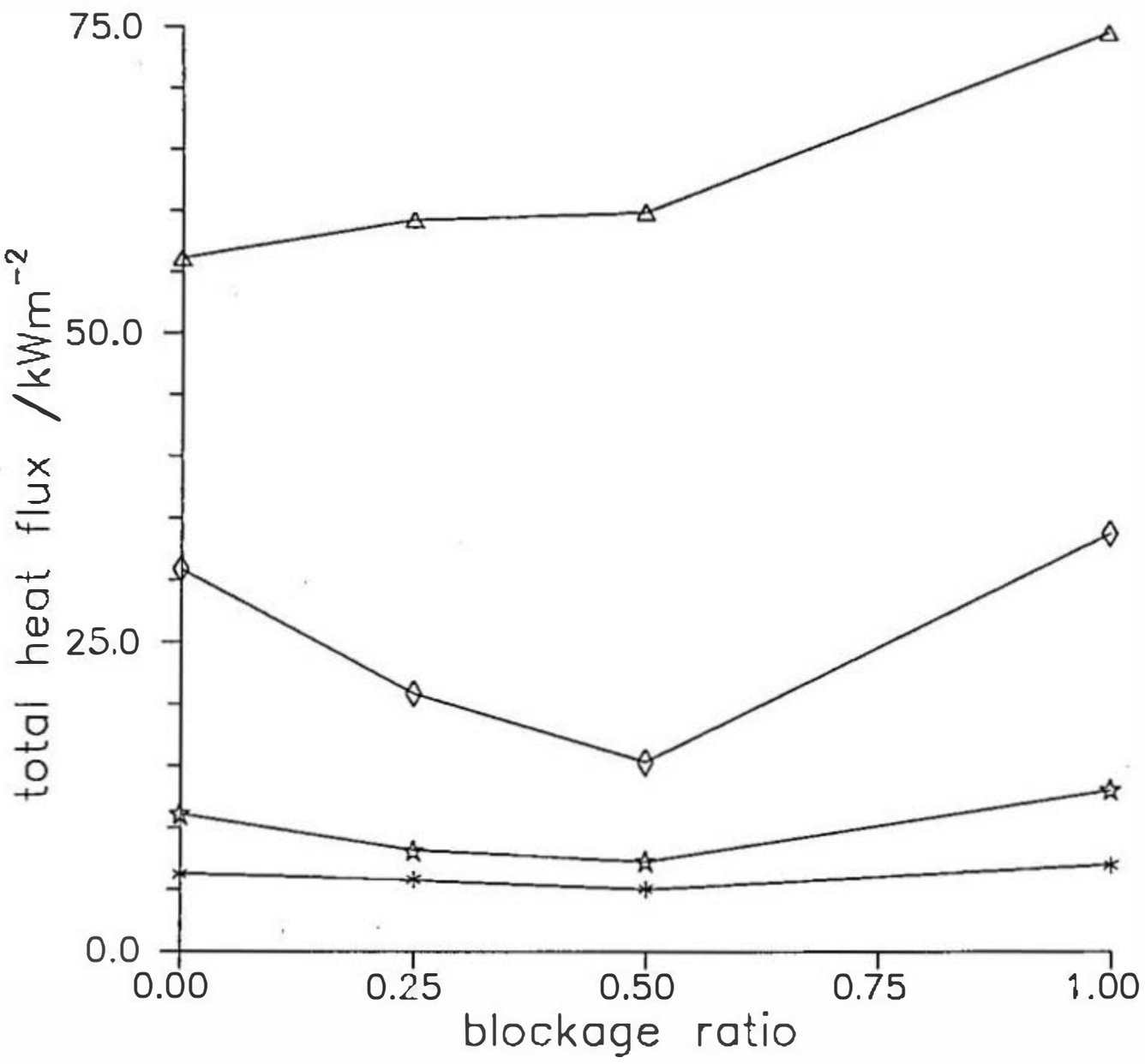

Figure (6.22) Heat flux as a function of end blockage ratio,
100 mm separation, closed base, burner in centre of channel.
Height above burner: △ 108 mm, ◊ 308 mm, ☆ 508 mm, * 708 mm

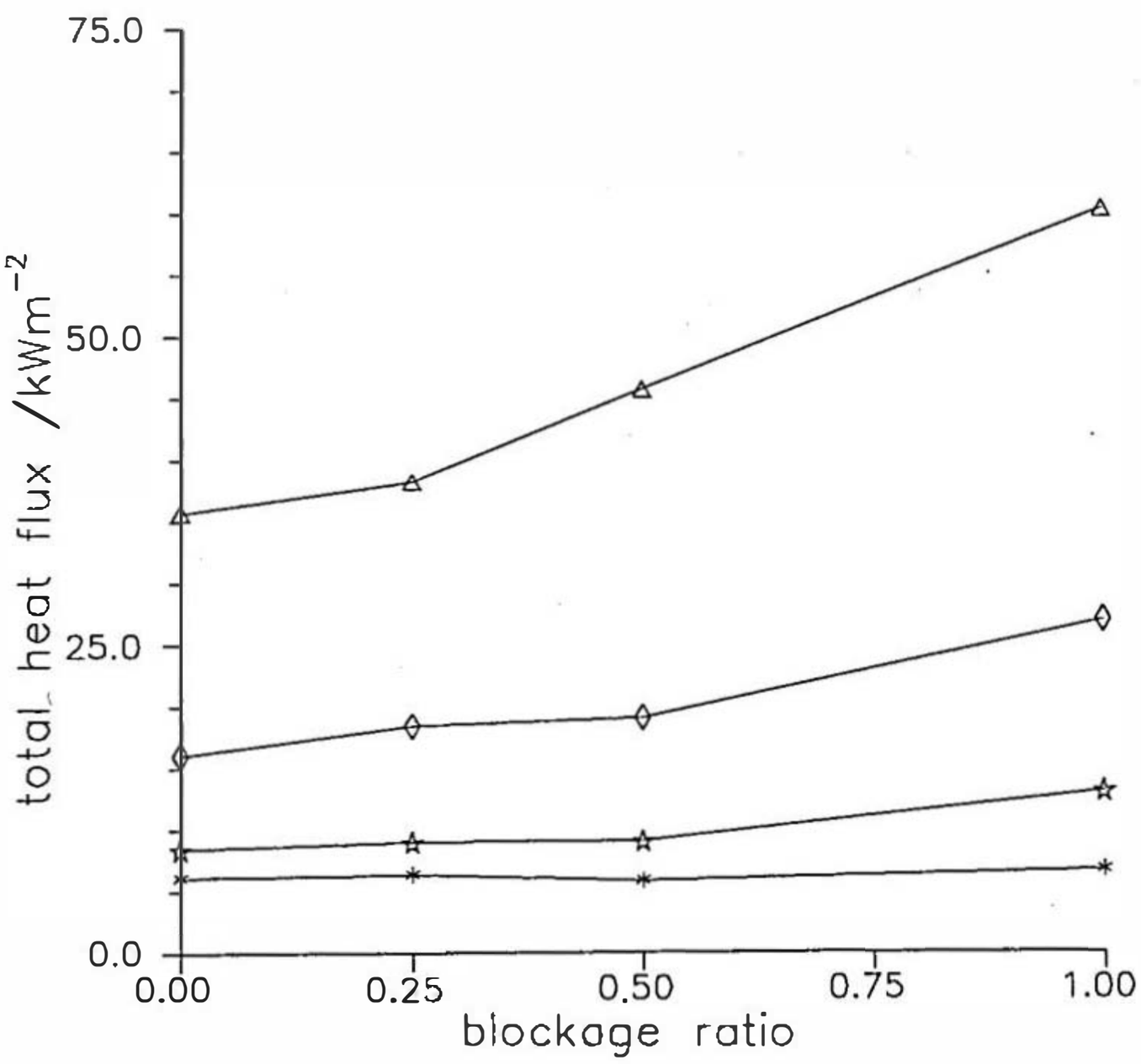

Figure (6.23) Grid for centreline heat fluxes

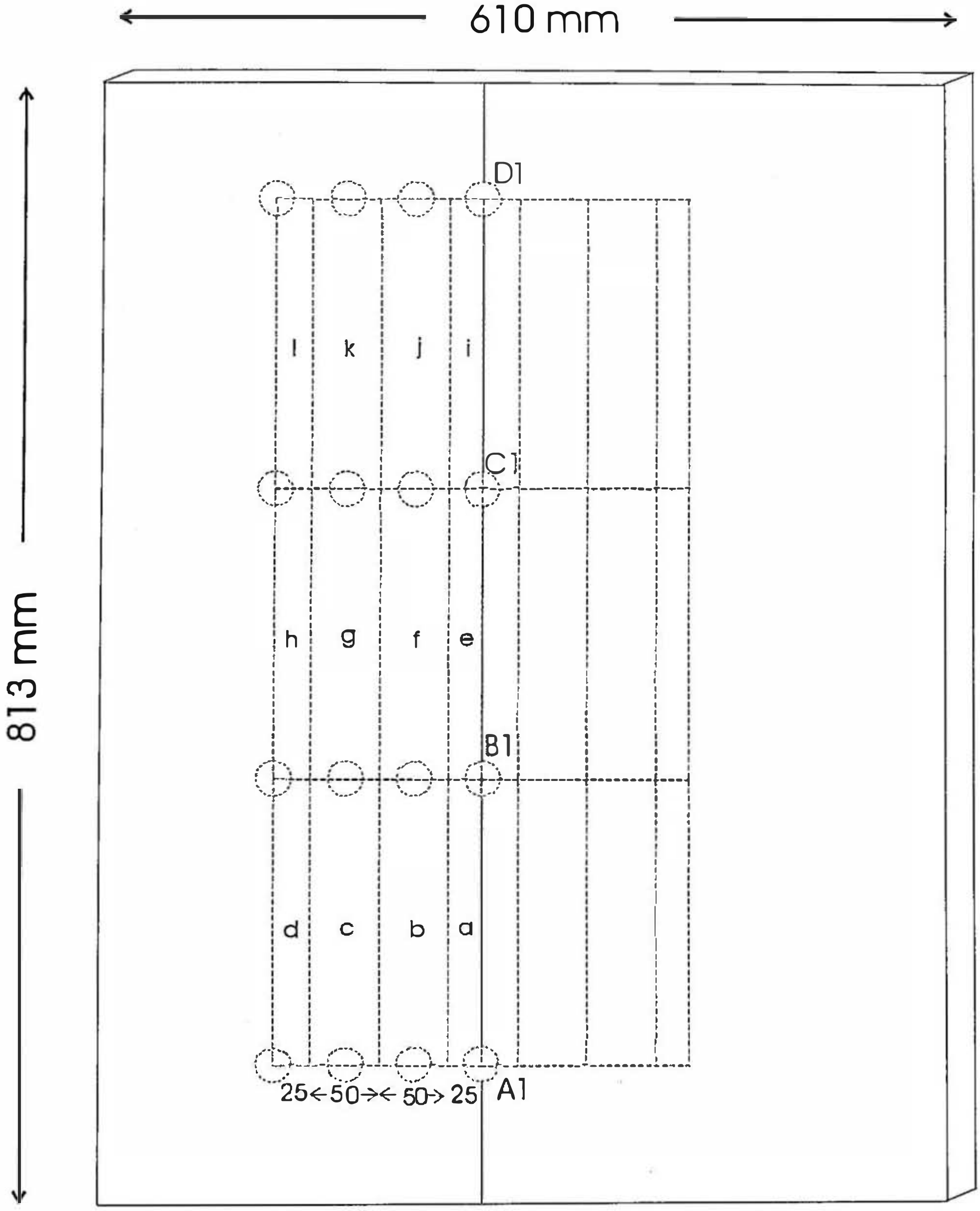

Figure (6.24) Grid for heat fluxes 50mm from centreline

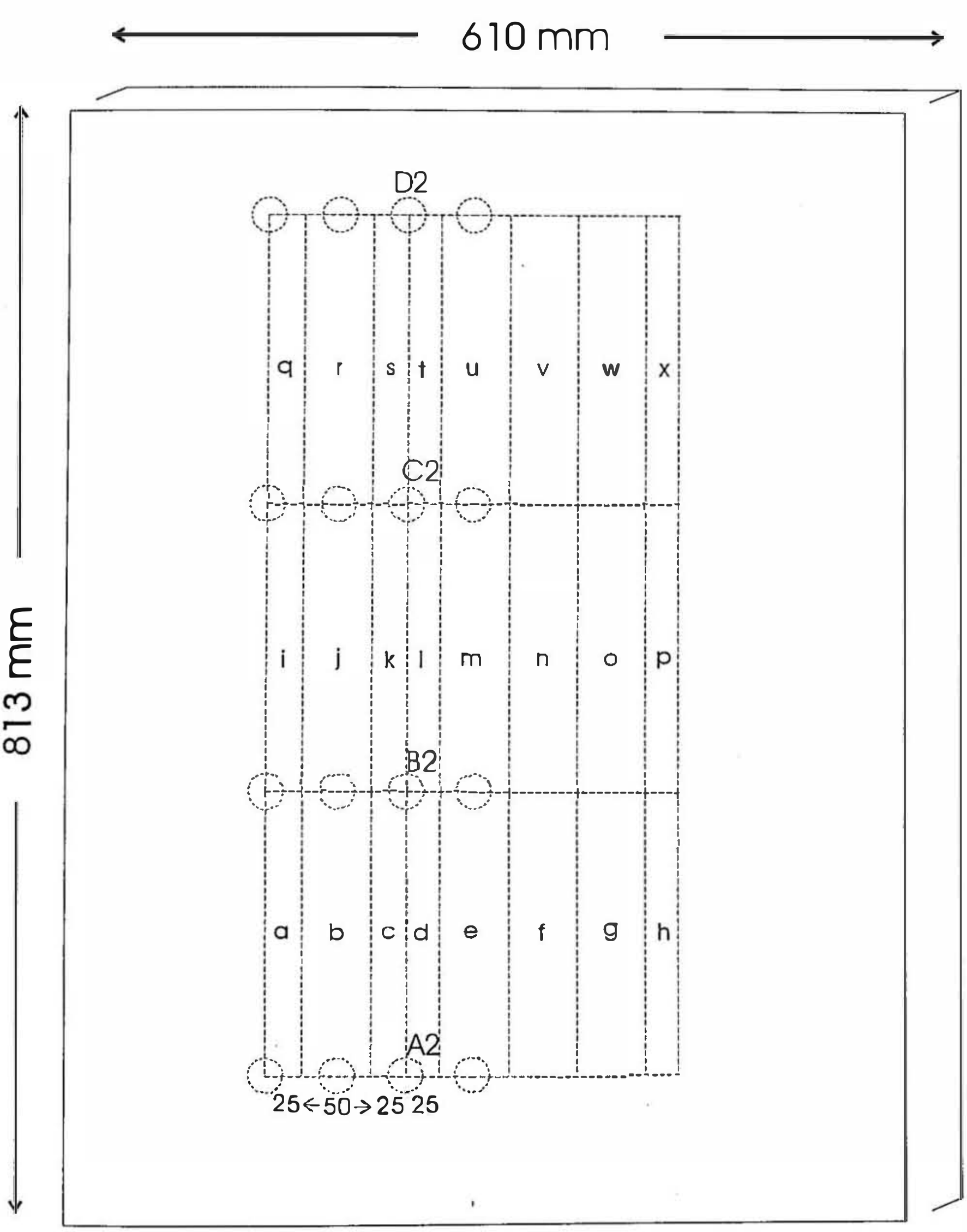

Figure (6.25) Grid for heat fluxes 100mm from centreline

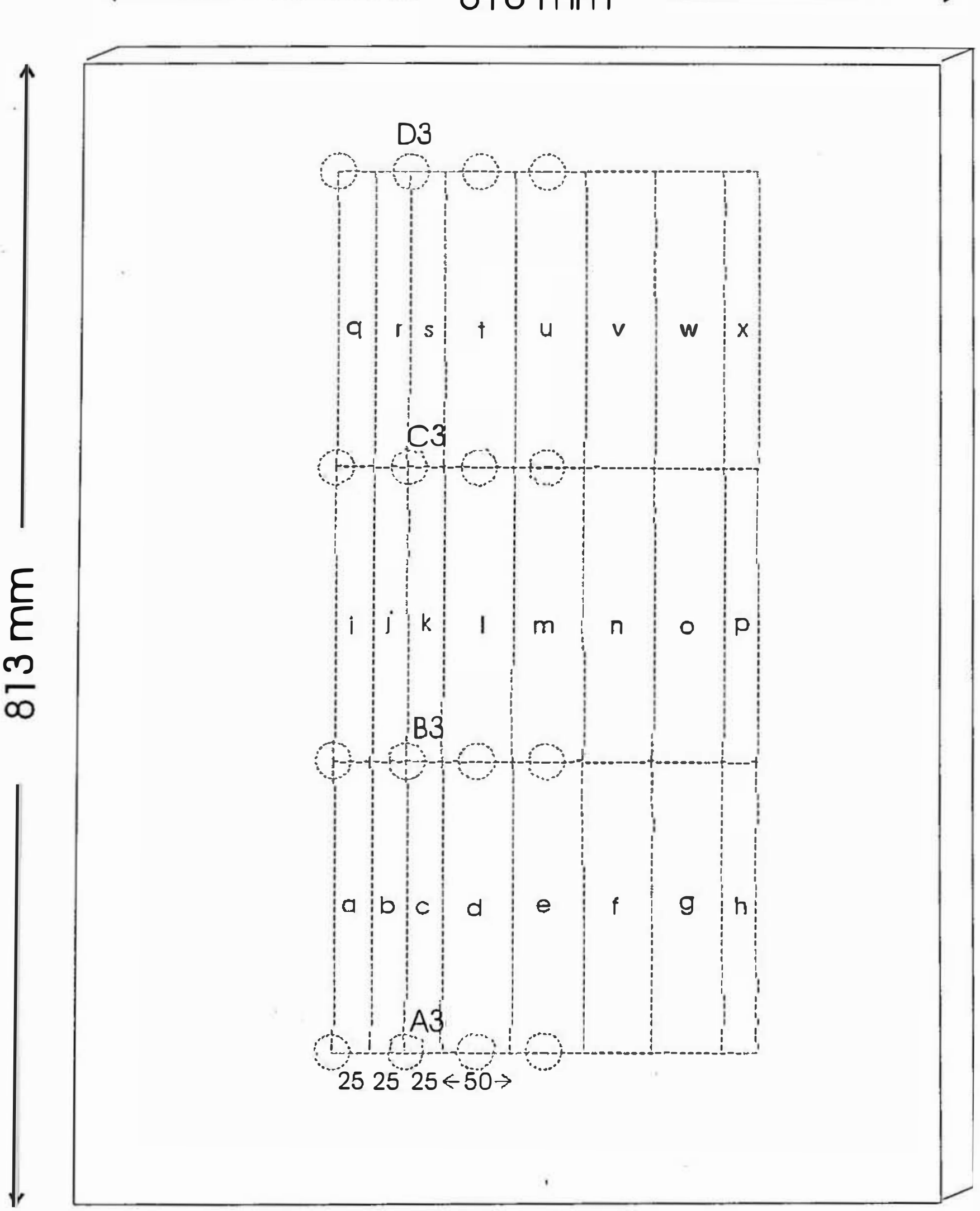

Figure (6.26) Grid for heat fluxes 150mm from centreline

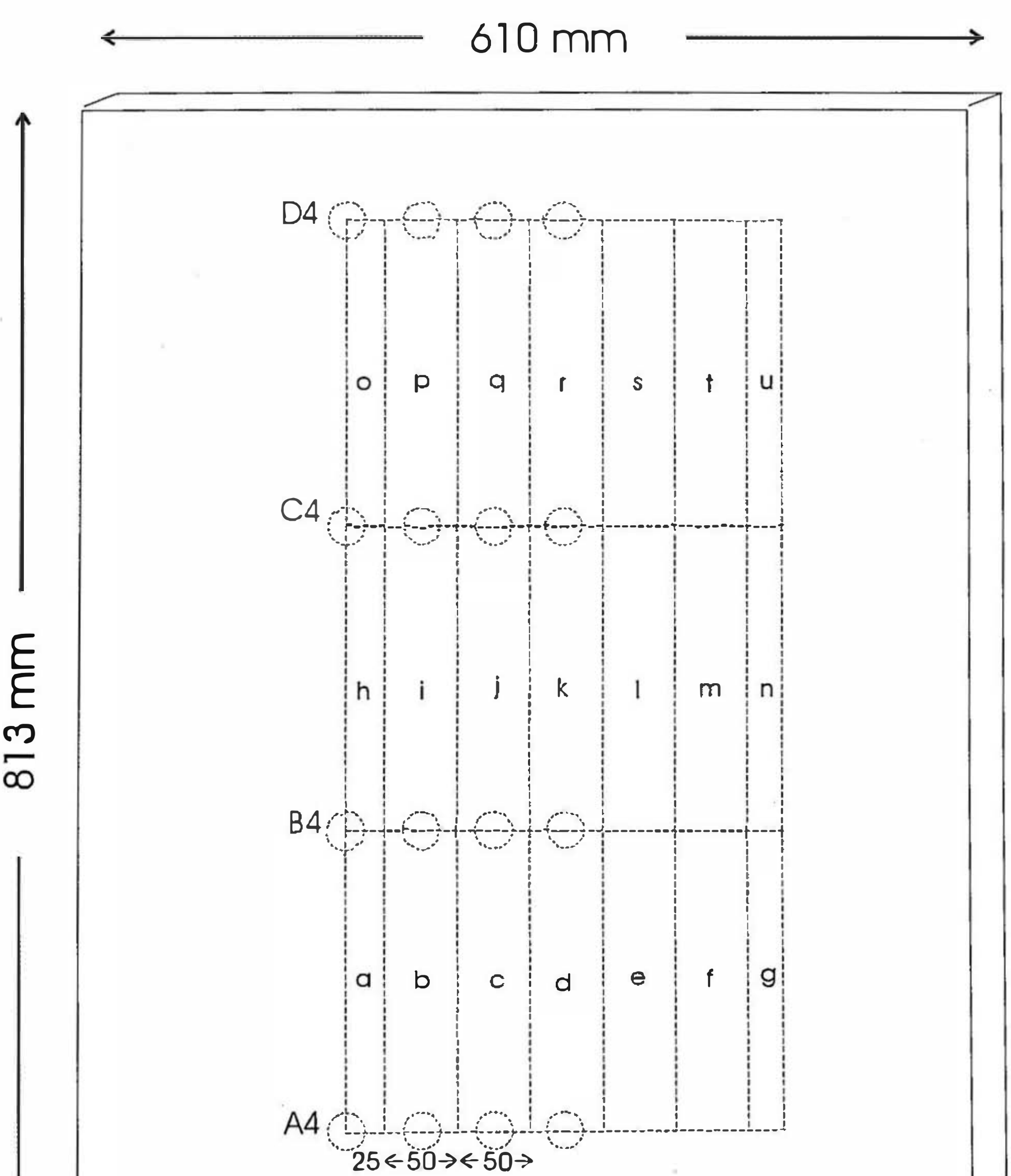

Figure (6.27) Centreline total heat flux as a function of correlation equation open base, burner against wall, 12.53 kW

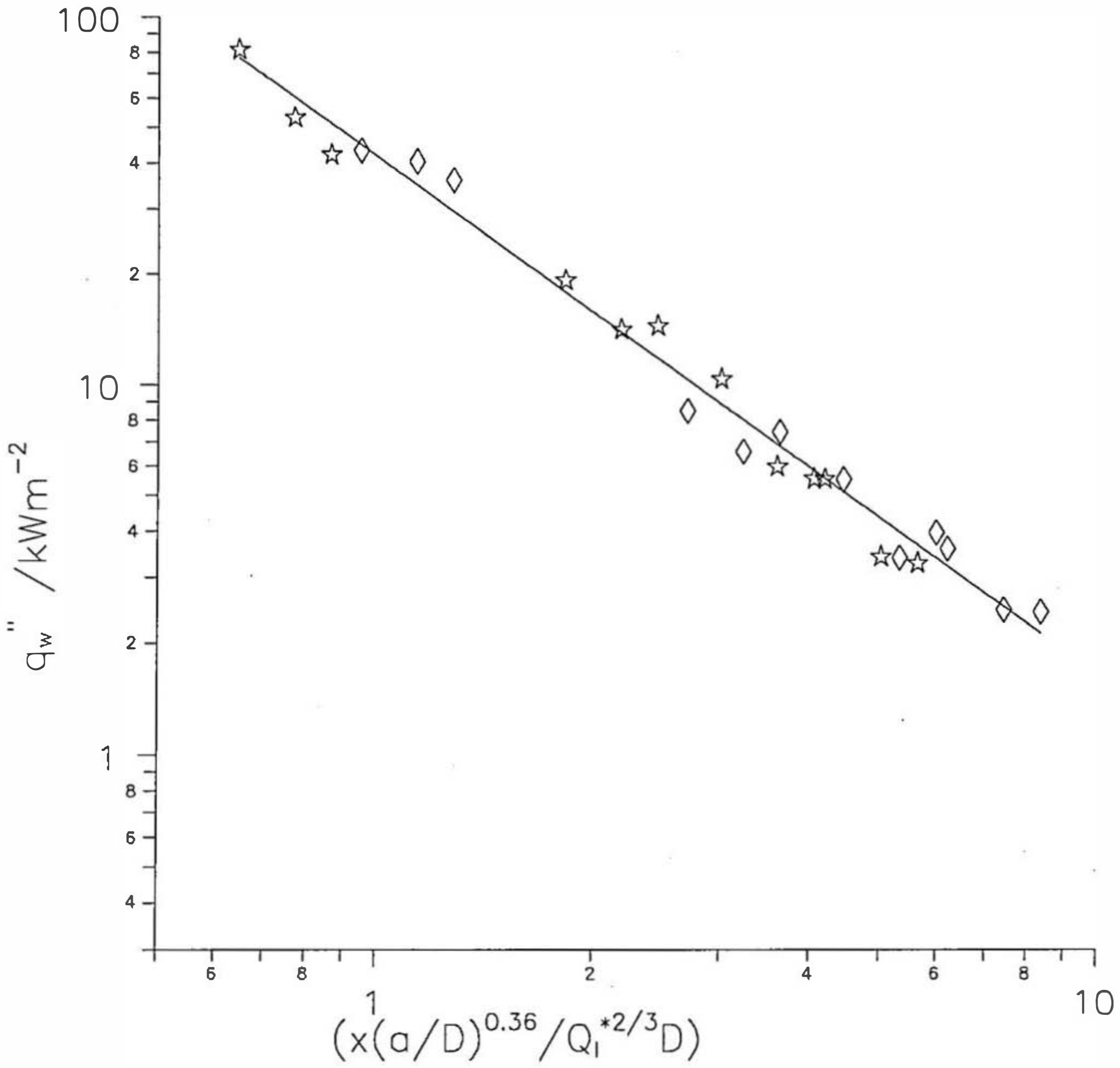

Figure (6.28) worksheet for regression calculation

number of points		24									
t-value at n-2		2.074									
	ln (x(a/D)^.36)	lnqw				(x-avg x)*					residuals
data point	/QI*^2/3D (x)	(y)		(x-avg x)	(y-avg y)	(y-avg y)	(x - avg x)^	fitted y	(y-fit y)^2	(y-avg y)^	(y-fitted y)
1	0.25	3.58		-0.79	1.30	-1.02	0.62	3.39	0.04	1.68	0.20
2	1.30	2.01		0.26	-0.28	-0.07	0.07	1.92	0.01	0.08	0.09
3	1.80	1.38		0.76	-0.91	-0.70	0.58	1.22	0.02	0.83	0.16
4	2.13	0.88		1.10	-1.40	-1.54	1.20	0.75	0.02	1.97	0.13
5	-0.14	3.75		-1.18	1.46	-1.72	1.39	3.94	0.04	2.13	-0.19
6	0.91	2.68		-0.13	0.39	-0.05	0.02	2.47	0.04	0.15	0.21
7	1.41	1.72		0.37	-0.57	-0.21	0.14	1.77	0.00	0.32	-0.05
8	1.74	1.19		0.70	-1.09	-0.77	0.49	1.30	0.01	1.20	-0.11
9	0.14	3.70		-0.90	1.41	-1.28	0.82	3.55	0.02	2.00	0.15
10	1.18	1.88		0.15	-0.40	-0.06	0.02	2.08	0.04	0.16	-0.20
11	1.68	1.22		0.65	-1.06	-0.69	0.42	1.38	0.03	1.13	-0.16
12	2.02	0.90		0.98	-1.39	-1.36	0.96	0.92	0.00	1.92	-0.02
13	-0.26	3.98		-1.29	1.69	-2.19	1.68	4.10	0.01	2.86	-0.12
14	0.79	2.66		-0.25	0.37	-0.09	0.06	2.63	0.00	0.14	0.02
15	1.29	1.80		0.25	-0.49	-0.12	0.06	1.93	0.02	0.24	-0.14
16	1.62	1.24		0.59	-1.05	-0.62	0.34	1.47	0.05	1.11	-0.23
17	-0.04	3.77		-1.08	1.48	-1.60	1.17	3.80	0.00	2.19	-0.04
18	1.01	2.14		-0.03	-0.15	0.00	0.00	2.33	0.04	0.02	-0.19
19	1.51	1.71		0.47	-0.58	-0.27	0.22	1.63	0.01	0.33	0.08
20	1.84	1.28		0.80	-1.01	-0.81	0.64	1.17	0.01	1.02	0.11
21	-0.43	4.40		-1.47	2.12	-3.12	2.17	4.35	0.00	4.48	0.05
22	0.61	2.96		-0.43	0.68	-0.29	0.18	2.88	0.01	0.46	0.08
23	1.11	2.35		0.07	0.06	0.00	0.01	2.18	0.03	0.00	0.16
24	1.45	1.72		0.41	-0.57	-0.23	0.17	1.72	0.00	0.32	0.00
	avg x =	avg y =				sum =	sum =	avg fit =	sum =	sum =	
	1.04	2.29				-18.77	13.41	2.29	0.45	26.74	

		st. dev.	t-ratio
a =	3.742	0.04	93.8963
b =	-1.400	0.04	-35.8141
s =	0.143		
R^2(%) =	98.314		

(x)	y fit	(x-avg x)^2	s.d fit	95 % C. I.		95 % P. I.	
-0.45	4.37	2.22	0.07	4.24	4.51	4.05	4.70
0	3.74	1.08	0.05	3.64	3.85	3.43	4.06
0.45	3.11	0.35	0.04	3.03	3.19	2.81	3.42
0.9	2.48	0.02	0.03	2.42	2.54	2.18	2.78
1.35	1.85	0.10	0.03	1.79	1.92	1.55	2.16
1.8	1.22	0.58	0.04	1.13	1.31	0.91	1.53
2.25	0.59	1.47	0.06	0.48	0.71	0.27	0.91

Figure (6.29)-residual values versus input values
for the single factor regression

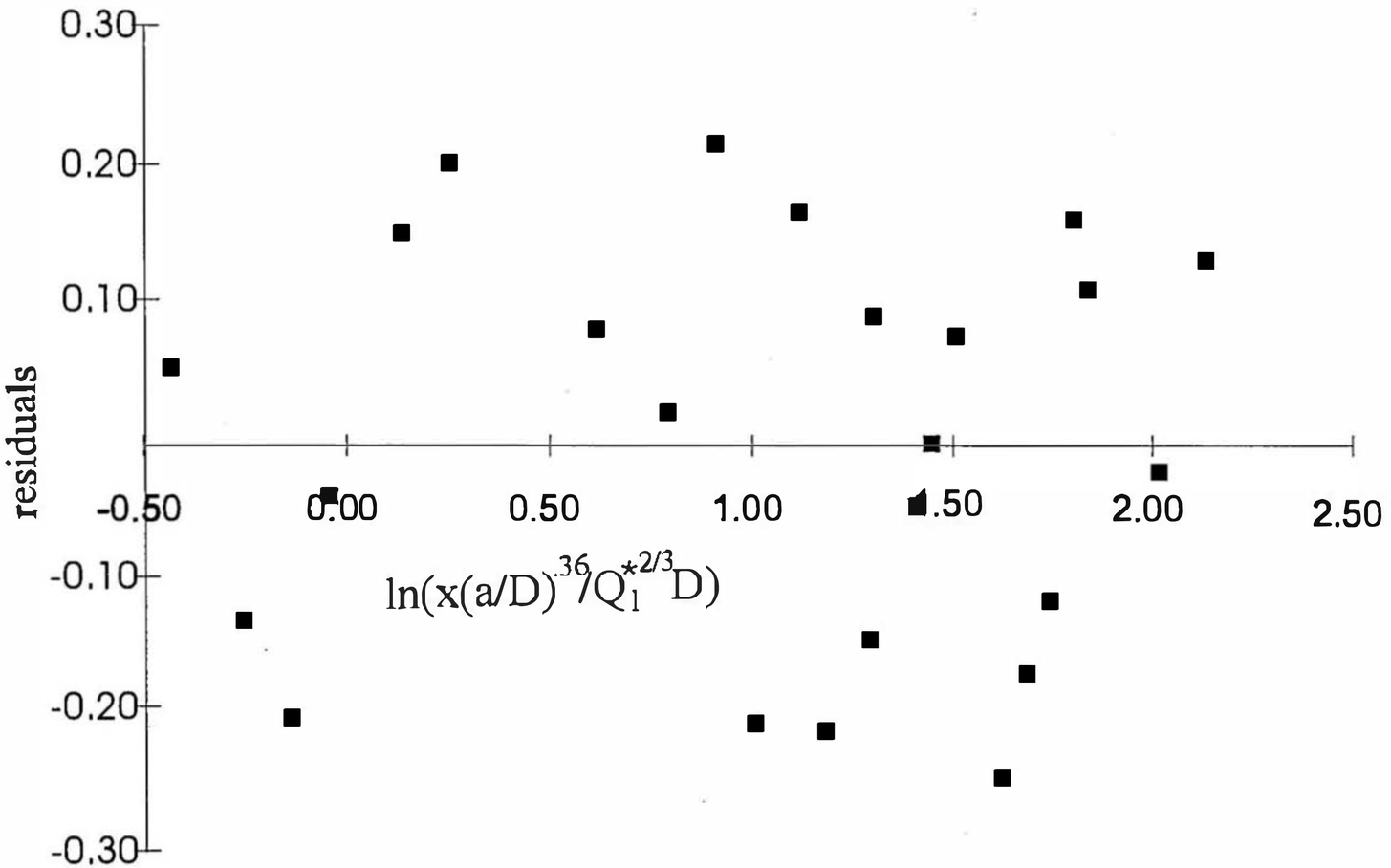

Figure (6.30)-showing 95 % confidence and predictive intervals for parallel walls, burner at instrumented wall and centreline wall heat fluxes

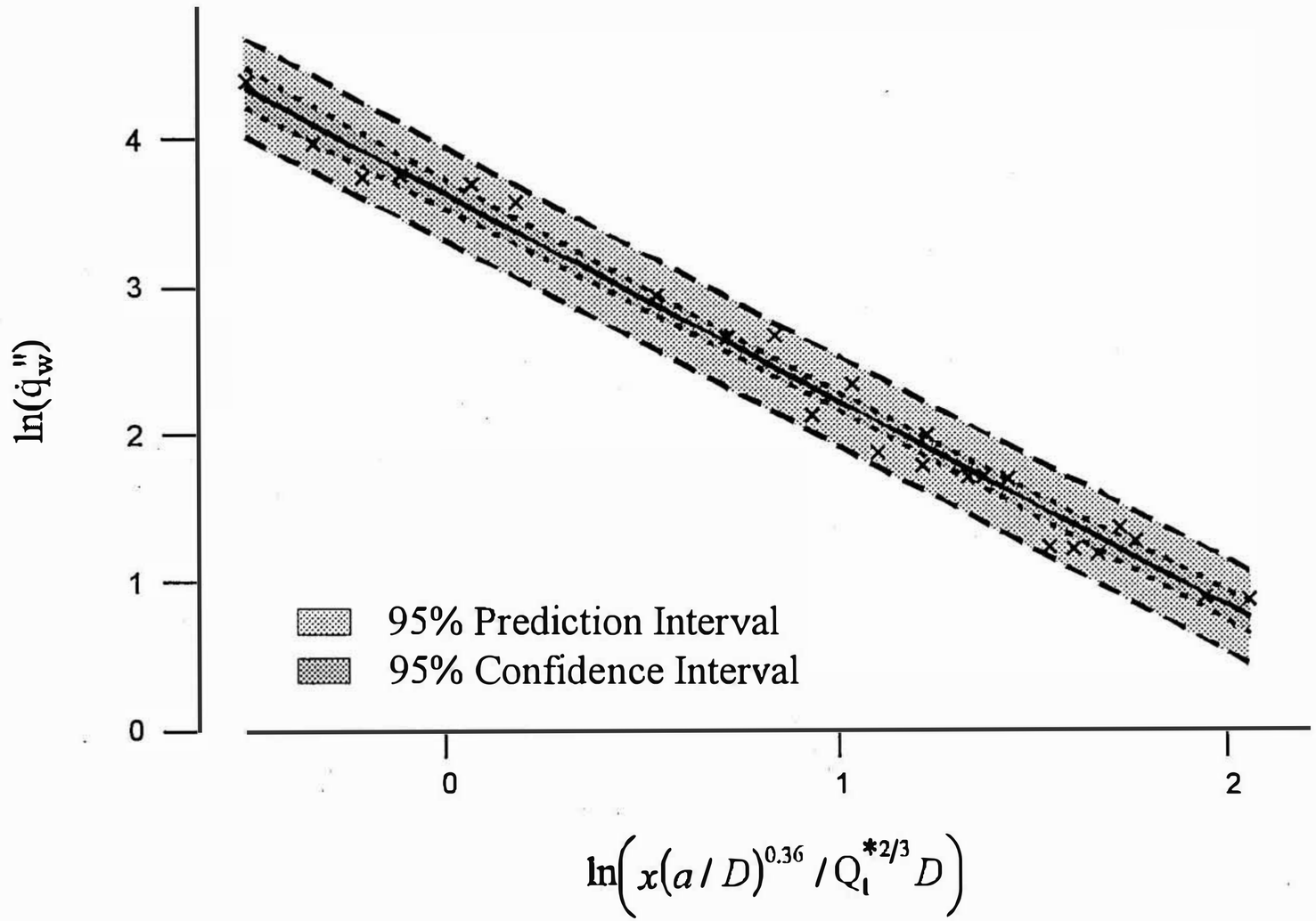

Figure (6.31)-95% confidence and predictive intervals for parallel walls, burner in centre of separation and all wall heat fluxes

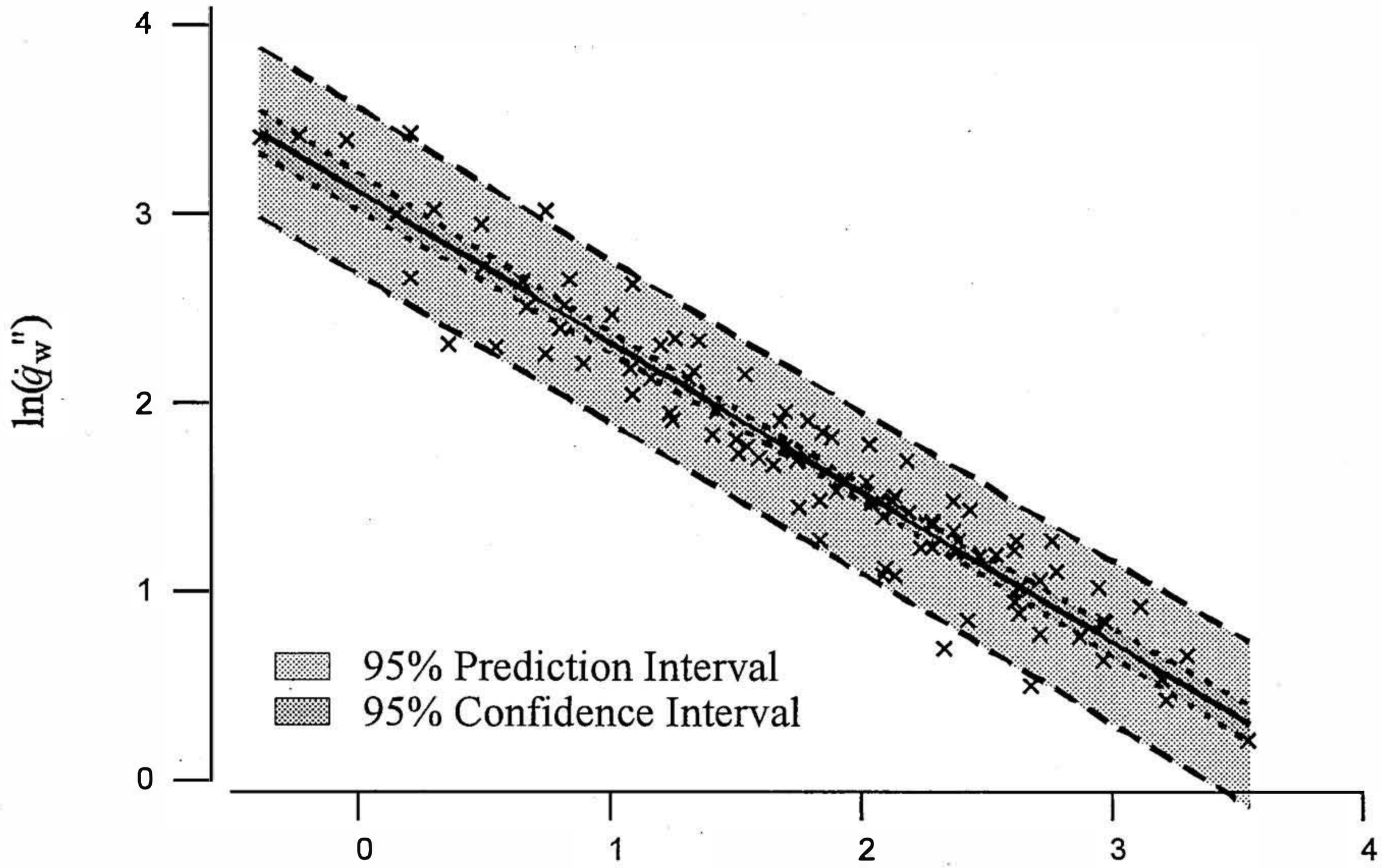

Figure (6.32) Heat flux as a function of $\left(x / Q_l^{*2/3} D \right)$, burner against the single wall, with the base open centreline heat fluxes only. ☆, $\dot{Q}_l$ = 11.6 kW/m, △, $\dot{Q}_l$ = 20.9 kW/m, ◇, data of Hasemi for thin wall.
Note: the correlation does not include Hasemi's results.

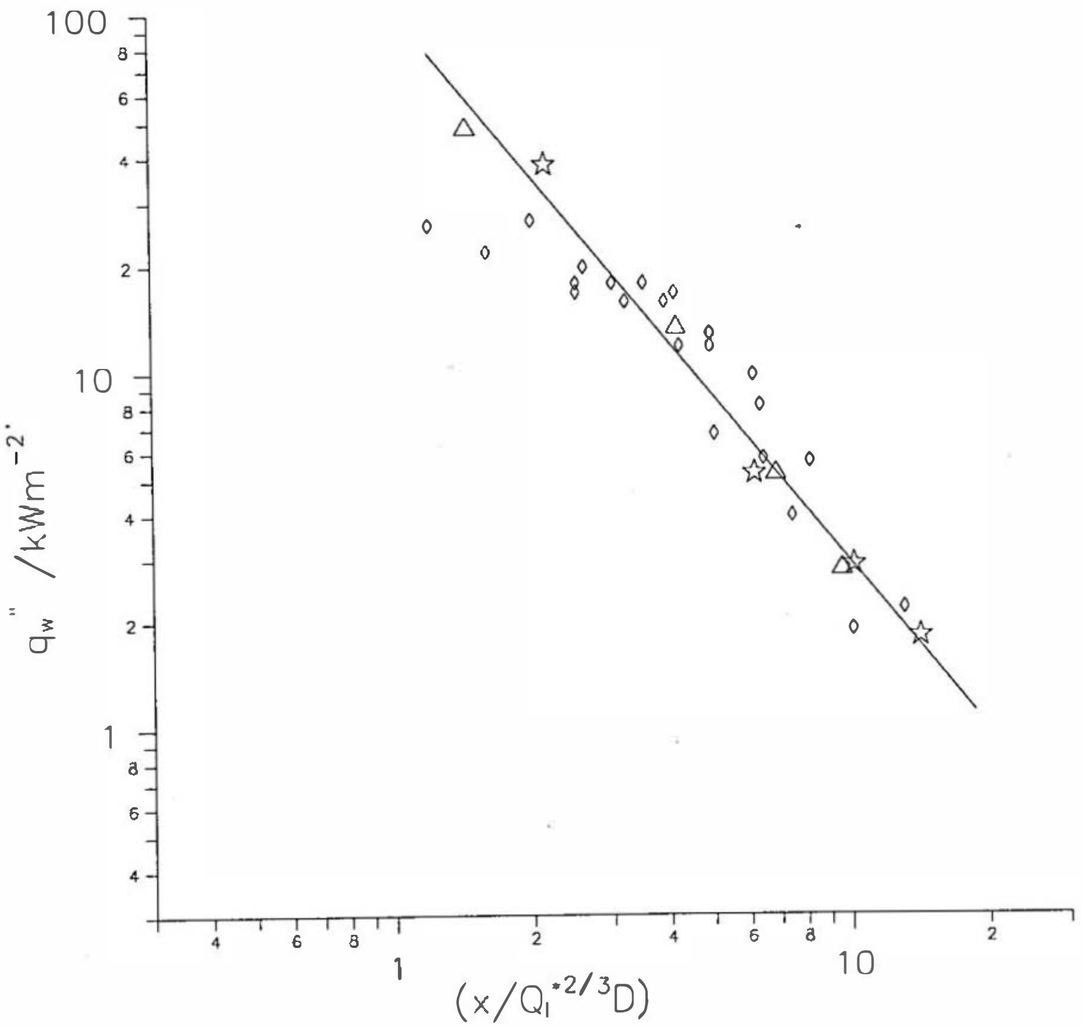

Figure (6.33) Heat flux as a function of $\left(x / Q_l^{*2/3} D\right)$, burner against the single wall, with the base closed, centreline heat fluxes only. ☆, $\dot{Q}_l = 11.6$ kW/m, ◇, $\dot{Q}_l = 20.9$ kW/m.

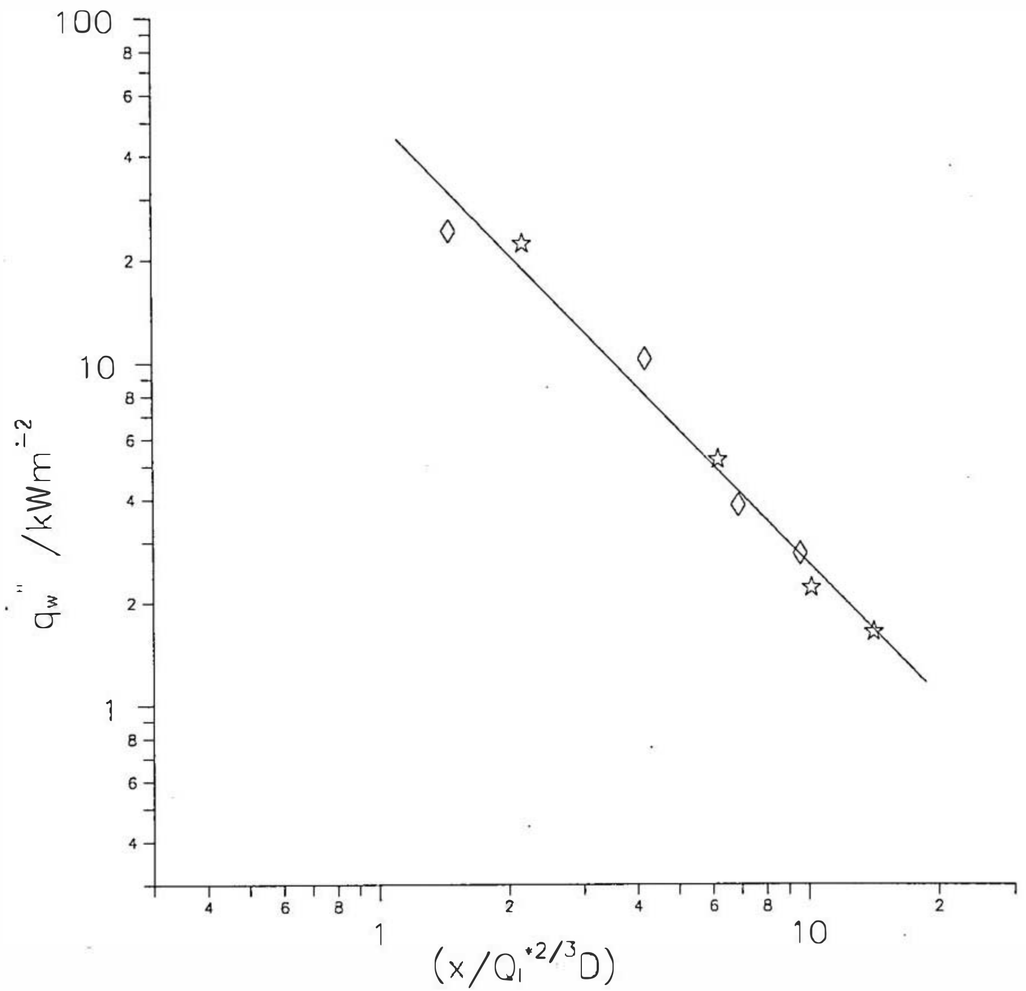

Figure (6.34) Heat flux as a function of $\left(x/\dot{Q}_l^{*2/3} D(y'/D)^{0.25}\right)$, burner against the single wall, with the base open all wall heat fluxes. ☆, $\dot{Q}_l = 11.6$ kW/m, ∆, $\dot{Q}_l = 20.9$ kW/m, ◇, data of Hasemi for thin wall
Note: the correlation does not include Hasemi's results

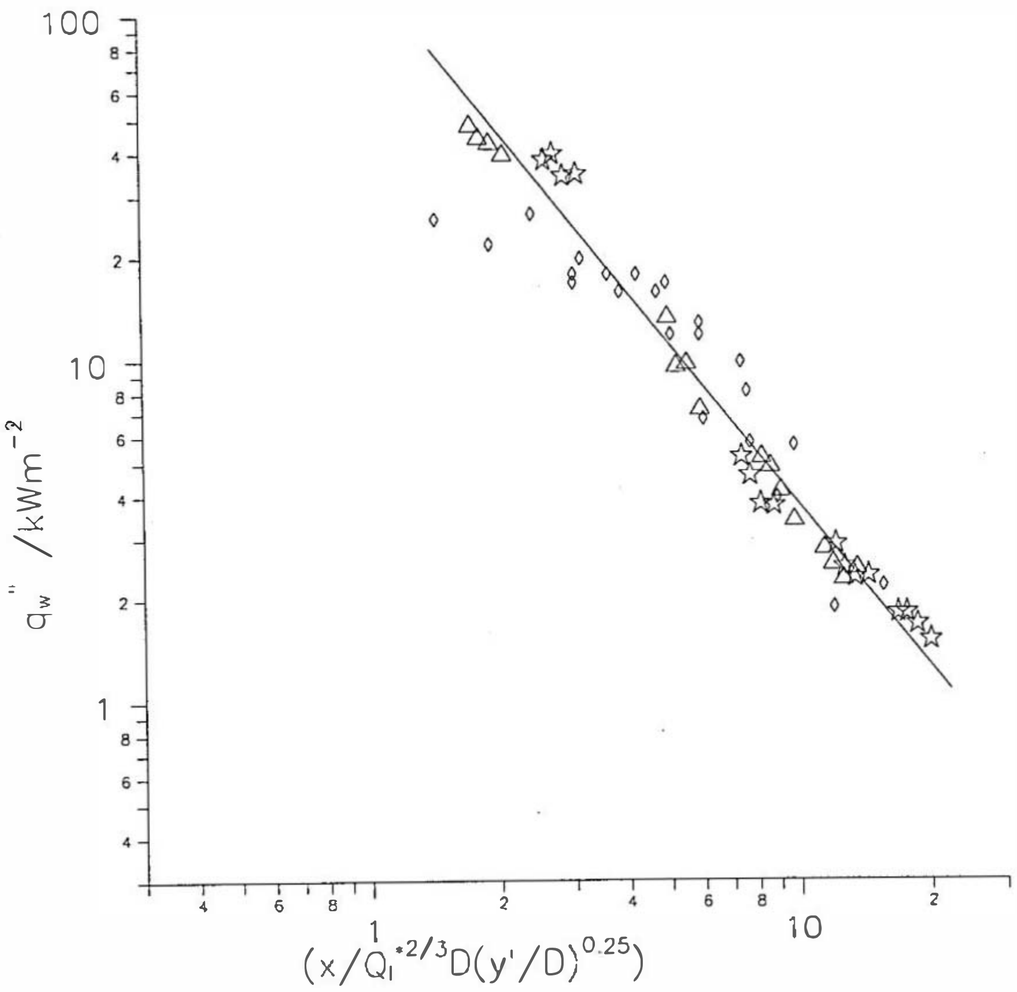

Figure (6.35) Heat flux as a function of $\left(x/\dot{Q}_l^{*2/3} D(y'/D)^{0.35}\right)$, burner against the single wall, with the base closed, all wall heat fluxes. ☆, $\dot{Q}_l = 11.6$ kW/m, ◇, $\dot{Q}_l = 20.9$ kW/m.

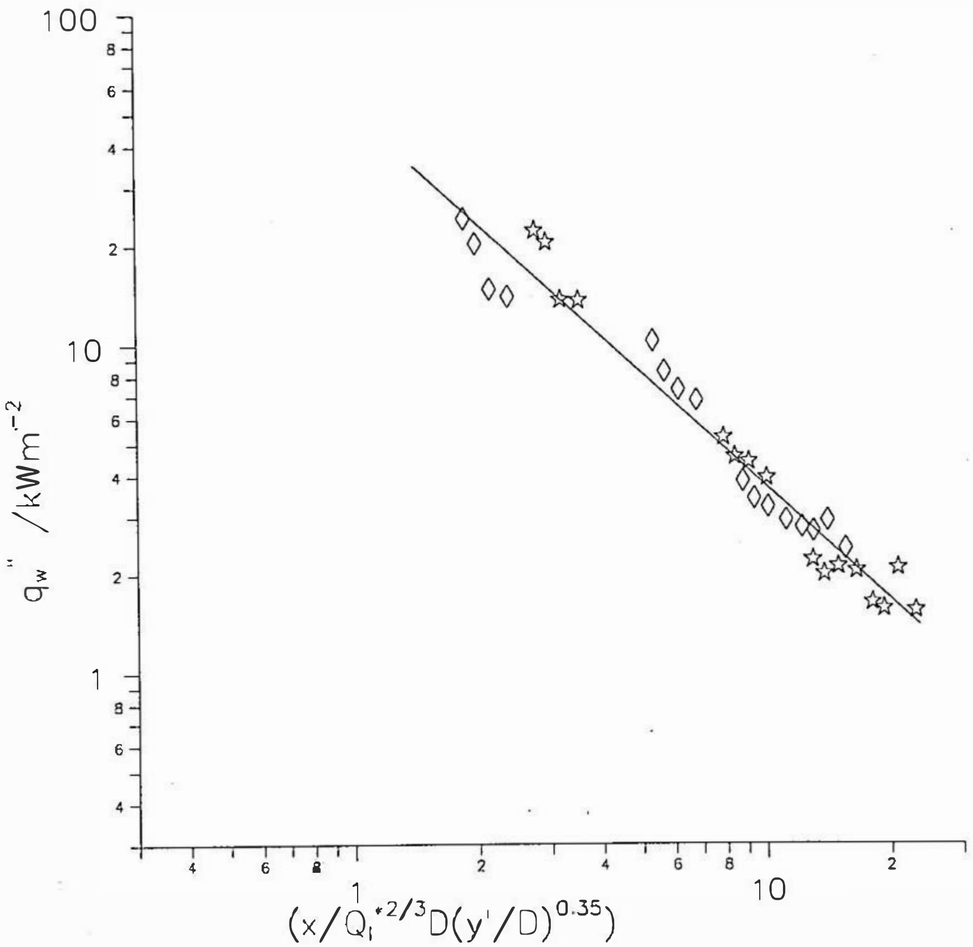

Figure (6.36) Heat flux as a function of $\left(x(a/D)^{n} / \dot{Q}_l^{*2/3} D \right)$, parallel walls, burner against the instrumented wall, with the base open, centreline heat fluxes only. ◊, $\dot{Q}_l$ = 11.6 kW/m, ☆, $\dot{Q}_l$ = 20.9 kW/m.

(a) no account taken of separation

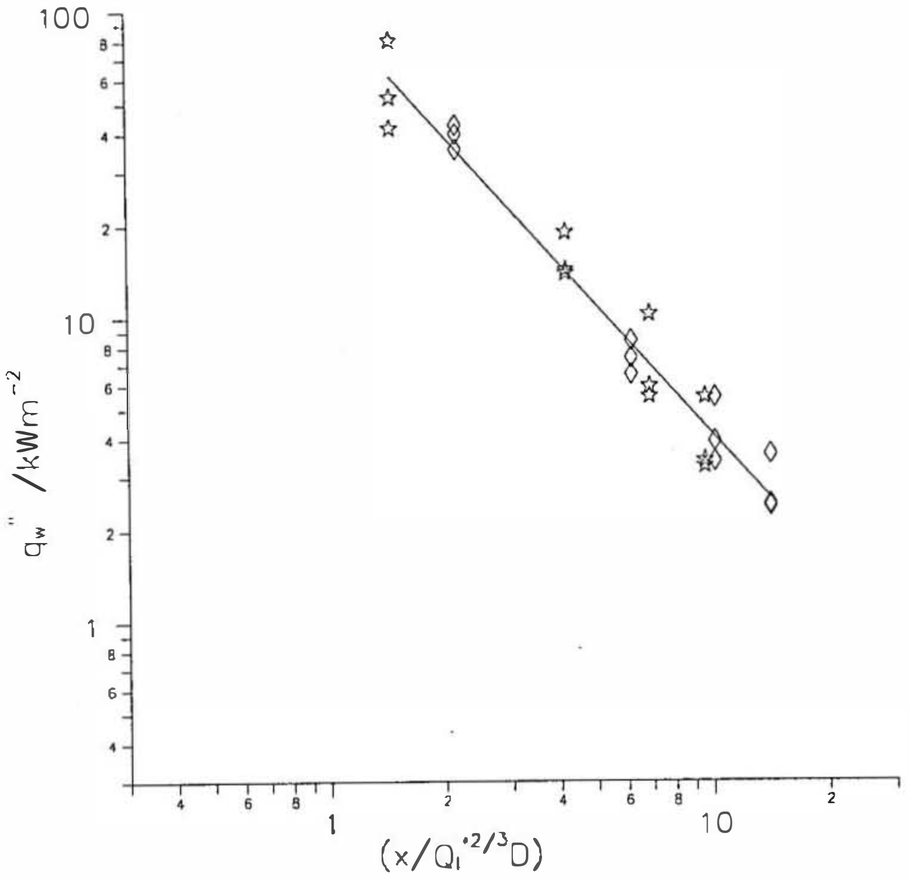

(b) abscissa includes separation term

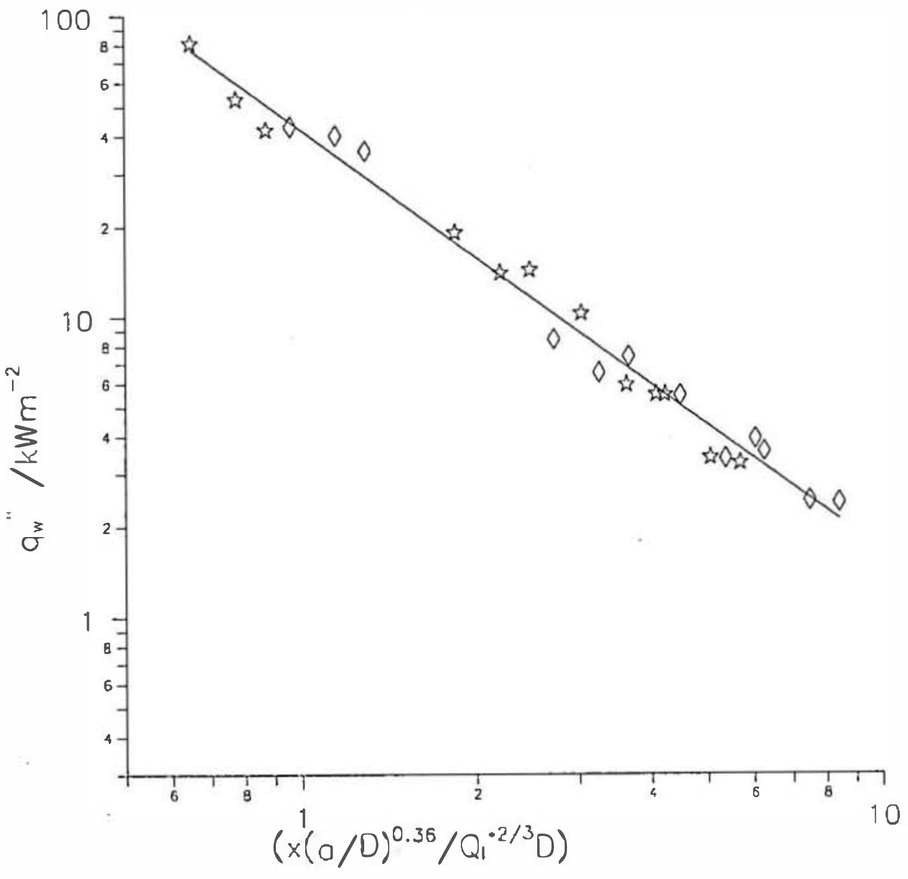

Figure (6.37) Heat flux as a function of $\left(x(a/D)^{n}/\dot{Q}_{l}^{*2/3}D\right)$,parallel walls, burner against the instrumented wall, with the base closed, centreline heat fluxes only. ◊, $\dot{Q}_l$ = 11.6 kW/m, ☆, $\dot{Q}_l$ = 20.9 kW/m.

(a) no account taken of separation

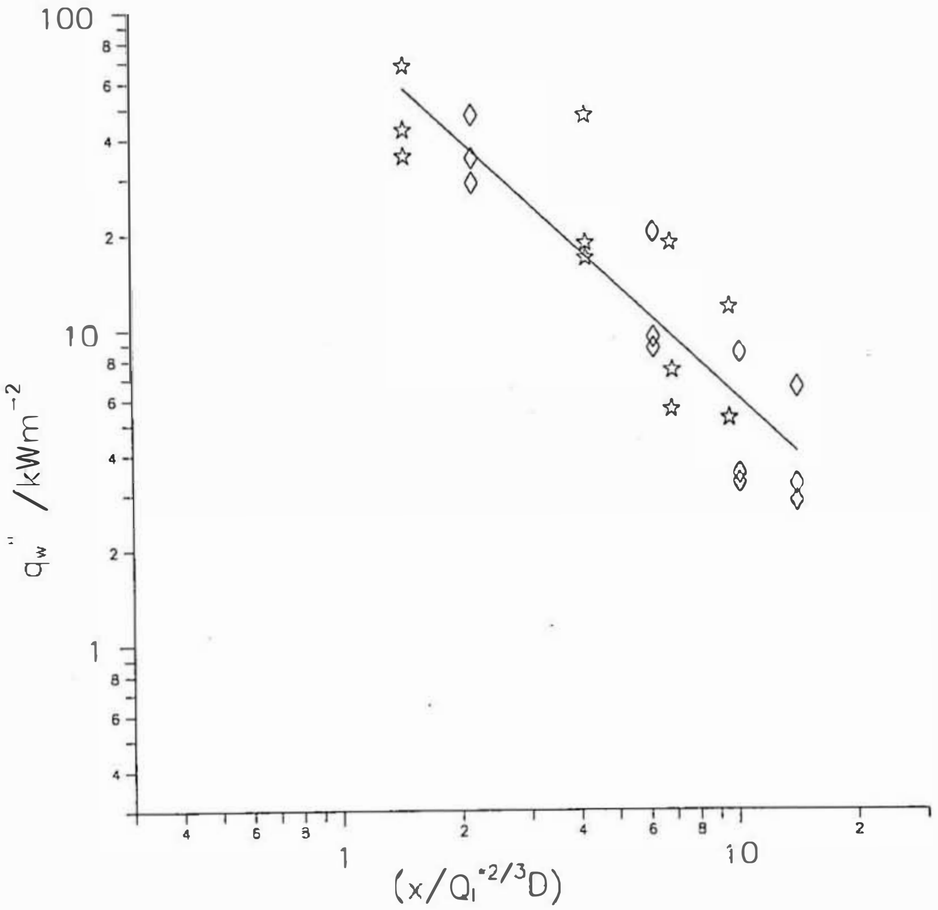

(b) abscissa includes separation term

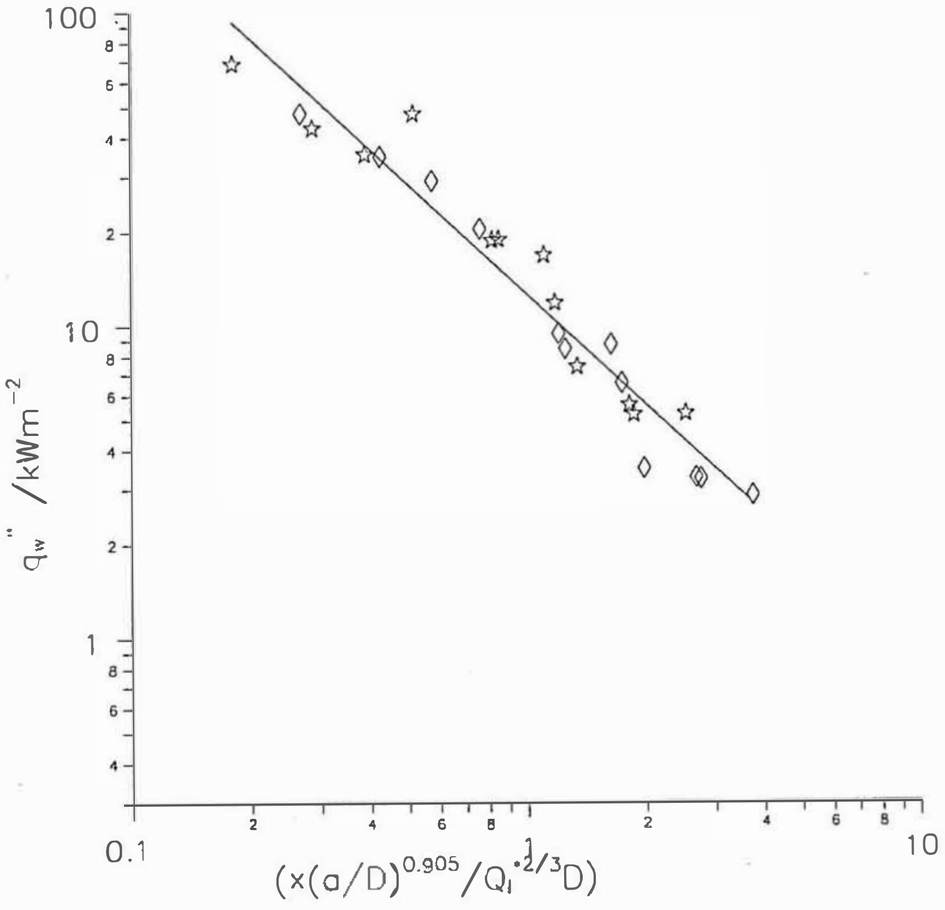

Figure (6.38) Heat flux as a function of $\left(x(a/D)^{n} / \dot{Q}_l^{*2/3} D(y'/D)^{m} \right)$, parallel walls, burner against the instrumented wall, all wall heat fluxes. ☆, 140 mm separation, ○ 100 mm separation, △ 60 mm separation, open symbols, $\dot{Q}_l$ = 11.6 kW/m, closed symbols $\dot{Q}_l$ = 20.9 kW/m

(a) open base

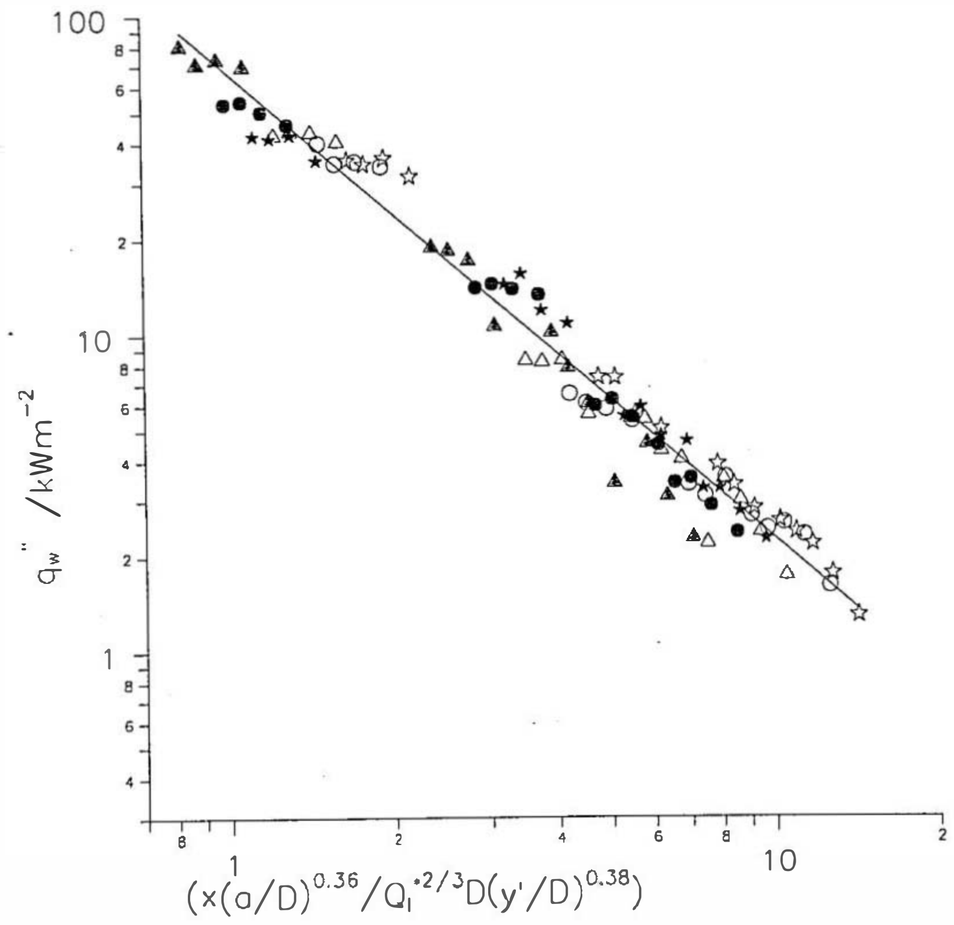

(b) closed base

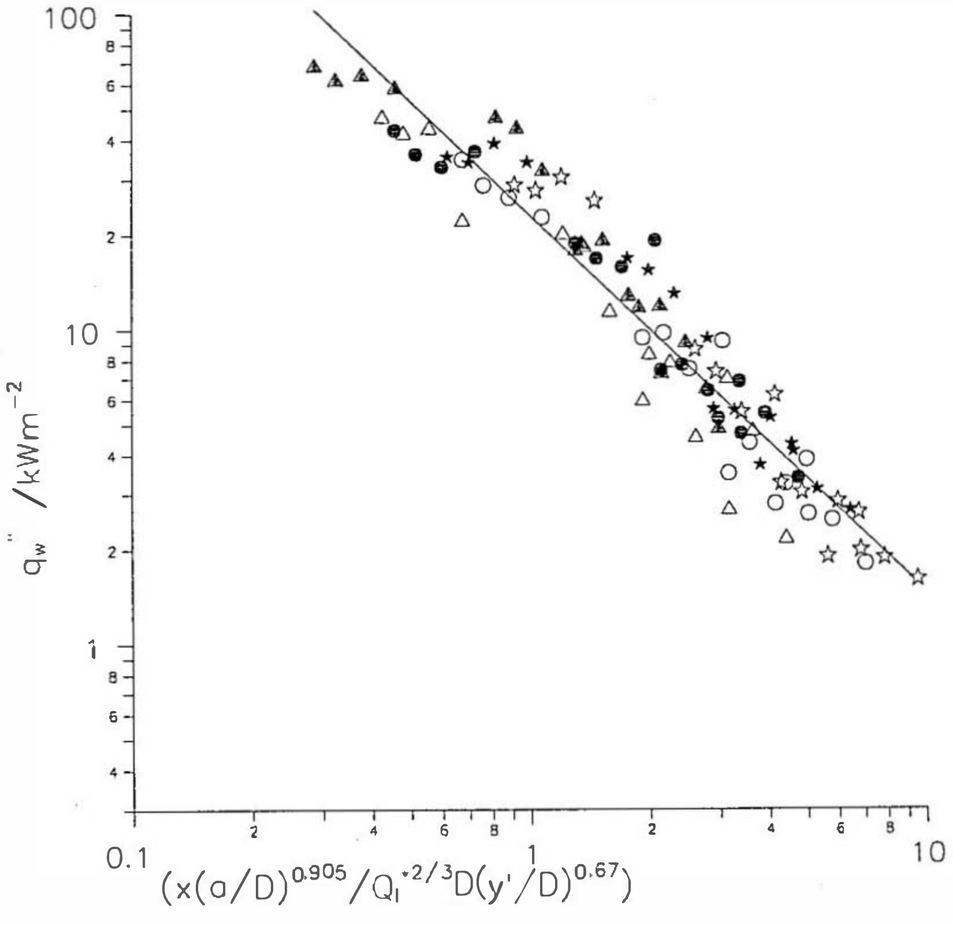

Figure (6.39) Heat flux as a function of $\left(x(a/D)^{n}/\dot{Q}_{l}^{*}D\right)$, parallel walls, burner in the centre of the channel, centreline heat fluxes only. ◊, $\dot{Q}_l = 11.6$ kW/m, ☆, $\dot{Q}_l = 20.9$ kW/m.

(a) open base

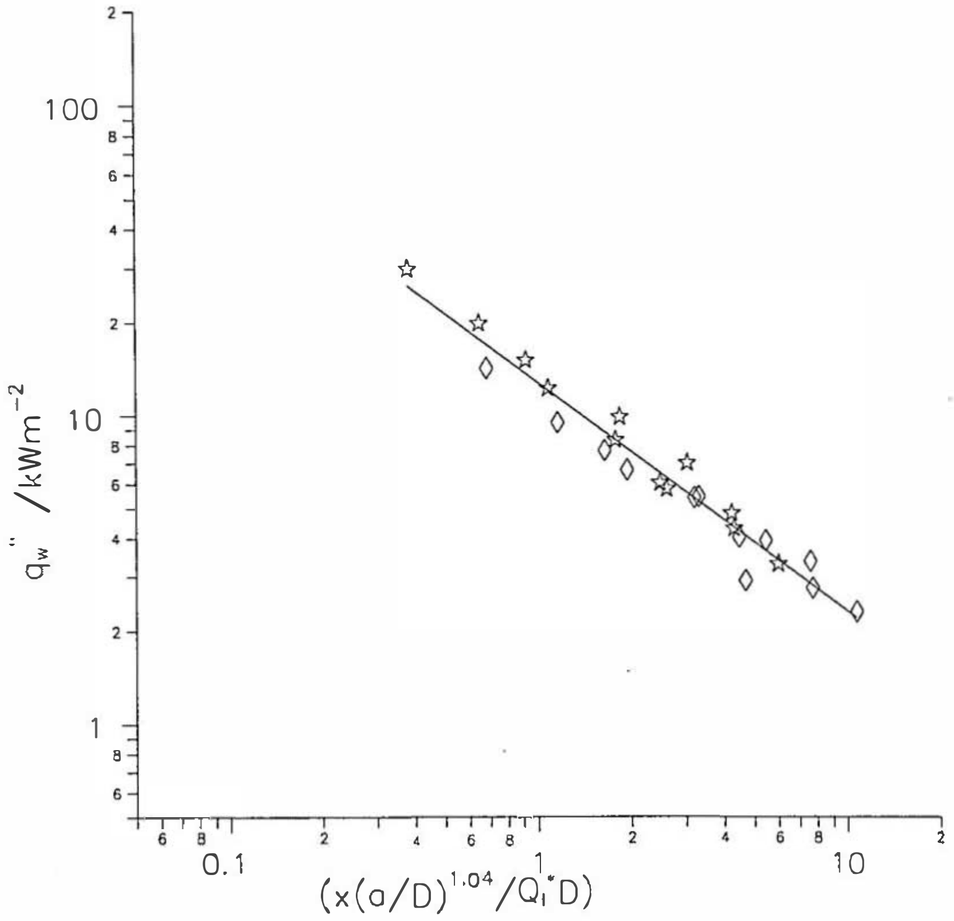

(b) closed base

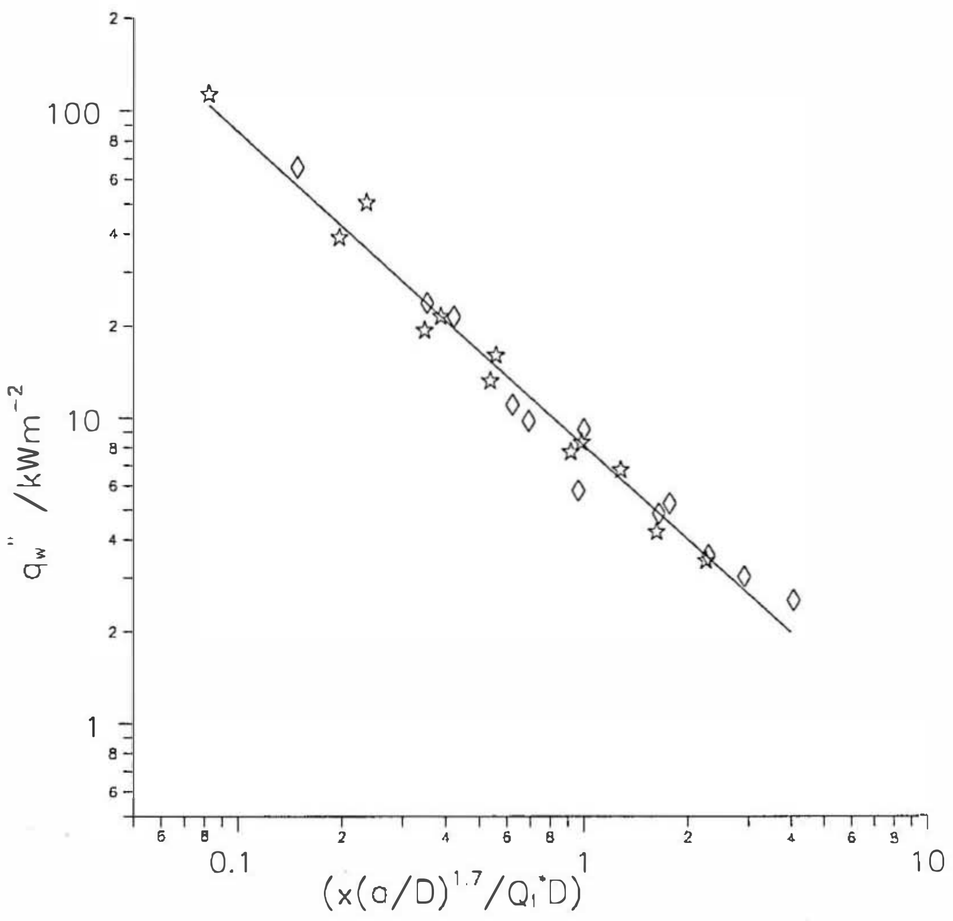

Figure (6.40) Heat flux as a function of $\left(x(a/D)^{n} / \mathrm{Q}_{l}^{*} D(y'/D)^{m} \right)$, parallel walls, burner in the centre of the channel, all wall heat fluxes. ☆, 140 mm separation, ○ 100 mm separation, △ 60 mm separation , open symbols, $\dot{\mathrm{Q}}_{l} = 11.6$ kW/m, closed symbols $\dot{\mathrm{Q}}_{l} = 20.9$ kW/m

(a) open base

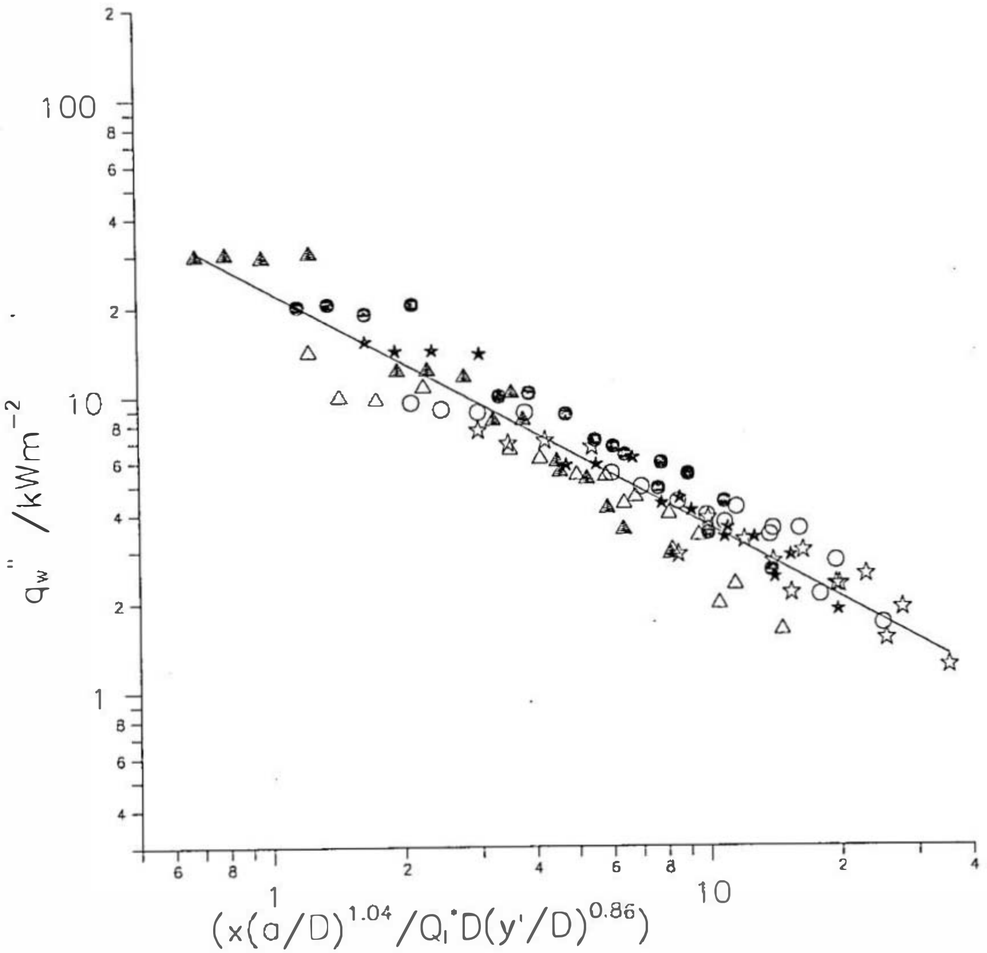

(b) closed base

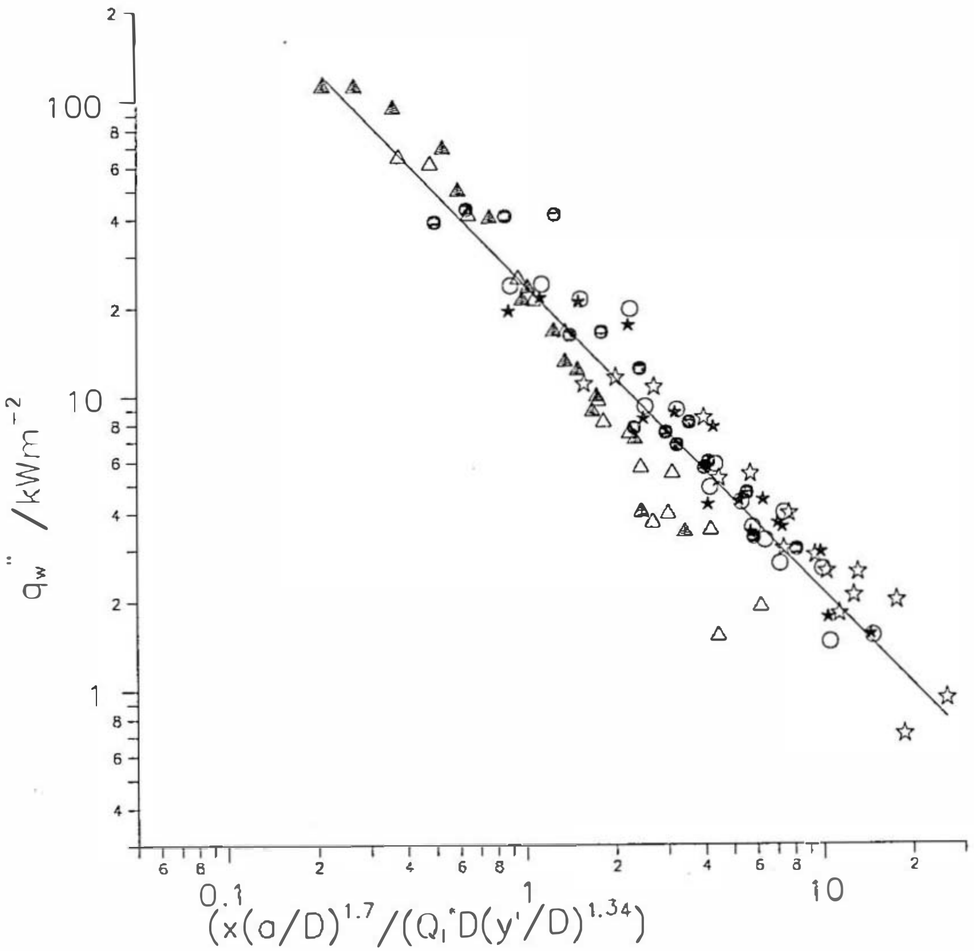

Figures (6.41)-(6.43): Graphs of centreline temperatures as functions of dimensionless height, separation and depth into the channel between the walls. The best fit lines are linear fits and polynomials to a degree of 4.

Figure (6.41) Centreline temperatures in the centre of the channel between the walls.

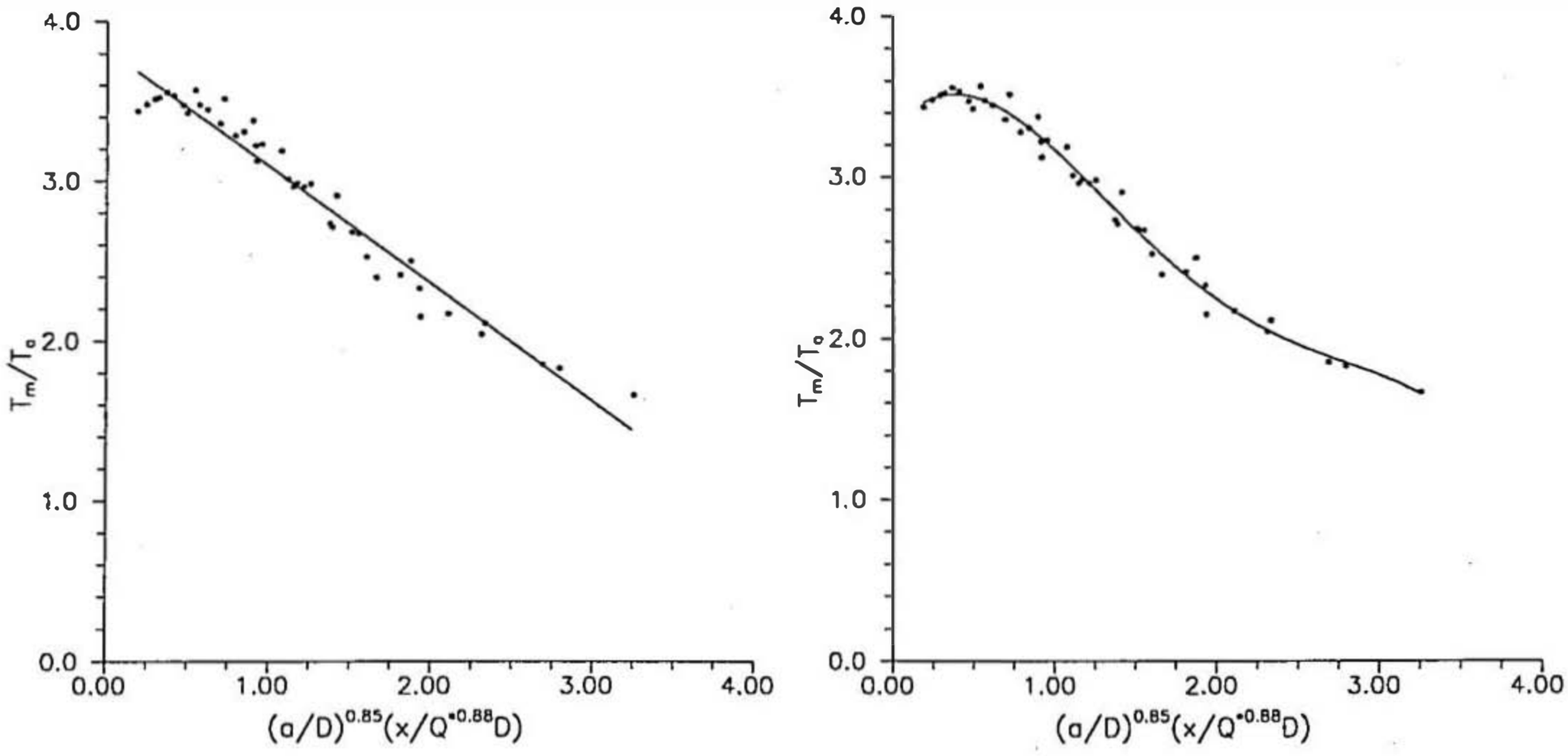

Figure (6.42) Centreline temperatures at different depths into the channel between the walls.

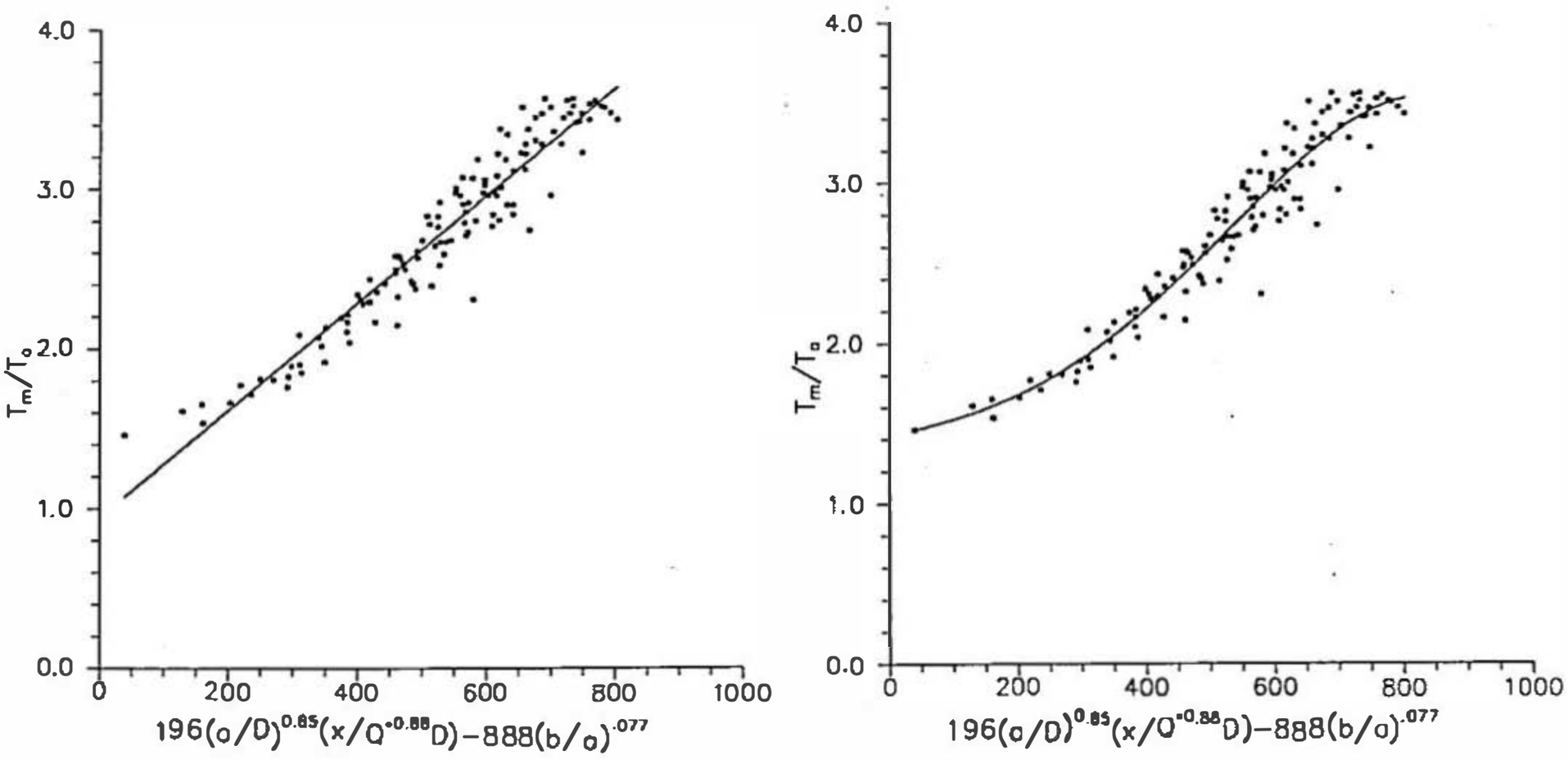

Figure (6.43) Graph of temperature in the channel between two walls as a function of depth into the channel, separation, height, horizontal distance, heat release and burner diameter

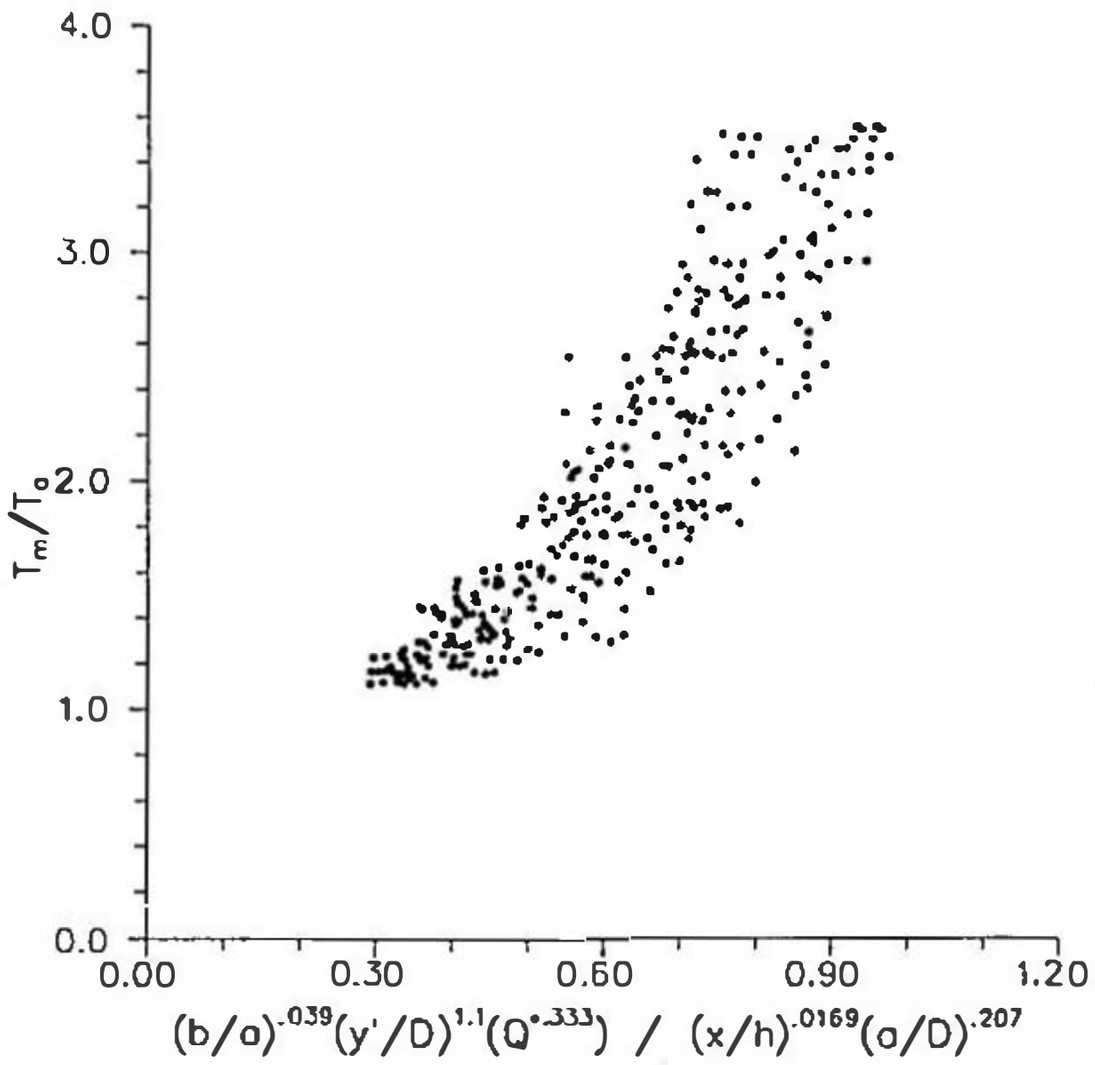

Figure (6.44) Single wall, open base, burner at instrumented wall

(a) correlation for radiative heat flux only

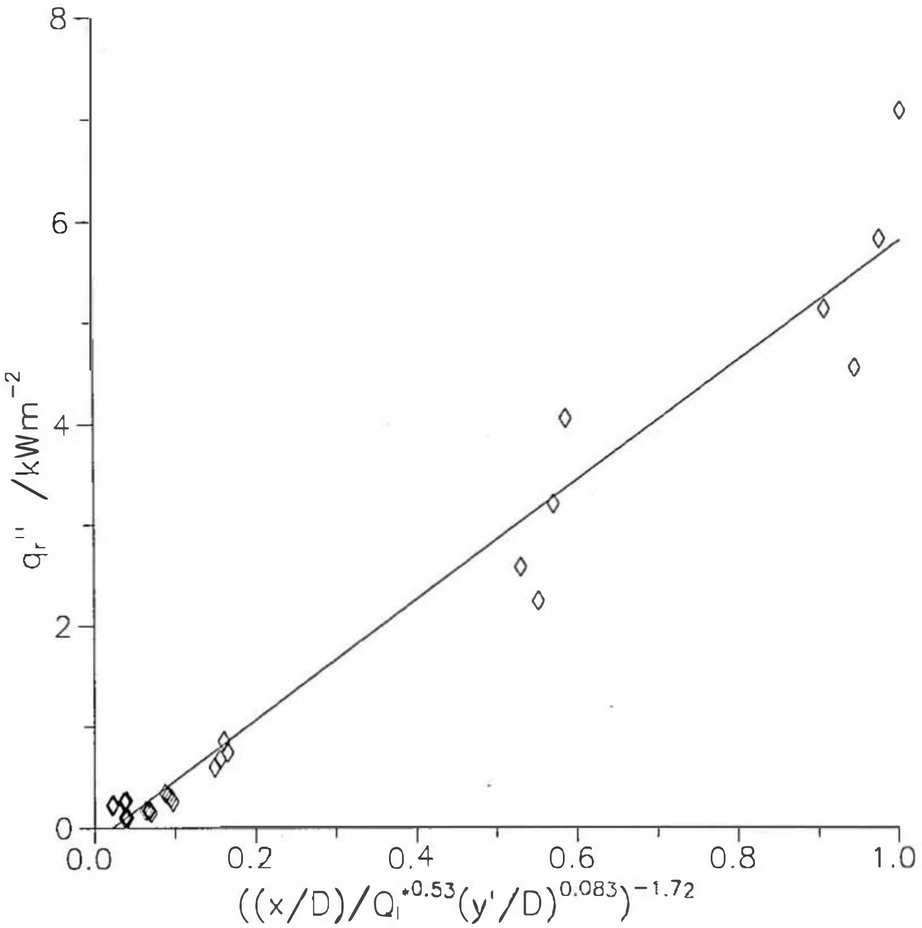

(b) correlation for radiative heat flux with total heat flux

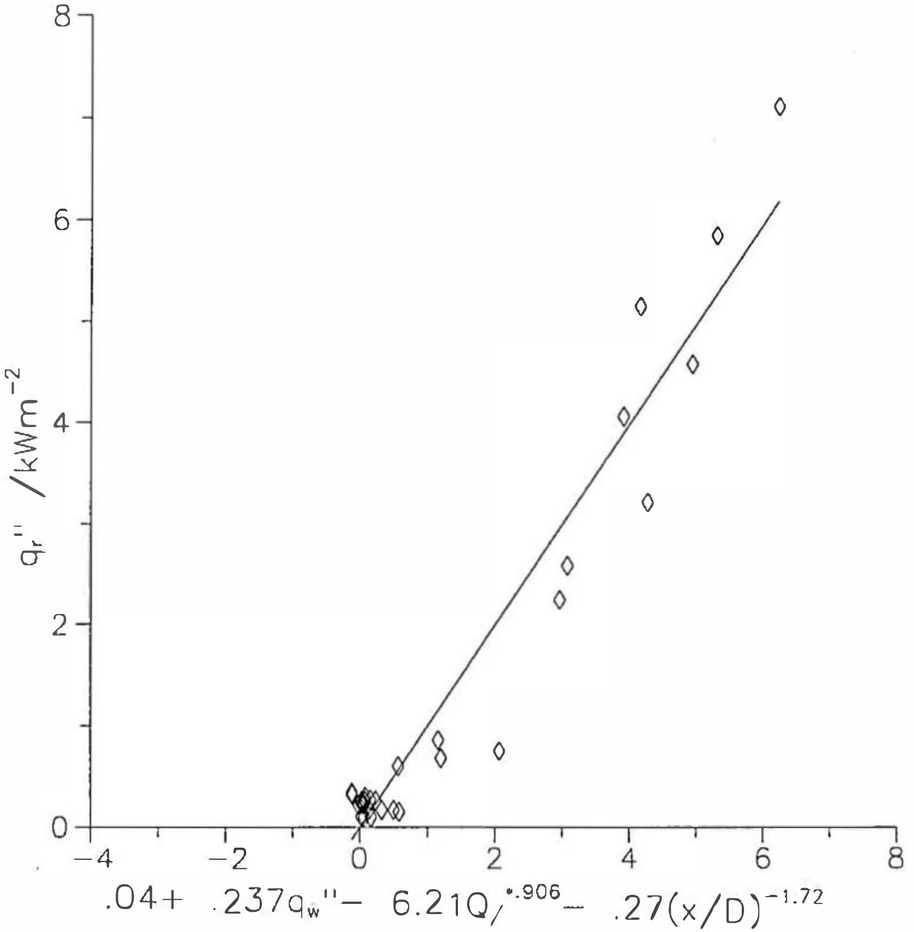

Figure (6.45) Parallel walls, open base, burner against instrumented wall

(a) correlation for radiative heat flux only

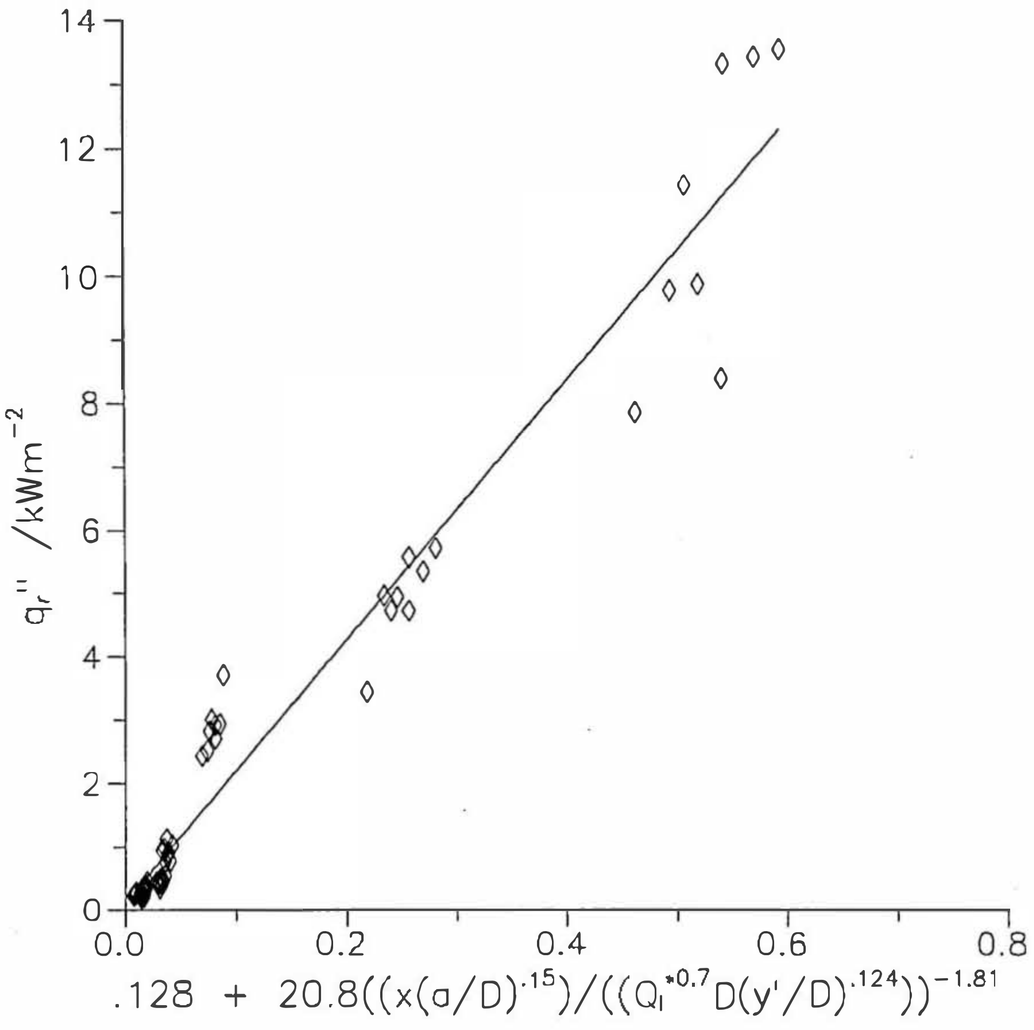

(b) correlation for radiative heat flux with total heat flux

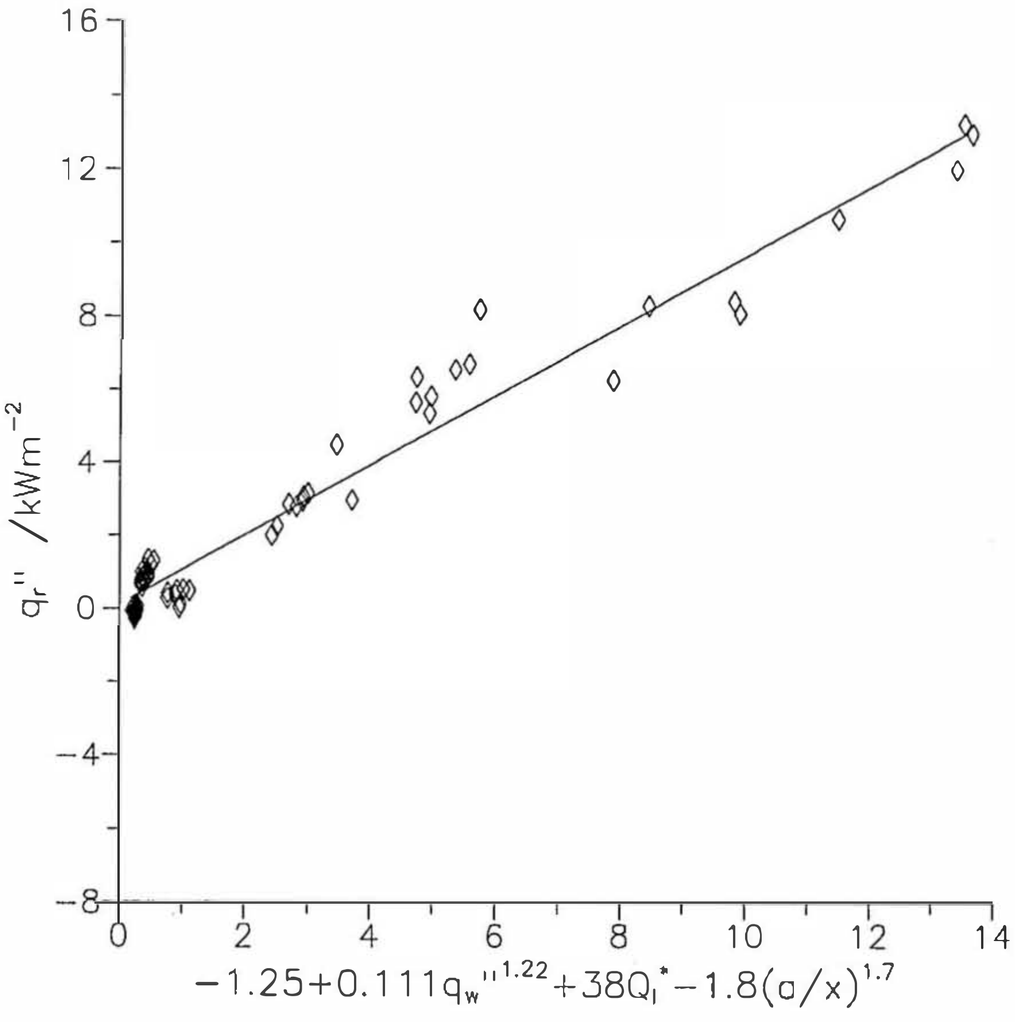

Figure (6.46) Parallel walls, open base, burner in the centre of the channel

(a) correlation for radiative heat flux only

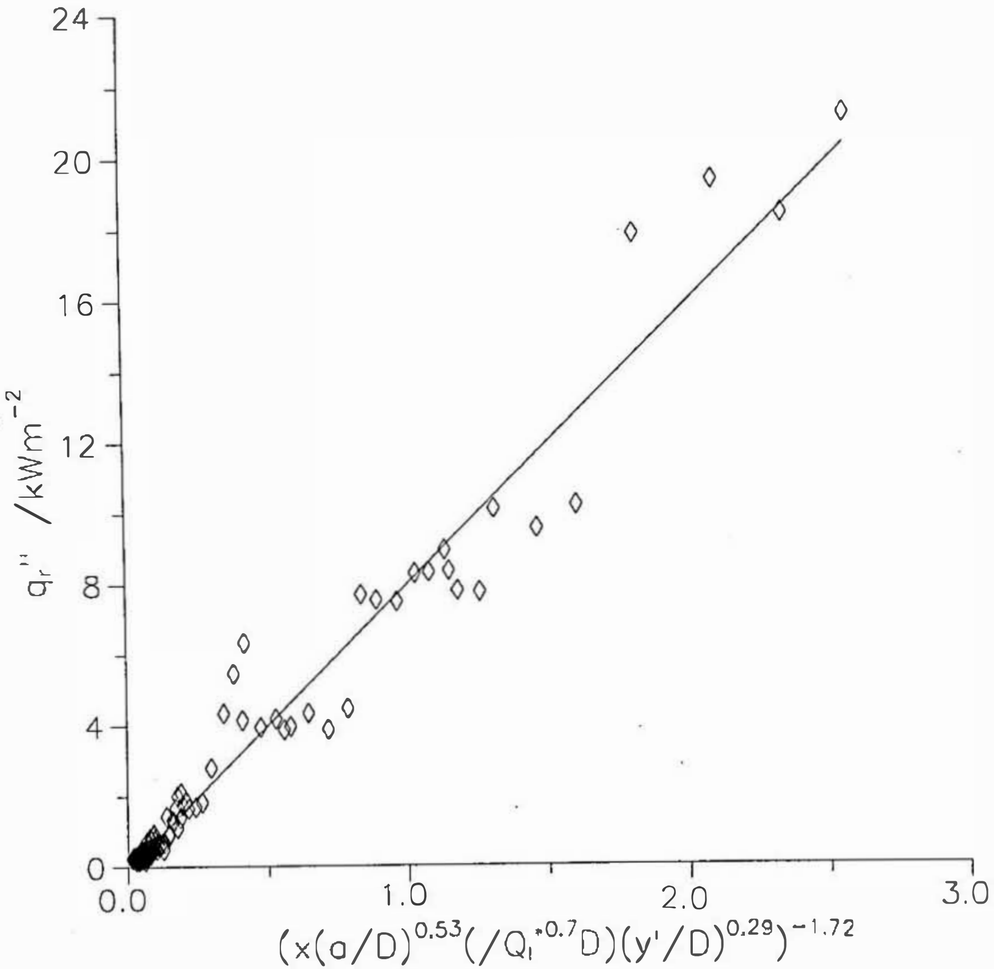

(b) correlation for radiative heat flux with total heat flux

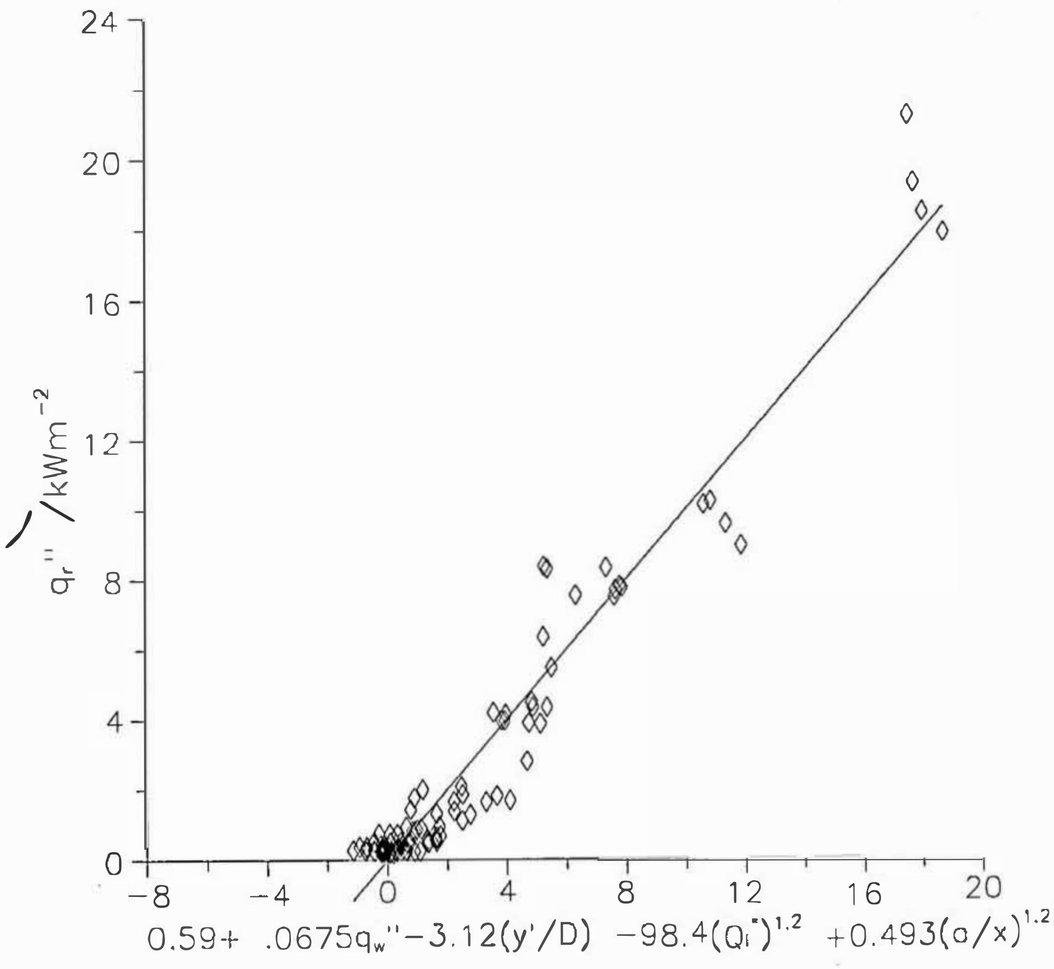

Figure (6.47) Parallel walls, closed base, burner in the centre of the channel

(a) correlation for radiative heat flux only

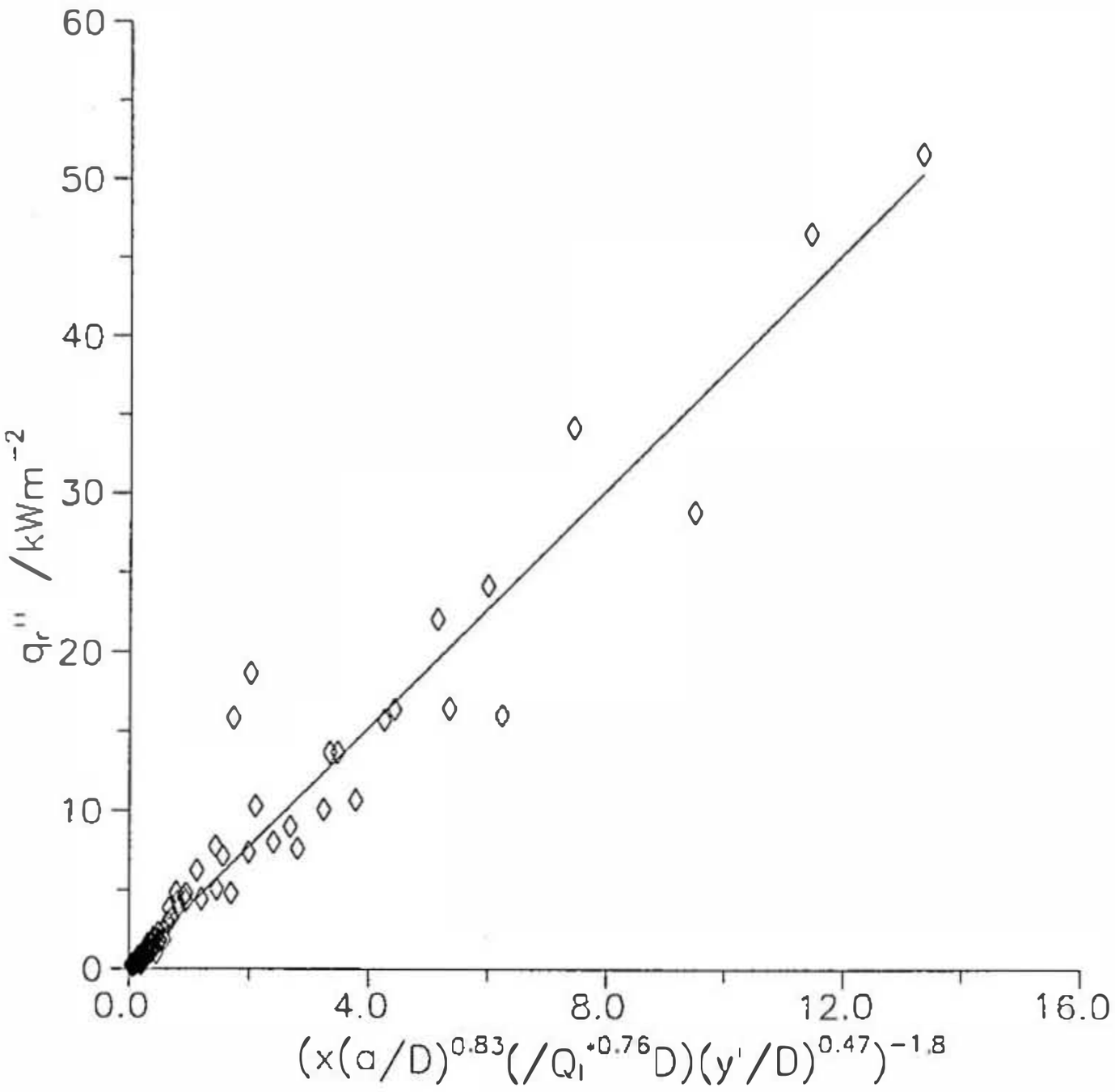

(b) correlation for radiative heat flux with total heat flux

(i) linear correlation

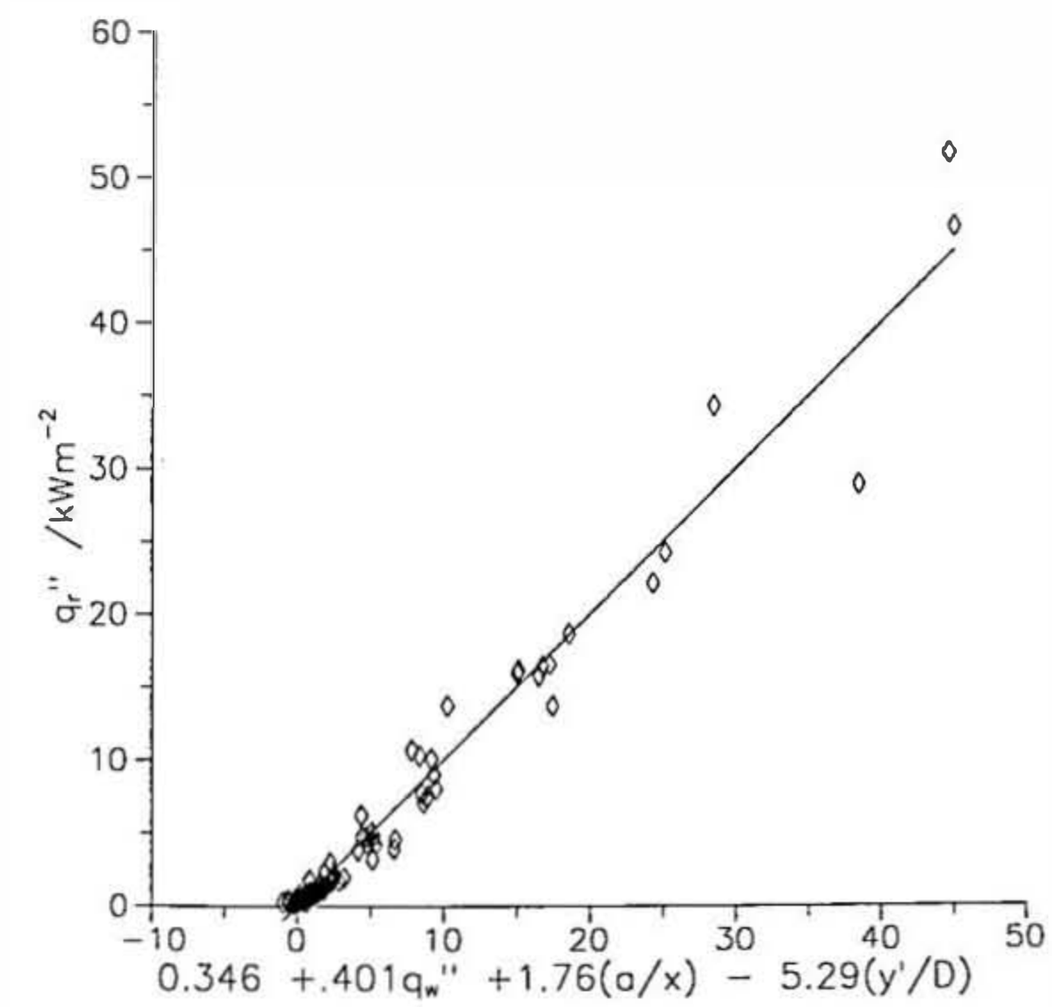

(ii) power terms included

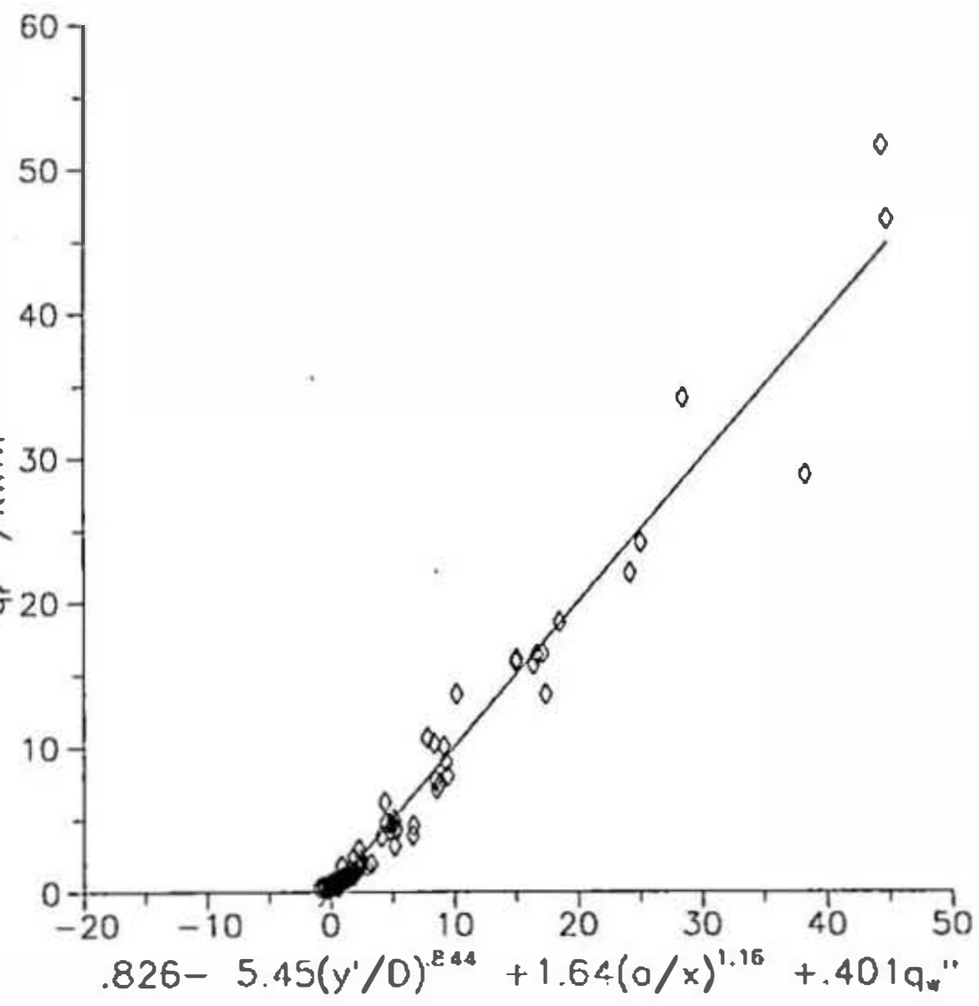

Figure (6.48) Position of the wall in a room

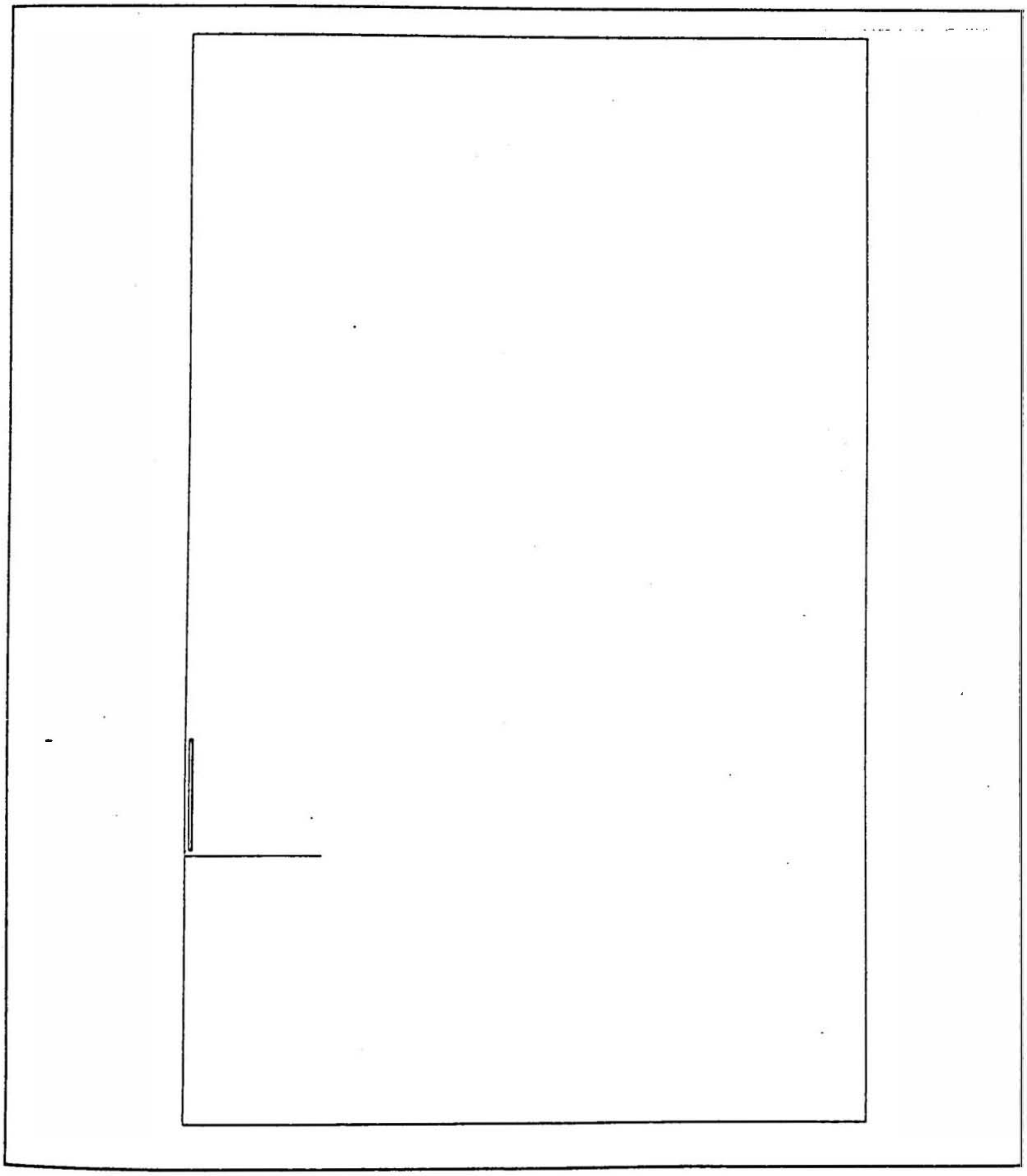

Figure (6.49) The geometry used for the simulation

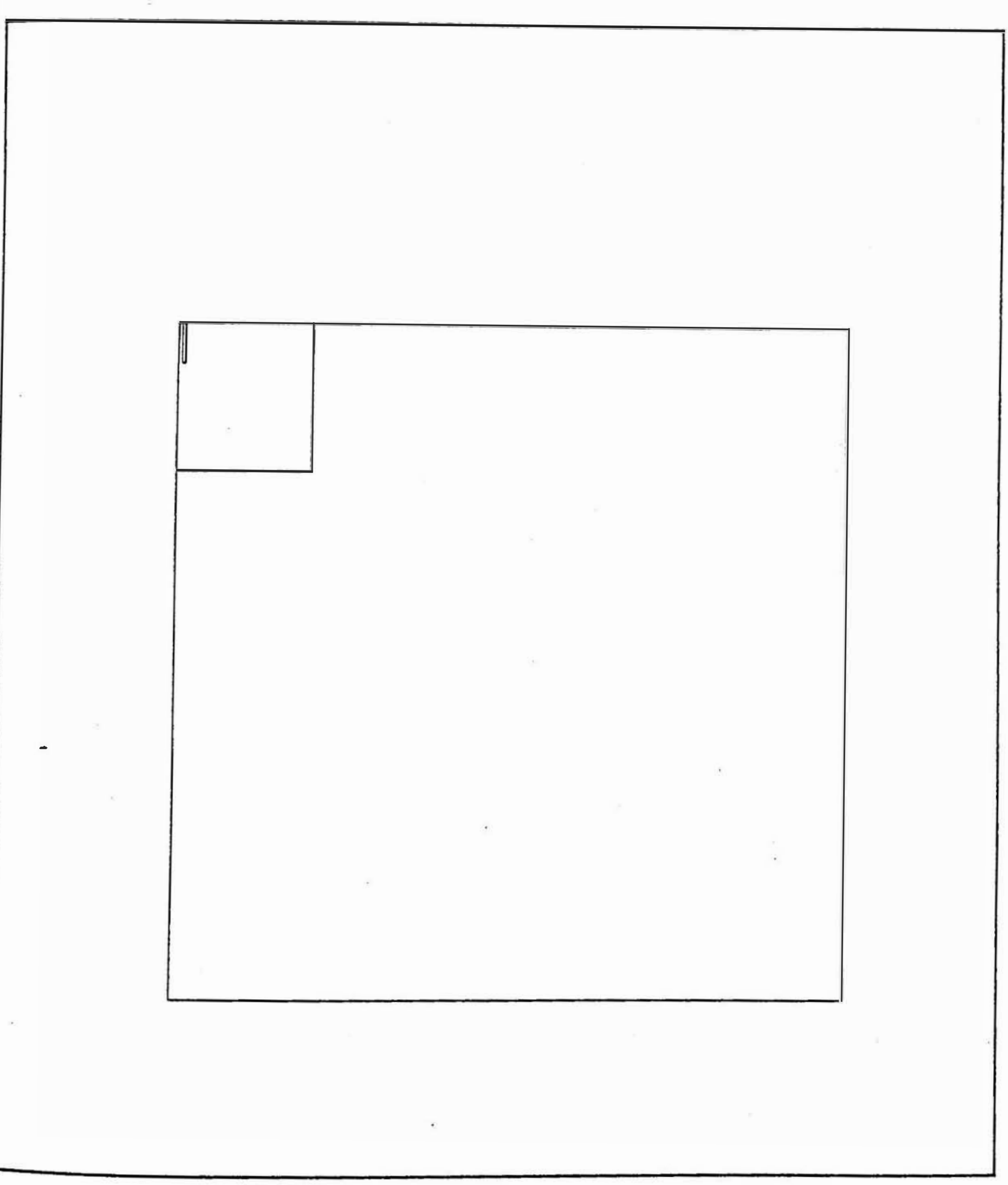

Figure (6.50) Grid at y=0m, looking across at the burner and parallel wall

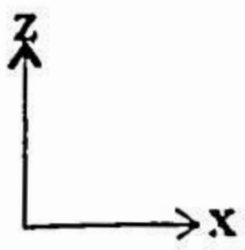

Figure (6.51) Grid (2), looking down onto the wall

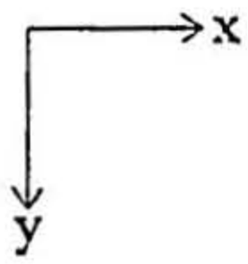

Figure (6.52) Grid (3), grid above burner

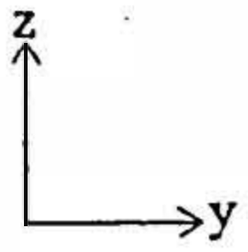

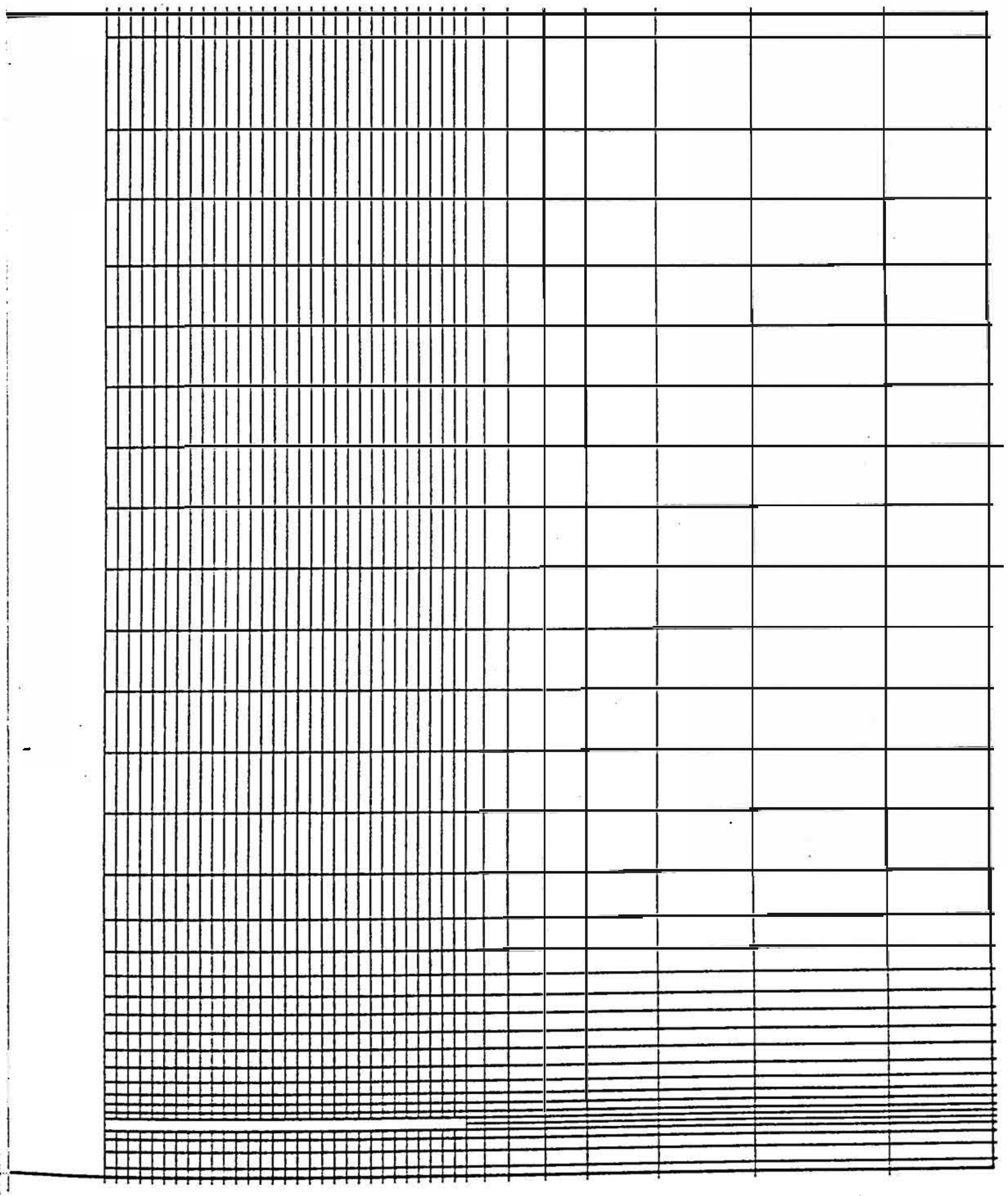

Figure (6.53) Open base

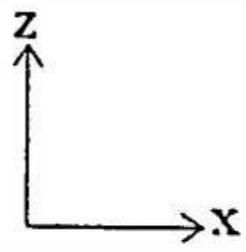

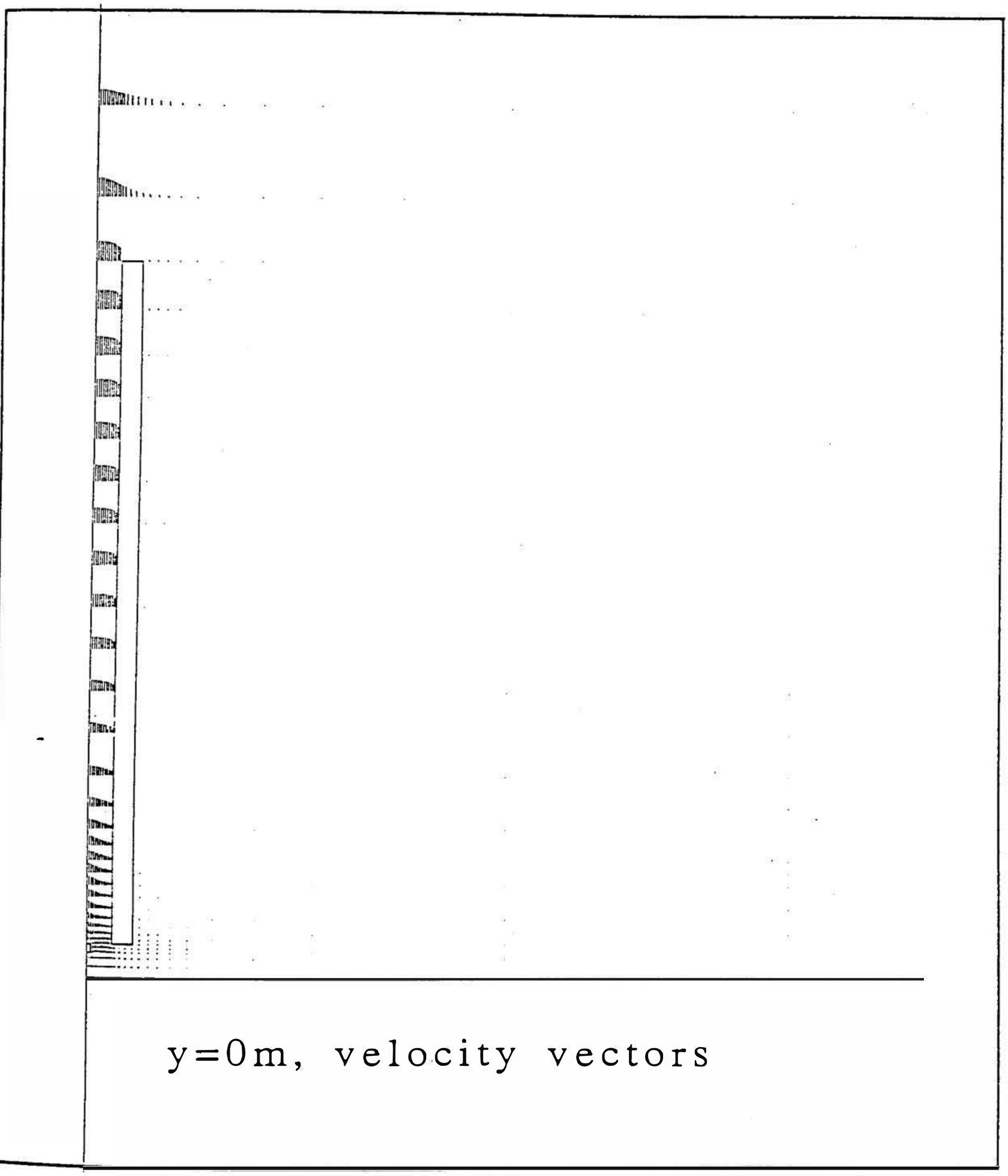

Figure (6.54) Open base

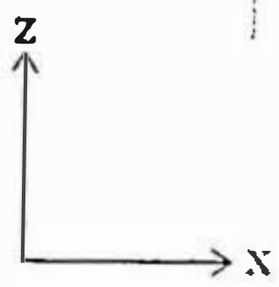

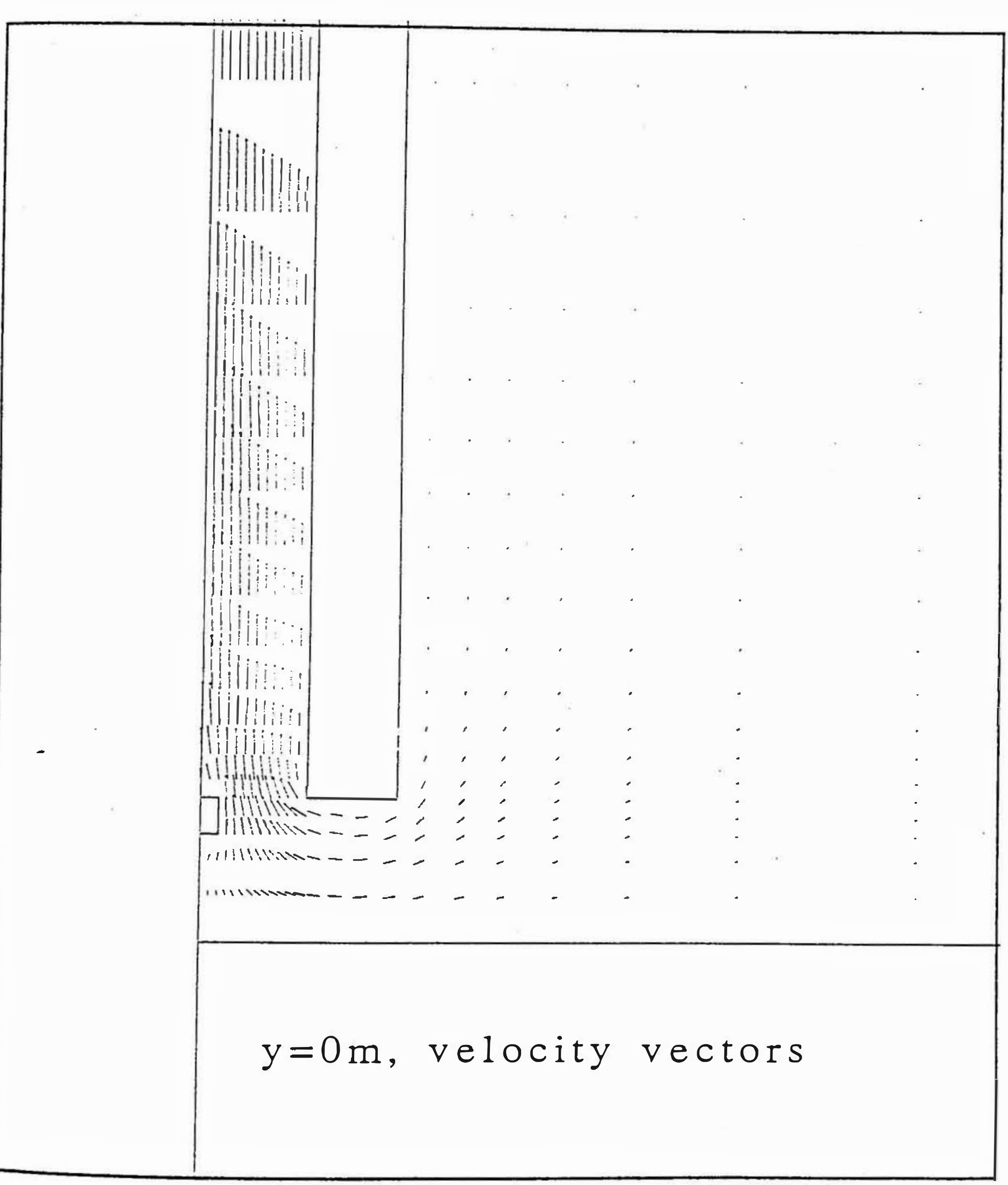

Figure (6.55) Open base

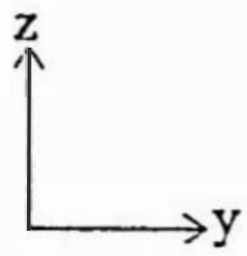

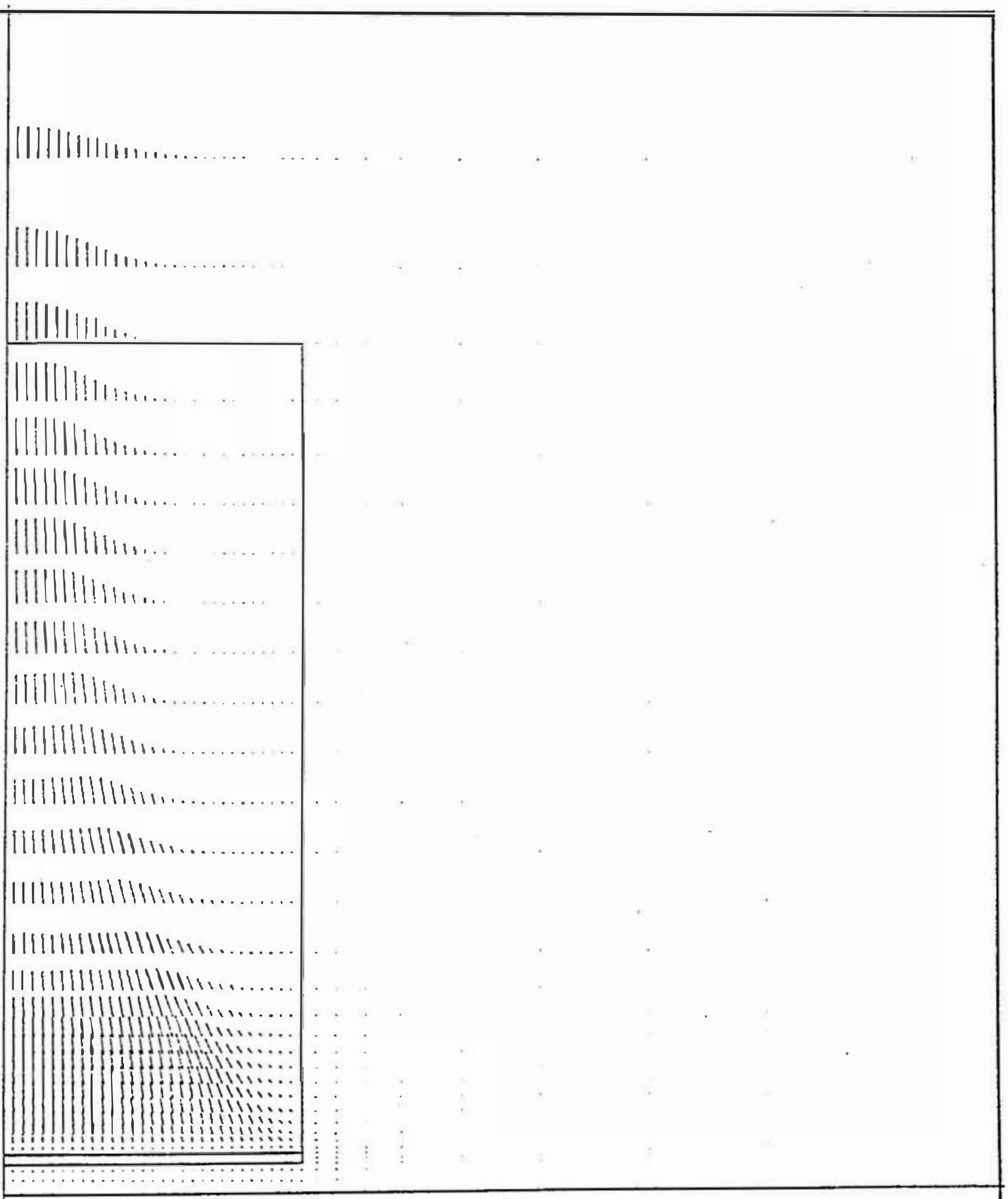

x=0m, velocity vectors

Figure (6.56) Closed base

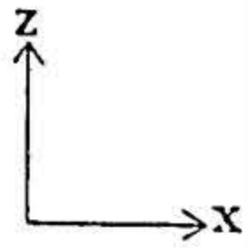

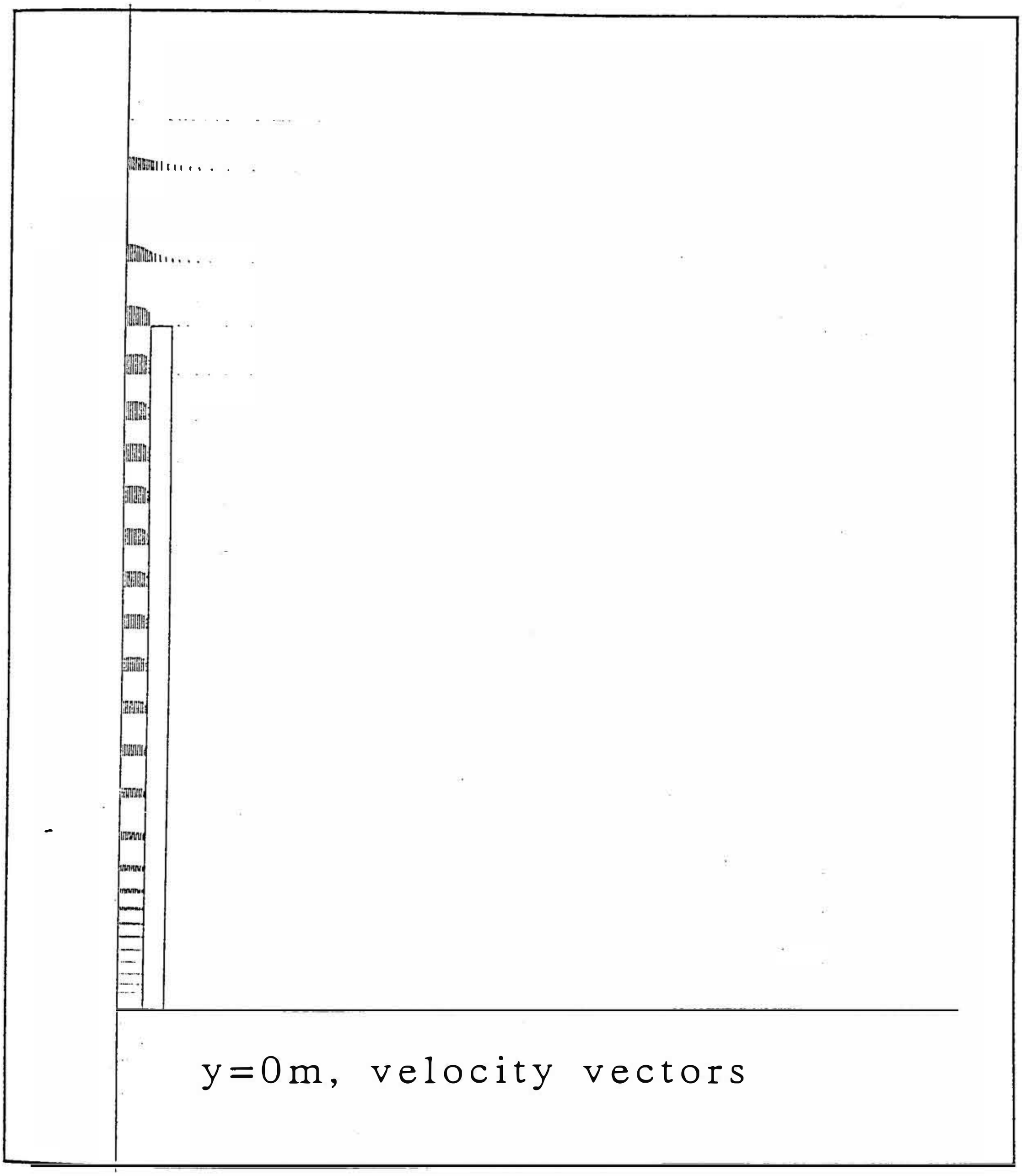

Figure (6.57) Closed base

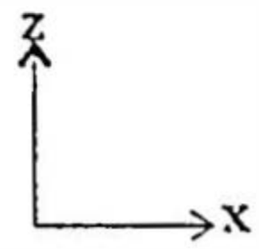

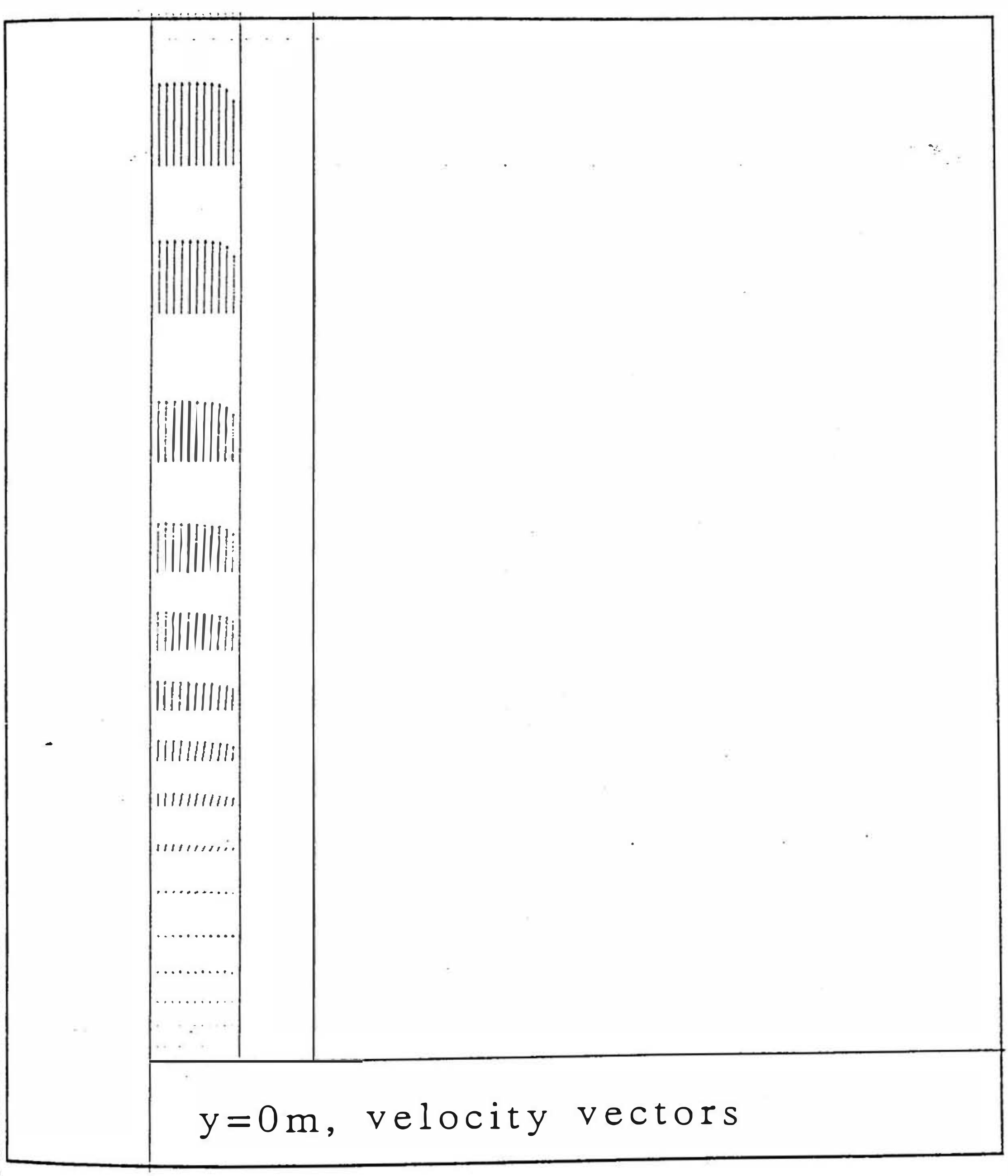

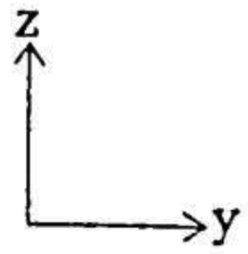

x=0m, velocity vectors

Figure (6.59) Closed base, flow at the top of the wall

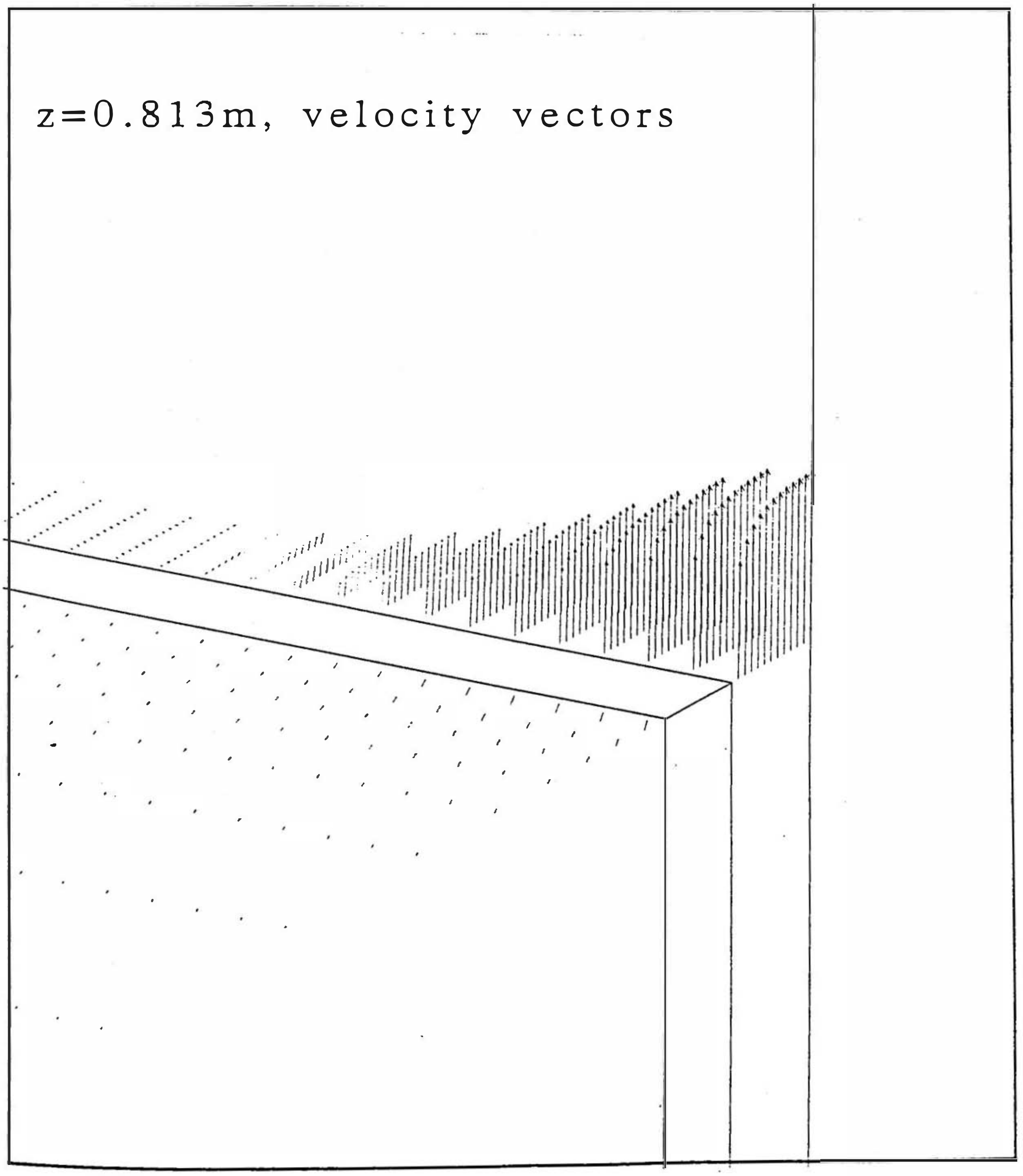

Figure (6.60) Open base, temperature contours,
y=0 m, 300-1600K, 100K contours

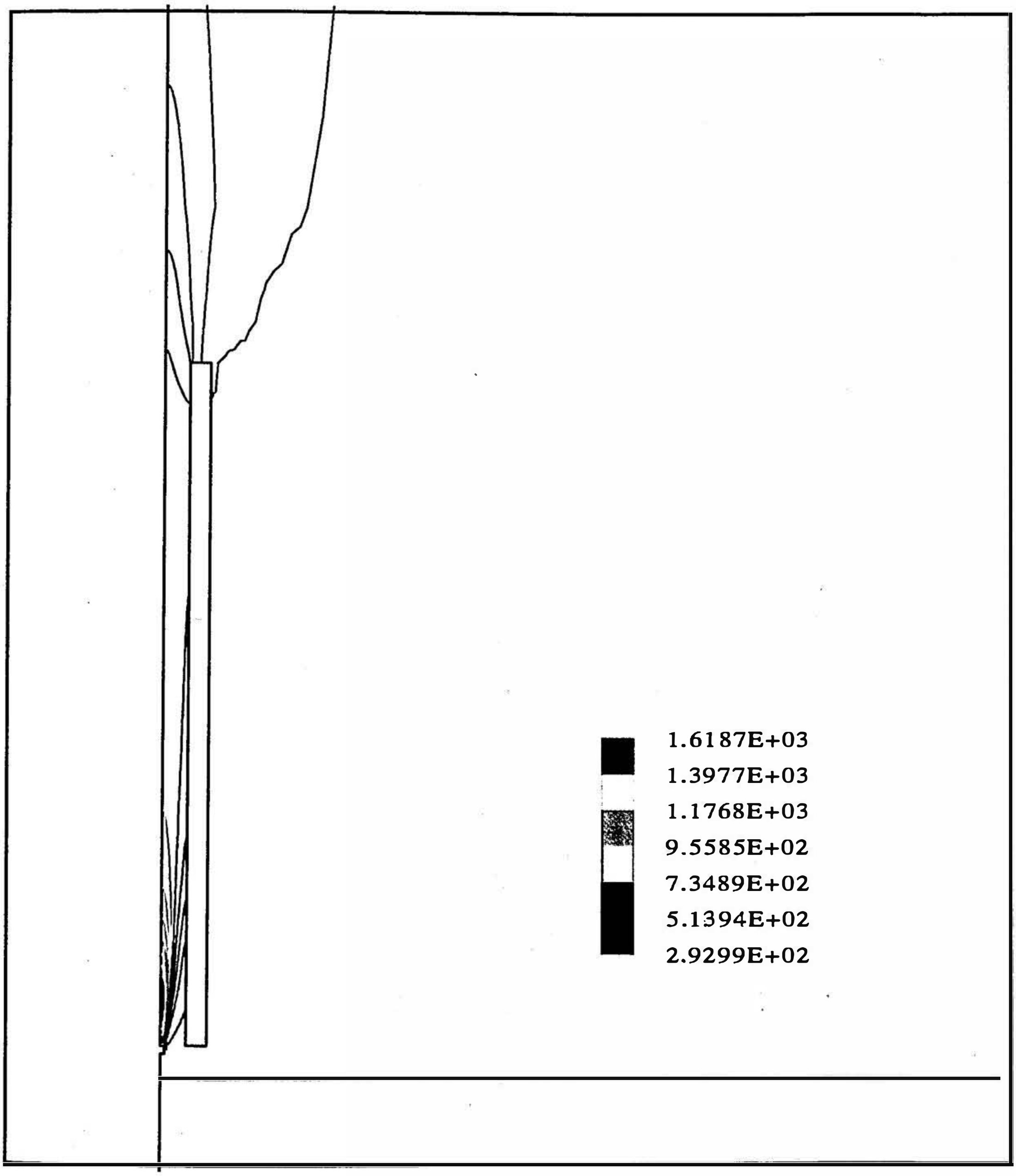

Figure (6.61) Open base, temperature contours,
y=0 m, 300-1600K, 100K contours

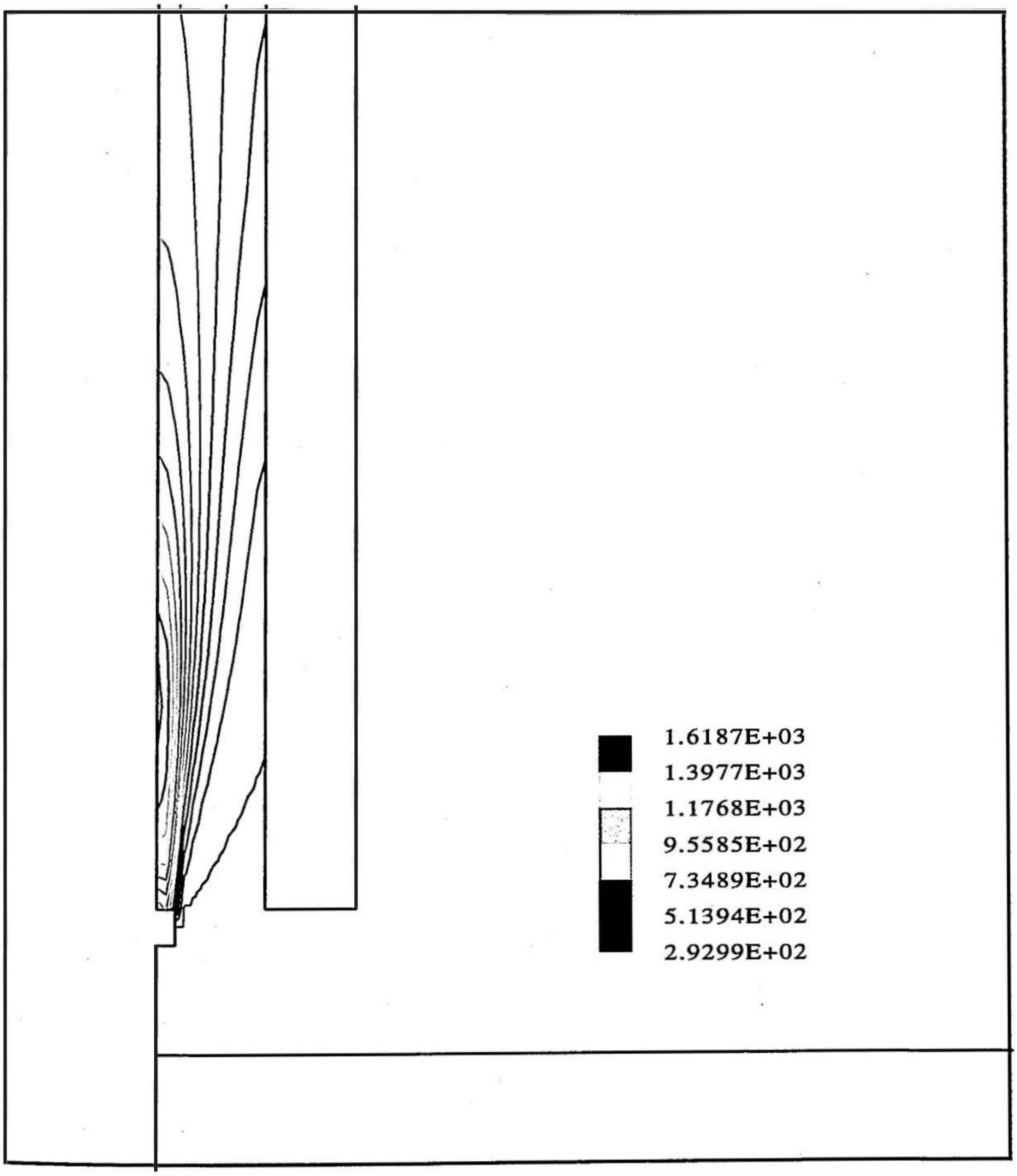

Figure (6.62) Open base, temperature contours,
x=0 m, 300-1600K, 100K contours

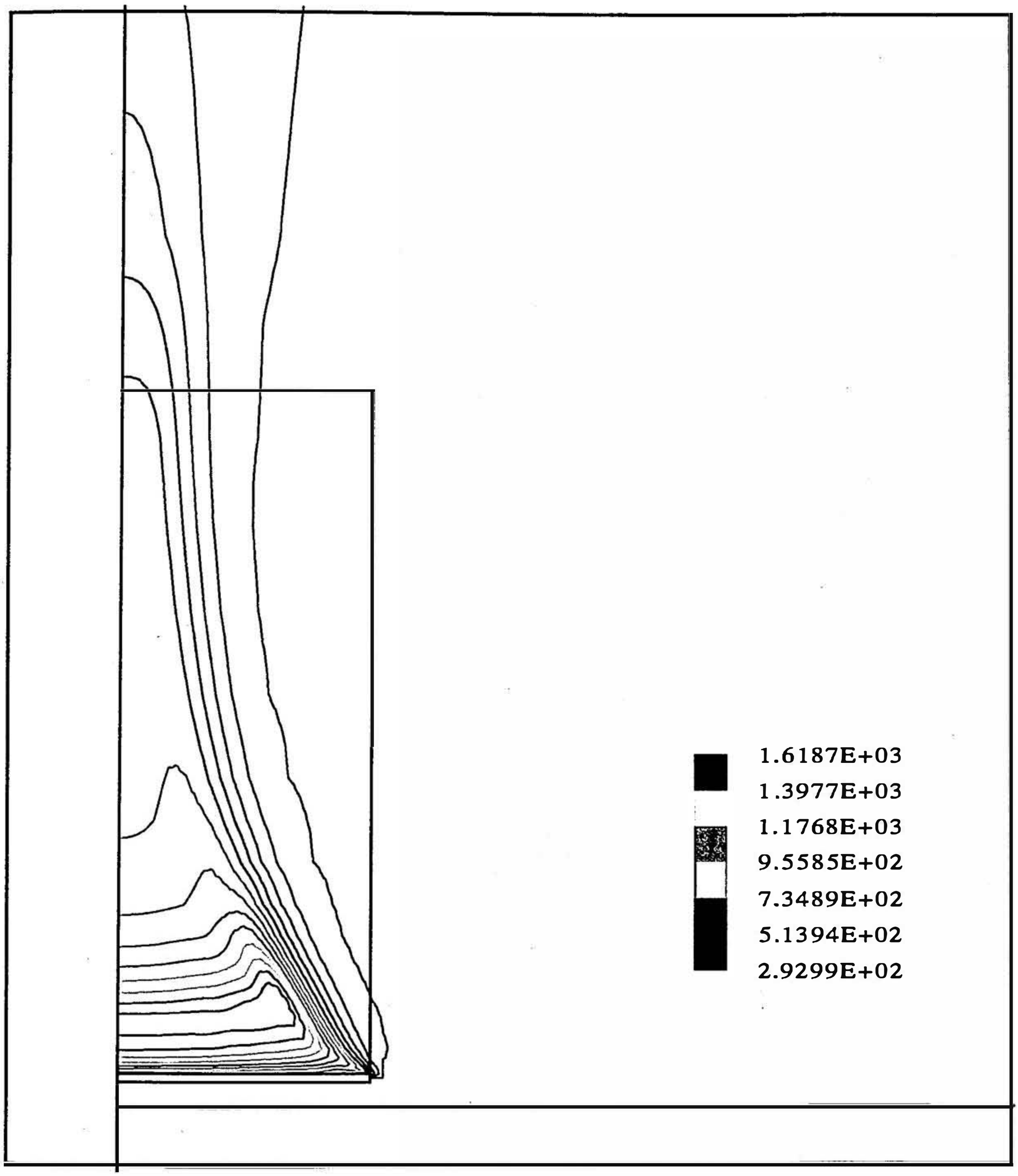

Figure (6.63) Closed base, temperature contours,
y=0 m, 300-1600K, 100K contours

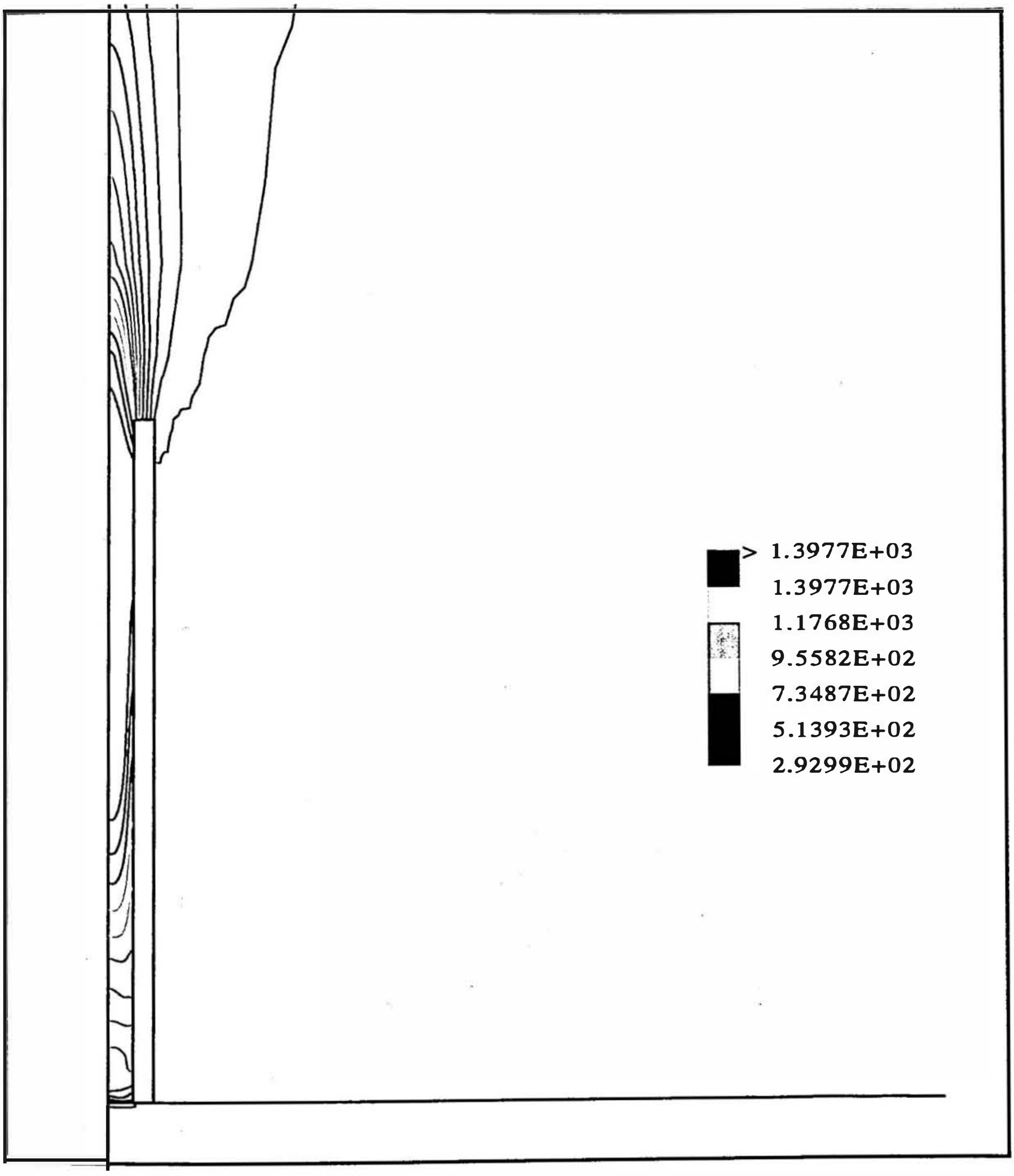

Figure (6.64) Closed base, temperature contours,
y=0 m, 300-1600K, 100K contours

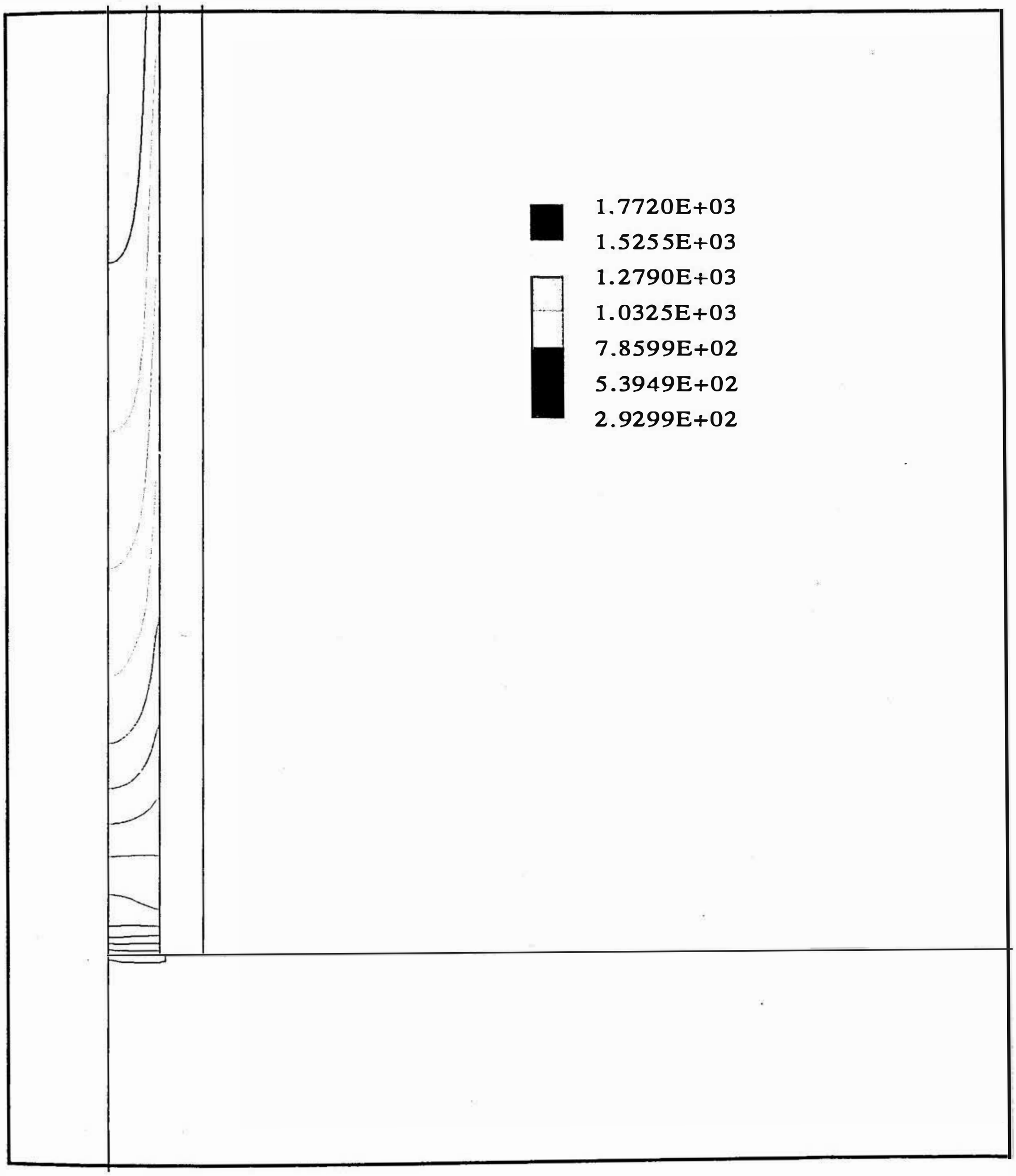

closed

Figure (6.65) Open base, temperature contours,
x=0 m, 300-1600K, 100K contours

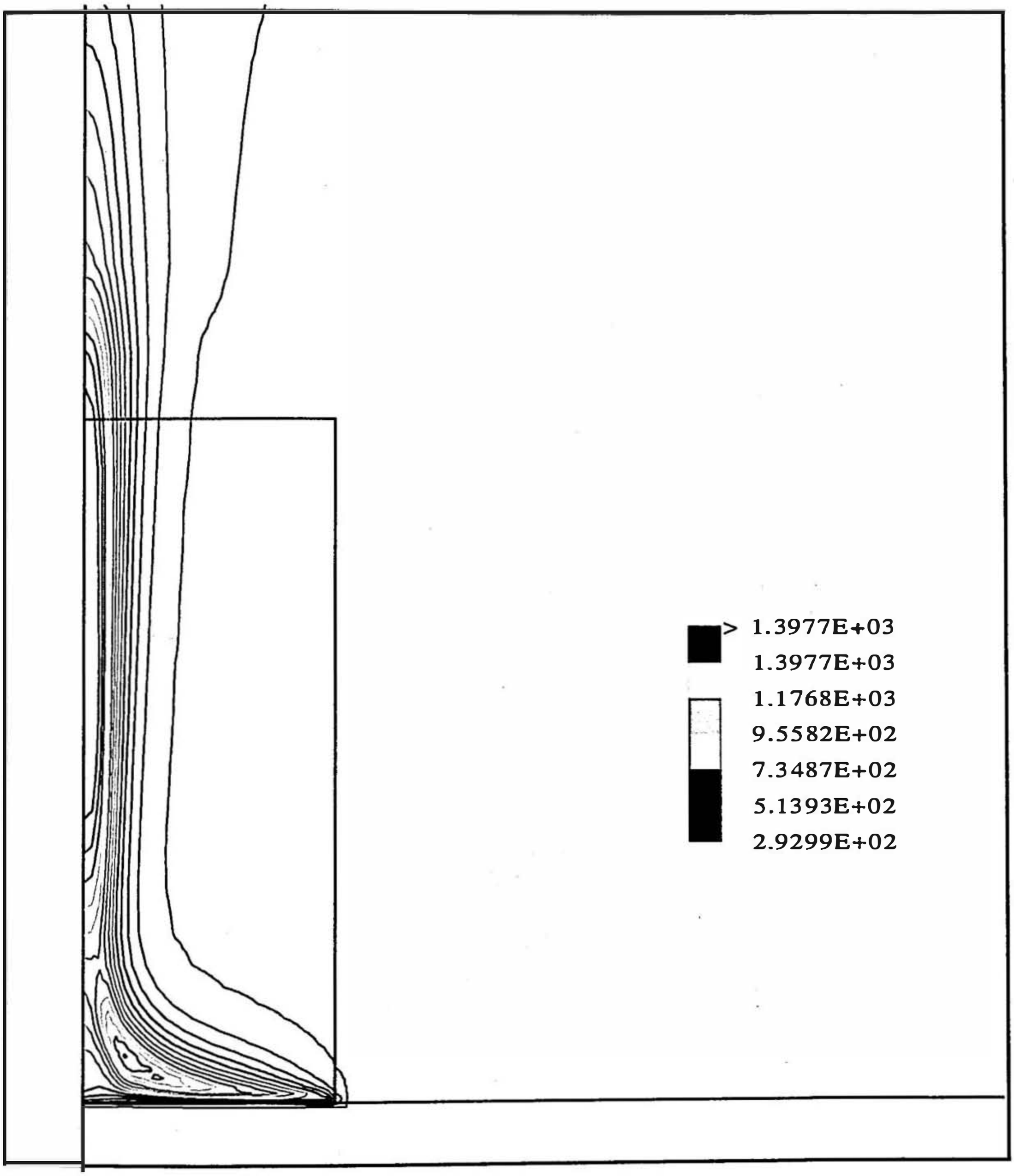

Figure (6.66) Open base, temperature contours,
x=0.03 m, 300-1600K, 100K contours

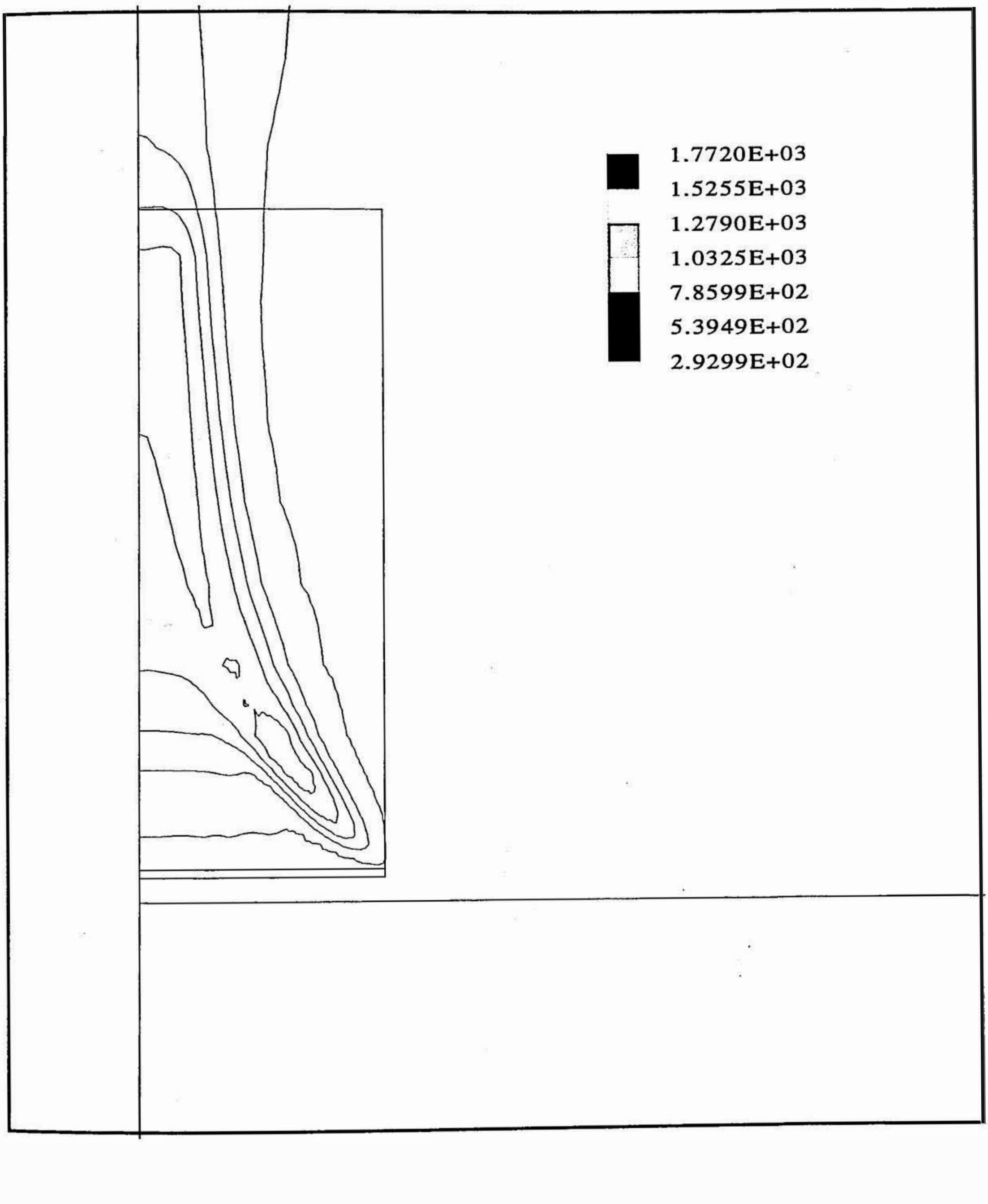

Figure (6.67) Closed base, temperature contours,
x=0.03 m, 300-1600K, 100K contours

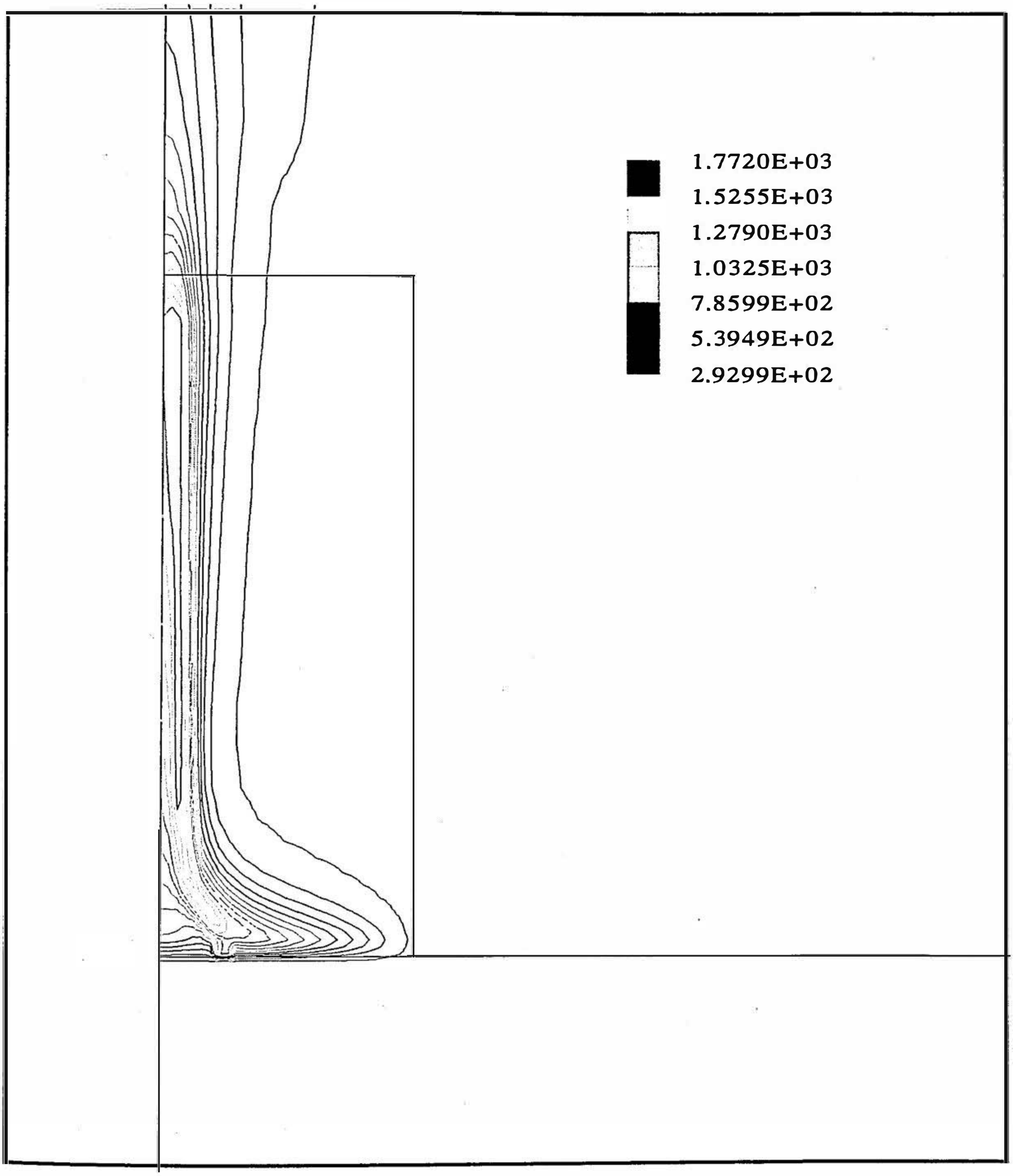

Chapter 7

Conclusions and Recommendations

7.1 Introduction

The objectives of this research were to contribute towards the understanding of fires in warehouses, specifically the sort of configurations which could lead to increased hazards, and to investigate fire testing for materials stored in warehouses. The HSE third scale room/corridor test is currently used to test materials that have been judged to present a possible problem in storage, whilst the Cone Calorimeter is becoming increasingly popular as a fire test. Experiments using these test methods were carried out, along with other tests, and the data examined. Research into flames between vertical parallel walls was carried out to increase understanding of fire spread in the storage configurations found in warehouses and as a first step towards identifying conditions that increase the ease of ignition and rates of fire growth.

7.2 Fire Testing of Flammable Solids

To interpret results from fire tests, both the conditions of test and the behaviour of the material under test need to be understood. Both of these have implications for understanding the behaviour of materials in real fires.

7.2.1 Test Conditions

The test conditions affect both the results and the ranking order or hazard assessment of materials. The ventilation provided in a fire test dramatically affects the results. Smoke production is higher for ventilation controlled burning than fuel controlled combustion. The rate of heat release in the ventilation controlled regime is determined by the amount of air available, whilst in the well ventilated regime it depends on the geometry and the burning characteristics of the fuel. The relative amounts of CO and CO_2 produced are also affected by the test conditions.

These differences mean that there is little logic in trying to compare results from tests under ventilation controlled conditions with results from those performed under well-ventilated burning. Many of the factors measured in the Cone Calorimeter tests did not compare well with results from the HSE third scale room/corridor test for this reason. However, analysis of the data from the early fire growth period in the third scale test, before the compartment began to have an effect, correlated well with the data from tests in the Cone Calorimeter under low irradiance levels. The factors included in these correlations were the rate of increase in heat release rate, the fire growth coefficient, and the rate of increase in smoke production rate. The rate of increase of heat release rate in the third scale tests up to the peak or the onset of ventilation control, where the compartment is having an effect but the fuel is still burning with sufficient oxygen, compared well with rate of increase of heat release data from the Cone Calorimeter at an irradiance of 30 kWm^{-2}. The rate of increase in smoke production rate could be treated in the same way; data up to the peak or ventilation controlled burning in the third scale room correlated well with Cone smoke data from ignition to peak under an irradiance of 40 kWm^{-2}.

Apart from the problem of comparing smoke produced under ventilation and fuel controlled burning, smoke data appears to be test dependent, from the smoke box and Cone Calorimeter experiments, and therefore not particularly useful for hazard assessment. It is, however, desirable to test materials for smoke production, as this is one of the principal hazards of a fire. Rather than simply using one of the current National or 'reaction-to-fire' tests, it is preferable to select a test based on the conditions that may be found in a fire involving the particular material or product, and the period of the fire of interest.

Both the ignition and heat source are important in determining early fire behaviour. The position of a flame was shown to be important in the parallel wall tests; this was also demonstrated in the third scale room tests with rigid polyurethane foam. Also in the third scale tests, the burner heat output was seen to be of greater influence for ignition of the foams than the duration of the flame.

Materials tested in the Cone Calorimeter changed ranking order when the irradiance level was altered. Again, it appears unsatisfactory to simply test and rank materials under a certain heat flux, rather it needs to be done with some knowledge of the stage of the fire of interest. For example is it required to know how easily a material

may be ignited with a small ignition source or is a high rate of heat release in a developing fire of more significance for the hazard assessment in a particular case? The rate of increase of rate of heat release is a potentially useful factor for fire growth that is not currently used. It may be possible to use this to identify materials with high flame spread rates or those that lead to flashover in compartment tests. Models for flame spread or flashover should take into account the real heat fluxes expected. The influence of the continuously changing heat flux levels in a compartment fire also needs to be considered for successful modelling.

Sample position and geometry have an influence over fire test results. Small scale tests do not always reveal material behaviour, whilst the thickness of a test specimen affects the heat losses. The sample orientation also plays a significant part in the heat transfer and therefore the flame spread. Models for flame spread generally use data from horizontal tests in predictions of upward vertical flame spread. Because of the difference in heat transfer, data from vertical tests should be used. A sample under a radiant heat flux of, e.g., 25 kWm^{-2} in the horizontal orientation may behave differently than a vertical sample, for example in rate of surface temperature rise and time to ignition. The results from a vertical sample tested under nominally the same heat flux arising from a flame against the sample will be different from either of the above. The latter case is the real situation of interest for upward flame spread. This forms part of ongoing work at Edinburgh University. The sample position is also important in other ways, for example, parallel specimens give rise to cross-radiation.

7.2.2 Material Behaviour

Fire test results are affected by the behaviour of a material under test, specifically, unusual behaviour which may be suppressed in order to maintain the test standard. Suppression of behaviour will decrease understanding of potential hazards or benefits. Materials which regress from a heat source reduce the chance of ignition, but preventing this behaviour could give very different fire behaviour, as in the example cited earlier (section 6.2.1.5.1) for vacuum packed thermally bonded wadding. Therefore, it is necessary for full hazard assessment to understand how any such material behaviour actually affects the fire hazard of a sample.

Melting is very important in hazard assessment. It has the potential to remove material from the area of a fire, thereby reducing the amount of material for

combustion. Alternatively melting may give a pool fire of large surface area which increases the material burning rate and the heat fluxes to nearby items. It is desirable therefore to know whether or not a material melts, and preferably also the viscosity of the melt and the amount of melt produced under different exposure levels. Most tests do not give information on whether a material exhibits melting or not, for example the Cone Calorimeter in the horizontal orientation. It is advisable instead to test for this behaviour separately, for example using a medium scale test in which the material is in a vertical orientation. Further testing of these materials may require a specially designed test, but the information would be valuable. Other unusual behaviour, such as swelling or spalling, should also be tested for. To aid in ranking or hazard assessment of materials, testing on a medium scale in the vertical orientation seems a better initial procedure than simply using one of the current standard tests.

7.2.3 Summary

Data from fire tests, even the new 'reaction-to-fire' generation, is test dependent. Although designed scientifically, and giving the useful heat release data, the Cone Calorimeter is itself not sufficient for a total hazard assessment. Furthermore, it seems unlikely that good correlations of data can be obtained from many different fire tests as the properties measured are not intrinsic and conditions vary widely between tests. It is preferable to concentrate on the 'real' fire conditions of interest in a certain situation, and test under representative heat fluxes, ventilation conditions etc.

The HSE third scale room/corridor test can provide some useful information on ventilation controlled fires, although a wider range of materials should be tested to assess whether or not it can be used to distinguish between materials that flashover and those that do not. Certainly, the averaging of rates of temperature rise over 4 second periods should be replaced by averaging over the period from ignition to peak temperature. This is more promising for distinguishing between the hazardous nature of various materials.

7.3 Geometry in Storage and Testing

Knowledge of the potential exposure conditions a material may experience during a fire is important for the appropriate testing of the material. It is also desirable to be able to identify those storage conditions which increase the possible hazard in order avoid them. Warehouses often have high rack storage with parallel face configurations. Reducing the separation between parallel walls with a flame between them, either against one face or in the centre of the channel, increases the heat fluxes to the walls. The temperatures at each height also increase, as do flame heights.

The highest heat fluxes, and flame heights, are generally seen with a burner in direct contact with the wall, as seen previously (Williamson *et al.*, 1991). Moving the burner into the centre of the channel between parallel walls reduced the convective heat transfer considerably, by a greater fraction than the reduction in radiation. For the open base configuration, the burner against the opposite wall gave higher heat fluxes than the burner in the centre of the channel, as the radiation was greater. The one case where the heat fluxes were higher with the burner in the centre of the channel than against the instrumented wall was with the smallest wall separation used and the closed base. Here the flame touched both walls and gave the higher heat fluxes.

Flame heights were compared to previous predictions (Hasemi and Tokunaga, 1984b) for unconfined flames and flames at walls. The open base and the flame at the wall gave good agreement, all others were higher than the predictions due to the influence of the second wall. The presence of the parallel wall increases the hazard associated with flames at walls.

The open base configuration gave lower heat fluxes than the closed, especially for the burner in the centre of the channel. The separation also had less of an influence on the heat flux for the open base. The results from the CFD simulations were used to help demonstrate the cause of these differences.

Restricting the air flow at the ends of the walls for the open base reduced the heat fluxes with the burner in the centre of the channel and increased them for the burner next to the wall, up to a flow restriction of half of the separation distance between the walls. The heat fluxes were much lower for the completely closed ends, due to

reduced combustion efficiency. Increases with partial end restriction will be due to increased turbulence and reduced entrainment giving higher convective heat transfer and increased radiation from flame thickening. For the closed base, with the burner in either position, increasing the end blockage ratio generally increased the heat fluxes, especially for the totally sealed ends. The differences between this case and the open base is caused by the different flow patterns giving different heat transfer rates. For warehouse storage, it is preferable to remove any flow restrictions in aisles, and to store materials raised on pallets.

The open and closed bases gave very different heat transfer patterns. Convective heat transfer was generally the dominant mode for all these tests, with radiation more important only for the open base configuration with the burner in the centre of the channel. The relative importance of convection increases with reducing separation, and the convective fraction was greater for the closed base than the open.

The use of regression analysis allowed the development of empirical correlations for both total and radiative heat fluxes and temperature, with excellent correlation coefficients. These provide a way forward for experimentalists to develop relationships for this complicated scenario, and may prove useful to fire engineers. This method of analysing data shows which of the many factors are important. Developing theoretical relationships will be more difficult. More data with different configurations are needed to extend the range of these correlations, especially different aspect ratios. At present they should only be used within the range of this study, but they do provide a basis for future development. The correlations help demonstrate the difference in burning behaviour between single and parallel walls. This is important both for understanding and modelling fire spread.

7.4 Summary

There should be a relationship between fire tests and the conditions materials may be exposed to in unwanted fires. Both the exposure conditions in fire tests and those in real fires under different conditions need to be understood for hazard assessment. This project has comprised of both an investigation into fire testing, using several test methods and materials, and an experimental study of flames between vertical parallel walls. These are of significance for understanding the fire hazards associated with the bulk storage of materials.

7.5 Recommendations for Future Work

1. An investigation into the melting of materials, with experiments to measure the rate of melting under different heat fluxes, will help provide useful data for hazard assessment of these materials. Information on the viscosity of the melts produced would also be valuable. A fire test designed specifically for materials that melt is preferable to using data from tests such as the Cone Calorimeter. Knowledge of the melting process and any consequent burning behaviour will help in the design of safety systems for warehouses, for example by including run-off drains for low viscosity melts or additional sprinklers where a melt would run to etc. for materials liable to create a pool fire.

2. The use of the rate of increase of heat release rate for hazard assessment warrants further investigation. As it shows the acceleration of the heat release towards the peak value, this data from Cone Calorimeter tests could be used to distinguish between those materials that will flashover and those that do not reach the heat release rate necessary, in given compartment tests. The rate of vent temperature rise is currently being used in this way in the HSE third scale room/corridor test. A wider range of materials would need to be studied, both in the Cone and in chosen compartment tests, but the rate of increase of heat release rate has potential for providing information on fire growth.

3. In order to test materials under appropriate exposure conditions, it is necessary to know what the conditions produced in various tests are. Apparatus such as the Cone Calorimeter incorporate easily controlled heat flux levels to the sample, but some of the tests relying on solid or gaseous heat and ignition sources have less well defined exposure conditions, e.g. in BS 5852 (BSI, 1982). A systematic experimental programme to measure the heat fluxes that samples are tested under in various of the standard tests, as well as heat fluxes from 'real' ignition sources, will increase understanding of the results from fire tests.

4. Burning behaviour of and heat transfer from flames between parallel walls are different from those of flames against a single wall, as shown in the experiments and correlations from this study. More data to identify the point at which the

second wall influences the heat transfer under different conditions would be valuable.

5. An investigation of the effects of scale and height to width aspect ratio is necessary to extend the range of the correlation equations developed for heat fluxes at walls. Different burner geometries and heat release rates should also be studied. The correlations need to be extended to identify common relationships and to increase understanding of the dynamics of these fires. Measurements should be made of both total and radiative heat transfer to show the relative importance of these under different conditions.

6. The heat transfer has been shown to be sensitive to the fluid mechanics of the system. This needs to be investigated further, both for the practical problems of reducing potential hazards and for increasing theoretical knowledge. The current tests employed sharp right angle corners, which will cause the flow to separate from the adjacent wall and increase the turbulence and heat transfer. Tests could be undertaken with a streamlined entrance around the periphery to reduce the turbulence and flow separation. This may lead to a change in flame appearance and heat transfer.

7. Further simulations using CFD would be of interest, especially making comparisons of predicted and experimental data. The use of techniques such as this could reduce the number of experiments necessary in many situations, particularly where a problem is perceived. It would first be necessary to validate various models against experimental data.

8. Finally, it would be desirable to obtain measurements of heat transfer from full scale experiments with the fuel configurations found in warehouses. Data for steady state heat transfer from flames, as for the parallel wall tests carried out as part of this research, and heat fluxes seen at ignition and during flame spread for combustible fuels would be helpful. These would be useful in validating or developing correlations with small scale test data, and would be valuable for helping determine the appropriate fire test conditions for materials stored in warehouses.

Chapter 8

References

AFNOR, Epiradiateur test. NF P 92-501, Association Francaise de Normalisation, Paris, 1975

Ahmed T. and Faeth G.M., Turbulent wall fires. *Fifteenth Symposium (International) on Combustion*, The Combustion Institute, pp. 1149-1160, 1974

Ahonen A.I., Holmlund C., and Kokkala, M.A., Effects of ignition source in room fire tests. *Fire Science and Technology*, Vol. 7, **1**, pp.1-13, 1987

Ahonen A.I., Kokkala M.A., and Weckman H., Burning characteristics of potential ignition sources of room fires. Technical Research Centre of Finland, Espoo, Finland. Research Report 285. 1984

ASTM, Rate of burning and/or extent and time of burning of self-supported plastics in a horizontal position. ANSI/ASTM D 635-77, American Society for Testing and Materials, Philadelphia, PA, 1977b

ASTM, Draft, Proposed test for heat and visible smoke release rates for materials and products. American Society for Testing and Materials, Philadelphia, PA, 1977

ASTM, Standard test method for measuring the minimum oxygen concentration to support candle-like combustion of plastics (oxygen index). ANSI/ASTM D 2863-77, American Society for Testing and Materials, Philadelphia, PA, 1977a

ASTM, Standard test method for specific optical density of smoke generated by solid material, ASTM E-662-79, American Society for Testing and Materials, Philadelphia, PA, 1979b

ASTM, Surface burning characteristics of building materials. ASTM E 84-79a, American Society for Testing and Materials, Philadelphia, PA, 1979a

ASTM, Proposed method for room fire test of wall and ceiling materials and assemblies. *Annual Book of ASTM Standards*, Pt.18, American Society for Testing and Materials, Philadelphia, PA, 1982

ASTM, Standard test method for determining material ignition and flame spread properties. ASTM E-1321-90, American Society for Testing and Materials, Philadelphia, PA, 1990a

ASTM, Standard test method for heat and visible smoke release rates for materials and products using an oxygen consumption calorimeter. ASTM E 1354 - 90a, American Society for Testing and Materials, Philadelphia, PA, 1990b

Atkinson G. and Drysdale D.D., A note on the measurement of smoke yields, *Fire Safety Journal*, **15**, pp.331-335, 1989

Atkinson, G., Assessment of the fire hazard of materials. *Report to Health and Safety Executive, contract no. 2319/RO4.21*, University of Edinburgh, 1989

Atkinson, G., *Private Communication*, 1992

Atkinson G., *Private Communication*, 1994

Babrauskas V., Development of the Cone Calorimeter - a bench-scale heat release rate apparatus based on oxygen consumption. (NBSIR 82-2611). [U. S.] Nat. Bur. Stand., 1982

Babrauskas V., Upholstered furniture heat release rates: measurements and estimation. *J. of Fire Sciences*, **1**, pp. 9-32, 1983

Babrauskas V., Development of the Cone Calorimeter - a bench-scale heat release rate apparatus based on oxygen consumption. *Fire and Materials,* **8**, pp.81-95, 1984

Babrauskas V., Effective measurement techniques for heat, smoke and toxic fire gases. *Fire: Control the Heat....Reduce the Hazard*, pp.4.1-4.10, 1988

Babrauskas V., Smoke and gas evolution rate measurements on fire-retarded plastics with the cone calorimeter. *Fire Safety Journal,* **14**, pp.135-142, 1989

Babrauskas V., Effective measurement techniques for heat, smoke and toxic fire gases. *Fire Safety Journal*, **17**, pp.13-26, 1991

Babrauskas V. and Krasny J.F., Prediction of upholstered chair heat release rates from bench-scale measurements. *Fire Safety Science and Engineering*, ed. T.Z. Harmathy. American Society for Testing and Materials, ASTM STP 882, pp.268-284, 1985

Babrauskas V. and Peacock R.D., Heat release rate: the single most important variable in fire hazard. *Fire Safety Journal*, **18**, pp.255-272, 1992

Babrauskas V., Lawson J.R., Walton W.D. and Twilley W.H., Upholstered furniture heat release rates measured with a furniture calorimeter (NBSIR 82-2604). [U.S.] Nat. Bur. Stand., 1982

Back G., Beyler C., DiNenno P., and Tatem P., Wall incident heat flux distributions resulting from an adjacent fire. *Fire Safety Science-Proceedings of the Fourth International Symposium*, pp.241-252, 1994

Beard A., A non-linear model of major fire spread in a tunnel. *To be published, Fire Safety Journal*, 1995a

Beard A., *personal communication*, 1995b

Bellin B., Upward turbulent fire spread and burning of fuel surface in the configuration of two PMMA surfaces facing each other. Report of Fire Research Institute, Japan, 1991

Bouhafid A., Vantelon J.P., Joulain P., and Fernandez-Pello A.C., On the flame structure at the base of a pool fire. *Twenty second Symposium (international) on Combustion*, The Combustion Institute, pp.1291-1298, 1988

Breazeale A.F., Wire and cable fire performance as determined by a Cone Calorimeter. *International Wire and Cable Symposium Proceedings*, pp.536-542, 1988

BSI, Fire tests for furniture. Part 1: Methods of test for the ignitability by smokers' materials of upholstered composites for seating. BS 5852 Part 1, 1979

BSI, Fire tests on building materials and structures. Part 6: Fire propagation test for materials. BS 476 Part 6: 1981

BSI, Methods of test for ignitability of upholstered composites for seating by flaming sources. BS 5852 : Part 2, 1982.

BSI, Fire tests on building materials and structures. Part 7: Surface spread of flame test for materials, BS 476 Part 7: 1987a

BSI, Fire tests on building materials and structures: Part 13. Method of measuring the ignitability of products subjected to thermal irradiance. BS476: Part 13: 1987b

BSI, Fire tests on building materials and structures. Part 15. Method for measuring the rate of heat release of products. BS 476: part 15: 1993

Bukowski R.W., Evaluation of furniture fire hazard using a hazard-assessment computer model. *Fire and Materials*, **9**, pp.159-166, 1985

Bukowski R.W., Peacock R.D., Jones W.W., and Forney C.L., HAZARD I Assessment method-software users guide, and example cases. NIST Handbook 146, NIST, 1989

Cetegen B.M., Zukoski E.E., and Kubota T., Entrainment in the near and far field of fire plumes. *Comb. Sci. and Tech.* **39**, p.305-331, 1984

Chatfield, C., Statistics for technology, Third Edition, (Chapman and Hall), London 1983.

Delichatsios M.A., Air entrainment into buoyant jet flames and pool fires. *The SFPE Handbook of Fire Protection Engineering*, Section 1/Chapter 19, SFPE, NFPA, 1988

Delichatsios M.A., Panagiotou Th., and Kiley F., The use of time to ignition data for characterising the thermal inertia and the minimum (critical) energy for ignition or pyrolysis. *Combustion and Flame*, **84**, pp.323-332, 1991

De Ris J.N., Spread of a laminar diffusion flame. *12th Symposium on Combustion*, Comb. Inst., Pittsburgh, pp.241-252, 1969

DIN, 53 437 Draft, Prüfung von Kunststoffen. Rauchdichtemessung., 1966

DIN, Small burner test. DIN 54332, February, 1975

DIN, Model introductory decree, DIN 4102; Mitt. IfBt 9, 1978

Drysdale D.D., *An Introduction to Fire Dynamics*, (John Wiley and Sons Ltd.), 1985

Drysdale D.D., *Private Communication*, 1995

Drysdale D.D. and Abdul-Rahim F.F., Smoke production in fires: small scale experiments. *Fire Safety: Science and Engineering*, ASTM STP 882, ed. T.Z. Harmathy (American Society for Testing and Materials, Philadelphia), pp.285-300, 1985

Drysdale D.D. and Thomson H.E., Heat transfer characteristics of common ignition sources. University of Edinburgh Report, 1990

Emmons H. W., Heat transfer in fire. *Journal of Heat Transfer*, **95**, pp. 145-151, 1973

Emmons H. W.,Fire and fire protection, *Scientific American*, **231**, No. 1, pp.21-27, 1974

Feizlmayr, A.H., Research in Austria on tunnel fires., *Int. Symp. on Aerodynamics and Ventilation of Vehicle Tunnels*, paper J2, pp. 19-27, 1976

Foley M. and Drysdale D.D., Smoke measurement and the Cone Calorimeter. *Fire and Materials*, **18**, pp. 385-387, 1994

FPA Casebook of Fires., *Fire Prevention* **121**, pp.33-34, 1977

FPA Casebook of Fires., *Fire Prevention* **164**, pp.38-41, 1983

FPA Casebook of Fires., *Fire Prevention* **166**, pp.38-39, 1984

FPA Casebook of Fires., *Fire Prevention* **181**, pp.42-44, 1985

Goff L.J., Analysis of polymers using the Cone Calorimeter. *Integr. Fundam. Polym. Sci. Technol.* **5**, pp.311-315, 1991

GOST, 12.1.017-80, Appendix 19. Method for the experimental determination of the smoke production coefficient of solid materials. 1980

Green A. R. and Bilger R. W., A review of flammability test methods for evaluating fire resistance of materials used underground (Technical report LISC RR-C-1). Londonderry Industrial Safety Centre, Londonderry, Australia, 1984

Hallman J.R., Welker J.R., and Sliepcevich C.M., Ignition characteristics of polymers. *S. P. E. Journal*, **28**, pp.43-47, 1972

Hasemi Y., Experimental wall flame heat transfer correlations for the analysis of upward wall flame spread. *Fire Science and Technology*, **4** No. 2, pp.75-89, 1984

Hasemi Y., Thermal modeling of upward flame spread. *Fire Safety Science-Proceedings of the First International Symposium*, pp. 87-96, 1985

Hasemi Y., *Private Communication*, 1994

Hasemi Y. and Tokunaga T., Flame geometry effects on the buoyant plumes from turbulent diffusion flames. *Fire Science and Tech.* **4**, pp.15-26, 1984a

Hasemi Y. and Tokunaga T., Some experimental aspects of turbulent diffusion flames and buoyant plumes from fire sources against a wall and in a corner of walls. *Comb. Science and Technology*, **40**, pp.1-17, 1984b

Heskestad G., Peak gas velocities and flame heights of buoyancy-controlled turbulent diffusion flames. *18th Symposium on Combustion*, Comb. Inst., Pittsburgh, pp.951-60, 1981

Heskestad G., Engineering relations for fire plumes. *Society of Fire Protection Engineers, Technology Report,* pp. 82-88, 1982

Heskestad G., Virtual origins of fire plumes. *Fire Safety Journal*, **5**, pp.109-114, 1983a

Heskestad G., Luminous heights of turbulent diffusion flames. *Fire Safety Journal*, **5**, pp.103-108, 1983b

Heskestad G., Engineering relations for fire plumes. *Fire Safety Journal*, 7, pp. 25-32, 1984

Heskestad G., *The SFPE Handbook of Fire Protection Engineering*, Section 1/Chapter 6, SFPE, NFPA, 1988

Heskestad A.W. and Hovde P.J., Assessment of smoke production from building products. *Fire Safety Science-Proceedings of the Fourth International Symposium*, pp.527-538, 1994

Hinkley P.L., Wraight H.G.H. and Wadley A., Rates of heat output and heat transfer in the fire propagation test. Fire Research Note No. 709, Fire Research Station, Borehamwood, England, 1968

Hirschler M.M., How to measure smoke obscuration in a manner relevant to fire hazard assessment: use of heat release calorimetry test equipment. *Journal of Fire Sciences*, **9**, pp.183-222, 1991b

Hirschler M.M., The measurement of smoke in rate of heat release equipment in a manner related to fire hazard. *Fire Safety Journal*, **17**, pp.239-258, 1991a

Hirschler M.M., Smoke and heat release and ignitability as measures of fire hazard from burning of carpet tiles. *Fire Safety Journal*, **18**, pp.305-324, 1992

Hognon B., Etude en vrai grandeur de la toxicité des effluents de la combustion de produits de construction. Centre Scientifique et Technique du Bâtiment, Marne la Vallée, France, 1992

HSE, Assessment of fire hazards from solid materials and the precautions required for their safe storage and use. HMSO, London, 1991

Huggett C., Estimation of rate of heat release by means of oxygen consumption measurements. *Fire and Materials*, **4**, No. 2, pp.61-65, 1980

Hume J. and Pettett K., Cone calorimetry of CMHR polyurethane foam: an evaluation of the effects of melamine additive. *Flame Retardents '90*, pp.234-241, 1990

Hymes, I. and Flynn, J. F., The probability of fire in warehouses and storage premises. Safety and Reliability Directorate. HSE Report No. HSE/SRD/089/ 00001/89/ Draft A., 1989

Ingason H., Fire experiments in a two dimensional rack storage. BRANDFORSK-project 701-917, SP Report 1993:56, 1993

ISO, Reaction to fire test-smoke generated by solid materials. ISO/DP 5659 (Edition 3), International Organisation for Standardisation, 1977a

ISO, (Preliminary proposal). Fire test-reaction to fire, spread of flame of building materials. ISO/DP 5658, International Organisation for Standardisation, 1977b

ISO, Fire Tests-Reaction-to-Fire. Ignitability of building products, ISO 5657, International Organisation for Standardisation, 1979

ISO, Fire tests-reaction to fire-smoke generated by building products, technical report TR 5924, International Organisation for Standardisation, 1980

ISO, Room fire test in full scale for surface products. ISO/TC 92/SC 1/WG7 -Doc N 40, International Organisation for Standardisation, 1986

ISO, International Standard-fire tests-reaction to fire, rate of heat release from building products (cone calorimeter), ISO 5660, International Organisation for Standardisation, 1990

Janssens M., Measuring the rate of heat release by oxygen consumption. *Fire Technology* **27**, pp.234-249, 1991

Janssens, M., Determining flame spread properties from Cone Calorimeter measurements - General concepts. Heat Release in Fires, eds. V. Babrauskas and S.J. Grayson, (Elsevier Applied Science, London), pp.265-281, 1992

Janssens M. and Minne R., Survey of rate of heat release test methods and apparatuses. Document ISO/TC 92/SC1-104, International Organisation for Standards, 1982

Jianmin Q., Prediction of flame spread test results from the test data of the cone calorimeter. SP REPORT 1990:38, Fire Technology, Boras, Sweden, 1990

Jianmin Q., Prediction of LIFT data from cone calorimeter measurements. *Heat Release in Fires*, eds. V. Babrauskas and S.J. Grayson, (Elsevier Applied Science, London), pp.293-306, 1992

JIS, Testing method for incombustibility of thin materials for buildings. JIS A 1322, Japanese Standards Association, 1966

Karlsson B., A mathematical model for calculating heat release rate in the room corner test. *Fire Safety Journal*, **20**, pp.93-113, 1993

Karlsson B and Magnusson S.E., An example room fire model. *Heat Release in Fires*, eds. V. Babrauskas and S.J. Grayson, (Elsevier Applied Science, London), pp.159-171, 1992

Kawagoe K., Fire behaviour in rooms. *Report No. 27*, Building Research Institute, Tokyo, 1958

Kim J. S., de Ris J., and Kroesser F. W., Laminar burning between parallel fuel surfaces. *Int. J. Heat Mass Transfer*, **17**, pp.439-451, 1974

Kishitani K., Sugawara, S., and Hamada, K., Upward flame spread of building materials. '*Saigai no Kenkyu*', **15**, pp.133, 1984

Krause R.F., Jn. and Gann R.G., Rate of heat release measurements using oxygen consumption. *J. of Fire and Flammability*, **12** , pp.117-130, 1980

Kumar S., Fire development and smoke spread in tunnels - some modelling considerations. *Proc. 1st Int. Conference, Safety in Road and Rail Tunnels, Switzerland.* pp. 379-393, 1992

Kung H. C. and Stavrianidis P., Buoyant plumes of large scale pool fires. *19th Symposium on Combustion*, Comb. Inst., Pittsburgh, pp. 905-912, 1983

Kurosaki Y., Akihiko I., and Chiba M., Downward flame spread along two vertical, parallel sheets of thin combustible solid. *Seventeenth Symposium (International) on Combustion*, The Combustion Institute, pp.1211-1220, 1978

Lawson D.I. and Simms D.L., The ignition of wood by radiation. *British Journal of Appied Physics*, **3**, pp. 288-292, 1952

Lee S.L. and Emmons H.W., A study of natural convection above a line fire. *Journal of Fluid Mechanics*, **11**, pp. 353-368, 1961

Levin B.C., Paabo M., Fultz M.L., Bailey C., Yin W., and Harris S.E., An acute inhalation toxicological evaluation of combustion products from fire retarded

and non-fire retarded flexible polyurethane foam and polyester. (NBSIR 83-2791). [U. S.] Nat. Bur. Stand., 1983

Magnusson S.E. and Sundström B., Combustible linings and room fire growth-a first analysis. *Fire Safety Science and Engineering*, ed. T.Z. Harmathy. American Society for Testing and Materials, ASTM STP 882, pp.45-69, 1985

Malhotra H.L., The philosophy and design of fire tests. *Int. Symp. on Fire Safety of Combustible Materials*. University of Edinburgh, 1975

Malhotra H.L., Full-scale Ad-hoc tests: Their meaning, limitations and role. VFDB; 5. *Int. Fire Protection Seminar*, Karlsruhe, p. 63-72, 1976

McCaffrey B. J., Purely buoyant diffusion flames: some experimental results. National Bureau of Standards, NBSIR 79-1910, 1979

McGuire J.H., Heat Transfer by Radiation, *Fire Research Special Report No. 2;* HMSO, London, 1953

Mikkola E., Smoke round robin on the cone calorimeter. ISO TC92/SC1/WG4, 1992

Mikkola E. and Wickman I.S., On the thermal ignition of combustible materials. *Fire and Materials*, **14**, pp.87-96, 1989

Morton B. R., Taylor G. I., and Turner J. S., Turbulent gravitational convection from maintained and instantaneous sources. *Proc. Royal Soc.(London),* A234, pp.1-23, 1956

Most J. M., Bellin B., Joulain P., and Sztal B., Interaction between two burning vertical walls. *Fire Safety Science-Proceedings of the Second International Symposium*, pp.285-294, 1988

Mulholland G.W., Henzel V., and Babrauskas V., The effect of scale on smoke emission. *Fire Safety Science-Proceedings of the Second International Symposium*, pp.347-357, 1988

Mulholland G.W., Janssens M., Yusa S., Twilley W., and Babrauskas V., The effect of oxygen concentration on CO and smoke produced by flames. *Fire Safety Science-Proceedings of the Third International Symposium*, pp. 585-594, 1991

NEN, 3881, Bepaling van de onbrandbaarheid van bouwmaterialen., 1975

Nordtest. NT Fire 004. Surfaces: Tendency to fire spread and smoke development. Nordtest Method, box 5103, S-10243, Stockholm 5, March 1976

Nordtest. NT Fire 013. Plastics - Candle-like combustion: Minimum oxygen concentration. Nordtest Method, box 5103, S-10243, Stockholm 5, June 1980

Nordtest NT Fire 025, Surface products: room fire test in full scale. Nordtest, Helsinki, 1986

Norme Experimentale, Essai de mesure de la densite optique specifique de la fumee. X 10-702, 1976

Orloff L., de Ris J., and Markstein G. H., Upward turbulent flame spread and burning of fuel surface. *Fifteenth Symposium (International) on Combustion*, The Combustion Institute, pp.183, 1974

Östman B., Comparison of smoke release rate from building products. Conference book, *Fire: Control the Heat, Reduce the Hazard*, Queen Mary College, Fire and Materials Centre, London, 1988

Östman B., Smoke measurements and predictions. *Proceedings of the Eurefic seminar*, Denmark. pub. Interscience Communications Ltd, London, pp. 37-45, 1991

Ostman B., Smoke and soot, *Heat Release in Fires*, eds. V. Babrauskas and S.J. Grayson, (Elsevier Applied Science, London) 1992

Östman B. and Nussbaum R., National standard fire tests in small scale compared with the full scale ISO room test (Rapport I 870217), Trateknik Centrum, Stockholm, 1987

Östman B. and Nussbaum R.M., Correlation between small-scale rate of heat release and full-scale room flashover for surface linings. *Fire Safety Science-Proceedings of the Second International Symposium*, pp.823-832, 1988

Östman B. and Tsantaridis L.D., Ignitability in the cone calorimeter and in the ISO ignitability test. *Interflam '90*, pp.175-182, 1990

Östman B. and Tsantaridis L.D., Smoke production in the cone calorimeter and the room fire test. *Fire Safety Journal*, **17**, pp.27-43, 1991

Parker W.J., An investigation of the fire environment in the ASTM E84 tunnel test. NBS Technical Note 945, Nat. Bur. Stand., Washington DC, 1977

Parker W.J., Calculations of the heat release rate by oxygen consumption for various applications. *Journal of Fire Sciences*, **2**, 1984

Parker W., Tu K-M., Nurbakhsh S., and Damant G., Chair burns in the TB133 room, the furniture calorimeter and the cone calorimeter. *Fire Safety Science-Proceedings of the Third International Symposium*, 1991

Paul K.T. and Christian S.D., Standard flaming ignition sources for upholstered composites, furniture and bed assembly tests. *J. Fire Sciences*, **5**, pp.178-211, 1987

Peacock RD. and Braun E., Fire tests of amtrak passenger rail vehicle interiors (NBS Tech. Note 1193). [U. S.] Nat. Bur. Stand., 1984

Porscht R., Uber das Flackern von Flammen. 6th International Seminar on the Problems of Automatic Fire Detection, Aachen, 1971

Quintiere J.G., A simplified theory for generalising results from a radiant panel rate of flame spread apparatus. *Fire and Materials*, **5**, No. 2, pp. 52-60, 1981

Quintiere J.G., Smoke measurements: an assessment of correlations between laboratory and full-scale experiments. *Fire and Materials*, **6**, Nos 3 and 4, pp.145-160, 1982

Quintiere J.G., Comments on 'Full-scale/bench-scale correlations of wall and ceiling linings' by Ulf Wickstrom and Ulf Goransson. *Fire and Materials*, **17**, pp. 149-150, 1993

Quintiere J. G. and Cleary T. G., Heat flux from flames to vertical surfaces. *Fire Technology*, second quarter, pp.209-231, 1994

Quintiere J.G. and Harkleroad M., New concepts for measuring flame spread properties. NBSIR 84-2943, National Bureau of Standards, Gaithersburg, MD, 1984

Quintiere J., Harkleroad M., and Hasemi Y., Wall flames and implications for upward flame spread. *Combust. Sci. and Tech*, **48**, pp.191-222., 1986

Rasbash D.J. and Phillips R.P., *Fire and Materials*, **2,** pp. 102 - 109, 1978

Rasbash D.J. and Pratt B.T., Estimation of the smoke produced in fires. *Fire Safety Journal*, **2**, pp.23-37, 1979/1980

Ross, S. M., Introduction to probability statistics for engineers and scientists, John Wiley and Sons, New York, 1987

Scoones, K., FPA large fire analysis 1991, *Fire Prevention* **268**, pp.18-26, 1994

Scudamore M.J., Briggs P.J., and Prager F.H., Cone calorimetry - a review of tests carried out on plastics for the association of plastics manufacturers in Europe. *Fire and Materials*, **15**, pp.65-84, 1991

Silcock A. and Hinkley P.L., Report on the spread of fire of Summerland in Douglas, Isle of Man, 2nd August 1973. B.R.E. Current paper CP74/74, 1974

Simms D.L., On the pilot ignition of wood by radiation. *Combustion and Flame*, **7**, pp. 253-261, 1963

Smith E.E., Heat release rate of building materials. *Ignition, Heat Release, and Non-combustibility of materials*, ASTM STP 502, American Society for Testing and Materials, Philadelphia, PA, pp.119-134, 1972

Steingeiser S., A Philosophy of Fire Testing. *J. Fire and Flammability*, **3**, p.238, 1972

Sugawa O., Satoh H., and Oka Y., Flame height from rectangular fire sources considering mixing factor. *Fire Safety Science-Proceedings of the Third International Symposium*, pp.435-444, 1991

Sussott R., Shafizadeh F. and Aanerud T.W., A quantitative thermal analysis technique for combustible gas detection. *J. of Fire and Flammability*, **10**, pp.94-104, 1979

Tamanini, F., Technical report: calculations and experiments on the turbulent burning of verticl walls in single and parallel configurations. Factory Mutual Research, No. OAOE7. BU-2, 1979

Tewarson A., Heat release rates from samples of polymethylmethacrylate and polystyrene burning in normal air. *Fire and Materials*, **1**, pp.90-96, 1976

TGL 10685/11. Determination of the combustibility group of building materials., Nov. 1975

Thomas P. H., Comments on the heat transfer in opposed flow flame spread. *Fire and Materials*, **17**, pp. 150-151, 1993

Thomas P. H., Webster C. T., and Raftery M. M., Some experiments on buoyant diffusion flames. *Combustion and Flame*, **5**, pp. 359-367, 1961

Thomson H.E. and Drysdale D.D., Flammability of plastics I: Ignition temperatures. *Fire and Materials*, **11**, pp.163-172, 1987

Thornton W.M., The relation of Oxygen to the heat of combustion of organic compounds. *Philosophical Magazine*, **33**, pp.196-203, 1917

Toong T. Y., A theoretical study of interactions between two parallel burning fuel plates. *Combustion and Flame.* **5**, No. 3, pp.221-227, 1961

Troitzsch J., International Plastics Flammability Handbook, Hanser Publishers, New York, 1983

Ward, R. B., The warehouse fire scandal. *Fire Prevention* **177**, pp.19-27, 1985

Watson A., Forensic pathology as an aid to fire investigation. *Fire Science and Fire Investigation Course Notes*, University of Edinburgh, Sept. 1994

Wharton R.K., A medium scale test method for assessing the fire hazard of flammable solid materials. *Journal of Loss Prevention in the Process Industries.* **3**, pp. 349-354, 1990

Whiteley R.H., Comments on the measurement of ignitability and on the calculation of critical heat flux. *Fire Safety Journal*, **21**, No.2, pp.177-183, 1993

Wickström U. and Göransson U., Full-scale/bench-scale correlations of wall and ceiling linings. *Fire and Materials*, **16**, pp.15-22, 1992

Wickström U., Sundström B. and Holmstedt G., The development of a full-scale room fire test. *Fire Safety Journal*, **5**, pp.191 - 197, 1983

Williamson R.B. and Baron F.M., A corner fire test to simulate residential fires. *J. Fire and Flammability*, **4**, pp. 99-105, 1973

Williamson R.B., Revenaugh A., and Mowrer F.W., Ignition sources in room fire tests and some implications for flame spread evaluation. *Fire Safety Science-Proceedings of the Third International Symposium*, pp.657-666, 1991

Woodward C.D. The industrial fire problem part 1. *Fire Prevention* **218**, pp.24-27, 1989a

Woodward C.D. The industrial fire problem part 2. *Fire Prevention* **219**, pp.28-33, 1989b

Zukoski E. E., Kubota T. and Cetegen B. M., Entrainment in Fire Plumes. *Fire Safety Journal*, **3**, pp.107-121, 1980/1981

Appendix A

Units of Smoke Measurement

There are various methods and units for the measurement of smoke from burning materials. The methods can be fitted into two main categories: dynamic and static smoke measurement. Static smoke measurement basically involves collecting the smoke produced in a container of known volume and measuring the decrease in light intensity of a beam passing through the smoke. The dynamic approach uses the same measurement, but the beam passes through the combustion products as they flow away from a fire. The volume flowrate of the combustion products, normally mixed with air, is known and the measurements are summed over the entire period of test.

The original unit used for the measurement of smoke is optical density, where:

$$D = \frac{1}{L}\log\left(\frac{I_0}{I}\right)$$

where D = optical density, m^{-1} (or ODm1)

L = pathlength over which measurement is made, m

I_0 = intensity of light in absence of smoke

I = intensity of light in presence of smoke

It is of more use to be able to say something about the amount of smoke produced by a material on a mass basis. The first unit to be used for this was 'mass optical density':

$$D_m = \frac{DV}{m}$$

where D_m = mass optical density, m^3 [ODm1]/kg

V = volume of static smoke chamber, m^3

m = total mass of material consumed in the test, kg

This corresponds to a light attenuation of one bel per metre of smoke path.

For dynamic and static conditions, the mass optical density can be calculated by similar equations:

$$D_m = \frac{\dot{V}}{\dot{m}L}\log\frac{I_0}{I} \qquad \text{dynamic}$$

$$D_m = \frac{V}{mL}\log\frac{I_0}{I} \qquad \text{static}$$

where $\dot{V}$ = volume flowrate past measuring device, m^3/s

$\dot{m}$ = mass loss rate of material, kg/s

The above can be thought of as the smoke yield expressed as the volume of smoke produced by 1 kg of material if this smoke were diluted (or concentrated) such that the intensity of light passing through it falls by a factor of 10 in every metre.

Another unit can be used to define the smoke produced per unit mass of volatiles, D_0, in terms of a new unit for smokiness, the obscura (ob), (Rasbash *et al*, 1979). The obscura corresponds to a smoke density when the measured light attenuation is one decibel per metre of smoke path. The main reason for defining it thus is that it is approximately the smokiness that will give rise to a visibility of about 10m under conditions of general illumination, this being approximately the smokiness at which people will begin to turn back from a smoke-filled path.

If the unit of obscura is used for smokiness, then the light attenuation in smoke may be expressed as obm; the quantity of smoke produced as obm^3; the smoke potential of materials as obm^3/g. The smoke potential here is fundamentally the same as the mass optical density above, but using a system of units based on the decibel (the normal measure of attenuation) rather than the bel.. The smoke potential, D_0, can be written as:

$$D_0 = \frac{10\dot{V}}{\dot{m}L}\log\frac{I_0}{I} \qquad \text{dynamic}$$

$$D_0 = \frac{10V}{mL}\log\frac{I_0}{I} \qquad \text{static}$$

The smokiness of 1 ob is one-tenth of the smokiness of the optical density per metre, D, as above and quoted as ODm1. These may be converted to obscura by multiplying by 10. Similarly, the mass optical density, D_m, in units of m^3[ODm1]/g may be converted to smoke potential (obm^3/g) by multiplying by 10.

The commonly used smoke test, the NBS Smoke chamber (see Chapter 2) measures smoke in terms of specific smoke density (bels/m)(m^3/m^2). This may also be converted to obscura by multiplying by 10.

An alternative unit, used to measure smoke in the Cone Calorimeter, is the specific extinction area (SEA). This is another measure of smoke yield per unit mass of material pyrolysed, measured as a function of time. The SEA can be calculated as

$$\sigma_f = \frac{k\dot{V}}{\dot{m}}$$

where σ_f = specific extinction area, m^2/kg

k = light extinction coefficient, m^{-1}

The extinction coefficient, k, comes from the fact that the specific extinction area is defined in natural logarithms rather than base 10 logarithms used by the obscura and the optical density based on decibels. This can be seen from the following equations:

$$\frac{I_0}{I} = e^{-kL}$$

giving

$$k = \frac{1}{L}\ln\left(\frac{I_0}{I}\right)$$

The meaning of specific extinction area and the m^2/kg units has been described as being visualised by imagining obscuring particles to be opaque spheres blocking the light (Östman, 1992). The attenuation of light will then be proportional to the projected area (m^2) of particles blocking the beam. This is then normalised by the mass of fuel burned.

The mass optical density, D_m, as defined above, uses logarithms to the base 10, whilst the specific extinction area uses natural logs. The relationship between them is therefore

$$\sigma_f = D_m \ln(10)$$

and that between the specific extinction area and the smoke potential, D_0, defined using the unit of obscura is

$$\sigma_f = \frac{D_0 \ln(10)}{10}$$

The rate of smoke production is of interest in many cases. It can be expressed as

$$SPR = k\dot{V}_f$$

where SPR is the smoke production rate in base e (m^2/s)

or

$$D_{sp} = D\dot{V}_f$$

where D_{sp} is the smoke production rate in base 10 (m^2/s).

Appendix B

Publications Arising from this Work

FIRE AND MATERIALS, VOL. 18, 385–387 (1994)

Note: Smoke Measurement and the Cone Calorimeter

Marianne Foley and Dougal Drysdale

Unit of Fire Safety Engineering, Department of Civil Engineering and Building Science, University of Edinburgh, The King's Buildings, Mayfield Road, Edinburgh EH93JL, UK

Fire testing has come under increasing scrutiny over the past decade with the realization that a set of internationally recognized standards is essential for the success of a free market within the European Union. This bas led to a move away from the 'traditional' standard tests, which are empirically based, towards tbe new generation of 'reaction to fire' tests which have been designed on scientific principles with a view to providing meaningful data on the fire properties of materials. The Cone Calorimeter is one such test which offers the opportunity to break away from empiricism.[1]

The greatest attribute of the Cone is its ability to measure the rate of heat release from combustible materials under a range of imposed radiant heat fluxes. Such results have been used to model flame spread on wall lining materials, with considerable success,[2,3] and offers the possibility that other fire scenarios may be modelled for the first time. However, this success has created a wider expectation within the fire test community which mirrors the way in which some of the 'old generation' of tests were used, i.e. it is assumed that the fire model of the new apparatus can be used to study a much wider range of 'fire properties', particularly the propensity of materials to produce smoke and toxic gases. Although designed to measure rate of heat release, the Cone has proved to be extremely versatile in that the fire effluents can readily be sampled and subjected to measurement. The relevance of data gained in this way, obtained under conditions of well-aerated, free burning, to real fires has still to be explored. This will be difficult as it will require careful analyses of the smoke yields from large-scale fire tests. This note describes a preliminary examination of the smoke measurements in the Cone Calorimeter in which they are compared with those obtained by burning materials in a 13.5 m^3 smoke chamber.

Smoke yield is very sensitive to the conditions of burning, and particularly to the availability of air. In the early stages of a fire, well-ventilated conditions are likely to exist and the yield of smoke will be relatively low. The situation will change with the approach and onset of flashover, and it is known that the yield of smoke will increase, as has been demonstrated by Abdul-Rahim.[4] It seems likely that measurement of smoke in the standard Cone Calorimeter can only be relevant to the early stages of a fire: however, this has never been put to the test.

Accordingly, a series of experiments was carried out to compare the smoke yields from three different fuels burning under conditions of adequate ventilation in a large smoke chamber with the smoke yields obtained in the Cone Calorimeter. This comparison is between a 'static' and a 'dynamic' measurement:[4,5] Atkinson and Drysdale[5] showed that there was good agreement between the static and dynamic measurements of smoke from the same fire, provided that the static measurement was made before the accumulated smoke had aged significantly. Accordingly in the present study, the maximum smoke yields in tbe 'smoke box' were compared with the Cone Calorimeter measurements.

The fuels used are listed in Table 1. Liquid *n*-hexane was identified as the most convenient as it could be burned in the open, without any imposed heat flux. The solid fuels had to be heated. This was achieved in the large smoke box using an apparatus originally constructed to study the ignition of combustible solids.[6] This, in effect, was a simplified version of the ISO Ignitability Test Apparatus,[7] using the same conical heater but with a smaller sample. The results, expressed as the 'specific extinction area' values are summarized in Table 1 in units of $m^2 kg^{-1}$. Specific extinction area is defined as the extinction area of the smoke produced per unit mass of volatile material burned. This method of presentation is used only because it is the one incorporated into the Cone Calorimeter software: the figures quoted in Table 1 are based on the cumulative smoke yield over the duration of the test, and are calculated by dividing the total smoke produced by the total mass consumed as specified in the ASTM standard[1] (cf. Rasbash's 'smoke potential'[8]). The results from measurements in the smoke box were calculated from the maximum optical density of the smoke which accumulated in the volume (13.5 m^3), using the expression

$$\mathrm{SEA} = -\frac{V}{ML}\ln\left(\frac{I}{I_0}\right)$$

where V is the volume of the smoke box (m^3), M is the mass of material burned (kg), L is the path length over which the optical density is measured (m), and I and I_0 are the intensities of light falling on a photocell L m from a light source, in the presence and absence of smoke, respectively. (Note: the relationship between SEA and Rasbash's ob.m^3.kg^{-1} [8] which is normally used by this group is through a simple conversion factor (4.34 ob. m^3. kg^{-1} = 1.0 $m^2 kg^{-1}$). The obscura (ob) expresses the smokiness of an atmosphere when the measured light attenuation is one decibel per metre of smoke path. It is approximately the smokiness that will give rise to a visibility of about 10 m under conditions of general illumination.)

It can be seen that significant differences exist, but the differences are not consistent. Thus, *n*-hexane consistently showed a lower smoke yield in the smoke box than in the Cone Calorimeter, although the same container (a 100 mm Petri dish) was used in both sets of expetiments. Of the solids, the results from the polyurethane foam were in reasonable agreement, but PMMA apparently gave *more* smoke when measured in the box, compared with the Cone. Unfortunately, the sample holder from the Cone Calorimeter was too large to be placed under the

CCC 0308–0501/94/060385–03
© 1994 by John Wiley & Sons, Ltd.

Received 15 November 1993
Accepted 10 March 1994

Table 1. Smoke yields measured in the Cone Calorimeter and the 'smoke box'[a]

Fuel	Heat flux/ kW m^{-2}	Cone Calorimeter SEA/m^{2}kg^{-1} 100 mm sample	Cone Calorimeter SEA/m^{2}kg^{-1} 60 mm sample	Smoke box SEA/m^{2}kg^{-1} 60 mm sample
Hexane[b]		101.9 (4.2)[b]	—	80.5 (1.5)[b]
PMMA	30	107.6	135.2 (4.9)	179.5 (2.0)
PMMA	25	98.8 (3.4)	128.9 (0.4)	171.1 (2.2)
PMMA	20	88.3 (4.8)	126.2 (3.4)	145.9 (4.8)
PMMA	15	90.9 (6.2)	115.3 (5.0)	141.8 (0.5)
PUF	30	188.2 (27.1)	—	203.8 (18.7)
PUF	25	196.6 (7.6)	—	177.2 (30.8)
PUF	20	143.7 (20.6)	—	148.9 (24.9)

[a] It was assumed that the amount of smoke produced before ignition could be ignored. Under the conditions of the tests, PMMA produces only monomer vapour, while PUF ignites within seconds, contributing a negligible amount to the total smoke yield. Figures in parentheses show the 'best estimate of the population standard deviation' from three replicates.
[b] Hexane = *n*-hexane burned as a pool in 100 mm diameter Petri dish in both the smoke box and the Cone Calorimeter.
PMMA = black polymethyl methacrylate.
PUF = melamine loaded polyurethane foam.
Cone Calorimeter 60 mm sample = this set of tests was carried out in the Cone Calorimeter using the sample holder and sample size as used in the smoke box tests.

Table 2. Smoke yields from *n*-hexane in the Cone Calorimeter with and without the heater in position

Heater position	SEA/m^{2}kg^{-1}
'Horizontal', 65 mm above sample	101.9 (4.17)
'Horizontal', 25 mm above sample	105.8 (5.56)
'Vertical'	127.5 (4.72)
Removed	135.1 (1.13)

conical heater in the smoke box, and a 60 mm diameter sample had to be used. To examine whether or not this could account for some of the differences observed in the PMMA results, the sample holder from the ignition apparatus was used to carry out some measurements in the Cone Calorimeter. As can be seen from Table 1, the smaller sample gave an increased SEA, but still not as high as the smoke box result.

Apart from the presence of the conical heater in the Cone Calorimeter, it is anticipated that the hexane results would be strictly comparable as the same 'sample holder' (Petri dish) was used in both sets of experiments, and no imposed heat flux was required. To determine the effect of the presence of the cone heater, a set of experiments was carried out in which the cone was moved into its vertical position, i.e. out of direct line of the flames rising from the Petri dish fire (although there was still some impingement), and the smoke measurements repeated. The smoke yield was observed to *increase* by about 20%, giving an even greater difference between the Cone and the smoke box tests. When the conical heater was completely removed from the Cone Calorimeter, a measured smoke yield was obtained which was even higher, 30% greater than with the heater in its 'horizontal orientation' (Table 2).

To examine the way in which the cone heater affects the yield of smoke from solid fuels, it is necessary to burn them in the absence of supporting radiation. It proved impossible to ignite PMMA slabs, but it was found that a 100 mm diameter tray containing 20 g of PMMA pellets could be ignited successfully using 20 ml of methanol as an 'accelerant'. Methanol had the additional advantage of yielding no smoke, so that the smoke yield could be attributed entirely to the plastic. Similar experiments were carried out with polystyrene pellets, but 6 ml of hexane had to be used to ensure reproducible burning of 15 g of the polystyrene. These tests showed that there was no significant difference in the smoke yield with the cone heater removed and with it in place 25 mm above the sample. This may be due to the fact that the flames produced from the solid fuels were very small, well below the level of the bottom of the heater. This contrasted with the tests using hexane (and with the solid plastics under an imposed heat flux) in which the flames were large, reaching up through the cone heater into the duct for the duration of the test. It would appear that the interaction between the cone heater and the flame interferes with the smoke production process, although it is impossible to investigate the magnitude of the effect for the solids as large flames can only be produced with an imposed heat flux.

The Cone Calorimeter is undoubtedly the most advanced laboratory-scale apparatus which we have for the measurement of the fire properties of materials. For the first time, test results are now available which can be used in fire models, but we must make haste slowly. The present results draw attention to the fact that there is still a need for a greater understanding of the processes occurring in the 'fire model', *particularly* if the use of the Cone is to be extended beyond the original purpose for which it was designed, i.e. the measurement of rate of heat

release for hazard assessment. Furthermore, more work is required on the mechanism of smoke formation in fires under a wide range of conditions before it will be possible to judge if and how estimates of smoke yield from the Cone Calorimeter can be used confidently as input to fire safety engineering design calculations.

REFERENCES

1. Standard Test Method for Heat and Visible Smoke Release Rates for Materials and Products using an Oxygen Consumption Calorimeter ASTM E1354-90. American Society for Testing and Materials, Philadelphia (1990).
2. B. Karlsson and S. E. Magnusson, *Heat Release in Fires*, ed. by V. Babrauskas and S. J. Grayson, pp. 159–72, Elsevier Applied Science, New York (1992).
3. U. Wickstrom and U. Goransson, *Heat Release in Fires*, ed. by V. Babrauskas and S. J. Grayson, pp. 461–78, Elsevier Applied Science, New York (1992).
4. D. D. Drysdale and F. F. Abdul-Rahim, *Fire Safety: Science and Engineering*, ASTM STP 882, ed. by T. Z. Harmathy, pp. 285–300, American Society for Testing and Materials, Philadelphia (1985).
5. G. Atkinson and D. D. Drysdale, *Fire Safety Journal* **15**, 331–35 (1989).
6. H. E. Thomson and D. D. Drysdale, *Fire and Materials* **11**, 163–72 (1987).
7. British Standards Institution. Fire tests on building materials and structures: Part 13. Method of measuring the ignitability of products subjected to thermal irradiance. BS 476: Part 13: 1987.
8. D. J. Rasbash and R. P. Phillips, *Fire and Materials* **2**, 102–9 (1978).

HEAT TRANSFER FROM FLAMES BETWEEN VERTICAL PARALLEL WALLS

M. FOLEY AND D. D. DRYSDALE
University of Edinburgh
Unit of Fire Safety Engineering
The Kings Buildings, Mayfield Rd
Edinburgh, Scotland EH9 3JL

Abstract

Measurements of total heat flux distribution across a wall have been made for propane flames between vertical parallel incombustible boards. The separation between the boards is seen to greatly affect the heat fluxes arising, with a small decrease in separation leading to a significant increase in heat flux at the wall. The burner geometry, position and heat output also alter the heat flux levels and distribution pattern. Altering the air flow into the system, by preventing the flow of air beneath the parallel walls is shown to have a dramatic effect on the heat transfer. The most severe case demonstrates an almost four fold increase in the maximum heat flux from an open base to a closed one. The results and findings have implications for the storage and hazard assessment of bulk materials in warehouses.

Introduction

A large proportion of warehouse fires are started deliberately, this being 'the most common *known* cause of fire outbreak'[1] for the storage of bulk materials. One study showed that this was the case for 37% of warehouse fires[2]. Fires started intentionally are usually serious because the perpetrator makes a conscious effort to locate the seat of the fire in a way that will lead to rapid flame spread.

There are two factors that need to be considered:
(a) how the storage configuration affects the ease with which stored materials can be ignited; and
(b) once ignited, how the configuration influences the rate of fire development.

The aim of this project is to characterise experimentally the heat flux distribution which can occur when a flame is burning between two parallel vertical walls, for various geometries. It is anticipated that the results will be of value in defining the exposure conditions to be used in test methods such as the Cone Calorimeter in order to predict the the behaviour of materials in storage arrays.

Experimental

Two vertical boards were used to represent the surfaces of materials, one instrumented as shown in diagram 1, the other blank. The apparatus was set up as shown, diagram 2, with the different conditions investigated shown in Table 1.

Diagram 1

Instrumented Board

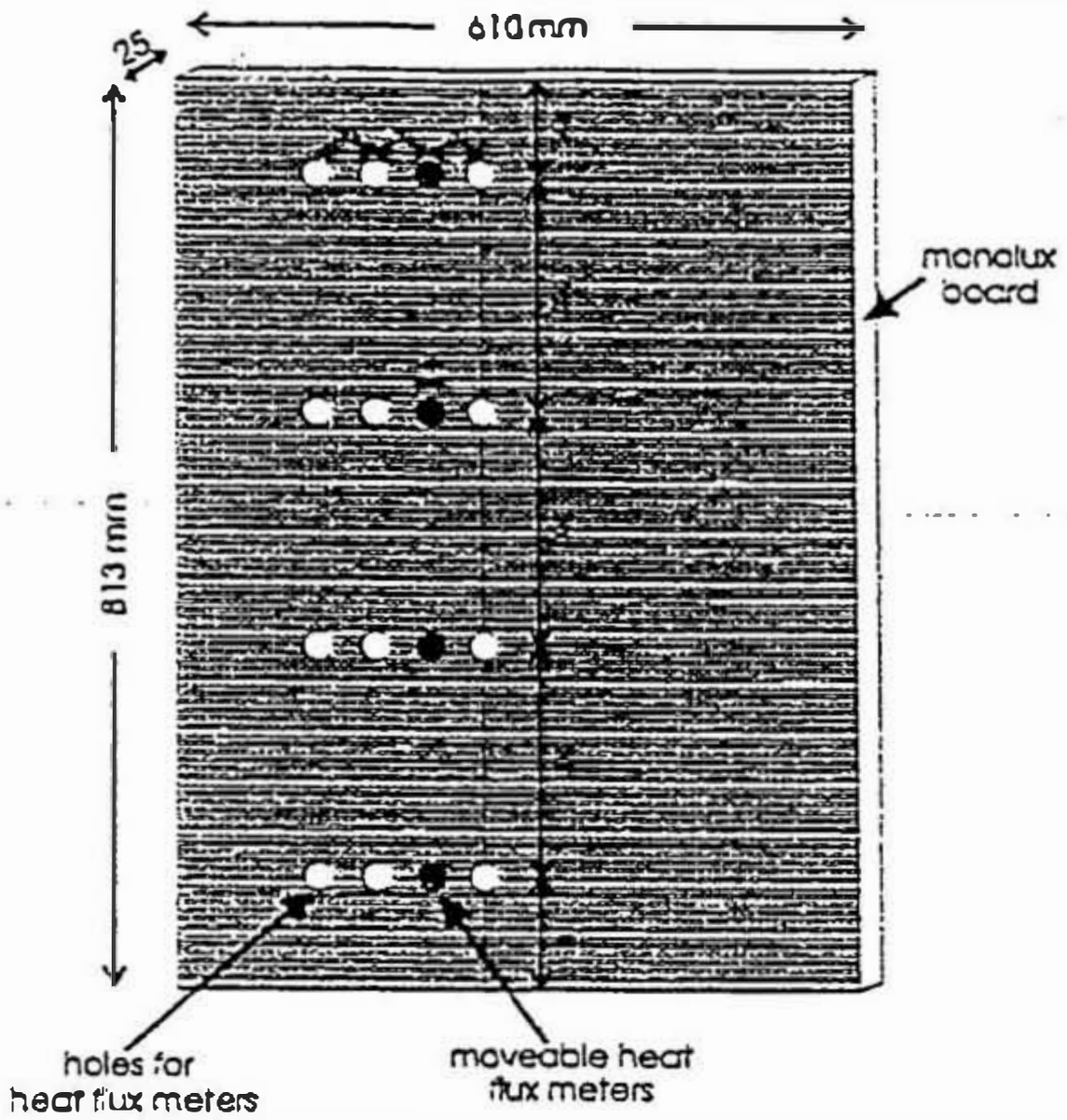

Table 1: experimental configurations

Burner Type	Line(jets), Line(sandbed), Circular(75 mm dia.)
Separation	60 mm, 100 mm, 120 mm[1], 140 mm, ∞[2]
Burner Position	Centre, Instrumented wall, Opposite wall
Base Type	Open[3], Closed
Propane Flowrate	5 l/min, 9 l/min

[1] Circular burner only
[2] Burner at the instrumented wall only
[3] Not for the circular burner
Most, but not all other combinations were investigated

The heat fluxes at sixteen positions on the board were obtained in four experiments by repositioning four heat flux meters as shown in diagram 1. The vacant holes were plugged with kaowool. Each experiment lasted approximately nine minutes: data readings were logged every second during the last three minutes and averaged over the last minute of the test. A number of experiments were duplicated to check the repeatability of the procedure.

Diagram 2

Experimental Setup

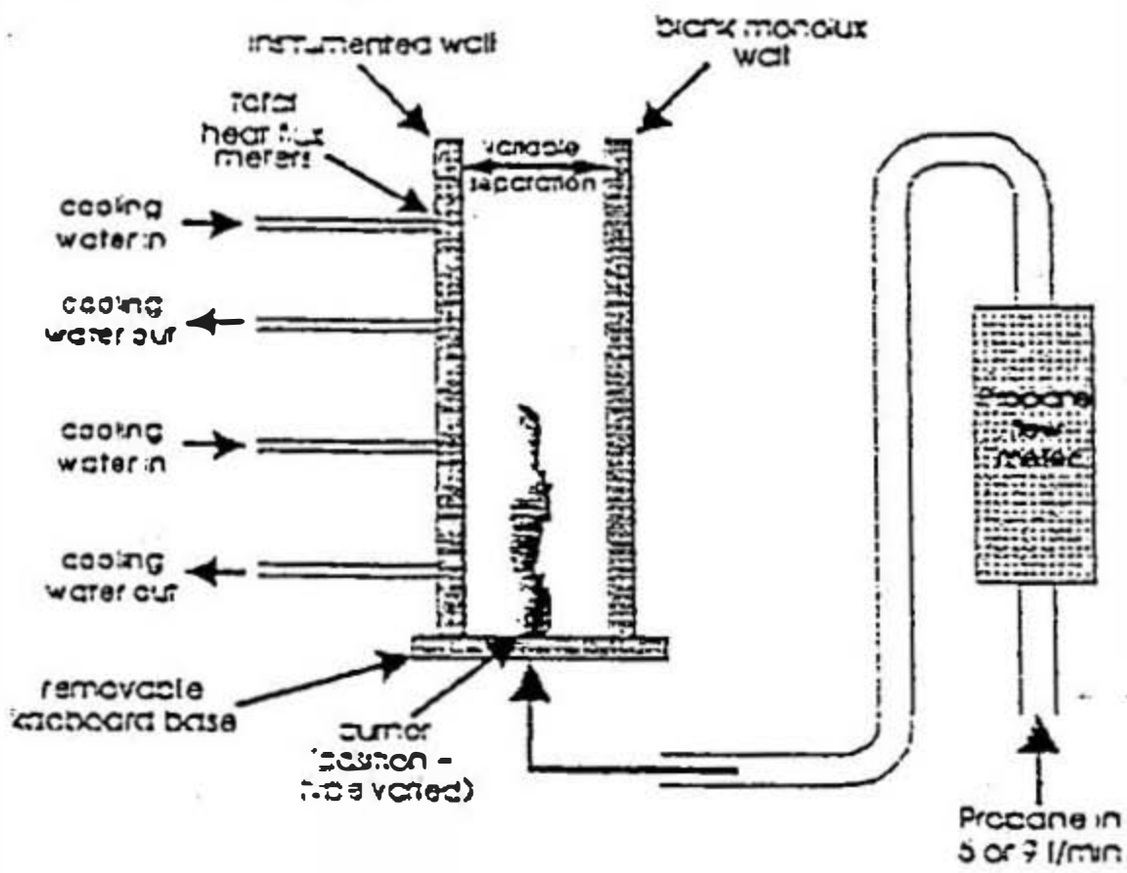

Results

1) The heat flux increases with decreasing separation between the boards for all three burner positions, as shown in diagram 3. This happens for both the open and closed base situations.
2) The contour maps of diagrams 4, 5 and 6 show the difference in heat flux distribution for the different burner types. For the circular burner, the flame is tall and narrow, being mainly in the centre of the boards. For both line burners, the flame covers the entire length of the boards, but is much shorter than for the circular burner.
3) The graphs in diagram 7 show how the position of an ignition source affects the heat fluxes at the wall.
4) Increasing the heat output of the burner or ignition source, as expected, increases the heat flux to the walls, as shown in diagram 8. The gas flow rates of 5 and 9 l/min correspond to heat release rates of 7.6 and 13.6 kW respectively.
5) The contour maps in diagrams 9 and 10 demonstrate the significant influence that air flow has on the flame and heat transfer characteristics of this type of system. In diagram 9, the base is left open whilst in diagram 10 the base is closed and air is unable to enter the system beneath the boards.

Discussion

It is necessary to understand the heat fluxes arising from fires in various different situations in order to be able to test whether materials will ignite and cause flame spread.

The cone calorimeter can give information on the ignitability of materials and, along with certain models, this can be used to assess flame spread. However, the irradiance level in the cone calorimeter must be appropriate to the end use or storage conditions of the material. The heat fluxes produced from flames under different conditions, and those situations which may lead to unexpected values must be fully understood.

A small decrease in the separation of the two walls in the above type of system is seen to cause significant increases in the heat fluxes experienced by the walls.
This is most noticeable for the closed base configuration which is probably affected more as air can only be entrained through the gap at the ends of the boards and not beneath them. This increase in heat flux with separation distance has obvious implications for the storage of bulk materials, as well as for the testing of materials with relation to their future storage conditions.

Burner geometry, varied by using a circular or a line burner, is seen to affect the heat flux distribution across the boards.
The line burners give higher fluxes close to the base of the boards, reasonably uniform across the board, whilst the circular one gives higher values at greater heights, with the heat flux falling across the board. The sandbed line burner gives a similar pattern as the line burner, with slightly higher fluxes near the base of the board. The higher the heat output from the burner, the greater the heat fluxes seen at the walls, for all burners.

The effect of burner position is that, for most separations, the heat flux is greatest for the burner against the instrumented wall.
Heat flux falls as the burner is moved away from the wall and the flame stops impinging on the wall, radiation is reduced and cool air can flow between the burner and the wall. The exception to this is for the line burner with the closed base and a 60 mm board separation, which shows higher heat fluxes with the burner in the centre of the gap than against the instrumented wall. This is probably because, for this situation, the flame fills the entire width of the gap, impinging on both walls, leading to high rates of heat transfer to which cross radiation contributes.

The choice of ignition source in a fire test can lead to different conclusions about the hazard of the material being tested, so selection of an appropriate ignition source is essential.
This decision must be made with knowledge of exposure conditions produced by different ignition sources as well as the end use of the material. Burner output and 'standoff' distance from a wall have also been shown to affect the heat flux distribution in a corner in work done on room fire test ignition sources, Williamson *et al*[4]. Burner size was also shown to be important by Ahonen *et al*[5], as the proportion of radiative and convective heat transfer can be altered by changing the burner size.

The different configurations of open and closed base give rise to different levels of heat flux
These configurations occur in warehouse storage when materials are stacked on pallets or directly on the ground. In these tests when the base is open, representing storage on a pallet, the air is able to flow under the boards to the flame. The heat fluxes produced are lower than they are for the closed base, when air may only enter at the ends. The most noticeable case is when the burner is in the centre of the separation. Cool air can then come between the flame and both walls for the open base, keeping the heat fluxes down. With the closed base, cool air cannot do this and the flame is thicker, filling the gap and giving rise, in the most severe case, to almost four times the heat flux of the open base.

Conclusions

1. For a configuration where cross radiation occurs between two parallel surfaces, the heat fluxes experienced by the surfaces increase significantly with decrease in separation between the surfaces.

2. The type and geometry of burner used as a heat or ignition source affects the heat flux distribution.

3. Burner / ignition source position has an important influence on heat flux distribution and it is not always the case that simply moving the burner away from the instrumented wall decreases the flux to that wall.

4. The higher the gas flow rate to the burner, the higher the heat fluxes at the wall

5. Reducing air flow to the flame, by preventing air entering under the boards, leads to significant increases in heat fluxes to the surfaces, which has implications for the storage of materials.

6. A precise understanding of the potential exposure conditions of materials in bulk storage is necessary in order that appropriate ignition sources and test methods are used to assess their hazard.

References

1. Hymes, I. and Flynn, J. F., The probability of fire in warehouses and storage premises. Safety and Reliability Directorate. HSE Report No. HSE/SRD/089/00001/89/ Draft A.

2. Ward, R. B., A survey of major fires in warehouses containing dangerous chemicals. Fire Prevention 175 pp 20-27, Dec. 1984.

3. Fire tests on building materials and structures. Part 1. Method for measuring the rate of heat release of products. British Standard BS 476 : Part 15 : 1993.

4. Williamson, R. B., Revenaugh, A. and Mowrer, F. W., Ignition sources in room fire tests and some implications for flame spread evaluation. Fire Safety Science, Proceedings of the Third International Symposium pp 657-666, 1991.

5. Ahonen, A. I., Holmlund, C. and Kokkala M. A., Effects of ignition source in room fire tests. Fire Science and Technology Vol. 7 No. 1 pp 1-13, 1987.

Diagram 3

Centreline Heat Flux versus 1/Board Separation,
Line Burner at Instrumented Wall, 9 l/min Propane

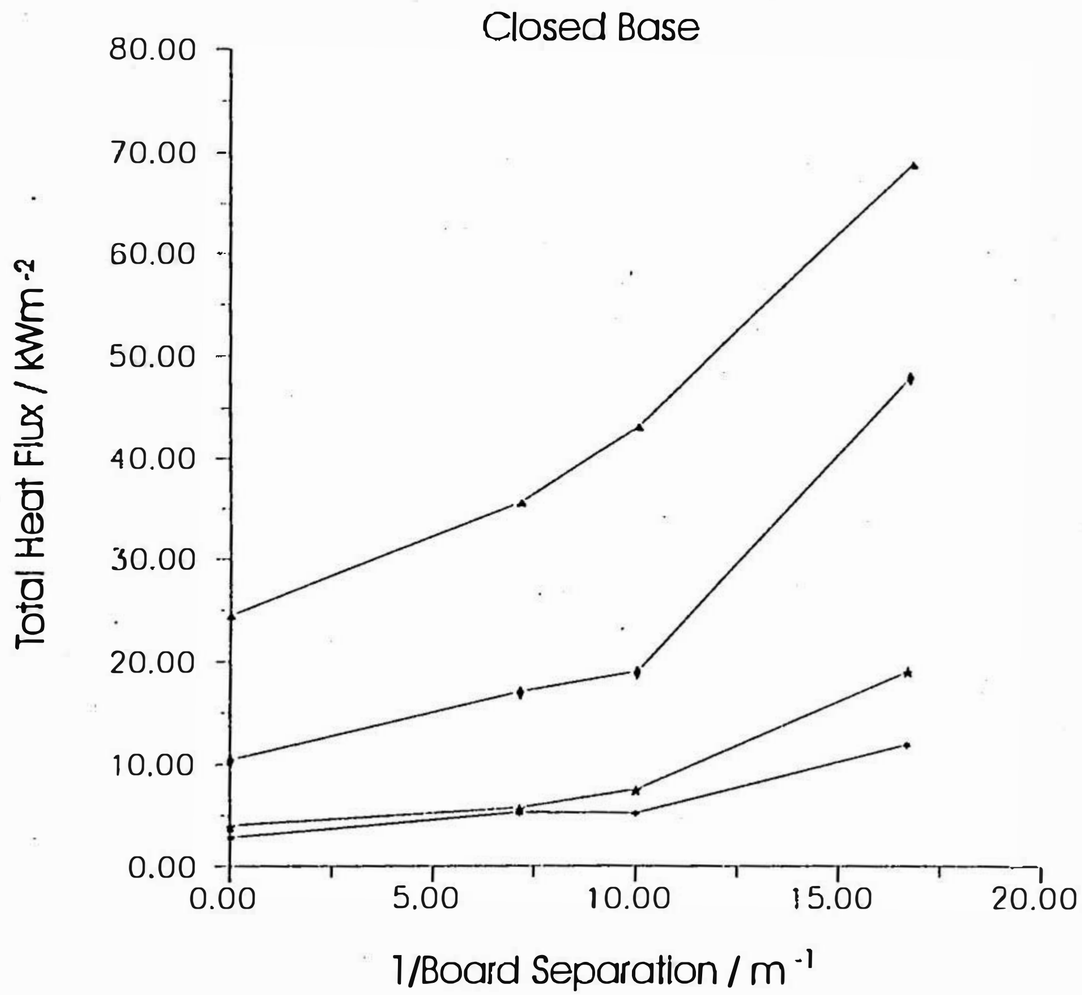

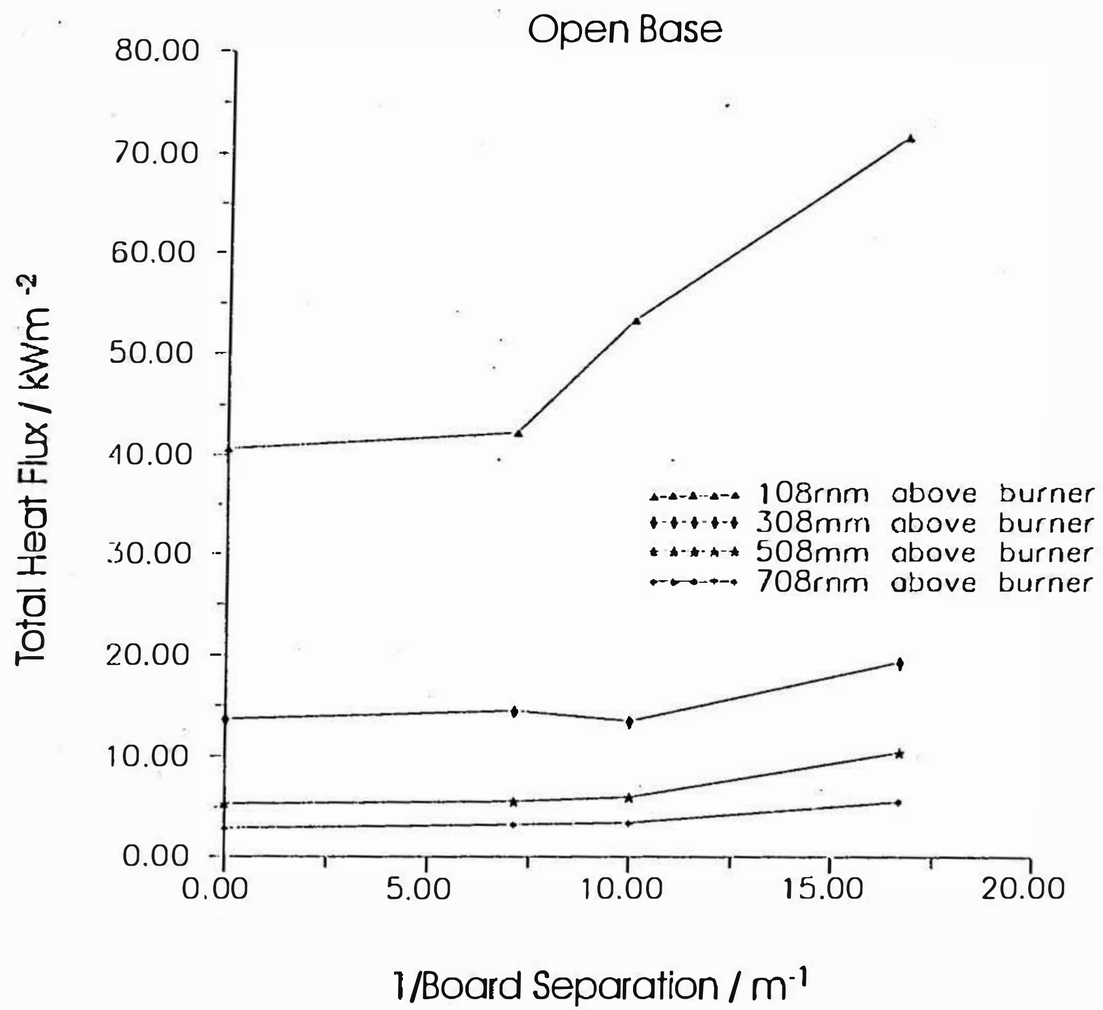

Diagram 4

Circular Burner

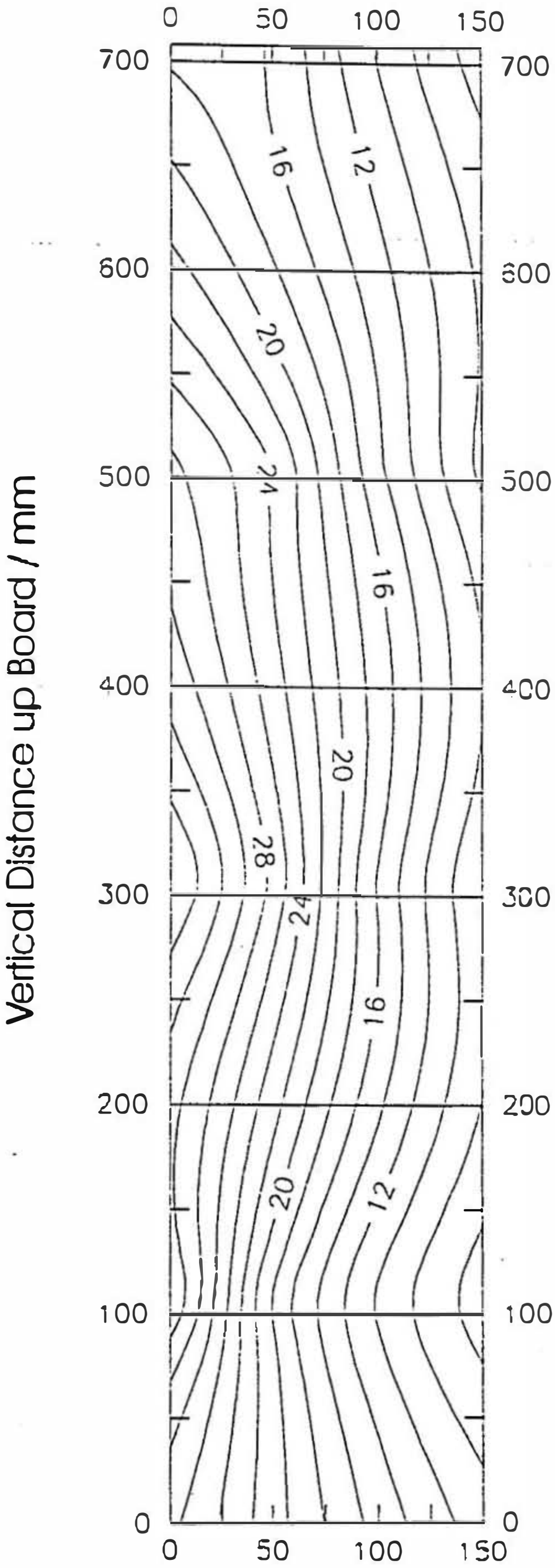

Diagram 5

Line Burner

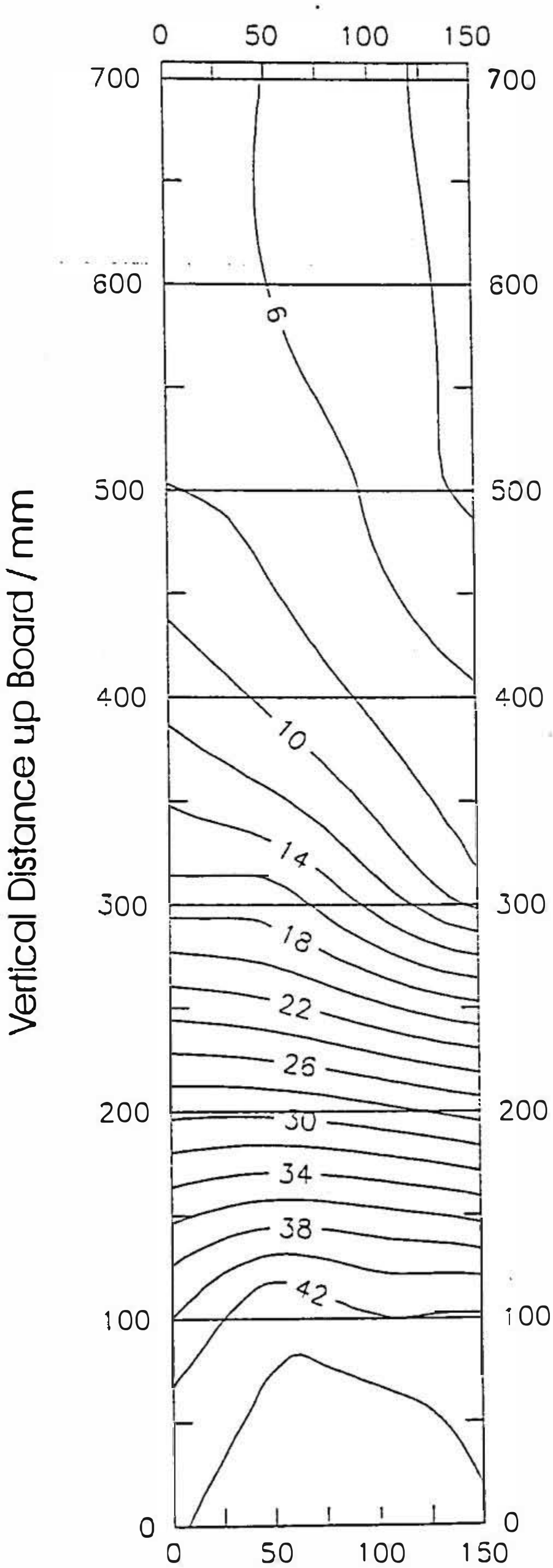

Diagram 6

Sandbed Burner

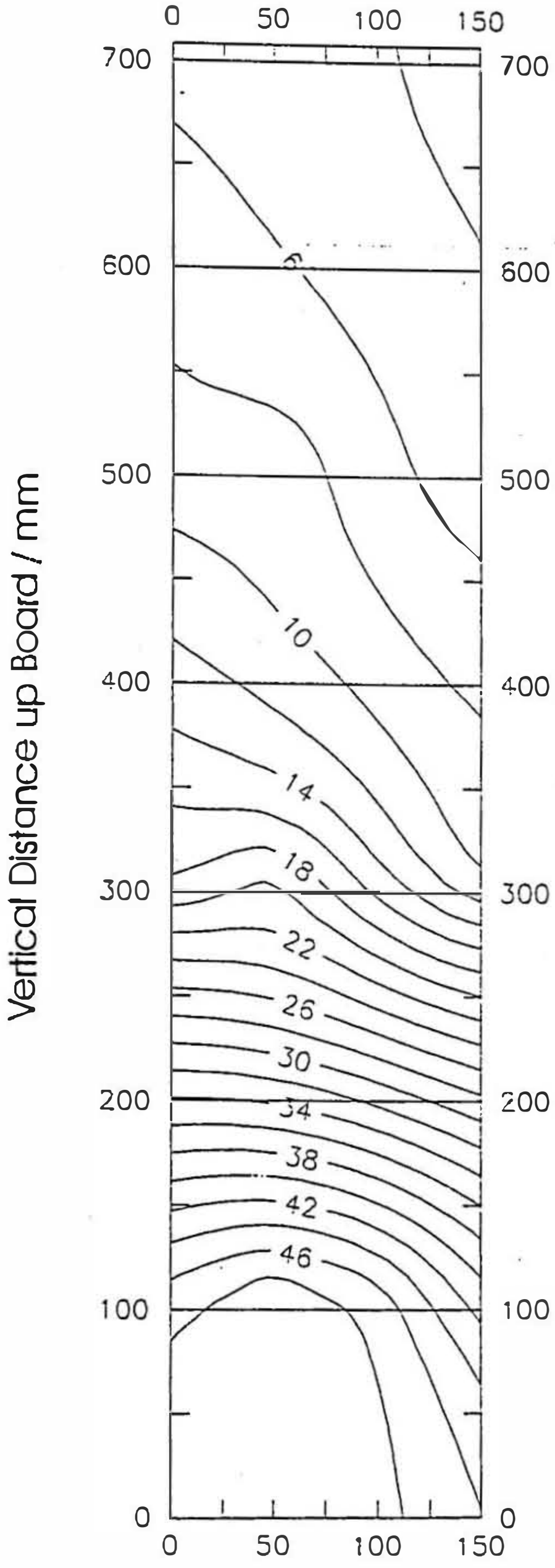

Diagram 7

Centreline Heat Flux versus Vertical Distance up the Board,
Line Burner at Different Positions, 5 l/min Propane

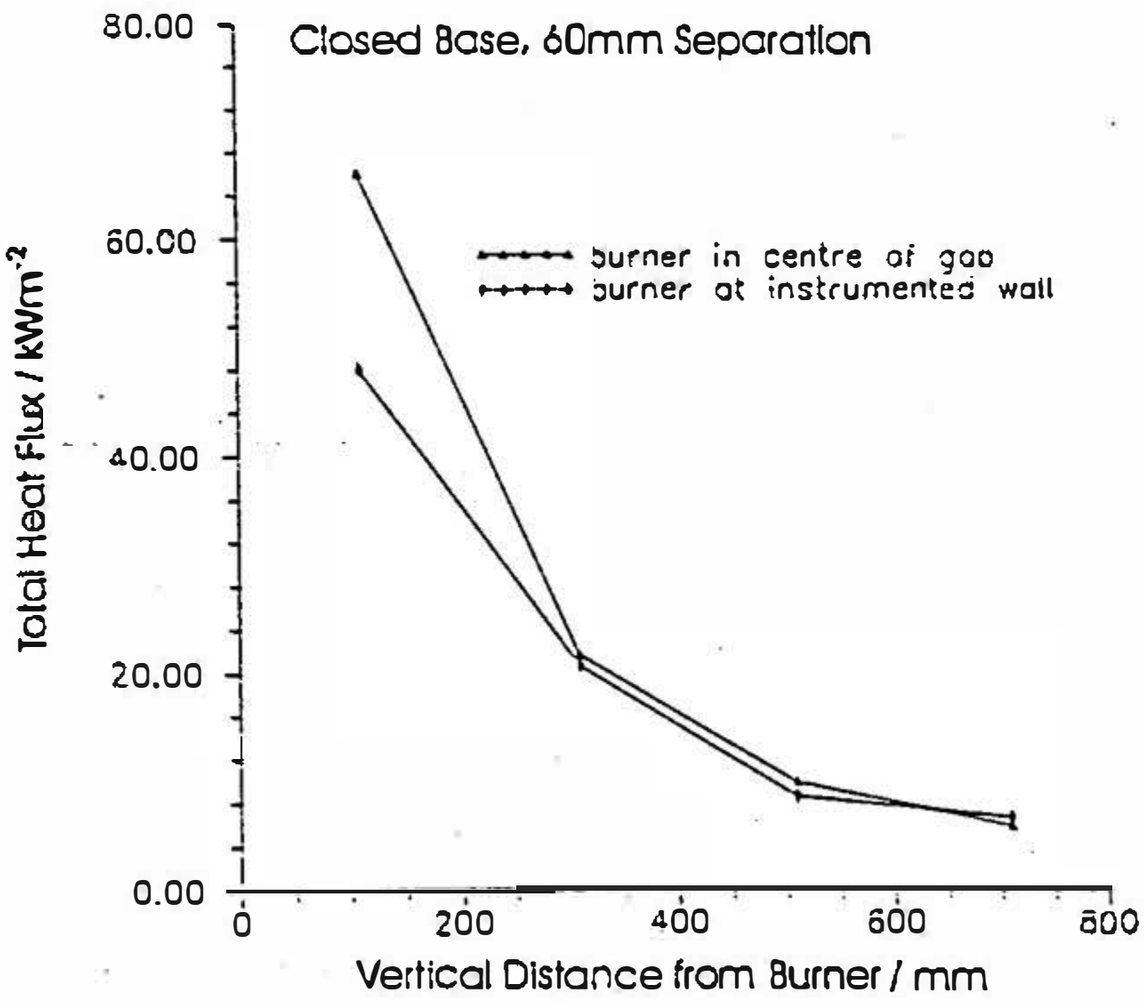

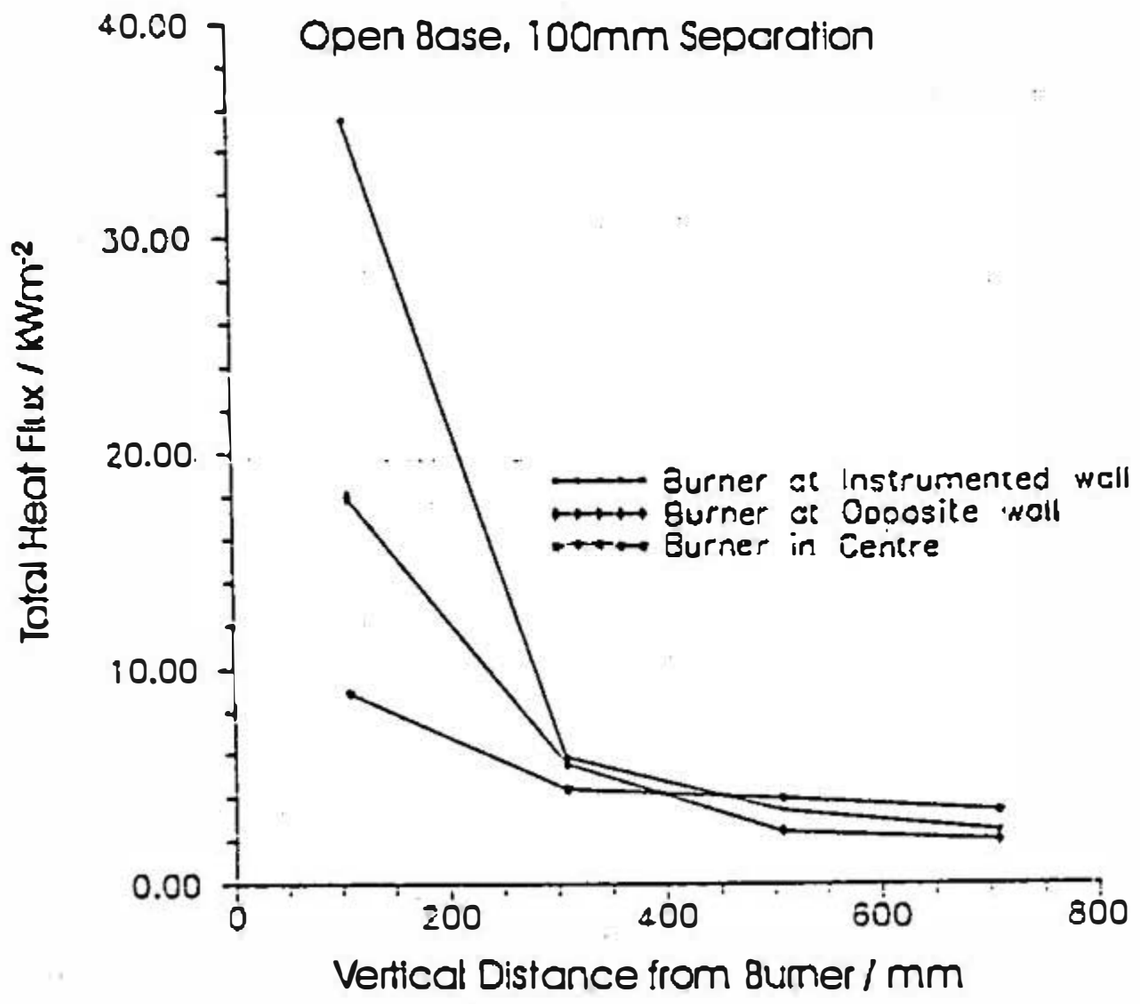

Diagram 8

Centreline Heat Flux versus Vertical Distance up the Board,
Line Burner in the Centre of the Gap, Open Base,
Variable Separation and Flowrate.

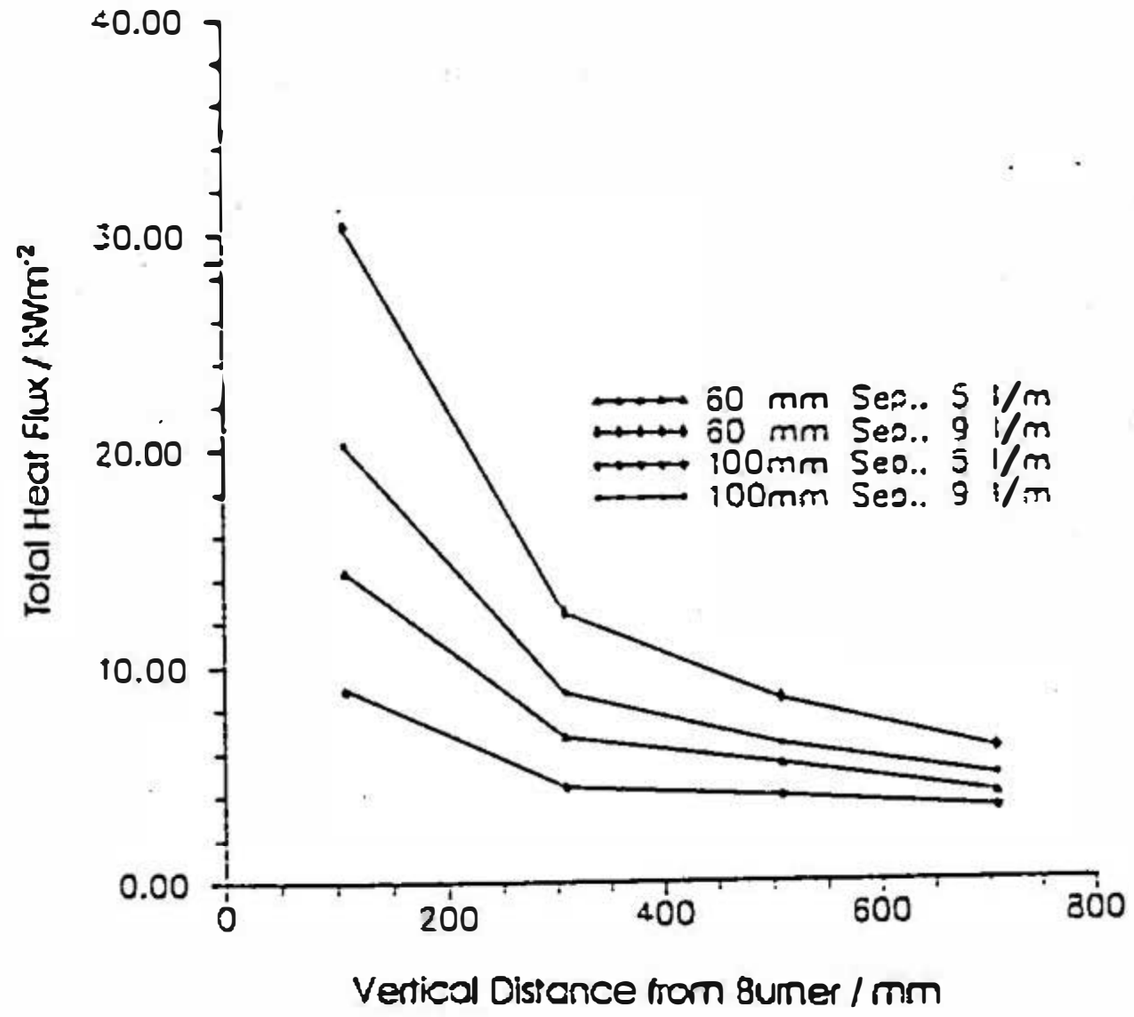

Contour plots of heat flux distribution over the Board /kWm^{-2} for 60 mm separation, 9 l/min

Diagram 9

Open Base

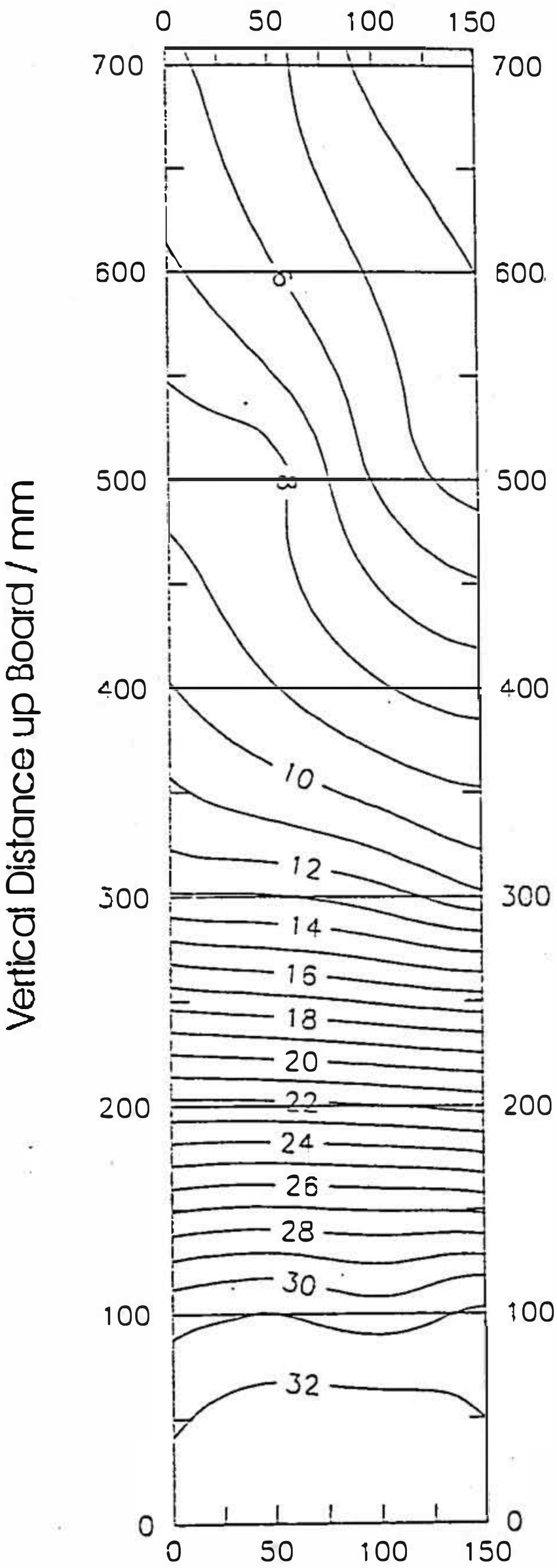

Diagram 10

Closed Base

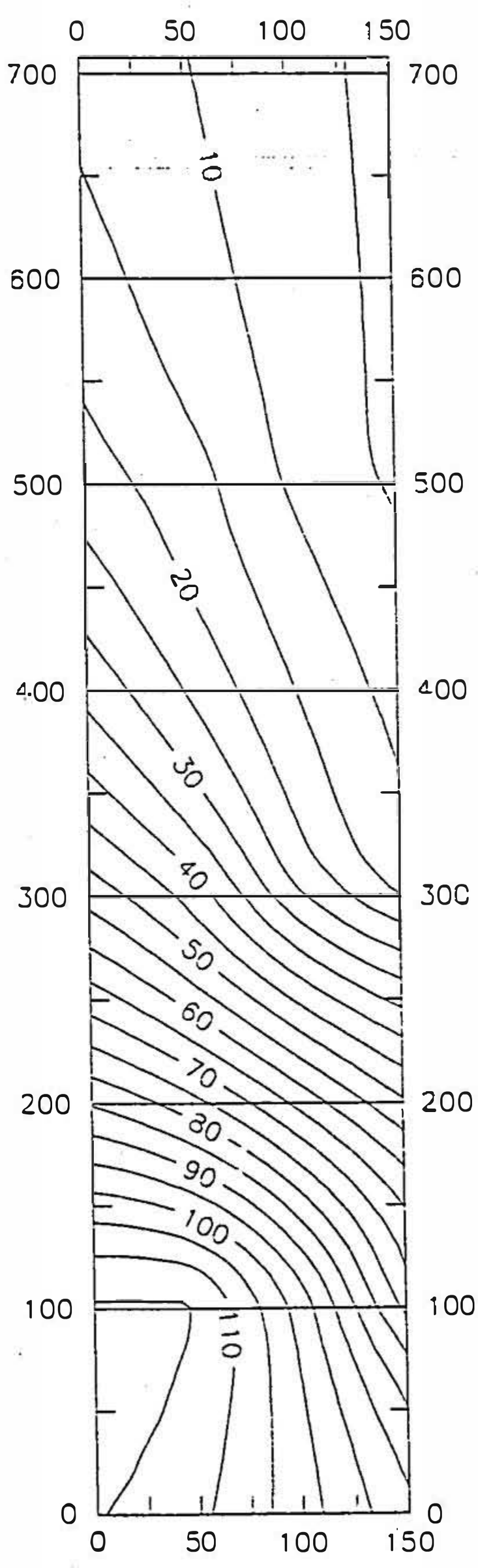

ELSEVIER

0379-7112(94)00000-0

Fire Safety Journal 00 (1995) 000–000
© 1995 Elsevier Science Limited
Printed in Northern Ireland. All rights reserved
0379-7112/95/$07·00

Heat Transfer From Flames Between Vertical Parallel Walls

M. Foley & D. D. Drysdale

University of Edinburgh, Unit of Fire Safety Engineering, The Kings Buildings, Mayfield Rd, Edinburgh, Scotland EH93JL

(Received 23 August 1994; revised version received and accepted 4 November 1994)

ABSTRACT

Measurements of the distribution of total heat flux on a wall exposed to a line burner have been carried out for a number of configurations in which the distance to a parallel wall has been varied. It has been shown that the heat fluxes increase as the separation between the walls is reduced. The burner position and heat output influence not only the levels of heat flux, but also the distribution pattern. Changing the air flow by blocking the ingress of air at the base of the walls is shown to have a dramatic effect. The most extreme case gave almost a four fold increase in the maximum heat flux when the base is closed off. Correlations have been obtained with a line burner symmetrically placed against an instrumented wall for q''_w *in terms of* $x/Q_l^{*2/3}D$, y'/D, *and* a/D, *with correlation coefficients of at least* 0·957. *The results and findings have implications for modelling flame spread in confined spaces, and for identifying and assessing the risks associated with the bulk storage of materials.*

NOTATION

a	separation distance between walls or boards, m
C_p	specific heat capacity, kJ/kg K
D	line burner length, m
g	acceleration due to gravity, m/s^2
h	height of vertical fuel surface, m
l	flame length, m
q''_w	wall total heat flux, kW/m^2

$\dot{Q}$	burner heat release rate, kW
$\dot{Q}_l$	burner heat release rate per unit length, kW/m
Q_l^*	dimensionless line burner heat release rate
T_∞	ambient temperature, K
x	height, m
y	horizontal distance from wall centreline, m
y'	horizontal distance, $y' = 0{\cdot}5D - y$; $(0 \leq y' \leq 0{\cdot}5D)$, m
ρ_∞	density of ambient air, kg/m^3
κ	flame absorption coefficient, m^{-1}
σ	Stefan–Boltzmann constant, kW/m^{2}K^4

INTRODUCTION

In recent years, a great deal of progress has been made in modelling flame spread over combustible materials.[1,2,3] Date from the Cone Calorimeter on the time to ignition and the rate of heat release can be used to model the rate of growth of the wall fire in which the rate of spread is determined by heat transfer from the vertical flame to the fuel above and ahead of the burning area.[4] This is considered to be the 'worst' orientation for rapid fire development over a combustible wall lining, but there are other configurations which can lead to even more rapid fire growth. One example is to be found in storage arrays in warehouses where the vertical channels between adjacent stacks offer an ideal pathway for fire growth.

Warehouse fires are particularly serious. A large proportion of these are started deliberately, this being 'the most common *known* cause of fire outbreak' for the storage of bulk materials.[5] One study has shown that this was the case for 37% of warehouse fires.[6] Fires started intentionally are usually serious because the perpetrator makes a concious effort to locate the seat of the fire in a way that will lead to rapid fire growth. Fire protection is difficult in such circumstances and there is a need to understand the fire spread mechanism in more detail to enable the risks to be quantified, and perhaps reduced by avoiding storage geometries which are particularly hazardous.

There is a dearth of information on vertical fires spread in confined spaces, despite the fact that it is recognised that this is a relatively common mechanism for rapid fire growth, sometimes leading to multiple fatalities in buildings. Assessing the hazard of combustible materials which may be used in such configurations requires an understanding of the effect of such geometries on ignition and flame spread characteristics. Two factors need to be considered:

(a) how the configuration affects the ease with which materials can be ignited by a given ignition source; and
(b) once ignited, how the configuration influences the rate of fire development.

There are no data available which may be used to quantify the hazard associated with this type of scenario. Consequently, work has been undertaken to determine the heat flux distributions which can occur when a flame is burning between two parallel, vertical surfaces, or walls, typical of the configurations which exist in warehouse storage.

Studies of the interaction of flames with vertical surfaces have been carried out, but the majority of the correlations which have been produced deal with flame height or temperature.[7,8,9] Hasemi[10] extended his research to the problem of heat fluxes from flames from a line burner to thermally thin and isothermal walls. He found the wall heat flux to be a function of $x/Q_l^{*2/3}D$, where x is the height above the burner, Q_l^* is a dimensionless heat release rate given by $Q_l^* = \dot{Q}_l/(\rho_\infty c_p T_\infty g^{1/2} D^{3/2})$ and D is the length of the line burner, within the range $0{\cdot}037 \leq D \leq 0{\cdot}082$ m, and $16{\cdot}7 \leq \dot{Q}_l \leq 218$ kW/m. Different expressions were found for wall fluxes at heights corresponding to different regions of the fire plume, *viz.* the near field (flame continuously present), the transition region and the buoyant plume. Quintiere *et al.*[11] performed experiments on six combustible materials in a similar manner to Hasemi[10] and compared their data to that for the incombustible walls. Measurements of wall heat flux showed an apparent universal distribution when plotted against the ratio of vertical distance (x) to flame height, although the authors expressed concern that this could be altered by changes in energy release rate and radiation effects for larger wall flames. Data from the burning materials showed the relationship $\dot{q}''_w \propto x^{-p}$, where $p \sim 2{\cdot}4$, which is consistent with findings of Ahmed & Faeth.[12] In 1994, Quintiere & Cleary[13] took data from several of the above sources for line fires against walls, square burner flames against walls and in corners, and window flames impinging on a wall. They investigated correlations for flame heat flux in terms of configuration and fuel properties. They deduced that

$$\frac{\dot{q}''}{\sigma T_\infty^4} = \mathrm{f}\left(\frac{x}{l}, \frac{y}{l}, \frac{l}{D}, \kappa D\right),$$

where l is flame length, x and y are the vertical and horizontal co-ordinates, κ is the flame absorption coefficient, and D is the characteristic burner dimension.

The interaction of flames with a wall has also been studied in

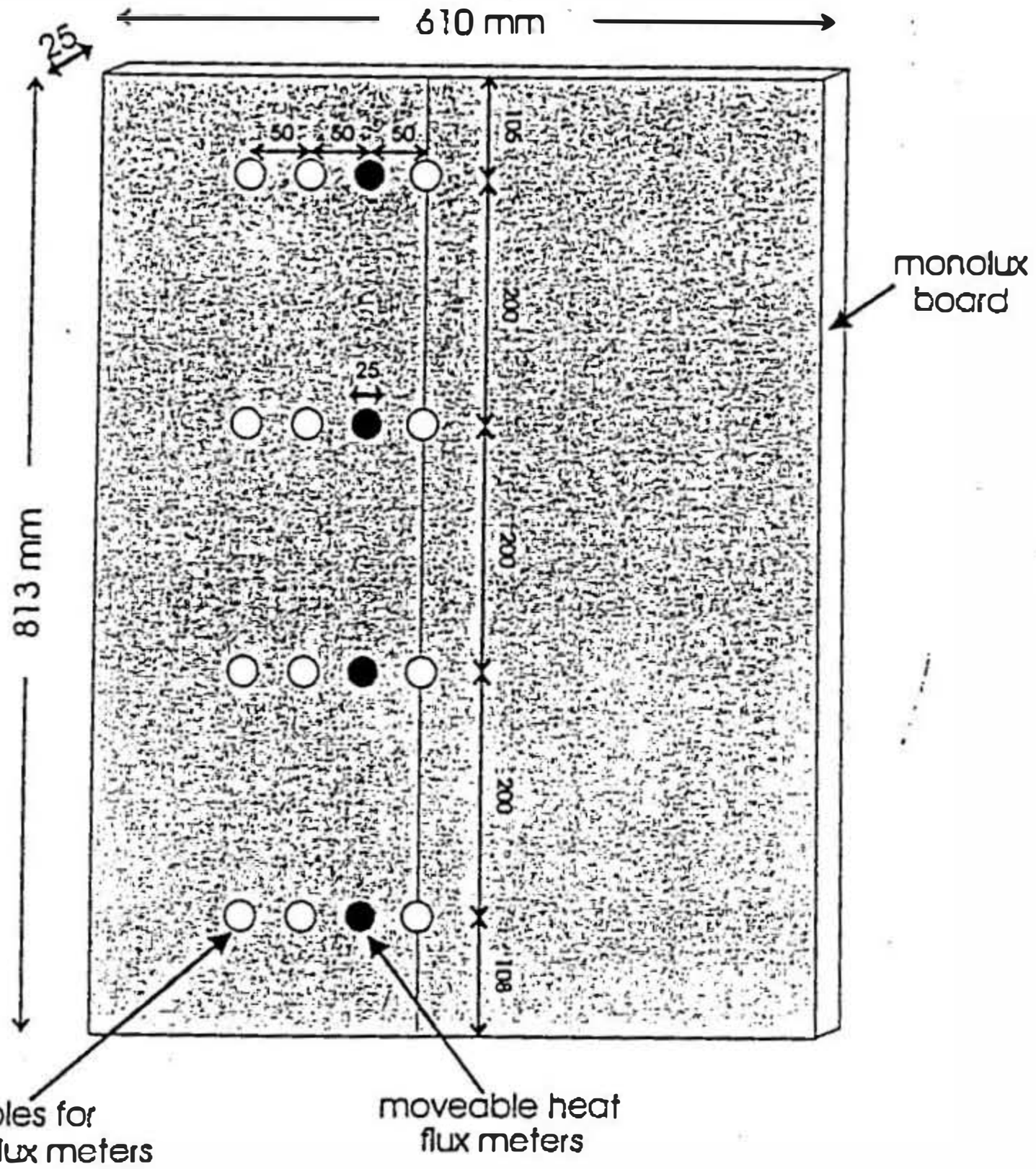

Fig. 1. Instrumented board.

boards (Monolux), 610 mm × 813 mm × 25 mm, one of which was instrumented with four Gardon-type total heat flux meters as shown in Fig. 1. the other board was blank. It was assumed that the heat flux distribution across the board was symmetrical about the board centre-line. Measurements of heat flux were obtained at four heights above the burner and at four horizontal positions, giving a sixteen point heat flux distribution across the wall. The apparatus was set up as shown in Fig. 2.

The separation between the boards was varied from infinity (the 'one wall' scenario) down to 60 mm. An incombustible base (600 mm × 500 mm × 40 mm Kaoboard) at the foot of the walls could be removed to allow air to flow vertically upwards into the space between the 'walls'. When the base was in place, air could only enter horizontally at the sides of the boards. Two burner flow rates were chosen, 5 and 9 l/min, corresponding to 7 and 12·5 kW, assuming complete combustion. The line burner was 600 mm long and 10 mm in diameter with

connection with exposure conditions produced by ignition sources and burners in fire tests, notably the Room Fire Test. Williamson *et al.*[14] examined the effects of burner location and intensity (heat output) on the heat fluxes at a wall and in a corner, and found both to be important although no correlations were obtained. The distance of the burner from the wall was particularly significant. Ahonen *et al.*[15] showed experimentally that the burner geometry also is an influencing factor in the wall exposure conditions.

No heat transfer measurements appear to have been made for flames at a vertical surface close to a parallel wall which would be relevant to a number of problems, including that of bulk storage in warehouses. The confinement provided by this type of configuration is known to have a significant effect on air flow patterns which in turn influence the heat transfer processes. Thus, Toong[16] found that when the separation of two parallel fuel plates burning in an oxidising stream was reduced, the burning rate increased significantly. Kim *et al.*[17] found that the burning rate of inward-facing combustible boards depended on the channel geometrical arrangement, $h/(a/2)^4$ where h is the height of vertical fuel surfaces and a is the separation between them. For small values of $h/(a/2)^4$ the total burning rate is proportional to $h^{3/4}$ and does not depend on the separation, whilst for large $h/(a/2)^4$ the total burning rate is independent of the channel height but proportional to a^3. Between these two extremes lies a transition region. The small scale of these tests meant that the flames were laminar. Further work,[18,19,20] on turbulent flames, has suggested that changes in the heat fluxes at walls (and the accompanying burning rate) in these configurations are caused by a change in the dominant heat transfer mechanism from radiative to convective as the separation is reduced. The most recent report[21] dealing with the issue of rack storage in warehouses demonstrates that the separation between the parallel walls is the most important geometrical parameter, whilst the positioning of horizontal flues for the air inflow was unimportant. However, no systematic heat transfer measurements were made, and there remains a dearth of relevant data. The present work was undertaken to study this aspect of heat transfer from flames.

EXPERIMENTAL

Measurements of the heat flux distribution at the surface of a vertical wall exposed to flames from a propane line burner were made for single and parallel wall arrangements. The 'walls' consisted of incombustible

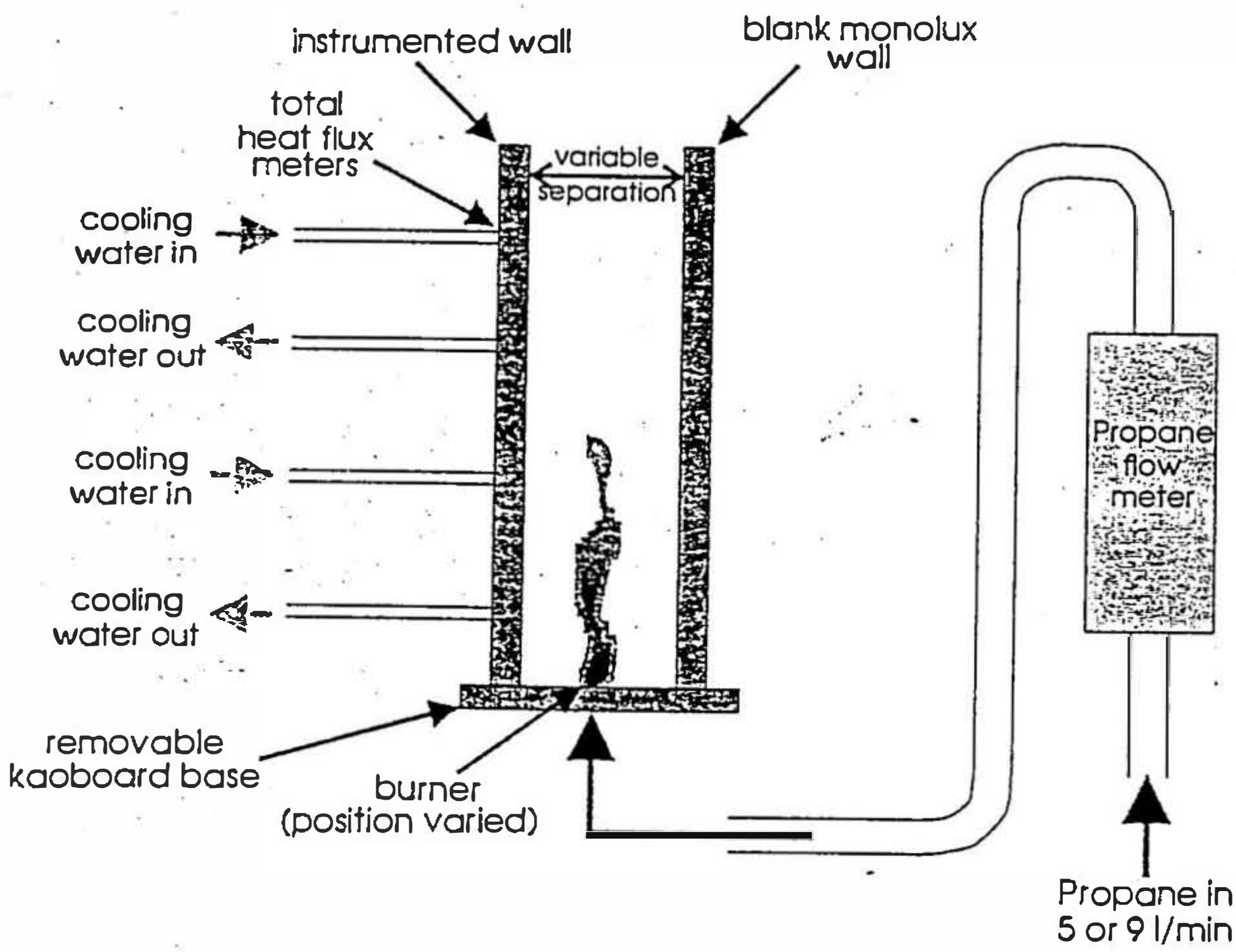

Fig. 2. Experimental setup.

1 mm holes at 10 mm intervals. The experimental configurations which were investigated are summarised in Table 1.

As only four Gardon gauges were available, the heat fluxes at sixteen positions on the board were obtained in four separate experiments by repositioning the heat flux meters as shown in Fig. 1. The vacant holes were plugged with Kaowool. Each experiment lasted approximately nine minutes: data readings were logged (using a Microlink system) every second during the last three minutes and averaged over the last minute of the test when steady state conditions were deemed to exist.

TABLE 1
Experimental Configurations

Separation	60 mm, 100 mm, ∝†
Burner position	Centre, Instrumented wall, Opposite wall
Base type	Open, Closed
Propane flowrate	5 l/min, 9 l/min

† Burner at the instrumented wall only. Most, but not all other combinations were investigated.

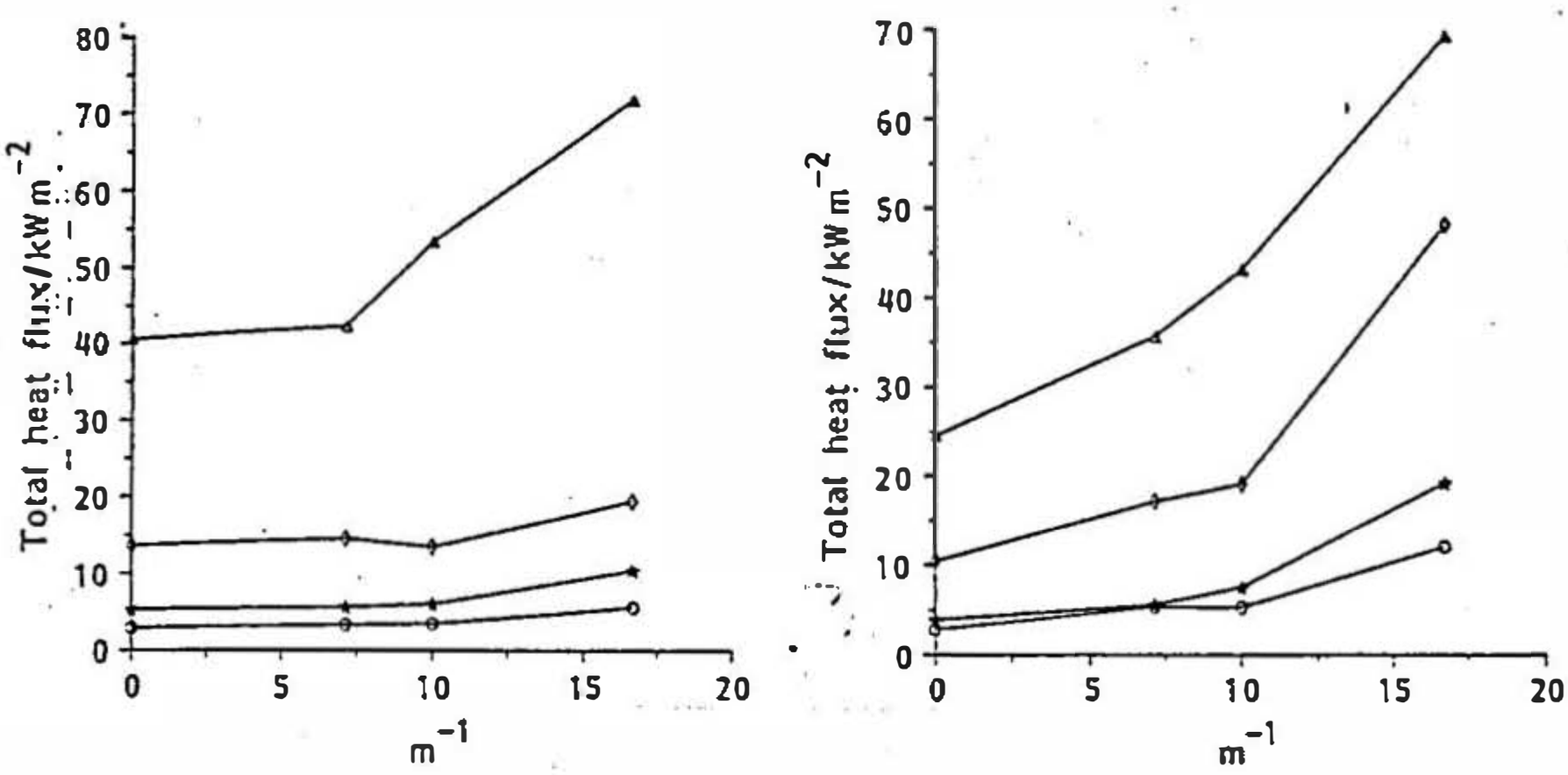

Fig. 3. Heat flux as a function of 1/board separation, burner against the instrumented wall. $\dot{Q}$ = 12·5 kW; Δ, 108 mm above burner; ◇, 308 mm above burner; ☆, 508 mm above burner; ○, 708 mm above burner.

Just over a quarter of the tests were duplicated to check the repeatability of the procedure: the maximum discrepancy was only 9%.

RESULTS AND DISCUSSION

The data were logged automatically and collected on disc for ease of processing. They are not included here in the interests of brevity: key aspects of the results may be presented most economically in graphical form.

The effect of reducing the separation between the boards is shown clearly by the centreline measurements in Fig. 3 for the open and closed base configurations. These results were obtained with the burner at the instrumented wall. The observed increase in heat flux with decreasing separation is consistent with the results of Toong[16] and Kim *et al.*[17]

Results for the different burner gas flow rates, and therefore heat release rates, are shown in Fig. 4. As would be expected, the higher burner heat release rate yields higher heat fluxes at the wall. The influence of the position of the line burner on the heat flux as a function of height on the centreline is shown in Fig. 5. For the 60 mm separation and a closed base the heat fluxes are highest for the burner in the centre of the gap. For all other cases, the highest heat fluxes are found with the burner against the instrumented wall. Subsets of the results are shown as contour maps in Fig. 6 for a 60 mm separation with the line burner at the centre of the gap. These demonstrate the significant

ωω 64288 adj = +5pts

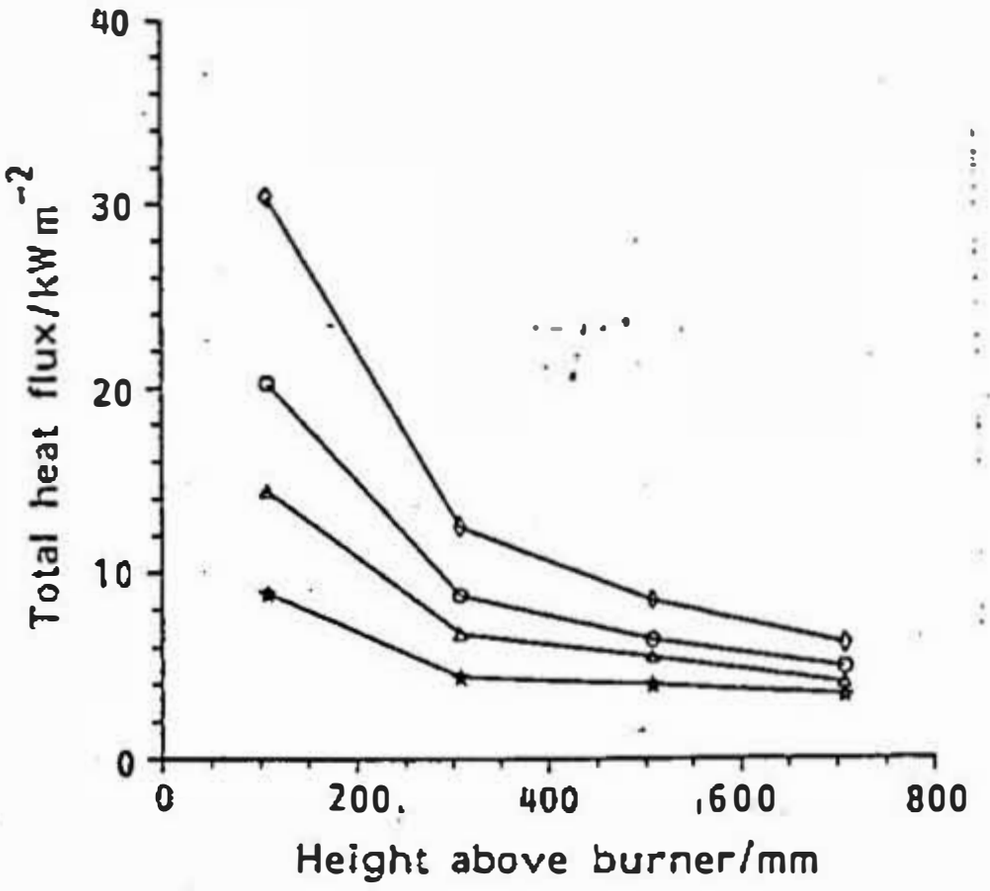

Fig. 4. Heat flux as a function of height, burner in the centre, with the base open, variable separation and burner heat release rate, centreline fluxes only. △, 60 mm separation, 7 kW; ◇, 60mm separation, 12·5kW; ☆, 100 mm separation, 7 kW; ○, 100 mm separation, 12·5 kW.

influence that air flow has on the flame and heat transfer characteristics of this type of system. These measurements are consistent with visual observations which showed that when the base is closed, the flame is gathered towards the centreline, influenced by the air flow induced from the open ends of the gap. With the base open, the flame was seen to behave more as a uniform sheet between the two walls. This behaviour is shown in the photographs in Fig. 7 with the closed base, the flame tends to fill the gap, impinging directly on both walls.

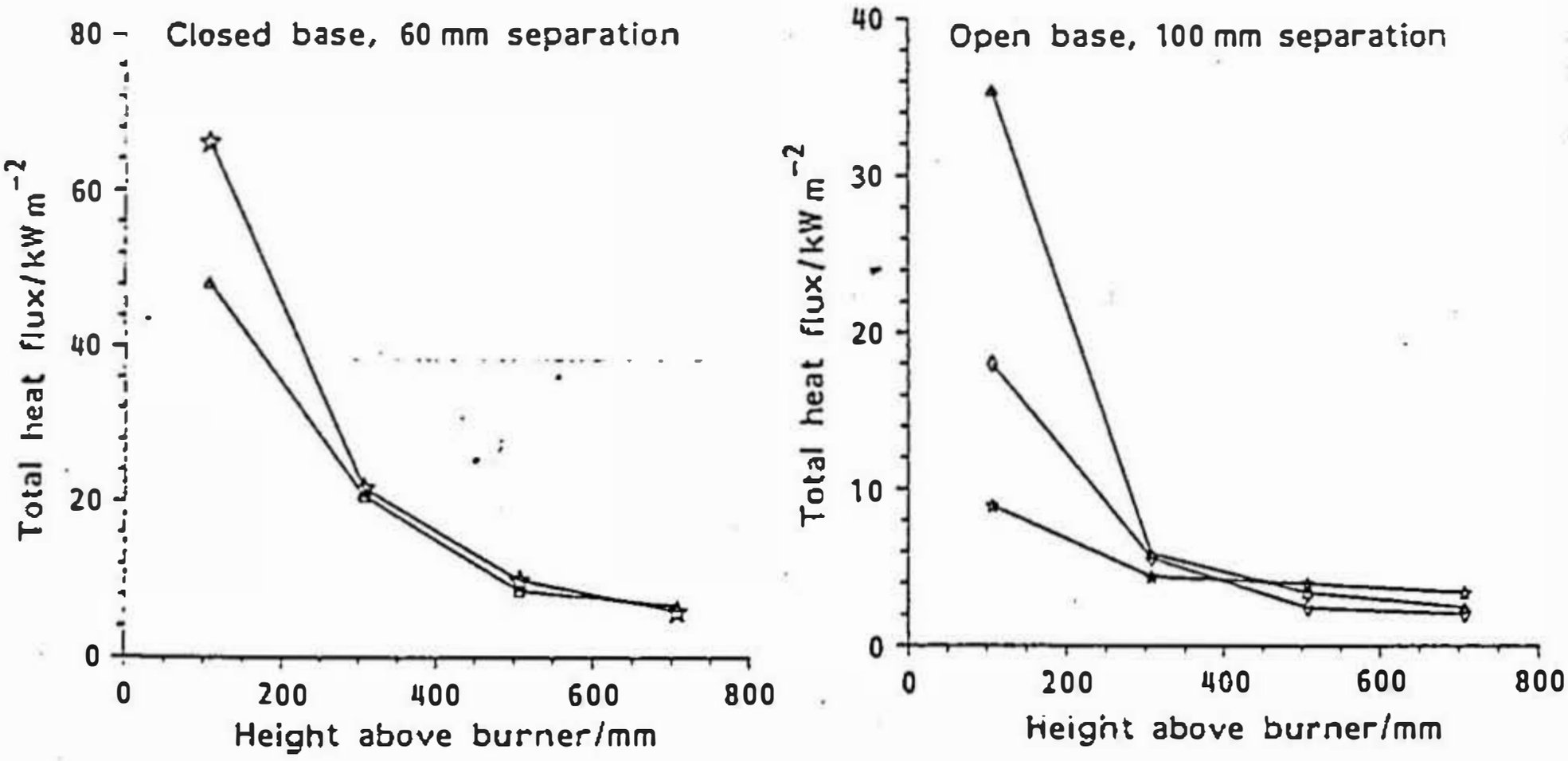

Fig. 5. Heat flux as a function of height, burner at different positions, $\dot{Q} = 12{\cdot}5$ kW, centreline fluxes only. △, burner at the instrumented wall; ☆, burner in the centre of the separation; ◇, burner against the opposite wall.

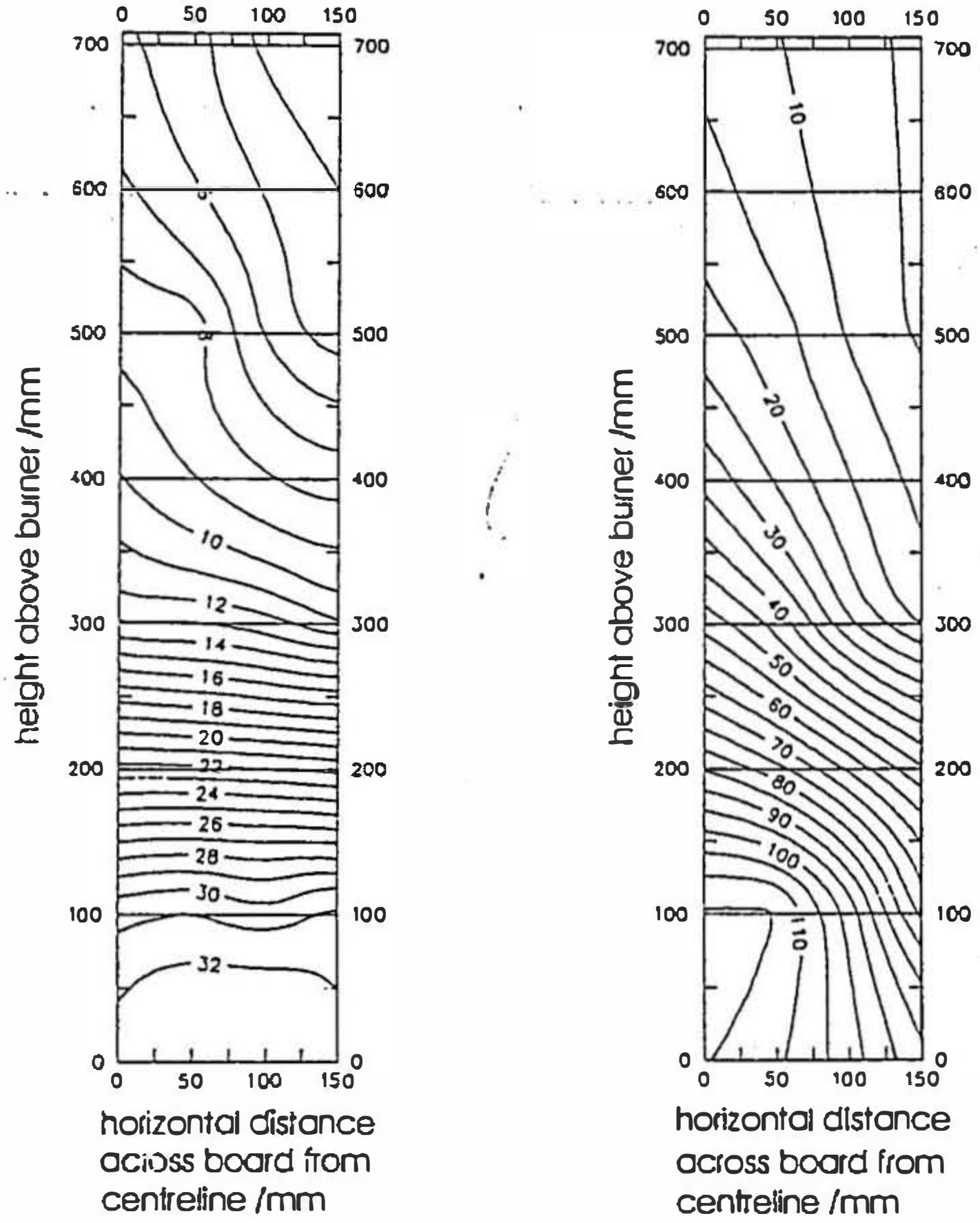

Fig. 6. Contour maps of total heat flux/kW m^{-2} over the board, 60 mm separation, burner in centre of separation, $\dot{Q} = 12{\cdot}5$ kW. (a) Open base; (b) closed base.

Correlations have been sought for the measured heat fluxes and their dependence on the experimental variables. Regression analysis was carried out (using the 'Minitab' software package) on subsets of the data, examining the dependence on Q_l^*, a/D, x/D and y'/D, and as well as the dimensionless groups identified by Quintiere & Cleary.[13] However, there was an insufficient range of data to make it worthwhile examining the effect of κD, and a preliminary check on using flame height in the dimensionless groups was not encouraging. The

000 64288 adj = +19pts

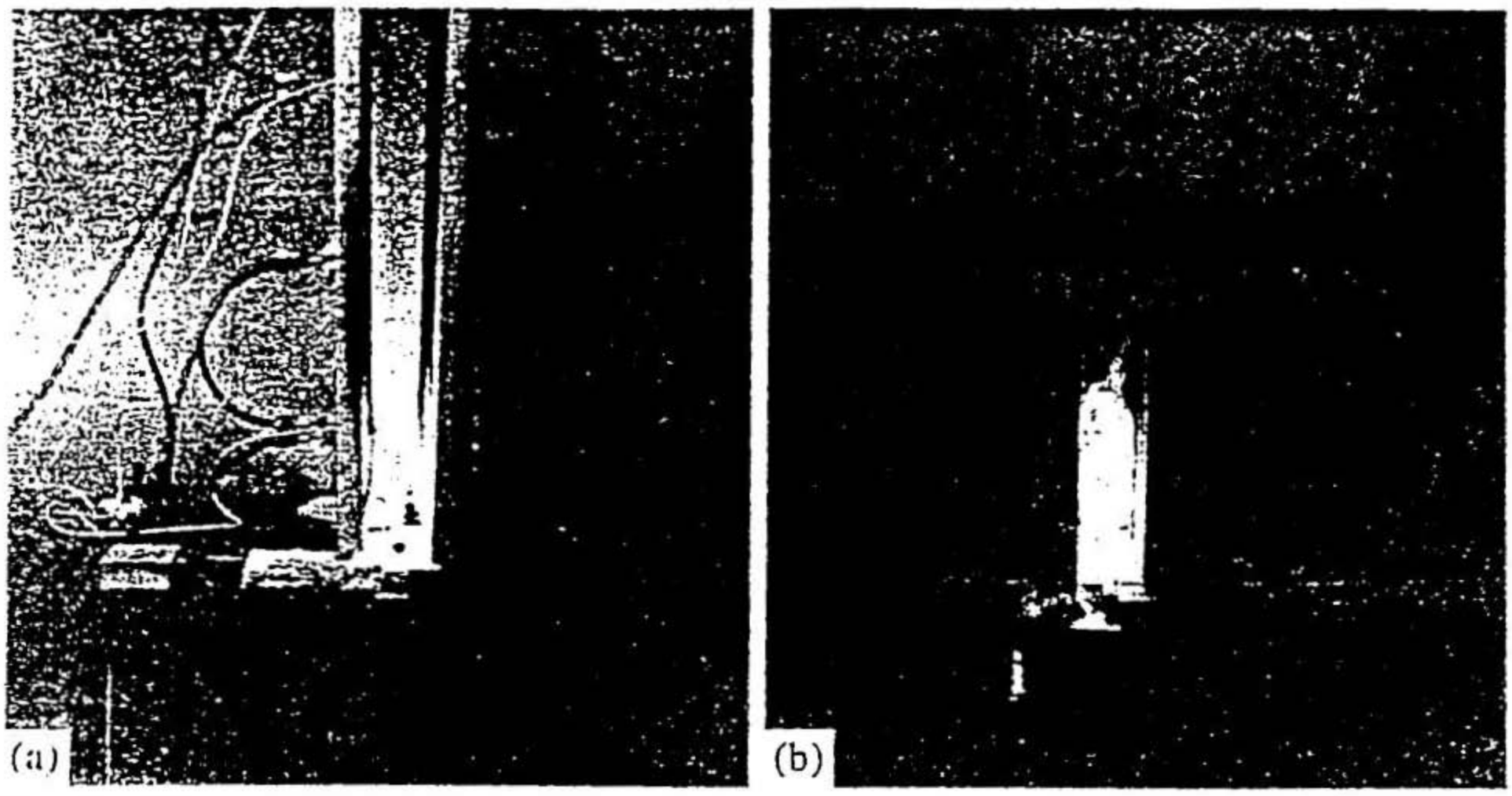

Fig. 7. Photographs of flames; 60 mm separation, burner in centre of separation, $\dot{Q} = 12{\cdot}5$ kW. (a) Open base; (b) closed base.

regression equations are presented below for the burner against the instrumented wall and in the centre of the gap (centreline heat fluxes only, and all heat fluxes). Separate correlations were obtained for the single wall and parallel wall configurations, as these are very different cases. When a second wall is in place, the air flows are different, affecting the convective heat transfer, and radiation from the opposite wall contributes to the overall heat transfer to the instrumented wall. Tests were not carried out to find the separation limit for which the parallel wall equations break down, where the system would effectively become a single wall case. Excellent correlations were obtained for the different cases using only the groups $x/Q_1^{*2/3}D$ (after Hasemi[10]), $x/Q_1^{*}D$, y'/D and a/D, with correlation coefficients greater than 0·95.

Single wall, burner against the instrumented wall

Open base, centreline fluxes only

$$\dot{q}''_w = 104{\cdot}95(x/Q_1^{*2/3}D)^{-1{\cdot}55}. \tag{1}$$

The correlation coefficient is 0·993 (Fig. 8).

Closed base, centreline fluxes only

$$\dot{q}''_w = 51{\cdot}07(x/Q_1^{*2/3}D)^{-1{\cdot}29}. \tag{2}$$

This has a correlation coefficient of 0·987 (Fig. 9).

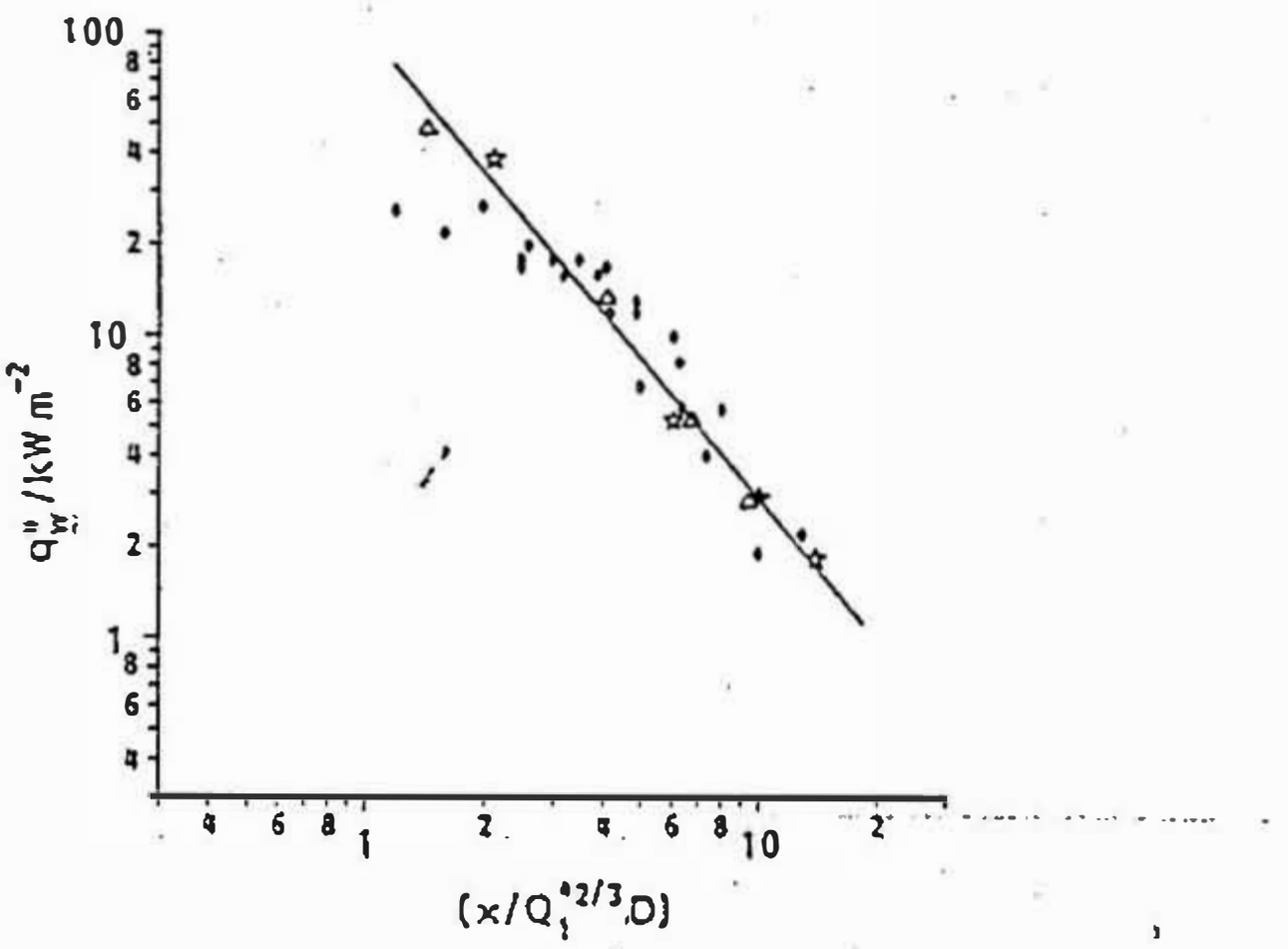

Fig. 8. Heat flux as a function of $[x/Q_1^{*2/3}D]$, burner against the single wall, with the base open centreline heat fluxes only. ☆, $\dot{Q}_1 = 11{\cdot}6$ kW/m; △, $\dot{Q}_1 = 20{\cdot}9$ kW/m; ◇, data of Hasemi for thin wall.[10] Note: the correlation does not include Hasemi's results.

Open base, all wall heat fluxes

$$\dot{q}''_w = 136{\cdot}8[x/(Q_1^{*2/3}D(y'/D)^{0{\cdot}25})]^{-1{\cdot}56}. \quad (3)$$

This has a correlation coefficient of 0·990 (Fig. 10). This shows that as (y'/D) increases to its maximum value of 0·5 (on the centreline, where $y = 0$), the heat flux increases to a maximum.

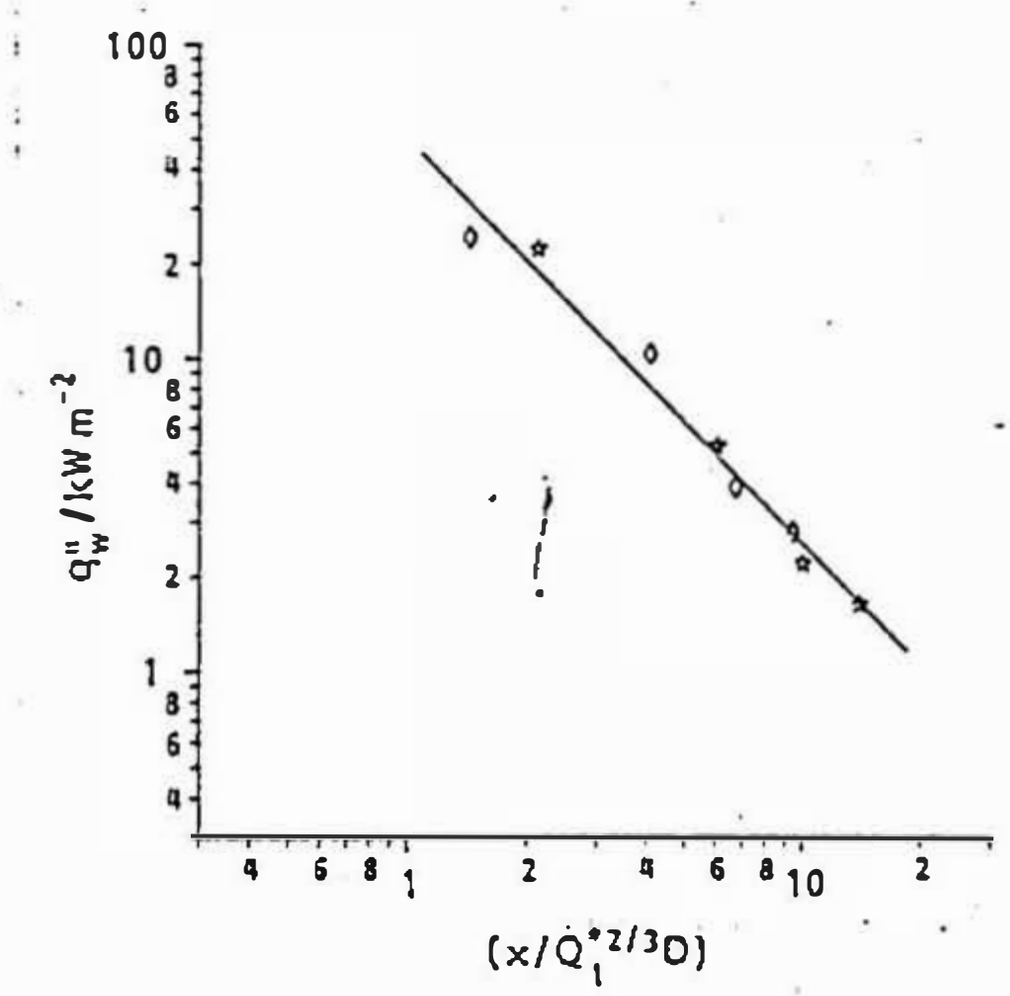

Fig. 9. Heat flux as a function of $[x/Q_1^{*2/3}D]$, burner against the single wall, with the base closed centreline heat fluxes only. ☆, $\dot{Q}_1 = 11{\cdot}6$ kW/m; ◇, $\dot{Q}_1 = 20{\cdot}9$ kW/m.

∞ 64288 adj = +4pts

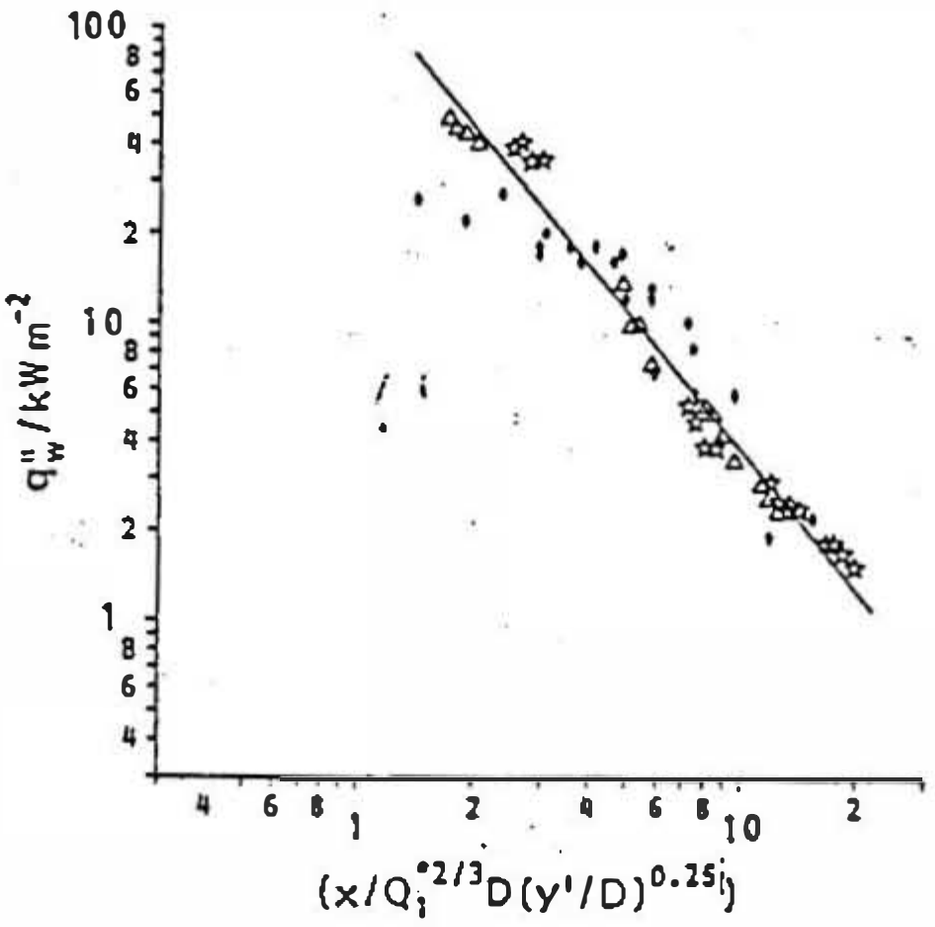

Fig. 10. Heat flux as a function of $[x/Q_1^{*2/3}D(y'/D)^{0.25}]$, burner against the single wall, with the base open all wall heat fluxes. ☆, $\dot{Q}_1 = 11{\cdot}6$ kW/m; △, $\dot{Q}_1 = 20{\cdot}9$ kW/m; ◇, data of Hasemi for thin wall.[10] Note: the correlation does not include Hasemi's results.

Closed base, all wall heat fluxes

$$\dot{q}''_w = 51{\cdot}81[x/(Q_1^{*2/3}D(y'/D)^{0.35})]^{-1.14}. \quad (4)$$

This has a correlation coefficient of 0·979 (Fig. 11).

Data from experiments on heat transfer from a line burner to a thin wall carried out by Hasemi[10] have been plotted in Figs 8 (centreline only) and 10 (all relevant results) for comparison with the present data, although the experimental conditions were different. Hasemi used a thermally thin wall which had an open base but closed sides: it was

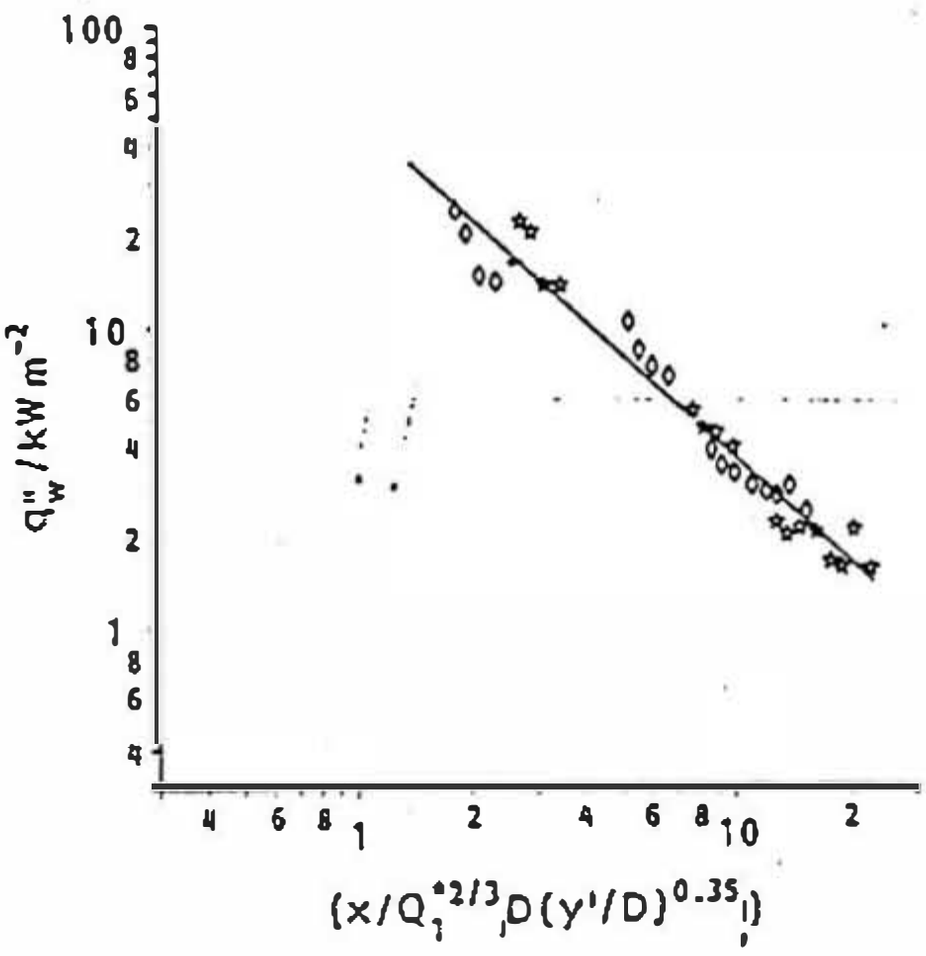

Fig. 11. Heat flux as a function of $[x/Q_1^{*2/3}D(y'/D)^{0.35}]$, burner against the single wall, with the base closed all wall heat fluxes. ☆, $\dot{Q}_1 = 11{\cdot}6$ kW/m; ◇, $\dot{Q}_1 = 20{\cdot}9$ kW/m.

considered[22] that this matched the present open base arrangement most closely, although the effect of the closed sides is not known. The agreement is very good. Not surprisingly, the data which he obtained for a line burner against an isothermal wall did not show the same correlation, falling well outside (below) the scatter of the present data.

Two parallel walls, burner against the instrumented wall

Open base, centreline heat fluxes

$$\dot{q}''_w = = 104{\cdot}53(x/Q_1^{*2/3}D)^{-1{\cdot}4}. \tag{5}$$

This has a correlation coefficient of 0·979 [Fig. 12(a)] although no allowance has been made for the different separations. A slight improvement is achieved if the separation is taken into account:

$$\dot{q}''_w = 42{\cdot}18[x(a/D)^{0{\cdot}36}/Q_1^{*2/3}D]^{-1{\cdot}4}. \tag{6}$$

If the separation term (a/D) is included, the correlation coefficient becomes 0·991 [Fig. 12(b)], showing that the separation does have some influence on the heat fluxes generated at the wall. Examination of eqn (6) shows that the heat flux depends on $(a/D)^{-0{\cdot}5}$, i.e. the inverse of the square root of the separation.

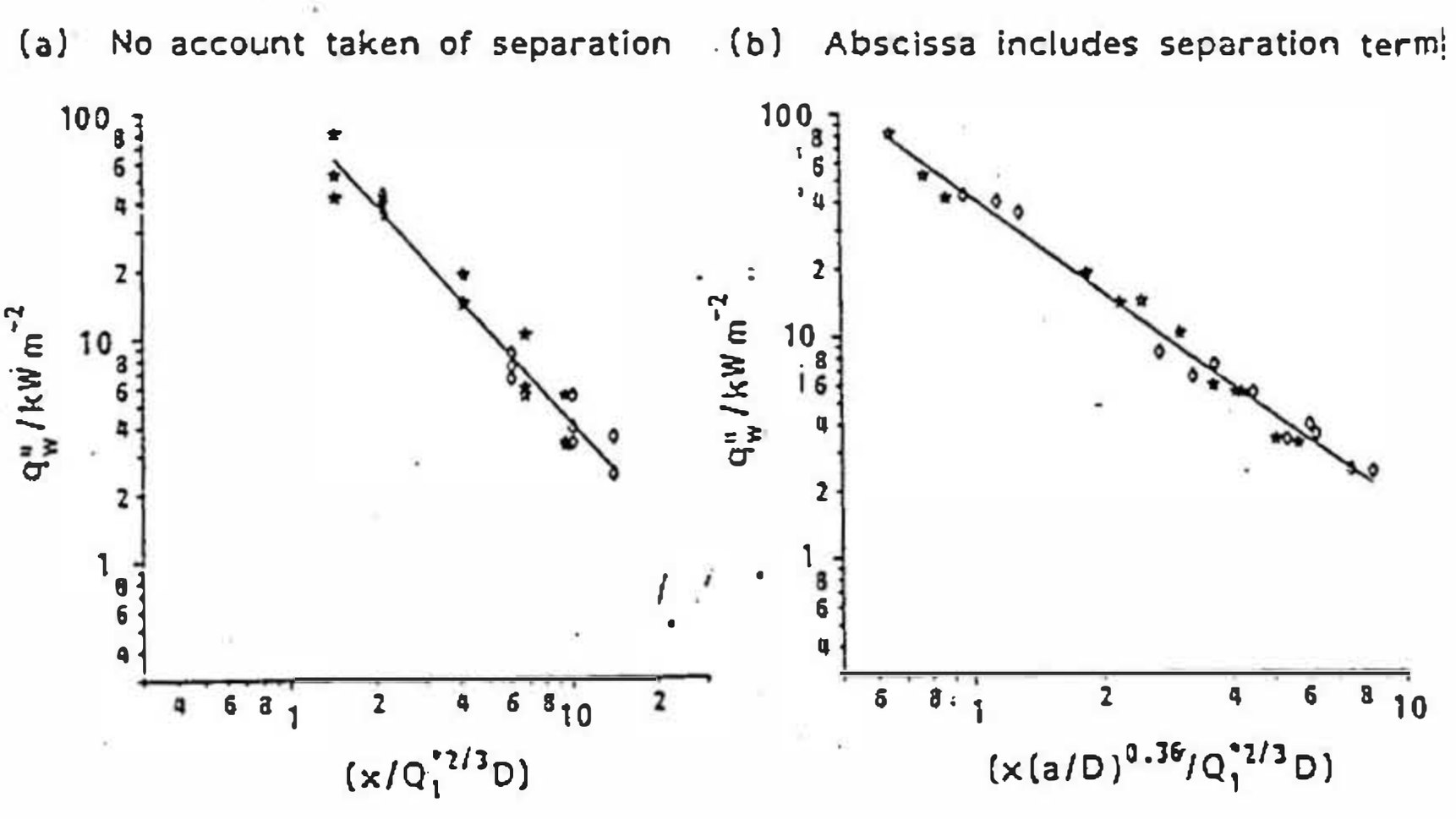

Fig. 12. Heat flux as a function of $[x(a/D)^n/Q_1^{*2/3}D]$, parallel walls, burner against the instrumented wall, with the base open, centreline heat fluxes only. ◇, $\dot{Q}_1 = 11{\cdot}6$ kW/m; ☆, $\dot{Q}_1 = 20{\cdot}9$ kW/m. (a) No account taken of separation; (b) abscissa includes separation term.

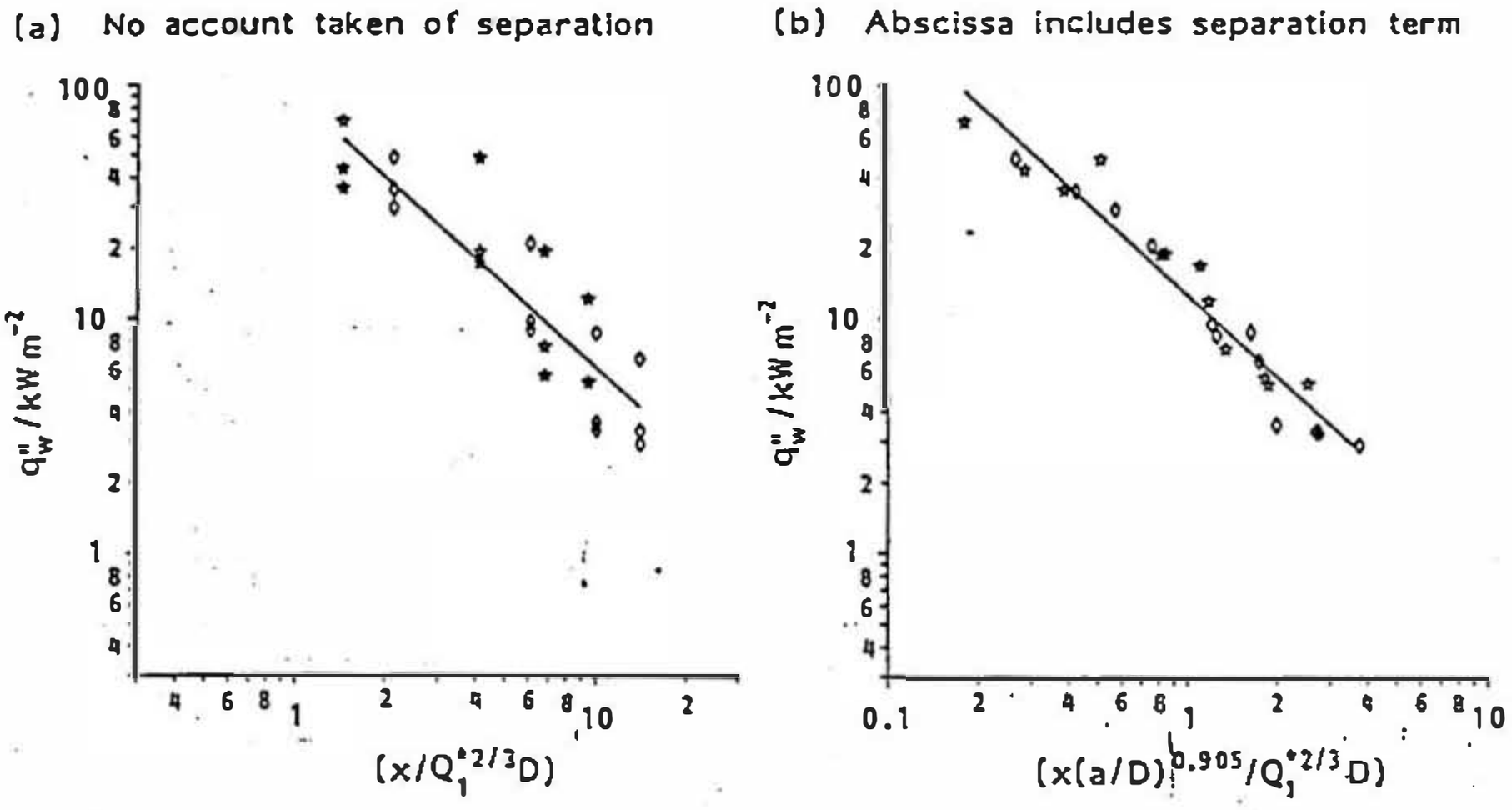

Fig. 13. Heat flux as a function of $[x(a/D)^n/Q_1^{*2/3}D]$, parallel walls, burner against the instrumented wall, with the base closed, centreline heat fluxes only. ◇, $\dot{Q}_1 = 11{\cdot}6$ kW/m; ☆, $\dot{Q}_1 = 20{\cdot}9$ kW/m. (a) No account taken of separation; (b) abscissa includes separation term.

Closed base, centreline heat fluxes

$$\dot{q}''_w = 89{\cdot}5(x/Q_1^{*2/3}D)^{-1{\cdot}16}. \tag{7}$$

This has a much lower correlation coefficient of 0·893 [Fig. 13(a)], suggesting a much greater dependence on the separation. Regression analysis leads to:

$$\dot{q}''_w = 12{\cdot}74[x(a/D)^{0{\cdot}905}/Q_1^{*2/3}D]^{-1{\cdot}16} \tag{8}$$

The improvement in the correlation with the addition of the separation term is considerable, the correlation coefficient now being 0·970 [Fig. 13(b)]. The heat flux is seen to depend on $(a/D)^{-1{\cdot}05}$.

The above equations for the parallel walls relate only to the centre line of the instrumented wall. In an attempt to correlate all the heat flux data from a given set of experiments, regression analyses were carried out including the term (y'/D) as used for the single wall case. The results are as follows:

Open base, all wall heat fluxes

The exponent of the separation term (a/D) introduced in eqn (6) is held constant, at 0·36, and the horizontal distance is included as (y'/D).

$$\dot{q}''_w = 67{\cdot}38[x(a/D)^{0{\cdot}36}/(Q_1^{*2/3}D(y'/D)^{0{\cdot}38})]^{-1{\cdot}47}. \tag{9}$$

The correlation coefficient is 0·987 [Fig. 14(a)]. The heat flux is proportional to $(y'/D)^{0{\cdot}56}$.

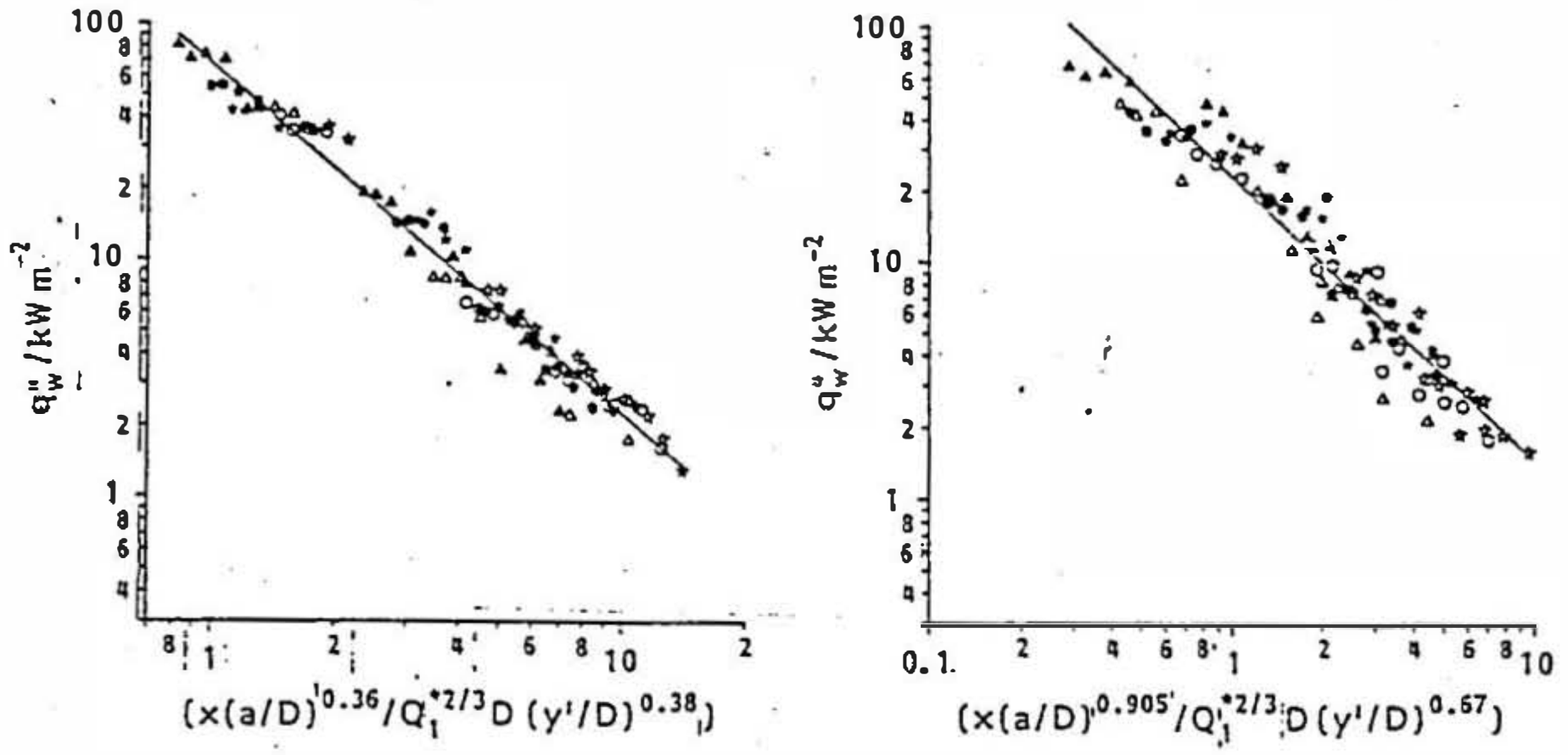

Fig. 14. Heat flux as a function of $[x(a/D)^n/Q_1^{*2/3}D(y'/D)^m]$, parallel walls, burner against the instrumented wall, all wall heat fluxes. ☆, 140 mm separation; O, 100 mm separation, Δ, 60 mm separation; open symbols, $\dot{Q}_1 = 11{\cdot}6$ kW/m; closed symbols, $\dot{Q}_1 = 20{\cdot}9$ kW/m. (a) Open base; (b) closed base.

Closed base, all wall heat fluxes

$$\dot{q}''_w = 23{\cdot}31[x(a/D)^{0{\cdot}905}/(Q_1^{*2/3}D(y'/D)^{2/3})]^{-1{\cdot}2}. \qquad (10)$$

The correlation coefficient is 0·962 [Fig. 14(b)]. The horizontal distance (y'/D) has a greater effect than in the case of the open base (as can be seen in the contour plots, Fig. 6). Air cannot enter the channel from beneath the boards, only from the sides, and so is entrained there at a higher velocity than for the open base configuration. This has the effect of pushing the flame over towards the centre and increasing the cooling close to the edges of the boards. This leads to the larger decreases in heat flux away from the wall centreline for the closed base. The heat flux is proportional $(y'/D)^{0{\cdot}8}$.

Two parallel walls, burner in the centre of the gap

For the burner in the centre of the gap, there is no equivalent to a single wall configuration. For the parallel board situation, equations have again been developed for the heat fluxes on the centreline and then extended to include the horizontal position. It was found that the separation term was always necessary in this case to obtain a satisfactory correlation. It was also found that the relationships best able to

ω 64288 adj = +38pts

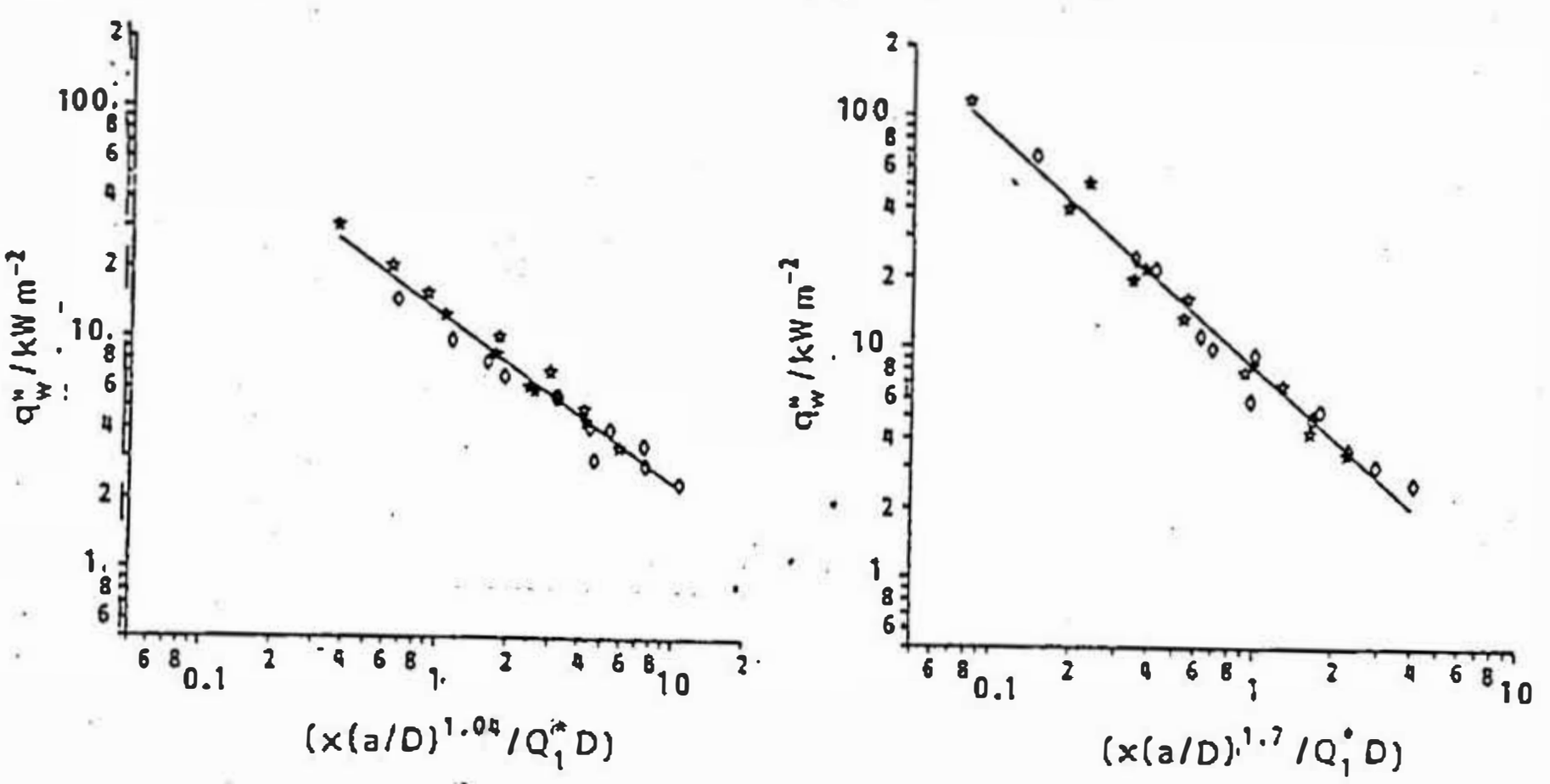

Fig. 15. Heat flux as a function of $[x(a/D)^n/Q_1^*D]$, parallel walls, burner in the centre of the separation, centreline heat fluxes only. ◇, $\dot{Q}_1 = 11{\cdot}6$ kW/m; ☆, $\dot{Q}_1 = 20{\cdot}9$ kW/m. (a) Open base; (b) closed base.

describe the data included the dimensionless group x/Q_1^*D rather than the previously used $x/Q_1^{*2/3}D$. These are shown in Figs 15 and 16.

Open base, centreline heat fluxes

$$\dot{q}''_w = 12{\cdot}85[x(a/D)^{1{\cdot}04}/Q_1^*D]^{-0{\cdot}741}. \tag{11}$$

This has a correlation coefficient of 0·979 [Fig. 15(a)]. The heat flux depends on $(a/D)^{-0{\cdot}77}$, whereas for the open base with the burner at the wall it was $(a/D)^{-0{\cdot}5}$. The separation has therefore greater influence in this case.

Closed base, centreline heat fluxes

$$\dot{q}''_w = 8{\cdot}23[x(a/D)^{1{\cdot}7}/Q_1^*D]^{-1{\cdot}02}. \tag{12}$$

The separation term is seen to be more important here than for the burner at the wall, as the heat flux depends on $(a/D)^{-1{\cdot}73}$, rather than $(a/D)^{-1{\cdot}05}$. This is confirmed by the fact that it was impossible to obtain a reasonable correlation coefficient without inclusion of the separation term. For this equation the correlation gives a coefficient of 0·987 [Fig. 15(b)].

These equations were then extended to the flux distribution across the wall and the term y'/D included.

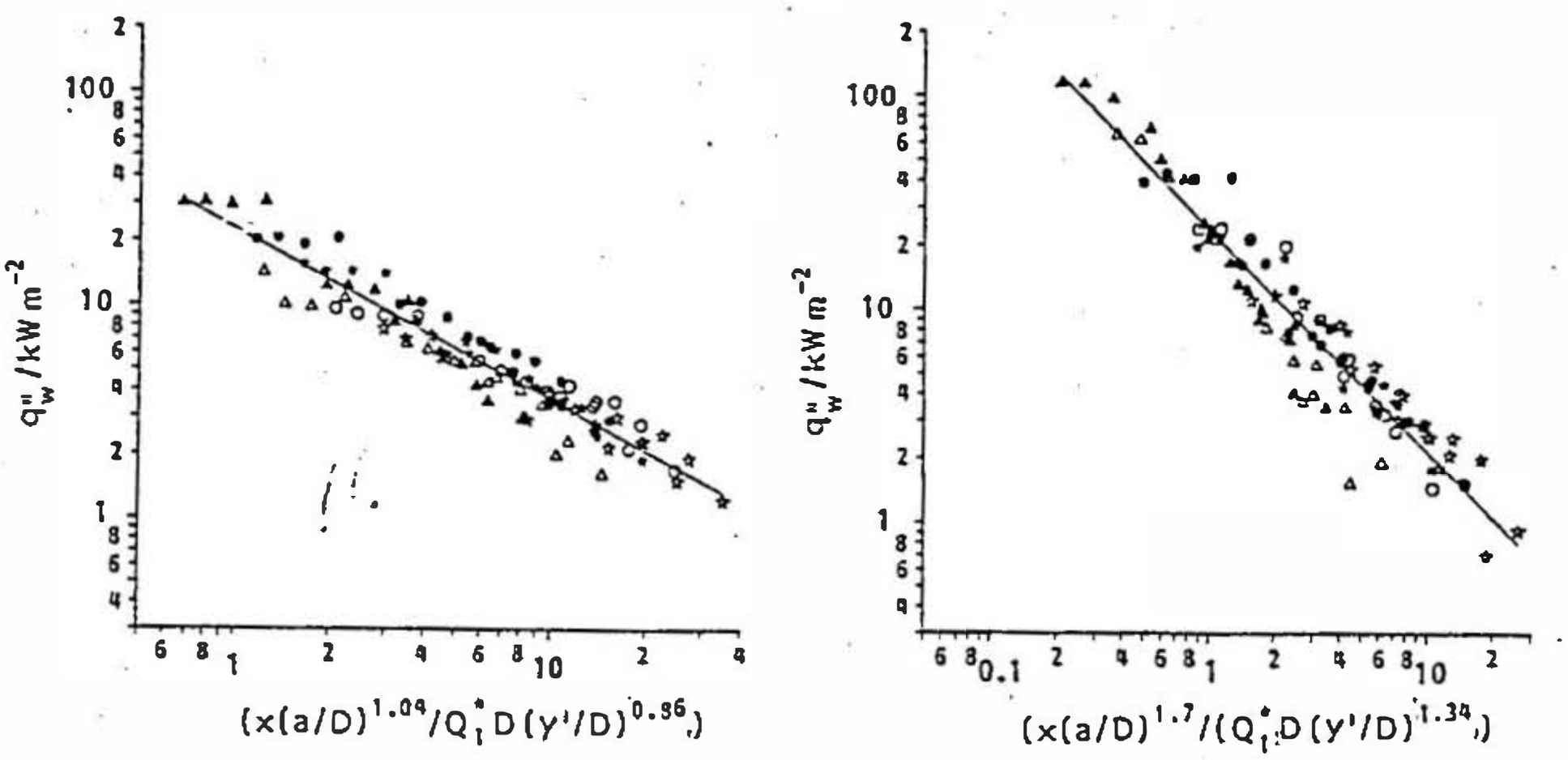

Fig. 16. Heat flux as a function of $[x(a/D)^n/Q_1^*D(y'/D)^m]$, parallel walls, burner in the centre of the separation, all wall heat fluxes, ☆, 140 mm separation; ○, 100 mm separation; △, 60 mm separation; open symbols, $\dot{Q}_1 = 11{\cdot}6$ kW/m; closed symbols, $\dot{Q}_1 = 20{\cdot}9$ kW/m. (a) Open base; (b) closed base.

Open base, all wall heat fluxes

$$\dot{q}''_w = 22{\cdot}71[x(a/D)^{1{\cdot}04}/(Q_1^*D(y'/D)^{0{\cdot}86})]^{-0{\cdot}797}. \qquad (13)$$

The horizontal distance has more influence with the burner away from the wall than against it, with the heat flux dependent on $(y'/D)^{0{\cdot}69}$. The correlation coefficient is 0·956 (Fig. 16a).

Closed base, all wall heat fluxes

$$\dot{q}_w = 23{\cdot}94[x(a/D)^{1{\cdot}7}/(Q_1^*D(y'/D)^{1{\cdot}34})]^{-1{\cdot}04}. \qquad (14)$$

This equation shows a dependence of heat flux on $(y'/D)^{1{\cdot}39}$, significantly greater than for the open base, and for the burner against the wall. The correlation coefficient in this case is 0·957 [Fig. 16(b)].

In general, the heat fluxes are greater when the line burner is against the instrumented wall, rather than in the centre of the gap. This is consistent with the hypothesis that direct flame impingement creates the highest heat transfer rate. The apparent exception is the case in which the base is closed and the separation is 60 mm: this gives a significantly higher heat flux for the burner at the central location than against the wall (Fig. 5). In this case, flame is seen to fill the entire width of the gap when the base is closed, giving direct flame impingement on both walls. The surface of the opposite wall will increase in temperature and radiate, thus contributing to the measured heat flux at the

instrumented wall. The effect of radiation from the opposite wall is being investigated, and will be published in due course. Direct radiation from the flame will also be increased due to the greater radiative pathlength, but the overall contribution to the heat flux from this source will remain small.

The different configurations of open and closed base give rise to different levels of wall heat flux. For the burner against the instrumented wall, the maximum heat fluxes are usually seen close to the base of the boards for the open base. This changes with increasing height, where the closed base demonstrates higher fluxes. Generally, the closed base configuration exhibits the higher heat fluxes: this becomes very noticeable when the burner is in the centre of the gap. When the base is open, cool air can flow upwards from the base and come between the flame and the walls, preventing direct flame impingement and reducing the heat flux. This cannot occur with the closed base, and higher heat fluxes are observed. The large dependence that the heat flux has on separation, given in eqn (14), is a consequence of the effect becoming very pronounced as the separation is reduced. In the most extreme case, 60 mm separation, the heat flux for the closed base is almost four times that for the open base (see Fig. 5).

These observations are of direct relevance to problems of ignition and upward flame spread in confined spaces which have inward-facing combustible surfaces. The implications for the storage of bulk materials are clear, but they are equally applicable to any situation involving vertical ducts and cavities which have combustible linings. The correlations presented in this paper provide a first step towards the analysis of the hazard associated with such scenarios. However, a wider database should be sought to test these correlations and extend their range, in particular, the effects of overall scale and height to width aspect ratio. The current study maintains as constant the wall height and width, and burner length.

CONCLUSIONS

1. For a line burner against a single wall, the heat flux at the wall is a function of $x/Q_{\dagger}^{*2/3}D$ and y'/D, the normalised horizontal distance from the edge of the burner, with different correlations existing for open and closed base configurations.

2. For a parallel wall situation, with the burner against the instrumented wall, the wall heat flux is a function of $x/Q_{\dagger}^{*2/3}D$, y'/D, and a/D, the nondimensional separation between the walls. The heat flux is

more dependent on separation for a closed base than the open base, where a small change in separation can cause a significant change in heat flux. The heat flux falls towards the edge of the wall for the closed base, whilst this is less pronounced for the open base. This is shown by the higher dependence on y'/D for the closed base.

3. With the burner in the centre of the gap between the boards, the heat flux is a function of x/Q^*d, y'/D, and a/D. The separation has a greater influence in this configuration than for the burner against the wall.

4. The burner position has an important influence on the heat flux distribution, and it is not always the case that simply moving the burner away from the wall decreases the heat flux at that wall.

5. Within the range of separations and conditions studied, altering the air flow pattern to the flame by preventing air entering under the boards leads to significant increases in heat fluxes to the surfaces. This is further enhanced by reducing the separation between the boards.

6. A precise understanding of the potential exposure conditions of materials in bulk storage is necessary in order that appropriate ignition sources and test methods are used to assess their hazard.

7. Correlations of wall heat fluxes for different conditions are necessary in order to understand further the parameters influencing heat flux and help identify possible hazardous storage conditions. This work has shown that simple correlations exist which can be used in the development of flame spread models and for prediction of fire behaviour.

ACKNOWLEDGEMENTS

The authors wish to thank SERC and HSE for a Case Studentship to Ms Foley. They acknowledge the technical assistance of Les Russell, Dave Bagshaw, and Ed Belfield, and are grateful to Dr Graham Atkinson, Dr John de Ris and Dr George Grant for helpful discussions.

REFERENCES

1. Fernandez-Pello, A. C. & Hirano, T., Flame spread modeling. *Combust. Sci. Technol.*, 39 (1984) 119–134.
2. Saito, K., Quintiere, J. G. & Williams, F. A., Upward turbulent flame spread. In *Fire Safety Science—Proceedings of the First International Symposium.* Hemisphere Publishing Co., 1985, pp. 75–86.

αn 64288 adj = +0pts change = -18pts

3. Hasemi, Y., Thermal modeling of upward flame spread. In *Fire Safety Science—Proceedings of the First International Symposium.* Hemisphere Publishing Co., 1985, pp. 87–96.
4. Janssens, M., Determining flame spread properties from cone calorimeter measurements—General concepts. In *Heat Release in Fires,* ed. V. Babrauskas & S. J. Grayson. Elsevier Applied Science, London, 1992, pp. 265–281.
5. Hymes, I. & Flynn, J. F., The probability of fire in warehouses and storage premises. Safety and Reliability Directorate. HSE Report No. HSE/SRD/089/00001/89/Draft A.
6. Ward, R. B., A survey of major fires in warehouses containing dangerous chemicals. *Fire Prevention,* 175 (1984) 20–27.
7. Ahmed, T. & Faeth, G. M., Turbulent wall fires. In *Fifteenth Symposium (International) on Combustion.* The Combustion Institute, 1974, pp. 1149–1160.
8. Hasemi, Y. & Tokunaga, T., Some experimental aspects of turbulent diffusion flames and buoyant plumes from fire sources against a wall and in a corner of walls. *Comb. Sci. Technol.,* 40 (1984) 1–17.
9. Sugawa, O., Satoh, H. & Oka, Y., Flame height from rectangular fire sources considering mixing factor. In *Fire Safety Science—Proceedings of the Third International Symposium.* pp. 435–444.
10. Hasemi, Y., Experimental wall flame heat transfer correlations for the analysis of upward wall flame spread. *Fire Sci. Technol.,* 4 (1984) 75–89.
11. Quintiere, J., Harkleroad, M., & Hasemi, Y., Wall flames and implications for upward flame spread. *Combust. Sci. Technol.* 48 (1986) 191–222.
12. Ahmed, T. & Faeth, G. M., Turbulent wall fires. In *Fifteenth Symposium (International) on Combustion.* The Combustion Institute 1974, pp. 1149–1160.
13. Quintiere, J. G. & Cleary, T. G., Heat flux from flames to vertical surfaces. *Fire Technol.,* 30 (1994) 209–231.
14. Williamson, R. B., Revenaugh, A. & Mowrer, F. W., Ignition sources in room fire tests and some implications for flame spread evaluation. In *Fire Safety Science—Proceedings of the Third International Symposium.* 1991, pp. 657–666.
15. Ahonen, A. I., Holmlund, C. & Kokkala, M. A., Effects of ignition source in room fire tests. *Fire Sci. Technol.,* 7 (1987) 1–13.
16. Toong, T. Y., A theoretical study of interactions between two parallel burning fuel plates. *Combust. Flame,* 5 (1961) 221–227.
17. Kim, J. S., de Ris, J. & Kroesser, F. W., Laminar burning between parallel fuel surfaces. *Int. J. Heat Mass Transfer,* 17 (1974) 439–451.
18. Tamanini, F., Calculations and experiments on the turbulent burning of vertical walls in single and parallel configurations. Technical Report No. OAOE7. BU-2, Factory Mutual Research, May 1979.
19. Kurosaki, Y., Ito, A. & Chiba, M., Downward flame spread along two vertical, parallel sheets of thin combustible solid. In *Seventeenth Symposium (International) on Combustion.* The Combustion Institute, 1978, pp. 1211–1220.
20. Most, J. M., Bellin, B., Joulain, P. & Sztal, B., Interaction between two

000 64288 adj = +48opts change = +48opts all = +opts

burning vertical walls. In *Fire Safety Science—Proceedings of the Second International Symposium.* pp. 285–294.
21. Ingason, H., Fire experiments in a two dimensional rack storage. BRANDFORSK-project 701–917, SP Report 1993: 56, 1993.
22. Hasemi, Y., Private communication.

MECHANISMS OF HEAT TRANSFER FROM FLAMES BETWEEN PARALLEL VERTICAL SURFACES

M. FOLEY* , D. D. DRYSDALE* AND C. J. LEA#

Abstract

Measurements of the distribution of total heat flux on a wall exposed to a propane line burner have been carried out for a number of configurations in which the distance to a parallel wall has been varied. Incombustible monolux boards, 813 x 610 mm were used to make the walls, and tests were performed with wall separation distances of ∞ (single wall case), 60 mm, 100 mm and 140 mm. The burner position and heat release rate were altered and the effect of air flow into the system investigated by having either an air gap between the base of the walls and the bench, or by closing the gap with an incombustible base.

The heat fluxes were seen to increase as the separation between the walls was reduced. With one exception, the heat fluxes were greatest with the burner against the instrumented wall. Changing the air flow by blocking the ingress of air at the base of the walls was shown to have a dramatic effect. The most extreme case gave almost a four fold increase in the maximum heat flux when the base is closed off. This was for the burner in the centre of the channel between the walls, at the smallest wall separation.

Correlations have been obtained, for both the single wall and the parallel wall configurations, for wall heat flux, which show its dependence on separation distance, height, distance across the wall and the dimensionless burner heat release rate Correlation coefficients of at least 0.956 were obtained for all cases. The single wall case showed good agreement with heat flux data from a line burner to a thin wall carried out by Hasemi[1]. For the parallel walls, the heat flux showed a greater dependence on separation for the closed base than the open, and the

---

* University of Edinburgh, Department of Civil Engineering, The Kings Buildings, Mayfield Rd, Edinburgh, Scotland, EH9 3JL

Health and Safety Laboratory, Health and Safety Executive, Fire and Thermofluids Section, Harpur Hill, Buxton, Derbyshire, U.K., SK17 9JN

[1] Hasemi, Y., Experimental wall flame heat transfer correlations for the analysis of upward wall flame spread.

separation had a greater influence with the burner in the centre of the channel than against the wall.

The parallel wall heat flux correlations, with the burner flush with the wall, were found to be:

open base: $$\dot{q}''_w = 67.38\left[x(a/D)^{0.36} \Big/ \left(Q_l^{*2/3} D(y'/D)^{0.38}\right)\right]^{-1.47}$$

closed base: $$\dot{q}''_w = 23.31\left[x(a/D)^{0905} \Big/ \left(Q_l^{*2/3} D(y'/D)^{2/3}\right)\right]^{-1.2}$$

The correlations for the burner in the centre of the channel are:

open base: $$\dot{q}''_w = 22.71\left[x(a/D)^{1.04} \Big/ \left(Q_l^{*} D(y'/D)^{0.86}\right)\right]^{-0.797}$$

closed base: $$\dot{q}''_w = 23.94\left[x(a/D)^{1.7} \Big/ \left(Q_l^{*} D(y'/D)^{1.34}\right)\right]^{-1.04}$$

The extreme case of the 60 mm separation and the burner in the centre, where the closed base gives four times the heat flux of the open base, was studied in more detail using FLOW3D, a CFD package. Both the computer modelling and experimental observations revealed very different flow patterns for the two cases. With the open base, the flame was relatively thin and did not spread to the walls. The closed base gave a much thicker flame which filled the entire width of the channel, touching both walls and giving much higher heat fluxes. The flame was pushed over towards the wall centreline by the air entering at the sides of the walls.

Measurements were also made of radiation, in order that the relative importance of radiation and convection could be assessed. The radiation was seen to be more important in the parallel wall configuration than for a single wall, due to cross-radiation. Radiation was the dominant mode of heat transfer for the open base with the burner in the centre, whilst convection was more important with the burner against the wall. Both radiation and convection were higher for the closed base, but the relative influence of convection was increased. In this case, convection was the dominant mode of heat transfer even for the burner in the centre of the channel.

These results show the importance of air flow and convection for ignition and flame spread.

There is a difference in burning behaviour between single and parallel walls, which requires further research to increase understanding. The results and findings of this study have implications for modelling flame spread in confined spaces, and for identifying the risks associated with the bulk storage of materials.

Nomenclature

a	wall separation distance, m
c_p	specific heat capacity, kJ/kgK
D	line burner length, m
g	acceleration due to gravity, ms^{-2}
$\dot{q}''_w$	wall heat flux, kWm^{-2}
$\dot{Q}_l$	burner heat release rate per unit length, kW/m
Q^*_l	dimensionless line burner heat release rate, $(Q^*_l = \dot{Q}_l / (\rho_\infty c_p T_\infty g^{1/2} D^{3/2})$
T_∞	ambient temperature, K
x	height, m
y	horizontal distance from wall centreline, m
y'	horizontal distance, $y' = 0.5D - y$; $(0 \leq y' \leq 0.5D)$
ρ_∞	density of ambient air, kgm^{-3}